PLANT ADAPTATIONS TO PHOSPHATE DEFICIENCY

EDITED BY: Alex Joseph Valentine, Alejandra Zúñiga-Feest, Aleysia Kleinert, Pablo Cornejo and Vagner A. Benedito

PUBLISHED IN: Frontiers in Plant Science

frontiers Research Topics

frontiers

ISSN 1664-8714
ISBN 978-2-88966-779-6
DOI 10.3389/978-2-88966-779-6

About Frontiers

Frontiers is more than just an open-access publisher of scholarly articles: it is a pioneering approach to the world of academia, radically improving the way scholarly research is managed. The grand vision of Frontiers is a world where all people have an equal opportunity to seek, share and generate knowledge. Frontiers provides immediate and permanent online open access to all its publications, but this alone is not enough to realize our grand goals.

Frontiers Journal Series

The Frontiers Journal Series is a multi-tier and interdisciplinary set of open-access, online journals, promising a paradigm shift from the current review, selection and dissemination processes in academic publishing. All Frontiers journals are driven by researchers for researchers; therefore, they constitute a service to the scholarly community. At the same time, the Frontiers Journal Series operates on a revolutionary invention, the tiered publishing system, initially addressing specific communities of scholars, and gradually climbing up to broader public understanding, thus serving the interests of the lay society, too.

Dedication to Quality

Each Frontiers article is a landmark of the highest quality, thanks to genuinely collaborative interactions between authors and review editors, who include some of the world's best academicians. Research must be certified by peers before entering a stream of knowledge that may eventually reach the public - and shape society; therefore, Frontiers only applies the most rigorous and unbiased reviews.
Frontiers revolutionizes research publishing by freely delivering the most outstanding research, evaluated with no bias from both the academic and social point of view. By applying the most advanced information technologies, Frontiers is catapulting scholarly publishing into a new generation.

What are Frontiers Research Topics?

Frontiers Research Topics are very popular trademarks of the Frontiers Journals Series: they are collections of at least ten articles, all centered on a particular subject. With their unique mix of varied contributions from Original Research to Review Articles, Frontiers Research Topics unify the most influential researchers, the latest key findings and historical advances in a hot research area! Find out more on how to host your own Frontiers Research Topic or contribute to one as an author by contacting the Frontiers Editorial Office: frontiersin.org/about/contact

PLANT ADAPTATIONS TO PHOSPHATE DEFICIENCY

Topic Editors:
Alex Joseph Valentine, Stellenbosch University, South Africa
Alejandra Zúñiga-Feest, Austral University of Chile, Chile
Aleysia Kleinert, Stellenbosch University, South Africa
Pablo Cornejo, University of La Frontera, Chile
Vagner A. Benedito, West Virginia University, United States

Phosphate is an essential mineral to all plants, and its availability in soils is an increasing challenge for agriculture. Phosphate is abundant in soils but its biological availability is often low due to the complexes that it forms with soil minerals and compounds. The biological availability of Phosphate is further reduced in acidic soils, which represent approximately 40% of earth's arable agricultural lands. Agricultural systems compensate Phosphate deficiency with fertilizers coming from the mining of rock phosphate, which is estimated to exhaust within the next 50 years. For these reasons, Phosphate limitations in natural and agricultural ecosystems is going to become a global problem, and we urgently need to better understand how plants respond to Phosphate deficiency.

Citation: Valentine, A. J., Zúñiga-Feest, A., Kleinert, A., Cornejo, P., Benedito, V. A., eds. (2021). Plant Adaptations to Phosphate Deficiency. Lausanne: Frontiers Media SA. doi: 10.3389/978-2-88966-779-6

Table of Contents

frontiers in Plant Science

ORIGINAL RESEARCH
published: 22 December 2017
doi: 10.3389/fpls.2017.02197

OsPT4 Contributes to Arsenate Uptake and Transport in Rice

*Ying Ye, Peng Li, Tangqian Xu, Liting Zeng, Deng Cheng, Meng Yang, Jie Luo and Xingming Lian**

National Key Laboratory of Crop Genetic Improvement and National Center of Plant Gene Research, Huazhong Agricultural University, Wuhan, China

Arsenic (As) is toxic to organisms, and elevated As accumulation in rice (*Oryza sativa*) grain may pose a significant health risk to humans. The predominant form of As in soil under aerobic conditions is As(V), which has a chemical structure similar to that of PO_4^{3-}. Rice roots take up As(V) by phosphate (Pi) transporters, such as OsPT1 and OsPT8. In the present study, we investigated the contribution of *OsPT4*, belonging to the Pht1 family, on rice As(V) uptake and transport. We determined the mRNA amounts of *OsPT*s in rice seedlings, and expressions of *OsPT1*, *OsPT4,* and *OsPT8* were up-regulated under As(V) conditions. *OsPT4*-overexpressing plants were obtained to examine the As (V) transport activity of *OsPT4* in rice. When transgenic rice grew in hydroponic culture with 25 and 50 μM As(V), the plants showed sensitivity to As(V) stress with aboveground parts showing delayed growth and the roots stunted. The *OsPT4* CRISPR lines showed the opposite phenotype. When plants were grown in 5 μM As(V) solution for 7 days, the As accumulation of *OsPT4*-overexpressing plants increased up to twice in roots and shoots. Furthermore, the arsenate uptake rates of *OsPT4*-overexpressing lines were higher compared with wild type. The V_{max} of As(V) uptake in *OsPT4*-overexpressing plants increased 23–45% compared with Nipponbare. In the flooded soil, the As accumulation of OsPT4-overexpressing plants increased 40–66% and 22–30% in straw and grain, respectively. While in *OsPT4*-cr plants As accumulation in roots decreased 17–30% compared with Nipponbare. Therefore, the present study indicates that *OsPT4* is involved in As(V) uptake and transport and could be a good candidate gene to generate low As-accumulating rice.

Keywords: *OsPT4*, rice, arsenate, phosphate transporter, uptake

OPEN ACCESS

Edited by:
Vagner A. Benedito, West Virginia University, United States

Reviewed by:
Ahmad H. Kabir, University of Rajshahi, Bangladesh
Jitender Giri, National Institute of Plant Genome Research (NIPGR), India
Emilio Fernandez, Universidad de Córdoba, Spain

***Correspondence:**
Xingming Lian
xmlian@mail.hzau.edu.cn

Specialty section:
This article was submitted to Plant Nutrition, a section of the journal Frontiers in Plant Science

Received: *21 September 2017*
Accepted: *13 December 2017*
Published: *22 December 2017*

Citation:
Ye Y, Li P, Xu T, Zeng L, Cheng D, Yang M, Luo J and Lian X (2017) OsPT4 Contributes to Arsenate Uptake and Transport in Rice. Front. Plant Sci. 8:2197. doi: 10.3389/fpls.2017.02197

INTRODUCTION

Inorganic arsenic (As) is a highly toxic metalloid listed as a Class-1 carcinogen by the International Agency for Research on Cancer (Smith et al., 2002). Humans ingest As unintentionally in contaminated food and drinking water. Excessive ingestion of As causes a series of acute and chronic human health problems, including skin lesions, cancers and nervous exhaustion (Anawar et al., 2002; Abernathy et al., 2003; Meharg and Rahman, 2003; Das et al., 2004). Rice (*Oryza sativa*), the most important staple food for half of the world's people especially in South and Southeast Asia (Meharg, 2004; Alamdar et al., 2017), is a major dietary source of inorganic As because of higher As accumulation in rice than in other cereal crops (Meharg and Rahman, 2003). The As contamination in soil is made worse by non-ferrous mining, which has elevated As accumulation in rice grain up

to 723 ng g^{-1} – far in excess of the Chinese maximum concentration of 200 ng g^{-1} for inorganic As in rice (Zhu et al., 2008; Williams et al., 2009; Okkenhaug et al., 2012). It is necessary to understand the mechanism of rice As accumulation and to generate low-As rice to protect human health.

Inorganic As in soil is classified into two chemical species, depending on the redox status of the soil: arsenite [As(III)] and arsenate [As(V)] (Abedin et al., 2002). As(III) is the predominant form in anaerobic paddy soil and As(V) in soil under aerobic conditions. Plant roots take up different kinds of As by different pathways. As(III) can enter root cells through nodulin26-like intrinsic proteins. Previous studies suggested that nodulin26-like intrinsic proteins are involved in As(III) transport and determine the sensitivity to As(III) stress in *Arabidopsis thaliana* (Isayenkov and Maathuis, 2008; Kamiya et al., 2009; Xu et al., 2015). In rice, the silicon transporter OsNIP2;1 (Lsi1) is functional in As(III) uptake (Zhao et al., 2010), and As(III) efflux from rice root cells to the xylem is through OsLsi2 (Ma et al., 2008; Li et al., 2009). However, when rice is grown in non-flooded soil for a long time, the soils become aerobic and then the rice roots primarily absorb As(V). In addition, because rice roots release oxygen, As(III) can be oxidized to As(V) in the rice rhizosphere (Seyfferth et al., 2010). It was reported that the chemical structure of As(V) is similar to that of PO_4^{3-} (Das et al., 2004). In various plant species including rice, phosphorus (Pi) competes with As(V) for uptake, suggesting that they both have the same transporters (De la Rosa et al., 2006; Catarecha et al., 2007). In *Arabidopsis*, As(V) absorption is closely related to the expression of Pi transporters Pht1;1 and Pht1;4 (Shin et al., 2004; Gonzalez et al., 2005). In rice, the Pi transport pathway genes also contribute to As uptake and transport. Overexpressing the gene for the transcription factor OsPHR2 (phosphate starvation response 2) led to doubling of the As concentration in root and shoot compared with wild-type, suggesting that this gene was involved in As(V) uptake and root–shoot translocation (Wu et al., 2011). In contrast, the Pi transporter *OsPHF1* (*phosphate transporter traffic facilitator 1*) mutant lost more than half of its ability to take up As(V) (Wu et al., 2011). The Pht1 family genes (*OsPT1*–*OsPT13*) in the rice genome encode Pi transporters that localize in the plasma membrane. Kamiya et al. (2013) reported that the As accumulation in rice shoots is consistent with *OsPT1* expression, indicating that OsPT1 is involved in As(V) uptake from soil to apoplast. In addition, OsPT8 was found to have a high affinity for As(V) and was a key transporter for As(V) uptake into rice roots (Wu et al., 2011; Kamiya et al., 2013). Overexpressing *OsPT8* increased the maximum As(V) influx by fivefold and mutation of *OsPT8* partially lost As(V) uptake ability (Wang et al., 2016).

After being absorbed by rice roots, As(V) is then transported into xylem vessels (Gilbert-Diamond et al., 2011). Because of its chemical structure being similar to Pi, As(V) can compete with Pi during Pi absorption and phosphorylation, forming As(V) esters and leading to imbalance in Pi metabolism (Finnegan and Chen, 2012). The As(V) esters are much less stable and hydrolyze faster than Pi esters. For example, As(V) competes with PO_4^{3-} in ATP (adenosine triphosphate) synthesis and replaces it to form unstable adenosine diphosphate-As(V), resulting in disruption of energy flows in the cell (Hartley-Whitaker et al., 2001; Meharg and Hartley-Whitaker, 2002; Cozzolino et al., 2010). Besides, most As(V) should be reduced to As(III) inside plant cells (Su et al., 2010; Shi et al., 2016). OsACR2 has been suggested to be involved in As(V) reduction in rice (Duan et al., 2007). The latest study suggested that OsHAC1;1 and OsHAC1;2 function as As(V) reductase and were involved in the reduction of As(V) to As(III) in rice plants (Shi et al., 2016). Overexpression of OsHAC1;1 and OsHAC1;2 increased As(III) efflux and decreased As accumulation in rice shoots. The mode of action of As(III) differs from that of As(V), with As(III) acting as a cross-linking agent by binding to monothiol molecules, thiol-containing proteins and co-factors (Ha et al., 1999; Raab et al., 2005; Song et al., 2010). On the one hand, the binding of As(III) to proteins has negative effects on folding of these proteins, resulting in inactivation of many enzymes. On the other hand, As(III) complexation is the main detoxification pathway for both As(III) and As(V) (Xu et al., 2007).

Apart OsPT1 and OsPT8, it is unclear whether other Pht1 family genes are involved in As(V) uptake. The objective of the present study was to investigate the function of Pi transporter OsPT4 in rice As(V) uptake. The mRNA amount of *OsPT4* in Nipponbare was measured and *OsPT4* was induced by As(V) stress. Overexpressing *OsPT4* significantly increased the As concentration in roots and shoots, and showed higher As(V) sensitivity at high As(V) levels. This study shows that *OsPT4* plays an important role in As(V) absorption.

MATERIALS AND METHODS

Plant Materials and Growth Conditions

Five rice (*O. sativa*) lines, the wild type Nipponbare, *OsPT2* overexpression line (*OsPT2*-ov), *OsPT4* overexpression line (*OsPT4*-ov), *OsPT4* RNA interference line (*OsPT4*-Ri), and *OsPT4* CRISPR (Clustered regularly interspaced short palindromic repeats) line (*OsPT4*-cr), were used in this study. The generation of *OsPT4*-cr is described below. *OsPT2*-ov, *OsPT4*-ov, and *OsPT4*-Ri were characterized previously (Liu et al., 2010; Ye et al., 2015).

To generate the construct of OsPT4-CRISPR vector, we designed the DNA spacer in NEB cutter[1]. The amplified PCR product including U3 promoter, spacer of OsPT4 and sgRNA (small guide RNA) were cloned into vector PJE 45/pH-Ubi-cas9-7 (Miao et al., 2013). The primers were *OsPT4*-spcer-F:5′-AGCCGGGGCTCTTGGACGCCGTTTTAGAGCTA TGCTGAAA-3′, spacer-sgRNA-R: 5′-AAAAAGCAGGCTTAAA AAAAAAGCACCGACTCG- 3′, *OsPT4*-spcer-F: 5′- GGCGTC CAAGAGCCCCGGCTTGCCACGGATCATCTGCAC-3′ and Pu3-spacer-F: 5′- AGAAAGCTGGGTAAAGGGATCTTTAA ACATAC GAAC-3′. The construct was transformed into Nipponbare via *Agrobacterium tumefaciens*-mediated transformation (Wu et al., 2003).

Standard rice culture solution was used in hydroponic experiments. The composition of the culture solution follows: 1.44 mM NH_4NO_3, 0.5 mM K_2SO_4, 1.0 mM $CaCl_2$, 1.6 mM

[1]http://tools.neb.com/NEBcutter2/

$MgSO_4$, 0.17 mM Na_2SiO_3, 0.3 mM NaH_2PO_4, 50 μM Fe-EDTA, 0.06 μM $(NH_4)_6Mo_7O_{24}$, 15 μM H_3BO_3, 8 μM $MnCl_2$, 0.12 μM $CuSO_4$, 0.12 μM $ZnSO_4$, 29 μM $FeCl_3$, and 40.5 μM citric acid at pH 5.5 (Yoshida et al., 1976). The transgenic lines were grown in solution containing different concentrations of As using Na_3AsO_4. The solution was renewed every 5 days. The Nipponare and transgenic lines were grown in a greenhouse under 16 h/8 h, 30/22°C, day/night conditions after germination, with *c.* 60% relative humidity.

A soil experiment was performed in the experimental field in Huazhong Agricultural University, Wuhan, China. The experimental field was divided into two parts with or without Pi fertilizer. The Pi concentrations of these two fields were 15 mg kg^{-1} soil P (−P) and 30 mg kg^{-1} soil P (+P). Seedlings of Nipponbare and *OsPT4*-overexpressing plants (20-day-old) were transplanted into the soil and grown to maturity. Each treatment had 10 replicates.

RNA Extraction and Real-Time PCR

Plant tissue samples (50–100 mg) were cut and ground with a mortar and pestle to a fine powder in liquid nitrogen. Afterward, total RNA was extracted using TRizol regent (Invitrogen, Carlsbad, CA, United States). Then, the resulted total RNAs were checked by gel electrophoresis (**Supplementary Figure S1A**). According to the manufacturer's instructions, 3 μg of total RNA was used to synthesize the first-strand cDNA in 20 μL of reaction mixture using M-MLV reverse transcriptase (Invitrogen). Real-time PCR was performed using the SYBR Premix Ex TaqTM (TaKaRa, Shiga, Japan) with the following gene-specific primers (**Table 1**). The amplification reaction was performed on an Applied Biosystems (Foster City, CA, United States) 7500 PCR instrument. The rice *Ubiquitin 5* gene was used as the internal control.

TABLE 1 | Primers for Real-time PCR.

Gene name	Forward primer/reverse primer
OsPT1	AGGCGGCCTACCCGAAGTAATTT/ AGGCGGCCTACCCGAAGTAATTT
OsPT2	GCACAAACTTCCTCGGTATGCTCA/ ACTCACGTCGAGACGGCATGTTTA
OsPT3	TGGAGGAGGTGTCCAAGGAGAA/ CAATGAGCTCTGTTGAACCACCGT
OsPT4	GCAACGTCATCGGGTTCTTCTTCA/ ACATCGTCATCGTCCTCGTTCTCG
OsPT5	AACTAACTCCTACAGGCAGACCGT/ GAGGCAAGAATGGCAGAATGCAAC
OsPT6	CTGCAAACTGTACTGTAGCGCTGT/ TTCGATCGATCTTCTCTGGTCTCG
OsPT7	AGCCGTGATCCACCCGTTAATTC/ TCTCTAGTGGACTAACCACGCA
OsPT8	TCCAGAAGGACATCTTCACCAGCA/ ATGTCGATGAGGAAGACGGTGAAC
OsPT9	TAAATGTTCTCATGGAGGCGGCGA/ ATTGTCATAGAGACATCCGGTGCG
OsPT10	GTCTCCGTGTGAGTGAACTCGATCAT/ CATGCACTCTCTCTGACGCACAAA
OsPT12	TCGTCCGGAGTTGAGATGGTGTAA/ ACGCTACAAGTACGAGCTTCGCAT
ubiquitin	AACCAGCTGAGGCCCAAGA/ ACGATTGATTTAACCAGTCCATGA

As(V) Tolerance Assays

Rice seeds were soaked in deionized water overnight and germinated at 37°C in darkness for 3 days. Seedlings were transferred to 0.5 mM $CaCl_2$ solution containing a gradient of As(V) concentrations: 0, 25, and 50 μM. Each treatment was replicated with 10 seedlings. Seedlings were grown in a controlled-environment room at 25°C constant temperature and 12-h day length. After 7 days, we photographed the growth phenotype and measured root length and shoot height.

Determination of As Concentration

Shoots and roots were harvested separately and roots washed with distilled water before sampling. After drying at 80°C for 3 days, all samples were digested in 65% nitric acid in a MARS6 microwave (CEM) at a temperature gradient of 120–180°C for 45 min, and then diluted in deionized water. The As content of samples was determined with inductively coupled plasma-mass spectrometry (Agilent 7700 series, CA, United States).

Measurement of Pi Concentration in Plants

Fresh samples were milled in liquid nitrogen and kept at 4°C until samples thawed. The milled samples were homogenized in 10% (w/v) perchloric acid:5% (w/v) perchloric acid (1:9) and placed on ice for 30 min. Following centrifugation at 10 000 *g* for 10 min at 4°C, the supernatant was used for Pi measurement by molybdenum blue method. The working fluid was a 6:1 ratio 0.4% (w/v) ammonium molybdate dissolved in 0.5M H_2SO_4 mixed with 10% ascorbic acid. Of the working fluid, 2 mL was added to 1 mL of sample solution, incubated in a water bath at 42°C for 20 min, and then cooled on ice. Sample absorbance was measured at 820 nm, and Pi concentration was calculated by normalization to fresh-weight values.

Data Analysis

Data were examined using one-way ANOVA, followed by comparisons of means using the LSD test (Fisher's Least Significant Difference).

RESULTS

Expression Pattern of Pht1 Family Members under As(V) Conditions

As(V) is a chemical analog of Pi and can be taken up by Pi transporters, so we assayed expression levels of the Pht1 family members except for *OsPT11* and *OsPT13*, which are induced specifically during mycorrhizal symbiosis. The transcript levels of *OsPT1*, *OsPT2*, *OsPT4,* and *OsPT8* were significantly higher than that of other Pht1 family members (**Figure 1**). When rice had been grown in hydroponic conditions with 5 μM As(V) for 7 days, the expression levels of *OsPT1*, *OsPT4,* and *OsPT8* were

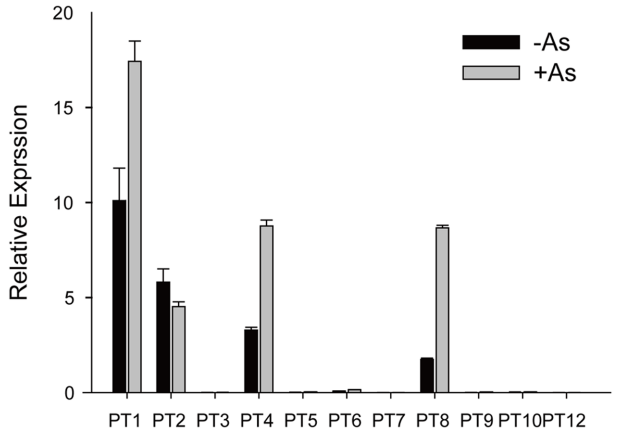

FIGURE 1 | Relative expression levels of Pht1 family members in roots of Nipponbare grown in culture solution with or without 5 μM arsenate for 3 days.

significantly increased by 1.7, 2.7, and 5.0 times, respectively. Considering that *OsPT1* and *OsPT8* are involved in As(V) uptake and transport in rice, *OsPT2* and *OsPT4* may also have roles in As(V) uptake and transport. The *OsPT2*- and *OsPT4*-overexpressing plants were obtained via *A. tumefaciens*-mediated transformation, and expression levels of *OsPT2* and *OsPT4* were measured using real-time PCR (**Supplementary Figures S1B,C**). When transgenic plants had been grown in culture solution with 5 μM As(V) for 3 days, differences in As concentration in both shoots and roots were observed in *OsPT4*-overexpressing but not *OsPT2*-overexpressing plants (**Supplementary Figures S1D,E**). Thus, we focused on the role of *OsPT4* in As(V) uptake and transport.

OsPT4-Overexpressing Rice Sensitive to As Toxicity

To examine the hypothesis that *OsPT4* was involved in As(V) absorption in rice plants, a phytotoxicity experiment was performed to observe growth of *OsPT4*-overexpressing rice. The Nipponbare and *OsPT4*-overexpressing lines were seeded in hydroponic conditions with 25 or 50 μM As(V). When exposed to the As(V) condition for 7 days, rice showed an As-toxicity phenotype in which growth of aboveground parts was delayed and the roots were stunted (**Figures 2A–C**). The *OsPT4*-overexpressing plants were more sensitive to As(V) and their root length and shoot height decreased 50 and 30% compared with wild-type, respectively (**Figures 2D,E**). Furthermore, As(V) uptake by *OsPT4*-overexpressing lines and wild-type roots were determined. At both 25 and 50 μM As(V), the As concentration in roots of *OsPT4*-overexpressing rice increased 10 and 33% compared with Nipponbare (**Figure 2F**).

The *OsPT4* Was Involved in the As(V) Uptake and Transport

A time-course experiment was used to investigate the ability of OsPT4 to take up As(V). The As accumulation was determined when plants were exposed to hydroponic culture with 5 μM As(V) for 2 h, 1 and 7 days. The concentration of As in rice roots and shoots increased significantly with the As(V) treatment time (**Figure 3**). When *OsPT4*-overexpressing lines grew in culture with 5 μM As(V) for 7 days, the As accumulation increased by twice in both roots and shoots.

Certainly, the overexpression lines of *OsPT4* accumulated more As both in shoots and roots. It is important to determine the As uptake rate of Nipponbare and *OsPT4*-overexpressing rice. Wild type and overexpression lines were cultured in the hydroponic solution with 1–50 μM As(V) concentration under +P (100 μM) and −P (0 μM). According to the results (**Figure 4**), the As(V) uptake rate of *OsPT4* overexpression lines was higher compared with wild type under the condition with or without Pi. In the absence of Pi, the As(V) uptake kinetics could be described by a Michaelis–Menten equation (**Table 2**). The V_{max} (maximum influx velocity) of As(V) uptake in *OsPT4*-overexpressing plants increased 23–45% compared with Nipponbare. Additionally, the K_m values of As(V) influx in overexpression lines were 8–28% higher than that in wild type. Under the +P condition, the As(V) uptake rates of rice were significantly lower compared with plants grown in the −P condition. Moreover, As(V) uptake rate was linear over the range of As(V) concentrations tested in the solution with Pi and the slopes of *OsPT4* overexpressing plants were 1.4 to 2 times greater compared with Nipponbare. The data suggested that *OsPT4* contributes to the As(V) uptake in rice root.

As(V) Concentration and Distribution in *OsPT4*-Overexpressing Rice

To further understand the role of *OsPT4* in As concentration and distribution in rice, the Nipponbare and *OsPT4*-overexpressing plants were grown to heading stage in hydroponic culture with 25 μM As(V). In this study, As accumulated mainly in the roots and to a lesser degree in aboveground organs (**Figure 5A**). In shoots, As was mainly in the nodes, which is the most important storage location for various metallic elements. The sum of As content in nodes accounted for 60% of total As in aboveground parts (**Figure 5B**). The As content in *OsPT4*-overexpressing lines increased in both roots and shoots by 22 and 47%, respectively. In addition, the As content of all organs in aboveground parts increased significantly, especially in nodes. The As content of the first node in *OsPT4*-overexpressing lines increased by twice that for the wild-type, while the second and third node only increased by 55 and 39% compared with wild-type, respectively. Furthermore, the As accumulation in flag leaf and flag sheath of *OsPT4*-overexpressing lines increased by 40 and 32%. The total As distribution of Nipponbare and *OsPT4*-overexpressing lines grown in the field soil was similar to that in the hydroponic experiment (**Supplementary Figure S2A**). This result was consistent with the expression pattern in different organs of rice, in which *OsPT4* was mainly expressed in root and flag leaf (**Supplementary Figure S2B**).

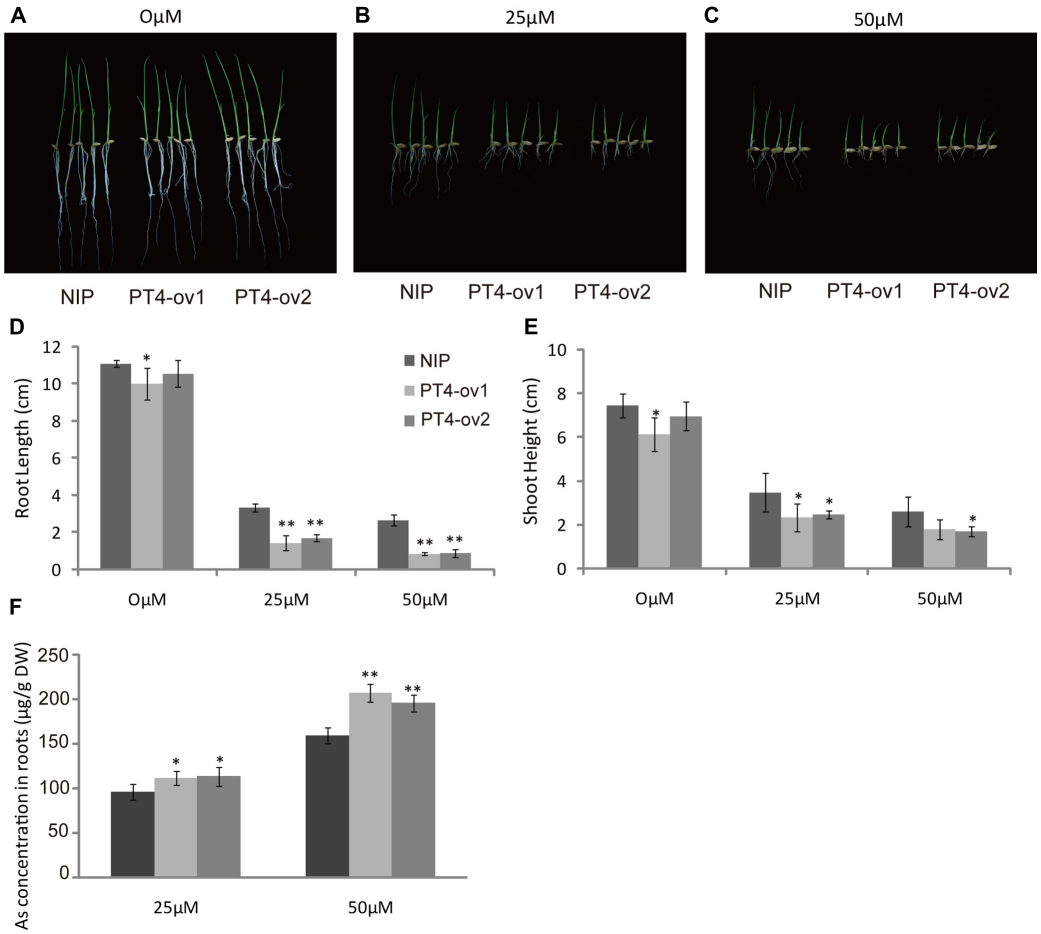

FIGURE 2 | Characterization of two *OsPT4*-overexpressing plants in Nipponbare background. **(A–C)** The growth phenotype of *OsPT4*-overexpressing plants and wild-type. Plants were grown in nutrient solutions to which 0, 25, and 50 μM arsenate were added for 7 days. **(D,E)** Phenotypic analysis of OsPT4-overexpressing plants. The root length and shoot height were obtained from the 7-day-old wild-type and overexpressing plants grown in nutrient solution with different arsenate concentrations. Five plants per line were measured. **(F)** The As concentration of roots in wild-type and transgenic plants. Data are means ± SD of five biological replicates. Values are significantly different from those of wild-type: $*P < 0.05$, $**P < 0.01$ (one-way ANOVA). DW, dry weight.

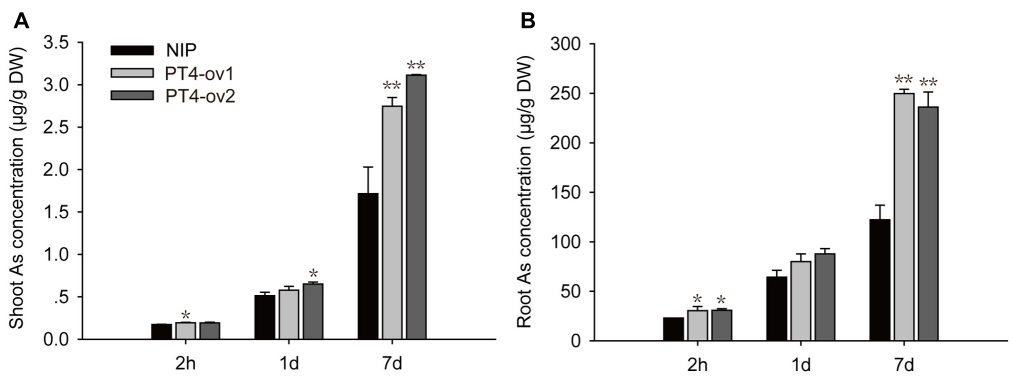

FIGURE 3 | The As concentration in shoots and roots **(A,B)** of Nipponbare and *OsPT4*-overexpressing seedlings after 2 h, 1 and 7 days of exposure to 5 μM arsenate. Data are means ± SD of three biological replicates. Values are significantly different from those of wild-type: $*P < 0.05$, $**P < 0.01$ (one-way ANOVA). DW, dry weight.

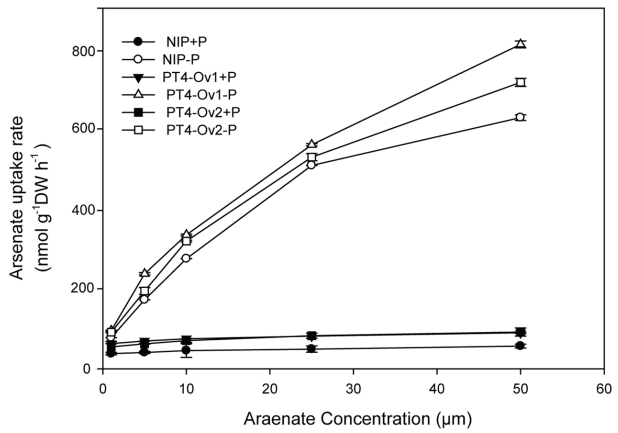

FIGURE 4 | Arsenate uptake kinetics of wild type and OsPT4 overexpressing plants. Data are means ± SD of four biological replicates. DW, dry weight.

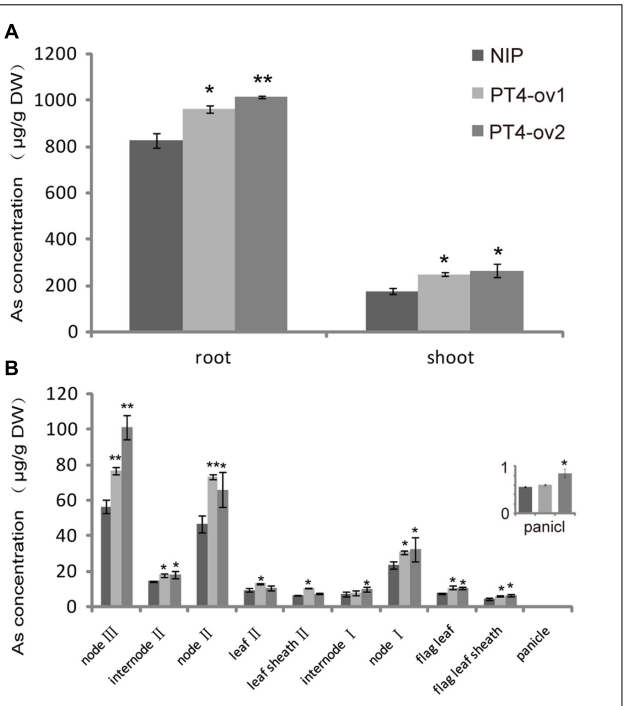

FIGURE 5 | The As concentration and distribution in Nipponbare and *OsPT4*-overexpressing lines grown in hydroponic culture with 5 μM arsenate. **(A)** The As concentration of shoots and roots of Nipponbare and *OsPT4*-overexpressing lines. **(B)** The As concentration of Nipponbare and *OsPT4*-overexpressing lines in different organs of shoots. Data are means ± SD of three biological replicates. Values are significantly different from those of wild-type: $^{*}P < 0.05$, $^{**}P < 0.01$ (one-way ANOVA). DW: dry weight.

Effect of Altered Expression of *OsPT4* on *OsPT1* and *OsPT8* under As(V) Conditions

Previous studies suggested that *OsPT1* and *OsPT8* were involved in As(V) uptake. The transcript levels of *OsPT1*, *OsPT4,* and *OsPT8* in rice grown in 5 μM As(V) for 2 h, 1 and 7 days were measured to determine any interaction between these genes. In roots, *OsPT8* expression rapidly increased by 10 times, then decreased and remained at a high level; however, *OsPT1* and *OsPT4* expression increased gradually and maintained a constant level until 7 days (**Figure 6A**). In the shoot, Real-time PCR analysis showed that expressions of these three genes were enhanced by As(V) (**Figure 6B**). *OsPT1* and *OsPT8* were significantly induced by 30 and 8 times, respectively, within a short period and then quickly returned to their original state. The transcript level of *OsPT4* increased gradually with treatment time, and finally increased 11 times at 7-days treatment. The induction of *OsPT1*, *OsPT4,* and *OsPT8* by As(V) raised the question of whether there was functional redundancy across the three genes. To determine this, the relative expression levels of *OsPT1* and *OsPT8* were evaluated in Nipponbare and *OsPT4*-overexpressing rice grown in hydroponic culture with or without As(V) (**Figures 6C,D**). Interestingly, expressions of *OsPT1* and *OsPT8* had no change in *OsPT4*-overexpressing rice cultured under normal conditions. The expression levels of *OsPT1* both in roots and shoots of *OsPT4*-overexpressing rice significantly increased in the As(V) condition. However, expression of *OsPT8* in *OsPT4*-overexpressing rice decreased over twofold in roots and was almost unchanged in shoots. The results suggest a lack of functional redundancy among *OsPT1*, *OsPT4* and *OsPT8*.

TABLE 2 | Fitted parameters of arsenate uptake kinetics of Nipponbare and the *PT4* overexpression line of rice.

Rice line and P treated	V_{max} (nmol g^{-1} root DW h^{-1})	K_m (μM)	Linear slope	r^2_{adj}
NIP+P	/	/	0.56 ± 0.12	0.950
PT4-Ov1+P	/	/	0.79 ± 0.05	0.912
PT4-Ov2+P	/	/	1.12 ± 0.21	0.906
NIP-P	625.0 ± 7.5	8.38 ± 0.3	/	0.965
PT4-Ov1-P	909.1 ± 11.2	10.72 ± 0.56	/	0.978
PT4-Ov2-P	769.2 ± 9.4	9.08 ± 0.04	/	0.955

Effects of *OsPT4* Overexpression on Pi and As Uptake by Rice Grown in Soil

A long-term experiment was used to investigate transgenic and wild-type plants grown to maturity in flooded soil conditions with two levels of P: −P (15 mg P kg^{-1} soil) and +P (30 mg P kg^{-1} soil). Overexpression of *OsPT4* significantly increased total Pi concentrations in both grain and straw both in −P field and +P field (**Figures 7A,B**). In −P field, *OsPT4* overexpression significantly enhanced grain and straw As accumulation by 22–30% and 40–66%, respectively, but no significant difference was shown in +P field (**Figures 7C,D**).

Phenotypes of OsPT4 CRISPR Plants under Arsenate Stress

In order to further study the role of *OsPT4* in rice As(V) uptake and transport, we studied the phenotype of *OsPT4*-Ri plants in solution with 0, 25, and 50 μM arsenate. The growth

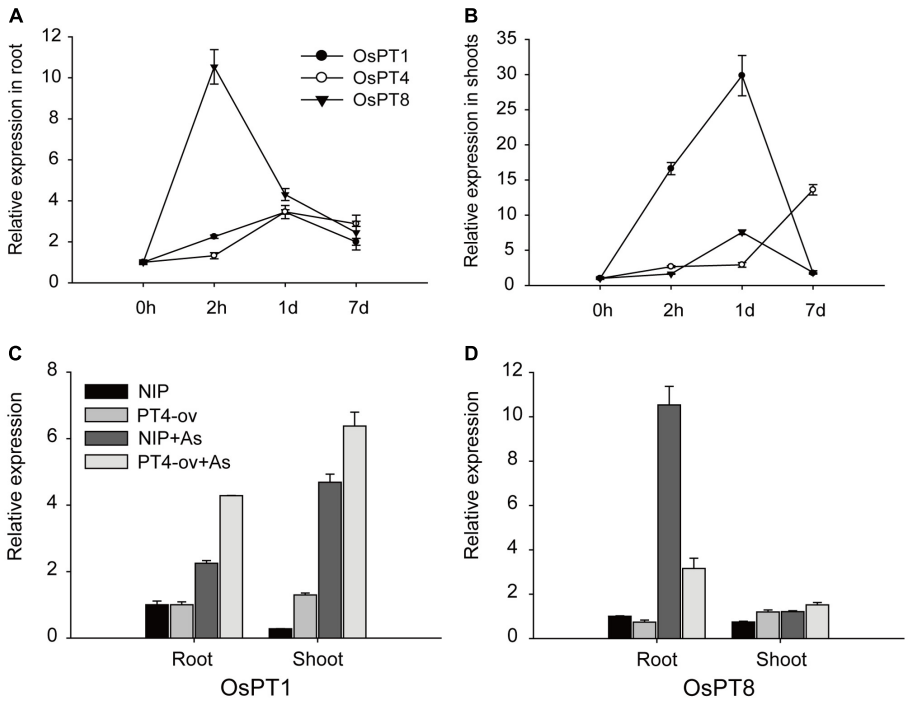

FIGURE 6 | Transcript levels of *OsPT1*, *OsPT4,* and *OsPT8* in Nipponbare under arsenate stress and the effect of altered expression of *OsPT4* on *OsPT1*, *OsPT8*. **(A,B)** Expression of *OsPT1*, *OsPT4,* and *OsPT8* in roots **(A,B)** of Nipponbare seedlings grown in nutrient solutions with 5 μM arsenate after 2 h, 1 and 7 days. **(C,D)** Expression of *OsPT1* and *OsPT8* in wild type and OsPT4-overexpressing lines grown in solution with or without arsenate. Error bars indicate ±SD (n = 3).

of *OsPT4*-Ri plants was similar to the wild type. No obvious difference in As concentration between NIP and *OsPT4*-Ri plants was observed (**Supplementary Figure S3**). Meanwhile, we obtained two different OsPT4 CRISPR lines that were treated with different As concentrations. As we expected, the *OsPT4*-cr lines showed stronger resistance to As(V) compared to wild type (**Figure 8**). The root length and shoot height of *OsPT4*-cr plants were significantly longer than wild type. Furthermore, the As accumulation of roots in *OsPT4*-cr plants decreased 17–30% compared with Nipponbare. The results obtained from *OsPT4*-cr plants confirmed that *OsPT4* is involved in As(V) uptake and transport.

DISCUSSION

As(V) is absorbed in roots and transported from vegetative tissues to rice grain. Elevated As accumulation in rice grain may pose a significant health risk to humans. It is important to determine how Pi transport genes contribute to As accumulation in rice. In the present study, we identified *OsPT4* as an important component of As(V) homeostasis and As tolerance in rice.

OsPT4 Involved in As(V) Uptake and Transport

As(V) is a toxic analog of Pi, so it can be absorbed and transported via Pi transport in plant (Xu et al., 2007). In *Arabidopsis*, previous studies suggested that AtPht1;1 and AtPht1;4 mediated a significant proportion of the As(V) uptake and a *AtPHF1* mutant was more resistant to As(V) than wild-type (Shin et al., 2004; Gonzalez et al., 2005). In rice, research has shown that Pht1 family genes participate in As(V) uptake – *OsPT1* was involved in As(V) transport from soil to apoplast and *OsPT8* functioned in As(V) uptake and resulted in a high affinity for As (Wu et al., 2011; Kamiya et al., 2013).

It was reported that the expression of *OsPT4* significantly increased in root of BRRT51 under As stress (Begum et al., 2016). In our study, the transcript levels of Pht1 family genes in Nipponbare grown in normal and As(V) conditions were measured. The expression level of *OsPT4* significantly increased in hydroponic culture containing As(V). The up-regulated expression of *OsPT4* hinted at a role in As(V) uptake. Furthermore, the ability of OsPT4 to absorb As was clearly demonstrated in the As phytotoxicity, hydroponic and field experiments. Root length and shoot height of *OsPT4*-overexpressing lines decreased 50 and 30%, respectively, compared with Nipponbare, and the As accumulation in roots of transgenic lines increased 33%. Meanwhile, the *OsPT4*-cr plants produced the opposite phenotype. Furthermore, the As(V) uptake rates of OsPT4-overexpressing plants were significantly higher than that in wild type under the growth condition with or without Pi. Differences in As concentration were also observed in grain and straw of *OsPT4*-overexpressing plants compared with wild-type in the flooded soil. All these results suggested that OsPT4 was a functional transporter in As(V) uptake.

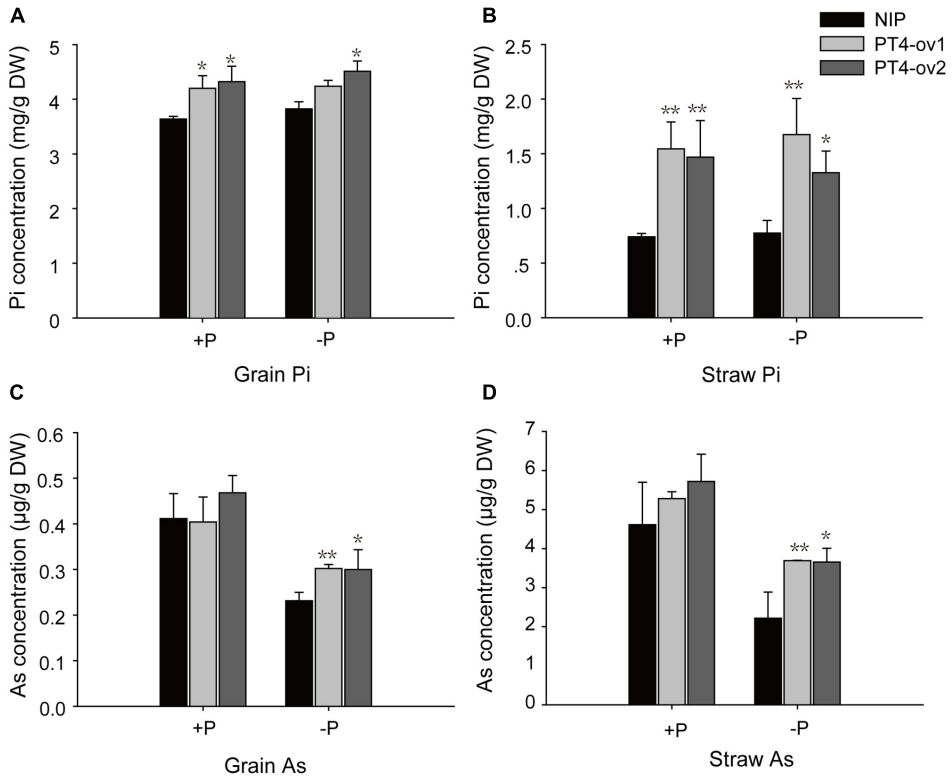

FIGURE 7 | The Pi and As concentrations of wild-type and *OsPT4*-overexpressing lines in the field. The rice was grown to maturity in soil under flooded conditions including two levels of P: –P (15 mg P kg^{-1} soil) and +P (30 mg P kg^{-1} soil). **(A,B)** The Pi concentration of grain **(A)** and straw **(B)** in wild-type and *OsPT4*-overexpressing lines. **(C,D)** The As concentration of grain **(C)** and straw **(D)** in wild-type and *OsPT4*-overexpressing lines. Data are means ± SD of three biological replicates. Values are significantly different from those of wild-type: $*P < 0.05$, $**P < 0.01$ (one-way ANOVA). DW: dry weight.

Previous studies showed that OsPT4, a Pi-influx transporter involved in Pi acquisition and mobilization in rice, facilitates embryo development (Ye et al., 2015; Zhang et al., 2015). *OsPT4* was highly expressed in roots, specifically in the exodermis cells and cortex. Although the sclerenchymatous cells at the exodermis in rice is the first apoplastic barrier to entry of toxic As, it does not completely stop entry of As because it shares transporters with essential Pi. The strong expression of *OsPT4* in the root exodermis cells and cortex (Ye et al., 2015) may explain the high As accumulation in roots and the heightened effect of As(V) in the As phytotoxicity experiment. Overall, the results suggested that *OsPT4* was a Pi transporter sharing an ion channel with As(V) and playing an important role in As(V) uptake.

In rice, *OsPT4* is constitutively expressed in roots and shoots (Ye et al., 2015), with the highest expression in flag leaves (**Supplementary Figure S2**). However, the As concentration in roots was much higher than that in shoots (**Figure 5**). The reason for this discrepancy is likely to be due to the mitigation strategies in rice As uptake and transport. The As(V) was absorbed by *OsPT4* and the other transporters, and then quickly reduced into As(III). OsHAC1;1 and OsHAC1;2 have been reported to act as arsenate reductases in rice (Shi et al., 2016). Most of As(III) was mainly fastened in root cortex and stele, forming complex with thiol (Su et al., 2010). The uncomplexed As(III) is transported to shoots and even to grain. The formation of As(III)-thiol complex in rice roots helps to explain the reason why the As concentration in roots is four times higher than that in shoots.

The flag leaf is an essential tissue for the growth and development of rice panicles, and plays a key role in remobilization of many mineral elements from leaves to developing grain. In addition, Zhang and his team reported that *OsPT4* was involved in Pi mobilization that facilitates embryo development in rice (Zhang et al., 2015). In our work, overexpressing *OsPT4* resulted in higher As concentration than wild-type in various organs of rice shoots, such as nodes, flag leaves and panicles Thus, we deduced that *OsPT4* was probably involved in As mobilization from flag leaf to panicles and immobilization in grain.

Many researches have reported that nodes are critical hubs in controlling the distribution of mineral elements including As. Nodes have a markedly larger concentration of As than the other tissues of rice shoots (Moore et al., 2014). This was confirmed in present study, showing that the As concentration of nodes represents 60% of the total As in shoot. The possible explanation is that a large portion of the node tissues are vascular bundles and that As accumulates strongly in the phloem (Chen et al., 2015). The nodes that produce or are near crown roots may accumulate higher concentrations of As accumulation. This may explain the

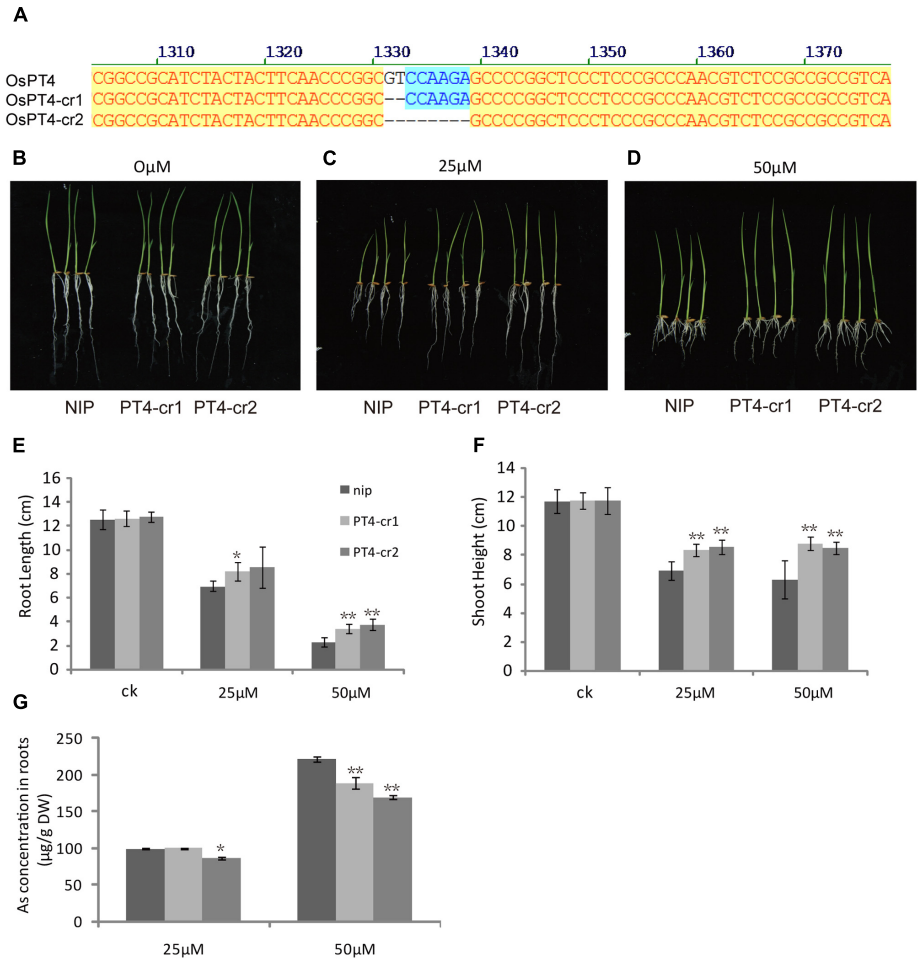

FIGURE 8 | Characterization of two *OsPT4* CRISPR plants in Nipponbare background. **(A)** Detection of mutations in OsPT4. The position of target site on the gene structure is indicated. **(B–D)** The growth phenotype of *OsPT4*-cr plants and wild-type. Plants were grown in nutrient solution to which 0, 25, and 50 μM arsenate were added for 7 days. **(E,F)** Phenotypic analysis of *OsPT4* CRISPR plants. The root lengths and shoot heights were obtained from the 7-day-old wild type and *OsPT4*-cr plants grown in nutrient solution with different arsenate concentrations. Five plants per line were measured. **(G)** As concentrations of roots in wild-type and transgenic plants. Data are means ± SD of five biological replicates. Values are significantly different from those of wild-type: $^{*}P < 0.05$, $^{**}P < 0.01$ (one-way ANOVA). DW: dry weight.

observation that *OsPT4*-overexpressing rice accumulated more As in node II and node III where generates crown roots. In the last few years, many mineral element transporters have been reported to function in rice nodes. A member of the rice C-type ATP-binding cassette (ABC) transporter family, *OsABCC1*, was reported as a As(III)-phytochelatin transporter. Knockout of *OsABCC1* in rice resulted in less As accumulation in the nodes and more As accumulation in the grain (Song et al., 2014). A strategy to prevent As accumulating in the grain is accumulate As in the nodes, especially those close to crown roots.

Interaction among Pht1 Family Proteins in As(V) Uptake

There are a reported 13 members of the rice Pht1 family and most share a similar protein structure and the same protein destination (localized to the plasma membrane). Among their encoding genes, *OsPT1*, *OsPT4,* and *OsPT8* were induced by As(V) stress. Individually overexpressing these three genes led to higher As accumulation than their background. These results raised the question of whether there is a network among these three Pi transporters playing specific and/or overlapping roles in As accumulation in rice.

The sensitivity to As(V) stress of *OsPT4*-overexpressing plants and *OsPT8* mutants, assessed in As phytotoxicity experiments, showed that both *OsPT4* and *OsPT8* were involved in As(V) uptake from roots (Wang et al., 2016) (**Figure 2**). Analyses of the GUS reporter gene driven by the promoters of *OsPT4* and *OsPT8* indicated a partial overlap in their spatial expression patterns, because the strongest expression of *OsPT4* and *OsPT8* were in the epidermis and cortex (Jia et al., 2011; Ye et al., 2015). Additionally, real-time PCR analysis revealed the same expression pattern of *OsPT4* and *OsPT8* in BRRI33 and BRRI51 under As stress along with lower regulation in BRRI33 and

higher regulation in BRRI51 (Begum et al., 2016). And both *OsPT4* and *OsPT8* were up-regulated in overexpression lines of *OsPAP21b* and *OsHAD1* under Pi-deficient conditions (Mehra et al., 2017; Pandey et al., 2017). Moreover, the transcript level of *OsPT8* in roots was dramatically attenuated in *OsPT4*-overexpressing plants grown in As(V) conditions (**Figure 6D**). These results indicated that there may be a functional overlap of OsPT4 with OsPT8. However, contrary to this assumption, *ospt8* mutants lost almost half of their As(V) uptake ability when seedlings were exposed to 1–2 μM As(V)(Wang et al., 2016). In our study, OsPT4-cr lines displayed significantly lower As concentrations in roots. The similar phenomenon has been observed in *ospt4* mutant (Cao et al., 2017). The attenuation of function of *OsPT8* was not compensated for by *OsPT4*, and so *OsPT4* and *OsPT8* were non-redundant in As(V) uptake. Furthermore, the expression variance of *OsPT4* and *OsPT8* in the time-course experiment also differed. In the present study, *OsPT8* expression in rice roots quickly increased by 10 times when plants were treated with As(V) for 2 h and then dropped (**Figure 6A**). Over the same time periods, the transcript level of *OsPT4* increased gradually and remained at a high level. In flooded soil, overexpressing *OsPT8* did not change the As accumulation in straw and grain (Wu et al., 2011), but the As accumulation in *OsPT4*-overexpressing plants increased in Pi-replete conditions (**Figures 7C,D**). These results strongly suggest that *OsPT4* and *OsPT8* had similar expression patterns but different regulation pathways in As uptake.

In *Arabidopsis*, there was a possible functional overlap of Pht1;1 with Pht1;4. In the As(V) condition, the double mutant showed a more resistant phenotype compared with background and the mutants for single genes (Shin et al., 2004). In rice, the promoters of *OsPT1* and *OsPT4*, unlike *OsPT8*, did not contain the P1BS element. The expression level of *OsPT1* and *OsPT4* was not effect by Pi supply conditions (Wu et al., 2013). Kamiya et al. (2013) reported that *OsPT1* was involved in As accumulation in shoots, a conclusion consistent with our result that the expression of *OsPT1* in shoots rapidly increased by 30 times (**Figure 6B**). The As accumulation in shoots of *ospt1* mutant was not significantly different to its background in Pi-replete condition (Kamiya et al., 2013), indicating that there may be a functional overlap between *OsPT1* and *OsPT4*. We also found that altered expression of *OsPT4* did affect expression of *OsPT1*. The transcript level of *OsPT1* in rice roots and shoots dramatically increased in *OsPT4*-overexpressing plants grown in normal and As(V) conditions (**Figure 6C**). Therefore, it was logical to assume that *OsPT1* and *OsPT4* shared a similar or the same pathway in rice As(V) uptake and translocation. Studies utilizing double mutants of these two genes are needed to test this hypothesis.

OsPT4 Could Be a Candidate Gene in Rice Breeding

Although there were significant increases of As concentration in *OsPT4*-overexpressing plants grown in hydroponic solution with Pi supplement, differences in As concentration in grain and straw were observed under −P but not +P flooded soil (**Figure 7**). The latest study showed that knockout of *OsPT4* could significantly decrease the inorganic As in rice grain (Cao et al., 2017). Since inorganic As is classified as Class-1 carcinogen, decreasing the concentration of inorganic As in rice grain is an important rice breeding target to protect human health. Under these circumstances, *OsPT4* which is involved in Pi and As uptake is a candidate gene to generate a high Pi-efficiency and low As-accumulating rice.

AUTHOR CONTRIBUTIONS

Experimental design: XL and YY. Experiments: YY, PL, TX, LZ, JL, and DC. Data analysis: YY and MY. Manuscript preparation: XL and YY. Supervision, funding and reagents: XL.

FUNDING

This work was supported by grants from the National High Technology Research and Development Program of China (2014AA10A603), Special Fund for Agro-Scientific Research in the Public Interest (201403015), the National Natural Science Foundation of China (31520103914 and 31471932).

ACKNOWLEDGMENTS

This research was conducted at the National Key Laboratory of Crop Genetic Improvement and National Center of Plant Gene Research (Wuhan), Huazhong Agricultural University, Wuhan. We thank Professor Lijia Qu for kindly providing the PJE 45/pH-Ubi-cas9-7 vector.

SUPPLEMENTARY MATERIAL

The Supplementary Material for this article can be found online at: https://www.frontiersin.org/articles/10.3389/fpls.2017.02197/full#supplementary-material

FIGURE S1 | The characteristics of *OsPT2*- and *OsPT4*-overexpressing plants. The expression levels and As contents of *OsPT2* and *OsPT4* were determined with real-time polymerase chain reaction and inductively coupled plasma mass spectrometry (ICP-MS), respectively. **(A)** Total RNA of wild type, *OsPT2*- and *OsPT4*-overexpressing plants. **(B)** Relative expression levels of *OsPT2* in *OsPT2*-overexpressing plants compared with background. **(C)** Relative expression levels of *OsPT4* in *OsPT4*-overexpressing plants compared with background. **(D,E)** The As accumulation in shoot **(D)** and root **(E)** of wild-type and transgenic plants after exposure to 5 μM arsenate for 7 days. Data are means ± SD of three biological replicates. Values are significantly different from those of wild-type: $^{*}P < 0.05$, $^{**}P < 0.01$ (one-way ANOVA). DW: dry weight.

FIGURE S2 | The As concentration in *OsPT4*-overexpressing plants and the expression pattern of *OsPT4* in Nipponbare. **(A)** The As concentration of wild-type and *OsPT4*-overexpressing plants grown to heading stage in flooded soil. Data are means ± SD of three biological replicates. Values are significantly different from those of wild-type: $^{*}P < 0.05$, $^{**}P < 0.01$ (one-way ANOVA). DW: dry weight. **(B)** The relative expression levels of *OsPT4* in different organs of Nipponbare. Error bars indicate ± SD ($n = 3$).

FIGURE S3 | Phenotypes of OsPT4 RNA interference plants. **(A–C)** The growth phenotype of OsPT4-Ri plants and wild type. Plants were grown in nutrient solution to which 0, 25, and 50 μM arsenate were added for 7 days. **(D)** As concentrations of roots in wild-type and OsPT4-Ri plants. Data are means ± SD of five biological replicates. Values are significantly different from those of wild-type: $^{*}P < 0.05$, $^{**}P < 0.01$ (one-way ANOVA). DW, dry weight.

REFERENCES

Abedin, M. J., Cotter-Howells, J., and Meharg, A. A. (2002). Arsenic uptake and accumulation in rice (*Oryza sativa* L.) irrigated with contaminated water. *Plant Soil* 240, 311–319. doi: 10.1023/A:1015792723288

Abernathy, C. O., Thomas, D. J., and Calderon, R. L. (2003). Health effects and risk assessment of arsenic. *J. Nutr.* 133(5 Suppl. 1), 1536S–1538S.

Alamdar, A., Eqani, S. A., Hanif, N., Ali, S. M., Fasola, M., Bokhari, H., et al. (2017). Human exposure to trace metals and arsenic via consumption of fish from river Chenab, Pakistan and associated health risks. *Chemosphere* 168, 1004–1012. doi: 10.1016/j.chemosphere.2016.10.110

Anawar, H. M., Akai, J., Mostofa, K. M. G., Safiullah, S., and Tareq, S. M. (2002). Arsenic poisoning in groundwater - Health risk and geochemical sources in Bangladesh. *Environ. Int.* 27, 597–604. doi: 10.1016/S0160-4120(01)00116-7

Begum, M. C., Islam, M. S., Islam, M., Amin, R., Parvez, M. S., and Kabir, A. H. (2016). Biochemical and molecular responses underlying differential arsenic tolerance in rice (*Oryza sativa* L.). *Plant Physiol. Biochen.* 104, 266–277. doi: 10.1016/j.plaphy.2016.03.034

Cao, Y., Ai, H., Mei, H., Liu, X., Sun, S., Xu, G., et al. (2017). Knocking out OsPT4 gene decreases arsenate uptake by rice plants and inorganic arsenic accumulation in rice grains. *Environ. Sci. Technol.* 51, 12131–12138. doi: 10.1021/acs.est.7b03028

Catarecha, P., Segura, M. D., Franco-Zorrilla, J. M., Garcia-Ponce, B., Lanza, M., Solano, R., et al. (2007). A mutant of the *Arabidopsis* phosphate transporter PHT1;1 displays enhanced arsenic accumulation. *Plant Cell* 19, 1123–1133. doi: 10.1105/tpc.106.041871

Chen, Y., Moore, K. L., Miller, A. J., McGrath, S. P., Ma, J. F., and Zhao, F.-J. (2015). The role of nodes in arsenic storage and distribution in rice. *J. Exp. Bot.* 66, 3717–3724. doi: 10.1093/jxb/erv164

Cozzolino, V., Pigna, M., Di Meo, V., Caporale, A. G., and Violante, A. (2010). Effects of arbuscular mycorrhizal inoculation and phosphorus supply on the growth of *Lactuca sativa* L. and arsenic and phosphorus availability in an arsenic polluted soil under non-sterile conditions. *Appl. Soil Ecol.* 45, 262–268. doi: 10.1016/j.apsoil.2010.05.001

Das, H. K., Mitra, A. K., Sengupta, P. K., Hossain, A., Islam, F., and Rabbani, G. H. (2004). Arsenic concentrations in rice, vegetables, a fish in Bangladesh: a preliminary study. *Environ. Int.* 30, 383–387. doi: 10.1016/j.envint.2003.09.005

De la Rosa, G., Parsons, J. G., Martinez-Martinez, A., Peralta-Videa, J. R., and Gardea-Torresdey, J. L. (2006). Spectroscopic study of the impact of arsenic speciation on arsenic/phosphorus uptake and plant growth in tumbleweed (*Salsola kali*). *Environ. Sci. Technol.* 40, 1991–1996. doi: 10.1021/es051526s

Duan, G. L., Zhou, Y., Tong, Y. P., Mukhopadhyay, R., Rosen, B. P., and Zhu, Y. G. (2007). A CDC25 homologue from rice functions as an arsenate reductase. *New Phytol.* 174, 311–321. doi: 10.1111/j.1469-8137.2007.02009

Finnegan, P. M., and Chen, W. H. (2012). Arsenic toxicity: the effects on plant metabolism. *Front. Physiol.* 3:182. doi: 10.3389/Fphys.2012.00182

Gilbert-Diamond, D., Cottingham, K. L., Gruber, J. F., Punshon, T., Sayarath, V., Gandolfi, A. J., et al. (2011). Rice consumption contributes to arsenic exposure in US women. *Proc. Natl. Acad. Sci. U.S.A.* 108, 20656–20660. doi: 10.1073/pnas.1109127108

Gonzalez, E., Solano, R., Rubio, V., Leyva, A., and Paz-Ares, J. (2005). PHOSPHATE TRANSPORTER TRAFFIC FACILITATOR1 is a plant-specific SEC12-related protein that enables the endoplasmic reticulum exit of a high-affinity phosphate transporter in *Arabidopsis*. *Plant Cell* 17, 3500–3512. doi: 10.1105/tpc.105.036640

Ha, S. B., Smith, A. P., Howden, R., Dietrich, W. M., Bugg, S., O'Connell, M. J., et al. (1999). Phytochelatin synthase genes from Arabidopsis and the yeast *Schizosaccharomyces pombe*. *Plant Cell* 11, 1153–1164. doi: 10.2307/3870806

Hartley-Whitaker, J., Ainsworth, G., Vooijs, R., Ten Bookum, W., Schat, H., and Meharg, A. A. (2001). Phytochelatins are involved in differential arsenate tolerance in *Holcus lanatus*. *Plant Physiol.* 126, 299–306. doi: 10.1104/pp.126.1.299

Isayenkov, S. V., and Maathuis, F. J. M. (2008). The *Arabidopsis thaliana* aquaglyceroporin AtNIP7;1 is a pathway for arsenite uptake. *FEBS Lett.* 582, 1625–1628. doi: 10.1016/j.febslet.2008.04.022

Jia, H., Ren, H., Gu, M., Zhao, J., Sun, S., Zhang, X., et al. (2011). The phosphate transporter gene OsPht1;8 is involved in phosphate homeostasis in rice. *Plant Physiol.* 156, 1164–1175. doi: 10.1104/pp.111.175240

Kamiya, T., Islam, M. R., Duan, G. L., Uraguchi, S., and Fujiwara, T. (2013). Phosphate deficiency signaling pathway is a target of arsenate and phosphate transporter *OsPT1* is involved in As accumulation in shoots of rice. *Soil Sci. Plant Nutr.* 59, 580–590. doi: 10.1080/00380768.2013.804390

Kamiya, T., Tanaka, M., Mitani, N., Ma, J. F., Maeshima, M., and Fujiwara, T. (2009). NIP1;1, an aquaporin homolog, determines the arsenite sensitivity of *Arabidopsis thaliana*. *J. Biol. Chem.* 284, 2114–2120. doi: 10.1074/jbc.M806881200

Li, R. Y., Ago, Y., Liu, W. J., Mitani, N., Feldmann, J., McGrath, S. P., et al. (2009). The rice aquaporin Lsi1 mediates uptake of methylated arsenic species. *Plant Physiol.* 150, 2071–2080. doi: 10.1104/pp.109.140350

Liu, F., Wang, Z., Ren, H., Shen, C., Li, Y., Ling, H.-Q., et al. (2010). OsSPX1 suppresses the function of OsPHR2 in the regulation of expression of *OsPT2* and phosphate homeostasis in shoots of rice. *Plant J.* 62, 508–517. doi: 10.1111/j.1365-313X.2010.04170.x

Ma, J. F., Yamaji, N., Mitani, N., Xu, X. Y., Su, Y. H., McGrath, S. P., et al. (2008). Transporters of arsenite in rice and their role in arsenic accumulation in rice grain. *Proc. Natl. Acad. Sci. U.S.A.* 105, 9931–9935. doi: 10.1073/pnas.0802361105

Meharg, A. A. (2004). Arsenic in rice - understanding a new disaster for South-East Asia. *Trends Plant Sci.* 9, 415–417. doi: 10.1016/j.tplants.2004.07.002

Meharg, A. A., and Hartley-Whitaker, J. (2002). Arsenic uptake and metabolism in arsenic resistant and nonresistant plant species. *New Phytol.* 154, 29–43. doi: 10.1046/j.1469-8137.2002.00363.x

Meharg, A. A., and Rahman, M. (2003). Arsenic contamination of Bangladesh paddy field soils: implications for rice contribution to arsenic consumption. *Environ. Sci. Technol.* 37, 229–234. doi: 10.1021/es0259842

Mehra, P., Pandey, B. K., and Giri, J. (2017). Improvement in phosphate acquisition and utilization by a secretory purple acid phosphatase (OsPAP21b) in rice. *Plant Biotechnol. J.* 15, 1054–1067. doi: 10.1111/pbi.12699

Miao, J., Guo, D. S., Zhang, J. Z., Huang, Q. P., Qin, G. J., and Zhang, X. (2013). Targered mutagenesis in rice using CRISPR-Cas system. *Cell Res.* 23, 1233–1236. doi: 10.1038/cr.2013.123

Moore, K. L., Chen, Y., Meene, A. M., Hughes, L., Geraki, T., Mosselmans, S. P., et al. (2014). Combined NanoSIMS and synchrotron X-ray fluorescence reveal distinct cellular and subcellular distribution patterns of trace elements in rice tissues. *New Phytol.* 201, 104–115. doi: 10.1111/nph.12497

Okkenhaug, G., Zhu, Y. G., He, J. W., Li, X., Luo, L., and Mulder, J. (2012). Antimony (Sb) and arsenic (As) in Sb mining impacted paddy soil from Xikuangshan, China: differences in mechanisms controlling soil sequestration and uptake in rice. *Environ. Sci. Technol.* 46, 3155–3162. doi: 10.1021/es2022472

Pandey, B. K., Mehra, P., Verma, L., Bhadouria, J., and Giri, J. (2017). OsHAD1, a haloacid dehaligenase-like APase, enhances phosphate accumulation. *Plant Physiol.* 174, 2316–2332. doi: 10.1104/pp.17.00571

Raab, A., Schat, H., Meharg, A. A., and Feldmann, J. (2005). Uptake, translocation and transformation of arsenate and arsenite in sunflower (*Helianthus annuus*): formation of arsenic-phytochelatin complexes during exposure to high arsenic concentrations. *New Phytol.* 168, 551–558. doi: 10.1111/j.1469-8137.2005.01519.x

Seyfferth, A. L., Webb, S. M., Andrews, J. C., and Fendorf, S. (2010). Arsenic localization, speciation, and co-occurrence with iron on rice (*Oryza sativa* L.) roots having variable Fe coatings. *Environ. Sci. Technol.* 44, 8108–8113. doi: 10.1021/es101139z

Shi, S. L., Wang, T., Chen, Z., Tang, Z., Wu, Z. C., Salt, D. E., et al. (2016). OsHAC1;1 and OsHAC1;2 function as arsenate reductases and regulate arsenic accumulation. *Plant Physiol.* 172, 1708–1719. doi: 10.1104/pp.16.01332

Shin, H., Shin, H. S., Dewbre, G. R., and Harrison, M. J. (2004). Phosphate transport in *Arabidopsis*: Pht1;1 and Pht1;4 play a major role in phosphate acquisition from both low- and high-phosphate environments. *Plant J.* 39, 629–642. doi: 10.1111/j.1365-313X.2004.02161.x

Smith, A. H., Lopipero, P. A., Bates, M. N., and Steinmaus, C. M. (2002). Public health - arsenic epidemiology and drinking water standards. *Science* 296, 2145–2146. doi: 10.1126/science.1072896

Song, W.-Y., Park, J., Mendoza-Cozatl, D. G., Suter-Grotemeyer, M., Shim, D., Hortensteiner, S., et al. (2010). Arsenic tolerance in Arabidopsis is mediated by two ABCC-type phytochelatin transporters. *Proc. Natl. Acad. Sci. U.S.A.* 107, 21187–21192. doi: 10.1073/pnas.1013964107

Song, W.-Y., Yamaki, T., Yamaji, N., Ko, D., Jung, K.-H., Fujii-Kashino, M., et al. (2014). A rice ABC transporter, OsABCC1, reduce arsenic accumulation in the grain. *Proc. Natl. Acad. Sci. U.S.A.* 111, 15699–15704. doi: 10.1073/pnas.1414968111

Su, Y. H., McGrath, S. P., and Zhao, F. J. (2010). Rice is more efficient in arsenite uptake and translocation than wheat and barley. *Plant Soil* 328, 27–34. doi: 10.1007/s11104-009-0074-2

Wang, P., Zhang, W., Mao, C., Xu, G., and Zhao, F. J. (2016). The role of OsPT8 in arsenate uptake and varietal difference in arsenate tolerance in rice. *J. Exp. Bot.* 67, 6051–6059. doi: 10.1093/jxb/erw362

Williams, P. N., Lei, M., Sun, G. X., Huang, Q., Lu, Y., Deacon, C., et al. (2009). Occurrence and partitioning of cadmium, arsenic and lead in mine impacted paddy rice: Hunan, China. *Environ. Sci. Technol.* 43, 637–642. doi: 10.1021/es802412r

Wu, C., Yuan, W., Chen, G., Kilian, A., and Li, J. (2003). Development of enhancer trap lines for functional analysis of the rice genome. *Plant J.* 35, 418–427. doi: 10.1046/j.1365-313X.2003.01808.x

Wu, P., Shou, H., Xu, G., and Lian, X. (2013). Improvement of phosphorus efficiency in rice on the basis of understanding phosphate signaling and homeostasis. *Curr. Opin. Plant Biol.* 16, 205–212. doi: 10.1016/j.pbi.2013.03.002

Wu, Z., Ren, H., McGrath, S. P., Wu, P., and Zhao, F. J. (2011). Investigating the contribution of the phosphate transport pathway to arsenic accumulation in rice. *Plant Physiol.* 157, 498–508. doi: 10.1104/pp.111.178921

Xu, W., Dai, W., Yan, H., Li, S., Shen, H., Chen, Y., et al. (2015). *Arabidopsis* NIP3;1 plays an important role in arsenic uptake and root-to-shoot translocation under arsenite stress conditions. *Mol. Plant* 8, 722–733. doi: 10.1016/j.molp.2015.01.005

Xu, X. Y., McGrath, S. P., and Zhao, F. J. (2007). Rapid reduction of arsenate in the medium mediated by plant roots. *New Phytol.* 176, 590–599. doi: 10.1111/j.1469-8137.2007.02195.x

Ye, Y., Yuan, J., Chang, X., Yang, M., Zhang, L., Lu, K., et al. (2015). The phosphate transporter gene OsPht1;4 is involved in phosphate homeostasis in rice. *PLOS ONE* 10:e0126186. doi: 10.1371/journal.pone.0126186

Yoshida, S., Forno, D. A., Cock, J. H., and Gomez, K. A. (1976). *Laboratory Manual for Physiological Studies of Rice*. Manila: International Rice Research Institute.

Zhang, F., Sun, Y., Pei, W., Jain, A., Sun, R., Cao, Y., et al. (2015). Involvement of OsPht1;4 in phosphate acquisition and mobilization facilitates embryo development in rice. *Plant J.* 82, 556–569. doi: 10.1111/tpj.12804

Zhao, F. J., Ago, Y., Mitani, N., Li, R. Y., Su, Y. H., Yamaji, N., et al. (2010). The role of the rice aquaporin Lsi1 in arsenite efflux from roots. *New Phytol.* 186, 392–399. doi: 10.1111/j.1469-8137.2010.03192.x

Zhu, Y. G., Sun, G. X., Lei, M., Teng, M., Liu, Y. X., Chen, N. C., et al. (2008). High percentage inorganic arsenic content of mining impacted and nonimpacted Chinese rice. *Environ. Sci. Technol.* 42, 5008–5013. doi: 10.1021/es8001103

Conflict of Interest Statement: The authors declare that the research was conducted in the absence of any commercial or financial relationships that could be construed as a potential conflict of interest.

frontiers in Plant Science

ORIGINAL RESEARCH
published: 13 April 2018
doi: 10.3389/fpls.2018.00463

Forest Soil Phosphorus Resources and Fertilization Affect Ectomycorrhizal Community Composition, Beech P Uptake Efficiency, and Photosynthesis

*Aljosa Zavišić[1], Nan Yang[1†], Sven Marhan[2], Ellen Kandeler[2] and Andrea Polle[1,3]**

[1] Forest Botany and Tree Physiology, University of Göttingen, Göttingen, Germany, [2] Institute of Soil Science and Land Evaluation, Soil Biology, University of Hohenheim, Stuttgart, Germany, [3] Laboratory for Radio-Isotopes, University of Göttingen, Göttingen, Germany

OPEN ACCESS

Edited by:
Pablo Cornejo,
Universidad de La Frontera, Chile

Reviewed by:
Saad Sulieman,
University of Khartoum, Sudan
Corina Carranca,
Instituto Nacional de Investigação Agrária e Veterinária, Portugal

***Correspondence:**
Andrea Polle
apolle@gwdg.de

†Present address:
Nan Yang,
College of Biology and the Environment, Nanjing Forestry University, Nanjing, China

Specialty section:
This article was submitted to Plant Nutrition, a section of the journal Frontiers in Plant Science

Received: *20 December 2017*
Accepted: *23 March 2018*
Published: *13 April 2018*

Citation:
Zavišić A, Yang N, Marhan S, Kandeler E and Polle A (2018) Forest Soil Phosphorus Resources and Fertilization Affect Ectomycorrhizal Community Composition, Beech P Uptake Efficiency, and Photosynthesis. Front. Plant Sci. 9:463. doi: 10.3389/fpls.2018.00463

Phosphorus (P) is an important nutrient, whose plant-available form phosphate is often low in natural forest ecosystems. Mycorrhizal fungi mine the soil for P and supply their host with this resource. It is unknown how ectomycorrhizal communities respond to changes in P availability. Here, we used young beech (*Fagus sylvatica* L.) trees in natural forest soil from a P-rich and P-poor site to investigate the impact of P amendment on soil microbes, mycorrhizas, beech P nutrition, and photosynthesis. We hypothesized that addition of P to forest soil increased P availability, thereby, leading to enhanced microbial biomass and mycorrhizal diversity in P-poor but not in P-rich soil. We expected that P amendment resulted in increased plant P uptake and enhanced photosynthesis in both soil types. Young beech trees with intact soil cores from a P-rich and a P-poor forest were kept in a common garden experiment and supplied once in fall with triple superphosphate. In the following summer, labile P in the organic layer, but not in the mineral top soil, was significantly increased in response to fertilizer treatment. P-rich soil contained higher microbial biomass than P-poor soil. P treatment had no effect on microbial biomass but influenced the mycorrhizal communities in P-poor soil and shifted their composition toward higher similarities to those in P-rich soil. Plant uptake efficiency was negatively correlated with the diversity of mycorrhizal communities and highest for trees in P-poor soil and lowest for fertilized trees. In both soil types, radioactive P tracing ($H_3{}^{33}PO_4$) revealed preferential aboveground allocation of new P in fertilized trees, resulting in increased bound P in xylem tissue and enhanced soluble P in bark, indicating increased storage and transport. Fertilized beeches from P-poor soil showed a strong increase in leaf P concentrations from deficient to luxurious conditions along with increased photosynthesis. Based on the divergent behavior of beech in P-poor and P-rich forest soil, we conclude that acclimation of beech to low P stocks involves dedicated mycorrhizal community structures, low P reserves in storage tissues and photosynthetic inhibition, while storage and aboveground allocation of additional P occurs regardless of the P nutritional status.

Keywords: fungal assemblage, nutrient stress, plant–microbe interaction, phosphorus nutrition, storage

INTRODUCTION

In temperate forest ecosystems nutrient availability is one of the most important drivers for tree growth and ecosystem functions (Elser et al., 2007). Soils vary considerably in plant-available phosphorus (P) because rock-derived mineral P is depleted over geological time scales (Chadwick et al., 1999; Turner and Condron, 2013). These biogeochemical processes require shifts in plant nutritional strategies from mineral-based P supply to recycling of organic P (Foster and Bhatti, 2006; Lambers et al., 2008; Lang et al., 2016). Plants take up P in its inorganic form as phosphate (Becquer et al., 2014). Since inorganic P is usually depleted in soil solutions, P is often the first limiting macronutrient for plant growth under natural conditions (Vitousek et al., 2010). Plants can acclimate to low P availabilities by P remobilization and recycling (Maillard et al., 2015; Netzer et al., 2016; Zavišić and Polle, 2018) and by increasing P uptake efficiency, for instance, by increasing activities and affinities of P transporters (Kavka and Polle, 2016; Zhang et al., 2016). Thereby, a relatively higher fraction of P is acquired by P-deficient plants from the available pool of P in the soil than by P-sufficient plants (Koide, 1991; Sattelmacher et al., 1994; Schmidt et al., 2015).

Beech (*Fagus sylvatica* L.) forests are the most important forest type in Central European Lowland (Leuschner and Ellenberg, 2017). As the potentially natural vegetation they are of immense ecological significance (Leuschner and Ellenberg, 2017). Beech trees produce valuable timber and are therefore also of economic relevance (von Wühlisch and Muhs, 2011). Beech forests occur across a wide range of soil types differing in P supply (Peters, 1997; Leuschner et al., 2006). Studies of foliar P concentrations in different European countries did not indicate excess supply in any of the study locations and even revealed decreasing trends over longer temporal scales (Duquesnay et al., 2000; Ilg et al., 2009; Jonard et al., 2015; Talkner et al., 2015). To assess tree nutrition, foliar element concentrations are commonly used (Mellert and Göttlein, 2012). Since P concentrations in beech leaves vary considerably during the growth season, often resulting in similar levels in the foliage of trees stocking on P-poor and P-rich soil types (Haußmann and Lux, 1997; Netzer et al., 2016; Zavišić and Polle, 2018), the evaluation of the nutritional status is difficult. Altogether, these observations call for a better understanding of how beech trees acclimate to low soil P resources.

Mycorrhizal fungi are key to tree nutrition (Alvarez et al., 2009; Plassard and Dell, 2010; Cairney, 2011; Becquer et al., 2014; Johri et al., 2015). Therefore, an obvious idea is that mycorrhizal diversity might be affected by soil P stocks similar as known for nitrogen (Lilleskov et al., 2002; Cox et al., 2010). However, P fertilization studies in tree plantations did not show clear effects on the ectomycorrhizal communities (Treseder, 2004). Field studies along natural P gradients neither uncovered clear relationships between mycorrhizal diversity and P stocks (Twieg et al., 2009; Horton et al., 2013; Teste et al., 2016; Zavišić et al., 2016) although the fungal assemblages varied considerably among site conditions. Since divergent climatic and chemical soil factors also influence fungal communities, the elucidation of causal effects is difficult in ecological studies.

To overcome these shortcomings and to gain additional knowledge on the physiological differences between beech trees acclimated to low or high P supply, we conducted a common garden experiment, in which trees from a P-rich and a P-poor forest were fertilized with triple superphosphate (TP). The trees were excavated with intact soil cores in two beech forests differing in soil P stocks (Zavišić et al., 2016; Lang et al., 2017) and kept under ambient conditions from fall of the sampling year to the following summer in the presence or absence of fertilizer. By the comparison of fertilized trees and non-fertilized controls, we disentangled the effects of P on free living soil microbes, mycorrhizal communities colonizing the roots, plant P uptake efficiency, P contents, and photosynthesis. By applying ^{33}P as a tracer, instantaneous plant uptake efficiency and P allocation were determined. Specifically, we addressed the following hypothesis: (i) P fertilization leads to increases in microbial biomass if microbes were P limited. We expected that an increase in microbial biomass might change belowground competition with roots for P. (ii) P fertilization causes shifts in the composition of mycorrhizal communities, regardless of soil types, if the communities were responsive to an increment in labile P (P_{labile}). (iii) P fertilization affects P uptake efficiency more strongly in P-sufficient than in P-deficient plants because the latter have a higher P demand than well-supplied beech trees. (iv) P is preferentially allocated to leaves leading to enhanced photosynthesis. We expected no stimulation of photosynthesis in trees in P-rich soil, if their P supply was sufficient.

MATERIALS AND METHODS

Plant Material and Triple Superphosphate Fertilizer Treatment

Beech seedlings (*Fagus sylvatica* L.) of ca. 0.4 m height were excavated in October 2014 in P-rich (Bad Brückenau, BBR) and in P-poor (Unterlüß, LUE) 120- and 137-year-old beech forests. The sites have been characterized in detail previously (Zavišić et al., 2016; Lang et al., 2017). Briefly, BBR is located in the natural biosphere reserve "Bayerische Rhön" (50°35′N, 9°92′E, 801–850 m above sea level. The climate is influenced by Atlantic air masses with an average long term sum of annual precipitation of 1000 mm, and a mean annual temperature of 5.8°C. The soil type is of volcanic origin (basalt), which is rich in minerals and nutrients. LUE is located in Lower Saxony (52°83′N, 10°36′E, 115 m above sea level) and has a mean annual temperature of 8.0°C, with an average annual precipitation of 730 mm. The soil type is sandy-loam with a low water capacity. A detailed description of the soils is given by Lang et al. (2017). Briefly, the soils of BBR/LUE contain 904/164 g P m^{-2}, 1.3/0.7 kg nitrogen m^{-2}, and 18/16 kg carbon m^{-2} to a depth of 1 m and have a pH value of 3.8/3.5 (Lang et al., 2017).

Young trees were collected inserting a polymer pipe (diameter 0.12 m, height: 0.2 m) into the soil around each individual and pulling it up with its intact soil core. The plants were exposed in a common garden experiment (Göttingen, 51°56′N, 9°96′E, 167 m above sea level) under ambient conditions under shading nets. The shading was necessary since all trees were collected

in the understory. After 1 month acclimation (until November 20, 2014), half of the trees from each site were fertilized with TP (46% (w/w) P_2O_5, AGRAVIS Raiffeisen AG, Obernjesa, Germany) which is moderately soluble $Ca(H_2PO_4)_2$ and typically used in agriculture for P-fertilization. TP was ground to a powder, sprinkled on the surface of the soil and subsequently dissolved by irrigation with tap water. Each tree obtained once a dose of 795 mg P. Control (CO) trees were irrigated with the same amount of tap water. These treatments resulted in the following experimental layout with 10 plants per treatment and site: CO beeches in P-poor soil, CO beeches in P-rich soil, TP beeches in P-poor soil, TP beeches in P-rich soil. The pipes, each containing plants of different treatments, were arranged in perforated crates and moved regularly to avoid positional effects. All trees were maintained under ambient conditions until harvest in the following summer in July and were watered regularly with tap water. For this experiment, a total of 40 plants were available (20 for radioactive treatments and 20 non-labeled controls).

Determination of Photosynthesis

Gas exchange was measured on June 29, 2015 using seven plants from each site and treatment. Net photosynthetic rates, transpiration, stomatal conductance, and the sub-stomatal and ambient CO_2 concentrations were determined using a portable photosynthesis system (LC Pro, ADC Bioscientific, Hoddesdon, United Kingdom). The light level was 350 μmol quanta m^{-2} s^{-1} of photosynthetically active radiation.

Radioactive Labeling and Plant Harvests

Non-labeled TP and CO trees were harvested on 15th and 16th July 2015 (5 per treatment and site). The remaining trees (5 per treatment and site) were labeled with $H_3{}^{33}PO_4$ (Hartmann Analytic GmbH, Braunschweig, Germany) to determine the P uptake rates. We used ^{33}P because of its longer half-life time of 25.4 days, thus, resulting in higher signals than ^{32}P (half-life time of 14.3 days) after 1 week of labeling. Further, the permitted limit of labeling outside of the control area (10^5 kBq for the whole experiment) had to be considered. Here, we added 1.912 MBq in 40 ml of tap water to each plant, amounting to a total of 0.017 nmol P per plant. This corresponded to less than 10^{-8} of the P content in the soil and thus, had no effect on P availability. Each plant was subsequently watered with tap water to distribute the radioactive marker throughout the soil core. To avoid loss of label via through-flow, a plastic saucer was placed underneath each soil core. Flow-through after labeling was collected and re-applied to the soil core. All plants were irrigated with 40 ml tap water to avoid drought stress when required. During the labeling period mean air temperatures were 20.8 ± 0.5°C and the relative air humidity was 69.9 ± 1.4 %. The trees were harvested 7 days after ^{33}P application. At harvest, the relative soil moisture across all treatments was 28 ± 6%.

Harvesting Procedures and Microbial Biomass Determination

At the harvesting time, main stem heights and stem diameters at the base were measured. The basal stem of each tree was cut approx. 0.01 m above the soil. The soil was subsequently pushed out of the polymer smooth walled pipe, and the organic layer separated from the mineral topsoil. The masses of each soil layer and of all plant fractions (buds, leaves, stem, fine roots, and coarse roots) were recorded for each plant. Before separation of the root system, the roots were gently shaken and the soil adhering to the roots thereafter was considered as rhizosphere soil. The rhizosphere soil was collected from the roots by brushing them carefully with toothpicks, thereafter weighed, dried and used for chemical analyses. The roots were briefly washed and used immediately for mycorrhizal analyses. Aliquots of soil and plant tissues were dried at 40°C for 1 week to determine the dry mass. Further aliquots were kept frozen at −80°C.

To obtain wood and bark exudates, an about 2 cm long basal segment of the stem was cut and debarked. The bark and the peeled xylem sample were incubated for 5 h in a solution of 10 mM Na_2EDTA (pH 7.0) and 15 mM chloramphenicol as described previously (Yang et al., 2016). The exudates were stored at −20°C.

Fresh soil samples were used for chloroform fumigation extraction and determination of microbial biomass (C_{mic} and N_{mic}) as described previously (Spohn et al., 2018). Data were calculated with conversion factors of 0.45 for C_{mic} and 0.54 for N_{mic}.

Mycorrhizal Morphotyping and Species Identification

All fine root tips (<2 mm diameter) were inspected under a dissecting microscope (Leica M205 FA; Leica, Wetzlar, Germany) and classified according to different fungal morphotypes as described before (Zavišić et al., 2016; Spohn et al., 2018). All mycorrhizal root tips of a given plant were inspected. Aliquots of unknown morphotypes were used for DNA extraction and identification based on sequencing of the rRNA ITS-region (White et al., 1990) and alignment of the sequences with GenBank or UNITE. Species names were accepted when the sequence identity was >97% and the score >900 bits. Sequences were deposited in GenBank (MG820044-MG820051, KX168637, KX168639, KX168640, KX168642, KX168647, KX168650, KX168651, KX168655, KX168659, KX168660, KX168661, KX168663, KX168664, and KX168665).

Determination of Labile and Total Phosphorus

For extraction of P_{labile} about 100 mg of dried, milled soil was used. The samples were suspended in 10 ml Bray-1 solution (1 M NH_4F, 0.5 M HCl) and shaken for 5 min at 180 rpm. The samples were afterwards filtered using phosphate free filter paper (MN $280\frac{1}{4}$, Macherey-Nagel, Düren, Germany). The filtrate was analyzed colorimetrically at 645 nm wavelength (Specord 205, Analytik Jena, Germany) using malachite green oxalate (Sigma, St. Louis, MO, United States) as reagent according to the procedure described by Lanzetta et al. (1979).

Total P (P_{tot}) was extracted from about 50 mg of dried, milled soil and plant material in 2 ml 65% HNO_3 at 160°C

for 12 h according to Heinrichs et al. (1986). Extracted samples were filtered using phosphate free filter paper (MN 280 $\frac{1}{4}$, Macherey-Nagel, Düren, Germany), and used for elemental analysis by inductively coupled plasma–optical emission spectroscopy (ICP–OES) (iCAP 6000 Series ICP–OES, Thermo Fisher Scientific, Dreieich, Germany). Bark and xylem exudates were directly used after filtration for P determinations.

Determination of ^{33}P in Soil and Plant Tissues

Extracts used for P_{tot} determination and bark and xylem exudates were used for measuring ^{33}P. Three ml of extract from each plant tissue and soil layer were mixed with 10 ml of scintillation cocktail (Rotiszint eco plus, Roth, Karlsruhe, Germany) and for detection of radioactivity in a Perkin-Elmer scintillation counter (Tri-Carb TR/SL 3180, Waltham, MA, United States). The non-labeled samples were also measured as controls and showed no background signal. The ^{33}P signal was corrected using QuantSmart (version 4.00, PerkinElmer) for its half-life of 25.34 days.

Calculations and Statistical Analyses

We refer to P (mg g^{-1} dry mass) as P concentration and to the amount of P (mg) in a given soil compartment or tissue as P content.

Whole-plant P content was determined as

$$\begin{aligned}&\text{Whole-plant P content} =\\ &P_{bud}\ (\text{mg g}^{-1}) \times \text{biomass of buds (g)} + P_{leaf}\ (\text{mg g}^{-1}) \times\\ &\text{biomass of leaves (g)} + P_{stem}\ (\text{mg g}^{-1}) \times \text{biomass of stem (g)}\\ &+ P_{coarse\ roots}\ (\text{mg g}^{-1}) \times \text{biomass of coarse roots (g)} +\\ &P_{fine\ roots}\ (\text{mg g}^{-1}) \times \text{biomass of fine roots (g)}.\end{aligned}$$

Whole-plant ^{33}P (Bq) was determined correspondingly with the tissue dry masses and their ^{33}P (Bq g^{-1} dry mass) concentrations.

P content of the soil per soil core was determined as

$$\begin{aligned}&\text{P content of the soil} =\\ &P_{organic\ layer}\ (\text{mg g}^{-1}) \times \text{dry mass of organic layer (g)}\\ &+ P_{mineral\ top\ soil}\ (\text{mg g}^{-1}) \times \text{dry mass of mineral top soil (g)}\\ &+ P_{\ Rhizosphere}\ (\text{mg g}^{-1}) \times \text{dry mass of rhizosphere soil (g)}.\end{aligned}$$

^{33}P content of soil was determined correspondingly. The labile ^{33}P content of the soil was calculated as:

$$\text{Soil } {}^{33}P_{labile} \text{ content (Bq)} = \frac{P_{labile} \text{ content of soil}}{P_{tot} \text{ content of soil}} \times {}^{33}\text{P content of soil}$$

Since P uptake rates of beech vary in different seasons (Zavišić and Polle, 2018), we distinguished between instantaneous uptake in summer determined 1 week after ^{33}P application as whole-plant ^{33}P content on the one hand and whole-plant P content as the result of life-time net P accumulation on the other hand. These measures were used to determine P uptake efficiencies according to Lang et al. (2017):

$$\text{Instantaneous P uptake efficiency} = \frac{\text{whole-plant } {}^{33}\text{P content}}{\text{soil} {}^{33}P_{labile} \text{ content}}$$

$$\text{P uptake efficiency} = \frac{\text{whole-plant P content}}{\text{whole soil } P_{labile} \text{ content}}$$

The plant P uptake rate was calculated as:

$$\text{P uptake rate (mg week}^{-1}) = \text{whole-plant } {}^{33}\text{P content after 1 week/(specific activity)}$$

with the following estimate:

$$\text{Specific activity (Bq mg}^{-1}\text{ P)} = \frac{\text{Soil } {}^{33}P_{labile} \text{ content (Bq)}}{P_{labile} \text{ content of soil core}}$$

Data are shown as means (± SE). Data were analyzed by ANOVA followed by comparisons of means with Tukey HSD (package: "multcomp") using R version 2.9.1 (R Core Development Team, 2012). Differences between means were considered to be significant when $p \leq 0.05$. Testing for homogeneity of variances and normal distribution was done by analyzing residuals of the models and performing a Shapiro-Wilk test. When the data violated the assumption of normal distribution, data were log-transformed, before ANOVA was performed. Correlation coefficients were calculated using Pearson moment product.

Diversity indices (Shannon, Dominance, Pielou's Evenness), ordination by non-metric multidimensional scaling (NMDS) and analysis of similarities (ANOSIM) were calculated for mycorrhizal assemblages using PAST software package 3.08[1] (Hammer et al., 2001). Because all ectomycorrhizal root tips of a plant were counted the sample sizes varied. Therefore, the Raup-Crick method for presence–absence data was employed for calculation of dissimilarities since this method can handle variable sample sizes.

RESULTS

Fertilization Increases the Labile Fraction of P in Soil but Has No Effect on Microbial Biomass

The P-poor soil contained the lowest concentrations of P_{tot} and P_{labile} in the organic layer as well as in the mineral top soil (**Table 1**). Fertilization resulted in significant increases in P_{labile} and P_{tot} in the organic layer in both the P-rich and the P-poor soil. In the mineral top soil, only the P-rich site exhibited higher P_{labile} concentrations after fertilization, whereas the increment in mineral soil from the P-poor sites was not significant (**Table 1**). P_{tot} concentrations in the mineral soil and in the rhizosphere were not affected by fertilization treatment

[1] https://folk.uio.no/ohammer/past/

(**Table 1**). Overall, fertilization resulted in about 3-times higher P_{tot} contents (per soil core) in P-poor soil than in non-fertilized control soil, whereas the P addition had no significant influence on P_{tot} content in the P-rich soil core (**Table 1**). However, in both soil types, fertilization increased the fraction of P_{labile} (**Table 1**).

The P-rich soil contained higher microbial biomass (C_{mic} and N_{mic}) than the P-poor soil (**Table 1**). In both soil types, microbial biomass was higher in the organic layer than in the mineral top soil (*t*-test, $p < 0.001$). Fertilization had no significant effects on microbial biomass (**Table 1**).

Mycorrhizal Community Structures of Beech in P-Poor Soil Are Influenced by P Fertilization

In total 16 fungal morphotypes were detected, of which 14 were identified by ITS sequencing (**Figure 1A**). The number of taxa differed among the sites and was higher on trees in P-rich than in

TABLE 1 | Phosphorus concentrations and microbial biomass in control and fertilized soil from a P-rich and a P-poor forest.

Parameter	Control		P-fertilized	
	P-rich	P-poor	P-rich	P-poor
P_{labile} in OL (mg g^{-1})	0.497 ± 0.118b	0.013 ± 0.003a	2.448 ± 0.122d	1.146 ± 0.054c
P_{tot} in OL (mg g^{-1})	1.673 ± 0.219b	0.211 ± 0.039a	2.096 ± 0.113d	1.149 ± 0.123c
P_{labile} in ML (mg g^{-1})	0.546 ± 0.101b	0.023 ± 0.001a	0.897 ± 0.088c	0.132 ± 0.028a
P_{tot} in ML (mg g^{-1})	1.432 ± 0.068b	0.069 ± 0.014a	1.515 ± 0.081b	0.157 ± 0.036a
P_{tot} in Rhizo (mg g^{-1})	1.385 ± 0.081b	0.151 ± 0.040a	1.885 ± 0.181b	0.614 ± 0.267a
P_{tot} content in soil core (mg)	1262 ± 186c	162 ± 27a	1482 ± 121c	510 ± 38b
P_{labile}/P_{tot} in soil	0.35 ± 0.05b	0.21 ± 0.04a	0.74 ± 0.04c	0.97 ± 0.04c
C_{mic} in OL (μg g^{-1})	1685 ± 114b	948 ± 89a	1572 ± 211b	1069 ± 93a
N_{mic} in OL (μg g^{-1})	300 ± 35c	177 ± 14a	281 ± 36bc	203 ± 39ab
C_{mic} in ML (μg g^{-1})	628 ± 61b	196 ± 42a	607 ± 73b	84 ± 17a
N_{mic} in ML (μg g^{-1})	101 ± 12b	27 ± 4a	107 ± 9b	18 ± 2a

Young beech trees in intact soil cores from the P-rich site (BBR, Bad Brückenau) and the P-poor site (LUE, Unterlüß) were fertilized once with 795 mg P in the form of TP or kept without fertilization (control) for 8 months in a common garden experiment. Soil P concentrations were measured at the final harvest [22nd (P-rich) and 23rd July 2015 (P-poor)] (n = 5, ± SE) and microbial biomass of carbon and nitrogen (C_{mic} and N_{mic}) twice (15th/16th and 22nd/23rd July 2015, n = 10 ± SE). Concentrations are expressed on the basis of soil dry mass. OL, organic layer, ML, mineral top soil layer, Rhizo, rhizosphere soil. Different letters indicate significant differences between means (Tukey's HSD pairwise comparisons) at p < 0.05.

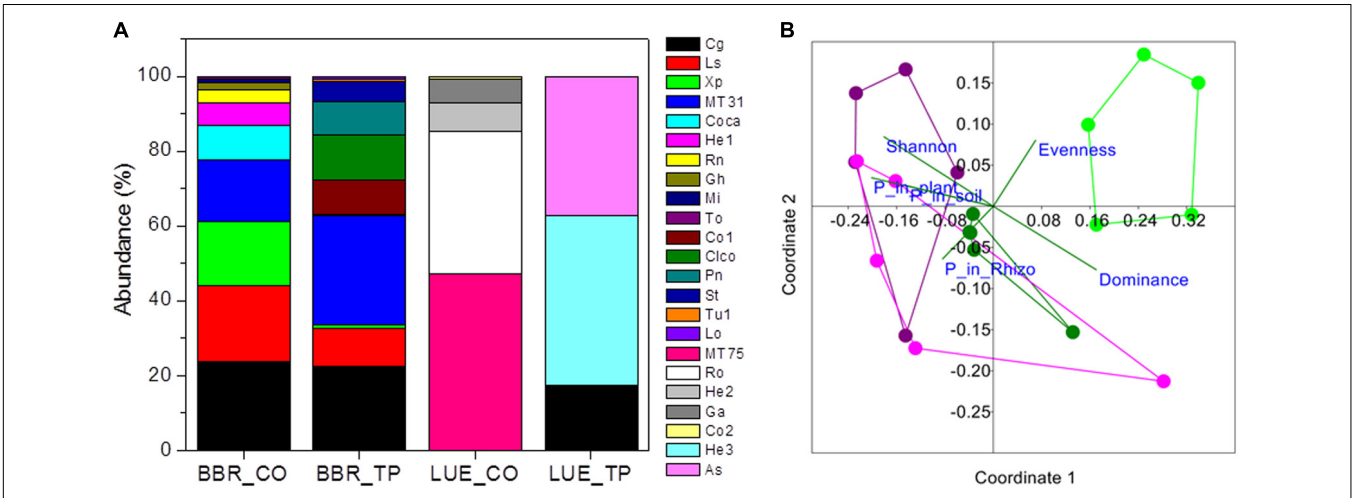

FIGURE 1 | Relative abundance of ectomycorrhizal fungal taxa colonizing root tips of beech trees in P-rich (BBR) or P-poor soil (LUE) without [Control (CO)] or with application triple superphosphate (TP) fertilizer **(A)** and non-metric multidimensional scaling (NMDS) of the fungal assemblages **(B)**. Stress: 0.194. Vectors indicate explanatory variables with the diversity indices (Shannon H, Evenness, and Dominance) and P contents (whole-plant P content, P content of soil, and P content of rhizosphere). Symbols refer to ectomycorrhizal communities from BBR_CO: pink, BBR_FP: purple, LUE_CO: light green, LUE_FP: dark green. In **(A)** abbreviations refer to the following fungal taxa: Cg, *Cenococcum geophilum*; Ls, *Lactarius subdulcis*; Xp, *Xerocomellus pruinatus*, MT31; Coca, *Cortinarius casimiri*; He1, *Helotiales* sp. 1; Rn, *Russula nigricans*; Gh, *Genea hispidula*; Mi, *Melanogaster intermedius*; To, *Tomentellopsis* sp.; Co1, *Cortinarius* sp_1.; Clco, *Clavulina coralloides*; Pn, *Pachyphlodes nemoralis*; St, *Solicoccozyma terricola*; Tu1, *Tuber* sp.; LO, *Leptodontidium orchidicola*, MT57; Ro, *Russula ochroleuca*; He2, *Helotiales* sp. 2; Ga, *Genea* cf. *anthracina*; Co2, *Cortinarius* sp. 2; He3, *Heliotales* sp. 3; As, Ascomycota; MT, morphotypes, for which sequencing failed.

P-poor soil (**Table 2**). *Cenococcum geophilum* was absent on roots of trees in P-poor soil but was an abundant species in P-rich soil (**Figure 1A**). *C. geophilum* also appeared after P fertilization on roots of beech trees in P-poor soil (**Figure 1A**). Further abundant taxa that appeared after fertilization of P-poor trees were an unknown ascomycete and *Cortinarius casimiri* (**Figure 1A**). In P-rich soil, fertilization also resulted in changes; among the abundant fungi *Lactarius subdulcis* and *Xerocomellus pruinatus* decreased and *Clavulina coralloides*, *Leptodontidium orchidicola* and an unspecified *Cortinarius* sp. 1 increased (**Figure 1A**). Shannon indices were higher and Dominance indices of the mycorrhizal communities lower in P-rich than in P-poor soil (**Table 2**).

Non-metric multidimensional scaling ordination showed strong dissimilarity of the ectomycorrhizal communities from P-poor controls compared with those from the P-rich site (ANOSIM, controls: $p < 0.05$, fertilized: $p < 0.01$) as well as those from those in P-poor soil after fertilization (ANOSIM, $p < 0.01$, **Figure 1B**). Fertilization of the P-rich soil did not change the ectomycorrhizal communities' structures (**Figure 1B**, ANOSIM, $p = 0.385$). The differences among the mycorrhizal communities in P-rich and P-poor soil were explained by higher Shannon diversity and higher P contents in soil, rhizosphere and plants for the ectomycorrhizal assemblages under P-rich conditions and by higher Evenness and dominance for the ectomycorrhizal assemblages in P-poor soil (**Figure 1B**).

P Nutrition and Uptake Efficiency in Relation to Mycorrhizal Diversity

Application of P fertilizer resulted in higher plant P contents in both, beech trees in P-poor and P-rich soil (**Table 3**). P fertilization increased P tissue concentrations of plants in P-poor soil but had no significant effects on those in P-rich soil (**Table 3**). The P uptake efficiency was highest for P-poor control beech trees and declined upon fertilization to levels similar to those of P-rich plants (**Table 3**).

Since the uptake efficiency for P_{tot} integrates over the whole life history of the plants, we were also interested in testing whether the results would hold for current P uptake. To determine instantaneous P uptake efficiency, ^{33}P was added as a tracer to the soil. Similar to the P uptake efficiency, the instantaneous P uptake efficiency was highest in control plants in the P-poor soil and lower in plants in P-rich soil and after fertilization (**Table 3**). Moreover, a strong decline in the instantaneous P uptake efficiency became apparent in fertilized plants resulting in about 10-fold lower values than those found for the P-poor conditions (**Table 3**). Despite lower uptake efficiencies, the estimated P uptake rates were generally higher for plants in P-rich than in P-poor soil and not significantly influenced by fertilization (**Table 3**).

Correlation analyses were conducted to test whether P contents or uptake were related to mycorrhizal diversity. Among the tested variables, Shannon diversity showed a strong linear negative correlation with P uptake efficiency (**Figure 2**), while the relationship with instantaneous P uptake efficiency was less strong ($R = -0.455$, $P = 0.044$) and those with whole plant P content ($R = 0.433$, $P = 0.056$) and P uptake rate ($R = 0.393$, $P = 0.086$) were not significant (Supplementary Figure S1).

P Fertilization Rescues Photosynthesis of P-Limited Beech Through Preferential Above-Ground Allocation

To investigate how beech plants handle the distribution of limiting or abundant P across different tissues, we determined the allocation of whole-plant P_{tot} and newly taken up P (^{33}P). The majority of whole-plant P_{tot} was present in coarse roots and stems (**Figure 3A**), while a large fraction of new P was also found in fine roots (**Figure 3B**). Fertilization shifted P_{tot} and ^{33}P allocation to stem tissue (**Figure 3A**).

Since the stem is both, transport and storage tissue, we wondered whether the additional P was mainly used for improved P supply to green tissues or indicated stronger accumulation of P reserves. Therefore, P concentrations in xylem and bark and in their respective exudates were determined. Both xylem and xylem exudates showed increased P concentrations after fertilization indicating higher transport (**Table 3**), but the relative P fraction in the xylem exudates was unaffected by fertilization amounting 6 ± 1% of the P concentration in the xylem. This finding indicates increased P storage. The bark concentrations of P also increased in response to fertilization (**Table 3**) but in this case, the fraction of P in the exudates also strongly increased from about 25% in controls to about 70% (P-rich) and 90% (P-poor) in fertilized plants ($p < 0.01$) suggesting enhanced P circulation in the fertilized compared with the control plants.

TABLE 2 | Diversity indices for mycorrhizal assemblages colonizing the roots beech trees from a P-rich (BBR) and a P-poor (LUE) site.

	Control		P-fertilized		$p_{(Treatment)}$	$p_{(Treatment)}$	$p_{(Sites)}$	$p_{(Sites)}$
	P-rich	P-poor	P-rich	P-poor	P-poor	P-rich	TP	CO
Taxa	11	5	12	3	0.012	0.001	0.001	0.001
Shannon H	1.933	1.133	1.915	1.030	0.531	0.006	0.001	0.001
Evenness	0.628	0.621	0.565	0.933	0.001	0.001	0.001	0.807
Dominance	0.168	0.377	0.179	0.375	0.029	0.801	0.001	0.001

Half of the trees were fertilized with TP; the other half served as the controls (CO). P-values obtained by permutation tests are indicated for the following pairwise comparisons: fertilized compared with controls at BBR: $p_{(Treatment)}$ BBR, fertilized compared with controls at LUE: $p_{(Treatment)}$ LUE, fertilized soil from BBR with fertilized soil from LUE: $p_{(Sites)}$ TP, control soil from BBR with control soil from LUE: $p_{(Sites)}$ CO.

TABLE 3 | Phosphorus contents, concentrations and uptake in beech trees grown control and fertilized soil from a P-rich and a P-poor forest.

	Control		P-fertilized	
	P-rich	**P-poor**	**P-rich**	**P-poor**
P content				
Whole-plant P_{tot} content (mg plant^{-1})	6.7 ± 1.2b	1.3 ± 0.2a	10.9 ± 1.6c	7.3 ± 0.5b
P concentrations				
Mean whole-plant P_{tot} (mg g^{-1})	1.32 ± 0.17b	0.47 ± 0.05a	1.60 ± 0.21b	0.78 ± 0.07a
P_{tot} in fine roots (mg g^{-1})*	1.03 ± 0.06b	0.55 ± 0.03a	1.46 ± 0.28b	1.97 ± 0.09b
P_{tot} in coarse roots (mg g^{-1})*	0.88 ± 0.14b	0.26 ± 0.02a	1.46 ± 0.16c	1.82 ± 0.33c
P_{tot} in stem (mg g^{-1})	0.84 ± 0.08b	0.26 ± 0.03a	1.12 ± 0.10b	0.98 ± 0.16b
P_{tot} in leaves (mg g^{-1})	1.15 ± 0.04ab	0.68 ± 0.06a	1.38 ± 0.11b	2.82 ± 0.33c
P_{tot} in buds (mg g^{-1})	1.02 ± 0.26a	1.09 ± 0.09a	1.43 ± 0.08a	2.54 ± 0.20b
P_{tot} in bark (mg g^{-1})	0.64 ± 0.02a	0.38 ± 0.02a	1.37 ± 0.22b	1.51 ± 0.30b
P in bark exudate (mg g^{-1})	0.15 ± 0.03a	0.09 ± 0.02a	1.04 ± 0.34b	1.38 ± 0.25b
P_{tot} in xylem (mg g^{-1})	0.84 ± 0.13b	0.16 ± 0.02a	1.36 ± 0.14c	1.11 ± 0.17bc
P_{tot} in xylem exudate (mg g^{-1})	0.040 ± 0.006b	0.011 ± 0.002a	0.067 ± 0.005c	0.075 ± 0.012c
P uptake				
P uptake efficiency (plant^{-1})*	0.018 ± 0.005a	0.047 ± 0.009b	0.010 ± 0.001a	0.015 ± 0.001a
Instant. P uptake efficiency (plant^{-1})*	0.016 ± 0.003b	0.069 ± 0.023c	0.006 ± 0.001a	0.005 ± 0.001a
Whole-plant P uptake rate (mg week^{-1})*	7.86 ± 2.78b	2.08 ± 0.77a	6.27 ± 1.32b	2.42 ± 0.28ab
P uptake rate (mg g^{-1} week^{-1})	1.52 ± 0.49b	0.79 ± 0.32ab	0.97 ± 0.25b	0.25 ± 0.03a

*Young beech trees in intact soil cores from the P-rich site (BBR, Bad Brückenau) and the P-poor site (LUE, Unterlüß) were fertilized with TP or kept without fertilization for 8 months in a common garden experiment. (n = 5, ± SE) Different letters in rows indicate significant differences between means (Tukey's HSD pairwise comparisons) for $p < 0.05$. For the definitions and calculations of P uptake efficiency, instantaneous (inst.) P uptake efficiency and P uptake rates refer to section "Materials and Methods". *Data were log-transformed for statistical analysis.*

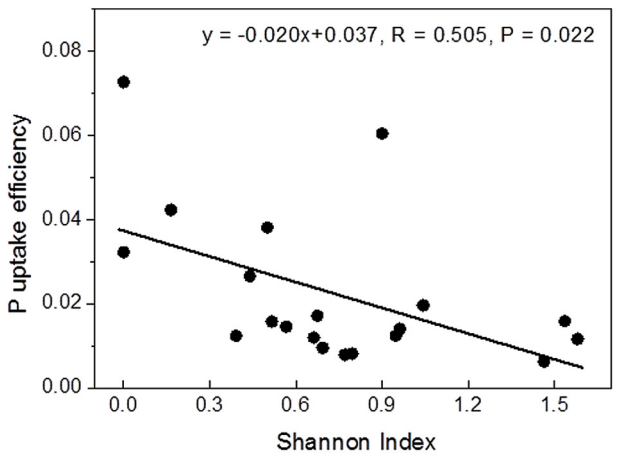

FIGURE 2 | Relationship between Shannon diversity of the mycorrhizal root tips and whole-plant P uptake efficiency.

The P_{tot} concentrations in leaves and buds of the plants in P-poor soil increased drastically in response to fertilization, whereas no significant changes in P_{tot} were found for the fertilized plants in P-rich soil (**Table 3**). However, regardless the soil type, the fraction of new ^{33}P was enhanced in leaves of fertilized compared with those of control plants (**Figure 3B**).

To investigate the physiological consequences of P fertilization, photosynthetic gas exchange was measured. CO_2 assimilation was higher in plants from the P-rich than in plants from the P-poor site (**Figure 4A**). Fertilization resulted in 60% increased photosynthesis rates in plants from the P-poor site but had no effect on plants from the P-rich site (**Figure 4A**). One reason for lower photosynthesis of P-poor plants was their lower stomatal conductance (**Figure 4B**). This reduction was not caused by water limitations because the overall soil moisture (28 ± 6%) in the soil cores did not differ among the treatments and soil types ($p > 0.05$). Limitations in CO_2 consumption can also lead to decreases in stomatal conductance as the result of increased substomatal CO_2 concentrations (Damour et al., 2010). However, this was not the case here (**Figure 4D**). Beech trees from the P-poor site exhibited higher water use efficiencies than fertilized trees from the P-rich site (**Figure 4C**).

DISCUSSION

Impact of P Fertilization on Soil Microbes and Mycorrhizal Communities

About 8 months after application of P fertilizer and regular irrigation of the plants with tap water, 77% (P-rich) and 64% (P-poor) of the added P had disappeared. Since we determined the P contents for all compartments in our experimental system and other leaks are unknown, the losses were most likely caused by leaching. Still, the concentrations of P_{labile} in the organic layer of P-fertilized soil were higher than those in non-treated soil, indicating persistent effects (**Table 1**). Since P is exchanged between microbial biomass and soil solution (Achat et al., 2010, 2012) microbial activities may influence tree nutrition. Seasonal

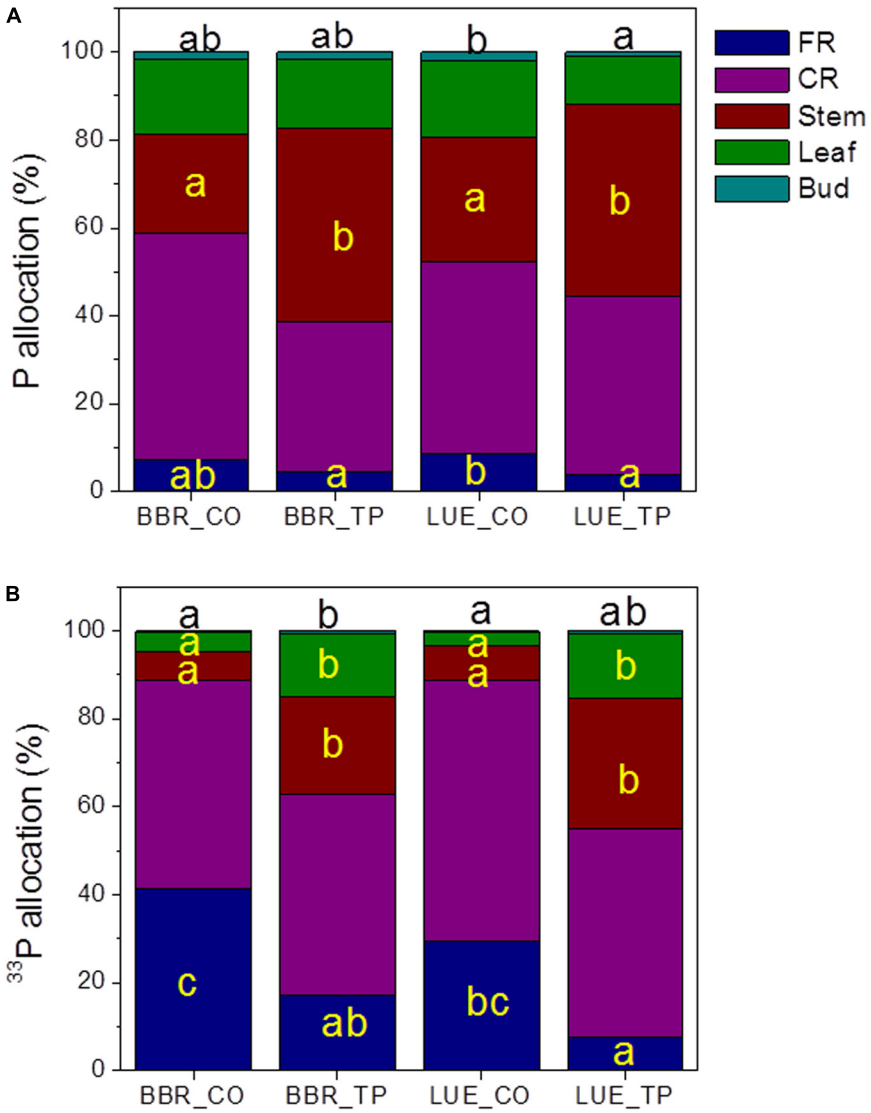

FIGURE 3 | Whole-plant P_{tot} **(A)** and ^{33}P **(B)** allocation in European beech trees (*Fagus sylvatica* L.) in P-rich (BBR) or P-poor soil (LUE) without (CO) or with application of TP fertilizer. The contents of P (mg) and of ^{33}P (Bq) were determined for each tissue 1 week after application of the radioactive label. For each plant, the sum of the tissue P_{tot} contents, respective the sum of the ^{33}P contents was set as 100%. Data indicate means (n = 5 per soil type and P treatment). Significant differences among the tissues at $p < 0.05$ are indicated by different letters. Black letters on top of the stacked bars refer to buds. Tissues without letters did not show any significant difference.

experiments with soil cores in a similar set-up as in the present study showed that a large fraction of P was bound in microbial biomass and, thus, not available for plant nutrition (Spohn et al., 2018). Therefore, a critical point in the current study was to clarify whether P concentrations resulted in enhanced microbial biomass. Here, no significant changes in microbial biomass were observed in response to P fertilization but microbial biomass was generally lower in P-poor than in P-rich soil (**Table 1**). A reduction of microbial biomass in P-poor compared to P-rich soil has also been reported in previous studies conducted in the forests at BBR and LUE (Zavišić et al., 2016; Zederer et al., 2017). Since we did not find an amelioration of microbial biomass in response to P fertilization, other nutrients such as carbon might have limited microbial biomass (Achat et al., 2012; Heuck et al., 2015). Lower carbon assimilation of plants in P-poor soil, as observed here (**Figure 4A**), would be expected to diminish belowground carbon flux and thereby, might limit microbial biomass carbon. Consequently, higher plant assimilation and biomass production in response to P additions could have positive feed-back effects on microbial biomass in the long run. Alternatively, microbial growth might also be limited by nitrogen in our sites. Using respiration measurements under different carbon, nitrogen and P amendments, Preusser et al. (2017) revealed that beech forest soils site were initially carbon limited, followed by subsequent nitrogen limitation. Only when nitrogen limitations were overcome by N amendments, addition of P

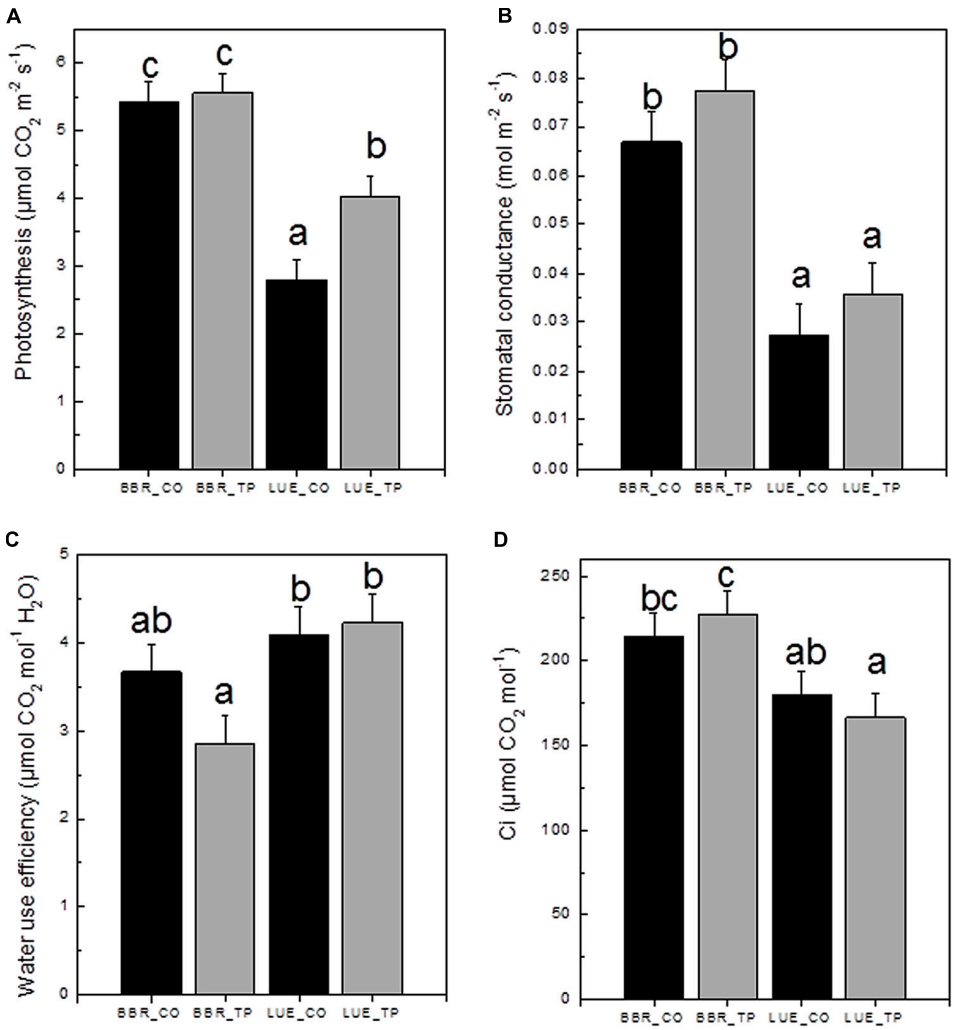

FIGURE 4 | Net photosynthetic rates **(A)**, stomatal conductance **(B)**, water use efficiency **(C)**, and substomatal CO_2 concentration c_i **(D)** of European beech trees (*Fagus sylvatica* L.) in P-rich (BBR) or P-poor soil (LUE) without (CO, black bars) or with application of triple superphosphate fertilizer (TP, gray bars). The trees were exposed in a common environment outdoors in October 2014 and fertilized in November 2014. The measurements were performed on June 29, 2015. Values for air temperature, relative air humidity, and ambient CO_2 concentrations during the times of the measurement were as follows: LUE_TP: 26.3°C, 69.3%, 379 ppm; LUE_CO: 27.1°C, 71.5%, 378 ppm; BBR_TP: 30.3°C, 64.7%, 379 ppm; BBR_CO: 30.4°C, 75.3%, 380 ppm. Bars represent means ± SE (n = 7). Different letters indicate significant differences at $p \leq 0.05$.

enabled a surplus of microbial growth response (Preusser et al., 2017).

Previous studies on beech roots from the old trees in the P-rich and P-poor forests revealed lower mycorrhizal species richness and compositional differentiation of the assemblages under low P availability (Zavišić et al., 2016). Here, we confirmed this observation for young beech trees from those sites (**Figure 1** and **Table 2**). Moreover, we clearly show that both diversity and composition were influenced by fertilization of P-poor beech trees (**Figure 1** and **Table 2**). This finding indicates that P availability is a driver for mycorrhizal fungal species composition in forest soil. The effect of fertilization on the mycorrhizal community was stronger in P-poor than in P-rich soil (**Figure 1B**). In P-rich soil, the fungal communities consisted of taxa typically found in beech forests such as *C. geophilum*, *L. subdulcis*, *X. pruinatus*, *Clavulina* sp., and *Cortinarius* sp. (Courty et al., 2010; Lang et al., 2011; Pena et al., 2017). In contrast to P-poor soil, P-fertilization did not result in significant shifts of the community structure in P-rich soil, despite some changes in abundances of fungal taxa (**Figure 1A**). To date, the few studies available on the influence of P fertilization on ectomycorrhizal communities have been conducted in plantations, also demonstrating P-induced changes in the communities (*Populus*: Baum and Makeschin, 2000; dipterocarps: Pampolina et al., 2002; *Eucalyptus*: Brearley et al., 2007). In our study, it was notable that only ascomycota were detected on the roots of fertilized trees in P-poor soil and that the abundance of this phylum also increased on roots of

fertilized trees in P-rich soil (**Figure 1A**). These shifts might indicate the development of mycorrhizal communities, which are more typical for disturbed conditions (Smith and Bonito, 2012). Furthermore, mycorrhizas formed by Ascomycota do not form widely extending extramatrical hyphae (Smith and Bonito, 2012), thus, relying on nutrients in their immediate vicinity. Our results suggest that larger P availability may favor such shifts because the similarity of mycorrhizal community structures of fertilized beeches in P-poor soil was closer to those of beeches in P-rich than to non-fertilized beeches in P-poor soil (**Figure 1B**).

Ectomycorrhizal communities are composed of functionally different taxa (Courty et al., 2010; Pritsch and Garbaye, 2011; Rineau and Courty, 2011; Pena et al., 2013; Pena and Polle, 2014). Here, we found that plant P uptake efficiency was strongly negatively correlated with the diversity of the fungal assemblage (**Figure 2**). A reason for this unexpected result could be that the fungal taxa associated with P-poor plants were more specialized for P acquisition and uptake than the communities of diverse taxa that colonized the well-supplied plants. For example, the fungal assemblages after fertilization as well as those in P-rich soil contained a significant fraction of *C. geophilum*. This fungus has lower phosphatase activities than many other mycorrhizal fungal taxa (Baxter and Dighton, 2005). This fungal trait might be less important under conditions of a high availability of P_{labile}. However, our suggestion that P limitation leads to functionally adapted, more specialized assemblages is speculative and should be tested in further P fertilization experiments combined with P uptake studies of distinct fungal taxa.

Beech Responses to P Fertilization

In the presence of high P availability, plants down-regulate their P uptake systems decreasing their uptake efficiency (Nussaume et al., 2011; Baker et al., 2015; Kavka and Polle, 2016; Kavka and Polle, 2017). It is, therefore, conceivable that regulation of P transport contributed to lower P uptake efficiencies observed here for trees in P-rich compared with those in P-poor soil. As expected, fertilization resulted in further decreases but in contrast to our working hypothesis that fertilized trees in P-poor soil would respond with less reduction in uptake efficiency, they showed a 10-fold decrease while that of P fertilized trees in P-rich soil was only threefold reduced (**Table 3**). The estimated P uptake rate (per unit of biomass) also dropped to its lowest level in fertilized beech trees in P-poor soil. This observation is surprising at the first glance. However, P uptake is regulated by long-distance signaling in response to transcription factors that survey the cellular P status (Chiou and Lin, 2011; Scheible and Rojas-Triana, 2015). In our study, P concentrations in leaves of fertilized plants in P-poor soil were strongly increased, from deficient (0.7 mg P g^{-1} dry mass) to excessive levels (2.8 mg P g^{-1}) according to the common classification scheme (P [mg g^{-1} dry mass]: deficient <1.1, normal 1.1–1.9, extreme >2.0, Mellert and Göttlein, 2012]. The fertilized trees on P-poor soil reached the highest foliar P concentrations among all conditions tested (**Table 3**). It is likely that this enrichment set off a regulatory cascade that shut down P uptake at the level of roots. The profound increase of P in bark exudate, which is a proxy for P transport (King and Zeevaart, 1974; Dambrine et al., 1995; Gessler et al., 1998; Yang et al., 2016), further supports this idea.

A word of caution is warranted regarding the estimated P uptake because the values are fairly high. In agreement with other studies (Morel and Fardeau, 1989; Bünemann et al., 2007; Oberson et al., 2010), we used the fraction of P_{labile} to determine the specific ^{33}P activity, required to accommodate for differences in tracer dilution in soil. P_{labile} indicates the maximum P fraction available, whereas the actual P concentrations in soil solutions are lower (e.g., Zavišić et al., 2016) and, thus, must result in lower *de facto* fluxes than those calculated here. Since the "true" P concentrations in the soil volume of the root tips are unknown and may vary spatially depending on P uptake by different mycorrhizal taxa, refined analyses of uptake rates are currently not possible. It is obvious that more information on the activities of distinct mycorrhizal taxa in their natural assemblages for P uptake and the molecular biology of these processes is urgently needed to better understand P fluxes.

Our P fertilization experiment was instrumental to distinguish between deficient and sufficient P supply of the young field-grown beech trees because the plants in P-rich soil did not respond with increases in photosynthesis although they exhibited increased P contents, whereas the plants in P-poor soil showed a strong stimulation of photosynthetic CO_2 assimilation (**Figure 4**). The positive response to P amendment is in agreement with many other studies showing that fertilization can increase photosynthetic rates in trees (Kirschbaum and Tompkins, 1990; Gough et al., 2004; Turnbull et al., 2007; King et al., 2008; Warren, 2011). Our results show that additional P taken up by fertilized trees in both soil types was preferentially allocated aboveground resulting in increased P accumulation in storage tissues (**Figure 3**). This is an important finding since P growth demand and P uptake are temporally decoupled in beech (Zavišić and Polle, 2018). P-deficient beech trees, as those studied her, develop a massive temporal P deficit during early growth, which is replenished in late summer and fall (Zavišić and Polle, 2018). In winter, almost no differences exist between the P nutritional status of P-deficient and P-sufficient trees (Zavišić and Polle, 2018). This balance is achieved by lower growth rates (Zavišić and Polle, 2018). In combination, those results and the current study highlight the importance of P storage pools and transport tissues for acclimation of beech to low P availabilities.

CONCLUSION

P fertilization shaped mycorrhizal fungal assemblages, shifting the community composition on roots in P-poor soil to a higher similarity to those on roots in P-rich soil but did not affect microbial biomass. Higher fungal taxa diversity in P-rich soil correlated with lower plant P uptake efficiency, which might indicate a higher specialization of fungal taxa colonizing roots in a stressful than in a less stressful environment.

In nature, beech can form closed stands even on the poorest geological substrates, thus, demonstrating large ecological amplitude for nutritional conditions (Leuschner and Ellenberg, 2017). Therefore, the diagnosis of nutrient deficiencies is difficult. Here, we found that P amendment increased the P contents of both, trees in P-poor and P-rich soil but enhanced photosynthesis only in trees in P-poor soil, thus, pin-pointing that young trees in P-rich soil were sufficiently P supplied, whereas those in P-poor soil suffered from P deficiency. Altogether the current studies (Netzer et al., 2016; Yang et al., 2016; Spohn et al., 2018; Zavišić and Polle, 2018) show that beech has a high metabolic flexibility to cope with low soil P stocks by growth adjustment. Since P deficiency results in drought stress-like photosynthetic responses such as decreased stomatal conductance, decreased substomatal CO_2 concentrations and a trend toward enhanced water use efficiency (Yang et al., 2016, this study), we suspect that P-deficient trees will be more vulnerable than P-sufficient trees when they encounter additional stresses in their long life span. Thus, climate change with longer periods of drought (IPCC, 2014) may endanger beech forests on P-limited soils. In future, it will be important to investigate the potential of nutrient-stressed beech trees to endure additional environmental constraints.

DATA AVAILABILITY STATEMENT

The raw data supporting the conclusions of this manuscript have been deposited in the central repositorium of Priority Program 1685 and will be made available by the authors, without undue reservation, to any qualified researcher.

AUTHOR CONTRIBUTIONS

AZ and AP contributed to the conception and design of the study. AZ, NY, and SM conducted the measurements and analyzed the data. AP and EK analyzed the data. AZ wrote the first draft of the manuscript. AP revised the draft. All authors contributed to manuscript revision and read and approved the submitted version.

FUNDING

We gratefully acknowledge funding from the Deutsche Forschungsgemeinschaft to the Priority Program 1685 "Ecosystem Nutrition" (Po362/22-2 and Ka1590/12-2). NY is grateful to the People's Republic of China for granting a CSC doctoral scholarship. The publication fund of the University of Göttingen and the Deutsche Forschungsgemeinschaft supported open access publication of this article.

ACKNOWLEDGMENTS

We thank M. Franke-Klein (Forest Botany and Tree Physiology, University of Göttingen), G. Lehmann (LARI, University of Göttingen), T. Klein (LARI, University of Göttingen), P. Gruner (University of Hohenheim), and M. Reichel (University of Göttingen) for helping with the sample collection and excellent technical assistance. Dr. M. Corre (Department for Tropical Soil Science, Göttingen) provided advice regarding the determination of mineral elements.

SUPPLEMENTARY MATERIAL

The Supplementary Material for this article can be found online at: https://www.frontiersin.org/articles/10.3389/fpls.2018.00463/full#supplementary-material

REFERENCES

Achat, D. L., Augusto, L., Bakker, M. R., Gallet-Budynek, A., and Morel, C. (2012). Microbial processes controlling P availability in forest podosols as affected by soil depth and soil properties. *Soil Biol. Biochem.* 44, 39–48. doi: 10.1016/j.soilbio.2011.09.007

Achat, D. L., Morel, C., Bakker, M. R., Augusto, L., Pellerin, S., Gallet-Budynek, A., et al. (2010). Assessing turnover of microbial biomass phosphorus: combination of an isotopic dilution method with a mass balance model. *Soil Biol. Biochem.* 42, 2231–2240. doi: 10.1016/j.soilbio.2010.08.023

Alvarez, M., Huygens, D., Olivares, E., Saavedra, I., Alberdi, M., and Valenzuela, E. (2009). Ectomycorrhizal fungi enhance nitrogen and phosphorus nutrition of *Nothofagus dombeyi* under drought conditions by regulating assimilative enzyme activities. *Physiol. Plant.* 136, 426–436. doi: 10.1111/j.1399-3054.2009.01237.x

Baker, A., Ceasar, S. A., Palmer, A. J., Paterson, J. B., Qi, W., Muench, S. P., et al. (2015). Replace, reuse, recycle: improving the sustainable use of phosphorus by plants. *J. Exp. Bot.* 66, 3523–3540. doi: 10.1093/jxb/erv210

Baum, C., and Makeschin, F. (2000). "Effects of nitrogen and phosphorus fertilization on mycorrhizal formation of two poplar clones (*Populus trichocarpa* and *P. tremula x tremuloides*). *J. Plant Nutr. Soil Sci.* 163, 491–497. doi: 10.1002/1522-2624(200010)163:5<491::AID-JPLN491>3.0.CO;2-3

Baxter, J. W., and Dighton, J. (2005). "Diversity–functioning relationships in ectomycorrhizal fungal communities," in *The Fungal Community. Its Role and Organization in the Ecosystem*, eds J. Dighton, J. F. White, and P. Oudemans (Boca Raton, FL: Taylor and Francis Group), 383–398.

Becquer, A., Trap, J., Irshad, U., Ali, M. A., and Claude, P. (2014). From soil to plant, the journey of P through trophic relationships and ectomycorrhizal association. *Front. Plant Sci.* 5:548. doi: 10.3389/fpls.2014.00548

Brearley, F. Q., Scholes, J. D., Press, M. C., and Palfner, G. (2007). How does light and phosphorus fertilisation affect the growth and ectomycorrhizal community of two contrasting dipterocarp species? *Plant Ecol.* 192, 237–249. doi: 10.1007/s11258-007-9325-6

Bünemann, E. K., Marschner, P., McNeill, A. M., and McLaughlin, M. J. (2007). Measuring rates of gross and net mineralisation of organic phosphorus in soils. *Soil Biol. Biochem.* 39, 900–913. doi: 10.1016/j.soilbio.2006.10.009

Cairney, J. W. G. (2011). Ectomycorrhizal fungi: the symbiotic route to the root for phosphorus in forest soils. *Plant Soil* 344, 51–71. doi: 10.1007/s11104-011-0731-0

Chadwick, O. A., Derry, L. A., Vitousek, P. M., Huebert, B. J., and Hedin, L. O. (1999). Changing sources of nutrients during four million years of ecosystem development. *Nature* 397, 491–497. doi: 10.1038/17276

Chiou, T.-J., and Lin, S.-I. (2011). Signaling network in sensing phosphate availability in plants. *Annu. Rev. Plant Biol.* 62, 185–206. doi: 10.1146/annurev-arplant-042110-103849

Courty, P. E., Franc, A., and Garbaye, J. (2010). Temporal and functional pattern of secreted enzyme activities in an ectomycorrhizal community. *Soil Biol. Biochem.* 42, 2022–2025. doi: 10.1016/j.soilbio.2010.07.014

Cox, F., Barsoum, N., Lilleskov, E. A., and Bidartondo, M. I. (2010). Nitrogen availability is a primary determinant of conifer mycorrhizas across complex environmental gradients. *Ecol. Lett.* 13, 1103–1113. doi: 10.1111/j.1461-0248.2010.01494.x

Dambrine, E., Martin, F., Carisey, N., Granier, A., Hällgren, J.-E., and Bishop, K. (1995). Xylem sap composition: a tool for investigating mineral uptake and cycling in adult spruce. *Plant Soil* 168, 233–241. doi: 10.1007/BF00029333

Damour, G., Simonneau, T., Cochard, H., and Urban, L. (2010). An overview of models of stomatal conductance at the leaf level. *Plant Cell Environ.* 33, 1419–1438. doi: 10.1111/j.1365-3040.2010.02181.x

Duquesnay, A., Dupouey, J. L., Clement, A., Ulrich, E., and Le Tacon, F. (2000). Spatial and temporal variability of foliar mineral concentration in beech (*Fagus sylvatica*) stands in northeastern France. *Tree Physiol.* 20, 13–22. doi: 10.1093/treephys/20.1.13

Elser, J. J., Bracken, M. E. S., Cleland, E. E., Gruner, D. S., Harpole, W. S., Hillebrand, H., et al. (2007). Global analysis of nitrogen and phosphorus limitation of primary producers in freshwater, marine and terrestrial ecosystems. *Ecol. Lett.* 10, 1135–1142. doi: 10.1111/j.1461-0248.2007.01113.x

Foster, N. W., and Bhatti, J. S. (2006). *Forest Ecosystems: Nutrient Cycling. Encyclopedia of Soil Science*. New York, NY: Taylor & Francis Group, 718–721.

Gessler, A., Schneider, S., Weber, P., Hanemann, U., and Rennenberg, H. (1998). Soluble N compounds in trees exposed to high loads of N: a comparison between the roots of Norway spruce (*Picea abies*) and beech (*Fagus sylvatica*) trees grown under field conditions. *New Phytol.* 138, 385–399. doi: 10.1046/j.1469-8137.1998.00134.x

Gough, C. M., Seiler, J. R., and Maier, C. A. (2004). Short-term effects of fertilization on loblolly pine (*Pinus taeda* L.) *physiology*. *Plant Cell Environ.* 27, 876–886. doi: 10.1111/j.1365-3040.2004.01193.x

Hammer, Ø., Harper, D. A. T., and Ryan, P. D. (2001). PAST: paleontological statistics software package for education and data analysis. *Palaeontol. Electron.* 4, 1–9.

Haußmann, T., and Lux, W. (1997). *Dauerbeobachtungsflächen zur Umweltkontrolle im Wald: Level II; erste Ergebnisse*. Bonn: Bundesministerium für Ernährung, Landwirtschaft und Forsten (BMELF), 148.

Heinrichs, R., Brumsack, H., Loftfield, N., and Konig, N. (1986). Improved pressure digestion system for biological and inorganic materials. *J. Plant Nutr. Soil Sci.* 149, 350–353.

Heuck, C., Weig, A., and Spohn, M. (2015). Soil microbial biomass C:N:P stoichiometry and microbial use of organic phosphorus. *Soil Biol. Biochem.* 85, 119–129. doi: 10.1016/j.soilbio.2015.02.029

Horton, B. M., Glen, M., Davidson, N. J., Ratkowsky, D., Close, D. C., Wardlaw, T. J., et al. (2013). Temperate eucalypt forest decline is linked to altered ectomycorrhizal communities mediated by soil chemistry. *For. Ecol. Manage.* 302, 329–337. doi: 10.1016/j.foreco.2013.04.006

Ilg, K., Wellbrock, N., and Lux, W. (2009). Phosphorus supply and cycling at long-term forest monitoring sites in Germany. *Eur. J. For. Res.* 128, 483–492. doi: 10.1007/s10342-009-0297-z

IPCC (2014). "Contribution of working groups I, II and III to the Fifth Assessment Report of the Intergovernmental Panel on Climate Change," in *Climate Change 2014: Synthesis Report*, eds R. K. Pachauri and L. A. Meyer (Geneva: **IPCC**), 151.

Johri, A. K., Oelmuller, R., Dua, M., Yadav, V., Kumar, M., Tuteja, N., et al. (2015). Fungal association and utilization of phosphate by plants: success, limitations, and future prospects. *Front. Microbiol.* 6:934. doi: 10.3389/fmicb.2015.00934

Jonard, M., Fürst, A., Verstraeten, A., Thimonier, A., Timmermann, V., Potočić, N., et al. (2015). Tree mineral nutrition is deteriorating in Europe. *Globe Change Biol.* 21, 418–430. doi: 10.1111/gcb.12657

Kavka, M., and Polle, A. (2016). Phosphate uptake kinetics and tissue-specific transporter expression profiles in poplar (Populus × canescens) at different phosphorus availabilities. *BMC Plant Biol* 16:206. doi: 10.1186/s12870-016-0892-3

Kavka, M., and Polle, A. (2017). Dissecting nutrient-related co-expression networks in phosphate starved poplars. *PLoS One* 12:e0171958. doi: 10.1371/journal.pone.0171958

King, N. T., Seiler, J. R., Fox, T. R., and Johnsen, K. H. (2008). Post-fertilization physiology and growth performance of loblolly pine clones. *Tree Physiol.* 28, 703–711. doi: 10.1093/treephys/28.5.703

King, R. W., and Zeevaart, J. A. D. (1974). Enhancement of phloem exudation from cut petioles by chelating agents. *Plant Physiol.* 53, 96–103. doi: 10.1104/pp.53.1.96

Kirschbaum, M. U., and Tompkins, D. (1990). Photosynthetic responses to phosphorus nutrition in *Eucalyptus grandis* seedlings. *Aust. J. Plant Physiol.* 17, 527–535. doi: 10.1071/PP9900527

Koide, R. T. (1991). Nutrient supply, nutrient demand and plant response to mycorrhizal infection. *New Phytol.* 117, 365–386. doi: 10.1111/j.1469-8137.1991.tb00001.x

Lambers, H., Raven, J. A., Shaver, G. R., and Smith, S. E. (2008). Plant nutrient-acquisition strategies change with soil age. *Trends Ecol. Evol.* 23, 95–103. doi: 10.1016/j.tree.2007.10.008

Lang, C., Seven, J., and Polle, A. (2011). Host preferences and differential contributions of deciduous tree species shape mycorrhizal species richness in a mixed Central European forest. *Mycorrhiza* 21, 297–308. doi: 10.1007/s00572-010-0338-y

Lang, F., Bauhus, J., Frossard, E., George, E., Kaiser, K., Kaupenjohann, M., et al. (2016). Phosphorus in forest ecosystems: new insights from an ecosystem nutrition perspective. *J. Plant Nutr. Soil Sci.* 179, 129–135. doi: 10.1002/jpln.201500541

Lang, F., Krüger, J., Amelung, W., Willbold, S., Frossard, E., Bünemann, E., et al. (2017). Soil phosphorus supply controls P nutrition strategies of beech forest ecosystems in Central Europe. *Biogeochem.* 136, 5–29. doi: 10.1007/s10533-017-0375-0

Lanzetta, P. A., Alvarez, L. J., Reinach, P. S., and Candia, O. A. (1979). An improved assay for nanomole amounts of inorganic phosphate. *Anal. Biochem.* 100, 95–97. doi: 10.1016/0003-2697(79)90115-5

Leuschner, C., and Ellenberg, H. (2017). *Ecology of Central European Forests. Vegetation Ecology of Central Europe*, Vol. 1. Cham: Springer, 919. doi: 10.1007/978-3-319-43042-3

Leuschner, C., Meier, I. C., and Hertel, D. (2006). On the niche breadth of *Fagus sylvatica*: soil nutrient status in 50 Central European beech stands on a broad range of bedrock types. *Ann. For. Sci.* 63, 355–368. doi: 10.1051/forest:2006016

Lilleskov, E. A., Fahey, T. J., Horton, T. R., and Lovett, G. M. (2002). Belowground ectomycorrhizal fungal community change over a nitrogen deposition gradient in Alaska. *Ecology* 83, 104–115. doi: 10.1890/0012-9658(2002)083[0104:BEFCCO]2.0.CO;2

Maillard, A., Diquelou, S., Billard, V., Laine, P., Garnica, M., Prudent, M., et al. (2015). Leaf mineral nutrient remobilization during leaf senescence and modulation by nutrient deficiency. *Front. Plant Sci.* 6:317. doi: 10.3389/fpls.2015.00317

Mellert, K. H., and Göttlein, A. (2012). Comparison of new foliar nutrient thresholds derived from van den Burg's literature compilation with established Central European references. *Eur. J. For. Res.* 131, 1461–1472. doi: 10.1007/s10342-012-0615-8

Morel, C. H., and Fardeau, J. C. (1989). Native soil and fresh fertilizer phosphorus uptake as affected by rate of application and P fertilizers. *Plant Soil* 115, 23–128. doi: 10.1007/BF02220702

Netzer, F., Schmid, C., Herschbach, C., and Rennenberg, H. (2016). Phosphorus-nutrition of European beech (*Fagus sylvatica* L.) during annual growth depends on tree age and P-availability in the soil. *Environ. Exp. Bot.* 137, 194–207. doi: 10.1093/treephys/tpx126

Nussaume, L., Kanno, S., Javot, H., Marin, E., Pochon, N., Ayadi, A., et al. (2011). Phosphate import in plants: Focus on the PHT1 transporters. *Front. Plant Sci.* 2:83. doi: 10.3389/fpls.2011.00083

Oberson, A., Tagmann, H. U., Langmeier, M., Dubois, D., Mäder, P., and Frossard, E. (2010). Fresh and residual phosphorus uptake by ryegrass from soils with different fertilization histories. *Plant Soil* 334, 391–407. doi: 10.1007/s11104-010-0390-6

Pampolina, N. M., Dell, B., and Malajczuk, N. (2002). Dynamics of ectomycorrhizal fungi in an Eucalyptus globulus plantation: effect of phosphorus fertilization. *For. Ecol. Manage.* 158, 291–304. doi: 10.1016/S0378-1127(00)00721-0

Pena, R., Lang, C., Lohaus, G., Boch, S., Schall, P., Schöning, I., et al. (2017). Phylogenetic and functional traits of ectomycorrhizal assemblages in top soil from different biogeographic regions and forest types. *Mycorrhiza* 27, 233–245. doi: 10.1007/s00572-016-0742-z

Pena, R., and Polle, A. (2014). Attributing functions to ectomycorrhizal fungal identities in assemblages for nitrogen acquisition under stress. *ISME J.* 8, 321–330. doi: 10.1038/ismej.2013.158

Pena, R., Tejedor, J., Zeller, B., Dannenmann, M., and Polle, A. (2013). Interspecific temporal and spatial differences for the acquisition of litter-derived nitrogen of ectomycorrhizal fungal assemblages. *New Phytol.* 199, 520–528. doi: 10.1111/nph.12272

Peters, R. (1997). *Beech Forests,* Vol. 24. The Hague: Springer, 170. doi: 10.1007/978-94-015-8794-5

Plassard, C., and Dell, B. (2010). Phosphorus nutrition of mycorrhizal trees. *Tree Physiol.* 30, 1129–1139. doi: 10.1093/treephys/tpq063

Preusser, S., Marhan, S., Poll, C., and Kandeler, E. (2017). Microbial community response to changes in substrate availability and habitat conditions in a reciprocal subsoil transfer experiment. *Soil Biol. Biochem.* 105, 138–152. doi: 10.1016/j.soilbio.2016.11.021

Pritsch, K., and Garbaye, J. (2011). Enzyme secretion by ECM fungi and exploitation of mineral nutrients from soil organic matter. *Ann. For. Sci.* 68, 25–32. doi: 10.1007/s13595-010-0004-8

R Core Development Team (2012). *R: A Language and Environment for Statistical Computing*. Vienna: R Foundation for Statistical Computing.

Rineau, F., and Courty, P. E. (2011). Secreted enzymatic activities of ectomycorrhizal fungi as a case study of functional diversity and functional redundancy. *Ann. For. Sci.* 68, 69–80. doi: 10.1007/s13595-010-0008-4

Sattelmacher, B., Horst, W. J., and Becker, H. C. (1994). Factors that contribute to genetic variation for nutrient efficiency of crop plants. *J. Plant Nutr. Soil Sci.* 157, 215–224. doi: 10.1111/pbi.12042

Scheible, W.-R., and Rojas-Triana, M. (2015). "Sensing, signalling, and control of phosphate starvation in plants: molecular players and applications," in *Annual Plant Reviews*, Vol. 48, eds W. C. Plaxton and H. Lambers (Hoboken, NJ: John Wiley & Sons), 23–63.

Schmidt, M., Veldkamp, E., and Corre, M. D. (2015). Tree species diversity effects on productivity, soil nutrient availability and nutrient response efficiency in a temperate deciduous forest. *For. Ecol. Manage.* 338, 114–123. doi: 10.1016/j.foreco.2014.11.021

Smith, M. E., and Bonito, G. M. (2012). "Systematics and ecology of edible ectomycorrhizal mushrooms," in *Edible Ectomycorrhizal Mushrooms, Soil Biology*, Vol. 34, eds A. Zambonelli and G. M. Bonito (Berlin: Springer), 17–39. doi: 10.1007/978-3-642-33823-6_2

Spohn, M., Zavišić, A., Nassal, P., Bergkemper, F., Schulz, S., Marhan, S., et al. (2018). Temporal variations of phosphorus uptake by soil microbial biomass and young beech trees in two forest soils with contrasting phosphorus stocks. *Soil Biol. Biochem.* 117, 191–202. doi: 10.1016/j.soilbio.2017.10.019

Talkner, U., Meiwes, K. J., Potočić, N., Seletković, I., Cools, N., De Vos, B., et al. (2015). Phosphorus nutrition of beech (*Fagus sylvatica* L.) is decreasing in Europe. *Ann. For. Sci.* 72, 919–928. doi: 10.1007/s13595-015-0459-8

Teste, F. P., Lalibert, E., Lambers, H., Auer, Y., Kramer, S., and Kandeler, E. (2016). Mycorrhizal fungal productivity and scavenging in nutrient-poor yet hyperdiverse plant communities: are the symbionts functionally ephemeral? *Soil Biol. Biochem.* 92, 119–132. doi: 10.1016/j.soilbio.2015.09.021

Treseder, K. K. (2004). A meta-analysis of mycorrhizal responses to nitrogen, phosphorus, and atmospheric CO_2 in field studies. *New Phytol.* 164, 347–355. doi: 10.1111/j.1469-8137.2004.01159.x

Turnbull, T. L., Warren, C. R., and Adams, M. A. (2007). Novel mannose-sequestration technique reveals variation in subcellular orthophosphate pools do not explain the effects of phosphorus nutrition on photosynthesis in Eucalyptus globulus seedlings. *New Phytol.* 176, 849–861. doi: 10.1111/j.1469-8137.2007.02229.x

Turner, B. L., and Condron, L. M. (2013). Pedogenesis, nutrient dynamics, and ecosystem development The legacy of TW Walker and JK Syers. *Plant Soil* 367, 1–10. doi: 10.1007/s11104-013-1750-9

Twieg, B. D., Durall, D. M., Simard, S. W., and Jones, M. D. (2009). Influence of soil nutrients on ectomycorrhizal communities in a chronosequence of mixed temperate forests. *Mycorrhiza* 19, 305–316. doi: 10.1007/s00572-009-0232-7

Vitousek, P. M., Porder, S., Houlton, B. Z., and Chadwick, O. A. (2010). Terrestrial phosphorus limitation: mechanisms, implications, and nitrogen-phosphorus interactions. *Ecol. Appl.* 20, 5–15. doi: 10.1890/08-0127.1

von Wühlisch, G., and Muhs, H. J. (2011). "Current state of European beech (*Fagus sylvatica* L.) forests in Germany," in *Genetic Resources of Beech in Europe – Current State*, Vol. 350, eds J. Frýdl, P. Novotný, J. Fennessy, and G. von Wühlisch (Braunschweig: VTI).

Warren, C. R. (2011). How does P affect photosynthesis and metabolite profiles of Eucalyptus globulus? *Tree Physiol.* 31, 727–739. doi: 10.1093/treephys/tpr064

White, T. J., Bruns, T., Lee, S., and Taylor, J. W. (1990). *Amplification and Direct Sequencing of Fungal Ribosomal RNA Genes for Phylogenetics*. New York, NY: Academic Press. doi: 10.1016/B978-0-12-372180-8.50042-1

Yang, N., Zavišiæ, A., Pena, R., and Polle, A. (2016). Phenology, photosynthesis, and phosphorus in European beech (*Fagus sylvatica* L.) in two forest soils with contrasting P contents. *J. Plant Nutr. Soil Sci.* 179, 151–158. doi: 10.1002/jpln.201500539

Zavišić, A., Nassal, P., Yang, N., Heuck, C., Spohn, M., Marhan, S., et al. (2016). Phosphorus availabilities in beech (*Fagus sylvatica* L.) forests impose habitat filtering on ectomycorrhizal communities and impact tree nutrition. *Soil Biol. Biochem.* 98, 127–137. doi: 10.1016/j.soilbio.2016.04.006

Zavišić, A., and Polle, A. (2018). Dynamics of phosphorus nutrition, allocation and growth of young beech (*Fagus sylvatica* L.) trees in P-rich and P-poor forest soil. *Tree Physiol.* 38, 37–51. doi: 10.1093/treephys/tpx146

Zederer, D. P., Talkner, U., Spohn, M., and Joergensen, R. G. (2017). Microbial biomass phosphorus and C/N/P stoichiometry in forest floor and A horizons as affected by tree species. *Soil Biol. Biochem.* 111, 166–175. doi: 10.1016/j.soilbio.2017.04.009

Zhang, C. X., Meng, S., Li, M. J., and Zhao, Z. (2016). Genomic identification and expression analysis of the phosphate transporter gene family in poplar. *Front. Plant Sci.* 7:1398. doi: 10.3389/fpls.2016.01398

Conflict of Interest Statement: The authors declare that the research was conducted in the absence of any commercial or financial relationships that could be construed as a potential conflict of interest.

frontiers in Plant Science

REVIEW
published: 05 June 2018
doi: 10.3389/fpls.2018.00752

Phosphorus Acquisition Efficiency Related to Root Traits: Is Mycorrhizal Symbiosis a Key Factor to Wheat and Barley Cropping?

Pedro Campos[1,2], *Fernando Borie*[1,3], *Pablo Cornejo*[1,3], *Juan A. López-Ráez*[2]*, *Álvaro López-García*[4] and *Alex Seguel*[1]*

[1] Scientific and Technological Bioresource Nucleus BIOREN-UFRO, Universidad de La Frontera, Temuco, Chile, [2] Department of Soil Microbiology and Symbiotic Systems, Estación Experimental del Zaidín-Consejo Superior de Investigaciones Científicas, Granada, Spain, [3] Departamento de Ciencias Químicas y Recursos Naturales, Universidad de La Frontera, Temuco, Chile, [4] Section Ecology and Evolution, Biological Institute, University of Copenhagen, Copenhagen, Denmark

OPEN ACCESS

Edited by:
Jose M. Garcia-Mina, Universidad de Navarra, Spain

Reviewed by:
Raffaella Balestrini, Consiglio Nazionale Delle Ricerche (CNR), Italy
Monica Calvo-Polanco, Montpellier SupAgro, France

***Correspondence:**
Juan A. López-Ráez
juan.lopezraez@eez.csic.es
Alex Seguel
alex.seguel@ufrontera.cl

Specialty section:
This article was submitted to Plant Nutrition, a section of the journal Frontiers in Plant Science

Received: *12 January 2018*
Accepted: *16 May 2018*
Published: *05 June 2018*

Citation:
Campos P, Borie F, Cornejo P, López-Ráez JA, López-García Á and Seguel A (2018) Phosphorus Acquisition Efficiency Related to Root Traits: Is Mycorrhizal Symbiosis a Key Factor to Wheat and Barley Cropping? Front. Plant Sci. 9:752. doi: 10.3389/fpls.2018.00752

Wheat (*Triticum aestivum* L.) and barley (*Hordeum vulgare* L.) are major crops cultivated around the world, thus playing a crucial role on human diet. Remarkably, the growing human population requires a significant increase in agricultural production in order to feed everybody. In this context, phosphorus (P) management is a key factor as it is component of organic molecules such as nucleic acids, ATP and phospholipids, and it is the most abundant macronutrient in biomass after nitrogen (N), although being one of the scarcest elements in the lithosphere. In general, P fertilization has low efficiency, as only a fraction of the applied P is acquired by roots, leaving a substantial amount to be accumulated in soil as not readily available P. Breeding for P-efficient cultivars is a relatively low cost alternative and can be done through two mechanisms: i) improving P use efficiency (PUE), and/or ii) P acquisition efficiency (PAE). PUE is related to the internal allocation/mobilization of P, and is usually represented by the amount of P accumulated per biomass. PAE relies on roots ability to acquire P from the soil, and is commonly expressed as the relative difference of P acquired under low and high P availability conditions. In this review, plant adaptations related to improved PAE are described, with emphasis on arbuscular mycorrhizal (AM) symbiosis, which is generally accepted to enhance plant P acquisition. A state of the art (1980–2018) of AM growth responses and P uptake in wheat and barley is made to discuss about the commonly accepted growth promoting effect and P increased uptake by AM fungi and the contrasting evidence about the generally accepted lack of positive responses in both plant species. Finally, the mechanisms by which AM symbiosis can affect wheat and barley PAE are discussed, highlighting the importance of considering AM functional diversity on future studies and the necessity to improve PAE definition by considering the carbon trading between all the directly related PAE traits and its return to the host plant.

Keywords: cereal, phosphorus, fungal diversity, mycorrhizae, nutrient uptake, PAE, root traits

INTRODUCTION

Cereals have been cultivated for more than 10,000 years, playing a crucial role in the development of human civilization. Today, cereals are still important, being the principal crops harvested in the world with more than 2.8 Gt of combined grain production (FAO, 2013). Among major cereals, the widespread and closely related wheat (*Triticum aestivum* L.) and barley (*Hordeum vulgare* L.) represents 31% of global grain yield (El Rabey et al., 2015). Cereals are also the major component of human diet worldwide with more than 50% of daily caloric intake, with values exceeding 80% in the poorest countries (Awika, 2011). Agricultural practices and technology have greatly improved over the last decades to reduce problems associated with food scarcity and to provide cereals for the daily diet. However, risks and unprecedented challenges still remain considering that global food, and grain production must increase a 70% by the year 2050 as world population is expected to be reach 9 billion people (FAO, 2012). Meanwhile, the slight increase in crop yields observed since the 1980s and the scarcity of available land suitable for production make the focus on reducing crop losses empirical due to various kinds of biotic and abiotic stresses factors, such as pathogen attack, cold, heat, drought, salt, deficiency of nutrients as phosphorous (P), and phytotoxicity by heavy metal stresses (Ray et al., 2012; Bhardwaj et al., 2014).

P fertilizers are manufactured from rock phosphate found only in a few places in the world, being Morocco the owner of 85% of the known active mining reserves. As a non-renewable resource, rock phosphate, as well as other non-renewable resources such as oil and coal is expected to become scarce near the 2030s (Cordell et al., 2009), or more optimistically within two to three centuries (Sattari et al., 2012). The market and countries are already responding to this scenario, which is reflected in the fact that both USA and China (the biggest P producer in the world) have stopped exporting this resource (van de Wiel et al., 2016). In addition, P fertilizers may cause environmental problems associated with eutrophication (Gaxiola et al., 2001) and can contain heavy metals such as cadmium that may accumulate in arable soils as a result of the addition of rock phosphate (van de Wiel et al., 2016). Remarkably, usually only about 10–30% of the P fertilizer applied in the first year is taken up by the roots, with a substantial part accumulated in the soil as residual P not readily available for plants (Syers et al., 2008). In alkaline soils, P can be bound to calcium, and in acidic soils it can be readily complexed to charged Al and Fe oxides and groups hydroxyls on clay surfaces (Kochian et al., 2004; Seguel et al., 2013), limitations that can occur in *ca*. 30% of arable soils worldwide (Kochian, 2012). Moreover, organic material present in the soil (e.g., from manure or crop residues) can also bind phosphate ions as well as phytate (inositol compounds).

Ideally, P taken up by agricultural products should represent the same amount of applied P fertilizer, achieving a neutral balance (Helyar, 1998; Syers et al., 2008). However, this situation is often only achieved in low input, low production farming systems (e.g., Burkitt et al., 2007; McIvor et al., 2011), on intrinsically low P-buffering capacity soils in productive agriculture (e.g., sands), or where P-buffering capacity is low because sorption sites for P are close to saturation and soil P availability is relatively high (e.g., Syers et al., 2008). Elsewhere, P-balance is relatively low, which contributes to an inefficient P use (Richardson et al., 2011). Thus, P management must be improved in order to enhance plant uptake in soils, as well as using the less available and bound-P through a better understanding of the processes happening in the soil-plant systems.

PHOSPHORUS IN THE SOIL-PLANT CONTINUUM

In general, P is present in plants either as organic phosphate esters or as free inorganic orthophosphate forms, representing up to *ca*. 0.2% of plants dry weight, making it the most abundant macronutrient in plants after nitrogen (N). However, unlike N, the amount of P available for agriculture is finite (Bovill et al., 2013). When compared to other essential macronutrients, P is one of the less-abundant elements in the lithosphere (0.1% of the total). P is an important component of organic molecules such as nucleic acids, ATP and phospholipids; thus playing a crucial role in energy metabolism of both plants and animals (Abel et al., 2002; Vance et al., 2003). Phosphate is also involved in signal-transduction pathways via phosphorylation/dephosphorylation, hence regulating key enzyme reactions in general cellular metabolism, including N fixation on N-fixing plants (Theodorou and Plaxton, 1996; Schachtman et al., 1998; Marschner, 2012).

Plants acquire P from the soil solution predominately as inorganic phosphate (Pi) ($H_2PO_4^-$/HPO_4^{-2}), having maximal uptake rates at pH 5-6 (Holford, 1997; Rae et al., 2003; Marschner, 2012). It acquisition occurs by a plasma membrane-localized phosphate transporter-mediated process, which has been suggested to operate as a H^+ co-transporter (Rae et al., 2003; Raghothama, 2005). Phosphate transporters are classified into four families: Pht1, Pht2, Pht3, and Pht4, which are located on the plasma membrane, plastidial membrane, mitochondrial membrane, and Golgi-compartment, respectively (Lopez-Arredondo et al., 2014). Two different uptake systems have been proposed: one with high-affinity, which is regulated by Pi availability and activated mainly under P deficiency, with a Km of 3–7 μM; and the other is a low-affinity system constitutively expressed system with Km of 50–300 μM (Bucher et al., 2001; Preuss et al., 2010; Liu et al., 2011; Tian et al., 2017). Despite of having a high-affinity acquisition system, P has a low availability and poor mobility in the soil, being one of the most inaccessible elements for plants (Holford, 1997). Concentrations of available P in soil solution are extremely low, being generally lower than 10 μM (Holford, 1997; do Nascimento et al., 2016), whereas in wheat leaves and stems concentrations of over 100 mM can be achieved (Bauer et al., 1987; Seguel et al., 2017). Therefore, as plants normally take up P faster than it is supplied by diffusion a depletion zone around the root system is quickly created, inducing P deprivation (**Figure 1A**; Hinsinger, 2001).

The rhizosphere encompasses the first millimeters of the soil surrounding plant roots, where biological and ecological complex processes occur. This is the critical zone for P dynamics as plants roots are capable of modifying this environment through their

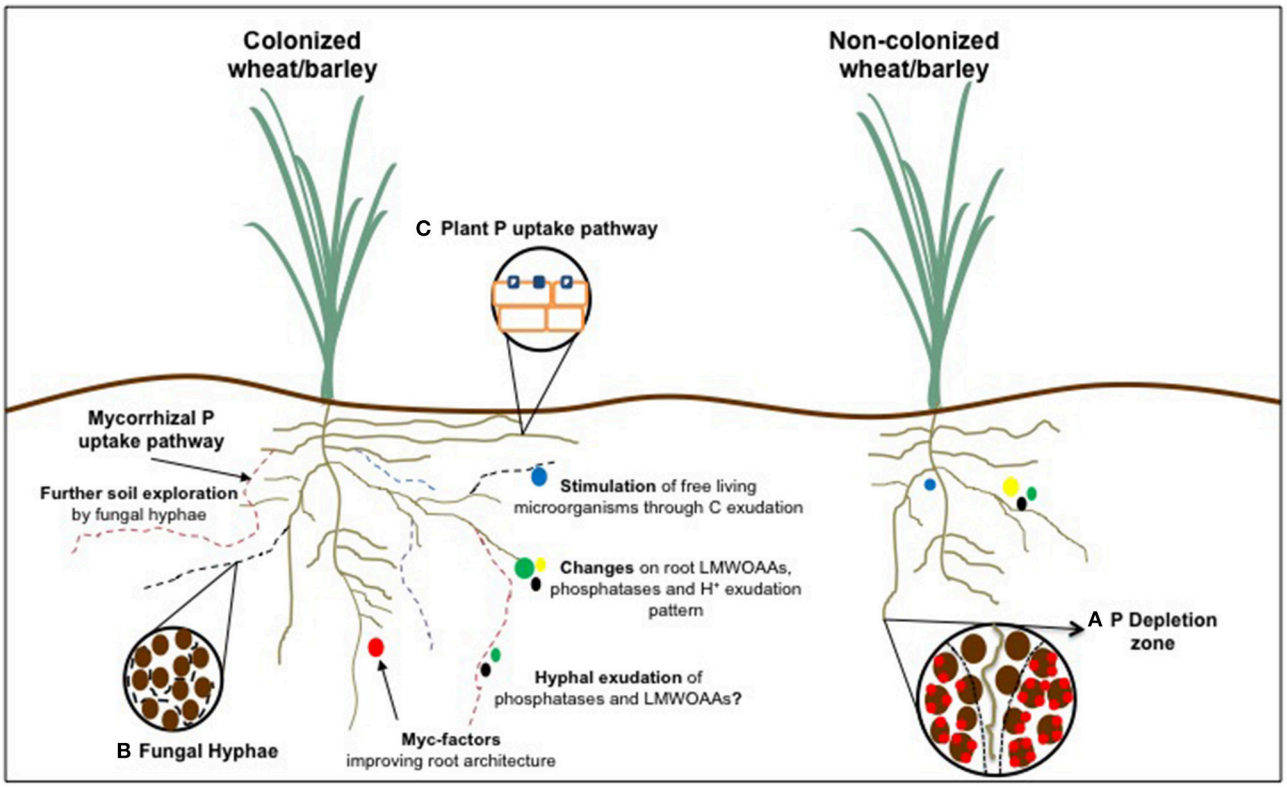

FIGURE 1 | Phosphorus acquisition efficiency related traits of wheat and barley roots affected by arbuscular mycorrhizal symbiosis in comparison to a non-colonized counterpart. **(A)** Representation of P depletion zone around the rhizosphere; **(B)** Access to smaller soil pores by AM fungal hyphae; and **(C)** Modulation of plant P transporters following colonization.

physiological activities, especially by exudation of organic acid anions, enzymes, secondary metabolites and sugars (Bais et al., 2006; Giles et al., 2017). These processes not only determine solubilization/mineralization, acquisition of soil nutrients and microbial dynamics, but also control the efficiency of nutrient use by plants and crops, therefore influencing productivity and sustainability of the agroecosystems (Hinsinger et al., 2009; Zhang et al., 2010).

PHOSPHORUS EFFICIENCY

Great efforts have been made in the last decade concerning P efficiency. In this sense, agronomic strategies for increasing P fertilizer availability to crops has been developed, for example, by applying liquid fertilizers (Holloway et al., 2001) or by localized fertilizer placement (Ma et al., 2009). However, those techniques require modern technologies and increase operational costs. On the other hand, breeding for P-efficient crop cultivars has been advocated due to its relatively low cost, providing benefits to both high and low-input systems (Rose et al., 2010).

Despite the growing knowledge in the field, there is still controversy in the concept and measurement of efficiency, as it has many definitions, and even different terms are often used although they are calculated in the same way (Bovill et al., 2013). Nowadays, P efficiency is understood as two different mechanisms: i) the internal efficiency of allocation/mobilization of P in order to produce higher biomass with lower input, and ii) plant ability to acquire P from the soil, also known as P acquisition efficiency (Wang et al., 2010; Rose and Wissuwa, 2012; Sandaña and Pinochet, 2016).

The internal use efficiency or P use efficiency (PUE) is here defined as the amount of P accumulated in the tissue per biomass unit (shoot and/or root) or grain produced (Rose and Wissuwa, 2012). It is related to a range of metabolic modifications that can occur for reducing P demand during plant development (Hammond et al., 2009; Vaneklaas et al., 2012). Improving internal PUE will lead to a more resource-efficient use of P rather than increasing uptake of potentially scarce P forms, as in theory less P will be acquired by crops, minimizing P fertilizer requirement and removal from fields. However, to date no crop species or genotypes within species are known to be capable of reducing its net P uptake if the demand is reduced (Rose and Wissuwa, 2012). This is operating in sandy or low P-soption capacity soils. On the contrary, in soils rich in sorbed P, which are observed in the majority of acid soils, breeding programs focused on the optimization of P scavenging mechanisms would be a key role to improve P efficiency. Consenquently, this review has been mainly focused on P acquisition efficiency.

Phosphorus Acquisition Efficiency

While PUE aims to produce more biomass with lesser P costs, P acquisition efficiency (PAE) is related to enhancing its acquisition from soil, especially from unavailable forms, and for this purpose root traits are a key factor. PAE is commonly expressed in the literature as the relative difference of P taken up in low and high P availability conditions (Vandamme et al., 2013; Seguel et al., 2015, 2017). However, this definition does not take into account the root traits involved. In this sense, Liao et al. (2008) made a more realistic approximation by integrating root length and root biomass. Nevertheless, other traits related to root architecture and physiolgy must be integrated in the PAE definition due to their key role in uptake as discussed below (**Figure 2**).

Root Architecture

P status is a major factor modulating root architecture, being a higher root-to-shoot ratio the most evident change in the majority of plants experiencing P deprivation (Wissuwa et al., 2005; Gruber et al., 2013). Phosphate, the available form of P, presents a heterogeneous distribution (patches) given its high affinity for the soil matrix. Root P gathering implies a continuous root growth due to the quickly depletion of rhizosphere P and the need of looking for new hotspots in soils (**Figure 1A**).

The upper soil layer (0–10 cm)—known as topsoil—is the zone where P availability for plants and microorganisms is generally higher, mainly due fertilizers input in the surface and its poor mobility throught soil profile. Important adaptations of plants to access this richer environment are the development of axial roots with shallower angle, enhancing adventitious rooting, and greater density and dispersion of lateral roots and root hairs (Wang et al., 2004; Lynch, 2007). These traits, together with root length, diameter and surface area comprise the most important inter- and intra-specifically functional variations of plant root adaptations for PAE for most plant species. During their screening for traits directly related to PAE, Manske et al. (2000) found that higher root length density in top soil of wheat crops was the most important root trait for P uptake, which was positively correlated with enhanced recovery of fertilized P. Basal roots in some legumes (as bean and soybean) appear in distinct nodes or "whorls," which affect root growth angles and therefore top soil exploration. Differences of up to 100% of improved P acquisition can be found in common bean cultivars as basal root whorl number varies among genotypes (Lynch, 2007; Miguel, 2011). However, a certain tradeoff occurs between P and water uptake since plants with higher density of roots in top soil and shallower angles have lower water use efficiency, as water is usually more abundant in deeper layers under drought conditions (Ho et al., 2005). Another obstacle in improving root density is the associated carbon cost of producing root hairs, that have to be compensated by producing either smaller or thinner hairs and/or increased proportion of aerenchyma in the cortex and less secondary growth of the stele (Lynch and Ho, 2005; Zhu et al., 2010). Plants would otherwise spare carbon allocated in developing "productive" parts.

Modeling root traits are clearly advantageous strategy for enhancing PAE. However, screening and phenotyping for these traits remain a complex challenge as soil-based study systems are high technology based, and hydroponic/aeroponic systems cannot totally emulate the complexity of the processes occurring in the soil. Therefore, genotypes selected in this way do not always show their superiority in field trials (van de Wiel et al., 2016).

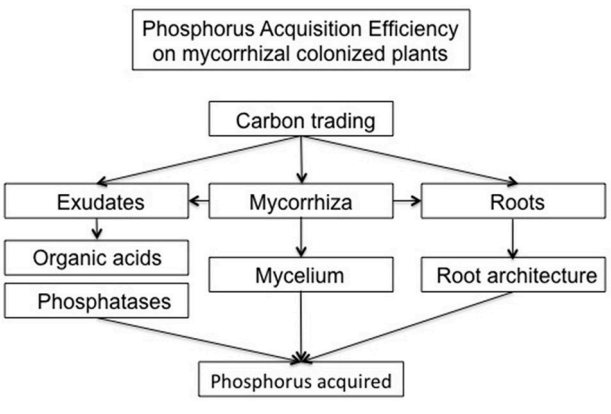

FIGURE 2 | General scheme showing the proposed PAE determination based on carbon trading between all directly related P acquisition traits in AM colonized plants.

Root Exudates

If P is present on fixed sources and/or unavailable forms, plants having larger and/or more branched root architecture do not significantly improve P acquisition. In this case, root physiology and biochemical responses play a major role on accessing P from sparingly available pools in soil. Hence, the exudation of low molecular weight organic acids (LMWOAAs), proton extrusion, phosphatase exudation and/or association with symbiotic and non-symbiotic microorganisms present in the rhizosphere are the most important adaptations developed by plants (**Figure 1**).

As inorganic P forms availability and enzymatic activity are strongly affected by soil pH (Hinsinger, 2001), P solubility can be increased by root-induced acidification in alkaline soils or by pH increase of the rhizosphere in acidic and deeply weathered soils (Gahoonia et al., 1992; Jones and Oburger, 2011). This process occurs mainly because changes in pH in the rhizosphere can influence surface charges on soil particles and therefore Pi availability (Geelhoed et al., 1999). Plants have the ability to either increase or decrease rhizospheric pH up to 2–3 pH units, mainly by absorption or release of protons in order to equilibrate cation/anion balance (Hinsinger et al., 2003). In the specific case of the cereals wheat and barley, Gahoonia and Nielsen (1996) observed that when rhizospheric pH was invariable, the plants displayed significant genotypic variation in terms of PAE, indicating that other mechanisms should also be involved in causing variation on P acquisition.

Carboxylates and the corresponding carboxylic acids, also known as LMWOAAs, constitute the major fraction of root exudates during P deficiency (**Figure 1**). Usually, the most common organic acid anions found in rhizosphere are lactate, acetate, oxalate, succinate, fumarate, malate, citrate, isocitrate, and aconitate (Jones, 1998). They have distinct functions on

energetic cell metabolism, maintaining charge balance or osmotic potential. It has been widely suggested that LMWOAAs can improve P availability by mobilizing sparingly available P forms in the soil solution. This occurs by chelating metals ions like Al, Fe or Ca involved in P sorption and occupying sorption sites on minerals (Jones, 1998). P mobilizing activity through LMWOAAs is based on their variable negative charge, which would allow the complexation of metal cations and the displacement of anions from the soil matrix. The above is supported by several studies reporting an increase of organic acids exudation by roots in response to P deprivation, especially in plants from Proteacea family that possess cluster roots (Jones, 1998; Vance et al., 2003; Delgado et al., 2013). In addition, the presence of LMWOAAs in solution has been seen to increased P availability compared to water treatments (Gerke, 1992; Khademi et al., 2009, 2010). The efficiency in mobilizing P differs across LMWOAAs as follows: citrate > oxalate > malate > acetate. However, organic acid anion-induced P release depends on many factors, such as pH, soil mineralogy and anion concentration (>100 mM for citrate, >1 mM for oxalate, malate and tartrate) (Bolan et al., 1994; Jones and Darrah, 1994; Lan et al., 1995). Indeed, the rates to which Pi and organic anions are replaced in soil solution make predictions of the real effect difficult. Organic acid anions have a fast turnover as they can be quickly adsorbed in acidic soils and rapidly degraded in alkaline counterparts, with half-lives of several hours (Wang et al., 2010). Contrasting evidence found that, despite exuding citrate, pea genotypes were not capable of mobilizing P from Al-P and Fe-P complexes (Pearse et al., 2007). Nevertheless, organic acid production constitutes an important carbon cost in plant metabolism, with 5–25% of total fixed carbon by photosynthesis being used to sustain exudation. However, this does not seem to significantly affect net biomass production as P deficiency can reduce growth to an even greater extent (Johnson et al., 1996; Keerthisinghe et al., 1998).

Sparingly available organic P forms represent between 30% and 90% of total P in some soils (Borie et al., 1989; Jones and Oburger, 2011). Substantial flows of P occur between inorganic and organic P pools in soil through immobilization and mineralization, being both processes mediated predominantly by soil microorganisms (Oberson and Joner, 2005; Richardson and Simpson, 2011). In order to utilize this P source, organic compounds have to be mineralized; that is, organic P substrates must be hydrolyzed by enzymatic activity of phosphatases to release Pi. This activity seems to be more pronounced in the rhizosphere and it is associated with a depletion of soil organic P (Gahoonia and Nielsen, 1992; Chen et al., 2002; Spohn and Kuzyakov, 2013). Phosphatases are enzymes responsible for catalyzing the hydrolysis of phosphoric acid anhydrides and esters (Schmidt and Laskowski, 1961). These are classified by the Nomenclature Committee of the International Union of Biochemistry and Molecular Biology into 5 groups: phosphomonoesterases (EC 3.1.3), phosphodiesterases (EC 3.1.4), triphosphoric monoester hydrolases (EC 3.1.5), enzymes acting on phosphoryl-containing anhydrides (EC 3.6.1) and on P–N bonds (EC 3.9) (Nannipieri et al., 2011). Phosphomonoesterases are the most abundant enzymes in soils and include acid and alkaline forms and phytases, among others. To date, there is no evidence that any plants produce alkaline phosphomonoesterases.

There is an increasing interest on phytases due to the fact that they hydrolyze inositol phosphates (isomers and lower order derivatives of inositol hexakisphosphate) which generally constitute a major component of soil total organic P. Ranging from 4 to 40% of total P in soils (Borie et al., 1989; Smernik and Dougherty, 2007; Turner, 2007), inositol phosphates are readily adsorbed to soil particles and can react with cations (Fe and Al in acidic soils and Ca in alkaline ones) depending on pH to form poorly soluble precipitates (Shang et al., 1992; Celi and Barberis, 2005). However, in most plant species phytase activity has limited capability to mineralize inositol phosphate due to its low production and exudation from roots and the poor availability of the substrate in solution (Richardson et al., 2001; George et al., 2007). Attempts to creating transgenic plants overexpressing phytases and/or other phosphatases have been achieved (Lung et al., 2005; Wasaki et al., 2009) with little successes under natural soil conditions, where substrate availability is restricted (Lung and Lim, 2006; Wang et al., 2009). Interestingly, phosphatase activities are higher near the rhizosphere, with maximum activities found from 2 to 3.1 mm to the root surface for acid and 1.2 to 1.6 mm for alkaline phosphomonoesterases, showing a negative correlation with rhizospheric organic P content in wheat plants (Nannipieri et al., 2011). Phosphatase activity is also regulated by other factors, such as soil mineralogy, organic matter content, P availability and bacterial communities present in the rhizosphere (Joner and Jakobsen, 1995; Snajdr et al., 2008; Stursova and Baldrian, 2011).

Microorganisms

Non-symbiotic soil microorganisms play a key role on organic P ecosystem dynamics (**Figure 1**; Harvey et al., 2009; Khan et al., 2010). It has been proposed that all alkaline phosphomonoesterases found in soil have a microbial origin, mainly bacterial (Tabatabai, 1994; Yadav and Tarafdar, 2003). Additionally, the majority of Pi mineralized from phytase activity is mediated by free-living bacteria and fungi (Unno et al., 2005; Richardson and Simpson, 2011). Spohn et al. (2013) using the ^{33}P isotopic approach found that the release of root exudates could be a plant strategy to increase P mineralization by enhancing microbial activity.

Free-living soil microorganisms are believed to be more efficient than plants in absorbing and incorporating P into their biomass. Therefore, microbial P represents an important soil sink (Xu et al., 2013) and a potential source of available P for most plants as microbial P is located in more labile intracellular compounds with a fast turnover (Oberson and Joner, 2005; Bünemann et al., 2013; Hinsinger et al., 2015). Despite having an important role in organic P dynamics, most research related to free-living soil microorganisms to enhance PAE has been focused on microorganisms capable of solubilizing sparingly available P (Wakelin et al., 2004; Leggett et al., 2007). Microorganisms can release protons, LMWOAAs, and other secondary organic metabolites that may contribute to P solubilization from minerals (Jones and Oburger, 2011). Indeed, between 1-50% of soil bacteria and about 0.5-0.1% of soil fungi can be classified as

P-solubilizing microorganisms (Kucey et al., 1989; Gyaneshwar et al., 2002). Fungal isolates (particularly the Genus *Penicillium*) have been largely studied due to their great capacity for solubilizing Pi in both solid and liquid media (Gyaneshwar et al., 2002; Leggett et al., 2007; Morales et al., 2011). A group of bacteria, usually denominated as plant-growth-promoting rhizobacteria (PGPR), are widely found in the rhizosphere of cropping and wild species and have the potential of enhancing PAE mainly through influencing nutrient availability, such as P, or via the indirect production of phytohormones, or plant growth regulators (Richardson et al., 2009). Among the latter, classical phytohormones as auxin, cytokinin, ethylene, gibberellin, and abscisic acid are included. These regulators influence root architecture and other features related to plant development (Peleg and Blumwald, 2011; Vacheron et al., 2013). Although the benefits of using PAE enhancing microorganisms have been evidenced in laboratory and glasshouse conditions, inconsistent results have been observed in field trials (Goos et al., 1994; Karamanos et al., 2010), with the exception of arbuscular mycorrhizal symbiosis established with certain soil fungi.

ARBUSCULAR MYCORRHIZAL SYMBIOSIS

Mycorrhizal symbiosis is an association between plant and some fungal species that generally colonize root or rhizoids, and is beneficial to both partners, at least under some circumstances (Jansa et al., 2011). Arbuscular mycorrhizal (AM) is the most common and widespread type of mycorrhizal symbiosis (Trappe, 1987; Wang and Qiu, 2006; Smith and Read, 2008), found in *ca.* 80% of plant species among all major plants lineages (Wang and Qiu, 2006; Brundrett, 2009) and in most of agricultural species (exceptions include *Brassica* spp., and *Lupinus* spp.). Although AM symbiosis is facultative for many plant species, fossil evidence indicates that the symbiosis matches with the first appearance of land plants, more than 400 million years ago, playing a crucial role in the development of terrestrial plants (Bonfante and Genre, 2008; Brundrett, 2009). AM fungi (subphylum Glomeromycotina) are obligate biotrophs that when associated with plant roots can provide an enhanced foraging system in order to improve acquisition of soil water and nutrients, particularly P, and to improve resistance to biotic and abiotic stresses in exchange of energy (using carbohydrates as trade) for fungal growth and reproduction (Jansa et al., 2003a; Smith and Read, 2008; Jung et al., 2012; Pozo et al., 2015; Armada et al., 2016; Santander et al., 2017). P appears to be one of major regulators of AM symbiosis establishment and efficiency, as root colonization, P uptake through fungal pathway (**Figure 1**) (See section Changes in P Transporters) and growth responses diminish with increasing soil P availability (Smith and Read, 2008; Richardson et al., 2011; Smith et al., 2011). However, plants can also modulate the symbiosis, by stimulating fungal metabolic activity and hyphal branching among other effects (Bücking and Shachar-Hill, 2005; Besserer et al., 2006), through the exudation of strigolactones (Akiyama et al., 2005; Parniske, 2006; López-Ráez et al., 2017) Accordingly, the production of these strigolactones is promoted by P deprivation, although in wheat can be also promoted in a small fraction by N deficiency (Yoneyama et al., 2007, 2012; López-Ráez et al., 2008).

Despite its broad host range and that its cosmopolitan distribution, AM diversity involves only ∼250 morphologically and 350 to 1000 molecularly defined AM fungi (Kivlin et al., 2011; Öpik et al., 2014), with low endemism patterns at global scale (Davison et al., 2015). The absence of AM fungal colonization is rare in natural conditions in plants able to perform the symbiosis, only being achieved in soils lacking AM fungal propagules or in non-mycorrhizal (NM) plant species (Smith et al., 2011). Commonly, the difference in plant growth in presence and absence of mycorrhizal fungal partners is defined as mycorrhizal growth responses (MGR) and vary widely from positive to negative depending on plant/fungi species and growth conditions (Johnson et al., 1997; Klironomos, 2003). When compared to MGR observed from other cereal crops [positives responses in maize (Sylvia et al., 1993; Karasawa et al., 2001) and rye (Baon et al., 1994a); and excluding rice, which is often not colonized or poorly colonized under continuous submersion (Vallino et al., 2009)], wheat and barley plants present a high variable response to AM colonization, being generally considered as low and sometimes showing even negative effects in plant growth (Hetrick et al., 1996; Grace et al., 2009). However, positive responses can also be found when applying different experimental conditions or analyzing at different growth stages, which indicates that AM fungal inoculation under appropiated circumstances can be an effective agronomic practice also in these crops (Borie and Rubio, 1999; Seguel et al., 2016a,b, 2017).

Interestingly, a recent meta-analysis by Pellegrino et al. (2015) looking at wheat responses to AM symbiosis inoculation under field conditions found out that although straw biomass was weakly correlated with root AM fungal colonization rate, grain yield and P accumulation correlated positively. A review of the main mycorrhizal growth responses and P uptake from mycorrhizal and NM treatments in wheat (**Table 1A**) and barley (**Table 1B**) are presented below highlighting the idea that growth responses associated to AM symbiosis are not directly related to P acquisition. Growth depletions upon AM fungal colonization are normally attributed to an excess of photosynthates shared with the fungal partner, which are estimated to be up to 20% of the C fixed by the host plant (Jakobsen, 1995; Ortas et al., 2002; Li et al., 2005; Morgan et al., 2005). However, some studies indicated that growth depletion resulting from C drain to the fungal symbiont do not apply in all cases. Hetrick et al. (1992) and Grace et al. (2009) reported that growth reductions in wheat and barley did not vary when associated with two different AM fungal partners with contrasting capacity to colonize their roots (e.g., 61 and 5%, respectively), and therefore, hypothetically different C demand from the host plant (Hetrick et al., 1992). Even so, cereals benefits from AM symbiosis despite growth and/or nutritional benefits (such as net P uptake) are not apparent. Special techniques such as isotopic labeling are necessary to demonstrate symbiosis functioning (nutrient, water and carbohydrate exchange) in these cases (Smith et al., 2004, 2009; Grace et al., 2009).

Table 1A | Mycorrhizal growth responses (MGR) and P uptake on mycorrhizal (+AM) and non-colonized (–AM) wheat (*T. aestivum* L.) cultivars under greenhouse or field conditions and at different days after sowing (DAS).

Wheat cultivar	AM specie	MGR (%)	P uptake (mg/g)		Exp. conditions	Harvest (DAS)	Observation	References
			+AM	−AM				
TAM-105	*G. etunicatum*	22	5.20	4.63	Field	175		Al-Karaki et al., 2004
Steardy	*G. etunicatum*	19	5.43	4.67	Field	175		Al-Karaki et al., 2004
Tam-105	*G. mossae*	6	4.73	4.63	Field	175		Al-Karaki et al., 2004
Steardy	*G. mossae*	6	5.20	4.67	Field	70		Al-Karaki et al., 2004
Tormes	*G. mossae*	36	1.6	1.2	Pot	70		Azcón and Ocampo, 1981
Anza	*G. mossae*	27	1.3	0.9	Pot	70		Azcón and Ocampo, 1981
Negrillo	*G. mossae*	−2	0.7	0.8	Pot	70		Azcón and Ocampo, 1981
7 Cerros	*G. mossae*	107	1.5	0.8	Pot	70		Azcón and Ocampo, 1981
Bastion	*G. mossae*	35	1.3	1.1	Pot	70		Azcón and Ocampo, 1981
Pane 247	*G. mossae*	15	2.0	1.3	Pot	70		Azcón and Ocampo, 1981
Lozano	*G. mossae*	28	1.9	1.6	Pot	70		Azcón and Ocampo, 1981
Cocorit	*G. mossae*	87	1.3	1.0	Pot	70		Azcón and Ocampo, 1981
Champlein	*G. mossae*	4	0.9	0.9	Pot	70		Azcón and Ocampo, 1981
Castan	*G. mossae*	3	1.9	1.8	Pot	70		Azcón and Ocampo, 1981
Tajo	*G. mossae*	4	1.8	1.6	Pot	70		Azcón and Ocampo, 1981
Boulmiche	*G. mossae*	3	1.1	1.0	Pot	70		Azcón and Ocampo, 1981
Jupateco	*G. mossae*	0	1.5	1.2	Pot	70		Azcón and Ocampo, 1981
Neepawa	*G. intraradices*	−27	1.5	1.1	Pot	42		Goh et al., 1997
Neepawa	*G. intraradices*	−29	2.6	2.9	Pot	42	50 mg P/kg	Goh et al., 1997
Neepawa	*G. intraradices*	−11	3.8	4.1	Pot	42	100 mg P/kg P	Goh et al., 1997
Neepawa	*G. intraradices*	−24	5.0	6.1	Pot	42	300 mg P/kg	Goh et al., 1997
Newton	*G. etunicatum* + *G. mosseae* + *G. intraradices*	−27	2.7	0.8	Pot	98		Hetrick et al., 1996
Turkey	*G. etunicatum* + *G. mosseae* + *G. intraradices*	160	1.4	0.8	Pot	98		Hetrick et al., 1996
Lewjain	*G. intraradices*	−7	1.56	1.33	Field	Tillering		Mohammad et al., 1998
Lewjain	*G. intraradices*	10	1.17	1.06	Field	Anthesis		Mohammad et al., 1998
Lewjain	*G. intraradices*	19	0.82	0.70	Field	Harvest		Mohammad et al., 1998
Lewjain	*G. intraradices*	5	1.76	1.80	Field	Tillering	30 kg P/ha	Mohammad et al., 1998
Lewjain	*G. intraradices*	−4	1.26	1.28	Field	Anthesis	30 kg P/ha	Mohammad et al., 1998
Lewjain	*G. intraradices*	11	0.93	0.71	Field	Harvest	30 kg P/ha	Mohammad et al., 1998

(Continued)

Table 1A | Continued

Wheat cultivar	AM specie	MGR (%)	P uptake (mg/g)		Exp. conditions	Harvest (DAS)	Observation	References
			+AM	−AM				
Diamondbird	*G. intraradices*	8	1.8	1.5	Field	122		Ryan and Angus, 2003
Diamondbird	*G. intraradices*	−9	2.3	2.3	Field	122	20 kg P/ha	Ryan and Angus, 2003
Diamondbird	*Scutellospora calospora*	8	2.1	1.5	Field	122		Ryan and Angus, 2003
Diamondbird	*Scutellospora calospora*	−5	2.1	2.3	Field	122	20 kg P/ha	Ryan and Angus, 2003
HPW-89	*G. mosseae* (local)	15	2.69	2.42	Field	150		Suri et al., 2011
HPW-89	*G. intraradices*	14	2.78	2.42	Field	150		Suri et al., 2011
HPW-89	*G. mosseae* (IARI)	13	2.79	2.42	Field	150		Suri et al., 2011
HPW-89	*G. mosseae* (local)	94	3.14	2.42	Field	150	50% P2O5 based on STCR	Suri et al., 2011
HPW-89	*G. intraradices*	103	3.36	2.42	Field	150	50% P2O5 based on STCR	Suri et al., 2011
HPW-89	*G. mosseae* (IARI)	95	3.34	2.42	Field	150	50% P2O5 based on STCR	Suri et al., 2011
HPW-89	*G. mosseae* (local)	154	3.67	2.42	Field	150	75% P2O5 based on STCR	Suri et al., 2011
HPW-89	*G. intraradices*	153	3.82	2.42	Field	150	75% P2O5 based on STCR	Suri et al., 2011
HPW-89	*G. mosseae* (IARI)	151	3.65	2.42	Field	150	75% P2O5 based on STCR	Suri et al., 2011
Laura	*G. clarum*	−10	1.42	1.10	Pot	95	0 mg P/kg	Xavier and Germida, 1997
Laura	*G. clarum*	−19	2.16	2.77	Pot	95	5 mg P/kg	Xavier and Germida, 1997
Laura	*G. clarum*	12	2.76	2.22	Pot	95	10 mg P/kg	Xavier and Germida, 1997
Laura	*G. clarum*	−7	2.43	2.67	Pot	95	20 mg P/kg	Xavier and Germida, 1997
Neepawa	*G. clarum*	17	0.42	0.57	Pot	95	0 mg P/kg	Xavier and Germida, 1997
Neepawa	*G. clarum*	−8	0.68	0.55	Pot	95	5 mg P/kg	Xavier and Germida, 1997
Neepawa	*G. clarum*	4	1.03	1.07	Pot	95	10 mg P/kg	Xavier and Germida, 1997
Neepawa	*G. clarum*	12	1.00	1.72	Pot	95	20 mg P/kg	Xavier and Germida, 1997
81(85)	*G. versiforme*	3	1.03	0.77	Pot	56		Yao et al., 2001
Fengxiao 8	*G. versiforme*	39	0.98	0.70	Pot	56		Yao et al., 2001
NC37	*G. versiforme*	21	1.06	0.91	Pot	56		Yao et al., 2001
HD 2204	*G. fasciculatum*	78	1.10	1.02	Field	135		Khan and Zaidi, 2007
HD 2204	*G. fasciculatum*	146	1.15	1.02	Field	135	A. chrococum	Khan and Zaidi, 2007
HD 2204	*G. fasciculatum*	155	1.89	1.02	Field	135	Bacillus	Khan and Zaidi, 2007
HD 2204	*G. fasciculatum*	295	1.76	1.02	Field	135	A. chrococum + Bacillus	Khan and Zaidi, 2007
HD 2204	*G. fasciculatum*	178	1.56	1.02	Field	135	A. chrococum + P. variable	Khan and Zaidi, 2007
HD 2204	*G. fasciculatum*	193	1.57	1.02	Field	135	A. chrococum + Bacillus + P. variable	Khan and Zaidi, 2007
WH 283	*Glomus* sp. 88	15	0.17	0.18	Pot	55		Singh and Kapoor, 1999
WH 283	*Glomus* sp. 88	42	0.20	0.18	Pot	55	B. circulans	Singh and Kapoor, 1999

(Continued)

Table 1A | Continued

Wheat cultivar	AM specie	MGR (%)	P uptake (mg/g)		Exp. conditions	Harvest (DAS)	Observation	References
			+AM	−AM				
WH 283	*Glomus* sp. 88	51	0.20	0.18	Pot	55	C. herbarum	Singh and Kapoor, 1999
WH 283	*Glomus* sp. 88	97	0.19	0.18	Pot	55	B. circulans + C. herbarum	Singh and Kapoor, 1999
Star	*G. mosseae*	17	2.5	2.2	Pot	60	Bavendorf soil, 200 mg P/kg	Tarafdar and Marschner, 1994b
Star	*G. mosseae*	16	1.4	0.8	Pot	60	Bavendorf soil, 200 mg organicP/kg	Tarafdar and Marschner, 1994b
Star	*G. mosseae*	28	2.3	2.0	Pot	60	Niger soil, 200 mg P/kg	Tarafdar and Marschner, 1994b
Star	*G. mosseae*	22	1.5	0.7	Pot	60	Niger soil, 200 mg organicP/kg	Tarafdar and Marschner, 1994b
UP 2003	*G. fasciculatum*	6	2.63	0.42	Pot	80		Zaidi and Khan, 2005
UP 2003	*G. fasciculatum*	136	1.0	0.42	Pot	80	A. chroococum	Zaidi and Khan, 2005
UP 2003	*G. fasciculatum*	142	1.61	0.42	Pot	80	P. striata	Zaidi and Khan, 2005
UP 2003	*G. fasciculatum*	236	1.10	0.42	Pot	80	A. chroococum + P. striata	Zaidi and Khan, 2005
UP 2003	*G. fasciculatum*	108	1.31	0.42	Pot	80	A. chroococum + P. variable	Zaidi and Khan, 2005
UP 2003	*G. fasciculatum*	122	1.5	0.42	Pot	80	A. chroococum + P. variable + P. striata	Zaidi and Khan, 2005

Mycorrhizal Influence on PAE Traits of Wheat and Barley

Root Architecture and Surface Area

The root systems of grain cereals as wheat and barley consist of two types of roots. The first type is known as primary or seminal roots, and comprises between three to seven roots growing from the seedling. They have 0.2–0.4 mm diameter, occupying 5–10% of total root volume in mature plants. The second type is the secondary roots, also called nodal, crown, or adventitious roots. These roots emerge from nodes at the base of main stem and tillers 1–3 months after germination, having a larger diameter (0.3–0.7 mm) than primary roots (Hoad et al., 2001). Significant genetic variation for root architectural traits has been found among cereal cultivars (Kujira et al., 1994; Marschener, 1998). Interestingly, it was found out that the number of tillers positively correlated with root length density and grain yield of semidwarf bread wheat cultivars grown under P deficiency (Manske et al., 2000). In addition, Gahoonia et al. (1997) showed that the presence of root hairs increased the total root surface of winter wheat by 95–341% and by up to 112–245% for barley.

Perhaps the main mycorrhizal-associated mechanism enhancing plant PAE is the increase of explored soil volume by the AM fungal hyphae, which can extend plant access from millimeters to centimeters from root surface. Fungal hyphae can also access soil pores that root hairs cannot due to their smaller diameter (20–50 um) (**Figure 1B**). Moreover, AM roots can improve water and nutrients uptake efficiency compared to non-colonized roots due to a lower C cost per unit of hyphal surface related to the root surface (Jansa et al., 2003a; Jakobsen et al., 2005; Gregory, 2006; Schnepf et al., 2008).

There is a complex interplay between root architecture and AM fungi and, as expected, root traits can influence how plants respond to mycorrhizal colonization (Newsham et al., 1995; Smith and Read, 2008). It is suggested that species with root systems characterized by low root hair length and density, and roots with relatively large diameters would display the greatest growth benefits from the symbiosis (Brundrett, 2002; Fitter, 2004; Smith and Read, 2008), especially under P-limiting conditions. Several studies have corroborated this assumption by making this comparison between wild and agricultural species, reporting associations between root traits and MGR (Baon et al., 1994a; Declerck et al., 1995; Schweiger et al., 1995; Jakobsen et al., 2005). However, a recent meta-analysis carried out by Maherali (2014) does not support this hypothesis.

Usually, root system architecture is also frequently modified before and following the establishment AM symbiosis (Scannerini et al., 2001; Hodge et al., 2009), especially through some fungal exudates, known as Myc-factors (**Figure 1**; Maillet et al., 2011; Mukherjee and Ané, 2011). These signal molecules are exuded even in the absence of a host plant and are involved not only in symbiotic signaling stimulating colonization, but also acting as plant growth regulators by modifying root development

Table 1B | Mycorrhizal growth responses (MGR) and P uptake on mycorrhizal (+AM) and non-colonized (–AM) barley (*H. vulgare* L.) cultivars under greenhouse or field conditions and at different days after sowing (DAS).

Barley cultivar	AM specie	MGR (%)	P uptake (mg/g)		Exp. conditions	Harvest (days)	Observation	References
			+AM	−AM				
Vodka	*G. intraradices*	−4	0.28*	0.18*	Pot	80	0 mg P/kg	Plenchette and Morel, 1996
Vodka	*G. intraradices*	−12	0.29*	0.21*	Pot	80	20 mg P/kg	Plenchette and Morel, 1996
Vodka	*G. intraradices*	−8	0.32*	0.24*	Pot	80	30 mg P/kg	Plenchette and Morel, 1996
Vodka	*G. intraradices*	−7	0.37*	0.27*	Pot	80	40 mg P/kg	Plenchette and Morel, 1996
Vodka	*G. intraradices*	−11	0.48*	0.34*	Pot	80	50 mg P/kg	Plenchette and Morel, 1996
Vodka	*G. intraradices*	−6	0.45*	0.41*	Pot	80	60 mg P/kg	Plenchette and Morel, 1996
Vodka	*G. intraradices*	−8	0.44*	0.42*	Pot	80	70 mg P/kg	Plenchette and Morel, 1996
Vodka	*G. intraradices*	−7	1.06*	0.76*	Pot	80	110 mg P/kg	Plenchette and Morel, 1996
Vodka	*G. intraradices*	−3	1.65*	1.06*	Pot	80	160 mg P/kg	Plenchette and Morel, 1996
Vodka	*G. intraradices*	3	3.07*	2.92*	Pot	80	310 mg P/kg	Plenchette and Morel, 1996
cv. SLB-6	*G. mosseae*	14	2.33	1.29	Pot	45	120 spores/100g dry soil	Al-Karaki and Clark, 1999
cv. SLB-6	*G. mosseae*	39	2.77	1.29	Pot	45	240 spores/100g dry soil	Al-Karaki and Clark, 1999
cv. SLB-6	*G. mosseae*	27	2.17	1.29	Pot	45	360 spores/100g dry soil	Al-Karaki and Clark, 1999
Pallas P02	*G. claroideum* + *G. intraradices*	−17	1.32	1.32	Pot	28		Jakobsen et al., 2005
brb	*G. claroideum* + *G. intraradices*	46	1.75	1.45	Pot	28	root hairless mutant	Jakobsen et al., 2005
UC 566	*G. constrictus*	49	0.83	0.88	Pot	80		Jensen, 1982
UC 566	*G. fasciculatus* n.185	38	0.97	0.88	Pot	80		Jensen, 1982
UC 566	*G. fasciculatus* n. 0–1	45	1.00	0.88	Pot	80		Jensen, 1982
UC 566	*Gigaspora margarita*	−14	0.73	0.88	Pot	80		Jensen, 1982
Rupal	*G. fasciculatus* no. 0–1	2	2.82	2.79	Pot	102		Jensen, 1984
Rupal	*G. fasciculatus* no. 92	6	3.20	2.79	Pot	102		Jensen, 1984
Rupal	*G. epigaeus*	19	3.02	2.79	Pot	102		Jensen, 1984
Rupal	*Gigaspora margarita*	1	2.62	2.79	Pot	102		Jensen, 1984
Rupal	*G. mosseae CA*	0	2.98	2.79	Pot	102		Jensen, 1984
Rupal	*G. mosseae DK*	5	3.07	2.79	Pot	102		Jensen, 1984
Rupal	*G. mosseae GB*	7	3.23	2.79	Pot	102		Jensen, 1984
Rupal	*G. caledonius*	3	3.43	2.79	Pot	102		Jensen, 1984
Rupal	*G. macrocarpus* CA	13	3.12	2.79	Pot	102		Jensen, 1984
Rupal	*G. macrocarpus* DK	6	3.36	2.79	Pot	102		Jensen, 1984
Rupal	*G. etunicatus*	4	3.74	2.79	Pot	102		Jensen, 1984
Lofa Abed	*G. mosseae*	0	4.38	4.35	Pot	23	No sterilized	Khaliq and Sanders, 1998
Lofa Abed	*G. mosseae*	0	2.26	2.46	Pot	52	No sterilized	Khaliq and Sanders, 1998

(Continued)

Table 1B | Continued

Barley cultivar	AM specie	MGR (%)	P uptake (mg/g)		Exp. conditions	Harvest (days)	Observation	References
			+AM	−AM				
Lofa Abed	*G. mosseae*	−14	2.07	1.95	Pot	67	No sterilized	Khaliq and Sanders, 1998
Lofa Abed	*G. mosseae*	−15	1.96	1.81	Pot	91	No sterilized	Khaliq and Sanders, 1998
Lofa Abed	*G. mosseae*	−13	2.17	2.08	Pot	116	No sterilized	Khaliq and Sanders, 1998
Lofa Abed	*G. mosseae*	−5	4.72	5.21	Pot	23	Sterilized	Khaliq and Sanders, 1998
Lofa Abed	*G. mosseae*	−20	2.29	2.59	Pot	52	Sterilized	Khaliq and Sanders, 1998
Lofa Abed	*G. mosseae*	−24	2.57	2.04	Pot	67	Sterilized	Khaliq and Sanders, 1998
Lofa Abed	*G. mosseae*	−23	2.33	1.64	Pot	91	Sterilized	Khaliq and Sanders, 1998
Lofa Abed	*G. mosseae*	−26	2.3	1.57	Pot	116	Sterilized	Khaliq and Sanders, 1998
Lofa Abed	*G. mosseae*	−3	0.17	0.16	Field	124	Sterilized 0 kg P/ha	Khaliq and Sanders, 2000
Lofa Abed	*G. mosseae*	−2	0.2	0.18	Field	124	Sterilized 100 kg P/ha	Khaliq and Sanders, 2000
Lofa Abed	*G. mosseae*	−2	0.13	0.12	Field	124	No sterilized 0 kg P/ha	Khaliq and Sanders, 2000
Lofa Abed	*G. mosseae*	−2	0.14	0.14	Field	124	No sterilized 100 kg P/ha	Khaliq and Sanders, 2000
ACSAD 6	Mix	37	2.27	1.97	Pot	35	Soil A	Mohammad et al., 2003
ACSAD 6	Mix	87	2.54	1.97	Pot	35	Soil A + 25 mg P/kg	Mohammad et al., 2003
ACSAD 6	*G. intraradices*	40	2.07	1.97	Pot	35	Soil A	Mohammad et al., 2003
ACSAD 6	Mix	28	2.76	2.29	Pot	35	Soil B	Mohammad et al., 2003
ACSAD 6	Mix	4	2.69	2.29	Pot	35	Soil B + 25 mg P/kg	Mohammad et al., 2003
ACSAD 6	*G. intraradices*	14	2.42	2.29	Pot	35	Soil B	Mohammad et al., 2003
ACSAD 6	Mix	22	2.63	1.80	Pot	35	Soil C	Mohammad et al., 2003
ACSAD 6	Mix	20	2.78	1.80	Pot	35	Soil C + 25 mg P/kg	Mohammad et al., 2003
ACSAD 6	*G. intraradices*	5	2.22	1.80	Pot	35	Soil C	Mohammad et al., 2003
Galleon	*G. intraradices*	−15	1.96	1.98	Pot	48	Soil temperature 10°C	Baon et al., 1994b
Galleon	*G. intraradices*	−26	2.45	2.3	Pot	48	Soil temperature 15°C	Baon et al., 1994b
Galleon	*G. intraradices*	−5	2.39	2.19	Pot	48	Soil temperature 20°C	Baon et al., 1994b

**Phosphorus concentration on grain.*

in some plant species (Maillet et al., 2011; Mukherjee and Ané, 2011). The formation of lateral roots has been found to be the most affected trait, making roots progressively more branched, probably to increase the number of suitable sites for colonization (Harrison, 2005). However, mycorrhizal-induced modifications on root traits are still poorly understood and seem to vary

according to specific plant-fungal combinations, (Schellenbaum et al., 1991; Berta et al., 2005; Fusconi, 2014). In the case of wheat and barley, evidences are controversial as well. Behl et al. (2003) found a significant increase of total root length in wheat colonized by *G. fasciculatum*, being up to 90% higher than control plants when co-inoculated with *Azotobacter*. The same pattern was found by Al-Karaki and Al-Raddad (1997), who studied the response of two durum wheat genotypes to AM colonization, detecting an increase of 25 and 20% in root length. On the other hand, AM fungal inoculation decreased wheat root length and surface area under high rates of P application in a calcareous soil (Mohammad and Malkawi, 2004).

Organic Acid Anion and Phosphatase Exudation

It has been suggested that AM fungi may have biochemical and physiological capacities to increase plant PAE through the uptake of P from sparingly available forms in soil, being the exudation of protons, phosphatases and LMWOAAs the suggested mechanisms involved in these processes (**Figure 1**; Tarafdar and Marschner, 1994a; Koide and Kabir, 2000; Klugh and Cumming, 2007).

AM fungi possess many genes encoding acid phosphatases (EC 3.1.3.2, ACP) in their genomes, with at least seven genes expressed in *Rhizophagus clarus* (Sato et al., 2015). However, exudation of phosphatases was mostly associated with the cell wall (Olsson et al., 2002) and their presence in the rhizosphere has been demonstrated only in limited cases (Tarafdar and Marschner, 1994a; Koide and Kabir, 2000). The magnitude of these processes is questioned as it is difficult to isolate the effects of plants, fungi and others microorganisms present in the experiments under unsterile conditions (Joner and Jakobsen, 1995; Joner et al., 2000). However, Sato et al. (2015) in an experiment with separated compartments for hyphal growth, collected exudates from soil solution, sand culture and *in vitro* monoxenic culture, providing strong evidence that the corresponding acid phosphatase activity was originated from *R. clarus*. Little information is available about the relationship between AM symbiosis and changes in enzymatic exudation and activity patterns in wheat and barley. Rubio et al. (1990) found out a positive correlation between wheat colonization by AM fungi and acid phosphatase activity in roots and soil, mainly under P-limiting conditions. Using a different experimental approach with separated compartments for hyphal growth, Tarafdar and Marschner (1994a,b) observed depletion in organic P content with a concomitant increase of phosphatase activity when wheat was colonized by *Glomus mosseae* (Nicol & Gerd) Gerd & Trappe. The same trend was found for barley in a 10 years' field trial where P-deprived plants presented higher colonization by AM fungi and higher phosphatase activity than fertilized treatments (Goicoechea et al., 2004). In this sense, Ye et al. (2018) in a recent report show the importance of phosphatase activity in P acquisition by non-AM colonized barley efficient genotypes through direct changes of rhizosphere P fractions. Nevertheless, the interaction of AM association with the phosphatase activity and the subsequent P acquisition by efficient genotypes is still unclear.

The phosphate-solubilizing activities of AM fungi are still controversial although AM plants have generally been shown to increase the uptake of insoluble Pi (Yao et al., 2001; Tawaraya et al., 2006; Klugh-Stewart and Cumming, 2009). In many studies, mycorrhizal inoculants proved to alter the composition and/or amount of total LMWOAAs exuded by *Liriodendron tulipifera* and *Andropogon virginicus*, respectively (**Figure 1**; Klugh and Cumming, 2007; Klugh-Stewart and Cumming, 2009). However, direct evidence for solubilization of P by AM fungi has not been obtained so far. Despite that AM fungi might not exude LMWOAAs by themselves, they can, however, improve P solubilization and/or mineralization indirectly by stimulating the surrounding soil microbes via the exudation of labile C, thus increasing local nutrient availability in the hyphosphere and in soil patches beyond the root hairs (Hodge et al., 2010; Cheng et al., 2012; Jansa et al., 2013). Recently, Kaiser et al. (2015) using nanoscale secondary ion mass spectrometry imaging and ^{13}C-phospho and neutral lipid fatty acids, traced the flow of recently photoassimilated C and found out that a significant and exclusive proportion of photosynthates was delivered through AM pathway and used by different microbial groups compared to C directly released by the roots.

The interaction between phosphate-solubilizing microorganisms with AM wheat and barley plants has been assessed by some researchers, with positive responses on growth and P uptake. Omar (1998) observed that the interaction between *Funneliformis constrictum* and the rock-phosphate-solubilizing *Aspergillus niger* and *Penicillium citrinum* fungi significantly increased biomass production of wheat plants under all experimental conditions tested. The effect was more evident in non-sterilized conditions. Bacteria from the *Azotobacter* and *Pseudomonas* genera also improved AM wheat growth under field and pot conditions, with positive correlation between AM colonization and *Azotobacter* survival in the rhizosphere (Kucey, 1987; Behl et al., 2003; Zaidi and Khan, 2005; Yousefi et al., 2011). Singh and Kapoor (1999) analyzed the effect of *Bacillus circulans*, *Cladosporium herbarum* and an isolated AM fungus in wheat where larger populations of phosphate-solubilizing microorganisms in the rhizosphere of mycorrhizal roots and an enhanced P acquisition in combined inoculation were found. Similarly, the inoculation with *Penicillium variable* alone negatively affected the biomass production of wheat. However, when applied in combination with *Azotobacter chroococcum*, *Pseudomonas striata* and the AM fungus *G. fasciculatum*, grain yield significantly increased compared with the other treatments (Zaidi and Khan, 2005).

In another study, wheat grain yield was enhanced by 92.8% in the presence of the rhizobacteria *Pseudomonas fluorescens* and *Burkholderia cepacia* and the AM fungus *Claroideoglomus etunicatum* (Saxena et al., 2013). The synergistic effect of combined inoculation with plant growth-promoting rhizobacteria and AM fungi on wheat was also proved to be effective under field conditions. It was shown that the combination of *A. chroococcum* and *Bacillus sp.* with *G. fasciculatum* significantly increased the dry matter by 2.6-fold and grain yield by 2-fold when compared to the control (Khan and Zaidi, 2007). In another field study, Mehrvarz et al. (2008)

found that although bacterial inoculation alone achievied the maximum biological yield, its application combined with AM fungi produced grains with higher weight.

Changes in P Transporters

In general, AM plants have two different pathways for P uptake from the soil (**Figure 1C**) with different P transporters involved in both of them. The direct P uptake is the plant endogenous pathway, which occurs via root epidermis and root hairs, while in the AM pathway the external hyphae is the responsible for acquiring P from the medium and transport to intracellular symbiotic interfaces where it finally goes to the plant (Grace et al., 2009; Smith et al., 2011). According to their function, plant transporters involved in the direct pathway are expressed mostly in the root apex and root hairs (Gordon-Weeks et al., 2003) and down-regulated in more mature regions. However, up-regulation of genes encoding phosphate transporters proved to have little influence on P acquisition. Rae et al. (2004) studying transgenic barley plants over-expressing a gene encoding for a phosphate transporter found no improvement on P uptake under any of the tested conditions, suggesting that post-transcriptional mechanisms could be involved affecting the activity of these transporters. AM transporters are less known due to their obligate biotrophic nature, coupled with the fact that they are multinuclear and heterocaryotic organisms (Sanders, 1999), which make the use of traditional genetic approaches difficult (Maldonado-Mendoza et al., 2001). These authors observed that the expression of a phosphate transporter gene from the extra-radical mycelium of *Rhizofagus intraradices* was regulated in response to P concentrations in the environment surrounding the extra-radical hyphae and that it was modulated by the overall phosphate status of the AM fungus rather than the host plant (Maldonado-Mendoza et al., 2001). Another important aspect of the AM pathway is the presence of AM-inducible plant P transporters, which are generally present at much higher levels in AM roots than other P transporters (Javot et al., 2007). These transporters are responsible for the exchange of P between the fungal hyphae and plant cell. They have been found in all AM plants investigated, regardless their growth response to colonization, and are mainly expressed in the colonized cortical cells, specifically in the arbusculated cells which is the place where the nutrient exchange takes place (Bucher, 2007; Javot et al., 2007). Genes encoding for AM-inducible transporters have been described in cereals and include the HvPHT1.11 and HvPHT1.8 for barley and TaPHT1.8, TaPHT1.11, TaPHT1.12, and TaPHT1.14 for wheat (Teng et al., 2017).

The two P pathways were believed to be additive in their contribution to plant nutrient uptake, and it was assumed that direct pathway made a constant contribution to the total P uptake, while the AM pathway participated as an extra contribution in plants with positive growth responses (Pearson and Jakobsen, 1993). However, further investigations proved that AM colonization could reduce the direct uptake pathway in some species (even in plants that respond positively to the symbiosis as in *Medicago truncatula*), and deactivate completely in others (Liu et al., 1998; Smith et al., 2004). Therefore, in order to not become P deficient AM pathway should compensate the reduced contribution of direct pathway (Smith et al., 2011). Recent studies using radioactive P isotopes has shown that AM pathway contributed significantly to total P uptake on wheat and barley. In this sense, Smith et al. (2015) clearly demonstrated that indigenous AM fungi contribute to wheat P uptake in 6.5–21% of total plant P in field conditions and 3–40% when grown in pots. However, mycorrhizal wheat plants acquired less P and produced less biomass when compared to their non-mycorrhizal counterpart (Li et al., 2006; Grace et al., 2009). It was suggested that negative growth responses could be generated by suppression of the direct pathway in these species, especially in the plants with very low colonization. Conversely, Grace et al. (2009) found out that the magnitude of the negative responses of barley was independent of contrasting colonization by two AM fungal species (*R. intraradices* and *F. geosporum*). In addition, the expression of P transporters belonging to direct pathway in barley was not affected by the symbiosis as expected. Again, this indicated that possible post-translational modifications of regulatory components could be involved in the plant response.

AM FUNCTIONAL DIVERSITY

It is a general consensus that there is little specificity between AM fungal and host plant species, and that AM plants can be colonized by several AM fungal species at the same time (Merryweather and Fitter, 1998; Jansa et al., 2003b; Smith et al., 2011). However, the existence of different colonization patterns could imply certain preferences for specific AM fungal species, functional groups or the co-evolution strategies between specific plant-fungus associations (Smith et al., 2009; Chagnon et al., 2013; López-García et al., 2017). For instance, Mao et al. (2014) showed that these preferences can exist even across wheat cultivars as they found a variation in AM fungal community composition, displaying a complex pattern of cultivar-AM fungal interaction under experimental field conditions. Despite of the projection of this work, the study of the AM fungal diversity associated to wheat and barley is overall scarce. Considering the wide distribution and economic importance of these two species, only 131 and five AM fungal sequences in MaarjAM database, the most complete sequence database of Glomeromycota (Öpik et al., 2010), are associated to wheat (*Triticum* sp.) and barley (*Hordeum* sp.) respectively, out of 5,296 sequences belonging to Poaceae in the database. The few studies covering molecular diversity in roots of wheat have shown differences between in community composition associated to wheat and N-fixing crops (Bainard et al., 2014; Higo et al., 2016). Communities associated to wheat have also been found to vary during the growing season and depend on P fluxes and degree of fertilization (Wu et al., 2011; Bainard et al., 2014; Qin et al., 2015). The diversity of AM fungal communities associated directly with roots of wheat is overall high, including members of different taxonomic families (e.g., Manoharan et al., 2017), but being predominatly associated with *Funneliformis* spp., in conventional cropping, and *Claroideoglomus* spp., in organically managed systems (Dai et al., 2014). In agreement, with this result, one of the few studies analyzing AM fungi in roots if barley, found that the abundance

of *Funneliformis* spp. were associated with high levels of P in soil, meanwhile *Claroideoglomus* spp. with lower levels of P (Cruz-Paredes et al., 2017), but harboring a high phylogenetic diversity as well (Manoharan et al., 2017). N fertilization has been seen another affecting AM fungal community composition in barley and interacting with the plant-fungus P trade, as tends to decrease the efficiency in the interexchange (Williams et al., 2017).

The lack of information on molecular diversity has been in some manner compensated with morphological studies of spore communities. In this context, a high taxonomic diversity has been found. Aguilera et al. (2014, 2017) analyzing spore morphology on acidic soils under continuous wheat cropping, found 24 AM fungal species, being *Acaulospora* and *Scutellospora* the dominant genera. In another study under similar conditions in acidic soils, Castillo et al. (2016b) described 26 fungal species with a prevalence of *Acaulospora* and *Claroideoglomus*. This dominance of *Acaulospora* spores in soils cropped with wheat was also observed by Hu et al. (2015) in North China and by Nadji et al. (2017) in Algeria, however in the last study Glomeraceae species was also detected as highly abundant.

The mycorrhizal growth response of a single host plant species can differ across AM fungal species, and in the same way, colonization by the same AM fungal isolated can result in different growth responses in different plant species or genotypes (Feddermann et al., 2010; Smith et al., 2011; Castillo et al., 2016a). Indeed, previous studies have demonstrated a high variability in the symbiotic response of different combinations of host plant and AM fungi (e.g., Smith et al., 2004; Avio et al., 2006; Jansa et al., 2008). Variations in MGR have also been revealed across wheat cultivars, which can range from −2% to 107% in different genotypes (Azcón and Ocampo, 1981). On the other hand, Graham and Abbott (2000) showed a huge variation in MGR when testing several AM fungal isolates in symbiosis with wheat, being *Scutellospora calospora* the only one promoting higher plant biomass. In a study in wheat showed that MGR by different AM fungal species and their combination or with *F. mosseae* alone resulted in negative growth responses, while positive responses were reported when inoculated with *R. clarum* (Talukdar and Germida, 1994). This variability in mycorrhizal response comes from the fact that AM fungi are functionally diverse both inter- and intraspecifically (see for example Koch et al., 2004, 2017; Antunes et al., 2011). Differences among AM fungal species have been suggested to exist in the colonization rates in roots and soils depending on the AM fungal colonization pattern (Hart and Reader, 2002; Powell et al., 2009). Perhaps, although morphological traits seem to be well-conserved across AM fungal phylogeny, i.e. morphological traits into the same species and related clades are similar, most of variation in plant growth promotion and P uptake occurs indeed intraspecifically (Munkvold et al., 2004; Koch et al., 2017). In general, it had been assumed that morphological traits, such as the hyphal lenght in soil, could be good predictors of P uptake. However, the above mentioned results on huge variabilities in plant P uptake on morphological and phylogenetically similar fungal isolates redirects the question toward which fungal functional trait have to be measured to understand soil-plant P dynamics in agricultural systems. Therefore, functional diversity among AM fungal species and genotypes need to be considered.

FUTURE PERSPECTIVES

Despite displaying negative responses in some studies and being considered as non-responsive by many authors, wheat and barley plants presented positive growth and P responses by performing AM symbiosis (**Tables 1A,B** respectively). There could be factors involved in this large PAE variation and the processes affecting both AM function and its benefits are still unknown. The question is complex due to the many factors are involved: plant genotype and fungal functional diversity, as well as their mutual compatibility, soil variable conditions or agricultural management needs to be studied. Indeed, the fact is that a major part of the research carried out in the interaction between crop cereals and AM fungi has only involved a handful of AM fungal isolates. In addition, there is little information available regarding the effect of different -or combined- AM fungal taxa colonization and different genotypes of wheat and barley on root morphology, development, exudation pattern, interaction with PGPR and/or P-solubilizing fungi, and the interplay between the two pathways of P uptake.

It is widely accepted that AM plants access to poorly available sources more effectively than non-colonized plants, but the mechanisms by which they are operating at field are not well understood (Smith et al., 2015). Studies using more than one crop cultivar and multiple AM species and genotypes should be carried out in order to analyze the effect of fungal diversity on PAE related traits as root length, root hair angles, changes on root-mycorrhiza exudation patterns and degree of inhibition (or not) of plant P transporters. In addition, these studies should be traced along different stages of development, until grain production, as it was found that although mycorrhization could hamper biomass production, it enhanced P acquisition and final grain production (Pellegrino et al., 2015). Isotopic, spectroscopic and molecular techniques coupled to new experimental designs could help identify some of the mechanisms mentioned above and the genetic background behind the different responses. In this sense, we suggest an inclusion of the Carbon costs related to all P acquisition traits (not only root architeture), specially those involved and altered by mycorrhizal colonization, in order to support accurate phenotyping for breeding programs focused on lowering P fertilizer inputs (**Figure 2**).

AUTHOR CONTRIBUTIONS

PCa wrote the manuscript. FB was the main advisor and revisor of the document. PCo contributed on wheat and barley agronomical aspects and microorganisms effects on PAE. AS contributed to the construction of the document and the figures, and on all features related to phosphorus. JL-R provided insights on mycorrhizal signaling and the physiological effects upon colonization. AL-G also contributed on mycorrhizal aspects, highlighting the importance of functional diversity.

ACKNOWLEDGMENTS

We fully acknowledge the financial support of the FONDECYT 11160385 (AS) and FONDECYT 1170264 (PCo) grants from Comisión Nacional de Investigación Científica y Tecnológica (CONICYT-Chile) and the support granted by CONICYT scholarship 21161474 (PCa). JL-R is supported by the grant AGL2015-64990-C2-1R (MINECO-Spain). AL-G is supported by the grant 708530–DISPMIC (European Union's Horizon 2020 Marie Curie Individual Fellowship).

REFERENCES

Abel, S., Ticconi, C. A., and Delatorre, C. A. (2002). Phosphate sensing in higher plants. *Physiol. Plant*. 115, 1–8. doi: 10.1034/j.1399-3054.2002.1150101.x

Aguilera, P., Cornejo, P., Borie, F., Barea, J. M., von Baer, E., and Oehl, F. (2014). Diversity of arbuscular mycorrhizal fungi associated with *Triticum aestivum* L. plants growing in an Andosol with high aluminum level. *Agric. Ecosyst. Environ*. 186, 178–184. doi: 10.1016/j.agee.2014.01.029

Aguilera, P., Marín, C., Oehl, F., Godoy, R., Borie, F., and Cornejo, P. (2017). Selection of aluminum tolerant cereal genotypes strongly influences the arbuscular mycorrhizal fungal communities in an acidic Andosol. *Agric. Ecosyst. Environ.* 246, 86–93. doi: 10.1016/j.agee.2017.05.031

Akiyama, K., Matsuzaki, K., and Hayashi, H. (2005). Plant sesquiterpenes induce hyphal branching in arbuscular mycorrhizal fungi. *Nature* 435, 824–827. doi: 10.1038/nature03608

Al-Karaki, G., and Al-Raddad, A. (1997). Effects of arbuscular mycorrhizal fungi and drought stress on growth and nutrient uptake of two wheat genotypes differing in drought resistance. *Mycorrhiza* 7, 83–88. doi: 10.1007/s005720050166

Al-Karaki, G., McMichael, B., and Zak, J. (2004). Field response of wheat to arbuscular mycorrhizal fungi and drought stress. *Mycorrhiza* 14, 263–269. doi: 10.1007/s00572-003-0265-2

Al-Karaki, G. N., and Clark, R. B. (1999). Varied rates of mycorrhizal inoculum on growth and nutrient acquisition by barley grown with drought stress. *J. Plant Nutr.* 22, 1775–1784. doi: 10.1080/01904169909365753

Antunes, P. M., Koch, A. M., Morton, J. B., Rillig, M. C., and Klironomos, J. N. (2011). Evidence for functional divergence in arbuscular mycorrhizal fungi from contrasting climatic origins. *New Phytol.* 189, 507–514. doi: 10.1111/j.1469-8137.2010.03480.x

Armada, E., López-Castillo, O., Roldán, A., and Azcón, R. (2016). Potential of mycorrhizal inocula to improve growth, nutrition and enzymatic activities in Retama sphaerocarpa compared with chemical fertilization under drought conditions. *J. Soil Sci. Plant Nutr*. 16, 380–399. doi: 10.4067/S0718-95162016005000035

Avio, L., Pellegrino, E., Bonari, E., and Giovannetti, M. (2006). Functional diversity of arbuscular mycorrhizal fungal isolates in relation to extraradical mycelial networks. *New Phytol.* 172, 347–357. doi: 10.1111/j.1469-8137.2006.01839.x

Awika, J. M. (2011). "Major cereal grains production and use around the world," in Advances in Cereal Science: Implications to Food Processing and Health Promotion, J. M. Awika, V. Piironen, and S. Bean (Washington, DC: ACS Symposium Series), 2–13,

Azcón, R., and Ocampo, J. A. (1981). Factors affecting the vesicular-arbuscular infection and mycorrhizal dependency of thirteen wheat cultivars. *New Phytol.* 87, 677–685. doi: 10.1111/j.1469-8137.1981.tb01702.x

Bainard, L. D., Bainard, J. D., Hamel, C., and Gan, Y. (2014). Spatial and temporal structuring of arbuscular mycorrhizal communities is differentially influenced by abiotic factors and host crop in a semi-arid prairie agroecosystem. *FEMS Microbiol. Ecol.* 88, 333–344. doi: 10.1111/1574-6941.12300

Bais, H. P., Weir, T. L., Perry, L. G., Gilroy, S., and Vivanco, J. M. (2006). The role of root exudates in rhizosphere interactions with plants and other organisms. *Annu. Rev. Plant Biol.* 57, 233–266. doi: 10.1146/annurev.arplant.57.032905.105159

Baon, J. B., Smith, S. E., and Alston, A. M. (1994a). Growth response and phosphorus uptake of rye with long and short root hairs: interactions with mycorrhizal infection. *Plant Soil* 167, 247–254. doi: 10.1007/BF00007951

Baon, J. B., Smith, S. E., and Alston, A. M. (1994b). Phosphorus uptake and growth of barley as affected by soil temperature and mycorrhizal infection. *J. Plant Nutr.* 17, 479–492. doi: 10.1080/01904169409364742

Bauer, A., Frank, A. B., and Black, A. L. (1987). Aerial parts of hard red spring Wheat. II. Nitrogen and phosphorus concentration and content by plant development stage 1. *Agron. J.* 79, 852–858. doi: 10.2134/agronj1987.00021962007900050020x

Behl, R. K., Sharman, H., Kumar, V., and Narula, N. (2003). Interactions amongst Mycorrhiza, *Azotobacter chroococcum* and root characteristics of wheat varieties. *J. Agron. Crop Sci*. 189, 151–155. doi: 10.1046/j.1439-037X.2003.00026.x

Berta, G., Sampò, S., Gamalero, E., Massa, N., and Lemanceau, P. (2005). Suppression of Rhizoctonia root-rot of tomato by *Glomus mosseae* BEG12 and *Pseudomonas fluorescens* A6RI is associated with their effect on the pathogen growth and on the root morphogenesis. *Eur. J. Plant Pathol*. 111, 279–288. doi: 10.1007/s10658-004-4585-7

Besserer, A., Puech-Pagès, V., Kiefer, P., Gomez-Roldan, V., Jauneau, A., Roy, S., et al. (2006). Strigolactones stimulate arbuscular mycorrhizal fungi by activating mitochondria. *PLoS Biol.* 4:e226. doi: 10.1371/journal.pbio.0040226

Bhardwaj, D., Ansari, M. W., Sahoo, R. K., and Tuteja, N. (2014). Biofertilizers function as key player in sustainable agriculture by improving soil fertility, plant tolerance and crop productivity. *Microb Cell Facts*. 13, 66–77. doi: 10.1186/1475-2859-13-66

Bolan, N. S., Naidu, R., Mahimairaja, S., and Baskaran, S. (1994). Influence of low-molecular-weight organic-acids on the solubilization of phosphates. *Biol. Fert. Soils* 18, 311–319. doi: 10.1007/BF00570634

Bonfante, P., and Genre, A. (2008). Plants and arbuscular mycorrhizal fungi: an evolutionary-developmental perspective. *Trends Plant Sci.* 13, 492–498. doi: 10.1016/j.tplants.2008.07.001.

Borie, F., and Rubio, R. (1999). Effects of arbuscular mycorrhizae and liming on growth and mineral acquisition of aluminum tolerant and aluminum sensitive barley cultivars. *J. Plant Nutr.* 22, 121–137. doi: 10.1080/01904169909365612.

Borie, F., Zunino, H., and Martinez, L. (1989). Macromolecule-p associations and inositol phosphates in some chilean volcanic soils of temperate regions. *Commun. Soil Sci. Plant Anal.* 20, 1881–1894. doi: 10.1080/00103628909368190.

Bovill, W. D., Huang, C. Y., and McDonald, G. K. (2013). Genetic approaches to enhancing phosphorus-use efficiency (PUE) in crops: challenges and directions. *Crop Pasture Sci.* 64, 179–198. doi: 10.1071/CP13135

Brundrett, M. C. (2002). Coevolution of roots and mycorrhizas of land plants. *New Phytol.* 154, 275–304. doi: 10.1046/j.1469-8137.2002.00397.x

Brundrett, M. C. (2009). Mycorrhizal associations and other means of nutrition of vascular plants: understanding the global diversity of host plants by resolving conflicting information and developing reliable means of diagnosis. *Plant Soil* 320, 37–77. doi: 10.1007/s11104-008-9877-9

Bucher, M. (2007). Functional biology of plant phosphate uptake at root and mycorrhiza interfaces. *New Phytol.* 173, 11–26. doi: 10.1111/j.1469-8137.2006.01935.x

Bucher, M., Rausch, C., and Daram, P. (2001). Molecular and biochemical mechanisms of phosphate uptake into plants. *J. Plant Nutr. Soil Sci.* 164:209–221. doi: 10.1002/1522-2624(200104)164:<209::AID-JPLN209>3.0.CO;2-F

Bücking, H., and Shachar-Hill, Y. (2005). Phosphate uptake, transport and transfer by the arbuscular mycorrhizal fungus *Glomus intraradices* is stimulated by increased carbohydrate availability. *New Phytol.* 165, 899–911. doi: 10.1111/j.1469-8137.2004.01274.x

Bünemann, E. K., Keller, B., Hoop, D., Jud, K., Boivin, P., and Frossard, E. (2013). Increased availability of phosphorus after drying and rewetting of a grassland soil: processes and plant use. *Plant Soil* 370, 511–526. doi: 10.1007/s11104-013-1651-y

Burkitt, L. L., Small, D. R., McDonald, J. W., Wales, W. J., and Jenkin, M. L. (2007). Comparing irrigated, biodynamic and conventionally managed dairy

farms. 1. Soil and pasture properties. *Aust. J. Experim. Agric.* 47, 479–488. doi: 10.1071/EA05196

Castillo, C. G., Borie, F., Oehl, F., and Sieverding, E. (2016a). Arbuscular mycorrhizal fungi biodiversity: prospecting in Southern-Central zone of Chile. A review. *J. Soil Sci. Plant Nutr.* 16, 400–422. doi: 10.4067/S0718-95162016005000036

Castillo, C. G., Oehl, F., and Sieverding, E. (2016b). Arbuscular mycorrhizal fungal diversity in wheat agro-ecosystems in Southern Chile and effects of seed treatment with natural products. *J. Soil Sci. Plant Nutr.* 16, 967–978. doi: 10.4067/S0718-95162016005000069

Celi, L., and Barberis, E. (2005). "Abiotic stabilization of organic phosphorus in the environment," in *Organic Phosphorus in the Environment,* eds B. L. Turner, E. Frossard, and D. Baldwin (Wallingford:CABI Publishing) 113–132.

Chagnon, P. L., Bradley, R. L., Maherali, H., and Klironomos, J. N. (2013). A trait-based framework to understand life history of mycorrhizal fungi. *Trends Plant Sci.* 18, 484–491. doi: 10.1016/j.tplants.2013.05.001

Chen, C. R., Condron, L. M., Davis, M. R., and Sherlock, R. R. (2002). Phosphorus dynamics in the rhizosphere of perennial ryegrass (*Lolium perenne* L.) and radiata pine (*Pinus radiata* D.Don). *Soil Biol. Biochem.* 34,487–499. doi: 10.1016/s0038-0717(01)00207-3

Cheng, L., Booker, F., Tu, C., Burkey, K. O., Zhou, L., Shew, H. D., et al. (2012). Arbuscular mycorrhizal fungi increase organic carbon decomposition under elevated CO_2. *Science* 2, 1084–1087. doi: 10.1126/science.1224304

Cordell, D., Drangert, J. O., and White, S. (2009). The story of phosphorus: global food security and food for thought. *Glob. Environ. Change* 19, 292–305. doi: 10.1016/j.gloenvcha.2008.10.009

Cruz-Paredes, C., López-García, Á., Rubæk, G. H., Hovmand, M. F., Sørensen, P., and Kjøller, R. (2017). Risk assessment of replacing conventional P fertilizers with biomass ash: residual effects on plant yield, nutrition, cadmium accumulation and mycorrhizal status. *Sci. Total Environ.* 575, 1168–1176. doi: 10.1016/j.scitotenv.2016.09.194

Dai, M., Hamel, C., Bainard, L. D., Arnaud, M. S., Grant, C. A., Lupwayi, N. Z., et al. (2014). Negative and positive contributions of arbuscular mycorrhizal fungal taxa to wheat production and nutrient uptake efficiency in organic and conventional systems in the Canadian prairie. *Soil Biol. Biochem.* 74, 156–166. doi: 10.1016/j.soilbio.2014.03.016

Davison, J., Moora, M., Öpik, M., Adholeya, A., Ainsaar, L., Bâ, A., et al. (2015). Global assessment of arbuscular mycorrhizal fungus diversity reveals very low endemism. *Nature* 349, 970–973. doi: 10.1126/science.aab1161

Declerck, S., Plenchette, C., and Strullu, D. G. (1995). Mycorrhizal dependency of banana (*Musa acuminata*, AAA group) cultivar. *Plant Soil* 176, 183–187. doi: 10.1007/BF00017688

Delgado, M., Zúñiga-Feest, A., Alvear, M., and Borie, F. (2013). The effect of phosphorus on cluster-root formation and functioning of *Embothrium coccineum* (R. et J. Forst.). *Plant Soil* 373, 765–773. doi: 10.1007/s11104-013-1829-3

do Nascimento, C. A., Pagliari, P. H., Schmitt, D., He, Z., and Waldrip, H. (2016). Phosphorus concentrations in sequentially fractionated soil samples as affected by digestion methods. *Sci. Rep.* 5:17967. doi: 10.1038/srep17967

El Rabey, H. A., Alshubaily, F., and Al-Otaibi, K. M. (2015). Phylogenetic relationships of some economically important cereal plants based on genome characterization using molecular markers. *Caryologia* 68, 225–232. doi: 10.1080/00087114.2015.1032612

FAO (2012). *World Agriculture: Towards 2030/2050. The 2012 Revision.* Available online at: http://www.fao.org/docrep/016/ap106e/ap106e.pdf (Accessed Jun 01, 2016).

FAO (2013). *World Agriculture Statistics.* Available online at: http://faostat3.fao.org/home/E (Accessed: June 01, 2016).

Feddermann, N., Finlay, R., Boller, T., and Elfstrand, M. (2010). Functional diversity in arbuscular mycorrhiza–the role of gene expression, phosphorous nutrition and symbiotic efficiency. *Fungal Ecol.* 3, 1–8. doi: 10.1016/j.funeco.2009.07.003

Fitter, A. H. (2004). Magnolioid roots–hairs, architecture and mycorrhizal dependency. *New Phytol.* 164, 15–16. doi: 10.1111/j.1469-8137.2004.01193.x

Fusconi, A. (2014). Regulation of root morphogenesis in arbuscular mycorrhizae: what role do fungal exudates, phosphate, sugars and hormones play in lateral root formation? *Ann. Bot-London* 113, 19–33. doi: 10.1093/aob/mct258

Gahoonia, T. S., Care, D., and Nielsen, N. E. (1997). Root hairs and phosphorus acquisition of wheat and barley cultivars. *Plant Soil* 191, 181–188. doi: 10.1023/A:1004270201418

Gahoonia, T. S., Claassen, N., and Jungk, A. (1992). Mobilization of phosphate in different soils by ryegrass supplied with ammonium or nitrate. *Plant Soil* 140, 241–248. doi: 10.1007/BF00010600

Gahoonia, T. S., and Nielsen, N. E. (1992). The effect of root induced pH changes on the depletion of inorganic and organic phosphorus in the rhizosphere. *Plant Soil* 143, 185–191. doi: 10.1007/BF00007872

Gahoonia, T. S., and Nielsen, N. E. (1996). Variation in acquisition of soil phosphorus among wheat and barley genotypes. *Plant Soil* 178, 223–230. doi: 10.1007/BF00011587

Gaxiola, R. A., Edwards, M., and Elser, J. J. (2001). A transgenic approach to enhance phosphorus use efficiency in crops as part of a comprehensive strategy for sustainable agriculture. *Chemosphere* 84, 840–845. doi: 10.1016/j.chemosphere.2011.01.062

Geelhoed, J. S., van Riemsdijk, W. H., and Findenegg, G. R. (1999). Simulation of the effect of citrate exudation from roots on the plant availability of phosphate adsorbed on goethite. *Eur. J. Soil Sci.* 50, 379–390. doi: 10.1046/j.1365-2389.1999.00251.x

George, T. S., Gregory, P. J., Simpson, R. J., and Richardson, A. E. (2007). Differential interactions of Aspergillus niger and Peniophora lycii phytases with soil particles affects the hydrolysis of inositol phosphates. *Soil Biol. Biochem.* 39, 793–803. doi: 10.1016/j.soilbio.2006.09.029

Gerke, J. (1992). Phosphate, aluminium and iron in the soil solution of three different soils in relation to varying concentrations of citric acid. *J. Plant Nut. Soil Sci.* 155, 339–343. doi: 10.1002/jpln.19921550417

Giles, C. D., Brown, L. K., Adu, M. O., Mezeli, M. M., Sandral, G. A., Simpson, R. J., et al. (2017). Response-based selection of barley cultivars and legume species for complementarity: Root morphology and exudation in relation to nutrient source. *Plant Sci.* 255, 12–28. doi: 10.1016/j.plantsci.2016.11.002.

Goh, T. B., Banerjee, M. R., Tu, S., and Burton, D. L. (1997). Vesicular arbuscular mycorrhizae-mediated uptake and translocation of P and Zn by wheat in a calcareous soil. *Can. J. Plant Sci.* 339–346. doi: 10.4141/P95-079

Goicoechea, N., Sánchez-Diaz, M., Sáez, R., and Irañeta, J. (2004). The Association of Barley with AM fungi can result in similar yield and grain quality as a long term application of P or P-K fertilizers by enhancing root phosphatase activity and sugars in leaves at tillering. *Biol. Agric. Hortic.* 22, 69–80. doi: 10.1080/01448765.2004.9754989

Goos, R. J., Johnson, B. E., and Stack, R. W. (1994). Penicillium bilaji and phosphorus fertilization effects on the growth, development yield and common root rot severity of spring wheat. *Fert. Res.* 39, 97–103. doi: 10.1007/BF00750908

Gordon-Weeks, R., Tong, Y., Davies, T. G., and Leggewie, G. (2003). Restricted spatial expression of a high-affinity phosphate transporter in potato roots. *J. Cell Sci.* 116, 3135–3144. doi: 10.1242/jcs.00615

Grace, E. J., Cotsaftis, O., Tester, M., Smith, F. A., and Smith, S. E. (2009). Arbuscular mycorrhizal inhibition of growth in barley cannot be attributed to extent of colonization, fungal phosphorus uptake or effects on expression of plant phosphate transporter genes. *New Phytol.* 181, 938–949. doi: 10.1111/j.1469-8137.2008.02720.x

Graham, J. H., and Abbott, L. K. (2000). Wheat responses to aggressive and non-aggressive arbuscular mycorrhizal fungi. *Plant Soil* 220, 207–218. doi: 10.1023/a:1004709209009

Gregory, P. J. (2006). *Plant Roots: Growth, Activity and Interaction With Soils.* Oxford: Blackwell.

Gruber, B. D., Giehl, R. F., Friedel, S., and von Wirén, N. (2013). Plasticity of the Arabidopsis root system under nutrient deficiencies. *Plant Physiol.* 163, 161–179. doi: 10.1104/pp.113.218453

Gyaneshwar, P., Naresh Kumar, G., Parekh, L. J., and Poole, P. S. (2002). Role of soil microorganisms in improving P nutrition of plants. *Plant Soil* 245, 83–93. doi: 10.1023/A:1020663916259

Hammond, J. P., Broadley, M. R., White, P. J., King, G. J., Bowen, H. C., Hayden, R., et al. (2009). Shoot yield drives phosphorus use efficiency in *Brassica oleracea* and correlates with root architecture traits. *J. Exp. Bot.* 60, 1953–1968. doi: 10.1093/jxb/erp083

Harrison, M. J. (2005). Signaling in the arbuscular mycorrhizal symbiosis. *Annu. Rev. Microbiol.* 59, 19–42. doi: 10.1146/annurev.micro.58.030603.123749

Hart, M. M., and Reader, R. J. (2002). Taxonomic basis for variation in the colonization strategy of arbuscular mycorrhizal fungi. *New Phytol.* 153, 335–344. doi: 10.1046/j.0028-646X.2001.00312.x

Harvey, P. R., Warren, R. A., and Wakelin, S. A. (2009). Potential to improve root access to phosphorus: the role of nonsymbiotic microbial inoculants in the rhizosphere. *Crop Pasture Sci*. 60, 144–151. doi: 10.1071/CP08084

Helyar, K. R. (1998). Efficiency of nutrient utilization and sustaining soil fertility with particular reference to phosphorus. *Field Crops Res*. 56, 187–195. doi: 10.1016/S0378-4290(97)00129-9

Hetrick, B. A. D., Wilson, G. W. T., and Todd, T. C. (1996). Mycorrhizal response in wheat cultivars: relationship to phosphorus. *Can. J. Bot.* 74, 19–25. doi: 10.1139/b96-003

Hetrick, B., Wilson, G., and Cox, T. (1992). Mycorrhizal dependece of modern wheat varieties, landraces, and ancestors. *Can. J. Bot.* 70, 2032–2040. doi: 10.1139/b92-253

Higo, M., Isobe, K., Miyazawa, Y., Matsuda, Y., Drijber, R. A., and Torigoe, Y. (2016). Molecular diversity and distribution of indigenous arbuscular mycorrhizal communities colonizing roots of two different winter cover crops in response to their root proliferation. *J. Microbiol.* 54, 86–97. doi: 10.1007/s12275-016-5379-2

Hinsinger, P. (2001). Bioavailability of soil inorganic P in the rhizosphere as affected by root-induced chemical changes: a review. *Plant Soil* 237, 173–195. doi: 10.1023/A:1013351617532

Hinsinger, P., Bengough, A. G., Vetterlein, D., and Young, I. M. (2009). Rhizosphere: biophysics, biogeochemistry and ecological relevance. *Plant Soil* 321, 117–152. doi: 10.1007/s11104-008-9885-9

Hinsinger, P., Herrmann, L., Lesueur, A. R., Robin, A., Trap, J., Waithaisong, K., et al. (2015). Impact of roots, microorganisms and microfauna on the fate of soil phosphorus in the rhizosphere. *Annu. Plant Rev*. 48, 77–408. doi: 10.1002/9781118958841.ch13

Hinsinger, P., Plassard, C., Tang, C., and Jaillard, B. (2003). Origins of root-mediated pH changes in the rhizosphere and their responses to environmental constraints: A review. *Plant Soil* 248, 43–59. doi: 10.1023/A:1022371130939

Ho, M. D., Rosas, J. C., Brown, K. M., and Lynch, J. P. (2005). Root architectural tradeoffs for water and phosphorus acquisition. *Funct. Plant Biol*. 32, 737–748. doi: 10.1071/FP05043

Hoad, S. P., Russell, G., Lucas, M. E., and Bingham, I. J. (2001). The management of wheat, barley, and oat root systems. *Adv. Agron*. 74, 193–246. doi: 10.1016/S0065-2113(01)74034-5

Hodge, A., Berta, G., Doussan, C., Merchan, F., and Crespi, M. (2009). Plant root growth, architecture and function. *Plant Soil* 321, 153–187. doi: 10.1007/s11104-009-9929-9

Hodge, A., Helgason, T., and Fitter, A. H. (2010). Nutritional ecology of arbuscular mycorrhizal fungi. *Fung. Ecol.* 3, 267–273. doi: 10.1016/j.funeco.2010.02.002

Holford, I. C. R. (1997). Soil phosphorus: its measurement, and its uptake by plants. *Aust. J. Soil. Res*. 35, 227–239. doi: 10.1071/S96047

Holloway, R. E., Bertrand, I., Frischke, A. J., Brace, D. M., McLaughlin, M. J., and Shepperd, W. (2001). Improving fertiliser efficiency on calcareous and alkaline soils with fluid sources of P, N and Zn. *Plant Soil* 236, 209–219. doi: 10.1023/A:1012720909293

Hu, J., Yang, A., Zhu, A., Wang, J., Dai, J., Wong, M. H., et al. (2015). Arbuscular mycorrhizal fungal diversity, root colonization, and soil alkaline phosphatase activity in response to maize-wheat rotation and no-tillage in North China. *J. Microbiol.* 53, 454–461. doi: 10.1007/s12275-015-5108-2

Jakobsen, I. (1995). "Transport of phosphorus and carbon in VA mycorrhizas," in *Mycorrhiza: Structure, Function, Molecular Biology and Biotechnology*, eds A. Varma and B. Hock (Berlin: Springer), 297–324.

Jakobsen, I., Leggett, M. E., and Richardson, A. E. (2005). "Rhizosphere microorganisms and plant phosphorus uptake," in Phosphorus, Agriculture and the Environment, eds J.T. Sims and A. N. Sharpley (Madison, WI: American Society for Agronomy), 437–494.

Jansa, J., Bukovská, P., and Gryndler, M. (2013). Mycorrhizal hyphae as ecological niche for highly specialized hypersymbionts–or just soil free-riders? *Front. Plant Sci.* 4:134 doi: 10.3389/fpls.2013.00134

Jansa, J., Finlay, R., Wallander, H., Smith, F. A., and Smith, S. E. (2011). "Role of mycorrhizal symbiosis in phosphorus cycling," in *Phosphorus in Action. Biological Processes in Soil Phosphorus Cycling*, eds E. K. Bunemann, A. Oberson, and E. Frossard (Berlin; Heidelberg: Springer-Verlag), 169–198.

Jansa, J., Mozafar, A., and Frossard, E. (2003a). Long-distance transport of P and Zn through the hyphae of an arbuscular mycorrhizal fungus in symbiosis with maize. *Agronomie* 23, 481–488. doi: 10.1051/agro:2003013

Jansa, J., Mozafar, A., Kuhn, G., Anken, T., Ruh, R., Sanders, I. R., et al. (2003b). Soil tillage affects the community structure of mycorrhizal fungi inmaize roots. *Ecol. Appl.* 13, 1164–1176. doi: 10.1890/1051-0761(2003)13[1164:STATCS]2.0.CO;2

Jansa, J., Smith, F. A., and Smith, S. E. (2008). Are there benefits of simultaneous root colonization by diferent arbuscular mycorrhizal fungi? *New Phytol.* 177, 779–789. doi: 10.1111/j.1469-8137.2007.02294.x

Javot, H., Pumplin, N., and Harrison, M. J. (2007). Phosphate in the arbuscular mycorrhizal symbiosis: transport properties and regulatory roles. *Plant Cell Environ.* 30, 310–322. doi: 10.1111/j.1365-3040.2006.01617.x

Jensen, A. (1982). Influence of four vesicular-arbuscular mycorrhizal fungi on nutrient uptake and growth in Barley (*Hordeum Vulgare*). *New Phytol.* 90, 45–50. doi: 10.1111/j.1469-8137.1982.tb03239.x

Jensen, A. (1984). Responses of barley, pea, and maize to inoculation with different vesicular-arbuscular mycorrhizal fungi in irradiated soil. *Plant Soil* 78, 315–323. doi: 10.1007/BF02450365

Johnson, J. F., Allan, D. L., Vance, C. P., and Weiblen, G. (1996). Root carbon dioxide fixation by phosphorus-deficient *Lupinus albus*: contribution to organic-acid exudation by proteoid roots. *Plant Physiol.* 112, 19–30. doi: 10.1104/pp.112.1.19

Johnson, N. C., Graham, J. H., and Smith, F. A. (1997). Functioning of mycorrhizal associations along the mutualism–parasitism continuum. *New Phytol.* 135, 575–586. doi: 10.1046/j.1469-8137.1997.00729.x

Joner, E. J., and Jakobsen, I. (1995). Growth and extracellular phosphatase activity of arbuscular mycorrhizal hyphae as influenced by soil organic matter. *Soil Biol. Biochem.* 27, 1153–1159. doi: 10.1016/0038-0717(95)00047-I

Joner, E. J., Van Aarle, I. M., and Vosatka, M. (2000). Phosphatase activity of extra-radical arbuscular mycorrhizal hyphae: a review. *Plant Soil* 226, 199–210. doi: 10.1023/A:1026582207192

Jones, D. L. (1998). Organic acids in the rhizosphere–a critical review. *Plant Soil* 205, 25–44. doi: 10.1023/A:1004356007312

Jones, D. L., and Darrah, P. R. (1994). Amino-acid influx at the soil-root interface of Zea mays L. and its implications in the rhizosphere.*Plant Soil* 163, 1–12. doi: 10.1007/BF00033935

Jones, D. L., and Oburger, E. (2011). "Solubilization of phosphorus by soil microorganisms," in *Phosphorus in Action. Biological Processes in Soil Phosphorus Cycling*, eds E. K. Bunemann, A. Oberson, and E. Frossard (Berlin; Heidelberg: Springer-Verlag), 169–198.

Jung, S. C., Martinez-Medina, A., Lopez-Raez, J. A., and Pozo, M. J. (2012). Mycorrhiza-induced resistance and priming of plant defenses. *J. Chem. Ecol.* 38, 651–664. doi: 10.1007/s10886-012-0134-6

Kaiser, C., Kilburn, M. R., Clode, P. L., Fuchslueger, L., Koranda, M., Cliff, J. B., et al. (2015). Exploring the transfer of recent plant photosynthates to soil microbes: mycorrhizal pathway vs direct root exudation. *New Phytol.* 205, 1537–1551. doi: 10.1111/nph.13138

Karamanos, R. E., Flore, N. A., and Harapiak, J. T. (2010). Re-visiting use of Penicillium bilaii with phosphorus fertilization of hard red spring wheat. *Can. J. Plant Sci.* 90, 265–277. doi: 10.4141/CJPS09123

Karasawa, T., Kasahara, Y., and Takebe, M. (2001). Variable response of growth and arbuscular mycorrhizal colonization of maize plants to preceding crops in various types of soils. *Biol. Fertil. Soils* 33, 286–293. doi: 10.1007/s003740000321

Keerthisinghe, G., Hocking, P. J., Ryan, P. R., and Delhaize, E. (1998). Effect of phosphorus supply on the formation and function of proteoid roots of white lupin (*Lupinus albus* L.). *Plant Cell Environ.* 21, 467–478. doi: 10.1046/j.1365-3040.1998.00300.x

Khademi, Z., Jones, D. L., Malakouti, M. J., and Asadi, F. (2010). Organic acids differ in enhancing phosphorus uptake by *Triticum aestivum* L.-effects of rhizosphere concentration and counterion. *Plant Soil* 334, 151–159. doi: 10.1007/s11104-009-0215-7

Khademi, Z., Jones, D. L., Malakouti, M. J., Asadi, F., and Ardebili, M. (2009). Organic acid mediated nutrient extraction efficiency in three calcareous soils. *Aust. J. Soil Res.* 47, 213–220. doi: 10.1071/SR07179

Khaliq, A., and Sanders, F. E. (1998). Effects of vesicular arbuscular mycorrhizal inoculation on growth and phosphorus nutrition of barley

in natural or methyl bromide-treated soil. *J. Plant Nutr.* 21, 2163–2177. doi: 10.1080/01904169809365552

Khaliq, A., and Sanders, F. E. (2000). Effects of vesicular-arbuscular mycorrhizal inoculation on the yield and phosphorus uptake of field-grown barley. *Soil Biol. Biochem.* 32, 1691–1696. doi: 10.1016/S0038-0717(00)00086-9

Khan, M. S., and Zaidi, A. (2007). Synergistic effects of the inoculation with plant growth-promoting rhizobacteria and an arbuscular mycorrhizal fungus on the performance of wheat. *Turkish J. Agric. For.* 31, 355–362. doi: 10.1002/jpln.200620602

Khan, M. S., Zaidi, A., Ahemad, M., Oves, M., and Wani, P. A. (2010). Plant growth promotion by phosphate solubilizing fungi—current perspective. *Arch. Agron. Soil Sci.* 56, 73–98. doi: 10.1080/03650340902806469

Kivlin, S. N., Hawkes, C. V., and Treseder, K. K. (2011). Global diversity and distribution of arbuscular mycorrhizal fungi. *Soil Biol. Biochem.* 43, 2294–2303. doi: 10.1016/j.soilbio.2011.07.012

Klironomos, J. N. (2003). Variation in plant response to native and exotic arbuscular mycorrhizal fungi. *Ecology* 84, 2292–2301. doi: 10.1890/02-0413

Klugh, K. R., and Cumming, J. R. (2007). Variations in organic acid exudation and aluminum resistance among arbuscular mycorrhizal species colonizing *Liriodendron tulipifera*. *Tree Physiol.* 27, 1103–1112. doi: 10.1093/treephys/27.8.1103

Klugh-Stewart, K., and Cumming, J. R. (2009). Organic acid exudation by mycorrhizal *Andropogon virginicus* L. (broomsedge) roots in response to aluminum. *Soil Biol. Biochem.* 41, 367–373. doi: 10.1016/j.soilbio.2008.11.013

Koch, A. M., Antunes, P. M., Maherali, H., and Klironomos, J. N. (2017). Evolutionary asymmetry in the mycorrhizal symbiosis: I. Conservatism in Glomeromycota fungal morphology does not predict host plant growth response. *New Phytol.* 214, 1330–1337. doi: 10.1111/nph.14465

Koch, A. M., Kuhn, G., Fontanillas, P., Fumagalli, L., Goudet, J., and Sanders, I. R. (2004). High genetic variability and low local diversity in a population of arbuscular mycorrhizal fungi. *Proc. Natl. Acad. Sci. U.S.A.* 101, 2369–2374. doi: 10.1073/pnas.0306441101

Kochian, L., Hoekenga, O., and Pineros, M. A. (2004). How do crop plants tolerate acid soils? Mechanisms of aluminum tolerance and phosphorus efficiency. *Annu. Rev. Plant Biol.* 55, 459–493. doi: 10.1146/annurev.arplant.55.031903.141655

Kochian, L. V. (2012). Rooting for more phosphorus. *Nature* 488:466. doi: 10.1038/488466a

Koide, R. T., and Kabir, Z. (2000). Extraradical hyphae of the mycorrhizal fungus Glomus intraradices can hydrolyse inorganic phosphate. *New Phytol.* 148, 511–517. doi: 10.1046/j.1469-8137.2000.00776.x

Kucey, R. M. (1987). Increased phosphorus uptake by wheat and field beans inoculated with a phosphorus-solubilizing penicillium bilaji strain and with vesicular-arbuscular mycorrhizal fungi. *Appl. Environ. Microbiol.* 53, 2699–2703.

Kucey, R. M. N., Jenzen, H. H., and Leggett, M. E. (1989). Microbially mediated increases in plant available phosphorus. *Adv. Agron.* 42, 199–228. doi: 10.1016/S0065-2113(08)60525-8

Kujira, Y., Grove, J. H., and Ronzelli, P. (1994). Varietal differences of root systems in winter-wheat seedlings. *Jap. J. Crop Sci.* 63, 524–530. doi: 10.1626/jcs.63.524

Lan, M., Comerford, N. B., and Fox, T. R. (1995). Organic anions effect on phosphorus release from spodic horizons. *Soil Sci. Soc. Am. J.* 59, 1745–1749. doi: 10.2136/sssaj1995.03615995005900060034x

Leggett, M., Cross, J., Hnatowich, G., and Holloway, G. (2007). "Challenges in commercializing a phosphate-solubilizing microorganisms: *Penicillium bilaiae*, a case history," in *First International Meeting on Microbial Phosphate Solubilization*, eds E. Velázquez, C. Rodríguez-Barrueco, E. Velázquez, and C. Rodríguez-Barrueco (Dordrecht: Springer), 215–222.

Li, H., Smith, S. E., Holloway, R. E., Zhu, Y., and Smith, F. A. (2006). Arbuscular mycorrhizal fungi contribute to phosphorus uptake by wheat grown in a phosphorus-fixing soil even in the absence of positive growth responses. *New Phytol.* 172, 536–543. doi: 10.1111/j.1469-8137.2006.01846.x

Li, H. Y., Zhu, Y. G., Marschner, P., Smith, F. A., and Smith, S. E. (2005). Wheat responses to arbuscular mycorrhizal fungi in a highly calcareous soil differ from those of clover, and change with plant development and P supply. *Plant Soil* 277, 221–232. doi: 10.1007/s11104-005-7082-7

Liao, M., Hocking, P. J., Dong, B., Delhaize, E., Richardson, A. E., and Ryan, P. R. (2008). Variation in early phosphorus-uptake efficiency among wheat genotypes grown on two contrasting Australian soils. *Aust. J. Agri. Res.* 59, 157–166. doi: 10.1071/AR06311

Liu, C., Muchhal, U. S., Uthappa, M., Kononowicz, A. K., and Raghothama, K. G. (1998). Tomato phosphate transporter genes are differentially regulated in plant tissues by phosphorus. *Plant Physiol.* 116, 91–99. doi: 10.1104/pp.116.1.91

Liu, F., Chang, X.-J., Ye, Y., Xie, W.-B., Wu, P., and Lian, X.-M. (2011). Comprehensive sequence and whole-life-cycle expression profile analysis of the phosphate transporter gene family in rice. *Mol. Plant* 4, 1105–1122. doi: 10.1093/mp/ssr058

López-Arredondo, D. L., Leyva-González, M. A., González-Morales, S. I., López-Bucio, J., and Herrera-Estrella, L. (2014). Phosphate nutrition: improving low-phosphate tolerance in crops. *Annu. Rev. Plant Biol.* 65, 95–123. doi: 10.1146/annurev-arplant-050213-035949

López-García, Á., Varela-Cervero, S., Vasar, M., Öpik, M., Barea, J. M., and Azcón-Aguilar, C. (2017). Plant traits determine the phylogenetic structure of arbuscular mycorrhizal fungal communities. *Mol. Ecol.* 26, 6948–6959. doi: 10.1111/mec.14403

López-Ráez, J. A., Charnikhova, T., Gómez-Roldán, V., Matusova, R., Kohlen, W., de Vos, R., et al. (2008). Tomato strigolactones are derived from carotenoids and their biosynthesis is promoted by phosphate starvation. *New Phytol.* 178, 863–874. doi: 10.1111/j.1469-8137.2008.02406.x

López-Ráez, J. A., Shirasu, K., and Foo, E. (2017). Strigolactones in plant interactions with beneficial and detrimental organisms: the Yin and Yang. *Trends Plant Sci.* 22, 527–537. doi: 10.1016/j.tplants.2017.03.011

Lung, S.-C., Chan, W.-L., Yip, W., Wang, L., Yeung, E. C., and Lim, B. L. (2005). Secretion of beta-propeller phytase from tobacco and *Arabidopsis* roots enhances phosphorus utilization. *Plant Sci.* 169, 341–349. doi: 10.1016/j.plantsci.2005.03.00.

Lung, S.-C., and Lim, B. L. (2006). Assimilation of phytate-phosphorus by the extracellular phytase activity of tobacco (*Nicotiana tabaccum*) is affected by the availability of soluble phytate. *Plant Soil* 279, 187–199. doi: 10.1007/s11104-005-1009-1

Lynch, J. P. (2007). Roots of the second green revolution. *Aust. J. Bot.* 55, 1–20. doi: 10.1071/BT06118

Lynch, J. P., and Ho, M. D. (2005). Rhizoeconomics: Carbon costs of phosphorus acquisition. *Plant Soil* 269, 45–56. doi: 10.1007/s11104-004-1096-4.

Ma, Q., Rengel, Z., and Rose, T. J. (2009). The effectiveness of deep placement of fertilisers is determined by crop species and edaphic conditions in Mediterranean-type environments: a review. *Aust. J. Soil Res.* 47, 19–32. doi: 10.1071/SR08105

Maherali, H. (2014). Is there an association between root architecture and mycorrhizal growth response? *New Phytol.* 204, 192–200. doi: 10.1111/nph.12927

Maillet, F., Poinsot, V., André, O., Puech-Pagès, V., Haouy, A., Gueunier, M., et al. (2011). Fungal lipochitooligosaccharide symbiotic signals in arbuscular mycorrhiza. *Nature* 469, 58–63. doi: 10.1038/nature09622

Maldonado-Mendoza, I. E., Dewbre, G. R., and Harrison, M. J. (2001). A phosphate transporter gene from the extra-radical mycelium of an arbuscular mycorrhizal fungus *Glomus intraradices* is regulated in response to phosphate in the environment. *Mol. Plant Microbe Interact.* 14, 1140–1148. doi: 10.1094/MPMI.2001.14.10.1140

Manoharan, L., Rosenstock, N. P., Williams, A., and Hedlund, K. (2017). Agricultural management practices influence AMF diversity and community composition with cascading effects on plant productivity. *Agric. Ecosyst. Environ,. Appl. Soil Ecol.* 115, 53–59. doi: 10.1016/j.apsoil.2017.03.012

Manske, G. G. B., Ortiz-Monasterio, J. I., Van Ginkel, M., González, R. M., Rajaram, S., Molina, E., et al. (2000). Traits associated with improved P-uptake efficiency in CIMMYT's semidwarf spring bread wheat grown on an acid Andisol in Mexico. *Plant Soil* 221, 189–204. doi: 10.1023/A:1004727201568

Mao, L., Liu, Y., Shi, G., Jiang, S., Cheng, G., Li, X., et al. (2014). Wheat cultivars form distinctive communities of root-associated arbuscular mycorrhiza in a conventional agroecosystem. *Plant Soil* 374, 949–961. doi: 10.1007/s11104-013-1943-2

Marschener, H. (1998). Role of root growth, arbuscular mycorrhiza, and root exudates for the efficiency in nutrient acquisition. *F. Crop. Res.* 56, 203–207. doi: 10.1016/S0378-4290(97)00131-7

Marschner, P. (ed.). (2012). "Phosphorus," in *Marschner's Mineral Nutrition of Higher Plant*, 3rd Edn (London: Academic Press; Elsevier Ltd.), 265–277.

McIvor, J. G., Guppy, C., and Probert, M. E. (2011). Phosphorus requirements of tropical grazing systems: the northern Australian experience. *Plant Soil.* 349, 55–67. doi: 10.1007/s11104-011-0906-8

Mehrvarz, S., Chaichi, M. R., and Alikhani, H. A. (2008). Effects of phosphate solubilizing microorganisms and phosphorus chemical fertilizer on yield and yield components of barley (*Hordeum vulgare* L.). *Am. Eur. J. Agric. Env. Sci.* 3, 822–828.

Merryweather, J., and Fitter, A. (1998). The arbuscular mycorrhizal fungi of Hyacinthoides non-scripta I. Diversity of fungal taxa. *New Phytol.* 138, 117–129. doi: 10.1046/j.1469-8137.1998.00888.x

Miguel, M. A. (2011). *Functional Role and Synergistic Effect of Root Traits for Phosphorus Acquisition Efficiency and Their Genetic Basis in Common Bean (Phaseolus vulgaris L.)*. Ph.D. thesis, Pennsylvania State University, University Park.

Mohammad, M. J., and Malkawi, H. I. (2004). Root, shoot and nutrient acquisition responses of mycorrhizal and nonmycorrhizal wheat to phosphorus application to highly calcareous soils. *Asian J. Plant Sci.* 3, 363–369. doi: 10.3923/ajps.2004.363.369

Mohammad, M. J., Malkawi, H. I., and Shibli, R. (2003). Effects of arbuscular mycorrhizal fungi and phosphorus fertilization on growth and nutrient uptake of barley grown on soils with different levels of salts. *J. Plant Nutr.* 26, 125–137. doi: 10.1081/PLN-120016500

Mohammad, M. J., Pan, W. L., and Kennedy, A. C. (1998). Seasonal mycorrhizal colonisation of winter wheat and its effect on wheat growth under dryland field conditions. *Mycorrhiza* 8, 139–144. doi: 10.1007/s005720050226

Morales, A., Alvear, M., Valenzuela, E., Castillo, C. E., and Borie, F. (2011). Screening, evaluation and selection of phosphate-solubilising fungi as potential biofertiliser. *J. Soil Sci. Plant Nut.* 11, 89–103. doi: 10.4067/S0718-95162011000400007

Morgan, J. A., Bending, G. D., and White, P. J. (2005). Biological costs and benefits to plant–microbe interactions in the rhizosphere. *J. Exp. Bot.* 56, 1729–1739. doi: 10.1093/jxb/eri205

Mukherjee, A., and Ané, J. M. (2011). Germinating spore exudates from arbuscular mycorrhizal fungi: molecular and developmental responses in plants and their regulation by ethylene. *Mol. Plant Microbe Interact.* 24, 260–270. doi: 10.1094/MPMI-06-10-0146

Munkvold, L., Kjøller, R., Vestberg, M., Rosendahl, S., and Jakobsen, I. (2004). High functional diversity within species of arbuscular mycorrhizal fungi. *New Phytol.* 164, 357–364. doi: 10.1111/j.1469-8137.2004.01169.x

Nadji, W., Belbekri, N., Ykhlef, N., and Djekoun, A. (2017). Diversity of arbuscular mycorrhizal fungi of durum Wheat (*Triticum durum* Desf.) fields of the East of Algeria. *J. Agric. Sci.* 9: 117. doi: 10.5539/jas.v9n3p117

Nannipieri, P., Giagnoni, L., Landi, L., and Renella, G. (2011). "Role of phosphatase enzymes in soil," in Phosphorus in Action. Biological Processes in Soil Phosphorus Cycling, eds E. K. Bünemann, A. Oberson, and E. Frossard (Berlin; Heidelberg: Springer-Verlag), 169–198.

Newsham, K. K., Fitter, A. H., and Watkinson, A. R. (1995). Multi-functionality and biodiversity in arbuscular mycorrhizas. *Trends Ecol. Evol.* 10, 407–411. doi: 10.1016/S0169-5347(00)89157-0

Oberson, A., and Joner, E. J. (2005). "Microbial turnover of phosphorus in soil," in Organic *Phosphorus* in the *Environment,* eds B. L. Turner, E. Frossard, and D. S. Baldwin (Wallingford: CABI), 133–164.

Olsson, P. A., van Aarle, I. M., Allaway, W. G., Ashford, A. E., and Rouhier, H. (2002). Phosphorus effects on metabolic processes in monoxenic arbuscular mycorrhiza cultures. *Plant Physiol.* 130, 1162–1171. doi: 10.1104/pp.009639

Omar, S. A. (1998). The role of rock-phosphate-solubilizing fungi and vesicular-arbusular-mycorrhiza (VAM) in growth of wheat plants fertilized with rock phosphate. *World J. Microbiol. Biotechnol.* 14, 211–218. doi: 10.1023/A:1008830129262

Öpik, M., Davison, J., Moora, M., and Zobel, M. (2014). DNA-based detection and identification of Glomeromycota: the virtual taxonomy of environmental sequences. *Botany* 92, 135–147. doi: 10.1139/cjb-2013-0110

Öpik, M., Vanatoa, A., Vanatoa, E., Moora, M., Davison, J., Kalwij, J. M., et al. Zobel, M. (2010). The online database MaarjAM reveals global and ecosystemic distribution patterns in arbuscular mycorrhizal fungi (*Glomeromycota*). *New Phytol.* 188, 223–241. doi: 10.1111/j.1469-8137.2010.03334.x

Ortas, I., Ortakci, D., Kaya, Z., Cinar, A., and Onelge, N. (2002). Mycorrhizal dependency of sour orange in relation to phosphorus and zinc nutrition. *J. Plant Nutr.* 25, 1263–1279. doi: 10.1081/PLN-120004387

Parniske, M. (2006). Plant–fungal associations: Cue for the branching connection. *Nature* 435, 750–751. doi: 10.1038/435750a

Pearse, S. J., Veneklaas, E. J., Cawthray, G., Bolland, M. D., and Lambers, H. (2007). Carboxylate composition of root exudates does not relate consistently to a crop species' ability to use phosphorus from aluminium, iron or calcium phosphate sources. *New Phytol.* 173,181–190. doi: 10.1111/j.1469-8137.2006.01897.x

Pearson, J. N., and Jakobsen, I. (1993). The relative contribution of hyphae and roots to phosphorus uptake by arbuscular mycorrhizal plants, measured by dual labelling with 32P and 33P. *New Phytol.* 124, 489–494. doi: 10.1111/j.1469-8137.1993.tb03840.x

Peleg, Z., and Blumwald, E. (2011). Hormone balance and abiotic stress tolerance in crop plants. *Curr. Opin. Plant Biol.* 14, 290–295. doi: 10.1016/j.pbi.2011.02.001

Pellegrino, E., Öpik, M., Bonari, E., and Ercoli, L. (2015). Responses of wheat to arbuscular mycorrhizal fungi: a meta-analysis of field studies from 1975 to 2013. *Soil Biol. Biochem.* 84, 210–217. doi: 10.1016/j.soilbio.2015.02.020

Plenchette, C., and Morel, C. (1996). External phosphorus requirement of mycorrhizal and non- mycorrhizal barley and soybean plants. *Biol. Fertil. Soils* 21, 303–308. doi: 10.1007/s003740050064

Powell, J. R., Parrent, J. L., Hart, M. M., Klironomos, J. N., Rillig, M. C., and Maherali, H. (2009). Phylogenetic trait conservatism and the evolution of functional trade-offs in arbuscular mycorrhizal fungi. *Proc. R. Soc. B Biol. Sci.* 276, 4237–4245. doi: 10.1098/rspb.2009.1015

Pozo, M. J., López-Ráez, J. A., Azcón-Aguilar, C., and García-Garrido, J. M. (2015). Phytohormones as integrators of environmental signals in the regulation of mycorrhizal symbioses. *New Phytol.* 205, 1431–1436. doi: 10.1111/nph.13252

Preuss, C. P., Huang, C. Y., Gilliham, M., and Tyerman, S. D. (2010). Channel-like characteristics of the low-affinity barley phosphate transporter Pht1;6 when expressed in xenopus oocytes. *Plant Physiol.* 152, 1431–1441. doi: 10.1104/pp.109.152009

Qin, H., Lu, K., Strong, P. J., Xu, Q., Wu, Q., Xu, Z., et al. (2015). Long-term fertilizer application effects on the soil, root arbuscular mycorrhizal fungi and community composition in rotation agriculture. *Agric. Ecosyst. Environ. Appl. Soil Ecol.* 89, 35–43. doi: 10.1016/j.apsoil.2015.01.008

Rae, A. L., Cybinski, D. H., Jarmey, J. M., and Smith, F. W. (2003). Characterization of two phosphate transporters from barley; evidence for diverse function and kinetic properties among members of the Pht1 family. *Plant Mol. Biol.* 53, 27–36. doi: 10.1023/B:PLAN.0000009259.75314.15

Rae, A. L., Jarmey, J. M., Mudge, S. R., and Smith, F. W. (2004). Over-expression of a high-affinity phosphate transporter in transgenic barley plants does not enhance phosphate uptake rates. *Funct. Plant Biol.* 31, 141–148. doi: 10.1007/s11104-007-9222-8

Raghothama, K. G. (2005). "Phosphorous," in Plant *Nutritional Genomics,* eds M. R. Broadley and P. J. White (Oxford: Blackwell Publishing Ltd.,), 112–126.

Ray, D. K., Ramankutty, N., Mueller, N. D., West, P. C., and Foley, J. A. (2012). Recent patterns of crop yield growth and stagnation. *Nat. Commun.* 3, 1293–1299. doi: 10.1038/ncomms2296

Richardson, A. E., Barea, J. M., McNeill, A. M., and Prigent-Combaret, C. (2009). Acquisition of phosphorus and nitrogen in the rhizosphere and plant growth promotion by microorganisms. *Plant Soil* 321, 305–339. doi: 10.1007/s11104-009-9895-2

Richardson, A. E., Hadobas, P. A., and Hayes, J. E. (2001). Extracellular secretion of Aspergillus phytase from *Arabidopsis* roots enables plants to obtain phosphorus from phytate. *Plant J.* 25, 641–649. doi: 10.1046/j.1365-313x.2001.00998.x

Richardson, A. E., Lynch, J. P., Ryan, P. R., Delhaize, E., Smith, F. A., Smith, S. E., et al. (2011). Plant and microbial strategies to improve the phosphorus efficiency of agriculture. *Plant Soil* 349, 121–156. doi: 10.1007/s11104-011-0950-4

Richardson, A. E., and Simpson, R. J. (2011). Soil microorganisms mediating phosphorus availability. *Plant Physiol.* 156, 989–996. doi: 10.1104/pp.111.175448

Rose, T. J., Pariasca-Tanaka, J., Rose, M. T., Fukuta, Y., and Wissuwa, M. (2010). Genotypic variation in grain phosphorus concentration; and opportunities to improve P-use efficiency in rice. *Field Crop Res.* 119, 154–160. doi: 10.1016/j.fcr.2010.07.004

Rose, T. J., and Wissuwa, M. (2012). *Rethinking Internal Phosphorus Utilization Efficiency. A New Approach Is Needed to Improve PUE in Grain Crops*. Burlington: 1st Edn. Elsevier Inc.

Rubio, R., Moraga, E., and Borie, F. (1990). Acid phosphatase activity and vesicular-arbuscular mycorrhizal infection associated with roots of four wheat cultivars. *J. Plant Nutr.* 13, 585–598. doi: 10.1080/01904169009364102

Ryan, M. H., and Angus, J. F. (2003). Arbuscular mycorrhizae in wheat and field pea crops on a low P soil: Increased Zn-uptake but no increase in P-uptake or yield. *Plant Soil* 250, 225–239. doi: 10.1023/A:1022839930134

Sandaña, P., and Pinochet, D. (2016). Phosphorus acquisition of wheat, pea and narrow-leafed lupin under different P supplies. *J. Soil Sci. Plant Nut.* 16, 537–549. doi: 10.4067/S0718-95162016005000044

Sanders, I. R. (1999). Evolutionary genetics: no sex please, we're fungi. *Nature* 399, 737–739. doi: 10.1038/21544

Santander, C., Aroca, R., Ruiz-Lozano, J. M., Olave, J., Cartes, P., and Borie, F. (2017). Arbuscular mycorrhiza effects on plant performance under osmotic stress. *Mycorrhiza* 27: 639–657. doi: 10.1007/s00572-017-0784-x

Sato, T., Ezawa, T., Cheng, W., and Tawaraya, K. (2015). Release of acid phosphatase from extraradical hyphae of arbuscular mycorrhizal fungus Rhizophagus clarus. *Soil Sci. Plant Nutr.* 61, 269–274. doi: 10.1080/00380768.2014.993298.

Sattari, S. Z., Bouwman, A.F.,Giller, K. E., and van Ittersum, M. K. (2012). Residual soil phosphorus as the missing piece in the global phosphorus crisis puzzle. *Proc. Natl. Acad. Sci. U.S.A.* 109, 6348–6353. doi: 10.1073/pnas.1113675109

Saxena, J., Chandra, S., and Nain, L. (2013). Synergistic effect of phosphate solubilizing rhizobacteria and arbuscular mycorrhiza on growth and yield of wheat plants. *J. Soil Sci. Plant Nutr.* 13, 511–525. doi: 10.4067/S0718-95162013005000040

Scannerini, S., Fusconi, A., and Mucciarelli, M. (2001). "The effect of endophytic fungi on host plant morphogenesis," in Symbiosis: *Organisms* and *Model Systems,* ed J. Seckback (Kluwer: Dordrecht), 427–447.

Schachtman, D. P., Reid, R. J., and Ayling, S. M. (1998). Phosphorus uptake by plants: from soil to cell. *Plant Physiol.* 116, 447–453. doi: 10.1104/pp.116.2.447

Schellenbaum, L., Berta, G., Raviolanirina, F., Tisserant, B., Gianinazzi, S., and Fitter, H. (1991). Influence of endomycorrhizal infection on root morphology in a micropropagated woody plant species (*Vitis vinifera* L.). *Ann. Bot. Lond.* 68, 135–141. doi: 10.1093/oxfordjournals.aob.a088231

Schmidt, G., and Laskowski, M. S. (1961). "Phosphatase ester cleavage (survey)," in *The enzymes*, 2nd Edn., eds P. D. Boyer, H. Lardy, and K. Myrback (New York, NY: Academic), 3–35.

Schnepf, A., Roose, T., and Schweiger, P. (2008). Impact of growth and uptake patterns of arbuscular mycorrhizal fungi on plant phosphorus uptake–a modelling study. *Plant Soil* 312, 85–99. doi: 10.1007/s11104-008-9749-3

Schweiger, P. F., Robson, A. D., and Barrow, N. J. (1995). Root hair length determines beneficial effect of a Glomus species on shoot growth of some pasture species. *New Phytol.* 131, 247–254. doi: 10.1111/j.1469-8137.1995.tb05726.x

Seguel, A., Barea, J. M., Cornejo, P., and Borie, F. (2015). Role of arbuscular mycorrhizal symbiosis in phosphorus-uptake efficiency and aluminium tolerance in barley growing in acid soils. *Crop Pasture Sci.* 66, 696–705. doi: 10.1071/CP14305

Seguel, A., Cornejo, P., Ramos, A., Von Baer, E., Cumming, J., and Borie, F. (2017). Phosphorus acquisition by three wheat cultivars contrasting in aluminium tolerance growing in an aluminium-rich volcanic soil. *Crop Pasture Sci.* 68, 305–316. doi: 10.1071/CP16224

Seguel, A., Cumming, J., Cornejo, P., and Borie, F. (2016a). Aluminum tolerance of wheat cultivars and relation to arbuscular mycorrhizal colonization in a non-limed and limed Andisol. *Agric. Ecosyst. Environ. Appl. Soil Ecol.* 108, 228–237. doi: 10.1016/j.apsoil.2016.08.014

Seguel, A., Castillo, C., Morales, A., Campos, P., Cornejo, P., and Borie, F. (2016b). Arbuscular Mycorrhizal symbiosis in four Al-tolerant wheat genotypes grown in an acidic Andisol. *J. Soil Sci. Plant Nutr.* 16, 164–173. doi: 10.4067/S0718-95162016005000013

Seguel, A., Cumming, J. R., Klugh-Stewart, K., Cornejo, P., and Borie, F. (2013). The role of arbuscular mycorrhizas in decreasing aluminium phytotoxicity in acidic soils: a review. *Mycorrhiza* 23, 167–183. doi: 10.1007/s00572-013-0479-x

Shang, C., Stewart, J. W. B., and Huang, P. M. (1992). pH effect on kinetics of adsorption of organic and inorganic phophates by short-range ordered aluminium and iron precipitates. *Geoderma* 53, 1–14. doi: 10.1016/0016-7061(92)90017-2

Singh, S., and Kapoor, K. K. (1999). Inoculation with phosphate-solubilizing microorganisms and a vesicular-arbuscular mycorrhizal fungus improves dry matter yield and nutrient uptake by wheat grown in a sandy soil. *Biol. Fertil. Soils* 28, 139–144. doi: 10.1007/s003740050475

Smernik, R. J., and Dougherty, W. J. (2007). Identification of phytate in phosphorus-31 nuclear magnetic resonance spectra: the need for spiking. *Soil Sci. Soc. Am. J.* 71, 1045–1050. doi: 10.2136/sssaj2006.0295

Smith, F. A., Grace, E. J., and Smith, S. E. (2009). More than a carbon economy: nutrient trade and ecological sustainability in facultative arbuscular mycorrhizal symbioses. *New Phytol.* 182, 347–358. doi: 10.1111/j.1469-8137.2008.02753.x

Smith, S. E., Jakobsen, I., Grønlund, M., and Smith, F. A. (2011). Roles of arbuscular mycorrhizas in plant phosphorus nutrition: interactions between pathways of phosphorus uptake in arbuscular mycorrhizal roots have important implications for understanding and manipulating plant phosphorus acquisition. *Plant Physiol.* 156, 1050–1057. doi: 10.1104/pp.111.174581

Smith, S. E., Manjarrez, M., Stonor, R., McNeill, A., and Smith, F. A. (2015). Indigenous arbuscular mycorrhizal (AM) fungi contribute to wheat phosphate uptake in a semi-arid field environment, shown by tracking with radioactive phosphorus. *Agric. Ecosyst. Environ. Appl. Soil Ecol.* 96, 68–74. doi: 10.1016/j.apsoil.2015.07.002

Smith, S. E., and Read, D. J. (2008). *Mycorrhizal Symbiosis*, 3rd Edn. New York, NY: Academic.

Smith, S. E., Smith, F. A., and Jakobsen, I. (2004). Functional diversity in arbuscular mycorrhizal (AM) symbioses: the contribution of the mycorrhizal P uptake pathway is not correlated with mycorrhizal responses in growth or total P uptake. *New Phytol.* 162, 511–524. doi: 10.1111/j.1469-8137.2004.01039.x

Snajdr, J., Valaskova, V., Merhautova, V., Herinková, J., Cajthaml, T., and Baldrian, P. (2008). Spatial variability of enzyme activities and microbial biomass in the upper layers of Quercus petraea forest soil. *Soil Biol. Biochem.* 40, 2068–2075. doi: 10.1016/j.soilbio.2008.01.015

Spohn, M., Ermak, A., and Kuzyakov, Y. (2013). Microbial gross organic-Phosphorus mineralization can be stimulated by root exudates a 33P isotopic dilution study. *Soil Biol. Biochem.* 65, 254–263. doi: 10.1016/j.soilbio.2013.05.028

Spohn, M., and Kuzyakov, Y. (2013). Distribution of microbial- and root-derived phosphatase activities in the rhizosphere depending on P availability and C allocation-Coupling soil zymography with 14C imaging. *Soil Biol. Biochem.* 67, 106–113. doi: 10.1016/j.soilbio.2013.08.015

Stursova, M., and Baldrian, P. (2011). Effects of soil properties and management on the activity of soil organic matter transforming enzymes and the quantification of soilbound and free activity. *Plant Soil* 338, 99–110. doi: 10.1007/s11104-010-0296-3

Suri, V. K., Choudhary, A. K., Chander, G., and Verma, T. S. (2011). Influence of vesicular arbuscular mycorrhizal fungi and applied phosphorus on root colonization in wheat and plant nutrient dynamics in a phosphorus-deficient acid alfisol of Western Himalayas. *Commun. Soil Sci. Plant Anal.* 42, 1177–1186. doi: 10.1080/00103624.2011.566962

Syers, J. K., Johnston, A. E., and Curtin, D. (2008). *Efficiency of Soil and Fertilizer Phosphorus Use—Reconciling Changing Concepts of Soil Phosphorus Behaviour With Agronomic Information. FAO Fertilizer and Plant Nutrition Bulletin 18*. Rome: United Nations. Available online at: http://www.fao.org/docrep/010/a1595e/a1595e00.htm (Accessed July 02, 2016).

Sylvia, D. M., Hammond, L. C., Bennett, J. M., Haas, J. H., and Linda, S. B. (1993). Field response of maize to a VAM fungus and water management. *Agron. J.* 85, 193–198. doi: 10.2134/agronj1993.00021962008500020006x

Tabatabai, M. A. (1994). "Soil enzymes," in *Methods of Soil Analysis. Part 2. Microbiological and Biochemical Properties*, eds R. W. Weaver, S. Angle, P. Bottomley, D. Bezdicek, S. Smith, A. Tabatabai, and A. Wollum (Madison, WI: Soil Science Society of America Journal), 775–833.

Talukdar, N. C., and Germida, J. J. (1994). Growth and yield of lentil and wheat inoculated with three Glomus isolates from Saskatchewan soils. *Mycorrhiza* 5, 145–152. doi: 10.1007/BF00202347

Tarafdar, J. C., and Marschner, H. (1994a). Phosphatase activity in the rhizosphere and hyphosphere of VA mycorrhizal wheat supplied with inorganic and organic phosphorus. *Soil Biol. Biochem.* 26, 387–395. doi: 10.1016/0038-0717(94)90288-7

Tarafdar, J. C., and Marschner, H. (1994b). Efficiency of vam hyphae in utilisation of organic phosphorus by wheat plants. *Soil Sci. Plant Nutr.* 40, 593–600. doi: 10.1080/00380768.1994.10414298

Tawaraya, K., Naito, M., and Wagatsuma, T. (2006). Solubilization of insoluble inorganic phosphate by hyphal exudates of arbuscular mycorrhizal fungi. *J. Plant Nutr.* 29, 657–665. doi: 10.1080/01904160600564428

Teng, W., Zhao, Y.-Y., Zhao, X.-Q., He, X., Ma, W.-Y., Deng, Y., et al. (2017). Genome-wide identification, characterization, and expression analysis of PHT1 phosphate transporters in wheat. *Front. Plant Sci.* 8, 1–14. doi: 10.3389/fpls.2017.00543

Theodorou, M. E., and Plaxton, W. C. (1996). Purification and characterization of pyrophosphate-dependent phosphofructokinase from phosphate-starved *Brassica nigra* suspension cells. *Plant Physiol.* 112, 343–351.

Tian, H., Yuan, X., Duan, J., Li, W., Zhai, B., and Gao, Y. (2017). Influence of nutrient signals and carbon allocation on the expression of phosphate and nitrogen transporter genes in winter wheat (*Triticum aestivum* L.) roots colonized by arbuscular mycorrhizal fungi. *PLoS ONE* 12:e0172154. doi: 10.1371/journal.pone.0172154

Trappe, J. M. (1987). "Phylogenetic and ecologic aspects of mycotrophy in the angiosperms from an evolutionary standpoint," in Ecophysiology of VA *Mycorrhizal Plants,* ed G. R. Safir (Boca Raton, FL: CRC), 5–25.

Turner, B. L. (2007). "Inositol phosphates in soil: amounts, forms and significance of the phosphorylated inositol stereoisomers," in *Inositol Phosphates: Linking Agriculture and the Environment*, eds B. L. Turner, A. E. Richardson and E. J. Mullaney (Wallingford: CABI Publishing), 186–206.

Unno, Y., Okubo, K., Wasaki, J., Shinano, T., and Osaki, M. (2005). Plant growth promotion abilities and microscale bacterial dynamics in the rhizosphere of Lupin analysed by phytate utilization ability. *Environ. Microbiol.* 7, 396–404. doi: 10.1111/j.1462-2920.2004.00701.x

Vacheron, J., Desbrosses, G., Bouffaud, M. L., Touraine, B., Moënne-Loccoz, Y., Muller, D., et al. (2013). Plant growth-promoting rhizobacteria and root system functioning. *Front. Plant Sci.* 4:356. doi: 10.3389/fpls.2013.00356

Vallino, M., Greppi, D., Novero, M., Bonfante, P., and Lupotto, E. (2009). Rice root colonisation by mycorrhizal and endophytic fungi in aerobic soil. *Ann. Appl. Biol.* 154, 195–204. doi: 10.1111/j.1744-7348.2008.00286.x

Vance, C. P., Uhde-Stone, C., and Allan, D. L. (2003). Phosphorus acquisition and use: Critical adaptations by plants for securing a nonrenewable resource. *New Phytol.* 157, 423–447. doi: 10.1046/j.1469-8137.2003.00695.x

Vandamme, E., Renkens, M., Pypers, P., Smolders, E., Vanlauwe, B., and Merckx, R. (2013). Root hairs explain P uptake efficiency of soybean genotypes grown in a P-deficient Ferralsol. *Plant Soil* 369, 269–282. doi: 10.1007/s11104-012-1571-2

van de Wiel, C. C. M., van der Linden, C. G., and Scholten, O. E. (2016). Improving phosphorus use efficiency in agriculture: opportunities for breeding. *Euphytica* 207, 1–22. doi: 10.1007/s10681-015-1572-3

Vaneklaas, E. J., Lambers, H., Bragg, J., Finnegan, P. M., Lovelock, C. E., Plaxton, W. C., et al. (2012). Opportunities for improving phosphorus-use efficiency in crop plants. *New Phytol.* 195, 306–320. doi: 10.1111/j.1469-8137.2012.04190.x

Wakelin, S. A., Warren, R. A., Harvey, P. R., and Ryder, M. H. (2004). Phosphate solubilization by *Penicillium* spp. Closely associated with wheat roots. *Biol. Fert. Soils* 40, 36–43. doi: 10.1007/s00374-004-0750-6

Wang, B., and Qiu, Y. L. (2006). Phylogenetic distribution and evolution of mycorrhizas in land plants. *Mycorrhiza* 16, 299–363. doi: 10.1007/s00572-005-0033-6

Wang, L., Liao, H., Yan, X., Zhuang, B., and Dong, Y. (2004). Genetic variability for root hair traits as related to phosphorus status in soybean. *Plant Soil* 261, 77–84. doi: 10.1023/B:PLSO.0000035552.94249.6a

Wang, X., Shen, J., and Liao, H. (2010). Acquisition or utilization, which is more critical for enhancing phosphorus efficiency in modern crops? *Plant Sci.* 179, 302–306. doi: 10.1016/j.plantsci.2010.06.007

Wang, X., Wang, Y., Tian, J., Lim, B. L., Yan, X., and Liao, H. (2009). Overexpressing AtPAP15 enhances phosphorus efficiency in soybean. *Plant Physiol.* 151, 233–240. doi: 10.1104/pp.109.138891

Wasaki, J., Maruyama, H., Tanaka, M., Yamamura, T., Dateki, H., Shinano, T., et al. (2009). Overexpression of the LaSAP2 gene for secretory acid phosphatase in white lupin improves the phosphorus uptake and growth of tobacco plants. *Soil Sci. Plant Nut*. 55, 107–113. doi: 10.1111/j.1747-0765.2008.00329.x

Williams, A., Manoharan, L., Rosenstock, N. P., Olsson, P. A., and Hedlund, K. (2017). Long-term agricultural fertilization alters arbuscular mycorrhizal fungal community composition and barley (Hordeum vulgare) mycorrhizal carbon and phosphorus exchange. *New Phytol.* 213, 874–885. doi: 10.1111/nph.14196

Wissuwa, M., Gamat, G., and Ismail, A. M. (2005). Is root growth under phosphorus deficiency affected by source or sink limitations? *J. Exp. Bot.* 417, 1943–1950. doi: 10.1093/jxb/eri189

Wu, F., Dong, M., Liu, Y., Ma, X., An, L., Young, J. P. W., et al. (2011). Effects of long-term fertilization on AM fungal community structure and Glomalin-related soil protein in the Loess Plateau of China. *Plant Soil* 342, 233–247. doi: 10.1007/s11104-010-0688-4

Xavier, L. J. C., and Germida, J. J. (1997). Growth response of lentil and wheat to Glomus clarum NT4 over a range of P levels in a Saskatchewan soil containing indigenous AM fungi. *Mycorrhiza* 7, 3–8. doi: 10.1007/s005720050156

Xu, X., Thornton, P. E., and Post, W. M. (2013). A global analysis of soil microbial biomass carbon, nitrogen and phosphorus in terrestrial ecosystems. *Global Ecol. Biogeogr.* 22, 737–749. doi: 10.1111/geb.12029

Yadav, R. S., and Tarafdar, J. C. (2003). Phytase of fungi in arid and semi-arid soils and their efficiency in hydrolysing different organic P compounds. *Soil Biol. Biochem.* 35, 1–7. doi: 10.1016/S0038-0717(03)00089-0

Yao, Q., Li, X. L., Feng, G., and Christie, P. (2001). Mobilization of sparingly soluble inorganic phosphates by the external mycelium of an arbuscular mycorrhizal fungus. *Plant Soil* 230, 279–285. doi: 10.1023/A:1010367501363

Ye, D., Zhang, X., Li, T., Xu, J., and Chen, G. (2018). Phosphorus-acquisition characteristics and rhizosphere properties of wild barley in relation to genotypic differences as dependent on soil phosphorus availability. *Plant Soil* 423, 503–516. doi: 10.1007/s11104-017-3530-4

Yoneyama, K., Xie, X., Kim, H. I., Kisugi, T., Nomura, T., Sekimoto, H., et al. (2012). How do nitrogen and phosphorus deficiencies affect strigolactone production and exudation? *Planta* 235, 1197–1207. doi: 10.1007/s00425-011-1568-8

Yoneyama, K., Xie, X., Kusumoto, D., Sekimoto, H., Sugimoto, Y., Takeuchi, Y., et al. (2007). Nitrogen deficiency as well as phosphorus deficiency in sorghum promotes the production and exudation of 5-deoxystrigol, the host recognition signal for arbuscular mycorrhizal fungi and root parasites. *Planta* 227, 125–132. doi: 10.1007/s00425-007-0600-5

Yousefi, A. A., Khavazi, K., Moezi, A. A., Rejali, F., and Nadian, H. A. (2011). Phosphate solubilizing bacteria and arbuscular mycorrhizal fungi impacts on inorganic phosphorus fractions and wheat growth. *World Appl. Sci. J.* 15, 1310–1318.

Zaidi, A., and Khan, M. S. (2005). Interactive effect of rhizotrophic microorganisms on growth, yield, and nutrient uptake of wheat. *J. Plant Nutr.* 28, 2079–2092. doi: 10.1080/01904160500320897

Zhang, Q., Blaylock, L. A., and Harrison, M. J. (2010). Two *Medicago truncatula* half-ABC transporters are essential for arbuscules development in arbuscular mycorrhizal symbiosis. *Plant Cell* 22, 1483–1497. doi: 10.1105/tpc.110.074955

Zhu, J., Brown, K. M., and Lynch, J. P. (2010). Root cortical aerenchyma improves the drought tolerance of maize (*Zea mays* L.). *Plant Cell Environ.* 33, 740–749. doi: 10.1111/j.1365-3040.2009.02099.x

Conflict of Interest Statement: The authors declare that the research was conducted in the absence of any commercial or financial relationships that could be construed as a potential conflict of interest.

frontiers in Plant Science

ORIGINAL RESEARCH
published: 05 June 2018
doi: 10.3389/fpls.2018.00735

Cellular Patterning of *Arabidopsis* Roots Under Low Phosphate Conditions

George Janes[1], *Daniel von Wangenheim*[1], *Sophie Cowling*[1], *Ian Kerr*[2], *Leah Band*[1], *Andrew P. French*[1,3] *and Anthony Bishopp*[1]*

[1] Centre for Plant Integrative Biology, School of Biosciences, University of Nottingham, Loughborough, United Kingdom, [2] Queen's Medical Centre, University of Nottingham Medical School, Nottingham, United Kingdom, [3] School of Computer Science, University of Nottingham, Nottingham, United Kingdom

Phosphorus is a crucial macronutrient for plants playing a critical role in many cellular signaling and energy cycling processes. In light of this, phosphorus acquisition efficiency is an important target trait for crop improvement, but it also provides an ecological adaptation for growth of plants in low nutrient environments. Increased root hair density has been shown to improve phosphorus uptake and plant health in a number of species. In several plant families, including Brassicaceae, root hair bearing cells are positioned on the epidermis according to their position in relation to cortex cells, with hair cells positioned in the cleft between two underlying cortex cells. Thus the number of cortex cells determines the number of epidermal cells in the root hair position. Previous research has associated phosphorus-limiting conditions with an increase in the number of cortex cell files in *Arabidopsis thaliana* roots, but they have not investigated the spatial or temporal domains in which these extra divisions occur or explored the consequences this has had on root hair formation. In this study, we use 3D reconstructions of root meristems to demonstrate that the radial anticlinal cell divisions seen under low phosphate are exclusive to the cortex. When grown on media containing replete levels of phosphorous, *A. thaliana* plants almost invariably show eight cortex cells; however when grown in phosphate limited conditions, seedlings develop up to 16 cortex cells (with 10–14 being the most typical). This results in a significant increase in the number of epidermal cells at hair forming positions. These radial anticlinal divisions occur within the initial cells and can be seen within 24 h of transfer of plants to low phosphorous conditions. We show that these changes in the underlying cortical cells feed into epidermal patterning by altering the regular spacing of root hairs.

Keywords: developmental biology, radial patterning, phosphate deficiency, root anatomy, *Arabidopsis*, root hair, cortex, light sheet microscopy

OPEN ACCESS

Edited by:
Alex Joseph Valentine, Stellenbosch University, South Africa

Reviewed by:
Taras P. Pasternak, Albert Ludwigs Universität Freiburg, Germany
Jitender Giri, National Institute of Plant Genome Research (NIPGR), India

***Correspondence:**
Anthony Bishopp
anthony.bishopp@nottingham.ac.uk

Specialty section:
This article was submitted to Plant Nutrition, a section of the journal Frontiers in Plant Science

Received: *15 February 2018*
Accepted: *15 May 2018*
Published: *05 June 2018*

Citation:
Janes G, von Wangenheim D, Cowling S, Kerr I, Band L, French AP and Bishopp A (2018) Cellular Patterning of Arabidopsis Roots Under Low Phosphate Conditions. Front. Plant Sci. 9:735. doi: 10.3389/fpls.2018.00735

INTRODUCTION

Phosphorus (P) is a critical macronutrient and essential for plant growth. Unlike nitrogen or ammonium, which are soluble and diffuse through the soil, phosphate (Pi) is immobile within the soil as it often binds clay particles and forms insoluble precipitates (Brady and Weil, 2008). This means that the region around roots becomes quickly depleted of phosphate. Plants have developed several strategies for increasing phosphate acquisition, including changes to root architecture

(López-Bucio et al., 2002) and through root hairs (Bates and Lynch, 1996; Ma et al., 2003). Studies in both *Arabidopsis* (using the *root hair defective - rhd2* - mutant) and barley (using the *bald root barley - brb* - mutant) have demonstrated reduced growth in low Pi soils of hairless mutants (Bates and Lynch, 2001; Gahoonia and Nielsen, 2004).

Plants may exhibit different root hair adaptations to low P. For example, tomato, spinach, rape and *Arabidopsis* all exhibit an increase in root hair length under low Pi (Foehse and Jungk, 1983; Ma et al., 2001; Bhosale et al., 2018). However, these species also respond by increasing their root hair density in low Pi conditions. A recent study of root hair traits in 166 accessions of *Arabidopsis thaliana* showed that root hair density and length were not correlated, and that the genotypes that showed the greatest increase in root hair density under low Pi were mostly those that had fewer and shorter root hairs under Pi replete conditions (Stetter et al., 2015).

Arabidopsis epidermal cells can acquire one of two fates, they can form trichoblasts that go on to produce root hairs, or they can form atrichoblasts that cannot form root hairs. In wild-type plants, these two cell types form continuous files extending through the root meristem. The cell fate decision is controlled through positional information transmitted from the cortex; trichoblasts form in epidermal cells that overly the cleft between to cortex cells, whilst atrichoblasts overlay just one cortical cell (**Figure 1**). In wild-type seedlings this results in a radial pattern in which files of trichoblasts are separated by one to three files of non-hair-bearing atrichoblasts (Dolan et al., 1993). The number of cells within each file is different, as trichoblasts are shorter than atrichoblasts (Dolan et al., 1993). Experimental analysis of master regulators of epidermal cell fate has shown that the differences in longitudinal cell length of trichoblasts is dependent upon the position of cells relative to the underlying cortex (Savage et al., 2013).

Pemberton et al. (2001) describe 3 types of epidermal patterning in angiosperms. They refer to the pattern in *Arabidopsis* of hair cells occurring in files separated by one to three files of non-hair cells as type 3. This type of patterning was found in all members of the Brassicaceae examined, as well as other families within the Brassicales and Caryophyllales. Most angiosperms displayed type 1 epidermal patterning, in which all epidermal cells can produce root hairs.

The molecular mechanism regulating epidermal cell fate is well understood in *Arabidopsis*. A transcriptional complex involving the transcription factors - WEREWOLF (WER), GLABRA 2 (GL2), ENHANCER OF GLABRA3 (EGL3), and TRANSPARENT TESTA GLABRA1 (TTGI) is required to specify atrichoblast identity (Grebe, 2012), and mutations in these genes result in plants with increased root hairs (Galway et al., 1994; Rerie et al., 1994; Masucci et al., 1996; Lee and Schiefelbein, 1999; Walker et al., 1999; Bernhardt, 2003). Whereas the transcription factors CAPRICE (CPC), TRIPTYCHON (TRY), and ENHANCER OF CAPRICE (ETC) promote trichoblast identity, and mutations in these genes result in few to no root hairs (Wada et al., 1997; Schellmann et al., 2002; Kirik et al., 2004). Together these components form a regulatory circuit, with CPC moving to trichoblasts where it competes with WER to bind the GL3-EGL3-TTG1 complex (Bernhardt, 2003). JACKDAW (JKD) acts in a non-cell-autonomous manner from the underlying cortex cells to specify trichoblast vs. atrichoblast fate by regulating *GL2*, *CPC*, and *WER* expression via the LRR kinase SCRAMBLED (SCM) (Kwak and Schiefelbein, 2008; Hassan et al., 2010).

A plant such as *Arabidopsis* that exhibits type 3 root hair patterning could increase root hair density either in the longitudinal domain by a reduction in cell elongation, or in the radial domain by increasing the number of epidermal cells that differentiate as trichoblasts. Indeed, phosphate deficiency has been shown to result in shorter epidermal cells and greater root hair production in *Arabidopsis* (Sánchez-Calderón et al., 2005).

Under normal conditions, *Arabidopsis* roots almost always have exactly eight cortical cells. However, when grown on low Pi media, *Arabidopsis* plants show an increase in the number of cortical cells and this results in an increase in the number of cells at the trichoblast position (Ma et al., 2003; Zhang et al., 2003; Cederholm and Benfey, 2015). Mathematical simulations of epidermal cell fate in which different signal inputs are supplied from the cortex, support a model where a time-evolving signal specifies the recruitment of atrichoblasts from a default trichoblast pathway to control cell length and therefore delay atrichoblast cell fate specification (Savage et al., 2013). These simulations suggest that even under Pi deficient conditions, the core mechanisms regulating epidermal cell fate is functional although plants show increased cell length and form additional trichoblast files (Savage et al., 2013).

In this manuscript, we use a combination of different microscopy techniques to investigate anatomical changes in root radial patterning of *Arabidopsis* in response to low Pi. We show that increases in cortical cell file number occur dynamically within the meristem and respond rapidly to reductions in Pi. Furthermore, we show that these changes in the cortical tissues result in alterations in the final root hair patterning.

MATERIALS AND METHODS

Plant Material and Growth Conditions

All *Arabidopsis* experiments were performed using *A. thaliana* (Columbia ecotype) seeds. All seeds were sterilized with 5% sodium hypochlorite for 5 mins before being rinsed with 70% ethanol with 0.01% Triton X-100 once and several times with sterile water. Seeds were then sown on agar plates, sealed with micropore tape (3 M) and cold treated overnight to synchronize germination. Plants were grown under 12 h light, 12 h dark conditions at 21°C. To ensure consistency of our experiments in relation to the photoperiod, all plants were moved into the growth room within the first 2 h of the light period. Harvesting of roots for microscopy and transfer between different media was always done within the same 2 h period at the start of the light cycle.

Low and high P/low and high Fe media was made using a modified Hoaglands medium consisting of the concentrations of minerals listed in **Table 1**. 0.5g/L of 2-(*N*-morpholino)ethanosulfonic acid (MES) was added and the pH of the media was adjusted to 5.7 using potassium hydroxide.

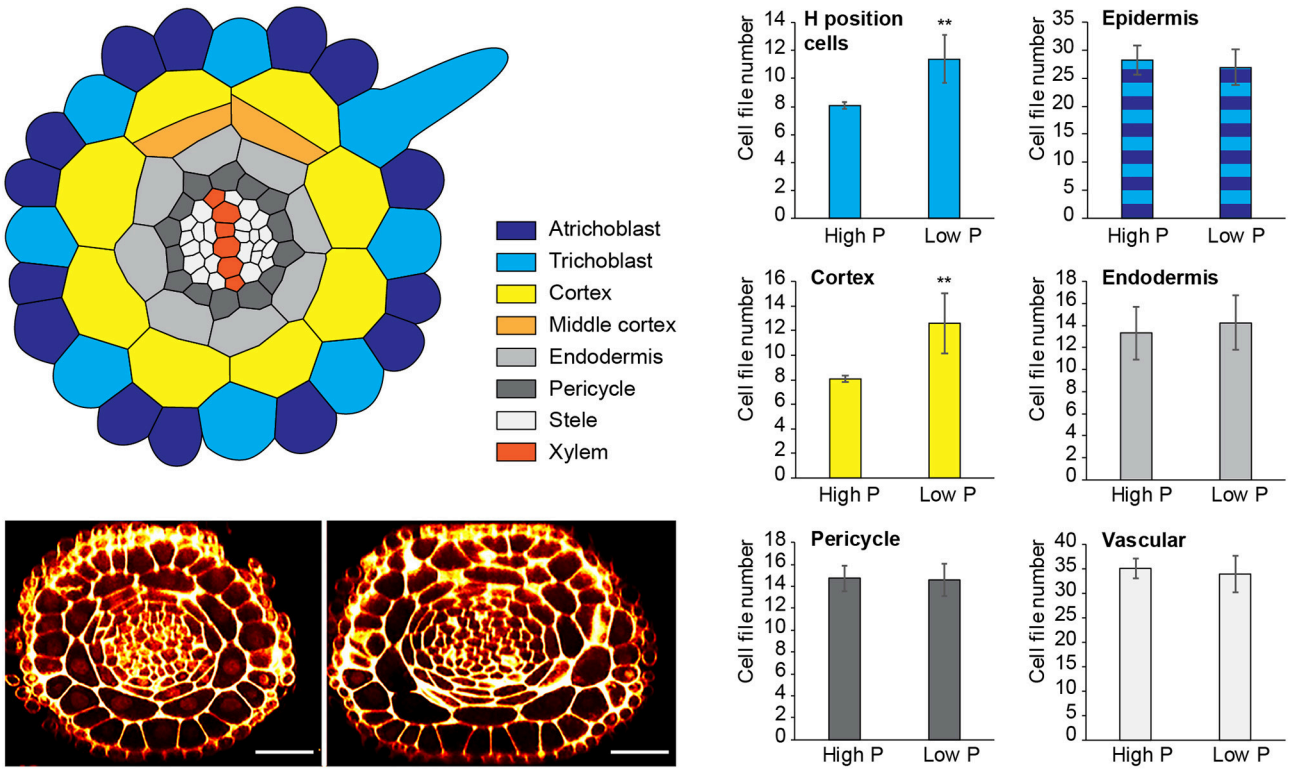

FIGURE 1 | Changes to radial anatomy under low phosphate are limited to changes in cortex and hair-cell number. Schematic diagram showing the radial organization of tissues in the *Arabidopsis* root. Concentric rings of tissues can be seen radiating out from the central vascular cylinder; trichoblast positions in epidermal cells at the cleft between two cortex cells can be seen (light blue). Layers of middle cortex can be seen beginning to form at the xylem poles (orange). Representative images of high Pi **(Left)** and low Pi **(Right)** treated roots in transverse section show how the radial organization differs between treatments, scale bar = 50 μm, Bar charts showing number of cells files in each tissue visualized in confocal microscope cross sections for two phosphate treatments: "high P" (1 mM), "low Pi" (50 μM). Roots of seedlings growing on high Pi (1 mM), or low Pi (50 μM) have, on average, 8 and 12 cortex cell files respectively ($p \leq 0.001$). This change corresponds to a change in the average number of hair position epidermal cell files (H cells) of 8 to 11 (**$p \leq 0.001$).

Media was then added to bottles containing Sigma purified agar (catalog number A1296) 8 g/L and autoclaved before being used to pour plates.

Pseudo-Schiff Propidium Iodide Staining

Roots for PS-PI staining were harvested from the plate and fixed immediately in a 50% methanol 10% acetic acid aqueous solution and kept at 4°C overnight. Roots were then rinsed in sterile, deionised water three times before being incubated at room temperature in 1% periodic acid for up to 40 min. Tissue was rinsed 2–3 times with sterile, deionised water and then left in PS PI solution for 1–2 h [0.015 N hydrochloric acid (HCl), 100 mM sodium metabisulphite; 50 μl/ml propidium iodide solution [1 mg/ml], freshly added each time]. Roots were again rinsed 2–3 times with water before being mounted on slides with 40% glycerol 30% chloral hydrate in water and left in the dark over night to clear.

Microscopy and Image Processing

Stained cleared roots were imaged using a Leica SP5 confocal microscope. A 488 nm laser was used to excite PI fluorescence for imaging, PI fluorescence was collected using either a photomultiplier tube (PMT) or hybrid detector at between 600 and 800 nm.

For the generation of optical sections from PS-PI stained/cleared roots, Z-stacks of roots were generated using LAS-X Leica software then dissected in orthogonal view using ImageJ image analysis software. An example z stack is shown in Supplemental Movie 1. Cell counts were performed using a cell counter function in the same software. We use post-mitotic cell positions to infer previous cell divisions.

Light-sheet microscopy was performed using a Zeiss Lightsheet Z.1. A 514 nm laser was used to excite YFP as well as propidium iodide. Emission wavelengths were filtered using a bandpass filter BP 525–545 for YFP and BP 575–615 for propidium iodide. Root tips were excised from plants and stained in 5–10 μl propidium iodide (PI)/ml in deionised H_2O and mounted in to a glass capillary (1 mm inner diameter) using low melting temperature agarose (Sigma-Aldrich) mixed with fluorescent beads from the PS-Speck Microscope Point Source Kit (ThermoFisher Scientific). Roots were imaged along six angles using the Multiview function in ZEN software. The ImageJ plugin Multiview-Reconstruction was used to assemble

TABLE 1 | Table showing concentrations of different nutrient components used in low Pi high Fe, high Pi high Fe, low Pi low Fe, and high Pi low Fe media preparations used for low and high P/low and high Fe treatments.

Nutrient	Low Pi high Fe	High Pi high Fe	Low Pi low Fe	High Pi low Fe
KNO_3	3 mM	3 mM	3 mM	3 mM
$Ca(NO_3)2\ 4H_2O$	2 mM	2 mM	2 mM	2 mM
$MgSO_4\ 7H_2O$	0.5 mM	0.5 mM	0.5 mM	0.5 mM
$(NH_4)_2S0_4$	425 μM	0	425 μM	0
$NH_4H_2PO_4$	50 μM	1 mM	50 μM	1 mM
H_3BO_3	25 μM	25 μM	25 μM	25 μM
ZnNa EDTA	2 μM	2 μM	2 μM	2 μM
$(NH_4)_6Mo_7O_{24}\ 4H_2O$	1 μM	1 μM	1 μM	1 μM
KCl	50 μM	50 μM	50 μM	50 μM
$MnSO_4\ H_2O$	2 μM	2 μM	2 μM	2 μM
$CuSO_4\ 5H_2O$	1 μM	1 μM	1 μM	1 μM
Fe-EDTA	50 μM	50 μM	5 μM	5 μM

multiview stacks in to a final stack using fluorescent beads as points of interest for registration (Preibisch et al., 2010, 2014).

Cell files of different cell types were counted by producing radial cross sections of roots from confocal Z-stacks assembled in ImageJ software, viewed in orthogonal views and counted using the cell counter plugin.

RESULTS

Changes in Radial Cell Proliferation in Response to Phosphate Are Limited to Cortex Cells

Although previous reports have shown that cortical cell proliferation is increased when *A. thaliana* plants are grown on low phosphate media (Ma et al., 2003; Cederholm and Benfey, 2015), it has been unclear whether the cortex is the only cell type to undergo additional radial anticlinal divisions to increase cell file number. In order to provide a greater understanding of precisely which cell lineages responded to low phosphate, we investigated this in higher resolution by generating 3D reconstructions of the root meristem based on a combination of fixation and labeling with pseudo-Schiff propidium idodide and generating z stacks using confocal microscopy (see Supplemental Movie 1 for an example). *Arabidopsis thaliana* seeds were sown on media containing 1 mM (high P), 50 μM (low P), or 1 μM (very low P) and grown for 12 days. We generated orthogonal projections through roots with which we could count cell file numbers of different cell types (stele, pericycle, cortex, and epidermis) within the meristem (**Figure 1**). At this age, *Arabidopsis* plants begin to mature, and we see the formation of some middle cortex cells. Previous studies have reported that this is the result of periclinal cell divisions within the endodermal layer (Baum et al., 2002; Lee et al., 2016). We have not included the middle cortex within these cell counts and only count cortex cell files that are in contact with the overlying epidermis.

We found no significant change in the number of stele, pericycle or endodermal cell files or in the total number of epidermal cell files (**Figure 1**), with the stele having between 30 and 35 cell files, and the pericycle, endodermis, and total epidermal cell files having 14–16, 12–14, and 26–28 cell files respectively. The only tissue that exhibited a change in cell file number was the cortex, where the number of cell files increased from 8 (1 mM P) to an average of 12 (50 μM P) or 11 (1 μM P).

These results show that the radial cell proliferation was restricted to the cortex, and differ from those shown previously by Cederholm and Benfey (2015), who also observed differences in the number of endodermal as well as cortical cells. This could be due to differences in the age of plants analyzed. as this study used 12 day old plants, whereas that by Cederholm and Benfey (2015) used approximately 6 day old plants or may be due to differences in the composition of the media.

The Root Cortex Response to Low Phosphate Is Concentration Dependent

Different studies by a variety of groups investigating low Pi stress in *Arabidopsis* seedlings have used a variety of Pi concentrations to mimic a stress scenario. We therefore considered it important to determine the specific concentration of Pi that will trigger cortical cell proliferation, to facilitate comparisons with the plethora of data already existing for architectural and anatomical changes.

To find the lowest concentration of phosphate, at which a response in cortical cell file number (CCFN) was seen, plants were grown under a concentration range from 0 M to 1 mM Pi. All concentrations between 0 and 400 μM Pi elicited an increase in CCFN. Within this range there was little difference in the number of cell files, with 0 M, 50, 100, 200, and 400 μM all showing ∼10–11 cortex cell files (**Figure 2**). Root length and lateral root density was also measured for these plants, and it was observed that plants grown on <50 μM phosphate typically exhibited more severe stress symptoms than those grown on higher concentrations, including dramatic inhibition of growth, anthocyanin accumulation and chlorosis. After 9 days root lengths were 69 ± 9 mm on high Pi and 26 ± 1 mm on low Pi. These general plant phenotypes were similar to those previously reported for plants grown in phosphate deficient conditions, such as Bates and Lynch (1996) and Trull et al. (1997). These results show that the changes in CCFN occur at Pi concentrations that do not severely affect plant growth, suggesting that this is an adaptive response rather than simply a disorganization of the meristem in response to phosphate starvation.

It has been shown previously that iron concentration in media affects root architectural responses to low phosphate (Hirsch et al., 2006; Svistoonoff et al., 2007; Ward et al., 2008; Dong et al., 2017; Gutiérrez-Alanís et al., 2017) as under low Pi conditions roots can accumulate high concentrations of free iron in the root meristem. This accumulation seems to be particularly high in the QC and surrounding initials and has been suggested to have a toxic effect that can lead to meristem disorganization and mis-localisation of key patterning regulators such as the transcription factors SHR and SCR (Ticconi et al., 2004, 2009). Whilst there

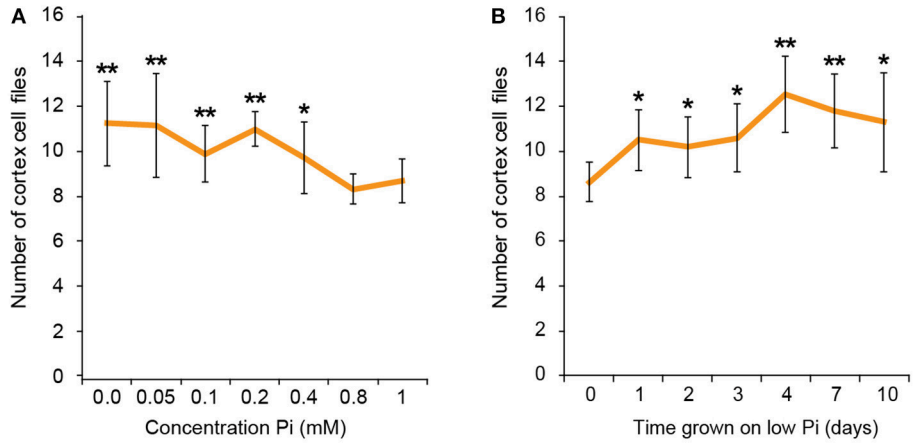

FIGURE 2 | Response to low phosphate is concentration and time dependent. Cortex cell file numbers increase when roots are exposed to medium containing 400 μM or lower. At lower concentrations the number of cortex cell files is as high as 13, but at 800 μM−1 mM the number of cortex cell files remains at 8 **(A)**. Error bars represent standard deviation. Number of plants used in cortex cell file counts 0 M: $n = 8$; 50 μM: $n = 12$; 100 μM: $n = 11$; 200 μM: $n = 10$; 400 μM: $n = 12$; 800 μM: $n = 11$; 1 mM: $n = 11$. **Statistically significant difference to 1 mM Pi ($p \leq 0.005$); *$p \leq 0.05$ **(A)**. Cortex cell file number increases to an average of 10 after 24 h exposure to low Pi, increasing to an average of 12 after 4 days. **(B)** Error bars represent standard error. Numbers of plants used in cell file counts 0 days: $n = 11$; 1 day: $n = 10$; 2 days: $n = 11$; 3 days: $n = 10$; 4 days: $n = 9$; 7 days: $n = 10$; 10 days: $n = 10$. **Statistically significant difference to 1 mM Pi ($p \leq 0.005$); *$p \leq 0.05$.

is increasing evidence that iron toxicity may be responsible for some of the extreme responses observed for *Arabidopsis* plants grown on agar plates under phosphate limiting conditions (such as a severe reduction in primary root length). More recent studies have mitigated this iron toxicity effect when using media with <1 μM Pi by reducing iron levels concomitantly with Pi reduction.

To test whether the response in CCFN to reduced phosphate in the media was primarily associated with a lack of Pi or an excess of iron, we set up experiments with *A. thaliana* sown on to agar plates containing media with high Pi high Fe (1 mM $NH_4H_2PO_4$, 50 μM Fe-EDTA), high Pi low Fe (1 mM $NH_4H_2PO_4$, 5 μM Fe-EDTA), low Pi high Fe (50 μM $NH_4H_2PO_4$, 50 μM Fe-EDTA), and low Pi low Fe (50 μM $NH_4H_2PO_4$, 5 μM Fe-EDTA). We counted CCFN in all these lines, and observed that when plants are exposed to low Pi, but also 10-fold less iron (5 μM Fe-EDTA) an increase in CCFN was still present. On this media, roots have a CCFN of 11; a result that is higher than on low Pi high Fe (**Figure 3**). This data supports the hypothesis that alterations in CCFN seen in Pi limiting conditions are primarily a response to low Pi and not due to an increase in Fe and/or Fe toxicity in the root.

Changes to Radial Cortex Anatomy Occur After 24 H Exposure to Low Phosphate Just Above the Cortex Endodermal Initial

Previous studies have shown that cortex proliferation in response to low Pi in *Arabidopsis* roots is visible within the root tip. However none of this work provided an explanation as to where exactly in the root meristem the proliferative divisions take place. In order to address this gap in the knowledge, we assembled 3-dimensional image stacks using confocal microscopy on chloral hydrate cleared pseudo-Schiff propidium iodide stained root tips grown on low or high P. By assembling these image stacks in ImageJ we determined the number of cortex cell files at specific cell tiers behind the quiescent center. Counting the number of cortex cell files at each tier revealed a trend for decreasing CCFN with distance from the QC in low Pi treated roots (**Figure 4**). Under high Pi conditions, CCFN was consistently 8 at each of the 10 tiers distal to the QC (**Figure 4**). However under low Pi the average number of CCFs at tier one is around 12, which then decreases to 11 at tier 10 (**Figure 4**). In order to reveal a clear view on the cortex cells only, we isolated the cortex cells from the rest of the cell layers by manually drawing a black mask in Adobe After Effects. We unrolled this layer (using ImageJ's function RadialReslice) to produce a longitudinal image of the cortical cell lineages (**Figure 5** and Supplemental Movie 2). Whilst 8 continuous cell files can be traced from just above the quiescent center until the start of the elongation zone for plants grown on high Pi, when grown on low Pi, we observe multiple events in which CCFN is increased in relatively small numbers of cells. From these images it was concluded that the proliferative divisions occur within the meristem, and as we saw many independent events altering CCFN in a relatively small longitudinal domain. We speculate that this is likely to be a dynamic processes perhaps responding to local levels of Pi.

We next asked if the changes in CCFN observed on low phosphate were a dynamic event capable of adapting rapidly to a low phosphate environment. We reasoned that if this cortical re-patterning is to confer an adaptive advantage to, then it should occur quickly, for example in the case of a root grows though a patch of soil low in P. To address the dynamics of this response, seedlings were grown on plates containing replete levels of Pi (1 mM). Plants were then transferred to 50 μM Pi containing medium after 4, 7, 10, 11, 12, and 13 days. Twenty four hours after the final transfer, when seedlings were 14 days old, roots were harvested from all the 50 μM Pi plates, alongside control

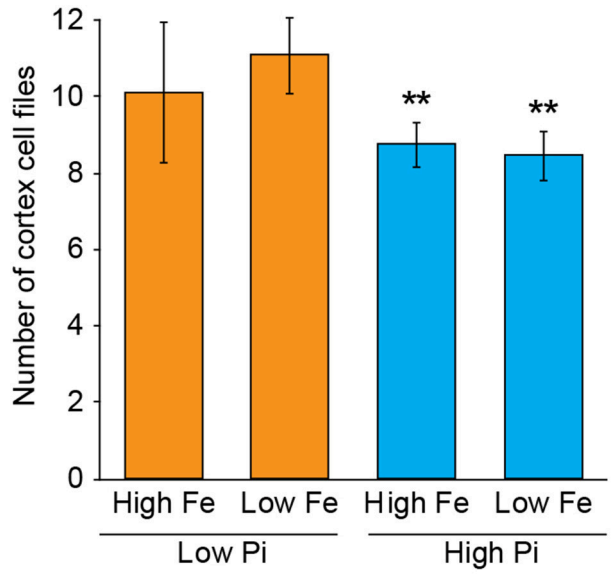

FIGURE 3 | Exposure to low Pi with low iron maintains the CCFN response of *Arabidopsis* roots to low Pi. Pseudo-Schiff propidium iodide stained roots imaged using confocal microscopy to generate optical transverse cross sections. Bar chart showing average CCFN for each treatment: LPHFe, CCFN = 10, $n = 11$; LPLFe, CCFN = 11, $n = 11$; HPHFe, CCFN = 8.75, $n = 12$; HPLFe, CCFN = 8.45, $n = 11$. Error bars represent standard deviation. **Statistically significant difference from HPHFe ($p \leq 0.001$); *statistically significant difference from HPHFe ($p \leq 0.05$).

plants from 1 mM Pi plates and roots imaged using pseudo-Schiff staining coupled with confocal microscopy. Strikingly, we observed a CCFN response to low Pi within 1 day of transferring plants to low Pi (**Figure 4**). Within this timeframe we saw a statistically significant increase in average CCFN from 8.6 to 10.5.

After this time point, the average CCFN remains between 9.5 and 12.5 with a small amount of variation depending on the transfer stage (**Figure 3**). These findings are broadly in line with other changes in plant response to low Pi as they occur much slower than changes in gene response. For example, changes in the expression of transcription factors such as WRKY75 occur within 3 h of transfer to low phosphate media (Devaiah et al., 2007).

Proliferation of Cortical Cells Alters Epidermal Patterning

Previously, it had been hypothesized that altering cortical cell file number would provide a mechanism through which root hair density can be increased in the radial dimension. We examined positions of epidermal cells laying in the H (trichoblast) position (i.e., spanning a junction between two cortical cells) and the N position (i.e., overlaying just one cortical cell). We found that the number of epidermal cells in the H position increased from 8 (1 mM P) to 11 (50 μM P) under Pi limiting conditions (**Figures 1**, **4B**). These results support previous observations by other researchers (Ma et al., 2001).

In order to confirm that this change in positional information for a selected subset of epidermal cells was sufficient to alter cell fate specification in these cells, we used light sheet microscopy to fully reconstruct 3D representations of mature tissues to evaluate the radial distribution of both expression of the root hair marker COBRA-like *COBL9* (Roudier et al., 2002) and the presence of the root hairs themselves in context of the underlying cortical cell geometry. We used light sheet microscopy because it enables a large volume to be imaged rapidly, it can be used with living samples and it does not require any clearing protocol which could change the cellular structural integrity. When plants were grown on high phosphate we observed a pattern as previously reported with files of trichoblasts over clefts between cortical cells, with these files being separated by 1–3 files of atrichoblasts (**Figures 6–8** and Supplemental Movies 3–5). We only occasionally saw deviations from this stereotypical pattern, with for example, occasional ectopic expression of *COBL9* in epidermal cells overlaying a single cortex cell. When plants were grown under low phosphate we saw a breakdown of this regular spacing and frequently found four non-typical root hair patterning scenarios. The first scenario was that we saw adjacent files of trichoblasts as a result of two neighboring epidermal cells overlying two adjacent cortex cell clefts (**Figure 5**). In reconstructions of roots grown on low Pi, we not only observed root hair forming cells forming at positions overlaying a cleft between two cortical cells, but in all reconstructions, we saw several examples where epidermal cells both expressing *COBL9* and forming root hairs were found over a single cortical cell (**Figures 6–8** and Supplemental Movies 3–5), which we denoted as scenario 2. We also observed several instances in which epidermal cells lying in the cleft between two cortex cells neither express *COBL9* nor form root hairs (scenario 3). Finally, the fourth scenario we noted was that of root hairs emerging from a file of epidermal cells overlaying cleft between more than two cortical cells. For roots grown on high or low Pi we observe examples in which cells expressing *COBL9* either fail to form root hairs or only produce very short root hairs, although this is likely to come in part from an asymmetry in the availability of water imposed by the agar plate (Bao et al., 2014). Using a conventional microscopy approach we measured the root hair length on the side of the root facing away from the agar plate and observed an increase in root hair length for plants grown on low Pi (High Pi, 153 ± 73 μm; Low Pi, 270 ± 128 μm) Collectively, these results suggest that rather than simply increasing trichoblast number, alterations in the cortical cell patterning file number have significant effects in which the regular root hair patterning mechanism of the mature root becomes unstable and a more chaotic pattern emerges (**Figures 6–8**).

DISCUSSION

Arabidopsis thaliana roots have previously been shown to respond to low phosphate by producing extra cortical cells (Ma et al., 2001; Cederholm and Benfey, 2015). However, although this phenomenon had been reported, it had not been explored in great detail. For example, it was unclear if the cortex was the

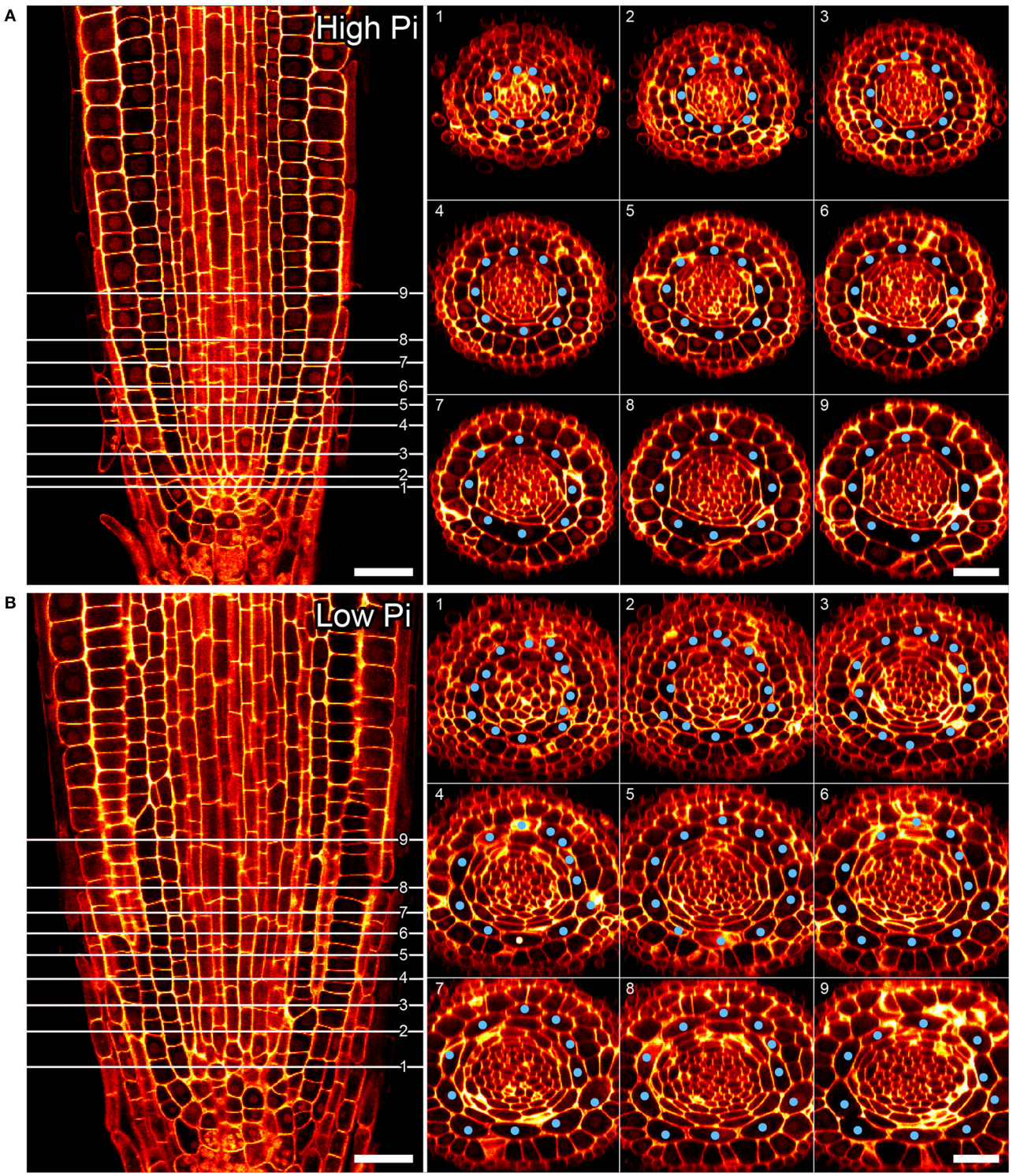

FIGURE 4 | Cortical cell proliferation occurs close to the root apical meristem. Reconstructed confocal Z-stacks of imaged pseudo-Schiff propidium iodide stained roots show that cortex cell file (blue spots) numbers are highest in proximity to the growing tip/cortex endodermis initial (CEI) cells in roots grown on 50 μM phosphate **(B)**. Plant roots grown on 1 mM phosphate containing medium exhibit 8 cortex cell files from 1 to 10 cell tiers (white lines) behind the cortex endodermal initial cell **(A)**. Cell file counts high P: $n = 17$; low Pi $n = 30$, differences between low and high Pi statistically significant $p \leq 0.001$. Scale bar = 25 μm.

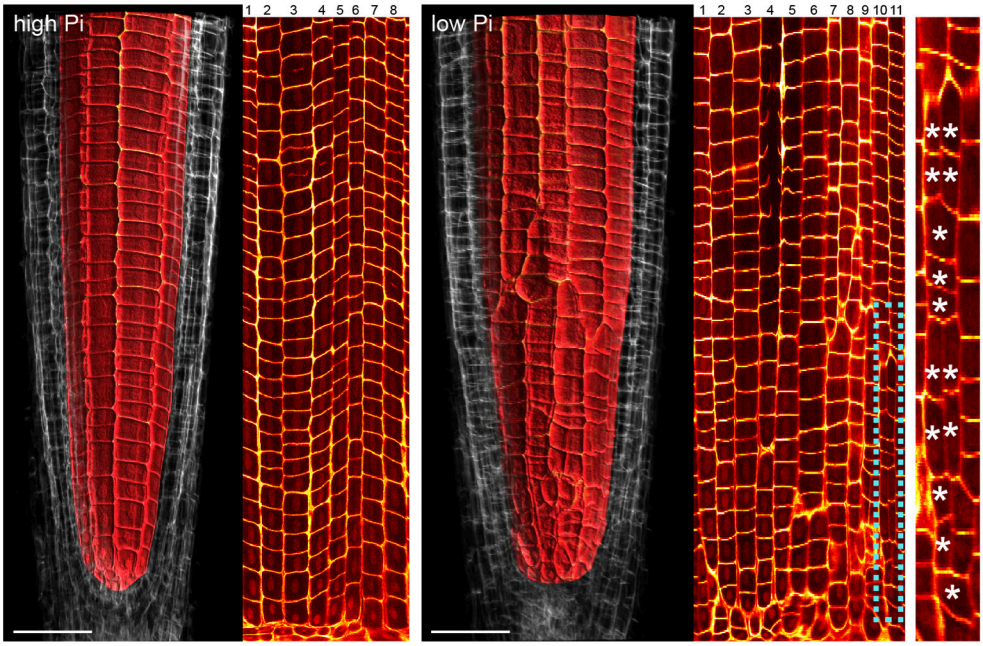

FIGURE 5 | Cell lineage analyses reveal multiple cell division events leading to increases in radial anticlinal cortical cell file number. Unrolled images showing cell lineages in the cortex of *Arabidopsis* roots under high Pi **(Left)** and low Pi **(Right)**. Using Adobe After Effects we digitally dissected the membranes between cortex cells. In ImageJ. We unrolled this data set in order to visualize the cortical cell lineages within the root meristem. The dissected cell layers unrolled are shown in Supplemental Movie 2. Whilst 8 continuous cell files can be traced from just above the quiescent center until the start of the elongation zone for plants grown on high Pi, when grown on low Pi, we observe multiple events in which CCFN is increased in relatively small numbers of cells. These events are marked with asterisks. Scale bars = 50 μm.

only cell type to show increased cell file number under low Pi, it was unknown which cortical cells underwent extra cell divisions, the exact timing of this response was unknown and it was unclear whether this was a specific response to low Pi or a result of iron toxicity. Furthermore, although changes in CCFN were reported, these were not correlated experimentally with alterations in root hair density or patterning.

To address these issues we exploited two methods for generating 3D reconstructions of the root meristem for plants grown under high and low Pi conditions. The first involved fixing roots and using a modified pseudo Schiff reagent to stain cell walls with propidium iodide. These stained roots were then visualized on a confocal microscope. This technique allowed us to image around 20–30 roots for each sample in a medium throughput manner. This confocal based approach allowed us to build upon the original data produced by Ma et al. (2003) that used just 6 roots. The second approach was based upon analysis using light sheet microscopy of roots stained with propidium iodide. In order to fully resolve the entire volume of the mature root we captured Z-stacks along six different angles coupled with the bead-based multiview reconstruction alignment (Preibisch et al., 2010). Four roots grown on low Pi and four roots grown on high Pi were analyzed, as well as a further 2 roots on high Pi and 3 roots on low Pi expressing the *COBL9* marker. This has allowed us to observe that trichoblasts can form in positions overlaying a single cortical cell, in plants grown on low Pi; a phenomenon that has not previously been described.

Collectively our data builds upon previous work showing files of extra cortical cells throughout the meristem (Cederholm and Benfey, 2015) by demonstrating that several rounds of radial anticlinal divisions occur close to the root apex. Our experiments transferring plants from Pi replete to Pi limiting conditions show that anatomical changes occur quickly, with the first changes occurring within 24 h of transfer. These results are in keeping with those required of an adaptive response evolved to maximize Pi acquisition from soil. For a root to maximize Pi capture from a heterogeneous soil environment, the developmental program controlling root hair patterning must be able to adapt quickly to changes in the local environment at a range of concentrations. We observed that changes in CCFN occurred at Pi concentrations between 0 and 400 μM, with the strongest effect seen at 50 μM. This was surprising as this concentration is far above what is seen is most soils (Raghothama, 1999), but this could be explained as the availability of Pi on plates is likely to be very different from that in the soil. Recently the relevance of traditional gel-based systems for investigating the effects of phosphate limitation on root growth has been challenged, and a new system has been developed in which Pi is adsorbed onto Al_20_3 particles (Hanlon et al., 2018). This has the advantage of delivering buffered levels of Pi to roots at concentrations closer to the Pi levels of natural soils. Although there are changes to *Arabidopsis* root architecture and anatomy when roots are grown on buffered vs. non-buffered medium, increases in CCFN on low Pi medium have been observed with both systems (Hanlon et al., 2018). This supports existing data showing that changes in CCFN are a direct response to low Pi, however it also indicates that alterations in the responses seen at different concentrations of Pi in this study cannot be

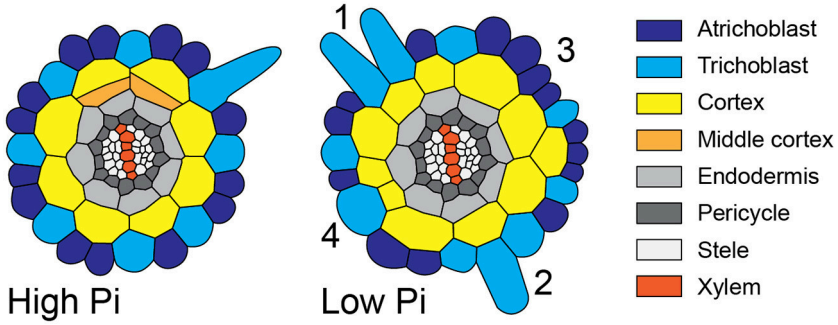

FIGURE 8 | Schematic diagram showing atypical root hair patterning scenarios found under low Pi conditions. Schematic representations of root radial cross sections under high Pi **(Left)** and low Pi **(Right)** conditions showing changes in tissue patterning including four atypical root hair patterning scenarios. These scenarios are: (1) the formation of 2 adjacent hair cells files forming over two adjacent cortical cells clefts, (2) the formation of a hair cell in a non-hair-cell position, (3) no root hairs forming from an H-cell file, and (4) one H cell file forming over two adjacent cortical cell clefts.

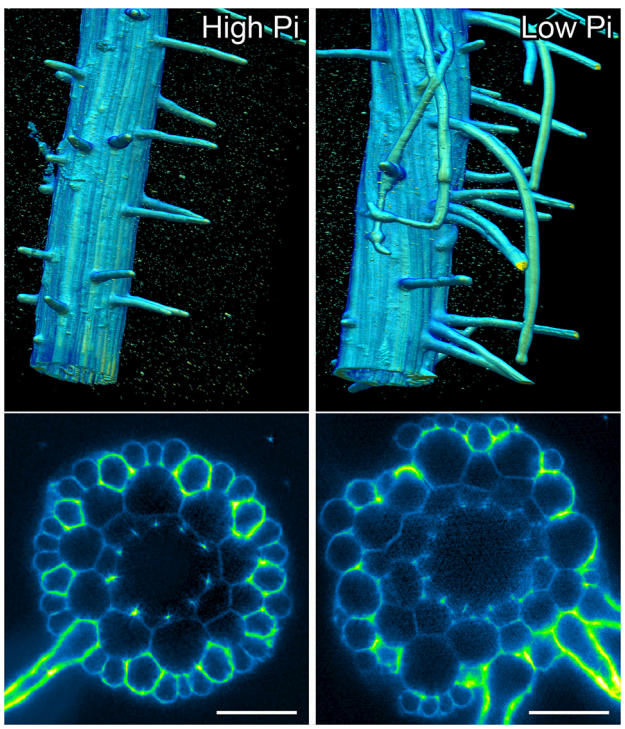

FIGURE 6 | Light sheet imaging reveals atypical root hair patterning scenarios under low Pi. Anatomy of a mature part of *Arabidopsis* under high Pi **(Left)** and low Pi conditions **(Right)**. Multi-view recording along six directions captured using Light Sheet Fluorescence Microscopy. A 3D reconstruction (Arivis Vision 4D software) of the fused image stack is shown in the upper panel and a single slice cross section is presented in the lower panel. Roots were stained with propidium iodide. Scale bars = 50 μm.

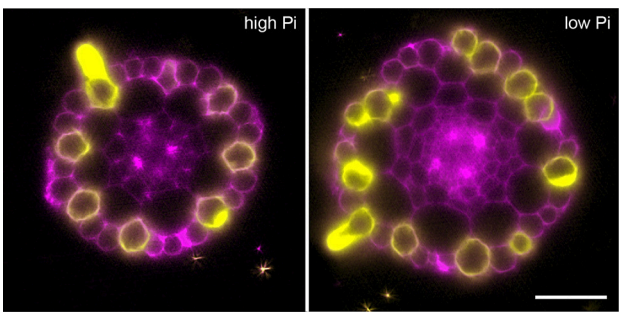

FIGURE 7 | Expression of the COBL9 marker shows atypical specification of trichoblast identity under low Pi. Anatomy of a mature part of *Arabidopsis* under high Pi **(Left)** and low Pi conditions **(Right)**. Multi-view recording along six directions captured using Light Sheet Fluorescence Microscopy to visualize the pCOBL9::GFP gene (yellow) and propidium iodide (magenta). Scale bars = 50 μm.

interpreted literally and do not represent levels found within soils.

Whilst our results were generally in keeping with those published previously (Ma et al., 2003; Cederholm and Benfey, 2015), they differed in a few minor aspects. Cederholm and Benfey (2015) reported changes in the number of endodermal cells. However in our assay the numbers of vascular cells, pericycle cells, endodermal cells and total epidermal cells did not differ significantly between low and high Pi conditions. We also observed changes in cortical cell file number on transfer to Pi limiting conditions earlier than has been reported by other authors. Cederholm and Benfey (2015) report changes in cortical cell file number at 2 days post-transfer, Ticconi et al. (2009) report changes in ground tissue in the Pi hypersensitive phosphate *deficient root 2* (*pdr2*) mutant after 2 days of transfer; whilst we observed the first changes occurring after only 24 h.

One limitation for performing studies limiting phosphate on agar plates, is that under low Pi conditions, roots can accumulate high concentrations of free iron in the root meristem (Hirsch et al., 2006; Svistoonoff et al., 2007; Ward et al., 2008; Dong et al., 2017; Gutiérrez-Alanís et al., 2017). This can have a toxic effect leading to meristem disorganization and ultimately termination. Our data demonstrates that the increased cortical cell file number, is direct a result of low Pi rather than extra iron.

Although increased CCFN has been proposed to offer an advantage to improving Pi acquisition under low nutrient conditions, it is only one of several traits employed by *Arabidopsis* to increase root hair density, as decreased epidermal cell size impacts root hair density in the longitudinal dimension and increased root hair length can increase uptake of Pi from the soil (Foehse and Jungk, 1983; Ma et al., 2001). However, when we followed the radial distribution of root hairs and compared it with the underlying pattern imposed by the cortex, we observed alterations in the regular spacing of root hair cell rather than a general increase. We frequently, observed multiple files of root hairs forming adjacently (scenario 1), we observed root hairs forming in positions where the epidermal cells overlay just one cortical cell (scenario two), epidermal cells overlaying a cleft between two cortical cells producing no root hairs (scenario three), and root hairs forming from single epidermal cell files overlying two adjacent cortical cell clefts (scenario four). These scenarios are summarized schematically in **Figure 8**. However, we did not see a significant increase in the radial density of root hairs. Our results challenge the assumption that the trait of increased CCFN has evolved in species that exhibit type 3 root hair patterning as a mechanism specifically to increase root hair density, although it is possible that different effects could be observed at different concentrations of Pi.

It is important to develop understanding of the mechanisms through which roots respond to low nutrient environments in order to develop new lines that can utilize nutrients existing in the soil more efficiently. In this paper, we perform a detailed anatomical study of how radial anatomy is altered under low phosphorus in *Arabidopsis* and the effect that modulating cortical cell file number has on controlling density of root hairs in the radial dimension. This study will inform future programmes that may seek to modulate root hair density in plants similar to *Arabidopsis* as it challenges the utility of focusing on CCFN. It opens up interesting questions regarding whether increased cortical cell file number offers an alternative adaptive advantage to growth on low Pi, and provides an intriguing example for future studies about how patterning events in one tissue can affect patterning in others.

AUTHOR CONTRIBUTIONS

AB, GJ, and DvW designed experiments. GJ, SC, and DvW performed experiments and analyzed results. AB, GJ, and DvW wrote the manuscript with input from LB, AF, and IK.

FUNDING

The Zeiss Z.1 LSFM used in this study was funded through a BBSRC Alert14 equipment grant BB/M012212/1.

ACKNOWLEDGMENTS

This work was supported by the Biotechnology and Biological Sciences Research Council [grant number BB/L023555]. GJ is funded through a Doctoral Training Programme award. SC was funded through a Gatsby summer placement. DvW and AF were funded through the BBSRC [grant number BB/N018575/1] and AB through a Royal Society University Research Fellowship.

SUPPLEMENTARY MATERIAL

The Supplementary Material for this article can be found online at: https://www.frontiersin.org/articles/10.3389/fpls.2018.00735/full#supplementary-material

REFERENCES

Bao, Y., Aggarwal, P., Robbins, N. E., Sturrock, C. J., Thompson, M. C., Tan, H. Q., et al. (2014). Plant roots use a patterning mechanism to position lateral root branches toward available water. *Proc. Natl. Acad. Sci. U.S.A.* 111, 9319–9324. doi: 10.1073/pnas.1400966111

Bates, T. R., and Lynch, J. P. (1996). Stimulation of root hair elongation in *Arabidopsis thaliana* by low phosphorus availability. *Plant Cell Environ.* 19, 529–538. doi: 10.1111/j.1365-3040.1996.tb00386.x

Bates, T. R., and Lynch, J. P. (2001). Root hairs confer a competitive advantage under low phosphorus availability. *Plant Soil.* 236, 243–250. doi: 10.1023/A:1012791706800

Baum, S. F., Dubrovsky, J. G., and Rost, T. L. (2002). Apical organization and maturation of the cortex and vascular cylinder in *Arabidopsis thaliana* (Brassicaceae) roots. *Am. J. Bot.* 89, 908–920. doi: 10.3732/ajb.89.6.908

Bernhardt, C. (2003). The bHLH genes GLABRA3 (GL3) and ENHANCER OF GLABRA3 (EGL3) specify epidermal cell fate in the *Arabidopsis* root. *Development* 130, 6431–6439. doi: 10.1242/dev.00880

Bhosale, R., Giri, J., Pandey, B. K., Giehl, R. F. H., Hartmann, A., Traini, R., et al.,. (2018). A mechanistic framework for auxin dependent *Arabidopsis* root hair elongation to low external phosphate. *Nat. Commun.* 9:1409 doi: 10.1038/s41467-018-03851-3

Brady, N. C., and Weil, R. R. (2008). *The Nature and Properties of Soil 14th Edn*. New Jersey, NJ: Prentice Hall, Upper Saddle River.

Cederholm, H. M., and Benfey, P. N. (2015). Distinct sensitivities to phosphate deprivation suggest that RGF peptides play disparate roles in *Arabidopsis thaliana* root development. *New Phytol.* 207, 683–691. doi: 10.1111/nph.13405

Devaiah, B. N., Karthikeyan, A. S., and Raghothama, K. G. (2007). WRKY75 transcription factor is a modulator of phosphate acquisition and root development in *Arabidopsis*. *Plant Physiol.* 143, 1789–1801. doi: 10.1104/pp.106.093971

Dolan, L., Janmaat, K., Willemsen, V., Linstead, P., Poethig, S., Roberts, K., et al. (1993). Cellular organisation of the *Arabidopsis thaliana* root. *Development*. *119*, 71–84.

Dong, J., Piñeros, M. A., Li, X., Yang, H., Liu, Y., Murphy, A. S., et al. (2017). An *Arabidopsis* ABC transporter mediates phosphate deficiency-induced remodeling of root architecture by modulating iron homeostasis in roots. *Mol. Plant*. 10, 244–259. doi: 10.1016/j.molp.2016.11.001

Foehse, D., and Jungk, A. (1983). Influence of phosphate and nitrate supply on root hair formation of rape, spinach and tomato plants. *Plant Soil* 74, 359–368. doi: 10.1007/BF02181353

Gahoonia, T. S., and Nielsen, N. E. (2004). Barley genotypes with long root hairs sustain high grain yields in low-P field. *Plant Soil*. 262, 55–62. doi: 10.1023/B:PLSO.0000037020.58002.ac

Galway, M. E., Masucci, J. D., Lloyd, A. M., Walbot, V., Favis, R. W., and Schiefelbein, J. W. (1994). The TTG gene is required to specify epidermal cell fate and cell patterning in the *Arabidopsis* root. *Dev Biol.* 166, 740–754. doi: 10.1006/dbio.1994.1352

Grebe, M. (2012). The patterning of epidermal hairs in *Arabidopsis*-updated. *Curr. Opin. Plant Biol.* 15, 31–37. doi: 10.1016/j.pbi.2011.10.010

Gutiérrez-Alanís, D., Yong-Villalobos, L., Jiménez-Sandoval, P., Alatorre-Cobos, F., Oropeza-Aburto, A., Mora-Macías, J., et al. (2017). Phosphate starvation-dependent iron mobilization induces CLE14 expression to trigger root meristem differentiation through CLV2/PEPR2 signaling. *Dev Cell. 41*, 555.e3–570.e3. doi: 10.1016/j.devcel.2017.05.009

Hanlon, M. T., Ray, S., Saengwilai, P., Luthe, D., Lynch, J. P., and Brown, K. M. (2018). Buffered delivery of phosphate to *Arabidopsis* alters responses to low phosphate. *J. Exp. Bot.* 69, 1207–1219. doi: 10.1093/jxb/erx454

Hassan, H., Scheres, B., and Blilou, I. (2010). JACKDAW controls epidermal patterning in the *Arabidopsis* root meristem through a non-cell-autonomous mechanism. *Development* 137, 1523–1529. doi: 10.1242/dev.048777

Hirsch, J., Marin, E., Floriani, M., Chiarenza, S., Richaud, P., Nussaume, L., et al. (2006). Phosphate deficiency promotes modification of iron distribution in *Arabidopsis* plants. *Biochimie* 88, 1767–1771. doi: 10.1016/j.biochi.2006.05.007

Kirik, V., Simon, M., Huelskamp, M., and Schiefelbein, J. (2004). The ENHANCER of TRY and CPC1 gene acts redundantly with TRIPTYCHON and CAPRICE in trichome and root hair cell patterning in *Arabidopsis*. *Dev. Biol.* 268, 506–513. doi: 10.1016/j.ydbio.2003.12.037

Kwak, S. H., and Schiefelbein, J. (2008). A feedback mechanism controlling SCRAMBLED receptor accumulation and cell-type pattern in *Arabidopsis*. *Curr Biol.* 18, 1949–1954. doi: 10.1016/j.cub.2008.10.064

Lee, M. M., and Schiefelbein, J. (1999). WEREWOLF, a MYB-related protein in *Arabidopsis*, is a position-dependent regulator of epidermal cell patterning. *Cell* 99, 473–483. doi: 10.1016/S0092-8674(00)81536-6

Lee, S. A., Jang, S., Yoon, E. K., Heo, J. O., Chang, K. S., Choi, J. W., et al. (2016). Interplay between ABA and GA modulates the timing of asymmetric cell divisions in the *Arabidopsis* root ground tissue. *Mol. Plant*. 9, 870–884. doi: 10.1016/j.molp.2016.02.009

López-Bucio, J., Hernández-Abreu, E., Sánchez-Calderó, L., Nieto-Jacobo, M. F., Simpson, J., and Herrera-Estrella, L. (2002). Phosphate availability alters architecture and causes changes in hormone sensitivity in the Arabidopsis root system. *Plant Physiol.* 129, 244–256. doi: 10.1104/pp.010934

Ma, Z., Baskin, T. I., Brown, K. M., and Lynch, J. P. (2003). Regulation of root elongation under phosphorus stress involves changes in ethylene responsiveness. *Plant Physiol.* 131, 1381–1390. doi: 10.1104/pp.012161

Ma, Z., Bielenberg, D. G., Brown, K. M., and Lynch, J. P. (2001). Regulation of root hair density by phosphorus availability in *Arabidopsis thaliana*. *Plant Cell Environ*. 24, 459–467. doi: 10.1046/j.1365-3040.2001.00695.x

Masucci, J. D., Rerie, W. G., Foreman, D. R., Zhang, M., Galway, M. E., Marks, M. D., et al. (1996). The homeobox gene GLABRA2 is required for position-dependent cell differentiation in the root epidermis of *Arabidopsis thaliana*. *Development* 122, 1253–1260.

Pemberton, L. M. S., Tsai, S.-L., Lovell, P. H., and Harris, P. J. (2001). Epidermal patterning in seedling roots of eudicotyledons. *Ann. Bot.* 87, 649–654. doi: 10.1006/anbo.2001.1385

Preibisch, S., Amat, F., Stamataki, E., Sarov, M., Singer, R. H., Myers, E., et al. (2014). Efficient Bayesian-based multiview deconvolution. *Nat. Methods* 11, 645–648. doi: 10.1038/nmeth.2929

Preibisch, S., Saalfeld, S., Schindelin, J., and Tomancak, P. (2010). Software for bead-based registration of selective plane illumination microscopy data. *Nat. Methods* 7, 418–419. doi: 10.1038/nmeth0610-418

Raghothama, K. G. (1999). Phosphate acquisition. *Annu. Rev. Plant Physiol. Plant Mol. Biol.* 50, 665–693. doi: 10.1146/annurev.arplant.50.1.665

Rerie, G. W., Feldmann, K., and Marks, M. D. (1994). The GLABRA2 gene encodes a homeodomain protein required for normal ovule development. *Genes Dev*. 8, 1388–1399. doi: 10.1101/gad.8.12.1388

Roudier, F., Schindelman, G., DeSalle, R., and Benfey, P. N. (2002). The COBRA family of putative GPI-anchored proteins in *Arabidopsis*. A new fellowship in expansion. *Plant Physiol*. 130, 538–548. doi: 10.1104/pp.007468

Sánchez-Calderón, L., López-Bucio, J., Chacón-López, A., Cruz-Ramírez, A., Nieto-Jacobo, F., Dubrovsky, J. G., et al. (2005). Phosphate starvation induces a determinate developmental program in the roots of *Arabidopsis thaliana*. *Plant Cell Physiol*. 46, 174–184. doi: 10.1093/pcp/pci011

Savage, N., Yang, T. J., Chen, C. Y., Lin, K. L., Monk, N. A. M., and Schmidt, W. (2013). Positional signaling and expression of ENHANCER OF TRY AND CPC1 are tuned to increase root hair density in response to phosphate deficiency in *Arabidopsis thaliana*. *PLoS ONE* 8:e75452. doi: 10.1371/journal.pone.0075452

Schellmann, S., Schnittger, A., Kirik, V., Wada, T., Okada, K., Beermann, A., et al. (2002). *TRIPTYCHON* and *CAPRICE* mediate lateral inhibition during trichome and root hair patterning in *Arabidopsis*. *EMBO J.* 21, 5036–5046. doi: 10.1093/emboj/cdf524

Stetter, M. G., Schmid, K., and Ludewig, U. (2015). Uncovering genes and ploidy involved in the high diversity in root hair density, length and response to local scarce phosphate in *Arabidopsis thaliana*. *PLoS ONE* 10:e0120604. doi: 10.1371/journal.pone.0120604

Svistoonoff, S., Creff, A., Reymond, M., Sigoillot-Claude, C., Ricaud, L., Blanchet, A., et al. (2007). Root tip contact with low-phosphate media reprograms plant root architecture. *Nat. Genet.* 39, 792–796. doi: 10.1038/ng2041

Ticconi, C. A., Delatorre, C. A., Lahner, B., Salt, D. E., and Abel, S. (2004). *Arabidopsis* pdr2 reveals a phosphate-sensitive checkpoint in root development. *Plant J.* 37, 801–814. doi: 10.1111/j.1365-313X.2004.02005.x

Ticconi, C. A., Lucero, R. D., Sakhonwasee, S., Adamson, A. W., Creff, A., Nussaume, L., et al. (2009). ER-resident proteins PDR2 and LPR1 mediate the developmental response of root meristems to phosphate availability. *Proc. Natl. Acad. Sci. U.S.A.* 106 14174–14179. doi: 10.1073/pnas.0901778106

Trull, M. C., Guiltinan, M. J., Lynch, J. P., and Deikman, J. (1997). The responses of wild-type and ABA mutant *Arabidopsis thaliana* plants to phosphorus starvation. *Plant Cell Environ.* 20, 85–92. doi: 10.1046/j.1365-3040.1997.d01-4.x

Wada, T., Tachibana, T., Shimura, Y., and Okada, K. (1997). Epidermal cell differentiation in *Arabidopsis* determined by a Myb homolog, CPC. *Science* 277, 1113–1116. doi: 10.1126/science.277.5329.1113

Walker, A. R., Davison, P. A., Bolognesi-Winfield, A. C., James, C. M., Srinivasan, N., Blundell, T. L., et al. (1999). The TRANSPARENT TESTA GLABRA1 locus, which regulates trichome differentiation and anthocyanin biosynthesis in *Arabidopsis*, encodes a WD40 repeat protein. *Plant Cell* 11, 1337–1349. doi: 10.1105/tpc.11.7.1337

Ward, J. T., Lahner, B., Yakubova, E., Salt, D. E., and Raghothama, K. G. (2008). The effect of iron on the primary root elongation of *Arabidopsis* during phosphate deficiency. *Plant Physiol.* 147, 1181–1191. doi: 10.1104/pp.108.118562

Zhang, Y. J., Lynch, J. P., and Brown, K. M. (2003). Ethylene and phosphorus availability have interacting yet distinct effects on root hair development. *J. Exp. Bot.* 54, 2351–2361. doi: 10.1093/jxb/erg250

Conflict of Interest Statement: The authors declare that the research was conducted in the absence of any commercial or financial relationships that could be construed as a potential conflict of interest.

frontiers in Plant Science

ORIGINAL RESEARCH
published: 06 June 2018
doi: 10.3389/fpls.2018.00723

Seasonal Alterations in Organic Phosphorus Metabolism Drive the Phosphorus Economy of Annual Growth in *F. sylvatica* Trees on P-Impoverished Soil

Florian Netzer[1†], *Cornelia Herschbach*[1,2*†], *Akira Oikawa*[3], *Yozo Okazaki*[3], *David Dubbert*[2], *Kazuki Saito*[3,4] and *Heinz Rennenberg*[1,5]

[1] Chair of Tree Physiology, Institute of Forest Sciences, Albert-Ludwigs-University Freiburg, Freiburg, Germany, [2] Ecosystem Physiology, Institute of Forest Sciences, Albert-Ludwigs-University Freiburg, Freiburg, Germany, [3] Metabolomics Research Group, RIKEN Center for Sustainable Resource Science, Yokohama, Japan, [4] Graduate School of Pharmaceutical Sciences, Chiba University, Chiba, Japan, [5] College of Science, King Saud University, Riyadh, Saudi Arabia

OPEN ACCESS

Edited by:
Aleysia Kleinert,
Stellenbosch University, South Africa

Reviewed by:
Ze-Xin Fan,
Xishuangbanna Tropical Botanical Garden (CAS), China
Steven Jansen,
Universität Ulm, Germany
Alex Joseph Valentine,
Stellenbosch University, South Africa

***Correspondence:**
Cornelia Herschbach
cornelia.herschbach@ctp.uni-freiburg.de

[†] These authors have contributed equally to this work.

Specialty section:
This article was submitted to Plant Nutrition, a section of the journal Frontiers in Plant Science

Received: 16 January 2018
Accepted: 14 May 2018
Published: 06 June 2018

Citation:
Netzer F, Herschbach C, Oikawa A, Okazaki Y, Dubbert D, Saito K and Rennenberg H (2018) Seasonal Alterations in Organic Phosphorus Metabolism Drive the Phosphorus Economy of Annual Growth in F. sylvatica Trees on P-Impoverished Soil. Front. Plant Sci. 9:723. doi: 10.3389/fpls.2018.00723

Phosphorus (P) is one of the most important macronutrients limiting plant growth and development, particularly in forest ecosystems such as temperate beech (*Fagus sylvatica*) forests in Central Europe. Efficient tree internal P cycling during annual growth is an important strategy of beech trees to adapt to low soil-P. Organic P (P_{org}) is thought to play a decisive role in P cycling, but the significance of individual compounds and processes has not been elucidated. To identify processes and metabolites involved in P cycling of beech trees, polar-metabolome and lipidome profiling was performed during annual growth with twig tissues from a sufficient (Conventwald, Con) and a low-soil-P (Tuttlingen, Tut) forest. Autumnal phospholipid degradation in leaves and P export from senescent leaves, accumulation of phospholipids and glucosamine-6-phosphate (GlcN6P) in the bark, storage of N-acetyl-D-glucosamine-6-phosphate (GlcNAc6P) in the wood, and establishing of a phospholipid "start-up capital" in buds constitute main processes involved in P cycling that were enhanced in beech trees on low-P soil of the Tut forest. In spring, mobilization of P from storage pools in the bark contributed to an effective P cycling. Due to the higher phospholipid "start-up capital" in buds of Tut beeches, the P metabolite profile in developing leaves in spring was similar in beech trees of both forests. During summer, leaves of Tut beeches meet their phosphate (P_i) needs by replacing phospholipids by galacto- and sulfolipids. Thus, several processes contribute to adequate P_i supply on P impoverished soil thereby mediating similar growth of beech at low and sufficient soil-P availability.

Keywords: phospholipids, metabolome, phosphorus nutrition, annual growth, whole plant nutrition

INTRODUCTION

Beside nitrogen (N), phosphorus (P) is one of the most important nutrients limiting plant growth and development in terrestrial ecosystems (Lambers et al., 2008, 2010, 2015; Lang et al., 2016). P limitation for terrestrial plants is a consequence of pedogenesis over thousands of years (Lambers et al., 2008; Lang et al., 2016), associated with erosion and leaching processes combined with

extremely low atmospheric P deposition (Peñuelas et al., 2013). Some of the most P impoverished soils of the world developed in Australia (Lambers et al., 2012, 2015; Lambers and Plaxton, 2015) and in South Africa at the fynbos biome (Vitousek et al., 2010). Also soils in Central Europe show low P availability as indicated by high foliar N to P ratios of vegetation growing on these soils (Talkner et al., 2009, 2015; Han et al., 2014; Jonard et al., 2015). P deficiency leads to morphological changes such as diminished growth, increased root/shoot ratio and altered root architecture (Lambers et al., 2006; Niu et al., 2013). In addition, physiological changes indicated by modified gene expression and proteome profiles (Lan et al., 2015) are thought to counteract P deficiency. The central consequence of these changes is an efficient phosphorus use in growth and development, photosynthesis, and respiratory energy production (Plaxton and Tran, 2011; Veneklaas et al., 2012; Ellsworth et al., 2015). For example, the replacement of membrane phospholipids by galactolipids, sulfolipids (Lambers et al., 2012), and glucuronosyldiacylglycerol (GlcADG) (Okazaki et al., 2013, 2015) constitutes a strategy providing phosphate (P_i) to other cellular applications in low P environments and, consequently, improves P_i abundance for metabolic processes in plants.

In addition, plants have developed strategies to cope with low P availability in the soil by improving P acquisition and internal P cycling (Côté et al., 2002; Netzer et al., 2017). P acquisition can be improved by (i) root exudation of organic acids and extracellular phosphatases for P solubilization from Al- and Fe-complexes containing P_i (Hinsinger et al., 2015; Smith et al., 2015; Tian and Liao, 2015), (ii) increasing P_i-uptake capacity by enhanced P_i-transporter expression (Chiou and Lin, 2011), (iii) cluster root formation as found in *Proteaceae* (Lambers et al., 2015), and (iv) mycorrhizal association for optimum soil exploitation (Bucher, 2006; Lambers et al., 2008; Smith et al., 2015). Improved internal P cycling during annual growth includes storage and mobilization of P as well as efficient recycling from leaves before abscission. Both together seem to be a strategy particularly of perennial plants to cope with low P in the environment (Côté et al., 2002; Netzer et al., 2017). This is reminiscent to N nutrition of trees in low-N environments (Rennenberg and Dannenmann, 2015; Sun et al., 2016) and seems a general adaptation strategy to enable high productivity of perennial plants on soil with low nutrient availability *via* relatively closed plant internal nutrient cycles (Rennenberg and Schmidt, 2010; Lang et al., 2016).

In a recent study with adult European beech trees on two field sites in Central Europe with sufficient Conventwald (Con) and low Tuttlingen (Tut) soil-P_i availability (Prietzel et al., 2016; Netzer et al., 2017), P (re)cycling was investigated during annual growth. In spring, P_i was provided to developing buds and leaves from the storage pools in bark and wood by xylem transport (Netzer et al., 2017) to cover the high amount of P needed for leaf growth and development (Dietz and Foyer, 1986; Plaxton, 1996; Rychter and Rao, 2005; Plaxton and Tran, 2011). Consequently, organic P (P_{org}) accumulated in the leaves during summer (Netzer et al., 2017). In autumn, P was re-mobilized from leaves and stored in the bark, wood and dormant buds mostly as P_{org} (Netzer et al., 2017). Similar results were observed for nitrogen with N-storage in the bark (Coleman et al., 1991; Wildhagen et al., 2010), increased occurrence of amino acids (AAs) in the xylem sap during spring (Schneider et al., 1994) and phloem allocation of amino compounds into storage tissues (Schneider et al., 1996; Geßler et al., 1998; Herschbach et al., 2012). These findings led to the hypothesis that also distinct components of the P_{org} fraction must contribute to P storage in stem tissues and to the seasonal dynamics of P_{org} to fulfill the P_i demand for metabolic processes needed for growth and development. P_{org} can be attributed to intermediates of photosynthesis, C metabolism, energy generation, and membrane components (Dietz and Foyer, 1986; Plaxton, 1996; Rychter and Rao, 2005; Lambers et al., 2012, 2015) that includes ribosomal RNA, sugar-Ps as well as phospholipids. However, the specific P metabolites that mediate seasonal alterations of the P_{org} fractions in plant tissues at different P_i availability in the soil are currently unknown.

The present study was aimed to identify P compounds contributing to the P_{org} pool in leaves, bark, wood, and transport saps as well as to address the specific functions of these metabolites in the seasonal dynamics of P cycling and its dependency on the P_i availability in the soil. It was hypothesized that (i) the profile of polar P metabolites and/or phospholipids is modulated by the season in leaves, bark and wood, (ii) independent of tree internal P cycling, the replacement of phospholipids by galacto- and sulfolipids contributes to maintain adequate P_i abundance in twig tissues at low-soil-P availability and, (iii) changes in the polar P metabolite and phospholipid profile by both season and P_i availability in the soil are associated with changes in central metabolic pathways. To test these hypotheses, polar metabolite and lipid profiles were analyzed in buds/leaves, bark, and wood during annual growth of beech. To understand the connection between metabolic reprogramming of polar P metabolite and phospholipid profiles with storage and mobilization processes, the abundance of P in long-distance transport fluids of xylem and phloem was investigated during spring growth and leaf senescence.

MATERIALS AND METHODS

Study Sites and Plant Material

Effects of plant available P_i in the soil on the polar metabolome and lipidome were investigated in buds/leaves, bark, and wood, as well as in xylem sap and phloem exudates of adult beech (*Fagus sylvatica* L.) trees. Two forest sites were compared which differ by a factor of eight in soil-P_i availability (Netzer et al., 2017). The beech forest site "Conventwald" (Con) represents a low but sufficiently P_i supplied forest, whereas "Tuttlingen" (Tut) represents an extremely low-soil-P_i forest due to different parent material (Prietzel et al., 2016; Netzer et al., 2017). Both forests are described as mature beech forests and the soils developed on Gneiss containing 0.29 mg P g^{-1} (Con) and on Limestone (Jurassic) (Tut) containing 0.37 mg P g^{-1}, respectively (Prietzel et al., 2016). Total P stock of the soil consist of different P species and amounted 162 g m^{-2} for the Con forest and 117 g m^{-2} for the Tut forest (Prietzel et al., 2016). P in the soil of the Tut forest mostly occurred as Ca-bound organic P (pH 6.4–7.4; Prietzel et al., 2016). The adult beech trees of the managed forests originated from natural regeneration and were 160–190 years old

at the Con forests (von Wilpert et al., 1996) and 80–90 years old at the Tut forest (Gessler et al., 2001; Pena et al., 2010). Twig tissues from five beech trees were harvested in October 2013, February 2014, April 2014 at bud burst and in June 2014. Xylem sap and phloem exudate were collected in autumn (October 2013) and spring (April 2014). Leaves (or buds in February and bursting buds in April), bark, wood, xylem sap, and phloem exudates were collected from ∼30 cm long sun exposed twigs of the beech crown (∼25–30 m above ground; Netzer et al., 2017). Xylem sap was collected by the method of Scholander et al. (1965) as modified by Rennenberg et al. (1996). For this purpose, at the cut end the bark of twigs was removed to uncover the wood. The wood was rinsed with $dd H_20$ to avoid contaminations and dried with paper tissue. Then, the twig was inserted in a sealed pressure chamber with the cut end protruding. The pressure in the chamber was slowly raised until shoot water potential was reached and kept constant slightly above the shoot water potential to collect xylem sap. The first appearing drops of xylem sap were discarded. The subsequently outrunning xylem sap was collected and frozen in liquid N_2 until further analyses.

Phloem exudation was performed with bark pieces of ∼60 mg on ice in the presence of PVPP (2:1, PVPP/ bark fresh weight) in 10 mM EDTA solution adjusted to pH 7.0 and supplemented with dithiothreitol and the antibiotic chloramphenicol (final concentrations 3 and 0.015 mM, respectively; Rennenberg et al., 1996). Phloem exudation was completed and terminated after 5 h of incubation (Schneider et al., 1996). Samples were shock frozen in liquid N_2 and stored at −80°C until further processing. Leaf and bark samples were homogenized under liquid N_2 using mortar and pestle, whereas wood samples were ground under liquid N_2 using a CryoMill (Retsch, Haan, Germany). All samples were freeze dried at −50°C, at a vacuum of 0.03 mbar for 72 h using the freeze drier Alpha 2–4 (Christ, Osterode am Harz; Germany).

Lipidome Analysis

Lipids in powdered, freeze-dried bud/leaf, bark and wood samples (from five trees at each time point) were extracted and analyzed as described (Okazaki et al., 2015). In total, 28 lipid classes including five P containing lipid classes were identified, i.e., lysophosphatidylcholines (lysoPC, 5 species), phosphatidylcholines (PC, 14 species), phosphatidylethanolamines (PE, 8 species), phosphatidylglycerols (PG, 4 species), and phosphatidylinositols (PI, 2 species). Besides, diacylglycerols (DAG, 8 species) and triacylglycerol (TAG, 39 species), the non-phospholipids sulfoquinovosyldiacylglycerols (SQDG, 7 species), glucuronosyldiacylglycerols (GlcADG, 5 species), glucosylceramides (GlcCer, 7 species), monogalactosyldiacylglycerols (MGDG, 9 species) known to be involved in phospholipid replacement upon P starvation in herbaceous plants (Lambers et al., 2012, 2015; Okazaki et al., 2013, 2015; Siebers et al., 2015) plus digalactosyldiacylglycerols (DGDG, 11 species), acyl steryl glucoside (ASG, 3 species), and sterol glucosides (SG, 3 species) were detected. In each lipid class, lipid species that differ in fatty acid composition, i.e., in total carbon length as well as in double bound abundance, were combined, presented and subjected to statistical analyses.

Polar Metabolome Analysis

The powdered and freeze-dried tissue samples as well as freeze dried xylem sap samples and phloem exudates (3 replicates per harvest, each) were analyzed by CE-MS according to Oikawa et al. (2011a,b).

IRMS Measurements

Three milligrams of dried, fine milled, and homogenized plant material was weight into tin boats using a precision scale. The samples were combusted in an elemental analyzer (Euro EA 3000, Hekatech, Wegberg, Germany) and analyzed in a continuous-flow isotope ratio mass spectrometer (IsoPrime, Elementar, Stockpor, UK) (Werner et al., 2006). The samples were measured against reference standard IAEA-600 caffeine and IAEA-NO-3 potassium nitrate (repeated measurement precision was 0.10) for nitrogen, and IAEA-600 caffeine and IAEA-CH-3 cellulose (repeated measurement precision was 0.12) for carbon.

Statistical Analyses

To characterize seasonal fluctuations and differences between field sites, polar metabolome, and lipidome data were subjected to partial least square discriminant analysis (PLS-DA) using MetaboAnalyst 3.0 (Xia et al., 2015). To reach maximum separation in PLS-DA plots, data were normalized by median, log transformed, and auto scaled (mean centered and divided by the standard deviation of each variable). Heat maps were created using the raw data subjected to Pearson's correlations analyses. As similarity measure Ward's clustering algorithm was used. Significant seasonal fluctuations of individual lipids ($n = 5$) or metabolites ($n = 3$) within one tissue and forest site were analyzed with One Way ANOVA (Holm–Sidak test as *post-hoc* test) in case of normal distributed data. In case of not normal distributed data or if data showed inhomogeneity of variances, the Kruskal–Wallis ANOVA test was applied (both $p \leq 0.05$, $\alpha = 0.95$). Normal distribution of the data was tested with the Shapiro–Wilk test; the homogeneity of variances was tested with the Levene² test (both $p \leq 0.05$). Statistically significant differences of individual lipids or polar metabolites within each season between study sites were analyzed by Student's *t*-test in case of normal distributed data. In the case of not normal distributed data or if homogeneity of variances was not given, the Mann–Whitney test was performed. Interactions between lipids and polar metabolites were analyzed by calculating Pearson's correlation coefficients. Statistical analyses were conducted with the Origin PRO 9.1 software (OriginLab Corporation, Northampton, USA). Venn diagrams were used to identify polar metabolites and lipids of tissues, which contribute to the separation of seasons and sites in each twig tissue (http://bioinformatics.psb.ugent.be/webtools/Venn/).

RESULTS

Total C, N, and P in Twig Leaves/Tissues Changed During Annual Growth

Total C, N (present study), and P (Netzer et al., 2017) analyses revealed clear seasonal changes indicating P and N storage in bark and wood during dormancy and its mobilization during spring (**Figure 1**). In leaves, C was highest in senescent leaves

and lowest in bursting buds. By contrast, N and P in leaves were lowest in autumn and highest in spring (**Figure 1**, Netzer et al., 2017). This pattern was observed in leaves of both forest sites, whereas the N increase in spring was less pronounced in leaves from the low-P and low-N forest site Tut. In leaves, P and N declined from summer until autumn indicating mobilization before leaf abscission. Bark and wood showed storage of P during dormancy at both field sites, but storage of N only in Con beeches (**Figure 1**, Netzer et al., 2017). Irrespective of seasonal changes, N in bark and wood was lower in Tut compared to Con beech trees in early summer (**Figure 1**). Surprisingly, the C content in the bark of both, Tut and Con beech trees showed lowest values during winter when C storage was expected. Analyses of the polar (P) metabolome and (P) lipidome were performed to identify distinct P and N compounds contributing to the seasonal fluctuations and site specific differences of P, N, and C in twig tissues.

The Contribution of P Metabolites to the Polar Metabolome and Lipidome of Beech Twigs

The polar metabolome and the polar P metabolome profile were first characterized by Venn analyses to get insight into differences between forests sites, twig organs/tissues and transport fluids (**Supplementary Figure S1**, **Supplementary Table S1**). While the overall number of polar (P) metabolites was equal in buds/leaves, bark, wood, xylem sap, and phloem exudates at both study sites, Venn-analyzes elucidated five leaf-specific, two xylem sap-specific [(G1P; Gal1P) and dAMP] and one phloem exudate specific (NaMN) polar P metabolite (**Table 1**). The lipidome of buds/leaves and wood showed 28 lipid classes, while 27 lipid classes were found in the bark. In leaves/buds, bark and wood all five classes of phospholipids (lysoPC, PC, PE, PG, PI) were found. Besides DAG and TAG, the non-phospholipids SQDG, GlcADG, GlcCer, and MGDG, all known to be involved in phospholipid replacement upon P starvation in herbaceous plants (Okazaki et al., 2013, 2015; Siebers et al., 2015), plus DGDG, ASG, and SG were detected (**Supplementary Table S2**).

Partial Least Square Distance Analyses (PLS-DA) identified seasonal differences in the lipidome and polar metabolome of beech twig leaves/tissues and revealed its dependency on P_i availability in the soil (**Supplementary Figure S2**). The lipidome and the polar metabolome of buds/leaves was different for all seasons and between levels of P_i availability in the soil. Phospholipids contributed 19–20%, P metabolites 13% to the differentiation of the metabolome and lipidome, respectively (**Supplementary Tables S3**, **S4**). The polar metabolome of bark and wood varied between seasons at both study sites, but with a lower contribution of P metabolites of 13% (Con) and 10% (Tut), whereas the lipidome of bark and wood showed only minor seasonal differences. The xylem sap and phloem exudate polar metabolome showed clear differences between spring and autumn as well as for both study sites (**Supplementary Figure S3**). The contribution of polar P metabolites to the metabolome variation was below 10%.

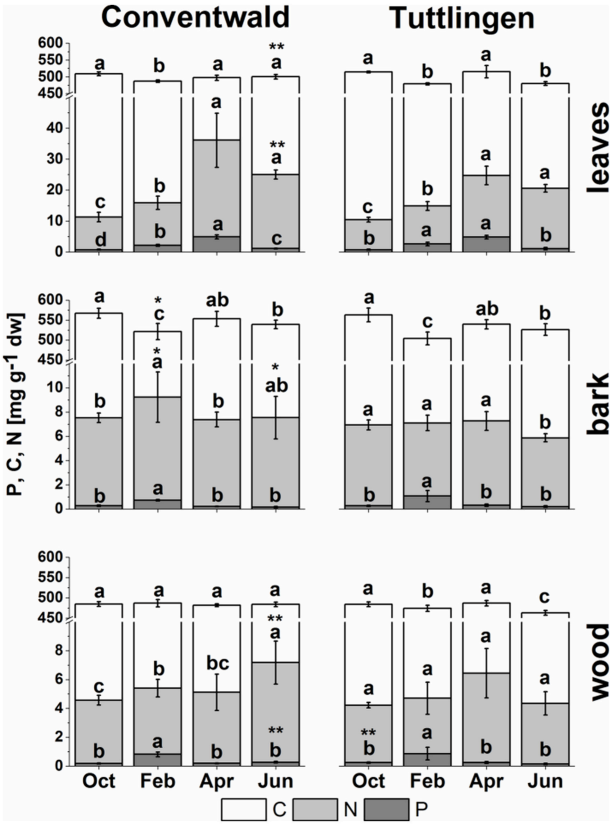

FIGURE 1 | Total C, N, and P in buds/leaves, bark, and wood of adult beech trees. The top of the bars represents mean values ± *S.D.* of total C (white bars), total N (light gray bars) and total P (dark gray bars) in beech twig organs/tissues. Data of total P were taken from Netzer et al. (2017). Lower case letters represent significant differences between seasons determined by Mann–Whitney-tests after Kruskal–Wallis-ANOVA as global test at the $p \leq 0.05$ level per tissue and site. Asterisks indicate significantly higher C, N, or P contents in the respective organ/tissue compared to the other field site. $^{*}p \leq 0.05$; $^{**}p \leq 0.01$ (results of Student's *t*-test or Mann–Whitney tests in case that the requirement of normal distribution of the data was not fulfilled). (Oct, October; Feb, February; Apr, April; Jun, June).

Differences in the polar metabolome and lipidome profile were also observed between both forest sites. The lipidome of leaves/buds was different in spring and autumn, while the polar metabolome was divergent in summer and autumn. The wood lipidome varied between sites in summer and autumn, while the polar metabolome of the wood differed between sites in spring, summer and autumn. VIP-scores of the PLS-DA analyses showed that the differentiation of the polar metabolome by season and site was mainly mediated by N containing metabolites rather than P metabolites (**Supplementary Table S3**). Several phospholipids were among the top 10 lipids contributing to the differentiation in PLS-DA plots (**Supplementary Tables S3**, **S4**). This clearly indicates phospholipids and N compounds as drivers to distinguish seasons and sites. Identification of distinct N compound(s) and phospholipids that differ between seasons and sites are elucidated below.

TABLE 1 | Organ/Tissue specific abundances of P metabolites.

	Season	Conventwald												Tuttlingen											
		Buds/leaves				Bark				Wood				Buds/leaves				Bark				Wood			
	Compound	o	f	a	j	o	f	a	j	o	f	a	j	o	f	a	j	o	f	a	j	o	f	a	j
1	2 Deoxy G6P																								
	T6P; L1P; Suc6P									B		B										B		B	
	G6P; F6P; M6P					C				B		B						C		C		B		B	
	UDP-Glc; UDP-Gal											B										B		B	
	Ino1P, Man1P					C		C		B		B						C		C		B		B	
	G1P; M6P																								
	Ribu5P; Rib5P, X5P																								
	GlcN6P																								
	GlcNAc6P					C				B		B						C				B		B	
	S7P											B										B		B	
	Suc6P																								
	GDP-glucose																								
	G1P, Gal1P									B		B										B		B	
2	DHAP																								
	Gly3P					C		C		B		B						C		C		B		B	
3	Pyridoxamine 5P																								
	Thiamine 5P																								
4	NAD																								
	NADP																								
	FAD																								
5	beta-NMN					C		C		B		B						C		C		B		B	
	AMP									B		B										B		B	
	AICAR											B										B		B	
	UMP									B		B										B		B	
	dCMP					C												C							
	ADP											B										B		B	
	ATP																								
	dTMP					C		C										C		C					
	GMP																								
	UDP												B											B	
	dTTP																								
	CTP																								
	GDP																								
	cGMP																								
	dUMP																								
	cAMP																								
	dAMP									B		B										B		B	
	NMN					C		C										C		C					

P metabolites in buds/leaves, bark and wood of Fagus sylvatica *in October (o), February (f), April (a), and June (j) of both forests, Conventwald (Con) and Tuttlingen (Tut). Gray shaded boxes = P metabolite is present in this tissue during this season. White boxes = not detected. 1 = sugar phosphates, 2 = triose phosphates, 3 = coenzymes, 4 = dinucleotides, 5 = nucleotides. B = present in the xylem sap. C = present in phloem exudates at this study site and during this season. The complete list of all metabolites is given in* ***Supplementary Table S1****.*

Polar P Metabolites and Phospholipids Responsible for Seasonal Fluctuations in Total P and N

Remodeling of the Polar Metabolome and Lipidome in Beech Twigs Until Autumn and Winter Indicates Mobilization and Storage

A special feature of the perennial life style of deciduous trees such as European beech is the remobilization of nutrients from senescent leaves for storage in bark and wood in autumn (Millard and Grelet, 2010; Rennenberg and Schmidt, 2010; Rennenberg et al., 2010). In the present study, decreased levels of chlorophyll and carotenoids in autumn leaves indicated leaf senescence (**Supplementary Figure S4**) and thus preparation of the adult beech trees for dormancy.

Leaves

P resorption from senescent leaves can occur either directly as P_{org} or as P_i after cleavage from organic P compounds. The latter was indicated by lower abundance of phospholipids (PE, PG, PC, and PI) in autumn compared to summer in senescent beech leaves from Tut, and for PG and PI in senescent beech leaves from Con beech trees (**Figure 2**). The simultaneous increase in the abundance of lysoPC, an indicator of phospholipid degradation (Nakamura, 2013; Boudière et al., 2014), supports this assumption (**Figure 2**).

In senescent leaves, the levels of most sugar-Ps remained unaffected compared to beech leaves in summer (**Figure 2**); products of glycolysis were either not detectable (DHAP) or lower (pyruvate) in autumn compared to summer. N remobilisation from senescent leaves after protein breakdown was indicated by the accumulation of both, numerous AAs (**Figure 2**) and the coenzyme pyridoxamine5P involved in the amino acid metabolism in autumn (Guo et al., 2004; Roje, 2007). In addition, the abundances of glutathione (GSH), the predominant transport form of reduced sulfur in the phloem of beech (Herschbach and Rennenberg, 1996), and 5-oxoproline, a degradation product of GSH (Bergmann and Rennenberg, 1993), in leaves were higher in autumn compared to summer. Accumulation of AAs, including sulfur (S) containing compounds, in phloem exudates in autumn compared to spring (**Figure 3**) coincide with their allocation to the storage tissues bark and wood via the phloem. Furthermore, raffinose, an important phloem mobile sugar (Rennie and Turgeon, 2009; Turgeon and Wolf, 2009), was ∼5-fold higher in phloem exudates in autumn compared to spring.

Bark

Changes in polar metabolite abundances that indicate nutrient storage in bark parenchyma cells during autumn were mostly driven by AAs (**Supplementary Table S3**). However, only the abundance of Val, Leu, and Gln was higher in autumn than in summer but significantly declined until dormancy. In case of amino-N storage in form of storage proteins, as previously reported for poplar (Wildhagen et al., 2010), this is not surprising and fits well with the higher total-N (**Figure 1**) content in the bark of Con beeches during dormancy.

In contrast, total-C in the bark was higher in autumn than in summer and was lowest during dormancy (**Figure 1**). Fat in oleosomes can constitute a C storage pool in the bark of deciduous trees (Sauter and van Cleve, 1994) and increased lipid levels can be expected in autumn and/or later during dormancy. Against this assumption, lipids, including phospholipids in the bark during autumn remained similar to summer levels (**Figure 4**). Nevertheless, the storage lipid TAG (Xu and Shanklin, 2016) and the phospholipids PC, PE and PG increased from autumn until winter. This effect was significant only for the bark of Tut beeches (**Figure 4**) and, this increase coincided with highest P_{tot} levels in the bark during dormancy (**Figure 1**). In addition, the abundances of MGDG, DGDG, SQDG, and of glucosamine-6-phosphate (GlcN6P, significant for Con beech twigs), one precursor of glycolipid synthesis (Furo et al., 2015), were higher in the twig-bark during dormancy compared to autumn.

Wood

The twig-wood revealed only minor changes in polar metabolite abundances between summer and autumn (**Figure 5**). Levels of sugar-Ps remained unaffected and the abundances of organic acids involved in glycolysis and the TCA-cycle, declined only in the wood of Con beeches. Significant changes were observed within the lipidome (**Figure 5**). The abundances of the phospholipids PG (both sites), PC, and PE (Con only) declined from summer to autumn, as also observed for the galactolipids DGDG and MGDG, while SQDG increased (Tut only). Later during dormancy, the abundance of PC, lysoPC and PE increased in the Con twig-wood, when P_i declined (Netzer et al., 2017). This indicates the use of P_i for phospholipid formation and phospholipid storage during dormancy. Furthermore, the P containing hexose N-acetyl-D-glucosamine 6-phosphate (GlcNAc6P), was highest in twig-wood and may contribute to P storage during dormancy as indicated by highest P_{tot} levels (**Figure 1**).

Remodeling of the Polar Metabolome and Lipidome in Spring Indicates Mobilization of Twig Storage Pools

In spring, growth of deciduous trees is characterized by the development of new leaves from buds and by stimulation of metabolic activity. Accordingly, the abundances of chlorophyll and carotenoids in buds increased compared to dormancy (**Supplementary Figure S4**), whereas ABA that keeps buds dormant in winter (Fladung et al., 1997) disappeared (**Supplementary Figure S5**). In the xylem sap lowered ABA, but higher levels of tZ (trans-zeatin), GA3 and GABA were observed in spring compared to autumn (**Supplementary Figure S9**) and correspond with their individual functions in dormancy release (Fladung et al., 1997; Zheng et al., 2015).

Developing buds

In developing buds, sugar-Ps and triose-Ps as products of hexose degradation by glycolysis, such as DHAP (only detectable in

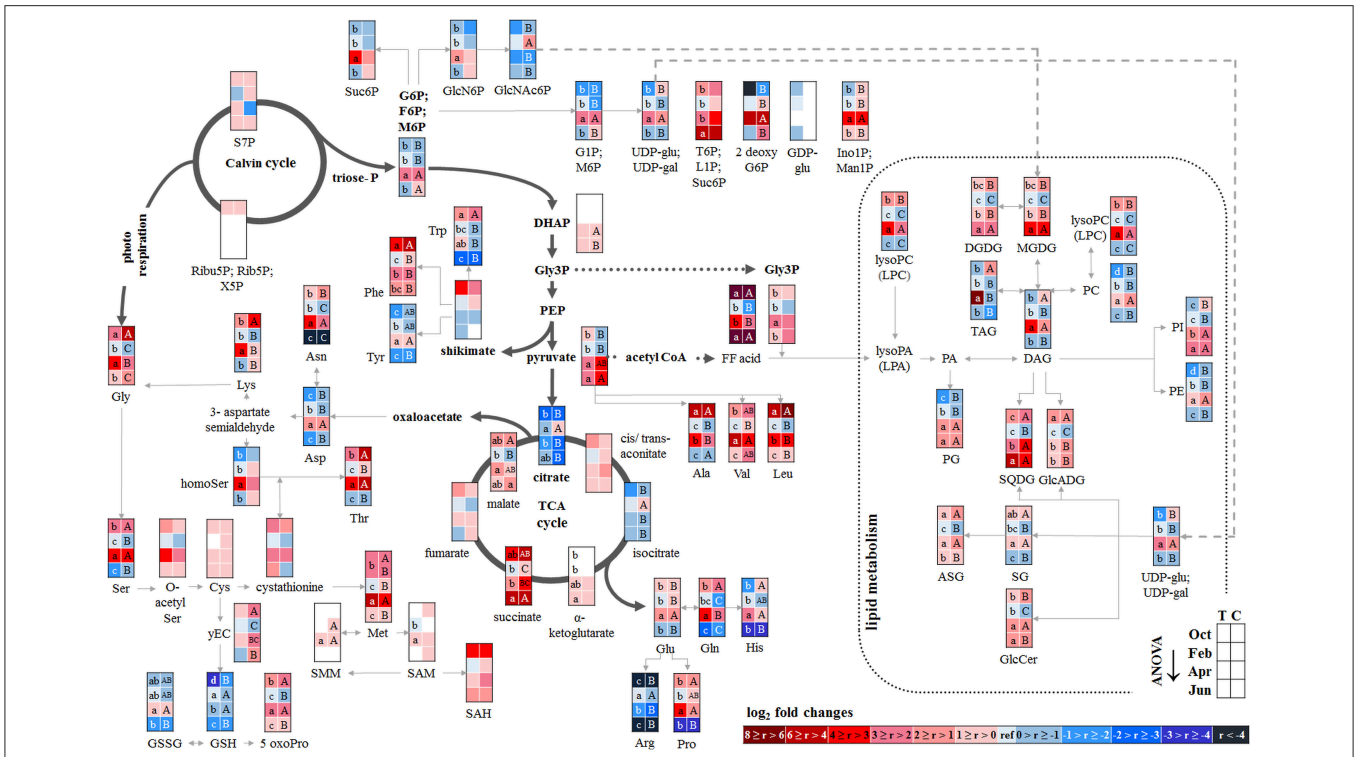

FIGURE 2 | Changes in polar metabolite and lipid abundances during annual growth in leaf buds and leaves. The figure shows heat maps of sugar-Ps, intermediates of central carbon metabolic pathways, and amino acids including sulfur compounds and lipids in senescent leaves (October) dormant leaf buds (February), bursting buds/developing leaves (April), and mature leaves (June) of adult beech trees from the Tut (T) and Con (C) forest. Mean values of seasonal fluctuations of metabolites ($n = 3$) and lipids ($n = 5$) were presented as $\log_2$ fold changes using Tut data in February as reference. Different minor (Tut) or capital (Con) letters indicate significantly different relative metabolite or lipid abundance between the four seasons per site (results of One-Way-ANOVA, or Kruskal–Wallis-ANOVA in case that the requirement of normal distribution and/or equal variances failed; $p < 0.05$). White = not detected. Abbreviations of metabolites: γ EC, γ-glutamylcysteine; GlcNAc6P, N-acetyl-D-glucosamine-6-phosphate; GlcN6P, glucosamine-6-phosphate; OPH, O-phospho-L-homoserine; SAH, S-adenosyl-L-homocysteine; SAM, S-adenosyl-L-methionine. Abbreviations of lipids: ASG, acyl steryl glucoside; DAG, diacylglycerol; DGDG, digalactosyldiacylglycerol; FF acid, free fatty acid; GlcADG, glucuronosyldiacylglycerol; GlcCer, glucosylceramide; Gly3P, glycerol-3-phosphate; lysoPA, lysophosphatidic acid; lysoPC, lysophosphatidylcholine; MGDG, monogalactosyldiacylglycerol; PA, phosphatidic acid; PC, phosphatidylcholine; PE, phosphatidylethanolamine; PG, phosphatidylglycerol; PI, phosphatidylinositol; SG, steryl ester; SQDG, sulfoquinovosyldiacylglycerol; TAG, triacylglycerol. Abbreviations of seasons: Oct, October; Feb, February; Apr, April; Jun, June. The pathways were designed based on Kegg pathways (http://www.genome.jp/kegg/pathway.html?sess=2764b8338258d6286de91bbebe6faf46) and on Hirabayashi and Ichikawa (2002), Gardocki et al. (2005), Li-Beisson et al. (2010), Boudière et al. (2014), Guschina et al. (2014), Okazaki et al. (2013, 2015), Furo et al. (2015), Kobayashi (2016), and Galili et al. (2016).

spring and summer) and pyruvate (**Supplementary Figure S6**), were higher in spring compared to dormancy. Simultaneously, AAs synthesized from phosphoenolpyruvate (Tyr, Phe, Try) and pyruvate (Ala, Leu, Val) also increased. The higher level of pyruvate coincides with enhanced malate and succinate levels in beech buds although citrate decreased (**Figure 2**). This fits well with increasing metabolic activities expected in spring during bud swelling and bud break. In accordance, AAs synthesized from TCA-cycle intermediates, i.e., 2-oxoglutarate (Glu-family) and oxaloacetate (Asp-family), peaked in spring (**Figure 2**). Although net photosynthesis is low in developing buds (Umeki et al., 2010), the AAs build from 2-phosphoglycolate via photorespiration, i.e., Ser and Gly, increased. Both AAs may also be synthesized via metabolic pathways different from photorespiration (Ho and Saito, 2001; Benstein et al., 2013) and/or may be supplied *via* xylem transport. Indeed, comparison of the xylem sap polar metabolome in spring with autumn revealed higher abundances of several organic acids, proteinogenic AAs including Ser and Gly, and several compounds of the TCA-cycle, namely citrate, isocitrate, succinate, fumarate, and malate, which can all be transported into the developing buds in spring.

In bursting buds, degradation of organic P compounds such as phospholipids to supply P_i for energy metabolism was not indicated. In opposite, in bursting buds, the abundances of all phospholipids, i.e., PC, PE, PG, PI, and lysoPC increased instead of decreased from dormancy until spring (**Figure 2**). Apparently, phospholipids in buds constitute sinks rather than sources for P_i at the beginning of the vegetation period. Another possible P_i source may be GlcNAc6P that is also a precursor of MGDG and DGDG synthesis (**Supplementary Figure S8**). GlcNAc6P declined in buds until spring although its precursor GlcN6P increased (**Figure 2**). This corresponds furthermore with high (UDP-Glc; UDP-Gal) levels in bursting buds. Hence, the present results indicate synthesis of non-phospholipid rather than phospholipid degradation.

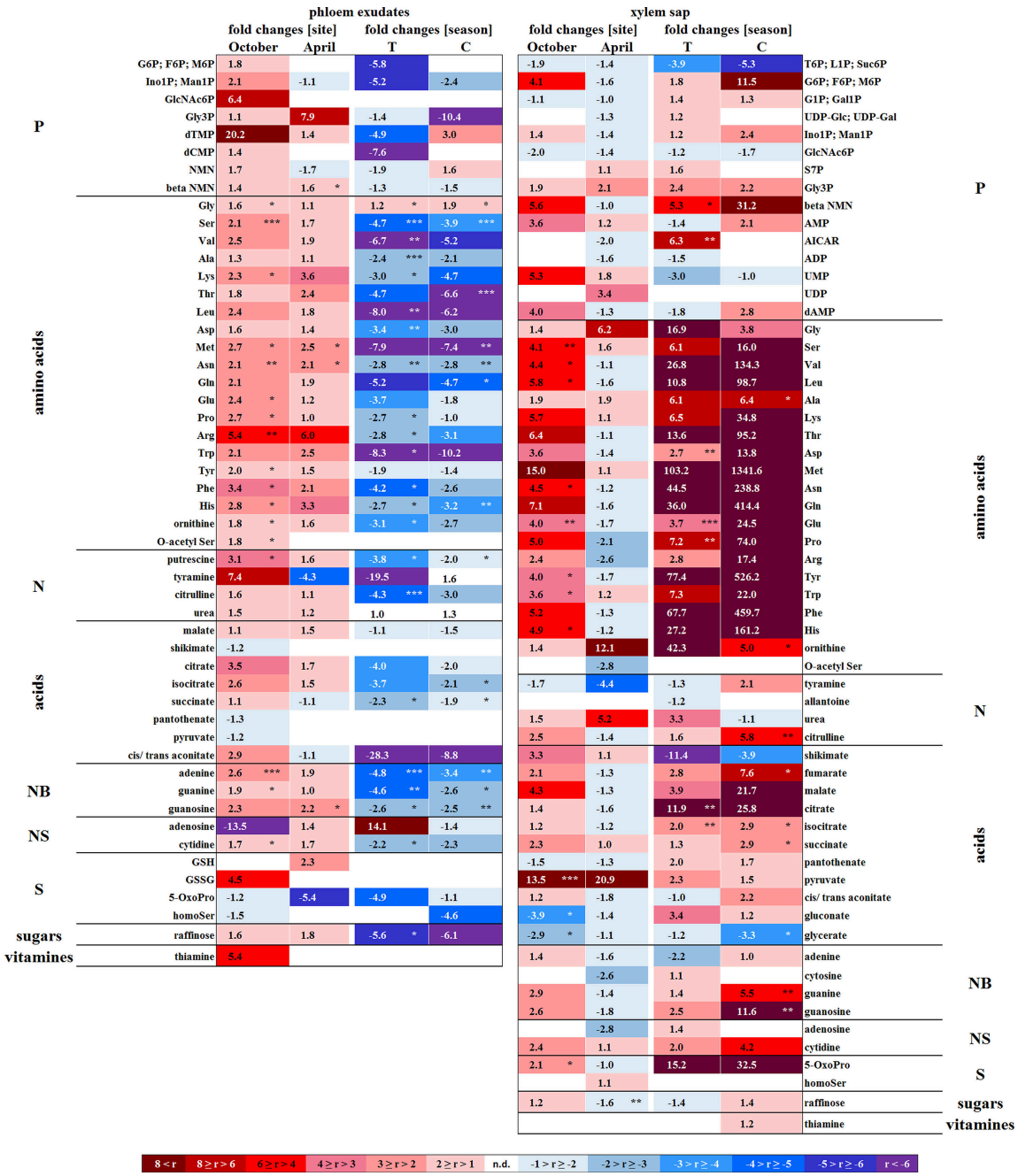

FIGURE 3 | Site and season effects on the polar metabolite abundance in xylem saps and phloem exudates. Phloem exudates (left) and xylem saps (right) from twigs of adult beech trees of the Tut (T) and Con (C) forest in autumn (October) and spring (April) are shown. Mean values ($n = 3$) of fold changes of relative peak areas are presented. The higher metabolite abundance in xylem saps and phloem exudates of Tut beeches at both seasons is indicated as Tut/Con ratios (red), while the lower abundance of metabolites in Tut samples is indicated by the reciprocal Con/Tut ratio (blue). Seasonal differences are presented as ratios of fold changes of relative peak values between April/October. Asterisks indicate significant differences for a particular metabolite between both field sites and between both seasons (results of Student's *t*-test or Mann–Whitney tests in case that the requirement of normal distribution of the data was not fulfilled). $^{*}p < 0.05$; $^{**}p < 0.01$; $^{***}p < 0.001$. nd = not detectable. Relative peak areas of all identified metabolites are given in the **Supplementary Table S1**.

Bark and wood

The polar metabolite and lipidome profile in both, bark and wood was mostly similar between dormancy and spring. Among sugar-Ps or organic acids involved in glycolysis and the TCA-cycle, only succinate in the bark and citrate in the wood increased in spring compared to dormancy (**Figure 4**). In the twig-wood, lipids were not involved in C-mobilization during spring, because MGDG (both field sites) as well as the storage fats TAG and DAG

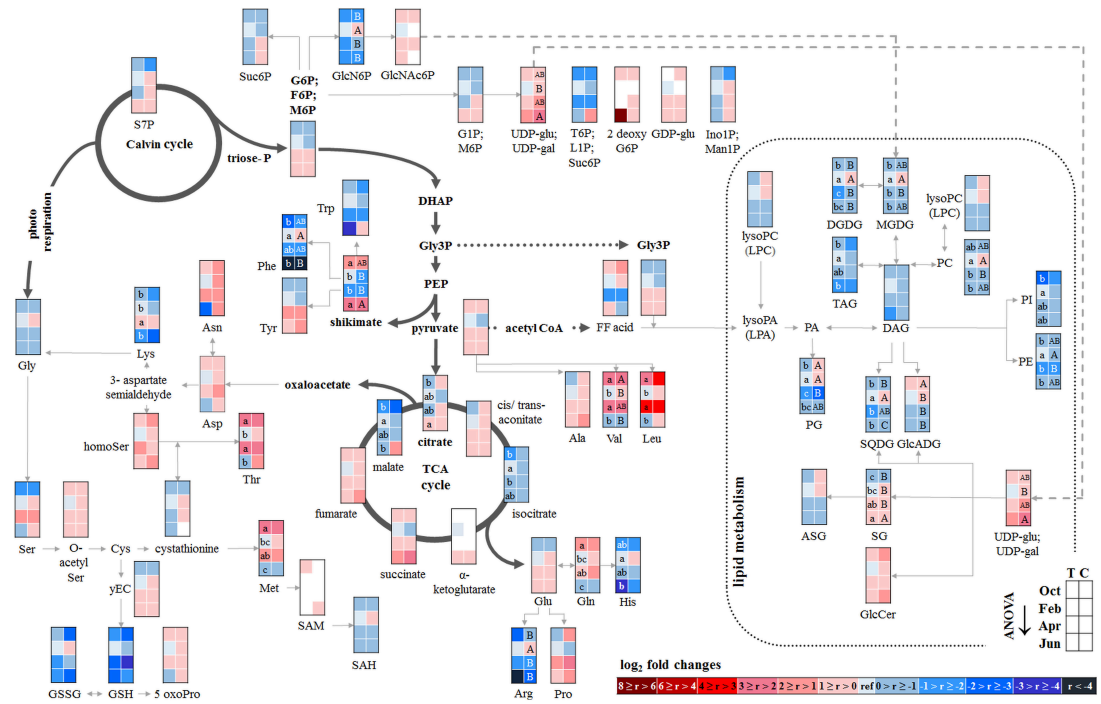

FIGURE 4 | Changes in polar metabolite and lipid abundances during annual growth in the bark. The figure shows heat maps of sugar-Ps, intermediates of central carbon metabolic pathways, and amino acids including sulfur compounds and lipids in the twig-bark of adult beech trees from the Tut (T) and Con (C) forest. Mean values of seasonal fluctuations of metabolites ($n = 3$) and lipids ($n = 5$) were presented as $\log_2$ fold changes using Tut data in February as reference. Different minor (Tut) or capital (Con) letters indicate significantly different relative metabolite or lipid abundance between the four seasons per site (results of One-Way-ANOVA, or Kruskal–Wallis-ANOVA in case that the requirement of normal distribution and/or equal variances was not fulfilled; $p < 0.05$). White = not detected. Abbreviations see **Figure 2**.

(Tut wood only) increased compared to dormancy (**Figure 5**). In contrast, protein breakdown in bark and wood during spring is indicated by enhanced abundances of AAs in these tissues (**Figures 4**, **5**). These AAs may be loaded into the xylem as denoted by the generally higher amino acid abundances in the xylem sap during spring (**Figure 3**).

In the xylem sap of adult beech trees also P_i strongly increased in spring (Netzer et al., 2017). GlcN6P in the bark and GlcNAc6P in the wood declined until bud burst and may constitute a source of xylem transported P_i. Further candidates providing P_i were the phospholipids PC, PG, and PE that declined in the bark during spring compared to dormancy. In contrast, phospholipids in the wood did not change between dormancy and spring or even increased and, thus, did not provide P_i for the xylem transport. beta-NMN that also increased in the bark, wood (**Supplementary Figure S10**) and xylem sap (**Figure 3**) during spring seems to be a candidate contributing to the enhanced P_{org} pool in the xylem sap at this time of the year.

Soil-P and Soil-N Influence the P/N Metabolome and Phospholipid Profile

The Polar Metabolome and the Lipidome in Beech Twigs During Autumn and Dormancy Depend on the P_i Availability in the Soil

Both, the low plant available soil-P_i (Netzer et al., 2017) and soil-N (Rennenberg and Dannenmann, 2015) at the Tut site caused particular differences in the polar metabolome and lipidome profile in beech twig organs/tissues from Tut compared to Con beech trees in autumn and dormancy.

Senescent leaves

Except for two sugar-Ps, (Ino1P; Man1P) and 2deoxyG6P, that were significantly lower in senescent Tut leaves (**Figure 6**), polar metabolites of central metabolic pathways were indifferent between both forest sites. By contrast, numerous AAs were significantly lower in senescent leaves from the low-soil-P_i (and N) forest Tut than in senescent leaves from Con beeches (**Figure 6**). This finding was accompanied by the higher abundance of numerous AAs, some nucleobases and nucleosides in phloem exudates of Tut beeches (**Figure 3**) and indicates enhanced phloem transport of mobilized N from Tut beech leaves. A similar result was obtained for P_i mobilization from phospholipids such as PC, PE, and PG, which were less abundant in senescent leaves of Tut compared to Con beech trees (**Figure 6**). Furthermore, the non-phospholipids MGDG, DGDG, and SQDG as well as glucosylceramide (GlcCer) and free fatty (FF) acids were lower in senescent leaves from Tut than from Con beech trees, whereas similar levels were found for DGDG and MGDG in summer. The lower levels of these constituents of chloroplast membranes (Kobayashi, 2016) correlated with lower chlorophyll and carotenoid contents in senescent leaves from Tut compared to Con leaves (**Supplementary Figure S4**). All

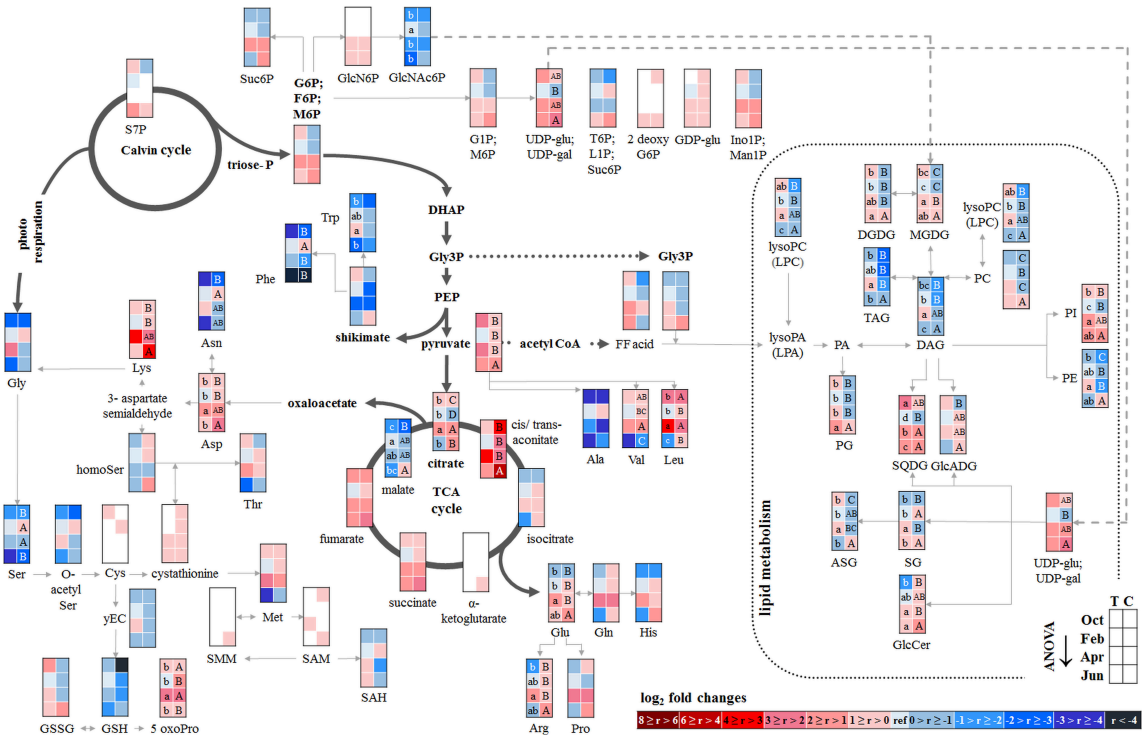

FIGURE 5 | Changes in polar metabolite and lipid abundances during annual growth in the wood. The figure shows heat maps of sugar-Ps, intermediates of central carbon metabolic pathways, and amino acids including sulfur compounds and lipids in the twig-wood of adult beech trees from the Tut (T) and Con (C) forest. Mean values of seasonal fluctuations of metabolites ($n = 3$) and lipids ($n = 5$) were presented as $\log_2$ fold changes using Tut data in February as reference. Different minor (Tut) or capital (Con) letters indicate significantly different relative metabolite or lipid abundance between the four seasons per site (results of One-Way-ANOVA, or Kruskal–Wallis-ANOVA in case that the requirement of normal distribution and/or equal variances was not fulfilled; $p < 0.05$). White = not detected. Abbreviations see **Figure 2**.

these findings indicate enhanced nutrient resorption from Tut compared to Con leaves.

Dormant buds

In both, dormant Tut and Con beech buds, ABA reached the highest level during the year (**Supplementary Figure S5**), as expected from the function of this phytohormone in setting and maintaining the dormant state (Fladung et al., 1997; Zheng et al., 2015). Although polar metabolites were not different between dormant Tut and Con buds, all phospholipids (PC, PE, PI, PG, lysoPC) showed higher abundances in dormant buds of Tut than of Con beech trees (**Figure 6**).

Bark and wood

With few exceptions, the polar metabolite profile was similar in the twig-bark and wood of beech trees from both forest sites during autumn (**Figure 6**). Only minor differences in metabolites involved in glycolysis and the TCA-cycle were observed. Nevertheless, abundances of several AAs were lower in twig-wood and/or bark of Tut beeches (**Figure 6**). Even the bark lipid profile showed only minor differences between the two forest sites in autumn whereas the wood lipid profile showed strong site-specific differences (**Figure 6**). Compared to Con beech trees, the abundances of phospholipids were higher in the wood of Tut beech trees during autumn (PC, PE, PG, and lysoPC) and dormancy (PC, PE, and lysoPC). The wood of Tut twigs also showed higher amounts of nearly all non-phospholipids, such as MGDG, DGDG, SQDG, TAG, DAG, ASG, and FF acids in autumn. These differences vanished during subsequent dormancy for MGDG, DGDG, and SQDG but PE, PC, the storage fats TAG, DAG, and FF acids remained higher in the wood of Tut beeches during dormancy (**Figure 6**). Altogether, this strongly indicates higher investment in P storage in form of phospholipids in the wood of Tut compared to Con beech trees as observed for the buds of Tut beeches (see above).

Mobilization of P From Twig Storage Pools in Spring Is Modulated by the P_i Availability in the Soil

Bursting buds

The polar metabolome profile of Con and Tut beech buds showed only few differences during spring. At the two forest sites the abundance of phospholipids was comparable, but the levels of TAG, DAG, and FF acid were higher in bursting buds of Tut compared to Con beech trees. Surprisingly, lipids involved in phospholipid replacement such as DGDG, SQDG, GlcADG, and GlcCER (Okazaki et al., 2013, 2015; Siebers et al., 2015) were higher in Con than in Tut buds in spring (**Figure 6**). Hence, swelling buds did not reveal any indication that low soil-P_i

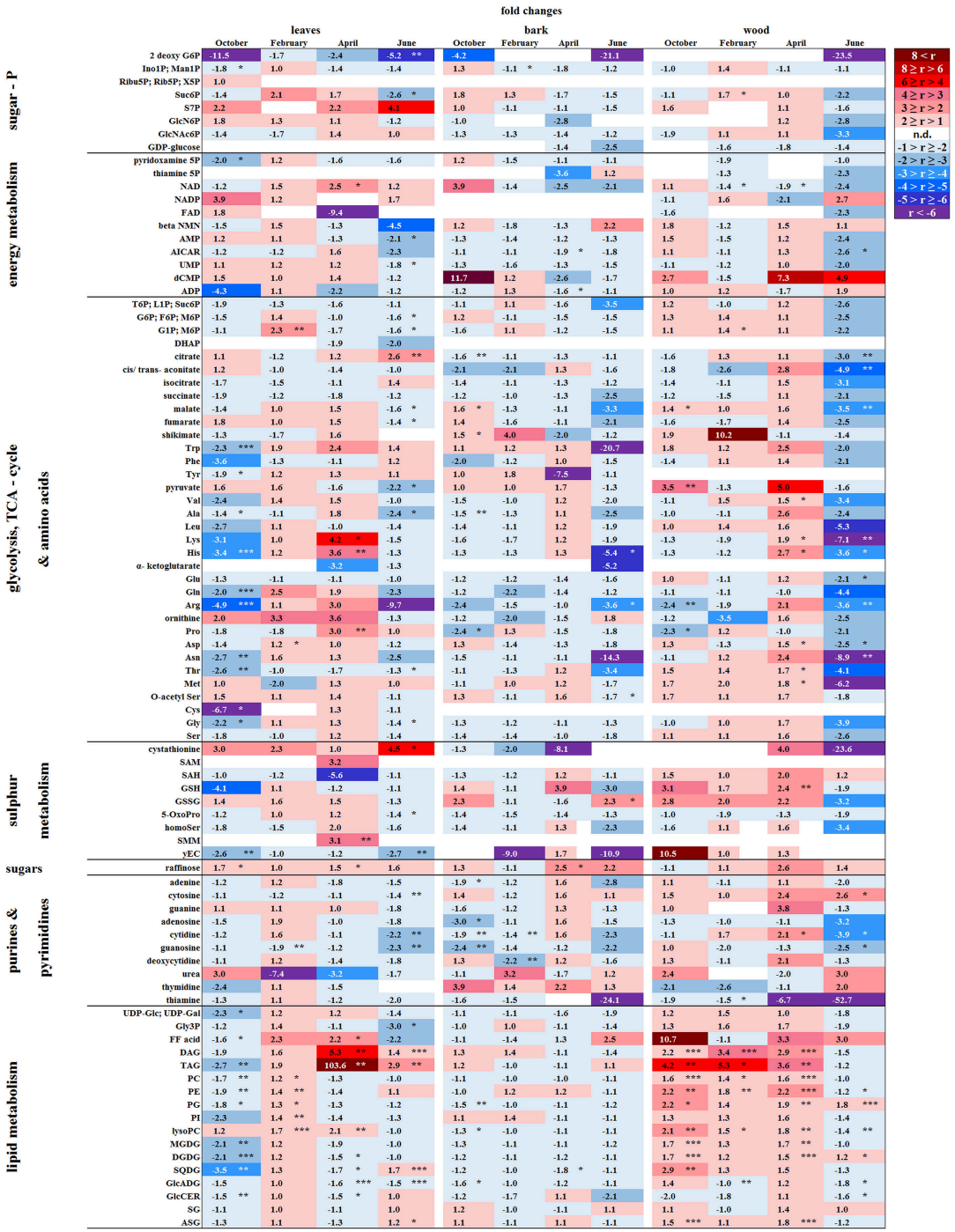

FIGURE 6 | Alterations in polar metabolite and lipid abundance due to P limitation. Fold changes of polar metabolites ($n = 3$) and lipids ($n = 5$) in buds/leaves, bark and wood of beech twigs from adult beeches of the Tut (low soil-P) and Con (sufficient soil-P) forests. Mean values of fold changes in relative peak areas are presented for the different seasons, i.e., autumn: October, dormancy: February, spring: April and early summer: June. The higher metabolite abundance in Tut tissues is given by Tut/Con ratios (red). The lower abundance of metabolites in Tut samples is presented by reciprocal Con/Tut ratios (blue). Asterisks indicate significant differences within one metabolite between both field sites during one season (results of Student's *t*-test or Mann–Whitney test in case that the requirement of normal distribution of the data was not fulfilled). $^{*}p < 0.05$; $^{**}p < 0.01$; $^{***}p < 0.001$; white boxes = not detectable. Relative peak areas of all identified metabolites are given in the **Supplementary Table S1**. AICAR, 5-aminoimidazole-4-carboxamide ribonucleotide; ASG, acyl steryl glucoside; DAG, diacylglycerol; DGDG, digalactosyldiacylglycerol; DHAP, dihydroxyacetone phosphate; FF acid, free fatty acid; γEC, γ-glutamylcysteine; GlcADG, glucuronosyldiacylglycerol; GlcCer, glucosylceramide; GlcN6P, glucosamine-6-phosphate; GlcNAc6P, N-acetyl-D-glucosamine-6-phosphate; Gly3P, glycerol-3-phosphate; lysoPA, lysophosphatidic acid; lysoPC, lysophosphatidylcholine; MGDG, monogalactosyldiacylglycerol; OPH, O-phospho-L-homoserine; PA, phosphatidic acid; PC, phosphatidylcholine; PE, phosphatidylethanolamine; PG, phosphatidylglycerol; PI, phosphatidylinositol; SAH, S-adenosyl-L-homocysteine; SAM, S-adenosyl-L-methionine; SG, steryl ester; SQDG, sulfoquinovosyldiacylglycerol; TAG, triacylglycerol.

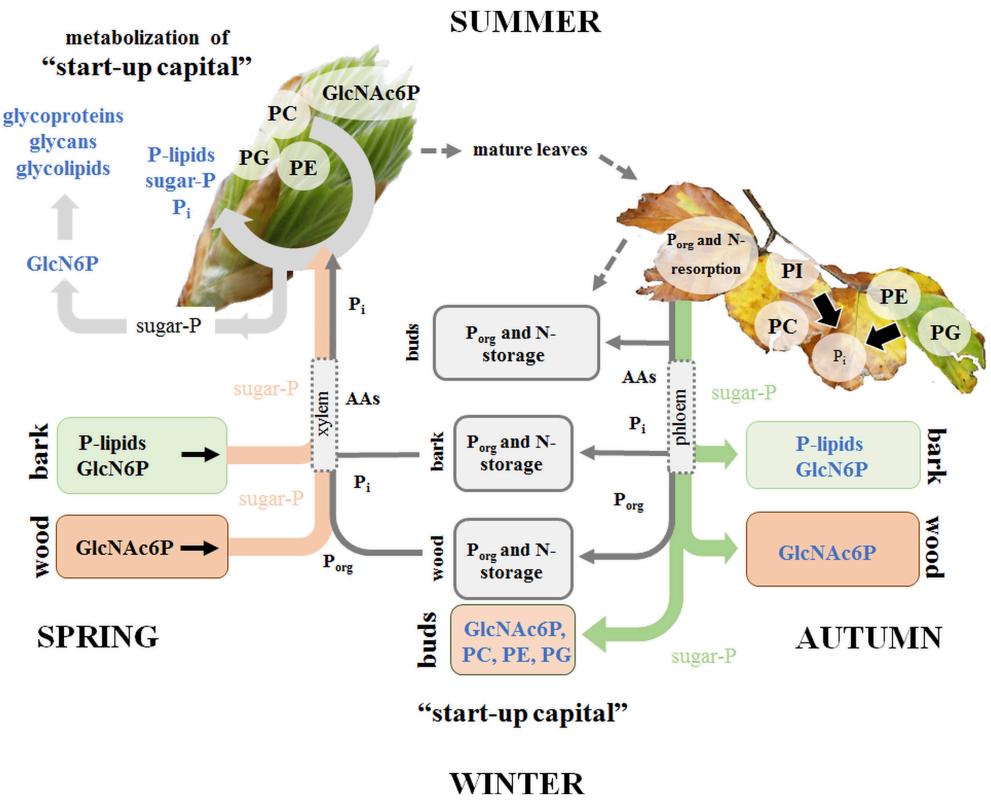

FIGURE 7 | P_{org} degradation in the stem contributes to fulfill P_i requirements for leaf development in spring. P and N storage, mobilization and fluxes are presented in gray. Storage and fluxes of distinct compounds of the polar (P) metabolom and (P) lipidome are presented in color. P mobilization in spring for the supply of P to developing buds, which require P_i for the energy metabolism and cell proliferation is achieved by three processes. (i) Phospholipid and GlcN6P degradation in the bark as well as GlcNAc6P mobilization in the wood; (ii) subsequent transport of released sugar-Ps and P_i to developing buds; and (iii) the use of the phospholipid "start-up capital" in buds built during autumn and/or dormancy. In the buds, GlcN6P can be synthesized from sugar-Ps and serves as a precursor for GlcNAc6P synthesis that can then be used in glycolipids, glycan and glycoprotein synthesis in spring buds (Furo et al., 2015). In autumn, phospholipid degradation and removal of P_i from senescent leaves take place prior leaf abscission. P_i is subjected to phloem transport and the formation of P-storage pools in bark and wood. In addition, P_i is used to build the P "start-up capital" in newly established buds. P_i supply of newly established buds in autumn is achieved by both, phloem and xylem transport. The dimension of arrows indicates the estimated contribution of either xylem or phloem transport in spring or autumn.

influenced their P metabolism. Regardless, the composition of the phloem sap that connects buds as sink tissues with stem tissues as nutrient sources showed few differences between beeches of both forests. During spring phloem exudates of Tut trees revealed higher abundances of beta-NMN, Met, Asn, and guanosine compared to Con beech trees (**Figure 3**).

Bark and wood

In the bark, polar metabolite abundances did not differ between beech trees of both forest sites in spring. In contrast, polar metabolites of the twig-wood revealed significant differences in AA levels. Val, Lys, His, Asp, Thr, and Met plus the sulfur containing peptide glutathione were higher in Tut than in Con twig-wood (**Figure 6**). Furthermore, the lipidome profile of the wood in spring showed strong differences between both forests as observed during autumn and dormancy. Several phospholipids and non-phospholipids were higher in the twig-wood of Tut compared to Con beech trees (**Figure 6**). These compounds included the phospholipids PC, PE, PG and lysoPC, the galactolipids DGDG, MGDG, and the storage lipids TAG and DAG (Bates and Browse, 2012; Manan et al., 2017) (**Figure 6**).

The Polar Metabolome and the Lipidome of Beech Twigs Are Modulated by the P_i Availability in the Soil During Vegetative Growth in Summer

Despite the lower soil-P_i availability at the Tut compared to the Con forest (Prietzel et al., 2016; Netzer et al., 2017), total P in leaves and other tissues was similar in beeches of both forests sites in summer indicating balanced P nutrition (**Figure 1**; Netzer et al., 2017). Still, distinct differences observed in the polar metabolome and lipidome indicate strategies to maintain adequate P_i levels in the leaves of Tut beech trees *via* bypassing the use of P_i in C metabolism and *via* phospholipid replacement by galacto- and sulfolipids.

Leaves

Leaf photosynthesis produces carbohydrates to supply leaf metabolism, and heterotrophic tissues/organs such as roots,

bark and wood with carbohydrates. Since chlorophyll and carotenoid levels were similar in both, Tut and Con beech leaves (**Supplementary Figure S4**) photosynthetic capacity can be expected to be equal in beech leaves of the two forest sites. Despite this similarity, several P containing hexoses involved in C metabolism, i.e., 2deoxyG6P, (G6P; F6P; M6P), (G1P; M6P), and sucrose-6P (Suc6P), were significantly lower in leaves from Tut compared to Con beech trees (**Figure 6**). These differences correspond to both, significantly lower C (**Figure 1**) and P_{org} (Netzer et al., 2017) contents in Tut leaves in summer. The abundance of sedoheptulose-7P (S7P) involved in ribulose-5P regeneration in the Calvin cycle was higher in Tut leaves. This might indicate insufficient P_i abundance for sugar-P synthesis via the Calvin cycle. In accordance, the abundance of the amino acids Gly and Ser, synthesized by photorespiration from 2-phosphoglycolate (**Supplementary Figure S7**), were slightly reduced in the leaves of Tut beech trees (**Figure 6**). Respectively, the abundance of the glutathione precursor γGluCys (γEC) that relies on Ser availability for the synthesis of its Cys moiety (Strohm et al., 1995), was also significantly lower in leaves of Tut beech trees.

On the other hand, the lower abundances of sugar-Ps such as (G6P; F6P; M6P) and (G1P; M6P) in Tut compared to Con leaves may indicate lower abundance of sugar-Ps for glycolysis. DHAP was only detectable in spring buds and summer leaves, and tended to be lower in beech trees of the Tut site. Although pyruvate, the product of glycolysis, was lower in Tut compared to Con in summer leaves, the level of citrate synthesized after pyruvate decarboxylation from acetyl-CoA and oxaloacetate was higher. Two TCA-cycle metabolites synthesized downstream of citrate, i.e., malate and fumarate (**Supplementary Figure S6**), were lower in Tut than in Con leaves. Down-regulation of carbohydrate degradation by glycolysis and the TCA-cycle may be concluded and is supported by reduced abundance of several AAs synthetized from intermediates of glycolysis and the TCA-cycle (Ala, Thr, Arg) for the beech leaves of the Tut forest (**Figure 6**, **Supplementary Figure S7**).

On the other hand, sugar-Ps such as (G1P; M6P) and pyruvate are precursors for lipid formation (**Supplementary Figure S8**). Several non-phospholipids are enhanced in Tut compared to Con leaves that are SQDG, GlcADG, and ASG, which replace phospholipids at low P availability (Okazaki et al., 2013; Lambers et al., 2015; Siebers et al., 2015). The storage lipids TAG, DAG, and their precursor glycerol-3P (Gly3P) showed higher abundance in Tut compared to Con leaves during summer.

Bark and wood

During summer, the polar metabolome and lipidome were largely similar for the twig-bark of Tut and Con beeches with exceptions of several N compounds (**Figure 6**). The AAs Arg (3.6-fold), His (5.4-fold), Asn (14.3-fold), and Trp (20.7-fold) and the Cys precursor O-acetylSer (1.4-fold) were higher in the bark of Con than of Tut beeches.

In the twig-wood the polar metabolome and the lipidome revealed strong differences between the two study sites (**Figure 6**). However, differences were not observed for sugar-Ps and metabolites of glycolysis, but for TCA-cycle intermediates (**Figure 6**). Lower malate, cis/trans-aconitate and citrate abundances were found in the twig-wood of Tut beeches that might indicate downregulation of the TCA-cycle. This view is supported by lower levels of nucleotides. Lower levels of 5-aminoimidazole-4-carboxamide ribonucleotide (AICAR) and AMP known to constitute activators of the "cell energy sensor" AMPK (AMP activated protein kinase; Theodorou et al., 1991; Hardie, 2011) support this assumption. The lipid composition of the wood showed strong differences between both forest sites, which were, however, not uniform. Higher abundances of PG and DGDG, but lower levels of PE, lysoPC and of the non-phospholipids GlcADG and GlcCER were detected in the wood of Tut compared to Con beeches.

DISCUSSION

This study provides a detailed view on the dynamics of P metabolism of the temperate climax forest tree species *F. sylvatica* during annual growth. It could be showed (i) that the profile of polar P metabolites and phospholipids is modulated by the season in leaves, bark and wood (hypothesis 1) for P storage and mobilization, and (ii) that these variations are linked to changes of central metabolic pathways (hypothesis 3). Phospholipids and GlcN6P in the bark, but solely GlcNAc6P in the wood as well as phospholipid accumulation in dormant leaf buds are the hallmarks of P storage during dormancy (**Figure 7**). The accumulated phospholipids in dormant buds provide the P "start-up capital" for shoot outgrowth in spring. Limitation of soil-P_i availability affected phospholipid storage and mobilization, thereby economizing P use in beech twigs *via* several processes (**Figure 7**). (i) P_i availability of leaves was economized in summer by diminished abundance of sugar-Ps and by phospholipid replacement (hypothesis 2). (ii) P resorption from phospholipids of senescent leaves in autumn and accumulation of phospholipids in leaf buds during dormancy was enhanced. (iii) Phospholipid storage in the twig-bark during dormancy was improved. The latter processes complemented the P "start-up capital" for shoot outgrowth in spring at low soil-P_i availability. Altogether, the results showed that seasonal changes of polar P metabolites and phospholipids and consequently the internal P-cycling efficiency were affected by the P_i availability in the soil (hypothesis 3). Thus, growth restriction by soil-P_i limitation was prevented in beech trees by economizing P_i availability in leaves and by efficient storage and mobilization of phospholipids.

Changes in Polar Metabolite and Lipid Composition Indicate Annual P (Re)cycling

Autumn and Winter: P Resorption From Beech Leaves and P Storage in Twig-Bark

The removal of nutrients from senescent leaves and storage pool formation in the stem constitutes a special feature of deciduous trees to restrict loss of nutrients by leaf abscission (Rennenberg and Schmidt, 2010). As a consequence, N (Millard and Grelet, 2010; Wildhagen et al., 2010), S (Herschbach et al., 2012), and P contents (Chapin and Kedrowski, 1983; Keskitalo et al., 2005;

Netzer et al., 2017) decrease in leaves and increase in stem tissues during autumn. Mobilization of nutrients from leaves during senescence requires metabolic remodeling to generate phloem mobile metabolites for its transport into storage tissues. Consistently, many proteinogenic AAs increased in senescent compared to summer leaves of adult beech trees (**Figure 2**). Simultaneously, AAs showed greater abundance in phloem exudates during autumn than in spring (**Figure 3**). The bark functions as sink organ for phloem-derived AAs and is the site of storage protein formation in autumn (Coleman et al., 1991; Millard and Grelet, 2010; Wildhagen et al., 2010). This is consistent with increased N in twig-bark and wood of beech trees in winter (**Figure 1**). Particularly prominent, the organic P compounds involved in P mobilization, phloem transport, and storage in the bark were identified in the present study. In beech leaves, phospholipids specifically PG and PI declined in autumn and, thus, constitute P_i sources. PG and PI degradation was supported by the increased abundance of lysoPC, an indicator of phospholipid degradation in senescent leaves (Nakamura, 2013; Boudière et al., 2014; Siebers et al., 2015). Consistently, in the arctic tundra forest tree *Betula papyrifera,* the phospholipid pool of leaves decreased by 50% and the nucleic acid P pool by 61% until senescence, thereby explaining 74% of the P resorption from birch leaves during senescence (Chapin and Kedrowski, 1983).

Depending on source-sink relations, resorbed and phloem transported nutrients are allocated to the roots, developing tissues such as apical meristems, to newly established buds or to stem tissues to fill up storage pools (Lough and Lucas, 2006; Lucas et al., 2013). Notably, sugar-Ps were identified as P_{org} compounds transported in the phloem and thereby mediating accumulation of P_{org} in beech buds during dormancy (Netzer et al., 2017). In dormant beech buds, however, phospholipids (PC, PE, PG) and GlcNAc6P rather than sugar-Ps contribute to P_{org} accumulation. Another sink of phloem allocated sugar-Ps are the twig-bark and wood that both accumulated P_{org} during dormancy (Netzer et al., 2017). In the bark, but not in the wood PC, PE, and PG contribute to P_{org} storage (**Figures 4**, **5**). In birch, P storage in stems during dormancy was mediated by nucleic acid-, lipid-, and ester-P (Chapin and Kedrowski, 1983). Hence, further P metabolites such as inositol-6-phosphate known as a common storage compound in grains may furthermore contribute to the P_{org} storage pool as described for poplar (Kurita et al., 2017). Development of an adequate and sophisticated technique for the analysis of IP6 in tree tissues needs further studies (Wu et al., 2009). Neither the extraction method of Lisec et al. (2006) nor a GC-MS approach (Du et al., 2016) nor a common photometric test using the "Ward-reagent" (Vaintraub and Lapteva, 1988; Konieczynski and Wesolowski, 2014) were suitable to quantify IP6 in beech tissues (data not shown). Nevertheless, the present study identified further P_{org} storage compounds; specifically GlcN6P in the bark and its acetylation product GlcNAc6P in the wood (**Figures 4**, **5**). GlcNAc6P, a precursor of glycolipid synthesis (Furo et al., 2015), was highest during dormancy and coincided with highest levels of the galactolipids DGDG and MGDG in beech bark (**Figure 4**). MGDG and DGDG are uncharged galactolipids and main constituents of the lipid bilayer matrix in thylakoid membranes (Shimojima and Ohta, 2011; Kobayashi, 2016). It may be speculated that increasing DGDG and MGDG play a role in chloroplasts development of bark parenchyma cells for photosynthesis. Bark photosynthesis is a phenomenon observed for several perennial plants including beech (Wittmann et al., 2001) and even in winter (Diehl et al., 1993; Aschan and Pfanz, 2003). Alternatively, increasing amounts of DGDG and MGDG may be involved in frost hardening during dormancy and/or in C storage (Yoshida and Sakai, 1973; Wang and Faust, 1988; Moellering et al., 2010).

Spring: P Mobilization From Twig-Bark and Xylem Transport to Developing Buds

Bud break in spring requires the release of dormancy to provide sufficient amounts of nutrients for energy production and building blocks for leaf growth and development. The present study shows that the decrease of P_{org} and P_{tot} (**Figure 1**, Netzer et al., 2017) in twig-bark is due to phospholipid degradation, since PC, PE, and PG declined from dormancy to spring (**Figure 4**). In addition, degradation of GlcN6P in the bark and GlcNAc6P in the wood could contribute to provide P_i. Hence, twig phospholipids, but also GlcN6P and GlcNAc6P, are strong candidates for supplying P_i to the buds after cleavage by phosphatases (Lan et al., 2015; Siebers et al., 2015) and P_i allocation *via* xylem transport. P_i was the main transport form of P in the xylem sap of beech in spring, but P_{org} still accounted for ∼40% of P_{tot} (Netzer et al., 2017). A number of polar P compounds, i.e., sugar-Ps, nucleotides, and beta-NMN, were identified in the xylem sap and thus contributed to the xylem transported P_{org} pool. The diversity of organic P metabolites was lower in the xylem sap compared to leaves, bark and wood (**Table 1**). This indicates restricted loading of P metabolites into the xylem sap. Mobilization of nutrients from storage pools of the stem and its transport to developing buds in spring was described for several tree species and may be the consequence of temperature restricted nutrient uptake from the soil (Geßler et al., 1998; Rennenberg et al., 2010; Budzinski et al., 2016). Degradation of bark storage proteins (BSP) during spring to release AAs for its allocation to developing buds *via* the xylem sap is a well-known feature of deciduous trees (Schneider et al., 1996; Nahm et al., 2006; Rennenberg et al., 2010) and was also evident in beech trees of the present study (**Figure 3**).

Spring: Metabolic Remodeling in Buds

During spring large amounts of P_{org} especially beta-NMN, sugar-Ps (**Figure 3**), P_i (Netzer et al., 2017), AAs and organic acids in the xylem sap coincided with peak levels of almost all AAs, sugar-Ps, lipids (present study), and P_i (Netzer et al., 2017) in beech buds. This identified bursting leaf buds as sinks for xylem derived nutrients. High levels of polar metabolites of glycolysis and the TCA-cycle in bursting buds indicated boosting of central pathways of C metabolism. Simultaneously, catabolic pathways involved in the production of building blocks for leaf growth and development as previously described for oak buds (Derory et al., 2006) are essential. Adequate P_i as a prerequisite for almost all anabolic and catabolic reactions in bursting buds can be provided via xylem transport into buds, and/or from *in situ* remobilization from sugar-Ps and

phospholipids by phosphatases (Tian and Liao, 2015). The only P_{org} compound that declined in buds until spring and thus constitutes a potential *in situ* source of P_i was GlcNAc6P that on the other hand is involved in the synthesis of glycolipids (**Supplementary Figure S8**, Furo et al., 2015). In bursting beech buds GlcNAc6P degradation went along with increasing GlcN6P, which is produced from F6P and serves as substrate for GlcNAc6P (Furo et al., 2015). Apparently, GlcNAc6P is used for both, glycolipid formation and as a substrate of P_i delivery. Thus, consumption of GlcNAc6P in buds during spring to allow leaf expansion might be enable by its regeneration via F6P and GlcN6P. Remarkable, in bursting beech buds sugar-Ps and phospholipids (PC, PE, PG, PI) increased and thus did not function as P_i source (**Figure 2**). Synthesis of phospholipids as major components of photosynthetic membranes in chloroplasts is highly significant in spring to fulfill the increasing need in energy and carbon compounds. Especially PG constitutes an important compound stabilizing photosynthetic membranes to maintain membrane polarity (Boudière et al., 2014; Siebers et al., 2015; Kobayashi, 2016). The increase of the chloroplast lipids DGDG and MGDG (Kobayashi, 2016) in developing buds provided additional evidence of chloroplast membrane formation at the beginning of the vegetation period that fits well with increased abundance of lipid precursors such as Gly3P, (UDP-Glc; UDP-Gal), DAG, and FF acids. Further support comes from positive correlations of phospholipids with ADP, sugar-6Ps, sugar-1Ps, and DHAP and phospholipid precursors specifically (UDP-Glc; UDP-Gal), DAG, CTP, and UDP. In addition, FF acid correlated significantly to each other (**Supplementary Figure S11**, **Supplementary Table S5**). Hence, phospholipid synthesis rather than phospholipid degradation to supply free P_i is evident in developing beech buds.

Annual P (Re)cycling Is Determined by Soil-P Availability

Autumn and Winter: Nutrient Resorption From Leaves, P Accumulation in Buds and Wood Are Enhanced in Beech Trees on P Impoverished Soil

It has been hypothesized that the lower plant available soil-P, the more pronounced will be tree internal P cycling (Lang et al., 2016). Consistent with this hypothesis, P_i resorption from the phospholipids PC, PE, and PG in senescent leaves was enhanced at the low-P (and N) forest site Tut compared to the Con site. Generally, higher nutrient resorption from senescing beech leaves in Tut was indicated by lower abundances of the non-P thylakoid membrane lipids MGDG, DGDG, and SQDG (Kobayashi, 2016), lower chlorophyll and carotenoid contents and lower levels of proteinogenic AAs (**Figure 2**, **Supplementary Figure S4**). Enhanced P resorption was, neither reflected by enhanced P_{tot} and P_{org} concentrations in phloem exudates nor in the bark in autumn and dormancy (Netzer et al., 2017). Consistently, similar polar (P)-metabolome profiles were determined for phloem exudates and twig-bark of both, Tut and Con, beeches. Nevertheless, the phospholipids PI, PE and PC were higher in the wood of Tut compared to Con twigs (**Figure 6**). Apparently, the twig-wood of Tut beeches constitutes a stronger sink for remobilized P from senescent leaves than the twig-wood of Con beeches, thereby contributing to uncouple P nutrition from P availability in the soil (Lang et al., 2016).

Different to P_{tot} and P_{org}, proteinogenic AAs in phloem exudates showed a higher abundance in Tut compared to Con twigs in autumn (**Figure 6**). This implies enhanced N transport into bark and wood probably for storage protein synthesis in Tut beech trees, as previously shown for poplar trees (Coleman et al., 1991; Millard and Grelet, 2010; Rennenberg et al., 2010; Wildhagen et al., 2010). Inconsistently, N storage was only observed in the bark of Con beech trees (**Figure 1**). The seasonal dynamic and spatial resolution of protein storage in beech bark and wood has not been studied and N allocation to the roots for storage cannot be excluded. The discrepancy of greater P and N resorption from senescent Tut leaves combined with equal P but higher N abundances in phloem exudates in comparison to Con beech twigs can be explained by different processes. First, higher phloem unloading and improved phloem-to-wood transport of phloem allocated P compounds may take place in Tut beeches. Second, P mobilized from senescent leaves may be consumed and stored in newly established buds (see below). Third, phloem allocated P compounds could have been transported to the main trunk and/or to the roots. Fourth, P resorption during senescence may take place prior or after N resorption. Hence, a high temporal resolution of polar (P) metabolome and lipidome analyses is needed to resolve timing of P vs. N resorption from senescent leaves in future studies.

Spring: The Polar (P) Metabolome and Lipidome in Beech Buds Indicates Adequate P and N Supply for Leaf Development in Spring Independent From Soil Properties

Although the Tut forest is limited by soil-P_i and soil-N (Rennenberg and Dannenmann, 2015; Prietzel et al., 2016; Netzer et al., 2017), similar abundances of polar metabolites, nucleotides and AAs were detected in buds during spring (**Figure 6**). Apparently, bursting buds were well prepared for an adequate energy metabolism and synthesis of membrane compounds, proteins, nucleoids, lignin etc. for its outgrowth independent of soil-P_i and soil-N availability. While during dormancy the P lipidome in buds differed between the low and the sufficient soil-P/N site, phospholipid abundance in spring was similar in the developing buds (**Figure 6**). This seems to be achieved by *de novo* phospholipid synthesis combined with sugar-P and P_i import *via* the xylem. The greater P "start-up capital" in the buds of Tut beeches was required, because of lower P_i levels in the xylem sap and, thus, lower P supply into the bursting buds in Tut compared to Con beeches (Netzer et al., 2017). Thus, formation of a higher P "start-up capital" in Tut buds constitutes a mechanism to avoid P shortage in case of restricted P supply *via* the xylem sap in spring.

Phosphorus Use in Tut Beech Leaves in Summer Is Economized by Metabolome and Lipidome Remodeling

In early summer, when leaf development of beech trees is completed and metabolic steady state can be expected, the lower

soil-P availability at the Tut compared to the Con forest was reflected by distinct differences in the P metabolome of mature leaves. Consistent with lower P_i and P_{org} levels (Netzer et al., 2017), diminished abundances of sugar-Ps in beech leaves of Tut trees were observed in the present study. The same was observed in leaves and roots of *Arabidopsis* plants and leaves of *Eucalyptus* trees upon P limitation (Warren, 2011; Pant et al., 2015a,b). Enhanced turnover or reduced synthesis of sugar-Ps in the leaves of Tut beeches could be a strategy to buffer cytosolic P_i (Veneklaas et al., 2012), either by releasing P_i from sugar-Ps, or by reducing sugar-P synthesis (Warren, 2011; Lambers et al., 2015). In Tut leaves, improved P_i availability may additionally be achieved through bypassing P_i consuming pyruvate production *via* pyruvate kinase (PK) (Plaxton and Tran, 2011). This assumption is supported by the lower abundance of AMP (**Figure 6**), an activator of the cytosolic pyruvate kinase (PKc) (Huppe and Turpin, 1994). Pyruvate can be produced from PEP either through pyruvate P_i-dikinase (PPDK) or *via* cytosolic phosphoenolpyruvate carboxylase (PEPCc) thereby synthesizing oxaloacetate that is converted to malate in the next step via malate dehydrogenase (MDH) in the cytosol (**Supplementary Figure S6**). After malate import into mitochondria, malate functions as a precursor for pyruvate synthesized *via* malic enzyme (ME) and, hence, for acetyl-CoA production without using P_i. Furthermore, malate in mitochondria itself can serve as a precursor for citrate synthesis in the TCA-cycle via rebuilding oxaloacetate, the acceptor of acetate from acetyl-CoA. This alternative pathway to fill up the TCA-cycle is thought to operate under P_i limitation (Plaxton and Tran, 2011; Plaxton and Shane, 2015). At the first view, such an alternative pathway in Tut beech leaves was not supported from the present data, because both, malate and pyruvate, were lower in Tut compared to Con leaves in summer. As PEPCc is inhibited by malate the lower malate content in Tut leaves may prevent down regulation of PEPCc at P limitation (Plaxton and Shane, 2015). On the other hand, the presented data did not distinguish between malate contents in the cytosol and mitochondria. However, the greater citrate accumulation in Tut than in Con leaves may indicate this alternative pathway but may also be caused by a reduced carbon flux through the TCA-cycle.

Alternatively, the lower abundance of pyruvate in Tut leaves can be explained by its enhanced conversion to acetyl-CoA for FF acid production (Troncoso-Ponce et al., 2016) and thus lipid biosynthesis. Although the abundance of FF acids in Tut beech leaves was significantly lower than in Con leaves, greater abundances of TAG and DAG that are synthesized from FF acids were found (**Figure 6**, **Supplementary Figure S8**). Both TAG and DAG can function as carbon storage pools at P deficiency and accordingly, were described as markers for P starvation in *Arabidopsis* (Pant et al., 2015a,b). Accumulation of DAG and TAG at P deficiency may be caused by their reduced export from chloroplasts into the cytosol. Antiporters that simultaneously import P_i (Rychter and Rao, 2005; Pant et al., 2015a,b) mediate the export of DAG, TAG, and triose phosphates from chloroplasts into the cytosol. Considering the lower P_i level in beech leaves of Tut compared to Con trees in early summer (Netzer et al., 2017), reduced DAG and TAG export from chloroplasts could explain their enrichment in Tut leaves. Furthermore, DAG and TAG are precursors for the synthesis of phospholipid replacing lipids such as MGDG, DGDG, SQDG, and GlcADG (**Supplementary Figure S8**). Gly3P needed in DAG and TAG synthesis was lower in Tut than in Con leaves (**Figure 6**) and finally, the higher abundance of the non-phospholipids SQDG and ASG in Tut leaves indicate phospholipid replacement (Lambers et al., 2012, 2015; Siebers et al., 2015). Especially SQDG is known to be involved in phospholipid replacement under P limitation to stabilize PSII in thylakoid membranes and thus to maintain photosynthetic capacity, especially at reduced PG abundance (Boudière et al., 2014). Thus, accumulation of SQDG can be taken as a strong hint for the adaptation of Tut beech leaves to low-soil-P_i availability. The replacement of phospholipids by non-phospholipids is consistent with lower P_{org} levels in Tut compared to Con leaves in early summer (Netzer et al., 2017). In summary, the present results strongly support the assumption that adequate P_i levels in leaves of Tut beech trees were achieved by (i) bypassing the P_i-consuming pyruvate synthesis via PKc, (ii) economized sugar-P availability, and (iii) phospholipid replacement by non-phospholipids.

CONCLUSION

Avoidance of P loss by autumnal leaf abcission was enabled by economized P cycling in the temperate climax forest tree species *F. sylvatica*. This is achieved by phospholipid degradation in senescent leaves and consecutive P_i export *via* the phloem. In the bark, phloem derived P_i is used to build P storage pools in form of phospholipids and GlcN6P, whereas in the wood solely GlcNAc6P fulfills the same function. During autumn, newly established buds are prepared for spring outgrowth by building a P "start-up capital" consisting of phospholipids and GlcNAc6P based on P_i mobilized from senescent leaves or delivered by xylem transport. In spring, buds are additionally supplied with P *via* the xylem sap in form of sugar-Ps, and in form of P_i mobilized from phospholipids stored in the bark during dormancy. P_i and sugar-P transported to the buds are channeled into energy metabolism and used for the synthesis of cellular metabolites, such as nucleotides, phospholipids etc., which are needed for growth and development. These processes are essential to economize tree-internal P cycling and are stimulated in trees growing on P impoverished soil. Under these conditions, P use in leaves is economized to establish adequate P_i abundance via phospholipid replacement through galacto- and sulfolipids.

AUTHOR CONTRIBUTIONS

FN did most of the research including tissue sampling in the field campaigns, sample preparation, data analyses, and the preparation of the figures. AO, YO, and KS performed lipid and metabolite analyses. DD performed the IRMS measurements. CH and HR designed the research and provided suggestions during data analyses. CH, FN, and HR wrote the manuscript.

FUNDING

The present research was performed in the context of the Deutsche Forschungsgemeinschaft (DFG) priority program SPP 1685 — Ecosystem nutrition: forest strategies for limited phosphorus resources. The Deutsche Forschungsgesellschaft (DFG) under project number RE 515/41-1 to HR and HE 3003/6-1; HE 3003/6-2 to CH financially supported the work, which is gratefully acknowledged. The article processing charge was funded by the German Research Foundation (DFG) and the University of Freiburg in the funding program Open Access Publishing.

ACKNOWLEDGMENTS

The authors owe special thanks to Oliver Itzel for supporting this work during the field campaigns in Tuttlingen and the Conventwald forest. Furthermore, Eduardo Federico Reppert López is acknowledged for preparing the samples for IRMS analyses of total N and C.

SUPPLEMENTARY MATERIAL

The Supplementary Material for this article can be found online at: https://www.frontiersin.org/articles/10.3389/fpls.2018.00723/full#supplementary-material

Supplementary Table S1 | Polar metabolites identified in buds/leaves, bark, wood, xylem sap, and phloem exudates.

Supplementary Table S2 | List of all lipid classes identified in buds/leaves, bark, and wood.

Supplementary Table S3 | Top 10 polar metabolites and lipids contributing to the differentiation in axis directions in the PLS-DA plots. Data are taken from PLS-DA analyses of beech tissues presented in **Supplementary Figures S2**, **S3**. Mean values [$n = 3$ for polar (P) metabolites], ($n = 5$ for lipids) of the VIP scores of all axis dimensions (X, Y, Z-dimension) are presented.

Supplementary Table S4 | Relative contribution of polar P metabolites or phospholipids to the overall separation in the PLS-DA plots. The relative contribution of P metabolites or phospholipids in the VIP score was calculated by summing up VIP score values of all polar P metabolites and phospholipids obtained from the respective PLS-DA analyzes presented in **Supplementary Figures S2**, **S3**.

Supplementary Table S5 | Pearson's correlation coefficients derived from of correlation analyses.

Supplementary Figure S1 | Distribution pattern of polar (P) metabolites in beech twig organs/tissues. Venn diagrams of all identified polar metabolites **(A)** and polar P metabolites **(B)** (irrespective of seasonal differences) in twig organs/tissues, i.e., buds/leaves, bark, wood, xylem sap, and phloem exudate of adult beech trees from the Con (first number) and Tut (second number) forest. A detailed overview of all polar (P) metabolites in the twig tissues is provided in **Table 1** and **Supplementary Table S1**.

Supplementary Figure S2 | Differentiation of the lipidome and the polar metabolome of organs/tissues by season and site. PLS-DA score plots of the lipidome **(A,C,E)** and the polar metabolome **(B,D,F)** for buds/leaves **(A,B)**, bark **(C,D)** and wood **(E,F)** of adult Tut (T) and Con (C) beech trees in October (O), February (F), April (A), and June (J). PLS-DA plots of the lipidome and polar metabolome were build using all identified compounds (**Supplementary Table S1**). The top 10 polar metabolites and lipids contributing to the separation in axis directions of the PLS-DA score plots are presented in the **Supplementary Table S3**. Statistical analyses were performed with MetaboAnalyst 3.0 (http://www.metaboanalyst.ca/, Xia et al., 2015).

Supplementary Figure S3 | Differentiation of the polar metabolome in xylem sap and phloem exudate by season and site. PLS-DA score plots of the polar metabolome of the xylem sap **(A)** and phloem exudates **(B)** collected from twigs of adult beech trees at the Tut (T) and the Con (C) forest in October (O) and April (A). All identified metabolites were included in the PLS-DA analyses and are presented in the **Supplementary Table S1**. The top three P metabolites causing the separation in the PLS-DA score plots are (i) for the xylem sap: beta-NMN, (T6P; L1P; Suc6P) and GlcNAc6P and (ii) for phloem exudates: (G6P; F6P; M6P), beta-NMN, dTMP. Statistical analyses were done with MetaboAnalyst 3.0 (http://www.metaboanalyst.ca/, Xia et al., 2015).

Supplementary Figure S4 | Changes in pigment abundance of leaves during annual growth. Chlorophyll **(A,B)** and carotenoids **(C,D)** of Con (**A,C**; black bars) and Tut beech leaves (**B,D**; gray bars) in autumn (October, Oct), winter (February, Feb), spring (April, Apr), and summer (June, Jun). Data represent mean values ± *S.D.* of five replicates. Different minor letters indicate significant differences between seasons at each forest site (One-Way-ANOVA, or Kruskal–Wallis-ANOVA in case that the requirement of normal distribution and/or equal variances was not fulfilled; $p < 0.05$). Asterisks indicate significant differences of a particular metabolite between both field sites during one season at $*p < 0.05$; $**p < 0.01$ (results of Student's *t*-test or Mann–Whitney tests in case that the requirement of normal distribution or homogeneity of variances of the data was not fulfilled).

Supplementary Figure S5 | Plant hormone abundance in beech twig organs/tissues during annual growth. GABA, ABA, GA3, tZ, and tZR in buds/leaves **(A,B)**, bark **(C,D)**, wood **(E,F)**, of Con (**A,C,E**; black bars) and Tut beeches (**B,D,F**; gray bars) in autumn (October, Oct), winter (February, Feb), spring (April, Apr), and summer (June, Jun). Data presented are mean values ± *S.D.* of three replicates. Different minor letters indicate significant differences between seasons at each forest site (One-Way-ANOVA, or Kruskal–Wallis-ANOVA in case that the requirement of normal distribution and/or equal variances was not fulfilled; $p < 0.05$). Asterisks indicate significant differences between both forest sites of a particular metabolite during the respective season. Statistics were done by Student's *t*-test or Mann–Whitney tests in case that the requirement of normal distribution or homogeneity of variances of the data was not fulfilled. $*p < 0.05$; $**p < 0.01$.

Supplementary Figure S6 | Central metabolic pathways including steps providing P_i at P starvation. The pathways were designed based on Kegg pathways http://www.genome.jp/kegg/pathway.html?sess=2764b8338258d6286de91bbebe6faf46). Abbreviations of metabolites: 3PGA, 3-phosphoglycerate; R5P, ribulose-5P, S7P, sedoheptulose-7P; F6P, fructose-6P; F1,6P_2, fructose-1,6P_2; G3P, glyceraldehyde-3P; DHAP, dihydroxyacetone-P; PEP, phosphoenolpyruvate; OAA, oxaloacetate. Abbreviations of enzymes: PFK, phosphofructokinase; PK, pyruvate kinase; PEPC, PEPcarboxylase; MDH, malate dehydrogenase; PDH, pyruvate dehydrogenase.

Supplementary Figure S7 | Synthesis of amino acids from metabolites of central metabolic pathways. The pathways were designed based on Kegg pathways (http://www.genome.jp/kegg/pathway.html?sess=2764b8338258d6286de91bbebe6faf46). Abbreviations of metabolites: 3PGA, 3-phosphoglycerate; R5P, ribulose-5P, S7P, sedoheptulose-7P; F6P, fructose-6P; F1,6P_2, fructose-1,6P_2; G3P, glyceraldehyde-3P; DHAP, dihydroxyacetone-P; PEP, phosphoenolpyruvate; OAA, oxaloacetate. Abbreviations of enzymes: PFK, phosphofructokinase; PK, pyruvate kinase; PEPC, PEPcarboxylase; MDH, malate dehydrogenase; PDH, pyruvate dehydrogenase.

Supplementary Figure S8 | Schematic overview of lipid metabolism independent of cellular compartmentation. Phospholipids are given in red, lipids known to be involved in phospholipid replacement in blue. Abbreviations: ASG, acyl steryl glucoside; DAG, diacylglycerol; DGDG, digalactosyldiacylglycerol; FF acid, free fatty acid; GlcADG, glucuronosyldiacylglycerol; GlcCer, glucosylceramide; GlcNAc6P, N-acetyl-glucosamine 6-phosphate; GlcN6P, glucosamine-6-phosphate; Gly3P, glycerol-3-phosphate; lysoPA, lysophosphatidic acid; lysoPC, lysophosphatidylcholine; MGDG, monogalactosyldiacylglycerol; PA, phosphatidic acid; PC, phosphatidylcholine; PE, phosphatidylethanolamine; PG, phosphatidylglycerol; PI, phosphatidylinositol; SG, steryl ester; SQDG, sulfoquinovosyldiacylglycerol; TAG, triacylglycerol. The Figure was created based on Okazaki et al. (2013, 2015), Siebers et al. (2015), Boudière et al. (2014), Hirabayashi and Ichikawa (2002), Guschina et al. (2014), Li-Beisson et al. (2010), Furo et al. (2015), and Kobayashi (2016).

Supplementary Figure S9 | Plant hormone abundance in transport tissues of beech twigs during annual growth. Plant hormones in the xylem sap and in phloem exudates of the Con (black bars) and the Tut (gray bars) beech twig organs/tissues. Data present mean values ± *S.D.* of three replicates. Different minor letters indicate significant differences between seasons at each forest site (One-Way-ANOVA, or Kruskal–Wallis-ANOVA in case that the requirement of normal distribution and/or equal variances was not fulfilled; $p < 0.05$). Asterisks indicate significant differences between both field sites of a particular metabolite during the respective season. Statistics were performed with Student's *t*-test or Mann–Whitney tests in case that the requirement of normal distribution of the data was not fulfilled $^{**}p < 0.01$; $^{***}p < 0.001$.

Supplementary Figure S10 | beta-NMN in twig organs/tissues of beech trees. Beta-NMN in leaves **(A)**, bark **(B)**, wood **(C)**, xylem sap **(D)**, and phloem exudates **(E)** of beech trees from the Con (black bars) and Tut (gray bars) forest. Data represent mean values ± *S.D.* of three replicates. Different minor letters show significant differences between the seasons per site (results of One-Way-ANOVA, or Kruskal–Wallis-ANOVA in case that the requirement of normal distribution and/or equal variances was not fulfilled; $p < 0.05$). Asterisks indicate significant differences of a particular metabolite between both field sites during the respective season at $^{*}p < 0.05$ (results of Student's *t*-test or Mann–Whitney tests in case that the requirement of normal distribution of the data was not fulfilled).

Supplementary Figure S11 | Visualized correlation analyzes.

REFERENCES

Aschan, G., and Pfanz, H. (2003). Non-foliar photosynthesis – a strategy of additional carbon acquisition. *Flora – Morphol. Distrib. Funct. Ecol. Plants* 198, 81–97. doi: 10.1078/0367-2530-00080

Bates, P. D., and Browse, J. (2012). The significance of different diacylgycerol synthesis pathways on plant oil composition and bioengineering. *Front. Plant Sci.* 3:147. doi: 10.3389/fpls.2012.00147

Benstein, R. M., Ludewig, K., Wulfert, S., Wittek, S., Gigolashvili, T., Frerigmann, H., et al. (2013). Arabidopsis phosphoglycerate dehydrogenase1 of the phosphoserine pathway is essential for development and required for ammonium assimilation and tryptophan biosynthesis. *Plant Cell* 25, 5011–5029. doi: 10.1105/tpc.113.118992

Bergmann, L., and Rennenberg, H. (1993). Glutathione metabolism in plants. *In* LJ De Kok, I Stulen, H Rennenberg, C Brunold, W Rauser, eds, Sulfur Nutrition and Sulfur Assimilation of Higher Plants. *SPB Academic Publishing, The Hague, Netherland, pp* 102–123.

Boudière, L., Michaud, M., Petroutsos, D., Rébeillé, F., Falconet, D., Bastien, O., et al. (2014). Glycerolipids in photosynthesis: composition, synthesis and trafficking. *Biochim. Biophys. Acta BBA - Bioenerg.* 1837, 470–480. doi: 10.1016/j.bbabio.2013.09.007

Bucher, M. (2006). Functional biology of plant phosphate uptake at root and mycorrhiza interfaces. *New Phytol.* 173, 11–26. doi: 10.1111/j.1469-8137.2006.01935.x

Budzinski, I. G. F., Moon, D. H., Morosini, J. S., Lindén, P., Bragatto, J., Moritz, T., et al. (2016). Integrated analysis of gene expression from carbon metabolism, proteome and metabolome, reveals altered primary metabolism in *Eucalyptus grandis* bark, in response to seasonal variation. *BMC Plant Biol.* 16:149. doi: 10.1186/s12870-016-0839-8

Chapin, F. S., and Kedrowski, R. A. (1983). Seasonal changes in nitrogen and phosphorus fractions and autumn retranslocation in evergreen and deciduous Taiga trees. *Ecology* 64, 376–391. doi: 10.2307/1937083

Chiou, T.-J., and Lin, S.-I. (2011). Signaling network in sensing phosphate availability in plants. *Annu. Rev. Plant Biol.* 62, 185–206. doi: 10.1146/annurev-arplant-042110-103849

Coleman, G. D., Chen, T. H. H., Ernst, S. G., and Fuchigami, L. (1991). Photoperiod control of poplar bark storage protein accumulation. *Plant Physiol.* 96, 686–692. doi: 10.1104/pp.96.3.686

Côté, B., Fyles, J. W., and Djalilvand, H. (2002). Increasing N and P resorption efficiency and proficiency in northern deciduous hardwoods with decreasing foliar N and P concentrations. *Ann. For. Sci.* 59, 275–281. doi: 10.1051/forest:2002023

Derory, J., Léger, P., Garcia, V., Schaeffer, J., Hauser, M., Salin, F., et al. (2006). Transcriptome analysis of bud burst in sessile oak (*Quercus petraea*). *New Phytol.* 170, 723–738. doi: 10.1111/j.1469-8137.2006.01721.x

Diehl, S., Kull, U., and Diamantoglou, S. (1993). Incorporation of ^{14}C-photosynthate into major chemical fractions of leaves and bark of *Ceratonia sillqua* L. at different seasons. *J. Plant Physiol.* 141, 657–662. doi: 10.1016/S0176-1617(11)81570-1

Dietz, K.-J., and Foyer, C. (1986). The relationship between phosphate status and photosynthesis in leaves. *Planta* 167, 376–381. doi: 10.1007/BF00391342

Du, B., Jansen, K., Kleiber, A., Eiblmeier, M., Kammerer, B., Ensminger, I., et al. (2016). A coastal and an interior douglas fir provenance exhibit different metabolic strategies to deal with drought stress. *Tree Physiol.* 36, 148–163. doi: 10.1093/treephys/tpv105

Ellsworth, D. S., Crous, K. Y., Lambers, H., and Cooke, J. (2015). Phosphorus recycling in photorespiration maintains high photosynthetic capacity in woody species. *Plant Cell Environ.* 38, 1142–1156. doi: 10.1111/pce.12468

Fladung, M., Grossmann, K., and Ahuja, M. R. (1997). Alterations in hormonal and developmental characteristics in transgenic *Populus* conditioned by the rolC gene from *Agrobacterium rhizogenes*. *J. Plant Physiol.* 150, 420–427. doi: 10.1016/S0176-1617(97)80092-2

Furo, K., Nozaki, M., Murashige, H., and Sato, Y. (2015). Identification of an N-acetylglucosamine kinase essential for UDP-N-acetylglucosamine salvage synthesis in *Arabidopsis*. *FEBS Lett.* 589, 3258–3262. doi: 10.1016/j.febslet.2015.09.011

Galili, G., Amir, R., and Fernie, A. R. (2016). The regulation of essential amino acid synthesis and accumulation in plants. *Annu. Rev. Plant Biol.* 67, 153–178. doi: 10.1146/annurev-arplant-043015-112213

Gardocki, M. E., Jani, N., and Lopes, J. M. (2005). Phosphatidylinositol biosynthesis: biochemistry and regulation. *Biochim. Biophys. Acta* 1735, 89–100. doi: 10.1016/j.bbalip.2005.05.006

Geßler, A., Schneider, S., Weber, P., Hanemann, U., and Rennenberg, H. (1998). Soluble N compounds in trees exposed to high loads of N: a comparison between the roots of Norway spruce (*Picea abies*) and beech (*Fagus sylvatica*) trees grown under field conditions. *New Phytol.* 138, 385–399. doi: 10.1046/j.1469-8137.1998.00134.x

Gessler, A., Schrempp, S., Matzarakis, A., Mayer, H., Rennenberg, H., and Adams, M. A. (2001). Radiation modifies the effect of water availability on the carbon isotope composition of beech (*Fagus sylvatica*). *New Phytol.* 150, 653–664. doi: 10.1046/j.1469-8137.2001.00136.x

Guo, Y., Cai, Z., and Gan, S. (2004). Transcriptome of *Arabidopsis* leaf senescence. *Plant Cell Environ.* 27, 521–549. doi: 10.1111/j.1365-3040.2003.01158.x

Guschina, I. A., Everard, J. D., Kinney, A. J., Quant, P. A., and Harwood, J. L. (2014). Studies on the regulation of lipid biosynthesis in plants: application of control analysis to soybean. *Biochim. Biophys. Acta* 1838, 1488–1500. doi: 10.1016/j.bbamem.2014.02.008

Han, W., Tang, L., Chen, Y., and Fang, J. (2014). Relationship between the relative limitation and resorption efficiency of nitrogen vs phosphorus in woody plants. *PLoS ONE* 9:e94515. doi: 10.1371/journal.pone.0094515

Hardie, G. D. (2011). AMP-activated protein kinase—an energy sensor that regulates all aspects of cell function. *Genes Dev* 25, 1895–1908. doi: 10.1101/gad.17420111

Herschbach, C., Gessler, A., and Rennenberg, H. (2012). "Long-distance transport and plant internal cycling of N- and S-compounds," in *Progress in Botany 73*, eds U. Lüttge, W. Beyschlag, B. Büdel, and D. Francis (Berlin; Heidelberg: Springer), 161–188.

Herschbach, C., and Rennenberg, H. (1996). Storage and remobilisation of sulphur in beech trees (*Fagus sylvatica*). *Physiol. Plant.* 98, 125–132. doi: 10.1111/j.1399-3054.1996.tb00683.x

Hinsinger, P., Herrmann, L., Lesueur, D., Robin, A., Trap, J., Waithaisong, K., et al. (2015). "Impact of roots, microorganisms and microfauna on the fate of soil phosphorus in the rhizosphere," in *Phosphorus Metabolism in Plants,* eds W. C. Plaxton and H. Lambers (Oxford, UK: John Wiley & Sons, Inc.), 375–407.

Hirabayashi, Y., and Ichikawa, S. (2002). "GlcCer synthase (UDP-Glucose:Ceramide Glucosyltransferase, UGCG)," in *Handbuch*

Glycosyltransferases Related Genes, eds N. Taniguchi, K. Honke, M. Fukuda, H. Clausen, K. Furukawa, G. W. Hart, R. Kannagi, T. Kawasaki, T. Kinoshita, T. Muramatsu, et al. (Tokyo: Springer), 3–8.

Ho, C.-L., and Saito, K. (2001). Molecular biology of the plastidic phosphorylated serine biosynthetic pathway in *Arabidopsis thaliana*. *Amino Acids* 20, 243–259. doi: 10.1007/s007260170042

Huppe, H., and Turpin, D. (1994). Integration of carbon and nitrogen metabolism in plant and algal cells. *Annu. Rev. Plant Biol.* 45, 577–607. doi: 10.1146/annurev.pp.45.060194.003045

Jonard, M., Fürst, A., Verstraeten, A., Thimonier, A., Timmermann, V., Potočić, N., et al. (2015). Tree mineral nutrition is deteriorating in Europe. *Glob. Change Biol.* 21, 418–430. doi: 10.1111/gcb.12657

Keskitalo, J., Bergquist, G., Gardeström, P., and Jansson, S. (2005). A cellular timetable of autumn senescence. *Plant Physiol.* 139, 1635–1648. doi: 10.1104/pp.105.066845

Kobayashi, K. (2016). Role of membrane glycerolipids in photosynthesis, thylakoid biogenesis and chloroplast development. *J. Plant Res.* 129, 565–580. doi: 10.1007/s10265-016-0827-y

Konieczynski, P., and Wesolowski, M. (2014). Phytate, inorganic and total phosphorus and their relations to selected trace and major elements in herbal teas. *Acta Pol. Pharm.* 71:85.

Kurita, Y., Baba, K., Ohnishi, M., Matsubara, R., Kosuge, K., Anegawa, A., et al. (2017). Inositol hexakis phosphate is the seasonal phosphorus reservoir in the deciduous woody plant *Populus alba* L. *Plant Cell Physiol.* 58, 1477–1485. doi: 10.1093/pcp/pcx106

Lambers, H., Brundrett, M. C., Raven, J. A., and Hopper, S. D. (2010). Plant mineral nutrition in ancient landscapes: high plant species diversity on infertile soils is linked to functional diversity for nutritional strategies. *Plant Soil* 334, 11–31. doi: 10.1007/s11104-010-0444-9

Lambers, H., Cawthray, G. R., Giavalisco, P., Kuo, J., Laliberté, E., Pearse, S. J., et al. (2012). Proteaceae from severely phosphorus-impoverished soils extensively replace phospholipids with galactolipids and sulfolipids during leaf development to achieve a high photosynthetic phosphorus-use-efficiency. *New Phytol.* 196, 1098–1108. doi: 10.1111/j.1469-8137.2012.04285.x

Lambers, H., Finnegan, P. M., Jost, R., Plaxton, W. C., Shane, M. W., and Stitt, M. (2015). Phosphorus nutrition in *Proteaceae* and beyond. *Nat. Plants* 1:15109. doi: 10.1038/nplants.2015.109

Lambers, H., and Plaxton, W. C. (2015). "Phosphorus: back to the roots," in *Phosphorus Metabolism in Plants*, eds W. C. Plaxton and H. Lambers (Oxford, UK: John Wiley & Sons, Inc.), 1–22.

Lambers, H., Raven, J. A., Shaver, G. R., and Smith, S. E. (2008). Plant nutrient-acquisition strategies change with soil age. *Trends Ecol. Evol.* 23, 95–103. doi: 10.1016/j.tree.2007.10.008

Lambers, H., Shane, M. W., Cramer, M. D., Pearse, S. J., and Veneklaas, E. J. (2006). Root structure and functioning for efficient acquisition of phosphorus: matching morphological and physiological traits. *Ann. Bot.* 98, 693–713. doi: 10.1093/aob/mcl114

Lan, P., Li, W., and Schmidt, W. (2015). "'Omics' approaches towards understanding plant phosphorus acquisition and use," in *Phosphorus Metabolism in Plants*, eds W. C. Plaxton and H. Lambers (Oxford, UK: John Wiley & Sons, Inc.), 65–97.

Lang, F., Bauhus, J., Frossard, E., George, E., Kaiser, K., Kaupenjohann, M., et al. (2016). Phosphorus in forest ecosystems: new insights from an ecosystem nutrition perspective. *J. Plant Nutr. Soil Sci.* 179, 129–135. doi: 10.1002/jpln.201500541

Li-Beisson, Y., Shorrosh, B., Beisson, F., Andersson, M. X., Arondel, V., Bates, P. D., et al. (2010). Acyl-lipid metabolism. *Arab. Book Am. Soc. Plant Biol.* 8:e0133. doi: 10.1199/tab.0133

Lisec, J., Schauer, N., Kopka, J., Willmitzer, L., and Fernie, A. R. (2006). Gas chromatography mass spectrometry-based metabolite profiling in plants. *Nat. Protoc.* 1, 387–396. doi: 10.1038/nprot.2006.59

Lough, T. J., and Lucas, W. J. (2006). Integrative plant biology: role of phloem long-distance macromolecular trafficking. *Annu. Rev. Plant Biol.* 57, 203–232. doi: 10.1146/annurev.arplant.56.032604.144145

Lucas, W. J., Groover, A., Lichtenberger, R., Furuta, K., Yadav, S.-R., Helariutta, Y., et al. (2013). The plant vascular system: evolution, development and functions. *J. Integr. Plant Biol.* 55, 294–388. doi: 10.1111/jipb.12041

Manan, S., Chen, B., She, G., Wan, X., and Zhao, J. (2017). Transport and transcriptional regulation of oil production in plants. *Crit. Rev. Biotechnol.* 37, 641–655. doi: 10.1080/07388551.2016.1212185

Millard, P., and Grelet, G. (2010). Nitrogen storage and remobilization by trees: ecophysiological relevance in a changing world. *Tree Physiol.* 30, 1083–1095. doi: 10.1093/treephys/tpq042

Moellering, E. R., Muthan, B., and Benning, C. (2010). Freezing tolerance in plants requires lipid remodeling at the outer chloroplast membrane. *Science* 330, 226–228. doi: 10.1126/science.1191803

Nahm, M., Holst, T., Matzarakis, A., Mayer, H., Rennenberg, H., and Geßler, A. (2006). Soluble N compound profiles and concentrations in European beech (*Fagus sylvatica* L.) are influenced by local climate and thinning. *Eur. J. For. Res.* 125, 1–14. doi: 10.1007/s10342-005-0103-5

Nakamura, Y. (2013). Phosphate starvation and membrane lipid remodeling in seed plants. *Prog. Lipid Res.* 52, 43–50. doi: 10.1016/j.plipres.2012.07.002

Netzer, F., Schmid, C., Herschbach, C., and Rennenberg, H. (2017). Phosphorus-nutrition of European beech (*Fagus sylvatica* L.) during annual growth depends on tree age and P-availability in the soil. *Environ. Exp. Bot.* 137, 194–207. doi: 10.1016/j.envexpbot.2017.02.009

Niu, Y. F., Chai, R. S., Jin, G. L., Wang, H., Tang, C. X., and Zhang, Y. S. (2013). Responses of root architecture development to low phosphorus availability: a review. *Ann. Bot.* 112, 391–408. doi: 10.1093/aob/mcs285

Oikawa, A., Fujita, N., Horie, R., Saito, K., and Tawaraya, K. (2011a). Solid-phase extraction for metabolomic analysis of high-salinity samples by capillary electrophoresis–mass spectrometry. *J. Sep. Sci.* 34, 1063–1068. doi: 10.1002/jssc.201000890

Oikawa, A., Otsuka, T., Jikumaru, Y., Yamaguchi, S., Matsuda, F., Nakabayashi, R., et al. (2011b). Effects of freeze-drying of samples on metabolite levels in metabolome analyses. *J. Sep. Sci.* 34, 3561–3567. doi: 10.1002/jssc.201100466

Okazaki, Y., Nishizawa, T., Takano, K., Ohnishi, M., Mimura, T., and Saito, K. (2015). Induced accumulation of glucuronosyldiacylglycerol in tomato and soybean under phosphorus deprivation. *Physiol. Plant.* 155, 33–42. doi: 10.1111/ppl.12334

Okazaki, Y., Otsuki, H., Narisawa, T., Kobayashi, M., Sawai, S., Kamide, Y., et al. (2013). A new class of plant lipid is essential for protection against phosphorus depletion. *Nat. Commun.* 4:1510. doi: 10.1038/ncomms2512

Pant, B.-D., Burgos, A., Pant, P., Cuadros-Inostroza, A., Willmitzer, L., and Scheible, W.-R. (2015a). The transcription factor PHR1 regulates lipid remodeling and triacylglycerol accumulation in *Arabidopsis thaliana* during phosphorus starvation. *J. Exp. Bot.* 66, 1907–1918. doi: 10.1093/jxb/eru535

Pant, B.-D., Pant, P., Erban, A., Huhmann, A., Kopka, J., and Scheible, W.-R. (2015b). Identification of primary and secondary metabolites with phosphorus status-dependent abundance in *Arabidopsis*, and of the transcription factor PHR1 as a major regulator of metabolic changes during phosphorus limitation. *Plant Cell Environ.* 38, 172–187. doi: 10.1111/pce.12378

Pena, R., Offermann, C., Simon, J., Naumann, P. S., Gessler, A., Holst, J., et al. (2010). Girdling affects ectomycorrhizal fungal (EMF) diversity and reveals functional differences in EMF community composition in a beech forest. *Appl. Environ. Microbiol.* 76, 1831–1841. doi: 10.1128/AEM.01703-09

Peñuelas, J., Poulter, B., Sardans, J., Ciais, P., van der Velde, M., Bopp, L., et al. (2013). Human-induced nitrogen–phosphorus imbalances alter natural and managed ecosystems across the globe. *Nat. Commun.* 4:2934. doi: 10.1038/ncomms3934

Plaxton, W. C. (1996). The organization and regulation of plant glycolysis. *Annu. Rev. Plant Physiol. Plant Mol. Biol.* 47, 185–214. doi: 10.1146/annurev.arplant.47.1.185

Plaxton, W. C., and Shane, M. W. (2015). "The role of post-translational enzyme modifications in the metabolic adaptations of phosphorus-deprived plants," in *Phosphorus Metabolism in Plants in the Post-Genomic Era: From Gene to Ecosystem,* eds W. C. Plaxton and H. Lambers (Oxford, UK: John Wiley & Sons, Inc.), 99–123.

Plaxton, W. C., and Tran, H. T. (2011). Metabolic adaptations of phosphate-starved plants. *Plant Physiol.* 156, 1006–1015. doi: 10.1104/pp.111.175281

Prietzel, J., Klysubun, W., and Werner, F. (2016). Speciation of phosphorus in temperate zone forest soils as assessed by combined wet-chemical fractionation and XANES spectroscopy. *J. Plant Nutr. Soil Sci.* 179, 168–185. doi: 10.1002/jpln.201500472

Rennenberg, H., and Dannenmann, M. (2015). Nitrogen nutrition of trees in temperate forests - the significance of nitrogen availability in the pedosphere and atmosphere. *Forests* 6, 2820–2835. doi: 10.3390/f6082820

Rennenberg, H., and Schmidt, S. (2010). Perennial lifestyle - an adaptation to nutrient limitation? *Tree Physiol.* 30, 1047–1049. doi: 10.1093/treephys/tpq076

Rennenberg, H., Schneider, S., and Weber, P. (1996). Analysis of uptake and allocation of nitrogen and sulphur compounds by trees in the field. *J. Exp. Bot.* 47, 1491–1498. doi: 10.1093/jxb/47.10.1491

Rennenberg, H., Wildhagen, H., and Ehlting, B. (2010). Nitrogen nutrition of poplar trees. *Plant Biol.* 12, 275–291. doi: 10.1111/j.1438-8677.2009.00309.x

Rennie, E. A., and Turgeon, R. (2009). A comprehensive picture of phloem loading strategies. *Proc. Natl. Acad. Sci. U.S.A.* 106, 14162–14167. doi: 10.1073/pnas.0902279106

Roje, S. (2007). Vitamin B biosynthesis in plants. *Phytochemistry* 68, 1904–1921. doi: 10.1016/j.phytochem.2007.03.038

Rychter, A. M., and Rao, I. M. (2005). "Role of phosphorus in photosynthetic carbon metabolism," in *Handbook of Photosynthesis Second Edition*, ed M. Pessarakli (Boca Raton, FL: Taylor & Francis Group, LLC), 123–148. doi: 10.1201/9781420027877.ch7

Sauter, J. J., and van Cleve, B. (1994). Storage, mobilization and interrelations of starch, sugars, protein and fat in the ray storage tissue of poplar trees. *Trees* 8, 297–304. doi: 10.1007/BF00202674

Schneider, A., Schatten, T., and Rennenberg, H. (1994). Exchange between phloem and xylem during long distance transport of glutathione in spruce trees [*Picea abies* [Karst.] L.). *J Exp Bot.* 45, 457–462. doi: 10.1093/jxb/45.4.457

Schneider, S., Gessler, A., Weber, P., von Sengbusch, D., Hanemann, U., and Rennenberg, H. (1996). Soluble N compounds in trees exposed to high loads of N: a comparison of spruce (*Picea abies*) and beech (*Fagus sylvatica*) grown under field conditions. *New Phytol.* 134, 103–114. doi: 10.1111/j.1469-8137.1996.tb01150.x

Scholander, P. F., Bradstreet, E. D., Hemmingsen, E. A., and Hammel, H. T. (1965). Sap pressure in vascular plants: negative hydrostatic pressure can be measured in plants. *Science* 148, 339–346. doi: 10.1126/science.148.3668.339

Shimojima, M., and Ohta, H. (2011). Critical regulation of galactolipid synthesis controls membrane differentiation and remodeling in distinct plant organs and following environmental changes. *Prog. Lipid Res.* 50, 258–266. doi: 10.1016/j.plipres.2011.03.001

Siebers, M., Dörmann, P., and Hölzl, G. (2015). "Membrane remodelling in phosphorus-deficient plants," in *Phosphorus Metabolism in Plants,* eds W. C. Plaxton and H. Lambers (Oxford, UK: John Wiley & Sons, Inc.), 237–263.

Smith, A. P., Fontenot, E. B., Zahraeifard, S., and Feuer DiTusa, S. (2015). Molecular components that drive phosphorus-remobilisation during leaf senescence. *Annu. Plant Rev.* 48, 159–186. doi: 10.1002/9781118958841.ch6

Strohm, M., Jouanin, L., Kunert, K. J., Pruvost, C., Polle, A., Foyer, C. H., et al. (1995). Regulation of glutathione synthesis in leaves of transgenic poplar (*Populus tremula* x *P. alba*) overexpressing glutathione synthetase. *Plant J.* 7, 141–145. doi: 10.1046/j.1365-313X.1995.07010141.x

Sun, Z., Liu, L., Peng, S., Peñuelas, J., Zeng, H., and Piao, S. (2016). Age-related modulation of the nitrogen resorption efficiency response to growth requirements and soil nitrogen availability in a temperate pine plantation. *Ecosystems* 19, 698–709. doi: 10.1007/s10021-016-9962-5

Talkner, U., Jansen, M., and Beese, F. O. (2009). Soil phosphorus status and turnover in central-European beech forest ecosystems with differing tree species diversity. *Eur. J. Soil Sci.* 60, 338–346. doi: 10.1111/j.1365-2389.2008.01117.x

Talkner, U., Meiwes, K., Potočić, N., Seletković, I., Cools, N., De Vos, B., et al. (2015). Phosphorus nutrition of beech (*Fagus sylvatica* L.) is decreasing in Europe. *Ann. For. Sci.* 72, 919–928. doi: 10.1007/s13595-015-0459-8

Theodorou, M. E., Elrifi, I. R., Turpin, D. H., and Plaxton, W. C. (1991). Effects of phosphorus limitation on respiratory metabolism in the green alga Selenastrum minutum. *Plant Physiol.* 95, 1089–1095. doi: 10.1104/pp.95.4.1089

Tian, J., and Liao, H. (2015). "The role of intracellular and secreted purple acid phosphatases in plant phosphorus scavenging and recycling," in *Phosphorus Metabolism in Plants,* eds W. C. Plaxton and H. Lambers (John Wiley & Sons, Inc.), 265–287.

Troncoso-Ponce, M. A., Nikovics, K., Marchive, C., Lepiniec, L., and Baud, S. (2016). New insights on the organization and regulation of the fatty acid biosynthetic network in the model higher plant *Arabidopsis thaliana*. *SI Lipids Biosynth. Funct.* 120, 3–8. doi: 10.1016/j.biochi.2015.05.013

Turgeon, R., and Wolf, S. (2009). Phloem transport: cellular pathways and molecular trafficking. *Annu. Rev. Plant Biol.* 60, 207–221. doi: 10.1146/annurev.arplant.043008.092045

Umeki, K., Kikuzawa, K., and Sterck, F. J. (2010). Influence of foliar phenology and shoot inclination on annual photosynthetic gain in individual beech saplings: a functional–structural modeling approach. *Ecol. Silvic Beech Gene Landsc.* 259, 2141–2150. doi: 10.1016/j.foreco.2009.12.011

Vaintraub, I. A., and Lapteva, N. A. (1988). Colorimetric determination of phytate in unpurified extracts of seeds and the products of their processing. *Anal. Biochem.* 175, 227–230. doi: 10.1016/0003-2697(88)90382-X

Veneklaas, E. J., Lambers, H., Bragg, J., Finnegan, P. M., Lovelock, C. E., Plaxton, W. C., et al. (2012). Opportunities for improving phosphorus-use efficiency in crop plants. *New Phytol.* 195, 306–320. doi: 10.1111/j.1469-8137.2012.04190.x

Vitousek, P. M., Porder, S., Houlton, B. Z., and Chadwick, O. A. (2010). Terrestrial phosphorus limitation: mechanisms, implications, and nitrogen–phosphorus interactions. *Ecol. Appl.* 20, 5–15. doi: 10.1890/08-0127.1

von Wilpert, K., Kohler, M., and Zirlewagen, D. (1996). *Die Differenzierung des Stoffhaushalts von Waldökosystemen durch die Waldbauliche Behandlung auf einem Gneisstandort des Mittleren Schwarzwaldes.* Ergebnisse aus der Ökosystemfallstudie Conventwald. Mitteilungen der Forstlichen Versuchs- und Forschungsanstalt, 197.

Wang, S., and Faust, M. (1988). Changes of fatty acids and sterols in apple buds during bud break induced by a plant bioregulator, thidiazuron. *Physiol. Plant.* 72, 115–120. doi: 10.1111/j.1399-3054.1988.tb06631.x

Warren, C. R. (2011). How does P affect photosynthesis and metabolite profiles of *Eucalyptus globulus*? *Tree Physiol.* 31, 727–739. doi: 10.1093/treephys/tpr064

Werner, C., Unger, S., Pereira, J. S., Maia, R., David, T. S., Kurz-Besson, C., et al. (2006). Importance of short-term dynamics in carbon isotope ratios of ecosystem respiration (δ13CR) in a Mediterranean oak woodland and linkage to environmental factors. *New Phytol.* 172, 330–346. doi: 10.1111/j.1469-8137.2006.01836.x

Wildhagen, H., Dürr, J., Ehlting, B., and Rennenberg, H. (2010). Seasonal nitrogen cycling in the bark of field-grown Grey poplar is correlated with meteorological factors and gene expression of bark storage proteins. *Tree Physiol.* 30, 1096–1110. doi: 10.1093/treephys/tpq018

Wittmann, C., Aschan, G., and Pfanz, H. (2001). Leaf and twig photosynthesis of young beech (*Fagus sylvatica*) and aspen (*Populus tremula*) trees grown under different light regime. *Basic Appl. Ecol.* 2, 145–154. doi: 10.1078/1439-1791-00047

Wu, P., Tian, J., Walker, C., and Wang, F. (2009). Determination of phytic acid in cereals–a brief review. *Int. J. Food Sci. Technol.* 44, 1671–1676. doi: 10.1111/j.1365-2621.2009.01991.x

Xia, J., Sinelnikov, I. V., Han, B., and Wishart, D. S. (2015). MetaboAnalyst 3.0—making metabolomics more meaningful. *Nucleic Acids Res.* 43, W251–W257. doi: 10.1093/nar/gkv380

Xu, C., and Shanklin, J. (2016). Triacylglycerol metabolism, function, and accumulation in plant vegetative tissues. *Annu. Rev. Plant Biol.* 67, 179–206. doi: 10.1146/annurev-arplant-043015-111641

Yoshida, S., and Sakai, A. (1973). Phospholipid changes associated with the cold hardiness of cortical cells from poplar stem. *Plant Cell Physiol.* 14, 353–359.

Zheng, C., Halaly, T., Acheampong, A. K., Takebayashi, Y., Jikumaru, Y., Kamiya, Y., et al. (2015). Abscisic acid (ABA) regulates grape bud dormancy, and dormancy release stimuli may act through modification of ABA metabolism. *J. Exp. Bot.* 66, 1527–1542. doi: 10.1093/jxb/eru519

Conflict of Interest Statement: The authors declare that the research was conducted in the absence of any commercial or financial relationships that could be construed as a potential conflict of interest.

The reviewer AJV and handling Editor declared their shared affiliation, and the handling Editor states that the process nevertheless met the standards of a fair and objective review.

frontiers in Plant Science

ORIGINAL RESEARCH
published: 27 June 2018
doi: 10.3389/fpls.2018.00883

Nutrient Use Efficiency of Southern South America Proteaceae Species. Are there General Patterns in the Proteaceae Family?

Mabel Delgado[1,2,3,4]*, *Susana Valle*[2,5], *Marjorie Reyes-Díaz*[3,4], *Patricio J. Barra*[4] and *Alejandra Zúñiga-Feest*[1,2]*

[1] Laboratorio de Biología Vegetal, Facultad de Ciencias, Instituto de Ciencias Ambientales y Evolutivas, Universidad Austral de Chile, Valdivia, Chile, [2] Centro de Investigación en Suelos Volcánicos, Universidad Austral de Chile, Valdivia, Chile, [3] Departamento de Ciencias Químicas y Recursos Naturales, Facultad de Ingeniería y Ciencias, Universidad de La Frontera, Temuco, Chile, [4] Center of Plant, Soil Interaction and Natural Resources Biotechnology, Scientific and Technological Bioresource Nucleus (BIOREN), Universidad de La Frontera, Temuco, Chile, [5] Facultad de Ciencias Agrarias, Instituto de Ingeniería Agraria y Suelos, Valdivia, Chile

OPEN ACCESS

Edited by:
Victoria Fernandez, Universidad Politécnica de Madrid (UPM), Spain

Reviewed by:
Maria A. Pérez-Fernádez, Universidad Pablo de Olavide, Spain
Anna Abrahão, Universidade Estadual de Campinas, Brazil

***Correspondence:**
Mabel Delgado
mabel.dt@gmail.com
Alejandra Zúñiga-Feest
alejandrazunigafeest@gmail.com

Specialty section:
This article was submitted to Plant Nutrition, a section of the journal Frontiers in Plant Science

Received: *08 February 2018*
Accepted: *06 June 2018*
Published: *27 June 2018*

Citation:
Delgado M, Valle S, Reyes-Díaz M, Barra PJ and Zúñiga-Feest A (2018) Nutrient Use Efficiency of Southern South America Proteaceae Species. Are there General Patterns in the Proteaceae Family? Front. Plant Sci. 9:883. doi: 10.3389/fpls.2018.00883

Plants from the Proteaceae family can thrive in old, impoverished soil with extremely low phosphorus (P) content, such as those typically found in South Western Australia (SWA) and South Africa. The South Western (SW) Australian Proteaceae species have developed strategies to deal with P scarcity, such as the high capacity to re-mobilize P from senescent to young leaves and the efficient use of P for carbon fixation. In Southern South America, six Proteaceae species grow in younger soils than those of SWA, with a wide variety of climatic and edaphic conditions. However, strategies in the nutrient use efficiency of Southern South (SS) American Proteaceae species growing in their natural ecosystems remain widely unknown. The aim of this study was to evaluate nutrient resorption efficiency and the photosynthetic nutrients use efficiency by SS American Proteaceae species, naturally growing in different sites along a very extensive latitudinal gradient. Mature and senescent leaves of the six SS American Proteaceae species (*Embothrium coccineum, Gevuina avellana, Orites myrtoidea Lomatia hirsuta*, *L. ferruginea,* and *L. dentata*), as well as, soil samples were collected in nine sites from southern Chile and were subjected to chemical analyses. Nutrient resorption (P and nitrogen) efficiency in leaves was estimated in all species inhabiting the nine sites evaluated, whereas, the photosynthetic P use efficiency (PPUE) and photosynthetic nitrogen (N) use efficiency (PNUE) per leaf unit were determined in two sites with contrasting nutrient availability. Our study exhibit for the first time a data set related to nutrient use efficiency in the leaves of the six SS American Proteaceae, revealing that for all species and sites, P and N resorption efficiencies were on average 47.7 and 50.6%, respectively. No correlation was found between leaf nutrient (P and N) resorption

efficiency and soil attributes. Further, different responses in PPUE and PNUE were found among species and, contrary to our expectations, a higher nutrient use efficiency in the nutrient poorest soil was not found. We conclude that SS American Proteaceae species did not show a general pattern in the nutrient use efficiency among them neither with others Proteaceae species reported in the literature.

Keywords: phosphorus and nitrogen use efficiency, photosynthesis rate, specific leaf area, cluster roots, chilean soils

INTRODUCTION

The flowering plant family Proteaceae is mostly constituted by non-mycorrhizal species that form specialized "proteoid" or cluster roots, which efficiently mobilize nutrients from the soil by releasing organic compounds (Lamont, 2003; Shane and Lambers, 2005; Lambers et al., 2006, 2015b). Naturally, Proteaceae species can be found in the Southern Hemisphere, where South Western (SW) Australian Proteaceae species are by far the most abundant, followed by South African Proteaceae species (Pate et al., 2001). In those regions, Proteaceae species inhabit some of the most phosphorus (P)-impoverished soils in the world (Shane and Lambers, 2005). Several studies have shown that the success of these plants relies on specific adaptations to thrive on severely P-impoverished soils. Lambers et al. (2015a) summarized very well several traits that SW Australian Proteaceae possess, highlighting: (i) "Efficient P resorption from senescing to mature leaves" and (ii) "Exceptionally high photosynthetic P use efficiency (PPUE)." The high levels of P resorption in leaves have been associated with up-regulation of extra and intracellular acid phosphatases and RNase activities in senescing leaves (Shane et al., 2014). Meanwhile, the high PPUE in these plants have been linked with differentiated P allocation patterns, such as extensive replacement of phospholipids by galactolipids and sulfolipids during leaf development (Lambers et al., 2012b) and with very low P allocation to rRNA in young leaves (Sulpice et al., 2014). In addition, a recent study by Hayes et al. (2018) compared leaf cell-specific nutrient concentrations and distributions for a phylogenetically disperse range of Proteaceae species from the extremely P-impoverished soils of SWA and the relatively P-rich soils of South America: Brazil and Chile. These authors assert that only those species from extremely P-impoverished habitats have higher PPUE by preferentially allocate P to photosynthetic mesophyll cells rather than epidermal cells, which suggests some functional divergence among Proteaceae species.

In Southern South America (SSA), where the soils are younger and nutrient richer than in SWA (Lambers et al., 2012a), only six members of the Proteaceae family can be naturally found. Three Southern South (SS) American species, *Embothrium coccineum* J.R. Forst. & G. Forst., *Lomatia hirsuta* Lam., and *Orites myrtoidea* Poepp. & Endl., are shade-intolerant and colonizers of young disturbed soils. Whereas, the other members, *L. ferruginea* Cav. R. Br., *L. dentata* Ruiz et Pavon R.Br., and *Gevuina avellana* Mol., are semi shade-tolerant, requiring protection from direct sunlight in the early stages of their life (Donoso, 2006). The geographical distribution varies among these species, being possible to find a large range of climatic and edaphic conditions in the sites where they inhabit. On the one hand, *L. hirsuta*, *L. dentata*, and *G. avellana* have their optimum distribution in the warm and deciduous forest biotopes of *Nothofagus obliqua* (35–44° S). While, *E. coccineum* and *L. ferruginea* have a wider distribution (35–56° S) with high presence in the cold biotopes of the Patagonian rainforests (Steubing et al., 1983). On the other hand, the endemic shrub *O. myrtoidea* is the Proteaceae species with the narrowest distribution, growing only in the Andes Mountains (35–38° S) (Hechenleitner et al., 2005). In general, there are few studies about SS American Proteaceae species and most of them have been focused on factors controlling cluster root formation (Donoso-Ñanculao et al., 2010; Zúñiga-Feest et al., 2010; Delgado et al., 2013; Piper et al., 2013). Thus, there are scarce and contradictory information about leaf traits of SS American Proteaceae and how this affects the cycling of nutrients, such as P and nitrogen (N), in their natural ecosystems. Lambers et al. (2012a), proposed that *E. coccineum* growing in P-rich volcanic soils can act as "ecosystem engineers," because maintain high P levels in senescent leaves, as a result of its low P resorption. Therefore, through the leaf drop provides P in the leaf litter to neighboring plants. However, this hypothesis has recently been refuted by Fajardo and Piper (2015), who found that *E. coccineum* growing in Chilean Patagonia have high foliar P and N resorption, and their shed litter is not richer in nutrient compared to that of other co-occurring species. These contrasting approaches are probably because the nutrient resorption is highly variable depending on the species and nutrient availability in the soil. In this context, Hayes et al. (2014) found that P concentration in leaves of several species (including Proteaceae) declined from youngest to oldest (P-poor) soils, while P resorption efficiency increases from 0 to 79%. The variation in leaf N concentration with soil age was less evident. However, leaf N-resorption efficiency was greatest on the youngest, N-poor soils. These authors also found that SW Australian Proteaceae shows higher leaf P resorption than other plant families inhabiting the same soil.

Although the evidence indicates that SW Australian Proteaceae species are efficient in the use of nutrients, there is no available information about the nutrient use efficiency of the SS American Proteaceae species naturally adapted to grow in a wide range of climatic and edaphic conditions. Therefore, we explored the nutrient (P and N) resorption efficiency and the photosynthetic use efficiency of P (PPUE) and N (PNUE) in leaves of six SS American Proteaceae species growing in a large geographical range ($\approx$ 1,800 km). We also evaluated the leaf N:P ratio to determine which is the limiting nutrient for

SS American Proteaceae species. We hypothesized that species growing in nutrient-poor soils have higher resorption efficiency and photosynthetic nutrient use efficiency (of P and N) in their leaves than species growing in nutrient-rich soils. The aim of this study was to evaluate leaf traits related to nutrient use efficiency of Proteaceae species naturally growing in different sites along a large latitudinal gradient (14°), and to compare our results with the literature on Proteaceae species from severely P-impoverished soils (e.g., SWA and South Africa).

MATERIALS AND METHODS

Collection Sites and Leaf Sampling

In Chile, there is a broad range of climatic and edaphic conditions where Proteaceae species grow naturally (**Tables 1**, **2**). We selected nine sites from different geographical locations during spring of 2015 and 2016 (**Table 1**). The weather conditions of the selected sites vary from cold (such as in Antuco, Aysén and Torres del Paine sites) to more temperate zones (all other evaluated sites), and from superhumid regions (e.g., Aysen) to regions with lower precipitation (e.g., Torres del Paine; **Table 1**). The soils where these species grow vary widely in origin and nutrient availability (**Table 2**). Most of the selected soils are of volcanic origin with different stages of development; from young rocky soils (e.g., Antuco, Ensenada) to more developed soils with well-defined horizons (e.g., Anticura, Cochamó, Aysen). Besides, we selected soils from different origins such as metamorphic rocks (Nahuelbuta; CIREN, 1999), fluvioglacial terraces (Chaiguata; CIREN, 2003), and glacial sediments (Torres del Paine; Díaz-Vial et al., 1960).

In order to evaluate leaf traits related to nutrient use efficiency on Proteaceae species naturally growing in different soils, we selected randomly 4–10 individuals of each species (*Embothrium coccineum, Gevuina avellana, Orites myrtoidea Lomatia hirsuta*, *L. ferruginea,* and *L. dentata*) present at each sampling site and collected leaf samples. The height of the trees ranged from 1.5 to 3.0 m and the branches holding the collected leaves were located at a maximum of 2 m above ground. The leaves were classified in mature: green leaves and without visible signs of damage, and senescent leaves: yellow-brown leaves still attached to the branch. The leaves collected were taken to the laboratory for further analysis.

Soil Collection and Chemical Analyses

A minimum of three soil samples were collected at 0–20 cm depth and taken to the laboratory for further chemical analysis (**Table 2**). Soil samples were sieved (2 mm) to remove organic material (e.g., roots, litter) and other large debris. Subsequently, homogenized soil samples were air-dried and chemical analyses were performed. Briefly, plant-available soil P (Olsen) was measured by extracting soil with 0.5 M $NaHCO_3$ at pH 8.5 (Olsen and Sommers, 1982) and determined colorimetrically applying the phospho-antimonyl-molybdenum blue complex method (Drummond and Maher, 1995). The soil's mineral N was determined after Kjeldalh acid-digestion. Organic matter was determined following the wet digestion method by Walkley and Black (1934). Total P was measured after soil ignition (550°C, 1 h) and subsequent digestion in nitric acid and perchloric acid (1:1), to spectrophotometrically determine the phospho-antimonyl-molybdenum blue complex. Soil pH was determined in a 1:2.5 soil to solution ratio in both, water and $CaCl_2$ (0.01 M). Exchangeable cations [potassium (K), sodium (Na), calcium (Ca), and magnesium (Mg)] and exchangeable aluminum (Al) were determined according to Sadzawka et al. (2004a) by extraction in ammonium acetate (1M, pH 7.0) and KCl (1 M) solutions, respectively, and measured by atomic absorption and emission spectrophotometer, AAES. Effective cation-exchange capacity (ECEC) was calculated by the sum of the cations.

Chemical Analysis in Leaves

The mature and senescent leaves were washed with distilled water and later dried at 60°C for 72 h. The dried samples were ground to a powder and used to analyze P and N concentrations. Phosphorus concentrations were determined colorimetrically using the vanado-phosphomolybdate method, once the grinded sample was calcined and digested in acid. Nitrogen concentrations, were determined by Kjeldahl distillation after acidic digestion (Sadzawka et al., 2004b). The N:P ratio of concentrations in leaves was used as an indicator of N or P limitation, where values below 10 are indicative of N limitation, values over 16 indicate P limitation, and values of between 10 and 16 indicate that plant growth is equally limited by N and P (Koerselman and Meuleman, 1996; Güsewell, 2004).

Photosynthetic Nutrient (P and N) Use Efficiency

In order to evaluate and compare the photosynthetic nutrient use efficiency per leaf unit, of phosphorus (PPUE) and nitrogen (PNUE), two sites, Ensenada (41.2° S) and Cochamó (41.5° S) were selected. We chose these sites because of the closeness between them, similar climatic conditions and flora composition and, especially, for their contrasting concentrations of total P and N in the soil. The PPUE and PNUE were calculated according to Hidaka and Kitayama (2009) by combining data on photosynthesis per unit leaf area divided by leaf P or N concentration, as shown in the following equation:

$$\text{PPUE or PNUE } \left(\mu\text{mol } CO_2\ g^{-1}\text{P or N } s^{-1}\right) = \frac{\left(A\left(\mu\text{mol } m^2\ s^{-1}\right) \times \text{SLA}(cm^2\ g^{-1})\right)/10,000}{[\text{P}] \text{ or } [\text{N}]}$$

Where A corresponds to measurements of photosynthesis rates, SLA to specific leaf area and [P] or [N] to P or N concentration.

The measurements of A were made in fully expanded green leaves (10 measurements for each plant, $n = 4$) using an infrared gas analyzer (ADC IRGA-LCA4—Analytical Development Co. Hoddesdon, UK) between 10:00 and 12:00 a.m. of a clear, sunny spring day. These determinations were performed in ambient CO_2 and temperature but the photosynthetic photon flux density (PPFD) was set to 400 μmol photons m^{-2} s^{-1}. We decided to use this PPFD because according to previous determinations of light

TABLE 1 | Geographical parameters from different studied populations where Chilean Proteaceae grow naturally.

Populations	Coordinates	Annual rainfall (mm)	Temperature (°C)			Elevation (m asl)	Edaphic Zone	Soil type*
			Annual	Min	Max			
Antuco	37° 23' S–71° 25'W	2012	6.8	1.1	14.0	1050	Wet mediterranean	Typic haploxerand
Nahuelbuta	37° 42' S–73° 13' W	1530	12.3	7.6	17.7	346	Wet mediterranean	Rhodic palehumult
Anticura	40° 3' S–72° 1' W	1641	13.9	9.2	18.7	350	Wet mediterranean	Acrudoxic Hapludand
Ensenada	41° 09' S–72°34' W	2021	10.7	7.3	14.6	39	Wet mediterranean	Andean recent terraces
Cochamó	41° 52' S–72° 28' W	1982	11.0	7.6	15.2	40	Wet mediterranean	Acrudoxic hapludand
Cucao	42° 07' S–73° 56' W	1942	10.4	6.9	14.4	14	Wet mediterranean	Typic hapludand
Tantauco	42° 37' S–74° 5.5' W	1942	10.4	6.9	14.4	150	Wet mediterranean	Fluvioglacial terraces
Aysén	45° 27' S–72° 44' W	2941	9.0	4.5	14.1	8	Rainy	Oxyaquic fulvudand
Torres del Paine	51° 22' S–72° 50' W	722	7.4	1.5	12.6	118	Magellan	Glacial sediments

The climatic variables were collected from the nearest Chilean weather stations reported by Luebert and Pliscoff (2006). Edaphic zones of Chile were described by Casanova et al. (2013).

**Whenever the classification of the soil taxonomy system (USDA) was missing, the soil type was described according to the origin of its material.*

TABLE 2 | Chemical analyses of soil collected in the natural habitats of Chilean Proteaceae.

Latitude S	37.23° (*n* = 15)	37.42° (*n* = 6)	40.30° (*n* = 8)	41.09° (*n* = 3)	41.52° (*n* = 15)	42.07° (*n* = 3)	42.37° (*n* = 3)	45.27° (*n* = 3)	51.22° (*n* = 5)
Mineral N (mg kg^{-1})	25.5 (1.9)	26.8 (1.2)	19.6 (1.5)	24.5 (2.1)	14.35 (0.5)	47.8 (8.7)	36.1 (1.1)	25.9 (1.4)	24.2 (1.2)
P-Olsen (mg kg^{-1})	17.3 (2.5)	2.0 (0.2)	12.4 (5.1)	2.5 (0.3)	2.56 (0.3)	6.8 (2.0)	3.65 (1.0)	11.4 (0.9)	2.92 (0.9)
pH (H_2O)	6.1 (0.1)	5.3 (0.1)	5.9 (0.2)	6.4 (0.1)	6.12 (0.0)	5.1 (0.2)	4.43 (0.0)	5.5 (0.0)	5.86 (0.1)
pH ($CaCl_2$)	5.3 (0.1)	4.3 (0.1)	4.9 (0.1)	5.6 (0.0)	5.15 (0.1)	4.0 (0.3)	3.32 (0.1)	4.8 (0.1)	5.09 (0.1)
Organic C (g 100 g^{-1})	6.2 (0.8)	4.5 (0.5)	7.52 (0.0)	0.04 (0.0)	6.30 (0.5)	16.0 (3.6)	5.24 (0.0)	19.2 (0.0)	2.89 (0.8)
Al ($cmol_c$ kg^{-1})	0.1 (0.0)	1.9 (0.2)	1.9 (0.5)	0.02 (0.0)	2.90 (0.9)	2.1 (1.1)	3.53 (0.5)	2.8 (0.6)	0.36 (0.2)
K ($cmol_c$ kg^{-1})	0.5 (0.1)	0.2 (0.0)	1.2 (0.1)	0.004 (0.0)	0.94 (0.0)	0.8 (0.2)	0.17 (0.0)	1.5 (0.0)	0.14 (0.0)
Na ($cmol_c$ kg^{-1})	0.1 (0.0)	0.01 (0.0)	1.2 (0.0)	0.01 (0.0)	1.16 (0.0)	1.1 (0.1)	0.14 (0.0)	1.4 (0.0)	0.03 (0.0)
Ca ($cmol_c$ kg^{-1})	9.9 (2.1)	0.6 (0.2)	9.0 (1.7)	0.10 (0.0)	5.63 (0.6)	3.2 (1.1)	0.28 (0.1)	12.9 (0.3)	1.85 (0.7)
Mg ($cmol_c$ kg^{-1})	2.0 (0.4)	0.3 (0.0)	3.0 (0.2)	0.01 (0.0)	2.71 (0.1)	3.7 (0.9)	0.62 (0.1)	4.6 (0.0)	0.25 (0.1)
Al saturation (%)	5.6 (2.9)	63.6 (6.1)	12.2 (3.3)	14.3 (8.2)	22.63 (6.7)	18.3 (7.3)	74.2 (3.8)	11.9 (2.3)	18.66 (6.0)
ECEC ($cmol_c$ kg^{-1})	12.5 (2.6)	3.0 (0.2)	16.3 (2.1)	0.13 (0.0)	12.71 (1.4)	10.9 (1.7)	4.74 (0.5)	22.3 (1.1)	2.62 (0.9)
Total N (g kg^{-1})	4.1 (0.8)	1.9 (0.2)	2.9 (0.6)	0.04 (0.0)	4.1 (0.3)	9.8 (1.2)	2.84 (0.0)	10.7 (0.1)	1.82 (0.5)
Total P (mg kg^{-1})	520 (48)	233.8 (23)	285.6 (35)	81.6 (7.2)	302.2 (19)	622 (172)	63.1 (8.5)	951.6 (45.8)	384.1 (98)

Each value corresponds to a mean of samples ± standard error in brackets.
ECEC, effective cation-exchange capacity.

saturation curves for photosynthesis all SS American Proteaceae species reach their maximum photosynthetic response at that value (Zúñiga-Feest, A. Unpublished data; Castro-Arevalo et al., 2008).

To determine SLA values, the area of some mature leaves were measured with an area folio-meter (LI-COR Model LI-3100 Area Meter). The leaves were then dried at 60°C for 72 h to determine the leaf dry mass (DM). SLA was calculated dividing the area of the leaf by its respective DM. Chemical analysis of N and P in leaves were performed as previously described.

Leaf Phosphorus and Nitrogen Resorption Efficiency

The percentage of P and N in leaves, which has been exported before dying, defines the leaf resorption efficiency of P and N, and was calculated according to Shane et al. (2014) by the difference between the P or N concentration of mature and senescent leaves, divided by the P or N of the mature leaves.

Statistical Analysis

One-way ANOVAs were applied separately with *post-hoc* Tukey tests to determine significant differences (P-value ≤ 0.05) in P and N concentrations in leaves, among species within the same site and among sites for the same species. The same test was applied to determine significant differences in P and N resorption efficiency, PNUE, PPUE, SLA, and P and N concentration per unit of leaf area. All data passed the normality and equal variance tests after natural logarithm transformations. Correlations between leaf traits and edapho-climatic conditions were tested by linear regression. A principal

component analysis (PCA) was performed to associate the edapho-climatic variables of the different locations with the plant variables. Only the variables having loads higher than 0.5 (loads > 0.5, Rodrigues de Lima et al., 2008) were considered as explanatory variables of the total variation among sites. ANOVAs analyses were performed using the Statistica 7.0 software, whereas the PCA was conducted in R Studio program.

RESULTS

Collection Sites and Species

From analyses performed on edapho-climatic and plant variables, we found that the groups of the species in the PCA were joined according to similar soil chemical characteristics and/or weather conditions of the sites where they grow (**Figure 1**). Thus, plants from Ensenada (41.2° S) and Torres del Paine (51.2° S) were grouped, likely since both are rocky sites with coarse soil material (mainly coarse sand) containing very low soil organic C content (**Table 2**). In contrast, plants growing in Anticura (40.3° S), Cochamó (41.5° S) and Cucao (42.1° S) were grouped together likely due to their similar weather conditions, organic C, sum bases and total P and N in the soil. The species from the sites of highest soil Al saturation content and low soil P availability (P-Olsen), Tantauco (42.4° S) and Nahuelbuta (37.4° S), were grouped in the upper quadrant of the left panel. Whereas, the species from Antuco (37.2° S), the site with the lowest Al saturation and highest soil P availability (P-Olsen), were located on the opposite side. Finally, plants from Aysén (45.3° S) were grouped alone because this site present the highest content of N and P in the soil. The PCA also revealed significant correlations ($P \leq 0.05$) between some plant variables with edapho-climatic conditions. Therefore, P resorption efficiency was correlated with maximum temperature ($R^2 = -0.42$) and soil pH (pH-H_2O, $R^2 = 0.42$; pH-$ClCa_2$, $R^2 = 0.44$). The N resorption efficiency was correlated with Al saturation ($R^2 = -0.46$) and soil pH (pH-H_2O, $R^2 = 0.46$; pH-$ClCa_2$, $R^2 = 0.40$). Meanwhile, the N:P ratio in mature leaves was positively correlated with annual ($R^2 = 0.60$) and minimum ($R^2 = 0.48$) temperature and negatively correlated with maximum temperature ($R^2 = -0.62$). Similar tendency was observed for N:P ratio in senescent leaves.

Leaf Phosphorus and Nitrogen Concentrations and Their Resorption Efficiency

The nutrient (P and N) concentrations and percentages of nutrient resorption differ among species and over their geographic and edaphic distributions. In general, *E. coccineum* showed the highest values of P and N concentrations in mature leaves compared to the other Proteaceae species evaluated. Thus, the concentrations of P and N were significantly higher in two and four of the nine sites evaluated, respectively (Supplementary Table S2). Thereby, P concentrations in *E. coccineum* ranged from 0.56 to 0.99 mg P g^{-1} and were followed by those for *L. ferruginea* (0.40–0.88 mg P g^{-1}), *G. avellana* (0.36–0.67 mg P g^{-1}), *L. hirsuta* (0.35–0.63 mg P g^{-1}), *L. dentata* (0.35 mg P g^{-1}), and *O. myrtoidea* (0.35 mg g^{-1}). The same tendency was found in N concentrations in mature leaves, where values for *E. coccineum* ranged from 10.4 to 18.9 mg N g^{-1} DW and were followed by *L. ferruginea* (6.89–13.38 mg N g^{-1}), *G. avellana* (8.19–12.1 mg N g^{-1}), *L. hirsuta* (5.99–12.3 mg N g^{-1}), *L. dentata* (9.96 mg N g^{-1}), and *O. myrtoidea* (7.11 mg N g^{-1}). In general, similar tendency was found in senescent leaves, where *E. coccineum* had the highest concentrations of P and N in leaves, whereas *O. myrtoidea* had the lowest (Supplementary Table S2). Correlation between total soil P and P in mature leaves ($R^2 = 0.028$; $P = 0.051$) and between total soil N and N in matures leaves ($R^2 = 0.064$; $P = 0.211$) was not found. Likewise, correlation between total soil P and P in senescent leaves ($R^2 = 0.173$; $P = 0.038$) and between total soil N and N in senescent leaves ($R^2 = 0.025$; $P = 0.068$) was not found either.

Combining all species and sites, mean P and N resorption efficiencies were 47.7 and 50.6%, respectively (**Figure 2**). *Embothrium coccineum* reached the highest values of P and N resorption efficiency (74.5 and 76.9%, respectively), whereas *L. dentata* showed the lowest values (28.5 and 37.0%, respectively). No correlation was found neither between total soil P and P resorption efficiency ($R^2 = 0.007$; $P = 0.347$) nor between total soil N and N resorption efficiency ($R^2 = 0.025$; $P = 0.074$) in leaves.

Nitrogen: Phosphorus Ratios for SS American Proteaceae

In general, all species studied had on average N:P ratios > 16 in mature and senescent leaves (**Figures 3A,B**) and, according to the limits of P and N for vegetation proposed by Koerselman and Meuleman (1996), this indicates P limitation in the leaves. Despite this, in some sites with young rocky soil (e.g., 41.2° S, the poorest site evaluated in this study), *L. hirsuta* and *E. coccineum* were co-limited by P and N.

Photosynthetic Nutrient Use Efficiency Per Unit Leaf Nitrogen (PNUE) and Phosphorus (PPUE)

In the nutrient richest site (41.5° S), the shade-intolerant species (*E. coccineum* and *L. hirsuta*) had the highest photosynthetic rates compared to the more shade-tolerant species (*G. avellana* and *L. ferruginea*), while in the nutrient poorest site no significant differences among species were found (**Table 3**). The PNUE and PPUE were significantly affected by the site, species and the interaction between them. Thus, for *E. coccineum,* the highest PNUE and PPUE was found in the nutrient richest site, which was significantly higher compared to the other species evaluated (except *L. ferruginea*, which had similar PPUE at both sites). The lowest PNUE and PPUE was found in *L. ferruginea* in the nutrient poorest site, whereas *G. avellana* and *L. hirsuta* had significantly higher PNUE in the nutrient poorest compared to that of the nutrient richest site, although no significant differences for the PPUE were found for these species (**Table 3**).

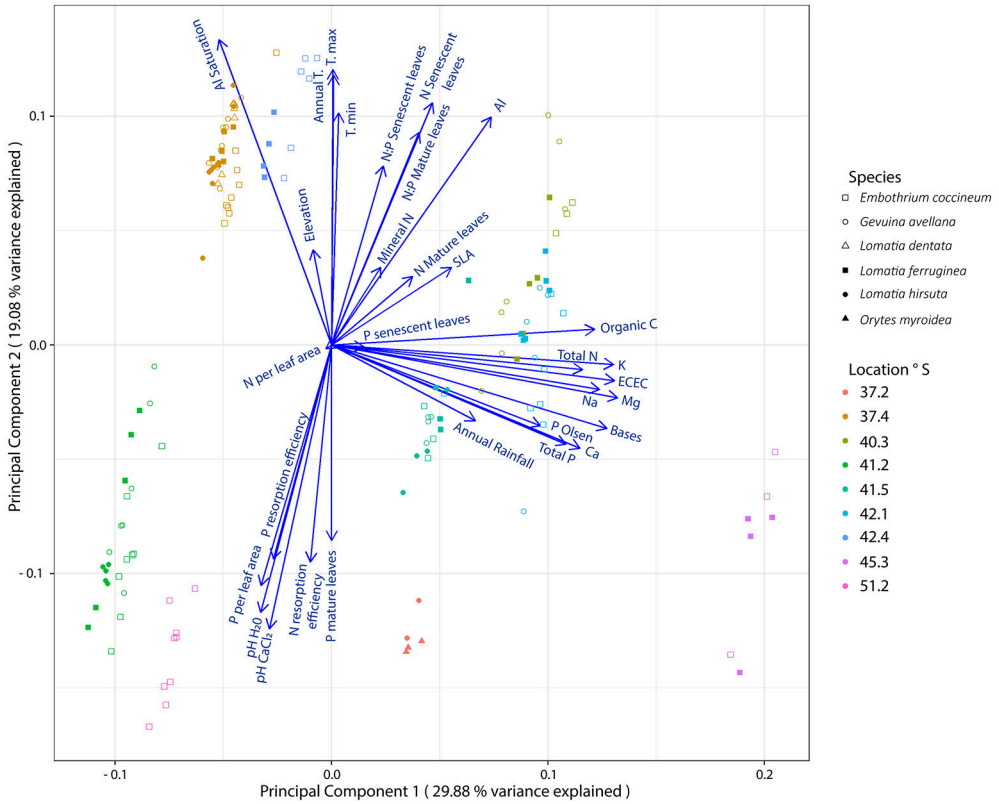

FIGURE 1 | Principal component analysis representing plant measurements from leaves of six Southern South American Proteaceae species and edapho-climatic variables of nine sites where these species grow naturally. Plant measurements: Phosphorus (P) in mature and senescent leaves (mg g^{-1}), Nitrogen (N) in mature and senescent leaves (mg g^{-1}), P and N resorption efficiency (%), N:P mature leaves, N:P senescent leaves, specific leaf area (SLA; cm^2 g^{-1}), P and N per leaf area (μg cm^2). Soil variables: mineral N (mg kg^{-1}), P Olsen (mg Kg^{-1}), pH (H_2O), pH ($CaCl_2$), Organic Carbon (Organic C; g 100 g^{-1}), Aluminum (Al; $cmol_c$ kg^{-1}), Potassium (K; $cmol_c$ kg^{-1}), Sodium (Na; $cmol_c$ kg^{-1}), Calcium (Ca; $cmol_c$ kg^{-1}), Magnesium (Mg; $cmol_c$ kg^{-1}) interchangeables, Sum of Bases (bases), Effective Cation-Exchange Capacity (ECEC), Al Saturation (%), total N (mg kg^{-1}) and total P (mg kg^{-1}). Climatic variables: annual rainfall (mm), annual temperature (Annual T., °C), minimal temperature (T. min; °C), maximal temperature (T. max; °C) and Elevation (meters above sea level; m asl).

DISCUSSION

Leaf Nitrogen and Phosphorus Concentrations and Resorption Efficiency of SS American Proteaceae Species

In our study, the semi-deciduous species *Embothrium coccineum* (Supplementary Table S1) reached the highest P and N concentration in the leaves (Supplementary Table S2) and the highest P and N resorption efficiency compared to the other evergreen Proteaceae species evaluated (**Figure 2**). In contrast, *Orites myrtoidea*, a shrub with perennial and coriaceous leaves, presented the lowest P and N concentration in the leaves (Supplementary Table S2). These results are in agreement with those of several other authors (Reich et al., 1999; Diehl et al., 2008; Gallardo et al., 2012), who reported that species having short leaf lifespan (e.g., broad-leaved deciduous species) have higher leaf P and N concentration due to higher nutrient requirements, and also higher nutrient resorption efficiency. This has been acknowledged as a nutrient conservation strategy, which is less obvious among species with a long leaf lifespan (e.g., broad-leaved evergreen).

Interestingly, the highest P and N resorption efficiency (74.5 and 76.9%, respectively) in *E. coccineum* (**Figure 2**) was found in the coldest environment of the highest latitude (55.22° S), similar to findings by Oleksyn et al. (2003) in six populations of *Pinus sylvestris* growing in a wide geographic distribution. These authors proposed that plant species inhabiting cold environments increase their internal nutrient cycling because low soil temperatures can limit the mineralization of organic matter and the nutrient release from mineral soils. Indeed, the southernmost site (55.22° S) of our study was one of the sites with the lowest organic carbon content and total N in the soil (**Table 2**). Thus, our results suggest that the interaction of low temperatures with low soil nutrient availability favor the high nutrient resorption in the leaves of *E. coccineum*, the only SS American Proteaceae species capable of growing in the southernmost, harsh environment (**Table 1**). Although, this tendency was not clearly observed in other species inhabiting cold environments (37.23° S site), such as *O. myrtoidea* and

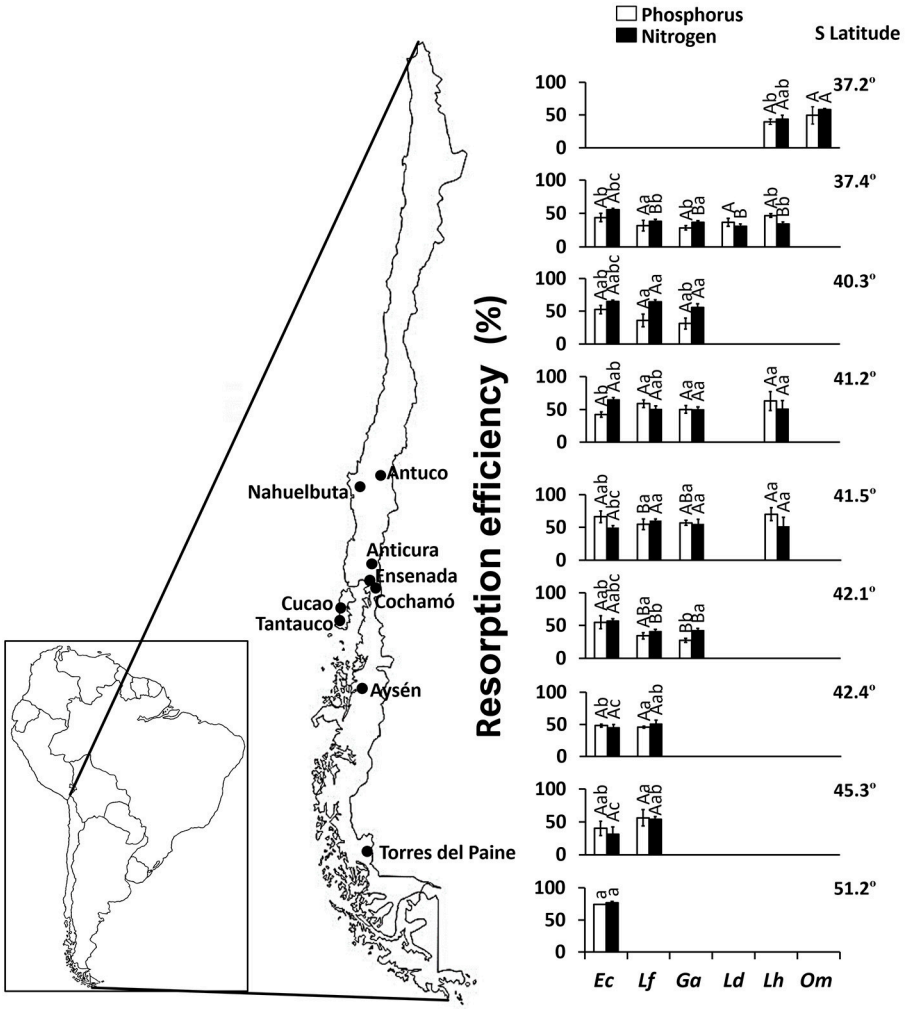

FIGURE 2 | Phosphorus (P) and nitrogen (N) resorption efficiencies in leaves of *Embothrium coccineum* (Ec), *Gevuina avellana* (Ga), *Lomatia ferruginea* (Lf), *Lomatia dentata* (Ld), *Lomatia hirsuta* (Lh), and *Orites myrtoidea* (Om) growing in their natural habitat. Each value corresponds to a mean of 4–10 samples ± standard error. Different capital letters indicate significant differences among species within the same site and different lower-case letters indicate significant differences among sites within the same species ($P \leq 0.05$).

L. hirsuta (**Table 1**, **Figure 2**), the results illustrated in the PCA (**Figure 1**) showed that the temperature is a driver of P resorption efficiency. Among the other edapho-climatic factors examined, those that influenced significantly the P and N resorption were soil pH and Al saturation, variables that have been commonly linked to nutrient availability in the soil (Lambers et al., 2008a)

In general, for all species and sites the P and N concentrations in mature leaves of SS American Proteaceae were on average 0.59 and 11.7 mg g^{-1}, respectively. These values are higher compared with P and N concentrations found in leaves of plants from SWA and South Africa (Lambers et al., 2010) and are 1.5 and 2.0 times higher, for N and P respectively, than those found in *Banksia* species (Proteaceae) growing in their natural habitat in SWA (Hayes et al., 2018). Probably this is because SS American Proteaceae species have evolved in nutrient richer soils than Proteaceae species from old, climatically buffered, infertile landscapes such as SWA and South Africa (Hopper, 2009; Lambers et al., 2012a). In this context, we found that, for all species and sites, the P and N resorption efficiencies of SS American Proteaceae were on average 47.7 and 50.6%, respectively, being these values lower compared to those in other Proteaceae species inhabiting ancient and severely P-impoverished soils, such as those in SWA. There, the species exhibit very high nutrient resorption efficiency, especially for P (Lambers et al., 2015a). Some examples of SW Australian Proteaceae species with extremely efficient P resorption are *Banksia chamaephyton* (82%, Denton et al., 2007), *Hakea prostrata* (85%, Shane et al., 2014), *B. attenuata* (90.8%, Hayes et al., 2014), and *B. menziesii* (90.2%, Hayes et al., 2014). These species are frequently found in old, nutrient-impoverished soils such as those along the two-million-year old dune chronosequence in SWA (Hayes et al., 2014).

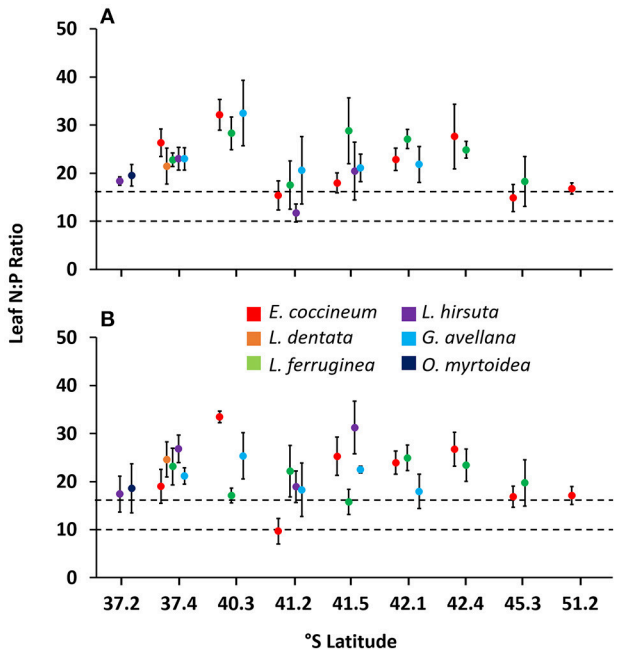

FIGURE 3 | Ratio of N:P concentrations in mature **(A)** and senescent **(B)** leaves of six Southern South American Proteaceae species growing in their natural habitat. Horizontal lines indicate N limitation (values <10), P limitation (values >16) or both, N and P limitation (values 10–16) in leaves. Each value corresponds to a mean of 4–10 samples ± standard error.

Studies on long-term soil development and its influence on the vegetation have come to the conclusion that nutrient resorption efficiency in leaves is widely linked to soil age and nutrient availability, and it becomes higher in old and highly weathered soils with low nutrient availability compared to nutrient richer and younger soils (Crews et al., 1995; Richardson et al., 2004; Hayes et al., 2014). However, this apparent negative correlation between nutrient resorption efficiency and nutrient availability in the soil does not always occur. Indeed, our results showed no correlation between nutrient resorption efficiency and soil nutrient availability. Similar results were found by Aerts (1996), who showed that there is no relationship between nutrient resorption efficiency and leaf nutrient status (defined by the author as soil fertility) in several evergreen shrubs and tree species from USA and Europe. Likewise, Gallardo et al. (2012), found that P and N concentrations in leaves and those in the soil are decoupled along a 60,000 years chronosequence in Llaima Volcano, Chile. Probably, in this young chronosequence and in our study sites the soil nutrient availability is not as poor as in ancient landscapes in SWA (Lambers et al., 2006, 2012a) due to rejuvenating catastrophic disturbances occurred in this region (e.g., volcanic eruptions, glaciation, and landslides caused by earthquakes) that have increased the soil nutrient content (Lambers et al., 2008b). Hayes et al. (2014) reported that Proteaceae species are dominant in the poorest and oldest soils along a two-million-year old dune chronosequence in SWA, with values of total soil P and N ranging from 6.6 to 20.3 mg P kg^{-1} and 240 to 288 mg N kg^{-1}, respectively. In contrast, our results showed that SS American Proteaceae species grow in soils containing total values of P and N ranging from 63.1 to 951.6 mg P kg^{-1} and 40 to 10,700 mg N kg^{-1}, respectively (**Table 2**). Despite the fact that Proteaceae species can grow in a wide range of soils, the general trend shows that the average values of total soil P and N are much higher in SSA than those in SWA. With this background information, we suggest that SS American Proteaceae have not developed the ability to be as efficient in nutrient resorption in leaves as SW Australian Proteaceae, probably due to the different evolutionary drivers (e.g., soil fertility) to which they have been exposed. The functional divergence between SS American and SW Australian Proteaceae species has been previously suggested by other authors, who have evidenced differences in cluster root functioning (Delgado et al., 2014) and in the accumulation of P and biomass in seeds (Delgado et al., 2015b). The notion of functional divergence, have recently been reinforced by Hayes et al. (2018), who compared the leaf cell-specific nutrient concentrations in Proteaceae species from SWA, Brazil, and Chile. These authors found that only species from extremely P-impoverished habitats preferentially allocated P to photosynthetic mesophyll cells, suggesting it has evolved as an adaptation to their habitat and that it is not a family-wide trait. Likewise, we suggest that the high nutrient resorption efficiency does not follow a general pattern for all species of the Proteaceae family.

Due to the low resorption efficiency of P and N (<20%) in *L. hirsuta* reported by Diehl et al. (2003) and other unpublished data for *E. coccineum* by Zuñiga-Feest A., Lambers et al. (2012a) proposed SS American Proteaceae species could act as ecosystem engineers in young soils since they provide nutrients through the deposition of leaf litter. However, recently, Fajardo and Piper (2015) claimed to have proof that *E. coccineum* is not an ecosystem engineer, because shows a higher P and N resorption efficiency (41.2 and 39.2%, respectively) compared to neighboring species in Chilean Patagonia (on average, 9.9 and 17.2%, respectively). Based on our results, where all species showed similar resorption efficiency and had higher or similar values of nutrient resorption than co-occurring natives species from the Andean Patagonia forest (as described by Diehl et al., 2003; Fajardo and Piper, 2015), we believe that there is not yet enough evidence to establish with certainty that SS American Proteaceae are ecosystem engineers. In addition, according to the benchmark levels established by Killingbeck (1996) for senescent leaves (concentration values <0.04% for P and <0.7% for N), our results showed that most SS American Proteaceae have a nearly complete resorption of P and N. These results demonstrate high resorption proficiency (expressed as the level to which species can reduce nutrient levels in senescent leaves) in SS American Proteaceae, contrasting with the results found by Diehl et al. (2003) in eight native woody species from Patagonian forest. These authors found that several species, including broad-leaved deciduous species, broad-leaved evergreens and conifers, co-occurring with some Proteaceae species in the south of Chile, were proficient in resorbing N but not P. Thus, we suggest that, although SS American Proteaceae species are not as efficient in the use of nutrients as other Proteaceae inhabiting old and severely P-impoverished soils (e.g., from SWA and South Africa),

TABLE 3 | Rates of photosynthesis, photosynthetic nitrogen use efficiency (PNUE) and photosynthetic phosphorus use efficiency (PPUE) per leaf unit in leaves of *Embothrium coccineum* (Ec), *Gevuina avellana* (Ga), *Lomatia ferruginea* (Lf), and *Lomatia dentata* (Ld) growing in their natural habitat.

Site	Species	Photosynthesis rate (μmol CO_2 m^{-2} s^{-1})	PNUE (μmol CO_2 g^{-1} N s^{-1})	PPUE (μmol CO_2 g^{-1} P s^{-1})
41.2° S	Ec	10.6 (0.3) Aa	6.1 (0.2) ABb	86.2 (2.8) Ab
(Poorest site)	Ga	7.9 (1.0) Aa	5.4 (0.7) ABa	69.5 (7.8) ABa
	Lf	7.7 (0.5) Aa	4.5 (0.3) Ba	58.8 (3.9) Bb
	Lh	8.7 (0.8) Aa	7.4 (0.7) Aa	85.7 (7.5) ABa
41.5° S	Ec	12.8 (0.5) Aa	9.9 (0.8) Aa	168.8 (11.3) Aa
(Richest site)	Ga	8.1 (0.5) BCa	4.5 (1.1) Bb	87.1 (12.2) Ca
	Lf	6.7 (0.3) Cb	5.5 (0.4) Ba	136.4 (10.0) ABa
	Lh	10.2 (0.7) ABa	4.5 (0.9) Bb	102.7 (15.2) BCa

Each value corresponds to a mean of four samples ± standard error in brackets. Different capital letters indicate significant differences among species within the same site and different lower-case letters indicate significant differences among sites within the same species ($P \leq 0.05$).

SSA Proteaceae species are proficient in P compared to other SS American species subjected to similar evolutionary pressures. Therefore, they are highly adapted to grow in P poor soils in this part of the world. Additionally, we suggest that these species could be potential ecosystem engineers in young soils however through different mechanisms, for example, by those involving their cluster roots. This could be, as proposed Delgado et al. (2015a), through the increase of nutrient availability at the rhizosphere level that could facilitate the establishment of species without such specialized roots.

Nitrogen: Phosphorus Ratios for SS American Proteaceae

Based on the range limits for P and N limitation of vegetation proposed by Koerselman and Meuleman (1996), almost all species were limited by P (N:P ratio >16, **Figure 3**). Similar results have been reported in other studies including *L. hirsuta* and *L. dentata* (Diehl et al., 2003, 2008; Gallardo et al., 2012). In these reports, the authors agreed that in general woody species growing in volcanic soils are limited by N, whereas the Proteaceae species are limited by P. These authors suggest that the cluster roots of this species are not as efficient in P uptake as those of other Proteaceae species growing in old, climatically buffered, infertile landscapes. Thus, they hypothesized that those root structures could be more likely involved in the uptake of N. Indeed, some studies reveal that N deficiency promotes cluster root formation in some Proteaceae species such as *Hakea actities* (W.R. Barker) (Schmidt et al., 2003) and in *E. coccineum* growing on moraine deposits originating from glacial erosion of the Exploradores Glacier, in Chilean Patagonia (Piper et al., 2013). Additionally, some authors reported that organic compounds released by cluster roots into the rhizosphere can become available as substrate for microorganisms (Ryan et al., 2001) and therefore, it could be that these plants are selecting their bacteria to actively benefiting from them. Along these lines, Lamont et al. (2014), further suggested that the formation of cluster roots is stimulated by the presence of plant-growth-promoting rhizobacteria, such as the N-fixing bacteria, which could have a positive effect on the uptake of N and help explain the P limitation we observed in the leaves instead of a limitation of N, as we expected. However, the mechanism by which cluster roots could be taking up N from the soil has not been studied yet in SS American Proteaceae species and further research is needed to understand functioning of cluster roots in these species.

Photosynthetic Nutrient Use Efficiency Per Leaf Unit, of Nitrogen (PNUE) and Phosphorus (PPUE)

The nutrient use efficiency found in some plants may be crucial to thrive in soils with nutrient limitations. For instance, SW Australian Proteaceae species are a good example of nutrient use efficient plants because they can successfully subsist with very low P concentrations in their mature leaves but still maintaining a very high PPUE (Denton et al., 2007; Lambers et al., 2010, 2012b, 2015a). In general, our results have revealed lower values of PPUE and PNUE for SS American Proteaceae species (**Table 3**) than those reported by Lambers et al. (2012a) for SW Australian Proteaceae species, for which PPUE and PNUE values reached 247 ± 30 μmol CO_2 g^{-1} P s^{-1} and 6.9 ± 0.9 μmol CO_2 g^{-1} N s^{-1}, respectively. These differences between Proteaceae species from SSA and SWA could be explained because they evolved in completely different habitats, with dissimilar climates and edaphic conditions, which in turn could be evidenced by differences in leaf traits. For example, some studies have associated high LMA with high nutrient use efficiency in plants from nutrient-poor habitats by reducing nutrient losses due to the decrease of herbivory (Lambers et al., 2010). In this context, we found that SS American Proteaceae species have lower LMA values (from 141 to 212 g m^{-2}, Supplementary Table S1) than plants from SW Australia (from 328 to 498 g m^{-2}) and South Africa (from 200 to 276 g m^{-2}), which exhibit the highest LMA values in the world (Lambers et al., 2010). These findings support the idea that SW Australian and South African Proteaceae are adapted to thrive in much more nutrient-poor soils than SS American Proteaceae species. In addition, it is interesting to note that the higher PPUE in thick leaves of SW Australian Proteaceae of the genus *Banksia* is associated with the presence of sunken stomata (Lambers et al., 2012b). These leaf structures increase

photosynthetic rates by reducing the diffusion pathway of CO_2 to mesophyll cells (Hassiotou et al., 2009; Lambers et al., 2015c). Sunken stomata are absent in species with thinner leaves such as *E. coccineum*, *G. avellana*, *L. ferruginea*, *L. hirsuta* (Hayes et al., 2018), which could explain, at least in part, the lower nutrient use efficiency in SS American Proteaceae species. High leaf lifespan values has also been associated with high nutrient use efficiency in plants from nutrient-poor soils by maintaining the nutrients for a longer period (Denton et al., 2007; Lambers et al., 2010). However, this assumption is not so clear for Proteaceae because SS American species (except *E. coccineum*) exhibit similar or higher leaf lifespan (Supplementary Table S1) than the SW Australian Proteaceae species described (Denton et al., 2007). This knowledge suggest that the strategy to use the nutrients efficiently of SS American Proteaceae species is through the maintenance of the nutrients in their leaves for longer period of time (especially *G. avellana*, Supplementary Table S1).

Contrary to our expectations, we found that *E. coccineum* and *L. ferruginea* have higher PPUE and PNUE in the nutrient richest site than in the nutrient poorest one. This probably occurs because in the nutrient richest site these species have significantly high SLA compared to the nutrient poorest site (**Table 4**). In concordance, Wright et al. (2004) stated that at a global scale, species with thinner leaves have shorter diffusion paths from stomata to chloroplasts favoring the photosynthesis process on an leaf area basis. Likewise, Poorter and Evans (1998) reported that several plant species (as trees, shrubs, and herbs) with high SLA have higher PNUE than that of low SLA species, mainly due to: lower N content per unit of leaf area, larger allocation of organic N to thylakoids and rubisco, and higher rubisco specific activity. Among our studied species, *E. coccineum* had the highest SLA in almost all studied sites (**Table 4**), and showed a negative correlation to N content per leaf area ($R^2 = -0.4942$), suggesting that the high PNUE present in *E. coccineum* could follow a similar physiological pattern to those species with high SLA reported by Poorter and Evans (1998). It should be noted that although *G. avellana* and *L. hirsuta* maintained their SLA values at both contrasting sites (41.2° S and 41.5° S, **Table 4**) their PNUE was higher in the poorest one (**Table 3**). These results showed that N use efficiency increases in the leaves of *G. avellana* and *L. hirsuta* when nutrient availability in the soil decreases, which has also been observed in other forest tree species (Boerner, 1984). This relationship was not observed in the PPUE neither in the other species studied, suggesting that a high nutrient use efficiency in the poorest soils is not a general response among all SS American Proteaceae species.

TABLE 4 | Specific leaf area (SLA) and P and N concentration per unit of leaf area of *Embothrium coccineum* (Ec), *Gevuina avellana* (Ga), *Lomatia ferruginea* (Lf), *Lomatia dentata* (Ld), *Lomatia hirsuta* (Lh), and *Orites myrtoidea* (Om) growing in their natural habitat.

Site (S Latitude)	Species	SLA ($cm^2\ g^{-1}$)	[P] per leaf area ($\mu g\ cm^{-2}$)	[N] per leaf area ($\mu g\ cm^{-2}$)
37.2° S	Om	50.1 (3.4) A-	9.9 (0.0) A-	170.0 (23.8) A-
	Lh	51.9 (1.3) Aa	9.6 (0.0) Aa	122.9 (11.5) Aa
37.4° S	Ec	79.6 (6.8) Aab	8.5 (0.4) Abc	202.3 (7.9) Aabc
	Ga	59.5 (1.3) Ba	7.0 (0.5) Aa	172.5 (12.9) Bb
	Lf	66.8 (3.3) ABbc	6.5 (0.3) Ab	142.9 (8.7) Bc
	Lh	59.8 (3.2) Ba	7.8 (1.1) Aa	168.7 (3.8) ABa
	Ld	71.3 (5.0) AB-	6.7 (0.8) A-	139.0 (4.3) AB-
40.3° S	Ec	133.4 (7.7) Aa	2.7 (0.4) Ac	134.1 (9.9) ABbc
	Ga	65.6 (1.6) Ba	7.2 (0.9) Aa	157.0 (21.3) Ab
	Lf	130.5 (2.7) Aa	3.7 (0.3) Ab	91.1 (5.4) Bc
41.1° S	Ec	63.2 (2.7) Acd	12.7 (1.7) Aa	177.6 (16.3) Aabc
	Ga	56.0 (1.0) ABa	10.4 (2.8) Aa	146.2 (15.6) Ab
	Lf	40.5 (0.8) Cc	13.1 (3.0) Aa	170.1 (25.2) Abc
	Lh	51.1 (3.5) BCa	12.4 (1.2) Aa	142.2 (20.6) Aa
41.5° S	Ec	88.4 (8.1) Ab	7.6 (1.0) ABbc	117.0 (7.7) Aa
	Ga	65.8 (5.3) Ba	9.0 (1.0) ABa	183.9 (1.1) Aab
	Lf	94.2 (9.1) Aab	4.9 (1.0) Bb	120.5 (2.7) Abc
	Lh	63.3 (4.5) Ba	9.9 (0.9) Aa	193.6 (46.1) Aa
42.1° S	Ec	72.6 (4.6) Abcd	11.1 (1.6) Aab	237.1 (18.3) Aab
	Ga	53.7 (2.6) ABa	12.5 (3.8) Aa	219.8 (16.1) Aa
	Lf	47.7 (2.0) Bbc	8.2 (0.3) Aab	221.6 (17.6) Aab
42.4° S	Ec	75.4 (1.6) Abcd	10.1 (2.17) Aabc	250.1 (13.6) Aab
	Lf	48.4 (2.5) Abc	11.6 (0.38) Aab	276.4 (13.2) Aa
45.3° S	Ec	69.4 (2.1) Abcd	14.4 (2.6) Aab	200.3 (4.2) Aabc
	Lf	89.3 (14.1) Aab	9.7 (1.6) Aab	155.7 (27.5) Abc
51.2° S	Ec	59.7 (2.2) d	15.0 (0.5) a	253.5 (20.2) a

Each value corresponds to a mean of 4–10 samples ± standard error in brackets. Different capital letters indicate significant differences among species within the same site and different lower-case letters indicate significant differences among sites within the same species ($P \leq 0.05$).

CONCLUSION

Our study showed a unique data set related to nutrient (P and N) resorption and photosynthetic nutrient (P and N) use efficiency in the six SS American Proteaceae species inhabiting across a large geographical range. First, we have showed that P and N resorption efficiency in leaves of Proteaceae species is not correlated to the P and N content of the soil. Second, SS American Proteaceae species are more limited by P than N as suggested by the N:P ratio in leaves. Third, PPUE and PNUE showed variations among the SS American Proteaceae evaluated, being *E. coccineum* the species presenting the highest values. Nevertheless, and contrary to our expectations, the PPUE and PNUE were, in general, higher in the nutrient richest soil. All these findings will help us to better understand the functioning of SS American Proteaceae species, which did not show a general pattern in the nutrient use efficiency among them neither with others Proteaceae species reported in the literature.

AUTHOR CONTRIBUTIONS

MD, this author contributed to the conception of this study, organized and carried out the field trips to collect the data. Besides, she organized (i.e., Graphs, tables) and interpreted the data along with writing the manuscript at all stages until the final version, given approval to be submitted. SV, this

author contributed to the field data collection, statistical analysis, valuables comments and revisions on the manuscript at all stages. MR, this author contributed with funding to do some chemical analysis in the leaf samples and revised critically the manuscript at the final stage. PB, this author contributed to statistical analysis, and helped in the design of figures, and writing of the manuscript. AZ-F, this author participated in the conception of this study. Besides contributed to the field data collection, funding to perform chemical analysis of soil and leaf samples and contributed with important intellectual content at all stages. All authors revised the manuscript and approved the final version.

FUNDING

This study was financed by the Comisión Nacional de Investigación Científica y Tecnológica (CONICYT) of Chilean government through FONDECYT Postdoctoral project N° 3150187 (MD) and N° 3170629 (PB), FONDECYT initiation project N° 11170368 (MD), and FONDECYT Regular project N° 1130440 and 1180699 (AZ-F) .

ACKNOWLEDGMENTS

The authors thanks Ariana Bertin, Andrea Ávila, and Gaston Muñoz for their enthusiastic support in field trips. Thanks also to Mauricio Rondanelli and Paulina Lobos for the collection of soil and leaf samples in Antuco and Aysén sites, respectively. Finally, we thanks Anticura National Park and Tantauco private park for allowing the collection of samples.

SUPPLEMENTARY MATERIAL

The Supplementary Material for this article can be found online at: https://www.frontiersin.org/articles/10.3389/fpls.2018.00883/full#supplementary-material

REFERENCES

Aerts, R. (1996). Nutrient resorption from senescing leaves of perennials: are there general patterns? *J. Ecol.* 84, 597–608. doi: 10.2307/2261481

Boerner, R. (1984). Foliar nutrient dynamics and nutrient use efficiency of four deciduous tree species in relation to site fertility. *J. Appl. Ecol.* 21, 1029–1040. doi: 10.2307/2405065

Casanova, M., Salazar, O., Seguel, O., and Luzio, W. (2013). *The Soils of Chile*. Santiago: Springer Science & Business Media.

Castro-Arevalo, M., Reyes-Diaz, M., Alberdi, M., Jara-Rodriguez, V., Sanhueza, C., Corcuera, L. J., et al. (2008). Effects of low temperature acclimation on photosynthesis in three Chilean Proteaceae. *Rev. Chil. Hist. Nat.* 81, 221–333. doi: 10.4067/S0716-078X2008000300002

CIREN (1999). *Estudio Agrológico VIII Región. Descripciones de suelos: Materiales y Símbolos*. *Santiago*.

CIREN (2003). *Estudio Agrológico X Región. Descripciones de suelos: Materiales y Símbolos*. Santiago.

Crews, T. E., Kitayama, K., Fownes, J. H., Riley, R. H., Herbert, D. A., Mueller-Dombois, D., et al. (1995). Changes in soil phosphorus fractions and ecosystem dynamics across a long chronosequence in Hawaii. *Ecology* 76, 1407–1424. doi: 10.2307/1938144

Delgado, M., Suriyagoda, L., Zúñiga-Feest, A., Borie, F., Lambers, H., and Field, K. (2014). Divergent functioning of Proteaceae species: the South American *Embothrium coccineum* displays a combination of adaptive traits to survive in high-phosphorus soils. *Funct. Ecol.* 28, 1356–1366. doi: 10.1111/1365-2435.12303

Delgado, M., Zúñiga-Feest, A., Almonacid, L., Lambers, H., and Borie, F. (2015a). Cluster roots of *Embothrium coccineum* (Proteaceae) affect enzyme activities and phosphorus lability in rhizosphere soil. *Plant Soil* 395, 189–200. doi: 10.1007/s11104-015-2547-9

Delgado, M., Zúñiga-Feest, A., Alvear, M., and Borie, F. (2013). The effect of phosphorus on cluster-root formation and functioning of *Embothrium* coccineum (R. et J. Forst.). *Plant Soil* 373, 765–773. doi: 10.1007/s11104-013-1829-3

Delgado, M., Zúñiga-Feest, A., and Borie, F. (2015b). Ecophysiological role of *Embothrium coccineum*, a Proteaceae species bearing cluster roots, at increasing Phosphorus availability in its rhizosphere. *J. Soil Sci. Plant Nutr*. 15, 307–320. doi: 10.4067/S0718-95162015005000028

Denton, M. D., Veneklaas, E. J., Freimoser, F. M., and Lambers, H. (2007). *Banksia* species (Proteaceae) from severely phosphorus-impoverished soils exhibit extreme efficiency in the use and re-mobilization of phosphorus. *Plant Cell Environ.* 30, 1557–1565. doi: 10.1111/j.1365-3040.2007.01733.x

Díaz-Vial, C., Aviles, C., and Roberts, R. (1960). Los Grandes Grupos de Suelos de la Provincia de Magallanes. *Agric. Técn.* 19, 224–308.

Diehl, P., Mazzarino, M., Funes, F., Fontenla, S., Gobbi, M., and Ferrari, J. (2003). Nutrient conservation strategies in native Andean-Patagonian forests. *J. Veg. Sci.* 14, 63–70. doi: 10.1111/j.1654-1103.2003.tb02128.x

Diehl, P., Mazzarino, M. J., and Fontenla, S. (2008). Plant limiting nutrients in Andean-Patagonian woody species: effects of interannual rainfall variation, soil fertility and mycorrhizal infection. *For. Ecol. Manage*. 255, 2973–2980. doi: 10.1016/j.foreco.2008.02.003

Donoso, C. (2006). *Las Especies Arbóreas de los Bosques Templados de Chile y Argentina, Autoecología*. Valdivia: Marisa Cúneo Ediciones.

Donoso-Ñanculao, G., Castro, M., Navarrete, D., Bravo, L. A., and Corcuera, L. J. (2010). Seasonal induction of cluster roots in *Embothrium coccineum* JR Forst. & G. Forst. in the field: factors that regulate their development. *Chil J Agric Res* 4, 559–566. doi: 10.4067/S0718-58392010000400005

Drummond, L., and Maher, W. (1995). Determination of phosphorus in aqueous solution via formation of the phosphoantimonylmolybdenum blue complex. Re-examination of optimum conditions for the analysis of phosphate. *Anal. Chim. Acta* 302, 69–74. doi: 10.1016/0003-2670(94)00429-P

Fajardo, A., and Piper, F. I. (2015). High foliar nutrient concentrations and resorption efficiency in *Embothrium coccineum* (Proteaceae) in southern Chile. *Am. J. Bot.* 102, 208–216. doi: 10.3732/ajb.1400533

Gallardo, M.-B., Pérez, C., Núñez-Ávila, M., and Armesto, J. J. (2012). Desacoplamiento del desarrollo del suelo y la sucesión vegetal a lo largo de una cronosecuencia de 60 mil años en el volcán Llaima, Chile. *Rev. Chil. Hist. Nat.* 85, 291–306. doi: 10.4067/S0716-078X2012000300004

Güsewell, S. (2004). N: P ratios in terrestrial plants: variation and functional significance. *New Phytol.* 164, 243–266. doi: 10.1111/j.1469-8137.2004.01192.x

Hassiotou, F., Evans, J. R., Ludwig, M., and Veneklaas, E. J. (2009). Stomatal crypts may facilitate diffusion of CO_2 to adaxial mesophyll cells in thick sclerophylls. *Plant Cell Environ*. 32, 1596–1611. doi: 10.1111/j.1365-3040.2009.02024.x

Hayes, P. E., Clode, P. L., Oliveira, R. S., and Lambers, H. (2018). Proteaceae from phosphorus-impoverished habitats preferentially allocate phosphorus to photosynthetic cells: an adaptation improving phosphorus-use efficiency. *Plant Cell Environ.* 41, 605–619. doi: 10.1111/pce.13124

Hayes, P., Turner, B. L., Lambers, H., Laliberté, E., and Bellingham, P. (2014). Foliar nutrient concentrations and resorption efficiency in plants of contrasting nutrient-acquisition strategies along a 2-million-year dune chronosequence. *J. Ecol.* 102, 396–410. doi: 10.1111/1365-2745.12196

Hechenleitner, P., Gardner, M., Thomas, P., Echeverría, C., Escobar, B., Brownless, P., et al. (2005). *Plantas Amenazadas del Centro-Sur de Chile. Distribución, Conservación y Propagación*. Valdivia: Universidad Austral de Chile y Real Jardín Botánico de Edimburgo.

Hidaka, A., and Kitayama, K. (2009). Divergent patterns of photosynthetic phosphorus-use efficiency versus nitrogen-use efficiency of tree leaves along nutrient-availability gradients. *J. Ecol.* 97, 984–991. doi: 10.1111/j.1365-2745.2009.01540.x

Hopper, S. D. (2009). OCBIL theory: towards an integrated understanding of the evolution, ecology and conservation of biodiversity on old, climatically buffered, infertile landscapes. *Plant Soil* 322, 49–86. doi: 10.1007/s11104-009-0068-0

Killingbeck, K. T. (1996). Nutrients in senesced leaves: keys to the search for potential resorption and resorption proficiency. *Ecology* 77, 1716–1727. doi: 10.2307/2265777

Koerselman, W., and Meuleman, A. F. (1996). The vegetation N: P ratio: a new tool to detect the nature of nutrient limitation. *J. Appl. Ecol.* 1441–1450. doi: 10.2307/2404783

Lambers, H., Bishop, J. G., Hopper, S. D.,Laliberté, E., and Zúñiga-Feest, A. (2012a). Phosphorus-mobilization ecosystem engineering: the roles of cluster roots and carboxylate exudation in young P-limited ecosystems. *Ann. Bot*. 110, 329–348. doi: 10.1093/aob/mcs130

Lambers, H., Brundrett, M. C., Raven, J. A., and Hopper, S. D. (2010). Plant mineral nutrition in ancient landscapes: high plant species diversity on infertile soils is linked to functional diversity for nutritional strategies. *Plant Soil* 334, 11–31. doi: 10.1007/s11104-010-0444-9

Lambers, H., Cawthray, G. R., Giavalisco, P., Kuo, J., Laliberté, E., Pearse, S. J., et al. (2012b). Proteaceae from severely phosphorus-impoverished soils extensively replace phospholipids with galactolipids and sulfolipids during leaf development to achieve a high photosynthetic phosphorus-use-efficiency. *New Phytol*. 196, 1098–1108. doi: 10.1111/j.1469-8137.2012.04285.x

Lambers, H., Chapin, F., and Pons, T. (2008a). *Plant Physiological Ecology*. New York, NY: Springer.

Lambers, H., Clode, P. L., Hawkins, H.-J., Laliberté, E., Oliveira, R. S., Reddell, P., et al. (2015c). "Metabolic adaptations of the non-mycotrophic proteaceae to soils with low phosphorus," in *Annual Plant Reviews, Phosphorus Metabolism in Plants,* eds W. C. Plaxton and H. Lambers (Chicester: John Wiley & Sons, Inc.), 289–335.

Lambers, H., Finnegan, P. M., Jost, R., Plaxton, W. C., Shane, M. W., and Stitt, M. (2015a). Phosphorus nutrition in Proteaceae and beyond. *Nat Plants* 1:15109. doi: 10.1038/nplants.2015.109

Lambers, H., Hayes, P. E., Laliberté, E., Oliveira, R. S., and Turner, B. L. (2015b). Leaf manganese accumulation and phosphorus-acquisition efficiency. *Trends Plant Sci.* 20, 83–90. doi: 10.1016/j.tplants.2014.10.007

Lambers, H., Raven, J. A., Shaver, G. R., and Smith, S. E. (2008b). Plant nutrient-acquisition strategies change with soil age. *Trends Ecol. Evol*. 23, 95–103. doi: 10.1016/j.tree.2007.10.008

Lambers, H., Shane, M. W., Cramer, M. D., Pearse, S. J., and Veneklaas, E. J. (2006). Root structure and functioning for efficient acquisition of phosphorus: matching morphological and physiological traits. *Ann. Bot.* 98, 693–713. doi: 10.1093/aob/mcl114

Lamont, B. B. (2003). Structure, ecology and physiology of root clusters – a review. *Plant Soil* 248, 1–19. doi: 10.1023/A:1022314613217

Lamont, B. B., Pérez-Fernández, M., and Rodríguez-Sánchez J, J. (2014). Soil bacteria hold the key to root cluster formation. *New Phytol.* 206, 1156–1162. doi: 10.1111/nph.13228

Luebert, F., and Pliscoff, P. (2006). *Sinopsis Bioclimática y Vegetacional de Chile*. Santiago: Editorial Universitaria.

Oleksyn, J., Reich, P. B., Zytkowiak, R., Karolewski, P., and Tjoelker, M. G. (2003). Nutrient conservation increases with latitude of origin in European *Pinus sylvestris* populations. *Oecologia* 136, 220–235. doi: 10.1007/s00442-003-1265-9

Olsen, S., and Sommers, L. (1982). "Phosphorus," in *Methods of soil analysis. Part 2. ASA Monograph,* ed A. L. Page (Madison: ASA and SSSA), 403–430.

Pate, J., Verboom, W., and Galloway, P. (2001). Co-occurrence of Proteaceae, laterite and related oligotrophic soils: coincidental associations or causative inter-relationships? *Aust. J. Bot.* 49, 529–560. doi: 10.1071/BT00086

Piper, F. I., Baeza, G., Zuniga-Feest, A., and Fajardo, A. (2013). Soil nitrogen, and not phosphorus, promotes cluster-root formation in a South American Proteaceae, *Embothrium coccineum*. *Am. J. Bot*. 100, 2328–2338. doi: 10.3732/ajb.1300163

Poorter, H., and Evans, J. R. (1998). Photosynthetic nitrogen-use efficiency of species that differ inherently in specific leaf area. *Oecologia* 116, 26–37. doi: 10.1007/s004420050560

Reich, P. B., Ellsworth, D. S., Walters, M. B., Vose, J. M., Gresham, C., Volin, J. C., et al.(1999). Generality of leaf trait relationships: a test across six biomes. *Ecology* 80, 1955–1969. doi: 10.1890/0012-9658(1999)080[1955:GOLTRA]2.0.CO;2

Richardson, S. J., Peltzer, D. A., Allen, R. B., McGlone, M. S., and Parfitt, R. L. (2004). Rapid development of phosphorus limitation in temperate rainforest along the Franz Josef soil chronosequence. *Oecologia* 139, 267–276. doi: 10.1007/s00442-004-1501-y

Rodrigues de Lima, A. C., Hoogmoed, W., and Brussaard, L. (2008). Soil quality assessment in rice production systems: establishing a minimum data set. *J. Environ. Qual*. 37, 623–630. doi: 10.2134/jeq2006.0280

Ryan, P. R., Delhaize, E., and Jones, D. L. (2001). Function and mechanism of organic anion exudation from plant roots. *Annu. Rev. Plant Physiol. Plant Mol. Biol*. 52, 527–560. doi: 10.1146/annurev.arplant.52.1.527

Sadzawka, A., Carrasco, M., Grez, R., and Ml, M. (2004a). *Métodos de Análisis Recomendados para los Suelos Chilenos*. Santiago: Sociedad Chilena de la Ciencia del Suelo.

Sadzawka, A., Grez, R., Carrasco, M., and Mora, M. (2004b). *Métodos de Análisis de Tejidos Vegetales*. Santiago: Comisión de Normalización y Acreditación Sociedad Chilena de la Ciencia del Suelo.

Schmidt, S., Mason, M., Sangtiean, T., and Stewart, G. (2003). Do cluster roots of *Hakea actities* (Proteaceae) acquire complex organic nitrogen? *Plant Soil* 248, 157–165. doi: 10.1023/A:1022352415728

Shane, M. W., and Lambers, H. (2005). Cluster roots: a curiosity in context. *Plant Soil* 274, 101–125. doi: 10.1007/s11104-004-2725-7

Shane, M. W., Stigter, K., Fedosejevs, E. T., and Plaxton, W. C. (2014). Senescence-inducible cell wall and intracellular purple acid phosphatases: implications for phosphorus remobilization in *Hakea prostrata* (Proteaceae) and *Arabidopsis thaliana* (Brassicaceae). *J. Exp. Bot.* 65, 6097–6106. doi: 10.1093/jxb/eru348

Steubing, L., Alberdi, M., and Wenzel, H. (1983). Seasonal changes of cold resistance of Proteaceae of the South Chilean laurel forest. *Vegetatio* 52, 35–44.

Sulpice, R., Ishihara, H., Schlereth, A., Cawthray, G. R., Encke, B., Giavalisco, P., et al. (2014). Low levels of ribosomal RNA partly account for the very high photosynthetic phosphorus-use efficiency of Proteaceae species. *Plant Cell Environ.* 37, 1276–1298. doi: 10.1111/pce.12240

Walkley, A., and Black, I. A. (1934). An examination of the Degtjareff method for determining soil organic matter, and a proposed modification of the chromic acid titration method. *Soil Sci.* 37, 29–38. doi: 10.1097/00010694-193401000-00003

Wright, I. J., Reich, P. B., Westoby, M., Ackerly, D. D., Baruch, Z., Bongers, F., et al. (2004). The worldwide leaf economics spectrum. *Nature* 428, 821–827. doi: 10.1038/nature02403

Zúñiga-Feest, A., Delgado, M., and Alberdi, M. (2010). The effect of phosphorus on growth and cluster-root formation in the Chilean Proteaceae: *Embothrium coccineum* (R. et J. Forst.). *Plant Soil* 334, 113–121. doi: 10.1007/s11104-010-0419-x

Conflict of Interest Statement: The authors declare that the research was conducted in the absence of any commercial or financial relationships that could be construed as a potential conflict of interest.

frontiers in Plant Science

MINI REVIEW
published: 11 July 2018
doi: 10.3389/fpls.2018.00922

Metabolomics and Transcriptomics in Legumes Under Phosphate Deficiency in Relation to Nitrogen Fixation by Root Nodules

Mostafa Abdelrahman[1,2], Magdi A. El-Sayed[2], Abeer Hashem[3,4], Elsayed Fathi Abd_Allah[5†], Abdulaziz A. Alqarawi[5], David J. Burritt[6] and Lam-Son Phan Tran[7,8]*

[1] Arid Land Research Center, Tottori University, Tottori, Japan, [2] Department of Botany, Faculty of Science, Aswan University, Aswan, Egypt, [3] Botany and Microbiology Department, College of Science, King Saud University, Riyadh, Saudi Arabia, [4] Mycology and Plant Disease Survey Department, Plant Pathology Research Institute, Agricultural Research Center, Giza, Egypt, [5] Plant Production Department, College of Food and Agriculture Sciences, King Saud University, Riyadh, Saudi Arabia, [6] Department of Botany, University of Otago, Dunedin, New Zealand, [7] Institute of Research and Development, Duy Tan University, Da Nang, Vietnam, [8] Stress Adaptation Research Unit, RIKEN Center for Sustainable Resource Science, Yokohama, Japan

OPEN ACCESS

Edited by:
Alex Joseph Valentine, Stellenbosch University, South Africa

Reviewed by:
Oswaldo Valdes-Lopez, Universidad Nacional Autónoma de México, Mexico
Aleysia Kleinert, Stellenbosch University, South Africa
Xia Li, Huazhong Agricultural University, China
Takuji Ohyama, Tokyo University of Agriculture, Japan

***Correspondence:**
Lam-Son Phan Tran
son.tran@riken.jp

[†]orcid.org/0000-0002-8509-8953

Specialty section:
This article was submitted to Plant Nutrition, a section of the journal Frontiers in Plant Science

Received: *22 January 2018*
Accepted: *11 June 2018*
Published: *11 July 2018*

Citation:
Abdelrahman M, El-Sayed MA, Hashem A, Abd_Allah EF, Alqarawi AA, Burritt DJ and Tran L-SP (2018) Metabolomics and Transcriptomics in Legumes Under Phosphate Deficiency in Relation to Nitrogen Fixation by Root Nodules. Front. Plant Sci. 9:922. doi: 10.3389/fpls.2018.00922

Phosphate (P_i) deficiency is a critical environmental constraint that affects the growth and development of several legume crops that are usually cultivated in semi-arid regions and marginal areas. P_i deficiency is known to be a significant limitation for symbiotic nitrogen (N_2) fixation (SNF), and variability in SNF is strongly interlinked with the concentrations of P_i in the nodules. To deal with P_i deficiency, plants trigger various adaptive responses, including the induction and secretion of acid phosphatases, maintenance of P_i homeostasis in nodules and other organs, and improvement of oxygen (O_2) consumption per unit of nodule mass. These molecular and physiological responses can be observed in terms of changes in growth, photosynthesis, and respiration. In this mini review, we provide a brief introduction to the problem of P_i deficiency in legume crops. We then summarize the current understanding of how P_i deficiency is regulated in legumes by changes in the transcriptomes and metabolomes found in different plant organs. Finally, we will provide perspectives on future directions for research in this field.

Keywords: legumes, metabolomics, transcriptomics, phosphate deficiency, nitrogen fixation

INTRODUCTION

Phosphorus(P) is a crucial element required for plant growth and development, playing a pivotal role in a diverse array of cellular processes, including photosynthesis, energy production, redox reactions, symbiotic nitrogen (N_2) fixation (SNF), and carbohydrate metabolism (Sulieman and Tran, 2015; Kleinert et al., 2017). However, more than 30–40% of the world's arable soils have low P

contents, and by 2050 rock phosphate (P_i) reserves, the most inexpensive form of P for fertilization of agricultural soils, may be exhausted (Vance et al., 2003; Herrera-Estrella and López-Arredondo, 2016; Kleinert et al., 2017). Uptake of P_i from some soils can be problematic for plants due to slow P_i diffusion rates and the formation of insoluble P_i complexes with cations, especially iron and aluminum in acid weathered soils (Valentine et al., 2010; Castro-Guerrero et al., 2016). In several cropping systems, P_i-containing fertilizers are applied frequently to soils to enhance P_i availability, and thus yield. With the increasing demand for food, P_i fertilizer demand has increased four- to five-fold in last few decades, and is expected to continue increasing[1] (**Figure 1**). This fact combined with a significant increase in P_i fertilizer production will add further pressure on the limited P_i reserve in the coming years (**Figure 1**). The use of P_i-containing fertilizers is a short-term solution to a much greater problem, as the real challenge for scientists and farmers is to deliver food with high nutritional quality using sustainable agricultural practices (Castro-Guerrero et al., 2016).

Grain legumes are an essential source of nutrition and income for a large number of consumers and farmers worldwide (Kleinert et al., 2017; Abdelrahman et al., 2018). Legumes can create symbiotic relationships with N_2-fixing rhizobia and arbuscular mycorrhizal fungi that facilitate the acquisition of nutrients; and thus, reduce the use of synthetic fertilizers, which is advantageous for sustainable agriculture (Considine et al., 2017; Valliyodan et al., 2017). SNF is an energetically expensive process, consuming ∼20 adenosine triphosphate (ATP) molecules for the production of two NH_3 molecules (Thuynsma et al., 2014). Because of the requirement for large amounts of ATP for SNF, P_i deficiency is a critical constraint for efficient SNF in legumes. There is substantial evidence demonstrating that P_i deficiency can more severely affect the N:P ratio in legume tissues when compared with non-leguminous crops (Sulieman and Tran, 2015; Guo et al., 2016). Enhanced nutrient acquisition by SNF nodules formed by plants of P_i-deficient soils is crucial for the efficient fixation of N_2 (Magadlela et al., 2015; Lazali et al., 2017). Legumes have evolved conserved acquisition and internal transport strategies for P_i detected in P_i-deficient soils in order to maintain nodule P_i-homeostasis and enable efficient SNF (**Figure 2**). These include decreased plant growth rates, modification of carbon metabolism, increased secretion of organic anions and phosphatases, changes in root architecture, expansion of root surface areas, and enhanced expression of P_i transporters (Sulieman and Tran, 2015; Considine et al., 2017; Kleinert et al., 2017; Uhde-Stone, 2017). Because of the diminishing reserves of inexpensive P_i fertilizers, plant acclimation to P_i deficiency has become a topic of considerable interest to plant researchers. Below we present recent advances in the transcriptomic and metabolomic changes that occur in legumes in response to P_i deficiency, which is essential if we are to understand the complex systemic metabolic mechanisms plants use to adapt to P_i deficiency.

[1] www.fao.org

A LEGUME TRANSCRIPTOME ATLAS UNDER P_i DEFICIENCY

Next-generation sequencing (NGS) technologies have become essential tools to help understand the regulation of gene expression and the molecular basis of cellular responses that occur in plants exposed to biotic and/or abiotic stressors (Abdelrahman et al., 2015, 2017a,b; Miao et al., 2015; Liese et al., 2017; Nasr Esfahani et al., 2017). A number of transcriptome studies of leguminous plant species, including white lupin (*Lupinus albus*), common bean (*Phaseolus vulgaris*), soybean (*Glycine max*), chickpea (*Cicer arietinum*), and *Medicago truncatula*, grown under P_i deficiency have been conducted in the last several years (Hernández et al., 2007; O'Rourke et al., 2013; Liese et al., 2017; Nasr Esfahani et al., 2017; Zhang et al., 2017). RNAseq-based transcriptome profiling of nodules of *Sinorhizobium meliloti*-inoculated *M. truncatula* plants grown under P_i deficiency has shown a strong down-regulation in the expression of genes encoding NODULE-SPECIFIC CYSTEINE-RICH peptides, LEGHEMOGLOBIN and NICOTIANAMINE SYNTHASE-LIKE PROTEIN, compared with nodules of control plants grown under P_i-replete conditions (Liese et al., 2017). The down-regulation of these genes disturbs normal cellular iron distribution, restricts the supply of oxygen for respiration and eventually lowers nitrogenase activity in nodules (Liese et al., 2017). This potential disruption of normal nodule metabolism caused by P_i deficiency greatly reduces SNF efficiency in legumes (Liese et al., 2017). In addition, a reduction in shoot and nodule dry matter, and tissue P_i levels was observed in P_i-deficient *M. truncatula* plants relative to P_i-replete control plants, indicating that P_i deficiency can severely limit legume growth and potential crop yields (Liese et al., 2017). However, while *S. meliloti*-inoculated *M. truncatula* plants grown under P_i deficiency had much lower stem and root tissue P_i concentrations compared with control (P_i-sufficient) plants, nodule P_i levels in P_i-deficient plants were maintained at relatively high levels and did not show the considerable loss of P_i as observed for stems and roots (Liese et al., 2017). Nasr Esfahani et al. (2017) examined transcriptome changes in the nodules of P_i-deficiency-more-susceptible *Mesorhizobium mediterraneum* SWRI9-(*Mm*SWRI9)-chickpea and P_i-deficiency-less-susceptible *M. ciceri* CP-31-(*Mc*CP-31)-chickpea associations under P_i-deficient and -sufficient conditions. The transcriptome profiles of these interactions showed that many genes related to several key cellular processes and metabolic pathways namely transcriptional regulation, detoxification, nodulation, ion/nutrient transport, and P_i signaling and remobilization were differentially expressed in *Mm*SWRI9-induced nodules relative to *Mc*CP-31-induced nodules (Nasr Esfahani et al., 2017). Changes in the expression of P_i starvation-related genes are likely to help improve acquisition and transport of P_i in the *Mm*SWRI9-chickpea association; and thus maintenance of the sufficient SNF capacity under P_i-deficient conditions (Nasr Esfahani et al., 2017). The above observations indicated that changes in legume transcriptomes under P_i starvation are mostly associated with facilitating P_i solubilization, acquisition and

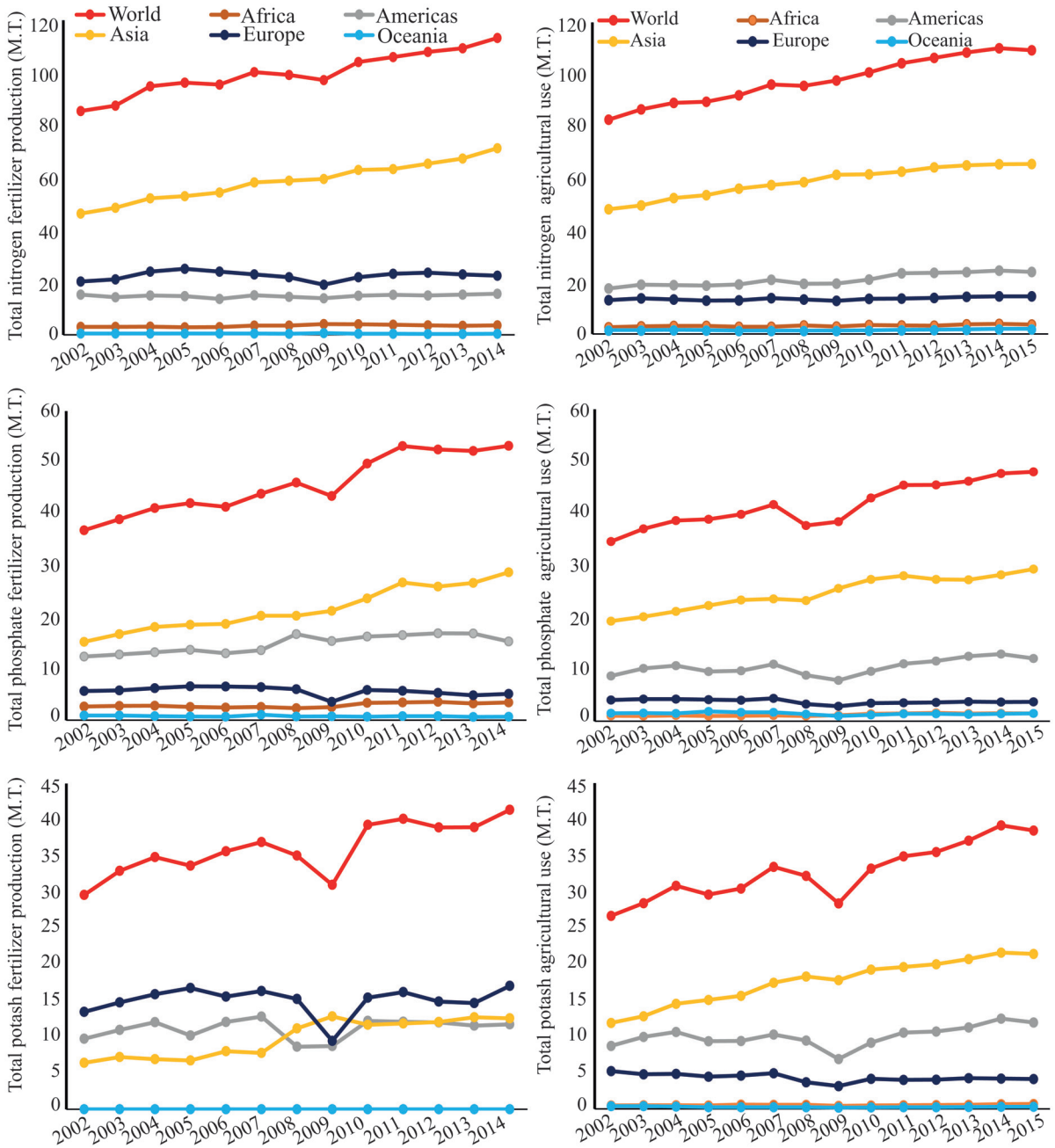

FIGURE 1 | World nitrogen, phosphate (P_2O_5), and potash (K_2O) fertilizer production from 2002 to 2014, and their agricultural use from 2002 to 2015 in millions of tonnes (M.T.), according to FAO (www.fao.org, accessed 2018).

transportation into nodules, which are significant sinks for P_i, contributing to more efficient SNF and therefore higher plant productivity.

Although most studies to date have focused on nodule transcriptomes, exploring the transcriptomes of other plant tissues is also important, as these may provide valuable insight into P_i deficiency acclimation mechanisms in legumes. For example, transcriptome analysis of leaves and roots (combined cluster and normal roots) of white lupine plants grown under P_i-deficient or -sufficient conditions identified 1,342 and 904 differentially expressed genes, respectively, in response to P_i deficiency (O'Rourke et al., 2013). In leaves, the most highly expressed transcripts were involved in amino acid metabolism, tetrapyrrole synthesis, photosynthesis, carbohydrate catabolism, and flavonoid biosynthesis; whereas in roots the most highly expressed transcripts were involved in sugar/nutrient signaling and transport, lignin biosynthesis, phospholipid and carbohydrate metabolism, and amino acid

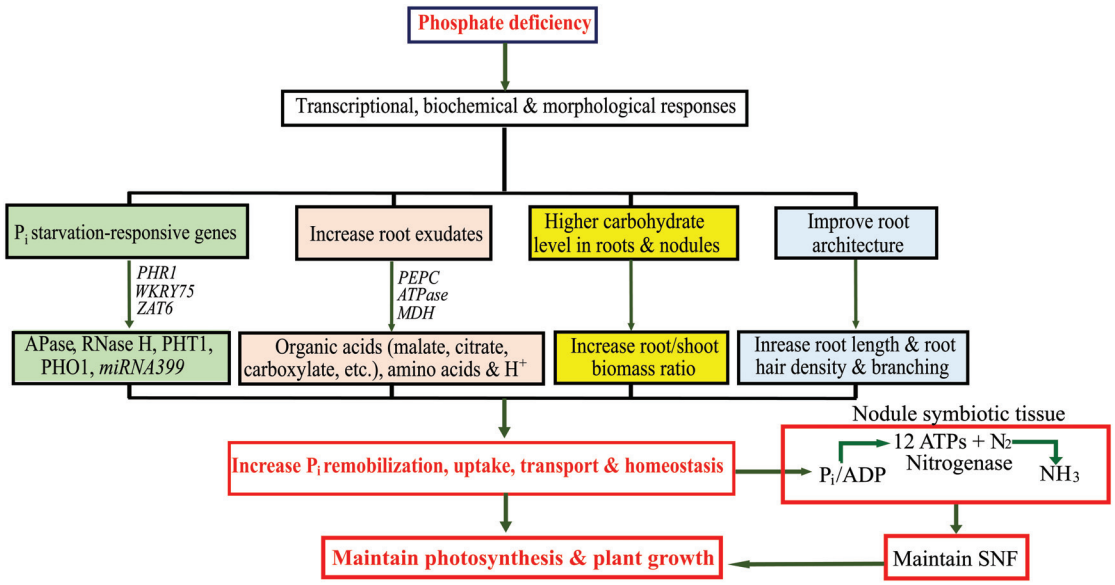

FIGURE 2 | Schematic representation of transcriptional, biochemical and morphological changes in legumes under phosphate (P_i) deficiency to increase P_i uptake and optimize P_i use efficiency. APase, ACID PHOSPHATASE; ATPase, Adenosine Triphosphatase; MDH, MALATE DEHYDROGENASE; PEPC, PHOSHOENOLPYRUVATE CARBOXYLASE; PHO1, PHOSPHATE TRANSPORTER 1; PHR1, PHOSPHATE STARVATION RESPONSIVE 1; PHT1, HIGH-AFFINITY PHOSPHATE TRANSPORTER 1; RNase H, RIBONUCLEASE H; SNF, symbiotic nitrogen fixation; ZAT6, ZINC FINGER OF *ARABIDOPSIS* 6.

synthesis. Interestingly, 12 transcripts identified in the above study were commonly induced by low-P_i stress across three species, white lupine, *Arabidopsis,* and potato (*Solanum tuberosum*), making them excellent candidates to investigate responses to P_i starvation in plants (O'Rourke et al., 2013). Among these 12 transcripts, three transcripts that were highly up-regulated in P_i-deficient lupine plants compared with P_i-sufficient ones (O'Rourke et al., 2013) encode SPX domain-containing proteins [RECOMBINANT *Saccharomyces cerevisiae* PROTEIN (SYG1)/PHOSPHATASE(PHO81)/XENOTROPIC and POLYTROPICRETROVIRUS RECEPTOR 1(XPR1)] that are essential regulators involved in P_i homeostasis and signaling responses to P_i deficiency (Chiou and Lin, 2011; Secco et al., 2012). In addition, P_i solubilization- and transport-related genes, encoding PHOSPHATE TRANSPORTER 1, PHOSPHOLIPASE, PYROPHOSPHATASE, PURPLE ACID PHOSPHATASE, and MONOGALACTOSYLDIACYLGLYCEROL SYNTHASE, were also up-regulated in lupine P_i-deficient relative to P_i-sufficient plants (O'Rourke et al., 2013). A recent study by Zhang et al. (2017) provided transcriptome datasets obtained from the roots and leaves of soybean plants grown under P_i-deficient and -sufficient conditions, and showed a significant role for the acid phosphatase-encoding gene *GmACP1* in regulating P_i use efficiency in soybean. These results were in agreement with a previous finding by the same research group (Zhang et al., 2014), who used a genome-wide association study of 192 soybean accessions to identify a quantitative trait locus (QTL) on soybean chromosome 8, namely *qPE8*, which was associated with improvement of soybean P_i use efficiency under P_i starvation. This *qPE8* QTL contained the candidate genes *Glyma08g20700*, *Glyma08g20710,* and *Glyma08g20800*, *Glyma08g20820*/*GmACP1* and *Glyma08g20830*, which encode CALCINEURIN B, PHOSPHOLIPASE D and putative PHOSPHATASES, respectively. *Glyma08g20820*/*GmACP1* was up-regulated under P_i deficiency; however, the transcript levels of the remaining genes were not changed (Zhang et al., 2014). In addition, overexpression study of *GmACP1* using hairy-root transformation showed that the transgenic hairy roots displayed a 2.3-fold increase in acid phosphatase activity and an 11.2–20.0% higher P_i use efficiency relative to wild-type plants under P_i starvation (Zhang et al., 2014).

Transcriptome analysis of wild legumes is also critical to aid in understanding the differences that exist between domesticated legumes and their wild progenitors (Abdelrahman et al., 2018). This could also help provide a better understanding of the P_i stress adaptation mechanisms present in wild legumes. In addition, transcriptome correlation analyses between different legume species under P_i deficiency may provide crucial information about the conserved P_i deficiency-responsive genes, which could be used as molecular markers for screening for low P_i- tolerant/susceptible cultivars or genetic engineering to enhance the growth and productivity of crop plants grown on low P_i soils.

TRANSCRIPTIONAL REGULATION AND MicroRNA UNDER P_i DEFICIENCY

Plants adapt to P_i starvation by an array of molecular responses in which transcription factors (TFs) are key components in the regulation of these processes (Jain et al., 2012).

The transcriptional regulations of the P_i starvation responses have been extensively studied in other plant species; however, these important processes have not much investigated yet in legumes. Four TF-encoding genes *BASIC HELIX-LOOP-HELIX 32* (*BHLH32*), *WRKY75*, *PHOSPHATE STARVATION RESPONSIVE 1* (*PHR1*), and *ZINC FINGER OF ARABIDOPSIS 6* (*ZAT6*) involved in P_i starvation signaling have been identified in *Arabidopsis* (Valdés-López and Hernández, 2008). *AtPHR1* and its orthologs from rice (*Oryza sativa*, *OsPHR1* and *OsPHR2*) are regarded as the key positive regulators controlling plant transcriptional responses to P_i deficiency (Rubio et al., 2001; Zhou et al., 2008). The overexpression of *AtPHR1* induced P_i-responsive genes involved in P_i remobilization (*ACID PHOSPHATASES and RIBONUCLEASE H*), transport [*HIGH-AFFINITY PHOSPHATE TRANSPORTER 1* (*PHT1*), *PHOSPHATE TRANSPORTER 1*(*PHO1*)] and homeostasis (*miRNA399* and *At4*), in addition to genes involved in anthocyanin biosynthesis (Valdés-López and Hernández, 2008). Hernández et al. (2007) reported 17 TF-encoding genes differentially expressed in common bean roots under P_i deficiency. Of these genes, *TC2883 MYB* gene was highly induced under P_i starvation and exhibited 63% homology to *AtPHR1*, suggesting an important role of PHR1 in common bean response to P_i deficiency. Likewise, the *Arabidopsis At4* plays a significant role in translocation of P_i from roots to shoots, and its ortholog from *M. truncatula*, the *Mt4*, showed strongly induced expression in roots under P_i deficiency (Valdés-López and Hernández, 2008). *WKRY75* and *ZAT6* are also up-regulated under P_i starvation, and both two genes are implicated in P_i remobilization, transport, and homeostasis as well as root architecture. In contrast, *BHLH32* is down-regulated under P_i deficiency, and its role in modification of root architecture has been proposed (Chen et al., 2007).

Overexpression of the rice *osa-miR827* and *Arabidopsis miR399*/*miRNA399* that target the SPX-MAJOR FACILITATOR SUPERFAMILY (MFS) protein-encoding genes and the P_i transporter genes, respectively, drastically impacts P_i homeostasis and accumulation in transgenic plants (Wang et al., 2012; Chen et al., 2017). During P_i starvation, *miR399*/*miRNA399* supresses its target gene *PHO2* and allows sufficient transcript of *PHT1* accumulated in the membrane of P_i-starved transgenic plants, thereby increasing P_i acquisition (Franco-Zorrilla et al., 2007). Recently, Chen et al. (2017) demonstrated a crucial role of the *TamiR167a* in mediating tobacco (*Nicotiana tabacum*) growth and adaptation to P_i starvation via regulation of various biological processes, including P_i acquisition and reactive oxygen species homeostasis. Thus, distinct miRNAs are also important regulators in mediating the plant response to P_i stress as well.

LEGUME METABOLOME PROFILE UNDER P_i DEFICIENCY

The development of crop plants that are able to produce good yield on nutrient-deficient soils requires an in-depth knowledge of physiological and biochemical processes that allow plants to survive under these stressful conditions. Integrated transcriptomic and metabolomic studies can aid in obtaining this knowledge (Hirai et al., 2004; Last et al., 2007; Hernández et al., 2009; Saito, 2013; Abdelrahman et al., 2014, 2015, 2017c,d; Jin et al., 2017). Plant metabolites are synthesized by numerous proteins/enzymes encoded in the plant genome, and integration of gene expression atlas with targeted/non-targeted metabolite profile is an innovative approach to identify gene-to-metabolite associations/networks (Hirai et al., 2004; Saito, 2013; Abdelrahman et al., 2017d). The use of metabolic profiling has been quite limited for legume crops, but this approach has recently been applied to help understand the metabolic changes associated with legume-rhizobial symbiosis. Symbiotic N_2-fixing bacteria secrete lipo-chitooligosaccharide signaling molecules, also known as Nod factors, upon perception of isoflavonoids and flavonoids secreted by legume roots (Zhang et al., 2012). The Nod factors are perceived by their receptors on the plasma membranes of root cells of leguminous plants, which then activate signaling processes within the nucleus and cytoplasm of target cells (Zhang et al., 2012). Untargeted metabolite profiling of the extracts of *M. truncatula* seedlings treated with rhizobial lipo-chitooligosaccharide molecules has shown a significant decrease in oxylipin-related compounds in *M. truncatula*. Oxylipins are precursors of the jasmonic acid biosynthesis pathway, and both oxylipins and jasmonic acids inhibit Nod factor signaling, suggesting that these oxylipin-related compounds act as negative regulators of the early stages of symbiosis (Zhang et al., 2012).

In an early study, Hernández et al. (2009) used integrated non-targeted metabolite profiling and transcriptome analysis to identify changes in the roots and nodules of common bean plants inoculated with *Rhizobium tropici* and grown under P_i-deficient and -sufficient conditions. They showed clear metabolic differences between plants grown under these two contrasting conditions. Integrative analysis of nodule transcriptome and metabolome allowed the authors to identify 13 metabolites that could be assigned to repressed or induced pathways in response to P_i deficiency. Of these 13 P_i starvation-responsive metabolites, a reduction in N metabolism-related metabolites, including spermidine, putrescine, urea, glycine, serine, glutamine, and threonine, was detected in nodules of P_i-deficient common bean plants relative to that of P_i-sufficient ones, and this change might contribute to a decrease in SNF efficiency (Hernández et al., 2009). In addition, P_i-deficient common bean roots show reduced levels of organic acids like tartaric acid and 2,4-dihydroxybutanoic acid, due to the secretion of these organic acids into the rhizosphere (Hernández et al., 2009). In contrast, alteration of carbon (C) metabolism in P_i-deficient common bean results in lower and higher carbohydrate levels in the shoots and roots, respectively, thereby contributing to the increased root/shoot biomass ratio and altering root morphology (Hernández et al., 2009). Similarly, Nasr Esfahani et al. (2016) showed lower SNF efficiency and decreased P_i level in the P_i-deficiency-more-susceptible *Mm*SWRI9-chickpea nodules than the P_i-deficiency-less-susceptible *Mc*CP-31-chickpea nodules under Pi deficiency, which was evident by significant differences in C and N metabolism-related metabolites. For example, in

*Mc*CP-31-inoculated plants, P_i deficiency increased total level of identified sugars by 68.8%, whereas that remained unchanged in *Mm*SWRI9-induced nodules (Nasr Esfahani et al., 2016). In addition, P_i deficiency induced a remarkable increase in total level of organic acids in *Mc*CP-31-nodulated roots, whereas it decreased that in *Mm*SWRI9-nodulated roots (Nasr Esfahani et al., 2016). These results revealed the existence of crosstalk among various signaling pathways involved in regulation of *Mesorhizobium*-chickpea adaptation to P_i deficiency, in-depth understanding of which at genetic level will be useful for genetic engineering of chickpea cultivars and other leguminous crops that can sustain efficient SNF under P_i deficiency. C and N metabolism is essential for SNF, and is a significant determinant of plant and nodule responses to P_i starvation (Kleinert et al., 2017). Some studies have shown that even under P_i deficiency, plant nodules continue to act as very strong nutrient sinks for C in order to maintain SNF, and underground biomass often continues to increase even at the expense of whole plant growth (Thuynsma et al., 2014; Magadlela et al., 2015). Interestingly, for white lupine plants grown under P_i-deficient and -sufficient conditions, no significant differences in the above and below ground biomass between P_i-deficient and -sufficient plants were observed, nor were any large differences in resource allocation (N and P_i) between the shoot and root/nodule systems (Thuynsma et al., 2014). However, white lupine plants produced more cluster root biomass, up to 24% of the root system under P_i deficiency; relative to approximately 5% increase of the root system with sufficient P_i supply. In contrast, less nodule biomass (up to 14% of the root system) was detected under P_i deficiency than (up to 20% of the root system) sufficient P_i supply. In addition, cluster roots exhibited a significant increase in P_i acquisition rates under deficient P_i than sufficient P_i conditions (Thuynsma et al., 2014). These results suggest that underground adaptations, rather than large changes in shoot/root biomass ratio, may underpin the ability of lupine plants to grow well on P_i-deficient soils, as more cluster root biomass would result in an improved P_i uptake rate; and hence help maintain high P_i level in the nodules, consequently efficient SNF under P_i deficiency (Thuynsma et al., 2014).

A recent metabolite profiling study of common bean root exudates grown in liquid culture media supplemented with P_i concentrations ranged from 0 to 8 mg L^{-1} showed that the levels of some organic acids, nucleic acids, and amino acids were much higher in common bean root exudates under P_i-deficient conditions than P_i-sufficient ones (Tawaraya et al., 2014). On the other hand, levels of phosphate esters, including glucose-6-phosphate, fructose-6-phosphate, and fructose-1, 6-phosphate, were lower in P_i-deficient relative to P_i-sufficient conditions (Tawaraya et al., 2014). The increase in amino acid and organic acid levels in the root exudates changed the respiration rate and influenced microsymbiont community in the root nodules, improving SNF under P_i deficiency (Tawaraya et al., 2014). While relatively few metabolomic profiling studies of legume crops under P_i deficiency have been conducted to date, future studies on legumes using an integrated metabolomic-transcriptomic approach may provide valuable information on the metabolic reprogramming at molecular level, which is required by plants for better adaptation to P_i deficiency.

SUMMARY AND FUTURE PERSPECTIVES

Legume crops are widely cultivated in many semi-arid and tropical parts of the world where P_i deficiency poses severe threats to crop productivity. To sustain legume cultivation under deficient P_i conditions, crop improvement programs require innovative methods, such as an integrated approach of transcriptomics and metabolomics to gain in-depth understanding of how plants respond to P_i deficiency at the molecular level. This mini review provides an overview of several transcriptomic and metabolomic studies conducted for legumes grown under P_i deficiency and their potential to help understand how legume crops respond to P_i deficiency (**Figure 2**). Transcriptomics and metabolomics have generated gigabyte-size data sets that require specialized computational software and bioinformatic tools to analyze them. To aid with this, several transcriptomic and metabolomic databases have been created; e.g., the MedicCyc for *M. truncatula*[2], which includes more than 250 pathways with related metabolites, enzymes and associated genes. Another database, the Soybean Knowledge Base (SoyKB)[3] has also been constructed. This resource is not only useful for soybean translational genomics, but also for legume proteomics and metabolomics. Identification of candidate genes and metabolic pathways important for the adaptation of legumes to P_i deficiency could be used in future for the marker-assisted selection of P_i-efficient genotypes. Characterizing the proteomes of legumes under P_i deficiency is also a significant task for the future. In addition, information generated from transcriptomics and metabolomics combined with information from other types of analyses, including reverse and forward genetic analyses, could lead to the long-elusive goal of improvement of N_2 fixation in agronomically essential grain legumes grown under P_i deficiency.

AUTHOR CONTRIBUTIONS

MA and L-SPT conceived the idea. MA, ME-S, AH, EA_A, AA, DB, and L-SPT wrote the manuscript. All authors read and approved the final manuscript.

ACKNOWLEDGMENTS

The authors would like to extend their sincere appreciation to the Deanship of Scientific Research at King Saud University for its funding to the Research Group number (RGP-271).

[2]https://www.plantcyc.org/typeofpublication/mediccyc

[3]http://soykb.org/

REFERENCES

Abdelrahman, M., Burritt, D. J., and Tran, L. P. (2017a). The use of metabolomic quantitative trait locus mapping and osmotic adjustment traits for the improvement of crop yields under environmental stresses. *Semin. Cell Dev. Biol.* doi: 10.1016/j.semcdb.2017.06.020 [Epub ahead of print].

Abdelrahman, M., El-Sayed, M., Jogaiah, S., Burritt, D. J., and Tran, L. P. (2017b). The "STAY-GREEN" trait and phytohormone signaling networks in plants under heat stress. *Plant Cell Rep.* 36, 1009–1025. doi: 10.1007/s00299-017-2119-y

Abdelrahman, M., El-Sayed, M., Sato, S., Hirakawa, H., Ito, S.-I., Tanaka, K., et al. (2017c). RNA-sequencing-based transcriptome and biochemical analyses of steroidal saponin pathway in a complete set of *Allium fistulosum-A. cepa* monosomic addition lines. *PLoS One* 12:e0181784. doi: 10.1371/journal.pone.0181784

Abdelrahman, M., Suzumura, N., Mitoma, M., Matsuo, S., Ikeuchi, T., Mori, M., et al. (2017d). Comparative *de novo* transcriptome profiles in *Asparagus officinalis* and *A. kiusianus* during the early stage of *Phomopsis asparagi* infection. *Sci. Rep.* 7:2608. doi: 10.1038/s41598-017-02566-7

Abdelrahman, M., Hirata, S., Ito, S.-I., Yamauchi, N., and Shigyo, M. (2014). Compartmentation and localization of bioactive metabolites in different organs of *Allium roylei*. *Biosci. Biotechnol. Biochem.* 78, 1112–1122. doi: 10.1080/09168451.2014.915722

Abdelrahman, M., Jogaiah, S., Burritt, D. J., and Tran, L.-P. (2018). Legume genetic resources and transcriptome dynamics under abiotic stress conditions. *Plant Cell Environ.* doi: 10.1111/pce.13123 [Epub ahead of print].

Abdelrahman, M., Sawada, Y., Nakabayashi, R., Sato, S., Hirakawa, H., El-Sayed, M., et al. (2015). Integrating transcriptome and target metabolome variability in doubled haploids of *Allium cepa* for abiotic stress protection. *Mol. Breed.* 35:195. doi: 10.1007/s11032-015-0378-2

Castro-Guerrero, N. A., Isidra-Arellano, M. C., Mendoza-Cozatl, D. G., and Valdés-López, O. (2016). Common bean: a legume model on the rise for unraveling responses and adaptations to iron, zinc, and phosphate deficiencies. *Front. Plant Sci.* 7:600. doi: 10.3389/fpls.2016.00600

Chen, X., Liu, Z., Shi, G., Bai, Q., Guo, C., and Xiao, K. (2017). MIR167a transcriptionally regulates *ARF6* and *ARF8* and mediates drastically plant Pi-starvation response via modulation of various biological processes. *Plant Cell Tissue Org. Cult.* 133, 177–191. doi: 10.1007/s11240-017-1371-8

Chen, Z. H., Nimmo, G. A., Jenkins, G., and Nimmo, H. G. (2007). BHLH32 modulates several biochemical and morphological processes that respond to Pi starvation in *Arabidopsis*. *Biochem. J.* 405, 191–198. doi: 10.1042/BJ20070102

Chiou, T.-J., and Lin, S.-I. (2011). Signaling network in sensing phosphate availability in plants. *Annu. Rev. Plant Biol.* 62, 185–206. doi: 10.1146/annurev-arplant-042110-103849

Considine, M. J., Siddique, K. H. M., and Foyer, C. H. (2017). Nature's pulse power: legumes, food security and climate change. *J. Exp. Bot.* 68, 1815–1818. doi: 10.1093/jxb/erx099

Franco-Zorrilla, J. M., Valli, A., Todesco, M., Mateos, I., Puga, M. I., Rubio-Samoza, I., et al. (2007). Target mimicry provides a new mechanism for regulation of microRNA activity. *Nat. Genet.* 39, 1033–1037. doi: 10.1038/ng2079

Guo, Y., Yang, X., Schöb, C., Jiang, Y., and Tang, Z. (2016). Legume shrubs are more nitrogen-homeostatic than non-legume shrubs. *Front. Plant Sci.* 8:1662. doi: 10.3389/fpls.2017.01662

Hernández, G., Ramírez, M., Valdés-López, O., Tesfaye, M., Graham, M. A., Czechowski, T., et al. (2007). Phosphorus stress in common bean: root transcript and metabolic responses. *Plant Physiol.* 144, 752–767. doi: 10.1104/pp.107.096958

Hernández, G., Valdés-López, O., Ramírez, M., Goffard, N., Weiller, G., Aparicio-Fabre, R., et al. (2009). Global changes in the transcript and metabolic profiles during symbiotic nitrogen fixation in phosphorus-stressed common bean plants. *Plant Physiol.* 151, 1221–1238. doi: 10.1104/pp.109.143842

Herrera-Estrella, L., and López-Arredondo, D. L. (2016). Phosphorus: the underrated element for feeding the world. *Trends Plant Sci.* 21, 461–463. doi: 10.1016/j.tplants.2016.04.010

Hirai, M. Y., Yano, M., Goodenowe, D. B., Kanaya, S., Kimura, T., Awazuhara, M., et al. (2004). Integration of transcriptomics and metabolomics for understanding of global responses to nutritional stresses in *Arabidopsis thaliana*. *Proc. Natl. Acad. Sci. U.S.A.* 1010, 10205–10210. doi: 10.1073/pnas.0403218101

Jain, A., Nagarajan, V. K., and Raghothama, K. G. (2012). Transcriptional regulation of phosphate acquisition by higher plants. *Cell. Mol. Life Sci.* 69, 3207–3224. doi: 10.1007/s00018-012-1090-6

Jin, J., Zhang, H., Zhang, J., Liu, P., Chen, X., Li, Z., et al. (2017). Integrated transcriptomics and metabolomics analysis to characterize cold stress responses in *Nicotiana tabacum*. *BMC Genomics* 18:496. doi: 10.1186/s12864-017-3871-7

Kleinert, A., Thuynsma, R., Magadlela, A., Benedito, V. A., and Valentine, A. J. (2017). "Metabolism and transport of carbon in legume nodules under phosphorus deficiency," in *Legume Nitrogen Fixation in Soils with Low Phosphorus Availability*, eds S. Sulieman and L. P. Tran (Cham: Springer International Publishing), 77–95.

Last, R. L., Jones, A. D., and Shachar-Hill, Y. (2007). Innovations: towards the plant metabolome and beyond. *Nat. Rev. Mol. Cell Biol.* 8, 167–174. doi: 10.1038/nrm2098

Lazali, M., Blavet, D., Pernot, C., Desclaux, D., and Drevon, J. J. (2017). Efficiency of phosphorus use for dinitrogen fixation varies between common bean genotypes under phosphorus limitation. *Agron. J.* 109, 283–290. doi: 10.2134/agronj2016.01.0034

Liese, R., Schulze, J., and Cabeza, R. A. (2017). Nitrate application or P deficiency induce a decline in *Medicago truncatula* N2-fixation by similar changes in the nodule transcriptome. *Sci. Rep.* 7:46264. doi: 10.1038/srep46264

Magadlela, A., Vardien, W., Kleinert, A., Dreyer, L. L., and Valentine, A. J. (2015). The role of phosphorus deficiency in nodule microbial composition, and carbon and nitrogen nutrition of a native legume tree in the Cape fynbos ecosystem. *Aust. J. Bot.* 63, 379–386. doi: 10.1071/BT14216

Miao, Z., Xu, W., Li, D., Hu, X., Liu, J., Zhang, R., et al. (2015). De novo transcriptome analysis of *Medicago falcata* reveals novel insights about the mechanisms underlying abiotic stress responsive pathway. *BMC Genomics* 16:818. doi: 10.1186/s12864-015-2019-x

Nasr Esfahani, M., Inoue, K., Chu, H. D., Nguyen, K. H., Ha, C. V., Watanabe, Y., et al. (2017). Comparative transcriptome analysis of nodules of two *Mesorhizobium*-chickpea associations with differential symbiotic efficiency under phosphate deficiency. *Plant J.* 95, 911–926. doi: 10.1111/tpj.13616

Nasr Esfahani, M., Kusano, M., Nguyen, K. H., Watanabe, Y., Ha, C. V., Saito, K., et al. (2016). Adaptation of the symbiotic *Mesorhizobium*–chickpea relationship to phosphate deficiency relies on reprogramming of whole-plant metabolism. *Proc. Natl. Acad. Sci. U.S.A.* 113, E4610–E4619. doi: 10.1073/pnas.1609440113

O'Rourke, J. A., Yang, S. S., Miller, S. S., Bucciarelli, B., Liu, J., Rydeen, A., et al. (2013). An RNA-Seq transcriptome analysis of orthophosphate-deficient white lupin reveals novel insights into phosphorus acclimation in plants. *Plant Physiol.* 161, 705–724. doi: 10.1104/pp.112.209254

Rubio, V., Linhares, F., Solano, R., Martín, A. C., Iglesias, J., Leyva, A., et al. (2001). A conserved MYB transcription factor involved in phosphate starvation signaling both in vascular plant and unicellular algae. *Genes Dev.* 15, 2122–2133. doi: 10.1101/gad.204401

Saito, K. (2013). Phytochemical genomics — a new trend. *Curr. Opin. Plant Biol.* 16, 373–380. doi: 10.1016/j.pbi.2013.04.001

Secco, D., Wang, C., Arpat, B. A., Wang, Z., Poirier, Y., Tyerman, S. D., et al. (2012). The emerging importance of the SPX domain-containing proteins in phosphate homeostasis. *New Phytol.* 193, 842–851. doi: 10.1111/j.1469-8137.2011.04002.x

Sulieman, S., and Tran, L. P. (2015). Phosphorus homeostasis in legume nodules as an adaptive strategy to phosphorus deficiency. *Plant Sci.* 239, 36–43. doi: 10.1016/j.plantsci.2015.06.018

Tawaraya, K., Horie, R., Saito, S., Wagatsuma, T., Saito, K., and Oikawa, A. (2014). Metabolite profiling of root exudates of common bean under phosphorus deficiency. *Metabolites* 4, 599–611. doi: 10.3390/metabo4030599

Thuynsma, R., Valentine, A., and Kleinert, A. (2014). Phosphorus deficiency affects the allocation of below-ground resources to combined cluster roots and nodules in *Lupinus albus*. *J. Plant Physiol.* 171, 285–291. doi: 10.1016/j.jplph.2013.09.001

Uhde-Stone, C. (2017). "White lupin: a model system for understanding plant adaptation to low phosphorus availability," in *Legume Nitrogen Fixation in Soils with Low Phosphorus Availability*, eds S. Sulieman and L. P. Tran (Cham: Springer International Publishing), 77–95.

Valdés-López, O., and Hernández, G. (2008). Transcriptional regulation and signaling in phosphorus starvation: what about legumes? *J. Integr. Plant Biol.* 50, 1213–1222. doi: 10.1111/j.1744-7909.2008.00758.x

Valentine, A. J., Benedito, V. A., and Kang, Y. (2010). "Legume nitrogen fixation and soil abiotic stress: from physiology to genomics and beyond," in *Nitrogen Metabolism in Plants in the Post-Genomic Era: Annual Plant Reviews*, Vol. 42, eds C. H. Foyer and H. Zhang (Oxford: Wiley-Blackwell).

Valliyodan, B., Ye, H., Song, L., Murphy, M., Shannon, J. G., and Nguyen, H. T. (2017). Genetic diversity and genomic strategies for improving drought and waterlogging tolerance in soybeans. *J. Exp. Bot.* 68, 1835–1849. doi: 10.1093/jxb/erw433

Vance, C. P., Uhde-Stone, C., and Allan, D. L. (2003). Phosphorus acquisition and use: critical adaptations by plants for securing a nonrenewable resource. *New Phytol.* 157, 423–447. doi: 10.1046/j.1469-8137.2003.00695.x

Wang, C., Huang, W., Ying, Y., Li, S., Secco, D., Tyerman, S., et al. (2012). Functional characterization of the rice SPX–MFS family reveals a key role of OsSPX–MFS1 in controlling phosphate homeostasis in leaves. *New Phytol.* 196, 139–148. doi: 10.1111/j.1469-8137.2012.04227.x

Zhang, D., Song, H., Cheng, H., Hao, D., Wang, H., Kan, G., et al. (2014). The acid phosphatase-encoding gene *GmACP1* contributes to soybean tolerance to low-phosphorus stress. *PLoS Genet.* 10:e1004061. doi: 10.1371/journal.pgen.1004061

Zhang, H., Chu, S., and Zhang, D. (2017). Transcriptome dataset of soybean (*Glycine max*) grown under phosphorus-deficient and -sufficient conditions. *Data* 2:17. doi: 10.3390/data2020017

Zhang, N., Venkateshwaran, M., Boersma, M., Harms, A., Howes-Podoll, M., den Os, D., et al. (2012). Metabolomic profiling reveals suppression of oxylipin biosynthesis during the early stages of legume–rhizobia symbiosis. *FEBS Lett.* 586, 3150–3158. doi: 10.1016/j.febslet.2012.06.046

Zhou, J., Jiao, F. C., Wu, Z. C., Li, Y. Y., Wang, X. M., He, X. H., et al. (2008). *OsPHR2* is involved in phosphorus-starvation signaling and excessive phosphate accumulation in shoot plants. *Plant Physiol.* 146, 1673–1686. doi: 10.1104/pp.107.111443

Conflict of Interest Statement: The authors declare that the research was conducted in the absence of any commercial or financial relationships that could be construed as a potential conflict of interest.

The reviewer AK and handling Editor declared their shared affiliation.

frontiers in Plant Science

ORIGINAL RESEARCH
published: 20 July 2018
doi: 10.3389/fpls.2018.00686

Overexpression of Phosphate Transporter Gene *CmPht1;2* Facilitated Pi Uptake and Alternated the Metabolic Profiles of Chrysanthemum Under Phosphate Deficiency

Chen Liu[1,2], Jiangshuo Su[1,2], Githeng'u K. Stephen[1,2], Haibin Wang[1,2], Aiping Song[1,2], Fadi Chen[1,2], Yiyong Zhu[3], Sumei Chen[1,2] and Jiafu Jiang[1,2]**

[1] College of Horticulture, Nanjing Agricultural University, Nanjing, China, [2] Key Laboratory of Landscape Agriculture, Ministry of Agriculture, Nanjing, China, [3] College of Resources and Environmental Sciences, Nanjing Agricultural University, Nanjing, China

OPEN ACCESS

Edited by:
Vagner A. Benedito, West Virginia University, United States

Reviewed by:
Fangsen Xu, Huazhong Agricultural University, China
Georgios Liakopoulos, Agricultural University of Athens, Greece
Ping Lan, Institute of Soil Science (CAS), China

***Correspondence:**
Sumei Chen
chensm@njau.edu.cn
Jiafu Jiang
jiangjiafu@njau.edu.cn

Specialty section:
This article was submitted to Plant Nutrition, a section of the journal Frontiers in Plant Science

Received: *23 January 2018*
Accepted: *04 May 2018*
Published: *20 July 2018*

Citation:
Liu C, Su J, Stephen GK, Wang H, Song A, Chen F, Zhu Y, Chen S and Jiang J (2018) Overexpression of Phosphate Transporter Gene CmPht1;2 Facilitated Pi Uptake and Alternated the Metabolic Profiles of Chrysanthemum Under Phosphate Deficiency. Front. Plant Sci. 9:686. doi: 10.3389/fpls.2018.00686

Low availability of phosphorus (P) in the soil is the principal limiting factor for the growth of cut chrysanthemum. Plant phosphate transporters (PTs) facilitate acquisition of inorganic phosphate (Pi) and its homeostasis within the plant. In the present study, *CmPht1;2* of the Pht1 family was cloned from chrysanthemum. CmPht1;2 is composed of 12 transmembrane domains and localized to the plasma membrane. Expression of *CmPht1;2* in roots was induced by Pi starvation. Chrysanthemum plants with overexpression of *CmPht1;2* (Oe) showed higher Pi uptake, as compared to the wild type (WT), both under Pi-starvation and Pi-sufficient conditions, and also showed a higher root biomass compared to WT in the Pi-starvation conditions. Seven days after the P-deficiency treatment, 85 distinct analytes were identified in the roots and 27 in the shoots between the Oe1 plant and WT, in which sophorose, sorbitol (sugars), hydroxybutyric acid (organic acids), and ornithine (amino acid) of *CmPht1;2* overexpressing chrysanthemum are specific responses to P-starvation.

Keywords: ***Chrysanthemum morifolium*, *CmPht1;2*, phosphate transporter, phosphorus, metabolome**

INTRODUCTION

As one of the major macronutrients, phosphorus (P) plays an important role in plant biochemical synthesis, energy transport, and signal transduction pathways (Wang et al., 2017). In addition, P is also involved in metabolism and the regulation of enzyme activity (Clarkson and Hanson, 1980). Although large amounts of phosphate-based fertilizer are applied in the agriculture system, most phosphorus in the soil becomes immobilized by precipitation or adsorption by soil minerals (Raghothama, 2000), resulting in a very low concentration of Pi in the soil solution available for plants (Vandamme et al., 2016). In this way, Pi-deficiency often limits plant growth and development (Raghothama and Karthikeyan, 2005).

PHOSPHATE TRANSPORTER1 (Pht1) family is plasma membrane-localized high-affinity Pi transporters and works on the uptake of inorganic phosphate (Pi) (Młodzińska and Zboińska, 2016). Nine Pi transporters in *Arabidopsis thaliana* were identified (Muchhal et al., 1996), and a

number of homologs of PHT1 transporters have been isolated from other species (Rausch and Bucher, 2002). In general, Pht1 members consist of 12 transmembrane (TM) domains with two parallel parts of six hydrophobic TM fragments (Saier, 2000). The functions of some Pht1 members have been identified. For example, Pht1;1 and Pht1;4 contribute to Pi uptake despite of the P status (Shin et al., 2004). Pht1;5 acts on the mobilization of Pi from P source to sink organs (Nagarajan et al., 2011).

Chrysanthemum (*Chrysanthemum morifolium* Ramat.) is one of the most important ornamental species. P deficiency in soil is one of the limitations hampering the growth and ornamental value of cut chrysanthemum to a great extent, such as causing yellow spotted leaves and slow growth rate (Liu et al., 2013). In our previous study, we found a putative high-affinity phosphate transporter CmPT1 in chrysanthemum (Liu et al., 2014). In this study, we further characterized one of the Pht1 members, *CmPht1;2*, from a phosphorus-deficiency-tolerant chrysanthemum cultivar 'Nannongyinshan'. The effects of its overexpression on the improvement of uptake of Pi and root dry weight of chrysanthemum was investigated. Moreover, the untargeted metabolic profiles were mined in *CmPht1;2* overexpressing chrysanthemum, to reveal information about plant biochemical biosynthesis, energy transfer reactions, and signal transduction events (Hernández et al., 2009; Bielecka et al., 2015; Ganie et al., 2015) under P starvation. This study provides the foundations for the improvement of phosphorus use efficiency in chrysanthemum.

MATERIALS AND METHODS

Plant Materials and Growth Conditions

The phosphorus-deficiency-tolerant chrysanthemum cultivar 'Nannongyinshan' (Liu et al., 2014) was obtained from the Chrysanthemum Germplasm Resource Preserving Centre, Nanjing Agricultural University, China. The cuttings were rooted in aerated water without any nutrition in a greenhouse for 2 weeks. Then, they were transferred to a hydroponic solution consisting of a diluted (1:4) and (1:2) Hoagland's solution for 3 days each (Bentonjones, 1982). Plants were maintained in the hydroponic solution with HP (300 μM, Pi) for 1 week, after which they were transferred to a hydroponic solution supplemented with either HP or –P (0 μM, Pi) for phosphate starvation treatment. The nutrient solution was renewed every 3 days. For *CmPht1;2* transcription profiles' analysis, leaf, stem, and root tissues were harvested 7 days after the phosphate treatment, snap-frozen in liquid nitrogen, and kept at −80°C. Experiments included three replicates. Each replicate contained nine seedlings.

Isolation and Sequence Analysis of *CmPht1;2*

The total RNA from the above sampled roots was extracted using Trizol reagent (Life Technologies) according to the manufacturer's instructions. To amplify a full-length sequence of *CmPht1;2*, PCR primers (Full-F/R; **Supplementary Table S1**) were designed according to the transcriptome of *Chrysanthemum nankingense* (Ren et al., 2014). The full-length *CmPht1;2* cDNA sequence was transcribed using *Pfu* DNA polymerase (TaKaRa Ex Taq®). The open reading frame (ORF) of *CmPht1;2* was identified using the sequence analysis program (BioXM2.6). Sequences of multiple peptides were aligned using the DNAMAN software version 6, and phylogenetic analyses were performed using the MEGA v5.0 software.

CmPht1;2 Expression Patterns

The total RNA was isolated from the above sampled root, stem, and leaf tissues of plants grown under the HP (300 μM, Pi) or –P (0 μM, Pi) treatments for 7 days by Trizol; 500 ng·μL^{-1} RNA was used for cDNA synthesis. For quantification of *CmPht1;2*, real-time quantitative PCR (qPCR) assays were performed using the SYBR Green master mix (SYBR Premix Ex Taq^{TM} II, TaKaRa Bio) and the primer pair q*GSP*-F/-R (**Supplementary Table S1**) (Gao J. et al., 2016). The reference gene, *CmEF1α*, was amplified using the primers *EF1A*-F/-R (sequences given in **Supplementary Table S1**). Relative transcription levels were calculated by the $2^{-\Delta\Delta C_t}$ method (Kenneth and Livak, 2001).

Construction of a GFP Fusion Vector and Intracellular Localization Analysis

The plasmid pENTR^{TM}1A-*CmPht1;2* was confirmed by restriction enzyme *Dra* I and *Not* I digestion and DNA sequencing. pENTR^{TM}1A-*CmPht1;2* was used to construct a C-terminus green fluorescent protein (GFP) fusion vector pMDC43-*CmPht1;2* by the LR reaction (as described in Gateway® Technology with Clonase® II). Plasmid DNA was bombarded into onion (*Allium cepa*) epidermal cells using a gene gun (PDS-1000; Bio-Rad, Hercules, CA, United States). The epidermal cells were incubated on Murashige and Skoog (MS) solid media plates in the dark for 16–20 h. The expression of GFP was monitored by confocal laser scanning microscopy at 488 nm (Zeiss, Germany) (Wan et al., 2008).

Regeneration of *CmPht1;2* Overexpressing Chrysanthemum

To further analyze the function of *CmPht1;2*, the pMDC43-*CmPht1;2* vector was transformed into leaf disks of the phosphate deficiency sensitive cultivar 'Jinba' (Liu et al., 2014) via *Agrobacterium tumefaciens*-mediated transformation, using strain EHA105 (Höfgen and Willmitzer, 1988) as previously described (Li et al., 2017). The hygromycin (Hyg)-resistant plants were verified by the PCR analysis using the vector primer *Hyg*-F/-R (sequences given in **Supplementary Table S1**), and the overexpression of *CmPht1;2* was validated by qRT-PCR using primer pairs of *qGSP*-F/-R (sequences given in **Supplementary Table S1**).

Phosphorus Uptake Assay of *CmPht1;2* Overexpressing Chrysanthemum

For phosphorus uptake velocity assay (^{32}P uptake assay), transgenic lines and non-transformed WT plants were cultured at HP (300 μM Pi) conditions for 1 week, followed by a 7-day hydroponic culture in HP (300 μM Pi) and LP (15 μM Pi)

solutions, respectively. Subsequently, plants were incubated in 100 mL hydroponic culture with HP (300 μM Pi) containing 1.2 μCi or LP (15 μM Pi) containing 0.06 μCi of $H_3{}^{32}PO_4$ for 3 and 6 h. Then, whole seedlings were rinsed thoroughly in sterile ddH_2O, dried at 80°C, and fine grounded. A scintillation solution was then added to the ground samples. The radioactivity of the mixture was detected with a Beckman LS6500 scintillation counter.

Transgenic lines and non-transformed wild-type (WT) plants were cultured at HP conditions for 1 week, followed by hydroponic culture in either P-sufficient (300 μM Pi; HP) or P-deficiency (15 μM Pi; LP) conditions for 7 days. The roots and shoots were harvested for the total phosphorus or inorganic phosphate concentration assay. The total plant phosphorus concentration was measured by a proton spectrometer from a ∼0.1 g dry sample as previously described (Chen et al., 2010). The inorganic phosphate concentration was calculated (Zhou et al., 2008). Experiments included three replicates, and each replicate contained three seedlings.

Morphological Characteristics of the *CmPht1;2* Overexpressing Chrysanthemum

Seedlings were subjected to HP or LP treatment as mentioned above. After 1-week HP or LP treatment, the root length and plant height of the seedlings were measured. The biomasses of roots and shoots were determined by dry weight. The root architecture was measured using a root scanner (Epson Color Image Scanner LA1600+). The experiments included three replicates, and each replicate included three seedlings.

Metabolomics Sample Preparation

CmPht1;2-overexpressing plants from the Oe1 line and WT plants were grown in a hydroponic solution under HP conditions for 1 week and then transferred to P-starvation (15 μM Pi; LP) medium for 7 days. The roots and leaves were harvested at 0, 2, and 7 days after the P-deficiency treatment. Six plants were included for each time point.

A root or shoot sample of 60 mg (dry weight) was transferred to 360 μL cold methanol, which was ground and ultrasonicated at the ambient temperature for 30 min immediately; 200 μL of chloroform was added, samples were vortexed, followed by adding 400 μL ddH_2O, and subsequently centrifuged at 12,000 rpm for 10 min at 4°C. The mean value of all samples were pooled to act as a quality control (QC). An aliquot of the 500 μL supernatant was taken as previously described (Peng et al., 2015) and incubated at 37°C for 90 min.

The analysis of metabolites was performed on an Agilent 7890B gas chromatography system coupled to an Agilent 5977A MSD system (Agilent Technologies Inc., Santa Clara, CA, United States). Derivatives were separated as described previously (Zhou et al., 2012). Helium (>99.999%) was used as the carrier gas at a constant flow rate of 1 mL/min. The injector temperature was maintained at 260°C. The injection volume was 1 μL by splitmode with a split ratio of 4:1. The initial oven temperature was 60°C, ramped to 125, 210, 270, and 305°C, and finally held at 305°C. The temperatures of the MS quadrupole and the ion source (electron impact) were set to 150 and 230°C, respectively. The mass data were obtained from a full-scan mode (m/z 50–500).

Data Preprocessing and Statistical Analysis of GC-MS

The differential metabolites were identified by the statistically significant threshold of variable influence on projection (VIP) values (VIP > 1, $P < 0.05$). OPLS-DA (orthogonal partial least-squares-discriminant analysis) was performed to visualize the metabolic difference of roots/shoots among the Oe plants and WT plants in response to LP stress after mean centering and unit variance scaling. Those differential metabolites between transgene lines and WT plants in response to LP were identified with a threshold (upregulate, FC > 1.2, and downregulate, FC < 0.8) as described previously (Lan et al., 2011). The relevant metabolic pathways were identified from the database of KEGG, and the significant changes were based on $P < 0.01$.

Statistical Analysis

All the significance discriminate analyses were carried out using the SPSS software (IBM SPSS Statistics Version 20), and the phenotypes of the Oe lines and WT were analyzed using Student's *t*-test at 5% level of probability. The figures were spliced using Photoshop software.

RESULTS

Cloning and Sequence Analysis of *CmPht1;2*

The full length of *CmPht1;2* was a 2,105 bp sequence, containing a 1,605 bp ORF which encodes a 534 amino acid polypeptide (**Figure 1A**). The calculated molecular mass and pI of the CmPht1;2 protein were 58.41 kDa and 8.12, respectively. The peptide was predicted to have 12 transmembrane domains (TMs), including a hydrophilic loop in the middle of the domains and a Pht1 signature sequence GGDYPLSATIxSE between TM4 and TM5 (**Figure 1A**). The identity level of the CmPht1;2 amino acid sequence with Pi transporters from other plant species ranged from 68.0% (*Hordeum vulgare* HvPT1, AAO32938) to 79.2% (*Lycopersicon esculentum* LePT1, AF022874). The sequence identity between chrysanthemum gene CmPht1;2 and CmPT1 (AGK29560) (Liu et al., 2014) is 90.8% (**Figure 1B**).

CmPht1;2 Transcription Induced by Pi-Deficient Conditions

CmPht1;2 transcriptions were present in roots, stems, and leaves, and were highest in the stem under Pi-sufficient (300 μM Pi; HP) conditions. However, it was strongly induced (5.3 times) in Pi-deficient (0 μM Pi; -P) conditions in the roots, while the induced expression was not obvious in the stems and leaves of chrysanthemum exposed to -P conditions (**Figure 2**).

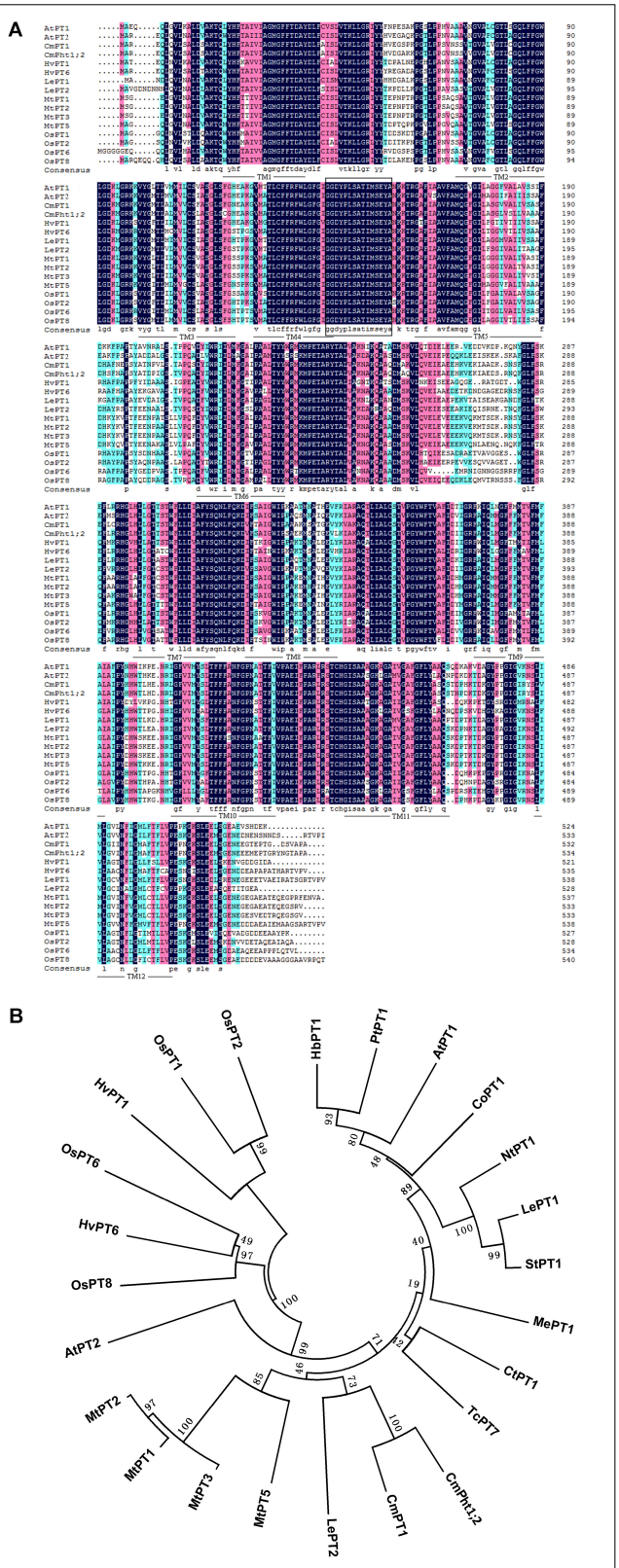

FIGURE 1 | Alignment and phylogenetic relationships of the peptide sequences of high-affinity Pi transporters. **(A)** Alignment of amino acid

(Continued)

FIGURE 1 | Continued

sequences of PT1 members. Identical peptides are highlighted in black and conserved substitutions in pink. Putative CmPht1;2 transmembrane domains are underlined. The Pht1 signature sequence is boxed. **(B)** Phylogenetic relationships of the peptide sequences of PT1s. AtPT1 (AED94948) and AtPT2 (AAC79607) from *Arabidopsis thaliana*; HvPT1 (AAO32938) and HvPT6 (AAN37901) from *Hordeum vulgare*; MtPT1 (AAB81346), MtPT2 (AAB81347), MtPT3(ABM69110), and MtPT5 (ABM69111) from *Medicago truncatula*; LePT1 (AAB82146) and LePT2 (AAB82147) from *Lycopersicon esculentum*; OsPT1 (Q8H6H4), OsPT2 (Q8GSD9), OsPT6 (Q8H6H0), and OsPT8 (Q8H6G8) from *Oryza sativa*; CtPT1 (AFY06657) from *Citrus trifoliata*; TcPT1 (EOY06027) from *Theobroma cacao*; CoPT1 (AFU07481) from *Camellia oleifera*; NtPT1 (AAF74025) from *Nicotiana tabacum*; StPT1 (AAD38859) from *Solanum tuberosum*; MePT1 (ADA83723) from *Manihot esculenta*; HbPT1 (ADL27918) from *Hevea brasiliensis*; PtPT1 (XP_002306844) from *Populus trichocarpa*; and CmPT1 (AGK29560) from *Chrysanthemum morifolium*.

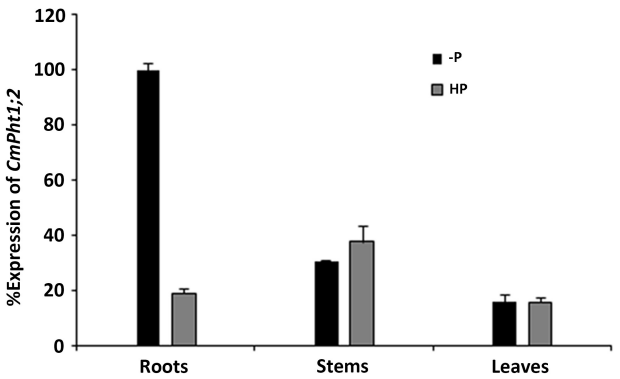

FIGURE 2 | Relative transcript abundance in the roots, stems, and leaves under HP (300 μM Pi) and -P (0 μM Pi).

Plasma Membrane Localization of CmPht1;2

To investigate the intracellular localization of the CmPht1;2 transporter, we analyzed a GFP-CmPht1;2 construct driven by the 35S promoter of the cauliflower mosaicvirus in onion epidermal cells. The GFP signals presented throughout the analyzed cells, including the nucleus, cytoplasm, and plasma membrane of the onion epidermal cell transformed with the pMDC43:35S-GFP empty vector (as control). The fluorescence signal was mainly observed on the plasma membrane of onion epidermal cells transformed with 35S:GFP-CmPht1;2, and this observation was confirmed by observing plasmolyzed cells (**Figure 3**).

Overexpression of *CmPht1;2* in Chrysanthemum Facilitated P Uptake

A genetic transformation system for 'Nannongyinshan' is not available. Therefore, to identify the function of *CmPht1;2*, *CmPht1;2* was introduced into the low Pi (15 μM Pi; LP) sensitive cultivar 'Jinba' by agrobacterium-mediated leaf disk transformation. Five putative transgenic plants were identified by the PCR analysis using *Hyg* primers (**Figure 4A** and **Supplementary Figure S1**). Five overexpression lines were

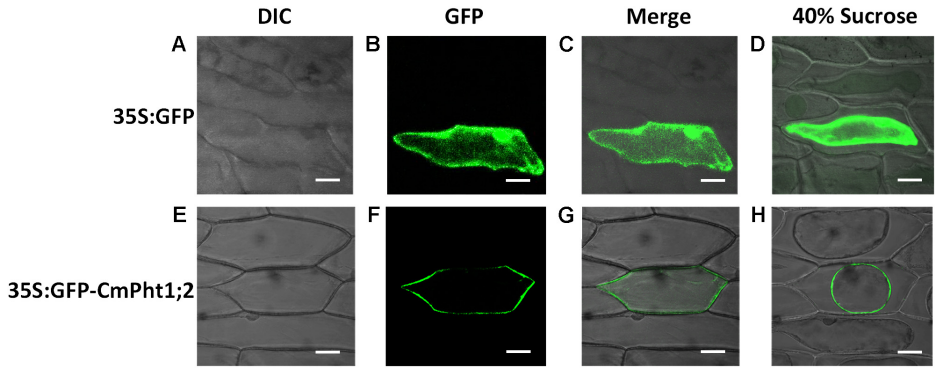

FIGURE 3 | Subcellular localization analysis of CmPht1;2. **(A–D)** Onion epidermal cells transformed with 35S:GFP. **(E–H)** Onion epidermal cells transformed with 35S:GFP-CmPht1;2. **(A,E)** Bright field microscopy images to display morphology. **(B,F)** Dark field images for detection of GFP fluorescence. **(C,G)** Superimposed light and dark field images. **(D,H)** Plasmolyzed onion epidermal cells. Bar: 50 μm.

validated by qRT-PCR, of which Oe1 and Oe2 lines displayed the highest *CmPht1;2* abundance (3.96- and 2.74-folds compared to that of WT), and were thus selected for further study (**Figure 4B**).

The Oe lines and WT plants were subjected to either HP or LP solutions for the functional analysis of *CmPht1;2*. Compared with WT plants, the Pi uptake of the overexpressing lines increased significantly under both HP and LP status (**Figure 5**).

Under HP status, the total P content in the roots of Oe1 and Oe2 plants increased by 64.7 and 73.7%, respectively, compared with WT plants, while no obvious difference in P concentrations of the shoots between Oe lines and WT plants was observed (**Figure 6A**). Under LP conditions, the total P concentrations in Oe lines were improved by 11.1 and 49.4%, respectively, in the roots compared with the WT plants, but the concentration of P in the shoots of Oe lines was comparable to that observed in the WT (**Figure 6B**). Inorganic phosphorus concentration in the roots of Oe1 and Oe2 increased by 40.0 and 27.0%, respectively, while those in the shoots had no obvious difference compared with the WT plants under HP conditions (**Figure 6C**). Under LP conditions, inorganic phosphorus concentrations in the roots of Oe1 and Oe2 plants were improved by 68.5 and 87.5%, respectively, and in the shoots, they increased by 133.8 and 45.4% compared with WT (**Figure 6D**).

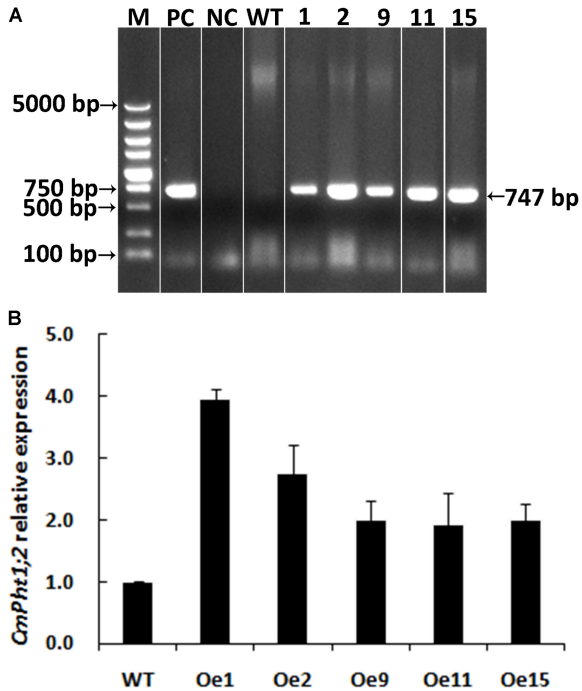

FIGURE 4 | Validation of transgenic plants. **(A)** PCR analysis of genomic DNA extracted from hygromycin-resistant regenerants. **(B)** Relative *CmPht1;2* transcript abundance in wild-type (WT) and transgenic plants. The figure was spliced and grouped using Photoshop software.

Overexpression of *CmPht1;2* Increased Shoot Height, Root Length, Root Biomass, and Number of Root Tips and Forks of Chrysanthemum

Under HP conditions, no significant differences in plant height, root length, and biomass of roots and shoots were observed between Oe lines and WT (**Figure 7**). In contrast, under LP conditions, the root length of Oe1 and Oe2 lines increased by 39.6 and 43.0%, respectively, and the plant height was enhanced by 42.7 and 38.8%, respectively (**Figures 7C,D**). The dry biomasses of roots of Oe1 and Oe2 were 4.27 and 4.45 times more than that of WT plants, and the biomasses of shoots were 1.15- and 1.26-folds more than that of WT under LP stress (**Figures 7E,F**). The root scanner analysis showed that root morphogenesis was similar in Oe lines and WT lines under HP conditions (**Figure 8**), except that the numbers of root tips slightly decreased by 29.3 and 36.7% in Oe1 and Oe2, respectively (**Figure 8G**). In contrast, under the LP conditions, the total lengths of roots of Oe1 and Oe2 increased by 37.2 and 41.1%, respectively, in comparison to WT (**Figure 8A**). Similarly, the projected area (ProjArea) of the two transgenic plants was increased by 50.7 and 24.5%, respectively, compared to WT (**Figure 8B**); the surface area (SurfArea) by 29.3 and

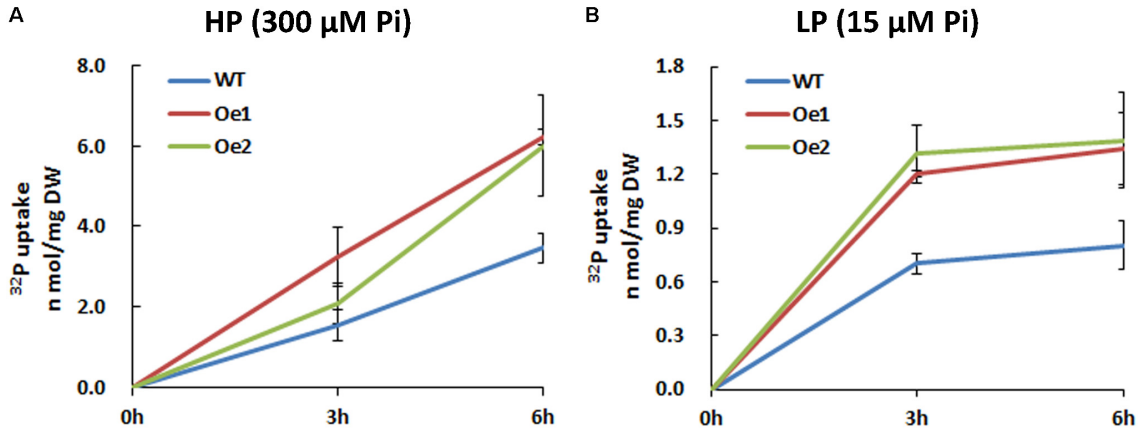

FIGURE 5 | ^{32}Pi uptake velocity in *CmPht1;2*-overexpressing lines. Pi uptake activity of WT and transgenic plants (Oe1 and Oe2) under HP (300 μM Pi) **(A)** and LP (15 μM Pi) **(B)** conditions. Error bars represent SD (n = 3). Three plants per line were included.

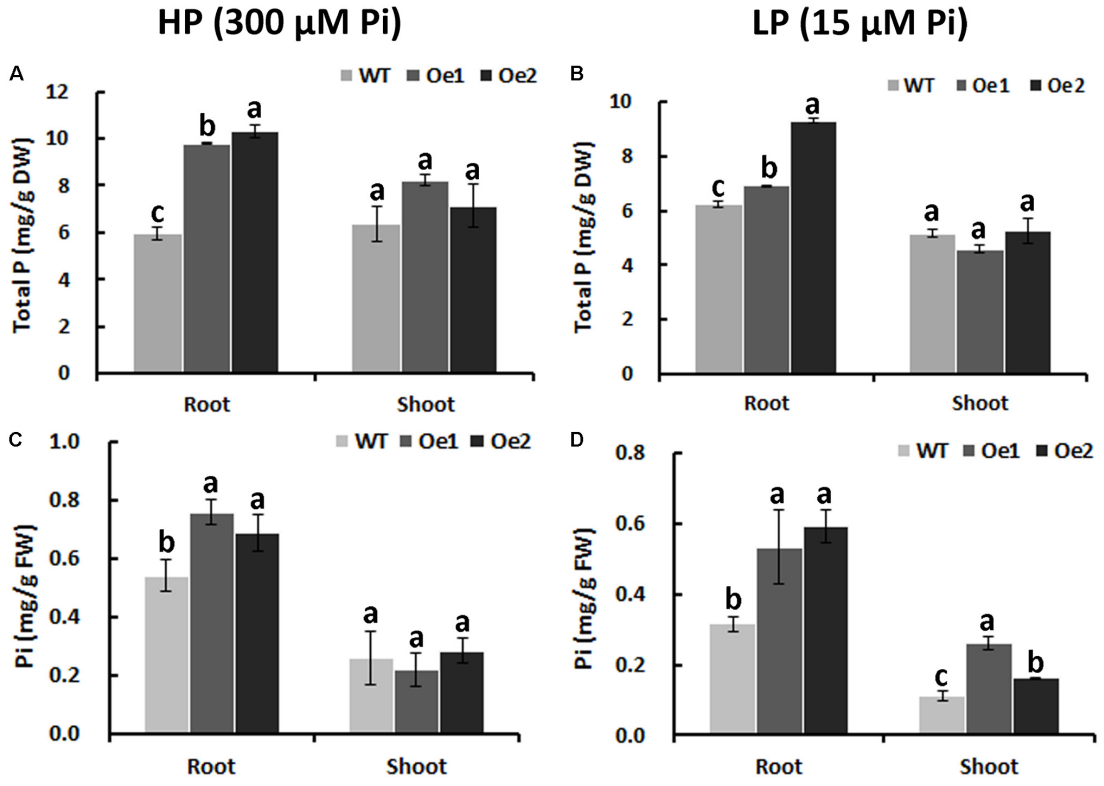

FIGURE 6 | Pi uptake in *CmPht1;2*-overexpressing lines. Total P contents in roots and shoots were measured in WT and transgenic plants (Oe1 and Oe2) under HP (300 μM Pi) **(A)** or LP (15 μM Pi) **(B)**. Error bars represent SD (n = 3). DW, dry weight. Pi contents in roots and shoots under HP (300 μM Pi) **(C)** or LP (15 μM Pi) **(D)**, respectively. Error bars represent SD (n = 3). FW, fresh weight. Three plants per line were included.

16.8% (**Figure 8C**), the length per volume (LenPerVol) by 37.2 and 60.0% (**Figure 8E**), the root volume by 100.3 and 37.0% (**Figure 8F**), the number of root tips by 69.6 and 55.8% (**Figure 8G**), and the number of root forks by 66.6 and 53.9% (**Figure 8H**). Instead, the average projected area (AvgDiam) and branch roots (Crossings) showed no obvious difference between Oe lines and WT (**Figures 8D,I**).

Differential Metabolites and Metabolic Pathways in *CmPht1;2* Overexpressing Plants in Response to Pi Deficiency

Non-targeted metabolite profiles were investigated in the roots and shoots of *CmPht1;2* overexpressing plants (Oe1 which have representative phenotypes) and WT subjected to LP treatment for

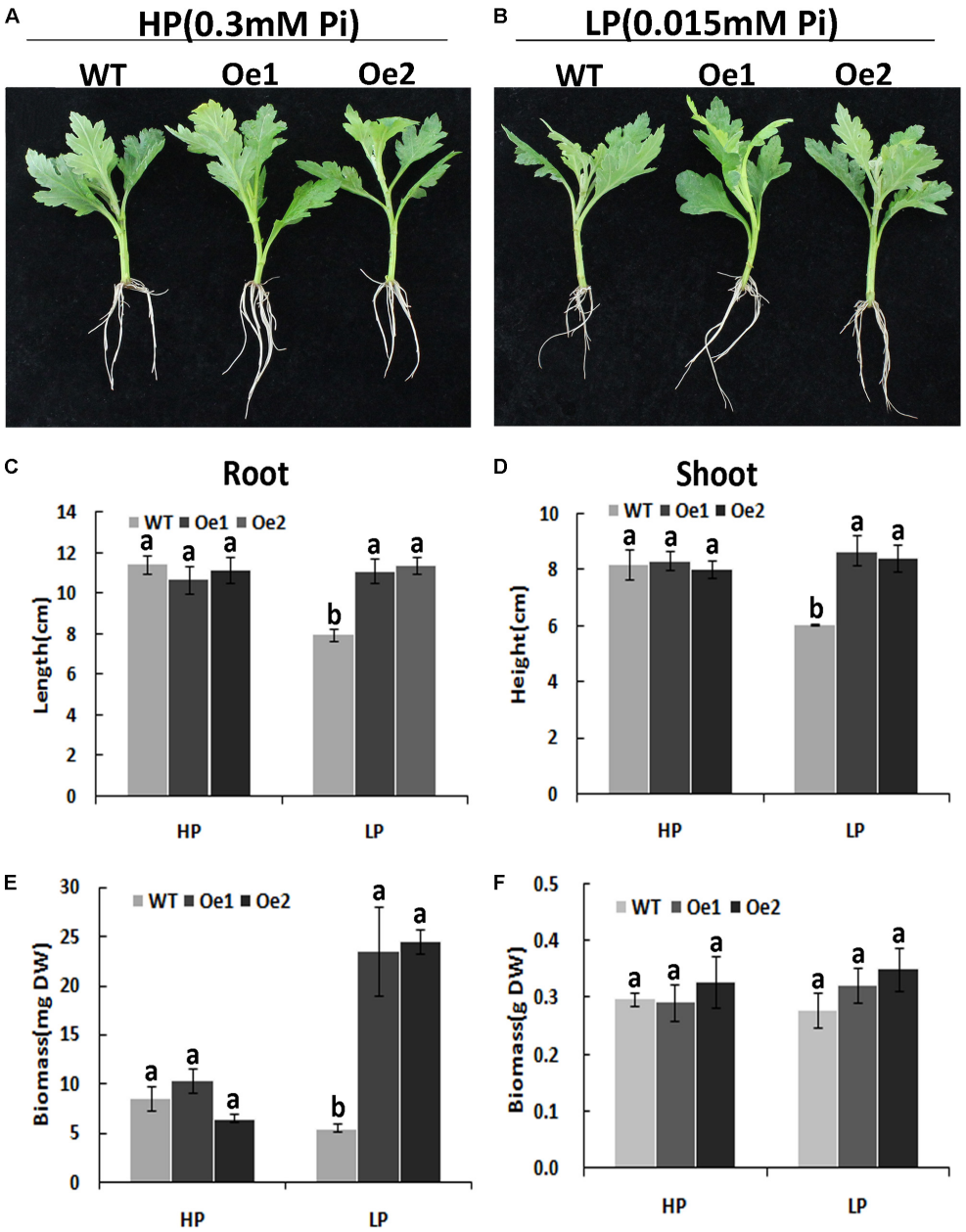

FIGURE 7 | Growth performance of the WT and *CmPht1;2*-Oe lines at different Pi levels in a hydroponics experiment. Growth performance of WT and *CmPht1;2*-overexpressing plants (Oe1 and Oe2) at HP (300 μM Pi) **(A)** and LP (15 μM Pi) **(B)** conditions. Roots **(C)** and shoots **(D)** height of WT and transgenic plants under HP and LP conditions. Biomass measurements of roots **(E)** and shoots **(F)** were obtained from WT and transgenic plants grown in nutrient solution to which 300 μM Pi (HP) or 15 μM Pi (LP) were added. DW, dry weight. Three plants per line were included.

0, 2, and 7 days. The principle component analysis (PCA) showed that the metabolite profiles in the roots and shoots of Oe1 plants differed from WT plants in response to LP stress (**Figure 9**). In the roots, there were 19 different metabolites between Oe1 and WT plants at day 0, 40 different metabolites at day 2, and 85 different metabolites at day 7 under the LP conditions (**Supplementary Table S2**). In the shoots, differential metabolites between Oe1 and WT plants at day 0 were 27, day 2 (43), and day 7 (27) under LP conditions (**Supplementary Table S3**).

There was an increase in amino acids including *N*-methyl-L-glutamic acid and tryptophan, organic acids of lactobionic acid, and dehydroshikimic acid in the roots of Oe1 compared with WT at day 0. Compared with WT, sugars such as galactinol, isopropyl-beta-D-thiogalactopyranoside, and sorbitol were upregulated in the roots of Oe1 plants at day 2 under LP conditions. While at day 7 under LP stress, the main compounds in the roots of the Oe1 plants that increased were the amino acid of *N*-alpha-acetyl-L-ornithine, phenol of 4-vinylphenol dimer, pigment of

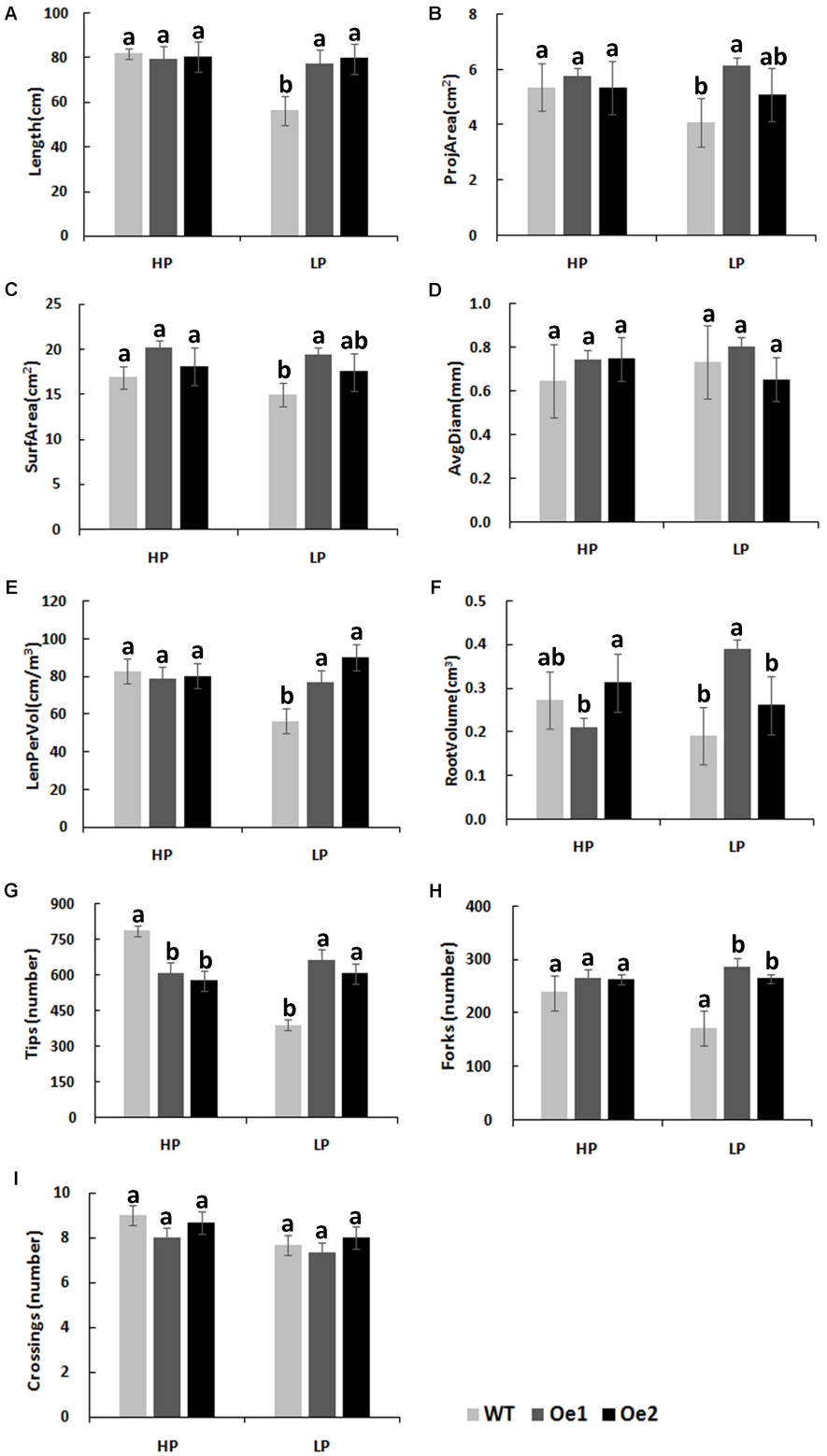

FIGURE 8 | Root architecture of *CmPht1;2* overexpressing plants under HP or LP conditions enhanced. **(A)** Total lengths (Length). **(B)** Projected area (ProjArea). **(C)** Superficial area (SurfArea). **(D)** Average projected area (AvgDiam). **(E)** Length per volume (LenPerVol). **(F)** Root volume. **(G)** Numbers of root tips (Tips). **(H)** Numbers of root forks (Forks). **(I)** The branch roots (Crossings). Error bars represent SD (n = 3). Three plants per line were included.

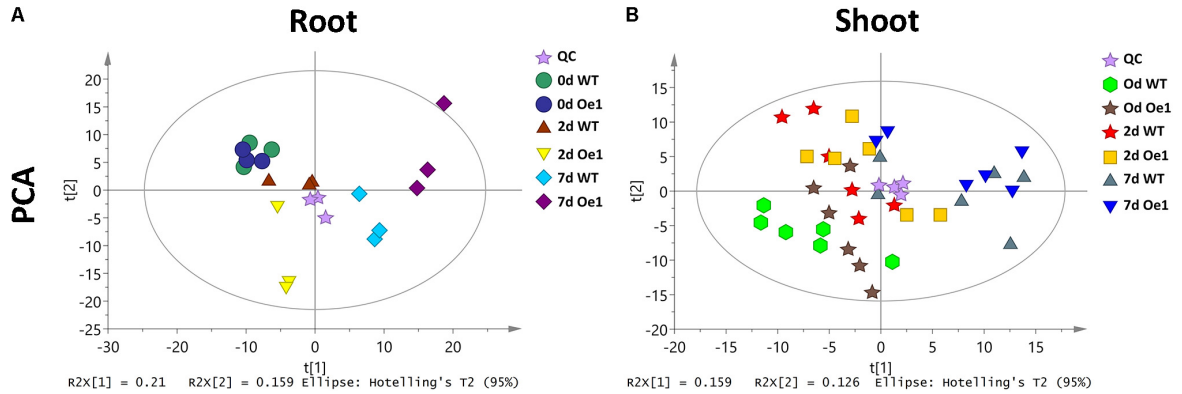

FIGURE 9 | Principle component analysis (PCA) score plot of WT and *CmPht1;2* Oe1 line. PCA score plot of roots **(A)** and shoots **(B)** of WT and *CmPht1;2* Oe1 line under 0, 2, and 7 days Pi stress, respectively.

alizarin, and organic acid of 3-hydroxybutyric acid compared with that of WT, whereas aminooxyacetic acid and *cis*-gondoic acid in the roots of Oe1 plants were less abundant than those in WT plants at day 0; 3-phenyllactic acid, butyraldehyde, cysteinylglycine, and nicotianamine in the roots of Oe1 plants showed a decline compared with those in WT plants at day 2. In addition, galactinol, glucoheptonic acid, nicotianamine, nicotinamide, salicylic acid, and sucrose decreased in the roots of Oe1 plants at 7-day post-treatment compared to the WT plants (**Supplementary Table S2**).

Compounds upregulated in the shoots of Oe1 plants relative to the WT plants included energy metabolites (glucose-6-phosphate and *O*-succinyl homoserine), amino acids (*N*-acetyltryptophan and L-glutamic acid), and organic acids (3-hydroxypropionic acid and 4-acetylbutyric acid) at 0 day, a slight increase in sugars (fructose, sophorose, and tagatose) at 2 days under LP stress, and increases in phenols (4-hydroxy-3-methoxybenzyl alcohol), nucleotide (adenosine), and amino acid (lysine) at 7 days after the LP treatment. However, amino acids (3-hydroxy-L-proline) and organic acids (3-hydroxybutyric acid) showed a decrease in the shoots of Oe1 plants in comparison to WT at 0 day. Most of the nucleotides and their degraded products (5,6-dihydrouracil, cytidine-monophosphate, and flavin adenine), in addition to amino acids (isoleucine) and organic acids (allylmalonic acid), decreased drastically in the shoots of Oe plants in comparison to WT plants following 2-day LP stress. Additionally, sterols (20-α-hydroxycholesterol and 4-cholesten-3-ketone) and organic acids (3-hydroxy-3-methylglutaric acid) also decreased in the 7-day-P-starved shoots of Oe1 plants compared to WT plants (**Supplementary Table S3**).

Significantly changed pathways in the roots of Oe1 plants vs. WT mainly consisted of hormone biosynthesis, sugar metabolism, alkaloid biosynthesis, and especially energy and amino acid metabolism pathways (**Supplementary Tables S4–S10**).

Compared with WT, significantly altered energy metabolism pathways in the roots of Oe1 plants after the LP treatment (especially at day 7) included the citrate cycle (TCA cycle), glyoxylate and dicarboxylate metabolism, carbon fixation in photosynthetic organisms, galactose metabolism, and glycolysis/gluconeogenesis (**Supplementary Table S4**). It is noteworthy that succinate, fumarate, malate, and pyruvate were all downregulated at 7-day LP stress in the Oe1 roots compared with WT (**Figure 10**).

Several amino acids related to metabolic pathways showed a clear change in response to LP treatment in the roots of Oe1 in comparison with WT (**Supplementary Table S4**). For example, tyrosine (a precursor of the tyrosine metabolism pathway) was present in a higher abundance in the roots of Oe1 plants compared to those found in WT at 7 days of LP stress (**Supplementary Table S2**). Other compounds such as fumarate and pyruvate, which act as products of tyrosine, decreased in most metabolic pathways of Oe1 roots compared to WT under LP conditions (**Figure 11**).

DISCUSSION

CmPht1;2 Is an Inducible Pi Transporter Located at the Plasma Membrane

Phosphorus in the plant, an essential nutrient, plays an important role both at the vegetative and reproductive stages (Shi et al., 2014). Various Pi transporters including the Pht1 family are identified to function on the Pi uptake and translocation throughout the plants (Nagarajan et al., 2011). We previously isolated a putative chrysanthemum Pi transporter CmPT1 which mediated Pi uptake in chrysanthemum (Liu et al., 2014). In this study, *CmPht1;2* was found to have the typical structure and signature sequence of Pht1 family members (**Figure 1A**), suggesting that *CmPht1;2* is also a member of the chrysanthemum Pht1 family. In addition, the predicted transmembrane domains based on the amino acid sequence, and localization at the plasma membrane in transfected onion cells, suggested that CmPht1;2 is a transmembrane protein (**Figure 3**), which is in consistent with previous studies that the Pht1 family consisted of a group of Pi transporters located in the plasma membrane (Nussaume et al., 2011). The majority of *Arabidopsis* PHT1 transporters are expressed exclusively in roots, where

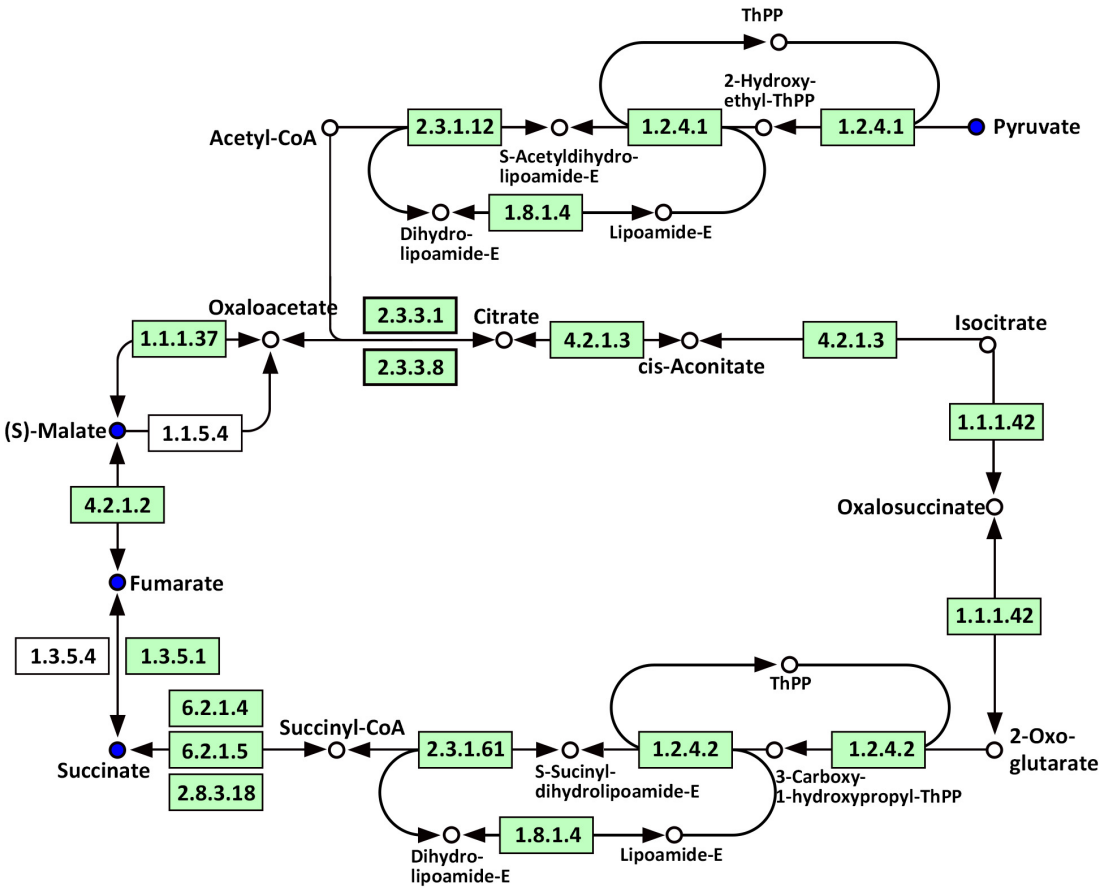

FIGURE 10 | Mapping of the TCA cycle pathways involved in *CmPht1;2* Oe1 in response to LP compared with WT based on KEGG. Blue circles indicate metabolites that were downregulated in *CmPht1;2* Oe1 compared with WT. Boxes indicate the enzymes involved in this pathway.

they are induced by P-starvation (Ai et al., 2009), consistent with their major function of Pi uptake from the rhizosphere (Teng et al., 2017). In the present study, the *CmPht1;2* transcript abundance was strongly induced in the roots under phosphate-deficient conditions (**Figure 2**), suggesting that CmPht1;2 might be associated with Pi uptake under LP stress.

CmPht1;2 *in Planta* Functions in Pi Uptake and Enhances Root Growth

The membrane transporters play key roles in plant nutrient uptake (Saia et al., 2015). In the present study, the Pi uptake rate was improved under both HP and LP conditions (**Figure 5**). In addition, the total content of phosphate in the root of Oe lines was notable higher than WT (**Figure 6**), indicating that CmPht1;2 is essential for Pi acquisition from rhizosphere, which is in line with the observation that double mutants of *pht1;1* and *pht1;4* or single mutant significantly decreased Pi uptake (Misson et al., 2004; Shin et al., 2004). Here, the growth of WT chrysanthemum was arrested under Pi-deficient conditions, similar to previous observations in rice (Jia et al., 2011), whereas the *CmPht1;2* overexpression could alleviate the arrest (**Figure 7**). Similarly, the growth of tobacco cells overexpressing high-affinity phosphate transporter PHT1 was increased under the phosphate-starvation conditions (Mitsukawa et al., 1997). The overexpression of the *CmPht1;2* directly or indirectly caused Pi-dependent root architecture alterations with enhanced root elongation and proliferated lateral root growth and increased root area and root tips under LP condition (**Figure 8**). These changes enabled exploration of soil Pi with an improvement in the absorptive surface area of roots (Nagarajan et al., 2011). It is noteworthy that the parallel increases of PT transcript and protein levels were observed in tomato, indicating the transcriptional and translational regulation of the phosphate transporter genes (Muchhal and Raghothama, 1999). In the present study, the phenotype of Oe1 and Oe2 is partly inconsistent with the transcripts levels of *CmPht1;2*, which might be due to the unknown level of protein expression and the positional effect of integration of *CmPht1;2* into genome or other unknown mechanisms.

Metabolic Profiles Are Altered in *CmPht1;2* Overexpression Line

Metabolomics provides tools to identify metabolic processes and analyze the physiological adaption of plants to different

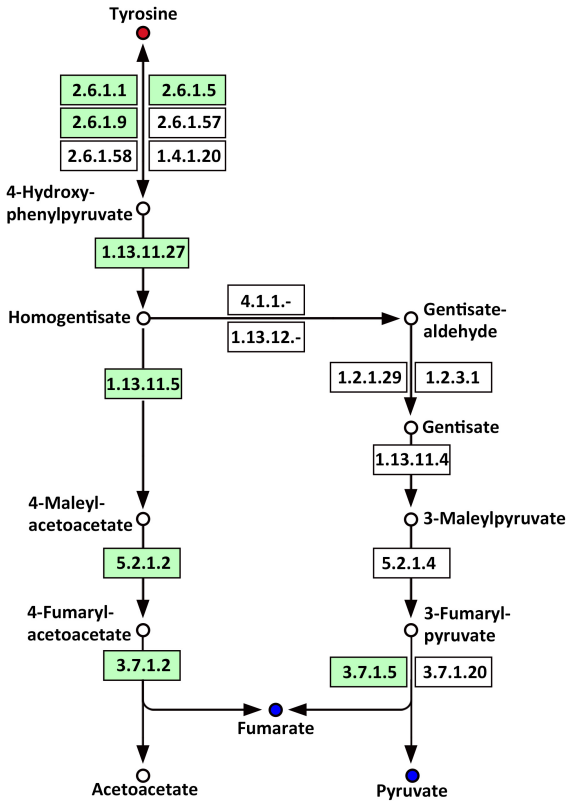

FIGURE 11 | Mapping of the tyrosine metabolism pathways involved in *CmPht1;2* Oe1 response to LP compared with WT based on KEGG. Blue circles indicate metabolites that were downregulated in the *CmPht1;2* Oe1 compared with WT. Red circles indicate metabolites that were upregulated in*CmPht1;2* Oe1 compared with WT. Boxes indicate the enzymes involved in this pathway.

nutrient availabilities (Hirai and Saito, 2004). For example, untargeted metabolomic profiling of plants under sulfate-limited conditions and resupply provided whole metabolome responses to sulfur nutrition in Arabidopsis (Bielecka et al., 2015). In the present study, Oe1 plants showed a number of different metabolites compared with WT plants under LP treatment. The identified differential metabolites were mostly primary metabolites including amino acids, nucleotides, sugar, energy metabolism compounds, and organic acids (**Supplementary Tables S2**, **S3**). These metabolites belong to different pathways, such as energy metabolism and the amino acid metabolism/biosynthesis pathways (**Figures 10**, **11**), indicating that the overexpression of *CmPht1;2* could affect the metabolic adaption of chrysanthemum to LP stress. Notably, a number of changes in the metabolism profiles were quite different from previous descriptions (Hernández et al., 2007; Hernández et al., 2009; Ganie et al., 2015). Where stress-related metabolites such as polyols accumulated in the P-deficient root of common bean (Hernández et al., 2007), glycerolipid metabolism and phenylalanine pathway have been identified in common bean under P stravation (Hernández et al., 2009). A sharp increase in asparagine, serine, and glycine was observed in both shoots and roots of maize under low P conditions (Ganie et al., 2015). To our knowledge, changes in sophorose, sorbitol (sugars), hydroxybutyric acid (organic acids), and ornithine (amino acid) are specific responses of *CmPht1;2* overexpressing chrysanthemum to LP conditions.

Phosphorus is the classical glycolysis-dependent cosubstrate (Plaxton, 2004) under LP conditions; higher availability of phosphorus in Oe1 plants may facilitate glycolysis in roots which is evidenced by the downregulation of disaccharides (sucrose) (**Supplementary Table S2**). Moreover, the upregulation of monosaccharides including galactinol, thiogalactopyranoside, and sorbitol implied that the roots of Oe1 plants might accumulate more carbohydrate for the growth (**Supplementary Table S2**). Sorbitol is a production of photosynthesis and an important translocated form of carbon, and is closely related to the growth and development of plants (Loescher et al., 1982). As a downstream pathway of glycolysis (Fernie et al., 2004), the contents of organic acids such as succinate, fumarate, malate, and pyruvate of the TCA cycle were less abundant in the roots of Oe1 plants than WT (**Figure 10**). These decreased organic acids in Oe1 plants under LP conditions could be the result of an enhanced secretion of organic acids into the rhizosphere, which in turn facilitated the Pi mobility in Oe1 plants' rhizosphere (Plaxton, 2004; Yao et al., 2011). Amino acids such as glutamic acid, tryptophan, and ornithine were increased in the root of Oe1 plant vs. WT (**Supplementary Table S2**), which might be a consequence of the increased amino acids' synthesis or repressed amino acids' degradation. Similar responses to P starvation have been reported in maize (Ganie et al., 2015), suggesting a conserved responses of those amino acids of plants to Pi starvation across different species. Glutamic acid and ornithine were involved in the supply of nitrogen for the growth of roots (Walker et al., 1984; Wright et al., 1995), and tryptophan is a precursor for auxin biosynthesis (Gao Y. et al., 2016). The aromatic amino acids' tyrosine which is a promoter of root length in plants (Bertin et al., 2007) was increased in Oe1 plants compared to WT under LP conditions (**Figure 11**). Taken together, the increases in glutamic acid, tryptophan, ornithine, and tyrosine might contribute to the enhanced root architecture in the roots of Oe1 than WT. Other compounds like nicotianamine (a chelator of metals) were increased as well (**Supplementary Table S2**), and it acts on the acquisition of iron in plants (Takahashi et al., 2003). If the Oe1 plant might possibly uptake more metals for the growth, additional evidence is needed before we could make a conclusion.

Twenty-seven compounds still had a sharp difference in shoots between Oe1 and WT plants under LP treatment (**Supplementary Table S3**). For example, fructose had a slight accumulation in the shoots of the Oe1 plant compared with WT, which possibly came from the degradation of phosphorylated polysaccharides, and consequently released more Pi (Morcuende et al., 2007). Similarly, most of the nucleotides, as organic P, significantly declined in the Oe plants vs. WT as well (**Supplementary Table S3**); similar changes have been found in maize (Ganie et al., 2015). Though the total P content had not obviously changed in the shoots between Oe1 and WT plants, the Pi concentration in the shoots of Oe1 plant increased (**Figure 6**).

We suggested that the overexpression of *CmPht1;2* might directly or indirectly enhance the Pi homeostasis in shoots rather than facilitating a transport of Pi from the root to the shoot (Wu et al., 2013).

CONCLUSION

In this study, we have identified the Pht1 family member *CmPht1;2,* whose expression is induced in the roots by P starvation. *CmPht1;2*-overexpressed chrysanthemum showed enhanced phosphorus uptake, suggesting that *CmPht1;2* may play a significant role in phosphate acquisition and root architecture reestablishment under LP. Metabolic profiles inferred that P participates in the regulation of amino acids and energy metabolism in chrysanthemum. The present study provides the basis for further studies on the Pi uptake modulation in chrysanthemum.

AUTHOR CONTRIBUTIONS

SC, FC, JJ, HW, and AS designed this study. CL did the main work of experimentation. All authors carried out the field experiments. YZ assisted deal with data of experiments. CL wrote the manuscript under the supervision of SC. JS and GS made a modification of the manuscript. All authors read and approved this manuscript.

FUNDING

This research was supported by the National Natural Science Foundation of China (Grant Nos. 31672192 and 31471913), the Fund for Independent Innovation of Agricultural Sciences in Jiangsu Province [CX (16) 1025].

SUPPLEMENTARY MATERIAL

The Supplementary Material for this article can be found online at: https://www.frontiersin.org/articles/10.3389/fpls.2018.00686/full#supplementary-material

FIGURE S1 | Original raw images of **Figure 4A**. Validation of transgenic plants. PCR analysis of genomic DNA extracted from hygromycinresistant regenerants.

TABLE S1 | Adaptor and primer sequences used.

TABLE S2 | Selected metabolites identified by GC-MS in roots of Oe1 under LP-treated conditions compared with WT.

TABLE S3 | Selected metabolites identified by GC-MS in the shoots of Oe1 under LP-treated conditions compared with WT.

TABLE S4 | Significant pathways identified by KEGG analysis.

TABLE S5 | Pathways involved in the roots of Oe1 under LP-treated conditions 0 day compared with WT identified by KEGG analysis.

TABLE S6 | Pathways involved in the roots of Oe1 under LP-treated conditions 2 days compared with WT identified by KEGG analysis.

TABLE S7 | Pathways involved in the roots of Oe1 under LP-treated conditions 7 days compared with WT identified by KEGG analysis.

TABLE S8 | Pathways involved in the shoots of Oe1 under LP-treated conditions 0 day compared with WT identified by KEGG analysis.

TABLE S9 | Pathways involved in the shoots of Oe1 under LP-treated conditions 2 days compared with WT identified by KEGG analysis.

TABLE S10 | Pathways involved in the shoots of Oe1 under LP-treated conditions 7 days compared with WT identified by KEGG analysis.

REFERENCES

Ai, P., Sun, S., Zhao, J., Fan, X., Xin, W., Guo, Q., et al. (2009). Two rice phosphate transporters, OsPht1;2 and OsPht1;6, have different functions and kinetic properties in uptake and translocation. *Plant J.* 57, 798–809. doi: 10.1111/j.1365-313X.2008.03726.x

Bentonjones, J. Jr. (1982). Hydroponics: its history and use in plant nutrition studies. *J. Plant Nutr.* 5, 1003–1030. doi: 10.1080/01904168209363035

Bertin, C., Weston, L. A., Huang, T., Jander, G., Owens, T., Meinwald, J., et al. (2007). Grass roots chemistry: meta-tyrosine, an herbicidal nonprotein amino acid. *Proc. Natl. Acad. Sci. U.S.A.* 104, 16964–16969. doi: 10.1073/pnas.0707198104

Bielecka, M., Watanabe, M., Morcuende, R., Scheible, W. R., Hawkesford, M. J., Hesse, H., et al. (2015). Transcriptome and metabolome analysis of plant sulfate starvation and resupply provides novel information on transcriptional regulation of metabolism associated with sulfur, nitrogen and phosphorus nutritional responses in Arabidopsis. *Front. Plant Sci.* 5:805. doi: 10.3389/fpls.2014.00805

Chen, A., Hu, J., Sun, S., and Xu, G. (2010). Conservation and divergence of both phosphate- and mycorrhiza-regulated physiological responses and expression patterns of phosphate transporters in solanaceous species. *New Phytol.* 173, 817–831. doi: 10.1111/j.1469-8137.2006.01962.x

Clarkson, D. T., and Hanson, J. B. (1980). The mineral nutrition of higher plants. *Annu. Rev. Plant Physiol.* 31, 239–298.

Fernie, A. R., Carrari, F., and Sweetlove, L. J. (2004). Respiratory metabolism: glycolysis, the TCA cycle and mitochondrial electron transport. *Curr. Opin. Plant Biol.* 7, 254–261. doi: 10.1016/j.pbi.2004.03.007

Ganie, A. H., Ahmad, A., Pandey, R., Aref, I. M., Yousuf, P. Y., Ahmad, S., et al. (2015). Metabolite profiling of low-P tolerant and low-P sensitive maize genotypes under phosphorus starvation and restoration conditions. *PLoS One* 10:e0129520. doi: 10.1371/journal.pone.0129520

Gao, J., Sun, J., Cao, P., Ren, L., Liu, C., Chen, S., et al. (2016). Variation in tissue Na^+ content and the activity of *SOS1* genes among two species and two related genera of Chrysanthemum. *BMC Plant Biol.* 16:98. doi: 10.1186/s12870-016-0781-9

Gao, Y., Dai, X., Zheng, Z., Kasahara, H., Kamiya, Y., Chory, J., et al. (2016). Overexpression of the bacterial tryptophan oxidase *RebO*, affects auxin biosynthesis and *Arabidopsis*, development. *Sci. Bull.* 61, 859–867. doi: 10.1007/s11434-016-1066-2

Hernández, G., Ramírez, M., Valdés-López, O., Tesfaye, M., Graham, M. A., and Czechowski, T. (2007). Phosphorus stress in common bean: root transcript and metabolic responses. *Plant Physiol.* 144, 752–767. doi: 10.1104/pp.107.096958

Hernández, G., Valdés-López, O., Ramírez, M., Goffard, N., Weiller, G., Aparicio-Fabre, R., et al. (2009). Global changes in the transcript and metabolic profiles during symbiotic nitrogen fixation in phosphorus-stressed common bean plants. *Plant Physiol.* 151, 1221–1238. doi: 10.1104/pp.109.143842

Hirai, M. Y., and Saito, K. (2004). Post-genomics approaches for the elucidation of plant adaptive mechanisms to sulphur deficiency. *J. Exp. Bot.* 55, 1871–1879. doi: 10.1093/jxb/erh184

Höfgen, R., and Willmitzer, L. (1988). Storage of competent cells for *Agrobacterium* transformation. *Nucleic Acids Res.* 16:9877. doi: 10.1093/nar/16.20.9877

Jia, H., Ren, H., Gu, M., Zhao, J., Sun, S., Zhang, X., et al. (2011). The phosphate transporter gene OsPht1;8 is involved in phosphate homeostasis in rice. *Plant Physiol.* 156, 1164–1175. doi: 10.1104/pp.111.175240

Kenneth, J., and Livak, T. D. (2001). Analysis of relative gene expression data using real-time quantitative PCR and the $2^{-\Delta\Delta C_t}$ method. *Methods* 25, 402–408. doi: 10.1006/meth.2001.1262

Lan, P., Li, W., Wen, T. N., Shiau, J. Y., Wu, Y. C., Lin, W., et al. (2011). iTRAQ protein profile analysis of Arabidopsis roots reveals new aspects critical for iron homeostasis. *Plant Physiol.* 155, 821–834. doi: 10.1104/pp.110.169508

Li, F., Zhang, H., Zhao, H., Gao, T., Song, A., Jiang, J., et al. (2017). Chrysanthemum *CmHSFA4* gene positively regulates salt stress tolerance in transgenic chrysanthemum. *Plant Biotechnol. J.* 16, 1311–1321. doi: 10.1111/pbi.12871

Liu, P., Chen, S., Song, A., Zhao, S., Fang, W., Guan, Z., et al. (2014). A putative high affinity phosphate transporter, CmPT1, enhances tolerance to Pi deficiency of chrysanthemum. *BMC Plant Biol.* 14:18. doi: 10.1186/1471-2229-14-18

Liu, P., Chen, S. M., Fang, W. M., Jiang, J. F., Guan, Z. Y., and Chen, F. D. (2013). Preliminary evaluation on tolerance to phosphorous deficiency of 32 cultivars of cut chrysanthemum. *Acta Ecol. Sin.* 33, 6863–6868. doi: 10.5846/stxb201207171016

Loescher, W. H., Marlow, G. C., and Kennedy, R. A. (1982). Sorbitol metabolism and sink-source interconversions in developing apple leaves. *Plant Physiol.* 70, 335–339.

Misson, J., Thibaud, M. C., Bechtold, N., Raghothama, K., and Nussaume, L. (2004). Transcriptional regulation and functional properties of *Arabidopsis* Pht1;4, a high affinity transporter contributing greatly to phosphate uptake in phosphate deprived plants. *Plant Mol. Biol.* 55, 727–741. doi: 10.1007/s11103-004-1965-5

Mitsukawa, N., Okumura, S., Shirano, Y., Sato, S., Kato, T., Harashima, S., et al. (1997). Overexpression of an *Arabidopsis thaliana* high-affinity phosphate transporter gene in tobacco cultured cells enhances cell growth under phosphate-limited conditions. *Proc. Natl. Acad. Sci. U.S.A.* 94, 7098–7102. doi: 10.1073/pnas.94.13.7098

Młodzińska, E., and Zboińska, M. (2016). Phosphate uptake and allocation – a closer look at *Arabidopsis thaliana* L. and *Oryza sativa* L. *Front. Plant Sci.* 7:1198. doi: 10.3389/fpls.2016.01198

Morcuende, R., Bari, R., Gibon, Y., Zheng, W. M., Pant, B. D., Blasing, O., et al. (2007). Genome-wide reprogramming of metabolism and regulatory networks of *Arabidopsis* in response to phosphorus. *Plant Cell Environ.* 30, 85–112. doi: 10.1111/j.1365-3040.2006.01608.x

Muchhal, U. S., Pardo, J. M., and Raghothama, K. G. (1996). Phosphate transporters from the higher plant *Arabidopsis thaliana*. *Proc. Natl. Acad. Sci. U.S.A.* 93, 10519–10523.

Muchhal, U. S., and Raghothama, K. G. (1999). Transcriptional regulation of plant phosphate transporters. *Proc. Natl. Acad. Sci. U.S.A.* 96, 5868–5872. doi: 10.1073/pnas.96.10.5868

Nagarajan, V. K., Jain, A., Poling, M. D., Lewis, A. J., Raghothama, K. G., and Smith, A. P. (2011). Arabidopsis Pht1;5 mobilizes phosphate between source and sink organs and influences the interaction between phosphate homeostasis and ethylene signaling. *Plant Physiol.* 156, 1149–1163. doi: 10.1104/pp.111.174805

Nussaume, L., Kanno, S., Javot, H., Marin, E., Pochon, N., Ayadi, A., et al. (2011). Phosphate import in plants: focus on the PHT1 transporters. *Front. Plant Sci.* 2:83. doi: 10.3389/fpls.2011.00083

Peng, Z. X., Wang, Y., Gu, X., Xue, Y., Wu, Q., Zhou, J. Y., et al. (2015). Metabolic transformation of breast cancer in a MCF-7 xenograft mouse model and inhibitory effect of volatile oil from *Saussurea lappa* Decne treatment. *Metabolomics* 11, 636–656. doi: 10.1007/s11306-014-0725-z

Plaxton, W. C. (2004). "Plant response to stress: biochemical adaptations to phosphate deficiency," in *Encyclopedia of Plant and Crop Science.*, ed. R. M. Goodman (New York, NY: Marcel Dekker, Inc.), 976–980.

Raghothama, K. G. (2000). Phosphate transport and signaling. *Curr. Opin. Plant Biol.* 3, 182–187. doi: 10.1016/S1369-5266(00)00062-5

Raghothama, K. G., and Karthikeyan, A. S. (2005). *Phosphate Acquisition*. Dordrecht: Springer.

Rausch, C., and Bucher, M. (2002). Molecular mechanisms of phosphate transport in plants. *Planta* 216, 23–37. doi: 10.1007/s00425-002-0921-3

Ren, L., Sun, J., Chen, S., Gao, J., Dong, B., Liu, Y., et al. (2014). A transcriptomic analysis of *Chrysanthemum nankingense* provides insights into the basis of low temperature tolerance. *BMC Genomics* 15:844. doi: 10.1186/1471-2164-15-844

Saia, S., Rappa, V., Ruisi, P., Abenavoli, M. R., Sunseri, F., Giambalvo, D., et al. (2015). Soil inoculation with symbiotic microorganisms promotes plant growth and nutrient transporter genes expression in durum wheat. *Front. Plant Sci.* 6:815. doi: 10.3389/fpls.2015.00815

Saier, M. H. Jr. (2000). Families of proteins forming transmembrane channels. *J. Membr. Biol.* 175, 165–180. doi: 10.1007/s002320001065

Shi, J., Hu, H., Zhang, K., Zhang, W., Yu, Y., Wu, Z., et al. (2014). The paralogous SPX3 and SPX5 genes redundantly modulate Pi homeostasis in rice. *J. Exp. Bot.* 65, 859–870. doi: 10.1093/jxb/ert424

Shin, H., Shin, H. S., Dewbre, G. R., and Harrison, M. J. (2004). Phosphate transport in *Arabidopsis*: Pht1;1 and Pht1;4 play a major role in phosphate acquisition from both low- and high-phosphate environments. *Plant J.* 39, 629–642. doi: 10.1111/j.1365-313X.2004.02161.x

Takahashi, M., Terada, Y., Nakai, I., Nakanishi, H., Yoshimura, E., Mori, S., et al. (2003). Role of nicotianamine in the intracellular delivery of metals and plant reproductive development. *Plant Cell* 15, 1263–1280. doi: 10.1105/tpc.010256

Teng, W., Zhao, Y. Y., Zhao, X. Q., He, X., Ma, W. Y., Deng, Y., et al. (2017). Genome-wide identification, characterization, and expression analysis of PHT1 phosphate transporters in wheat. *Front. Plant Sci.* 8:543. doi: 10.3389/fpls.2017.00543

Vandamme, E., Rose, T., Saito, K., Jeong, K., and Wissuwa, M. (2016). Integration of P acquisition efficiency, P utilization efficiency and low grain P concentrations into P-efficient rice genotypes for specific target environments. *Nutr. Cycl. Agroecosyst.* 104, 413–427. doi: 10.1007/s10705-015-9716-3

Walker, K. A., Givan, C. V., and Keys, A. J. (1984). Glutamic acid metabolism and the photorespiratory nitrogen cycle in wheat leaves: metabolic consequences of elevated ammonia concentrations and of blocking ammonia assimilation. *Plant Physiol.* 75, 60–66.

Wan, Y. L., Eisinger, W., Ehrhardt, D., Kubitscheck, U., Baluska, F., and Briggs, W. (2008). The subcellular localization and blue-light-induced movement of phototropin 1-GFP in etiolated seedlings of *Arabidopsis thaliana*. *Mol. Plant* 1, 103–117. doi: 10.1093/mp/ssm011

Wang, D., Lv, S., Jiang, P., and Li, Y. (2017). Roles, regulation, and agricultural application of plant phosphate transporters. *Front. Plant Sci.* 8:817. doi: 10.3389/fpls.2017.00817

Wright, P., Felskie, A., and Anderson, P. (1995). Induction of ornithine-urea cycle enzymes and nitrogen metabolism and excretion in rainbow trout (*Oncorhynchus mykiss*) during early life stages. *J. Exp. Biol.* 198, 127–135.

Wu, P., Shou, H., Xu, G., and Lian, X. (2013). Improvement of phosphorus efficiency in rice on the basis of understanding phosphate signaling and homeostasis. *Curr. Opin. Plant Biol.* 16, 205–212. doi: 10.1016/j.pbi.2013.03.002

Yao, Y., Sun, H., Xu, F., Zhang, X., and Liu, S. (2011). Comparative proteome analysis of metabolic changes by low phosphorus stress in two *Brassica napus* genotypes. *Planta* 233, 523–537. doi: 10.1007/s00425-010-1311-x

Zhou, J., Jiao, F., Wu, Z., Li, Y., Wang, X., He, X., et al. (2008). OsPHR2 is involved in phosphate-starvation signaling and excessive phosphate accumulation in shoots of plants. *Plant Physiol.* 146, 1673–1686. doi: 10.1104/pp.107.111443

Zhou, J., Zhang, L., Chang, Y., Lu, X., Zhu, Z., and Xu, G. (2012). Alteration of leaf metabolism in Bt-transgenic rice (*Oryza sativa* L.) and its wild type under insecticide stress. *J. Proteome Res.* 11, 4351–4360. doi: 10.1021/pr300495x

Conflict of Interest Statement: The authors declare that the research was conducted in the absence of any commercial or financial relationships that could be construed as a potential conflict of interest.

frontiers in Plant Science

ORIGINAL RESEARCH
published: 20 August 2018
doi: 10.3389/fpls.2018.01186

Overexpression of a Phosphate Starvation Response AP2/ERF Gene From Physic Nut in Arabidopsis Alters Root Morphological Traits and Phosphate Starvation-Induced Anthocyanin Accumulation

*Yanbo Chen[1,2], Pingzhi Wu[1], Qianqian Zhao[1,2], Yuehui Tang[1,2], Yaping Chen[1], Meiru Li[1], Huawu Jiang[1] and Guojiang Wu[1]**

[1] Key Laboratory of Plant Resources Conservation and Sustainable Utilization, South China Botanical Garden, Chinese Academy of Sciences, Guangzhou, China, [2] College of Life Sciences, University of Chinese Academy of Sciences, Beijing, China

OPEN ACCESS

Edited by:
Alex Joseph Valentine,
Stellenbosch University, South Africa

Reviewed by:
Ki-Hong Jung,
Kyung Hee University, South Korea
Liang Chen,
University of Chinese Academy of Sciences (UCAS), China
Ping Lan,
Institute of Soil Science (CAS), China

***Correspondence:**
Guojiang Wu
wugj@scbg.ac.cn

Specialty section:
This article was submitted to Plant Nutrition, a section of the journal Frontiers in Plant Science

Received: 01 February 2018
Accepted: 24 July 2018
Published: 20 August 2018

Citation:
Chen Y, Wu P, Zhao Q, Tang Y, Chen Y, Li M, Jiang H and Wu G (2018) Overexpression of a Phosphate Starvation Response AP2/ERF Gene From Physic Nut in Arabidopsis Alters Root Morphological Traits and Phosphate Starvation-Induced Anthocyanin Accumulation. Front. Plant Sci. 9:1186. doi: 10.3389/fpls.2018.01186

Physic nut (*Jatropha curcas* L.) is highly tolerant of barren environments and a significant biofuel plant. To probe mechanisms of its tolerance mechanisms, we have analyzed genome-wide transcriptional profiles of 8-week-old physic nut seedlings subjected to Pi deficiency (P−) for 2 and 16 days, and Pi-sufficient conditions (P+) controls. We identified several phosphate transporters, purple acid phosphatases, and enzymes of membrane lipid metabolism among the 272 most differentially expressed genes. Genes of the miR399/PHO2 pathway (*IPS*, miR399, and members of the SPX family) showed alterations in expression. We also found that expression of several transcription factor genes was modulated by phosphate starvation stress in physic nut seedlings, including an AP2/ERF gene (*JcERF035*), which was down-regulated in both root and leaf tissues under Pi-deprivation. In *JcERF035*-overexpressing Arabidopsis lines both numbers and lengths of first-order lateral roots were dramatically reduced, but numbers of root hairs on the primary root tip were significantly elevated, under both P+ and P− conditions. Furthermore, the transgenic plants accumulated less anthocyanin but had similar Pi contents to wild-type plants under P-deficiency conditions. Expression levels of the tested genes related to anthocyanin biosynthesis and regulation, and genes induced by low phosphate, were significantly lower in shoots of transgenic lines than in wild-type plants under P-deficiency. Our data show that down-regulation of the *JcERF035* gene might contribute to the regulation of root system architecture and both biosynthesis and accumulation of anthocyanins in aerial tissues of plants under low Pi conditions.

Keywords: AP2/ERF transcription factor, phosphate starvation, root morphology, anthocyanin, physic nut (*Jatropha curcas* L.)

INTRODUCTION

Phosphorus (P) is an important macro-element for higher plants in the processes of growth and development, which is absorbed by the root system from soil in the form of inorganic phosphate (Pi) (Raghothama, 1999). In plants, Pi starvation stimulates changes in root system architecture (RSA), including inhibition of primary root growth accompanied by increases in lateral root

number and both the length and number of root hairs (Péret et al., 2011). At the biochemical level, responses to Pi limitation include increases in production of phosphatases, RNases, Pi, H^+ and organic acid transporters that facilitates Pi acquisition by roots (Vance et al., 2003; Plaxton and Tran, 2011). Another common plant response to phosphate deficiency is anthocyanin accumulation in the shoot (Marschner, 1995; Morcuende et al., 2007), which probably protects the photosynthetic apparatus and DNA from oxidative damage (Zeng et al., 2010). Comparative global gene expression profiling studies have shown that many Pi starvation response (PSR) genes are involved in these processes in Arabidopsis and other plants (Wasaki et al., 2003, 2006; Misson et al., 2005; Morcuende et al., 2007; Müller et al., 2007; Calderon-Vazquez et al., 2008; Li et al., 2010; Thibaud et al., 2010). These profiling studies indicate that Pi deprivation also triggers activation of alternative non-phosphorylating metabolic pathways. Moreover, during Pi deficiency, Pi is released from reserves contained in phospholipids, via their hydrolysis and conversion into sulfolipids or galactolipids (Misson et al., 2005).

Several studies have revealed important components of the sensing and signaling networks involved in Pi deficiency responses in Arabidopsis and rice. The MYB-CC transcription factors (TFs) PHOSPHATE STARVATION RESPONSE1 (PHR1) family genes in Arabidopsis (Rubio et al., 2001) and rice (Zhou et al., 2008; Guo et al., 2015) play key regulatory roles in these responses. A loss-of-function mutation in *PHR1* influences a subset of Pi starvation responses, including anthocyanin accumulation, changes in root to shoot growth ratios and expression of a subset of Pi starvation-induced genes (Rubio et al., 2001). SPX proteins play essential functions in regulating the activity of *AtPHR1*/*OsPHR2* under Pi starvation in distinct subcellular levels (Secco et al., 2012). In Arabidopsis, the miR399/PHO2 pathway operates downstream of *PHR1*, and regulates several Pi-dependent responses, such as Pi allocation between the shoot and root. Thus, the miR399/PHO2 pathway is a significant component of the Pi-signaling network (Lin S.I. et al., 2008; Chiou and Lin, 2011; Guo et al., 2015).

Besides the PHR1 family, members of the AP2/ERF (Ramaiah et al., 2014), bHLH (Yi et al., 2005; Chen et al., 2007), G2-like (Liu et al., 2009), R2R3 MYB and MYB-like (Devaiah et al., 2009; Dai et al., 2012; Yang et al., 2014; Nagarajan et al., 2016; Zhou et al., 2017), WRKY (Devaiah et al., 2007a; Chen et al., 2009; Wang et al., 2014; Su et al., 2015; Dai et al., 2016), and zinc finger (Devaiah et al., 2007b) TF families play essential roles in the regulation of Pi starvation responses. They affect several morphological processes that respond to Pi availability, and expression levels of several Pi starvation-induced (PSI) genes.

Physic nut (*Jatropha curcas* L.) is a species of shrubs of the family Euphorbiaceae. It can tolerate semiarid, drought-prone and barren environments, including low Pi environments that are not suitable for crop cultivation (Gubitz et al., 1999; Dhillon et al., 2009; Parthiban et al., 2009). Zhao et al. (2012) found that even after growing in a Pi-deficient medium for 17 days, physic nut seedlings can maintain high net photosynthetic rates, equivalent to ca. 90% of the rate of seedlings grown under Pi-sufficient conditions, despite significant declines in total Pi contents of their roots (ca. 55%) and aerial parts (ca. 81%). The dry weight of aerial parts decrease ca. 4%, whereas that of roots increase ca. 10%, compared with plants grown under Pi-sufficient condition (Zhao et al., 2012). However, the Pi starvation response mechanisms of physic nut, which control Pi homeostasis, remain obscure. Therefore, to probe these mechanisms we applied next-generation sequencing to explore transcriptomic changes in physic nut roots and leaves under Pi deficiency. Interestingly, we found that *JcERF035*, a member of the DREB subfamily of TFs, responded to Pi starvation in both roots and leaves. The DREB TFs play important roles in the responses to cold, dehydration, salt stress, and regulation of GA biosynthesis, cell dedifferentiation, plant morphology and branching (Lata and Prasad, 2011; Rehman and Mahmood, 2015). Previous studies indicate that DREB genes play important roles in determination of root architecture and abiotic stress responses (Liu et al., 2015; Liao et al., 2017; Yang et al., 2017). However, no DREB subfamily genes have been functionally characterized in terms of their responses to Pi deficiency in plants. Therefore, we overexpressed the *JcERF035* gene in Arabidopsis, and found that it altered root morphology, anthocyanin accumulation and expression levels of some PSI genes, but it did not significantly influence the Pi content of transgenic plants.

MATERIALS AND METHODS

Plant Materials and Pi Starvation/Sufficiency Treatments

After disinfection with 1:5000 $KMnO_4$ solution, seeds of the inbred physic nut cultivar GZQX0401 were planted in sand to germinate. When cotyledons were fully expanded, seedlings were transferred to trays containing a 3:1 mixture of sand and soil soaked with half-strength Hoagland solution in a greenhouse illuminated with natural sunlight. After emergence of the first true leaf, the trays were each irrigated with 1 L of Hoagland nutrient solution (pH 6.0) every 2 days at dusk. Pi deficiency (P−) and sufficiency (P+) treatments were begun at the six-leaf stage (8 weeks after germination). The P− treatment was initiated by removing most nutrients from the environments of a group of randomly selected seedlings by five washes, each with 1 L of tap water. These seedlings were then irrigated daily with Hoagland nutrient solution without phosphate, while another group, assigned to the P+ treatment, were not washed and irrigated with complete Hoagland solution (Zhao et al., 2012).

On the basis of our previous observation of changes in net photosynthetic rate (Pn) in physic nut leaves under Pi deficiency treatment, seedlings of the P− and P+ groups were sampled after 2 and 16 days of the treatment. According to these observations, Pn began to decrease during the first 2 days of the P− treatment, but remained at ca. 90% of the control rate after 16-day treatment (Zhao et al., 2012). The Pi content in Pi-deficiency group decreased 54.8 ± 3.5% and 81.2 ± 2.6% of controls' contents in roots and shoots, respectively, while the root/shoot dry weight ratio increased from 0.047 ± 0.003 (control) to 0.054 ± 0.003 (Pi-deficiency) at the end of the treatment (17 days) (Zhao et al., 2012). In this study, roots and leaves of plants subjected to both

the P− and P+ treatments were sampled at 8 a.m. to 9 a.m. after 2 and 16 days. Root samples consisted of 5–10 mm root tips, while leaf samples consisted of the second fully expanded leaf from the apex. Samples of both Pi-deficient and control groups were frozen immediately in liquid nitrogen and stored at −80°C. RNA isolation and digital gene expression library preparation and sequencing were performed as previously described (Zhang et al., 2014). For gene expression analysis, the numbers of expressed tags normalized to TPM (number of transcripts per million tags) were calculated (Zhang et al., 2014). We would prefer, 'Data on the RNA-seq' sequencing saturation of all samples are provided in **Supplementary Figure S1**.

JcERF035 Transformation

The full-length *JcERF035* coding domain sequence was cloned into the pCAMBIA1301 vector under control of the CaMV35S promoter (Tang et al., 2017). The resulting construct was transferred into Arabidopsis plants (Columbia ecotype) by the floral-dipping method (Clough and Bent, 1998). Homozygous lines with single T-DNA insertions were selected for subsequent analysis.

Pi Deficiency/Sufficiency Treatments of Transgenic Arabidopsis Plants

Wild-type and transgenic Arabidopsis seeds were surface-sterilized and planted on half-strength Murashige and Skoog (MS) plates supplemented with 1% (w/v) sucrose and 1% (w/v) agar. The plates were placed at 4°C for 2 days in the dark, then positioned vertically in a growth chamber providing long-day photoperiod (16 h light/8 h dark) at 22 ± 2°C. Four days after germination (DAG), seedlings of all lines were transferred to new vertical Pi deficiency (P–) and Pi plus (P+) agar plates (Bates and Lynch, 1996), with the following macroelements: 3 mM KNO_3, 2 mM $Ca(NO_3)_2$, 0.5 mM $MgSO_4$, and 1 mM $NH_4H_2PO_4$ (P+) or 0.5 mM $(NH_4)_2SO_4$ (P−). After 7 days, the seedlings' root morphology was observed and they were sampled for RNA isolation, anthocyanin assays, and quantification of total Pi.

RNA Isolation, Semi-Quantitative RT-PCR, and Quantitative RT-PCR (qRT-PCR)

Total RNA was isolated from Arabidopsis leaves using Trizol® reagent according to the manufacturer's instructions (Invitrogen[1]), and from physic nut roots and leaves as previously described (Zhang et al., 2014). First-strand cDNAs were synthesized from 3 μg portions of total RNA, using M-MLV reverse transcriptase (Promega) following the manufacturer's instructions. The primers used for RT-PCR in this work are listed in **Supplementary Table S1**. The *AtActin2* gene of Arabidopsis and *JcActin* gene of physic nut were used as references. Three independent biological replicates were performed for each PCR assay.

For semi-quantitative RT-PCR, PCR products were separated on 1.5% agarose gels and stained with ethidium bromide. The gels were then photographed using a Gel Imaging System (Shanghai Bio-Tech[2]), and an LCS480 system (Roche[3]) was used for quantitative real-time PCR. Each 20 μL reaction solution contained 10 μL 2 × SYBR Premix ExTaq, 0.4 μL forward primer (10 μM), 0.4 μL reverse primer (10 μM), 2 μL diluted cDNA solution, and 7.2 μL ddH_2O. The thermal profile used for all PCR amplifications was: 10 min at 95°C for DNA polymerase activation, followed by 40 cycles of 5 s at 95°C, 20 s at 60°C and 20 s at 72°C. The $2^{-\Delta\Delta CT}$ method was used for calculating the expression levels of genes.

Measurements of Roots

A stereomicroscope (Leica M165C) equipped with a digital camera was used to capture images of root hairs within the zone 5 mm from the root tips of transgenic and wild-type seedlings at 4 DAG. The number and length of the root hairs of 30 seedlings from each line subjected to each treatment were measured using the ImageJ program[4]. The software was also used to record the primary root length, lateral root number, and lateral root length of 20 seedlings of each line subjected to each treatment.

Anthocyanin Estimation

Anthocyanin contents of shoots of Arabidopsis plants were determined following Rabino and Mancinelli (1986). The anthocyanin was extracted from the shoots by incubating them in acidic (1% HCl, w/v) methanol at 4°C for 2 days. The absorbance (A) of the centrifuged extract was determined at 530 nm and 657 nm (A_{530} and A_{657}, respectively), and the concentration of anthocyanin was expressed as $A_{530}-0.25A_{657}$ g^{-1} fresh weight.

Quantification of Total Pi

Phosphate content was determined according to Ramaiah et al. (2014). Fresh samples ca. 50 mg were each transferred into a pre-weighed crucible and oven dried. After washing by furnace, samples were subsequently dissolved in 100 μL of concentrated hydrochloric acid. Then each sample was prepared by adding 10 μL the sample solution from the previous step and 790 μL ddH_2O. A 200 μL portion of assay solution (35 mM ascorbic acid, 2.5 N H_2SO_4, and 4.8 mM NH_4MoO_4) was then added, and the resulting mixture was incubated at 45°C for 20 min. Appropriate standards were used to convert A_{650} values to total Pi contents, which were expressed as total Pi (nmol mg^{-1} dry weight).

Statistical Analysis

Three to six biological repeats were used for all experiments, and the means acquired for all variables were compared using Duncan tests (Duncan, 1955) implemented in the SAS software package version 9[5].

[1]http://www.thermofisher.com

[2]http://www.shbiotech.com

[3]http://www.roche.com/

[4]http://rsb.info.nih.gov/ij/

[5]http://www.sas.com/en_us/software/sas9.html

RESULTS

Changes in Transcriptomic Profiles of Roots and Leaves of Physic Nut Seedlings in Response to Pi Starvation

For a preliminary screening of genes responsive to Pi-starvation in physic nut plants, roots and leaves sampled after 2 and 16 days of the P− and P+ treatments were used to examine genome-wide changes in the transcriptomes. Using the physic nut genome sequence we previously acquired (Wu P. et al., 2015), we identified transcripts with clean tags for a total of 272 protein-encoding genes that were severely affected (with ≥3-fold difference in expression level between Pi-deficient and Pi-sufficient plants) at all time points (**Supplementary Table S2**). About half of the up-regulated transcripts in leaves were orthologs of Arabidopsis genes that have been reportedly upregulated under Pi-starvation (**Supplementary Table S2**), including lipid metabolism, phosphate transporter, some C-metabolism, various phosphatase and SPX domain-containing genes (Misson et al., 2005; Müller et al., 2007). Many of the up-regulated genes were orthologs of Arabidopsis genes that are involved in soil Pi release, Pi uptake and Pi scavenging-related metabolism (**Supplementary Table S3**). The severely affected genes in Pi scavenging metabolic pathways were related to the glycolytic bypass, sulfate assimilate and reduction, fatty acid biosynthesis, and sulfo/galactolipid biosynthesis (**Supplementary Table S3**). Many of the severely down-regulated genes were involved in cell expansion, cell wall biosynthesis, and leaf extension (**Supplementary Table S2B**). Four AUX/IAA transcriptional regulator genes (JCGZ_01304, JCGZ_02271, JCGZ_07276, and JCGZ_23499) and two gibberellin-regulated family protein genes were down-regulated (JCGZ_19847 and JCGZ_25966).

Several severely affected genes involved in the miR399/PHO2 pathway signaling pathway were also found. These included SPX domain-containing protein genes, miRNA399 precursor, ncRNAs of the IPS family, and *PHT1* transporter genes. Differential expression of ncRNAs, SPX domain-containing protein genes, and *PHT1* transporter genes in roots and shoots at 16 days after the onset of Pi deficiency was corroborated by RT-PCR and qRT-PCR (**Figure 1** and **Supplementary Figure S2**). According to the clean tags for these genes, no miRNA399 precursor was detected in roots and leaves under Pi-sufficient conditions, and there were low levels of transcripts for *MT4*/*IPS2*, *SPX* genes (JCGZ_06151 and JCGZ_14570), *PHT1* genes (JCGZ_08040 and JCGZ_02324) in Pi-sufficient leaves. In contrast, high levels of these transcripts were detected in Pi-deficient plants (**Figure 1**).

Changes in Expression of *JcERF035* Under Pi Deficiency

Several TF genes responded to Pi starvation in physic nut, including genes of the WRKY (Xiong et al., 2013), NAC (Wu Z. et al., 2015), GRAS (Wu Z.Y. et al., 2015), MYB (Zhou et al., 2015), and AP2/ERF (Tang et al., 2016) families. We observed that an AP2/ERF gene, designated *JcERF035* (Accession No. JCGZ_24071 in GenBank), was down-regulated in both leaves and roots under the Pi deficiency treatment. The changes in expression of the *JcERF035* gene were confirmed by qRT-PCR. This revealed 22–51% reductions in the gene's expression in leaves, and 20–44% reductions in roots, of seedlings after 2 h, 2, 4, and 16 days of the P− treatment, relative to those in Pi-sufficient seedlings (**Figure 2**).

Overexpression of *JcERF035* in Arabidopsis Altered Root Morphological Traits

Overexpression of *JcERF035* in Arabidopsis (*OeJcERF035*, or simply Oe lines hereafter) enhanced the sensitivity of transgenic seedlings to salt stress (**Supplementary Figure S3**), in accordance with reported results of overexpressing it in rice seedlings (Tang et al., 2017). To investigate functions of the physic nut *JcERF035* gene in response to Pi-deficiency *in planta*, three independent single insertion *OeJcERF035* lines (Oe1, Oe2, and Oe3) were used for detailed investigation. Semi-quantitative RT-PCR was used to detect the expression level of *JcERF035* in these transgenic Arabidopsis lines (**Figure 3A**). Apart from root morphology, no obvious developmental differences were detected between wild-type and transgenic lines under Pi-sufficient growth conditions on 1/2 MS medium in agar petri plates or vermiculite medium in pots (**Figures 3B**,**4A**). During growth in agar petri plates, we observed more root hairs in the basal 5-mm region of the primary root tip of *OeJcERF035* seedlings than in those of wild type plants (**Figures 3C,D**), accompanied by significant reductions in the number (**Figures 4A,B**) and total length (**Figure 4C**) of first-order lateral roots. Shoots of transgenic seedlings had ca. 20% lower dry weights than those of wild-type seedlings grown on vertically oriented agar plates (**Figures 4A,E**).

The *JcERF035* gene is a member of subgroup 1b of the ERF family and group A6 of the DREB subfamily (Tang et al., 2016). In Arabidopsis, several subgroup 1b ERF genes reportedly have roles in cell dedifferentiation and drought tolerance (Iwase et al., 2011; Zhu et al., 2014). In Arabidopsis lines overexpressing orthologs of *JcERF035* (At1g78080 or At1g36060), several aquaporin genes were found to be up-regulated more than twofold (Rae et al., 2011; Zhu et al., 2014). To determine whether these genes were also up-regulated in the *JcERF035*-overexpressing lines, we examined their expression levels in two *OeJcERF035* lines by qRT-PCR analysis. We found that the *AtTIP2;3* (At5g47450) gene was up-regulated more than twofold, whereas *AtPIP2;5* (At3g54820) was down-regulated more than twofold and the other three aquaporin genes—*AtPIP2;2* (At2g37170), *AtTIP1;1* (At2g36830), and *AtTIP2;2* (At4g17340)—showed less than twofold changes in expression in the *OeJcERF035* lines (**Figure 5**). Thus, the JcERF035 protein appears to regulate different genes from its Arabidopsis orthologs.

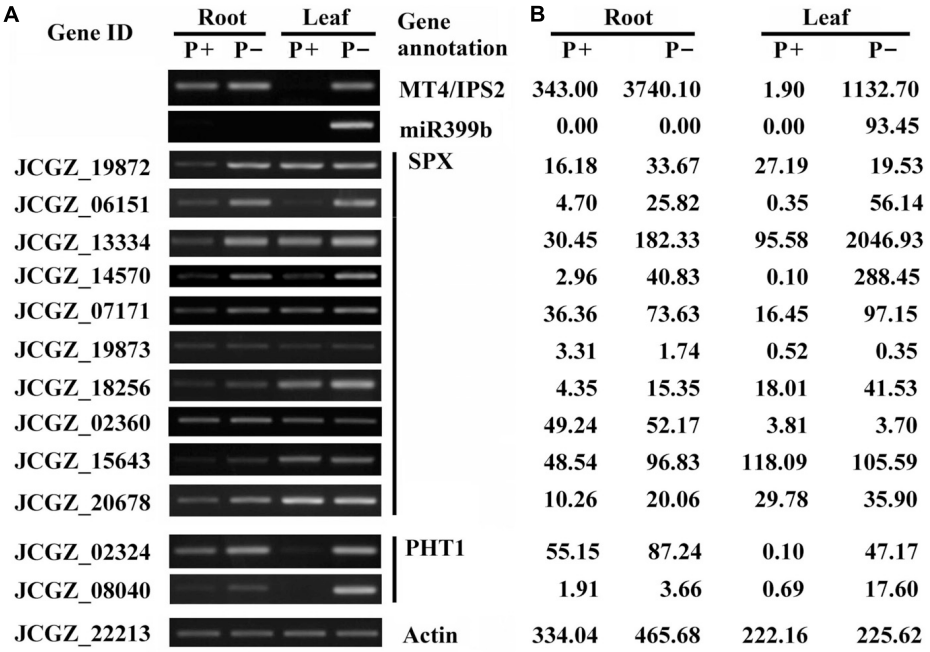

FIGURE 1 | Results of RT-PCR analysis of differences in expression levels of selected genes involved in the miR399/PHO2 pathway and SPX family genes between physic nut seedlings grown under Pi deficiency (P–) and Pi sufficiency (P+). Root and leaf samples from plants 16 days after the onset of P– and P+ treatments were tested. **(A)** Results of semi-quantitative RT-PCR analysis showing expression of indicated genes relative to a physic nut *Actin* gene (bottom). **(B)** Expression changes obtained from the digital gene expression tag profiling database.

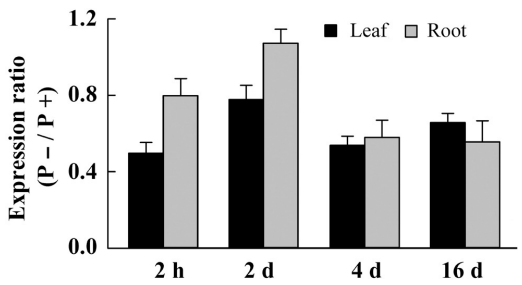

FIGURE 2 | Differences in expression level of the *JcERF035* gene between leaves (black column) and roots (gray column) of physic nut seedlings grown under Pi deficiency (P–) and Pi sufficiency (P+). A physic nut *JcActin* gene was used as a loading control. Fold changes indicate ratios of expression levels under P– conditions to those recored under P+ conditions at each time point. Bars represent means ± SD from three biological replicates, each with two technical replicates.

Overexpression of *JcERF035* in Arabidopsis Affected Seedlings' Responses to Phosphate Starvation

The *JcERF035* expression level was down-regulated in both roots and leaves of physic nut under Pi starvation stress. To examine the effect of this gene on phosphate starvation responses, 4-day-old wild-type and *OeJcERF035* Arabidopsis seedlings were transplanted into P− and P+ agar petri plates. *OeJcERF035* seedlings had fewer first-order lateral roots (**Figures 4A,B**), and lower shoot dry weights (**Figure 4E**) than the wild-type seedlings under both P+ conditions and P− conditions. Additionally, *OeJcERF035* seedlings had shorter primary roots and more root hairs on their primary root tips (**Figures 4A,D**), and lower root-shoot ratio (**Figure 4F**) under Pi deficiency.

The purple coloration induced by Pi starvation appeared lighter in *OeJcERF035* shoots than in wild-type shoots (**Figure 4A**), and the total anthocyanin content was notably lower in *OeJcERF035* shoots than in wild-type shoots under P− conditions (**Figure 4G**). To determine whether the lower anthocyanin content in *OeJcERF035* shoots was related to any effects of *JcERF035* overexpression on the maintenance of Pi homeostasis in the transgenic lines, we measured total Pi contents of shoots of the *OeJcERF035* and wild-type seedlings. Shoots of *OeJcERF035* seedlings had slightly lower Pi contents than the wild-type shoots under both P+ and P− conditions (**Figure 4H**). These results suggest that overexpression of *JcERF035* did not significantly modulate shoot Pi content in the transgenic seedlings.

Changes in Expression of Phenylpropanoid Metabolism-Related Genes and Some PSI Genes in Shoots

To better understand the mechanisms underlying the observed reduction in phosphate starvation-induced anthocyanin biosynthesis conferred by overexpression of *JcERF035* in Arabidopsis, we tested the expression of several genes involved in phenylpropanoid metabolism and its regulation. We found that

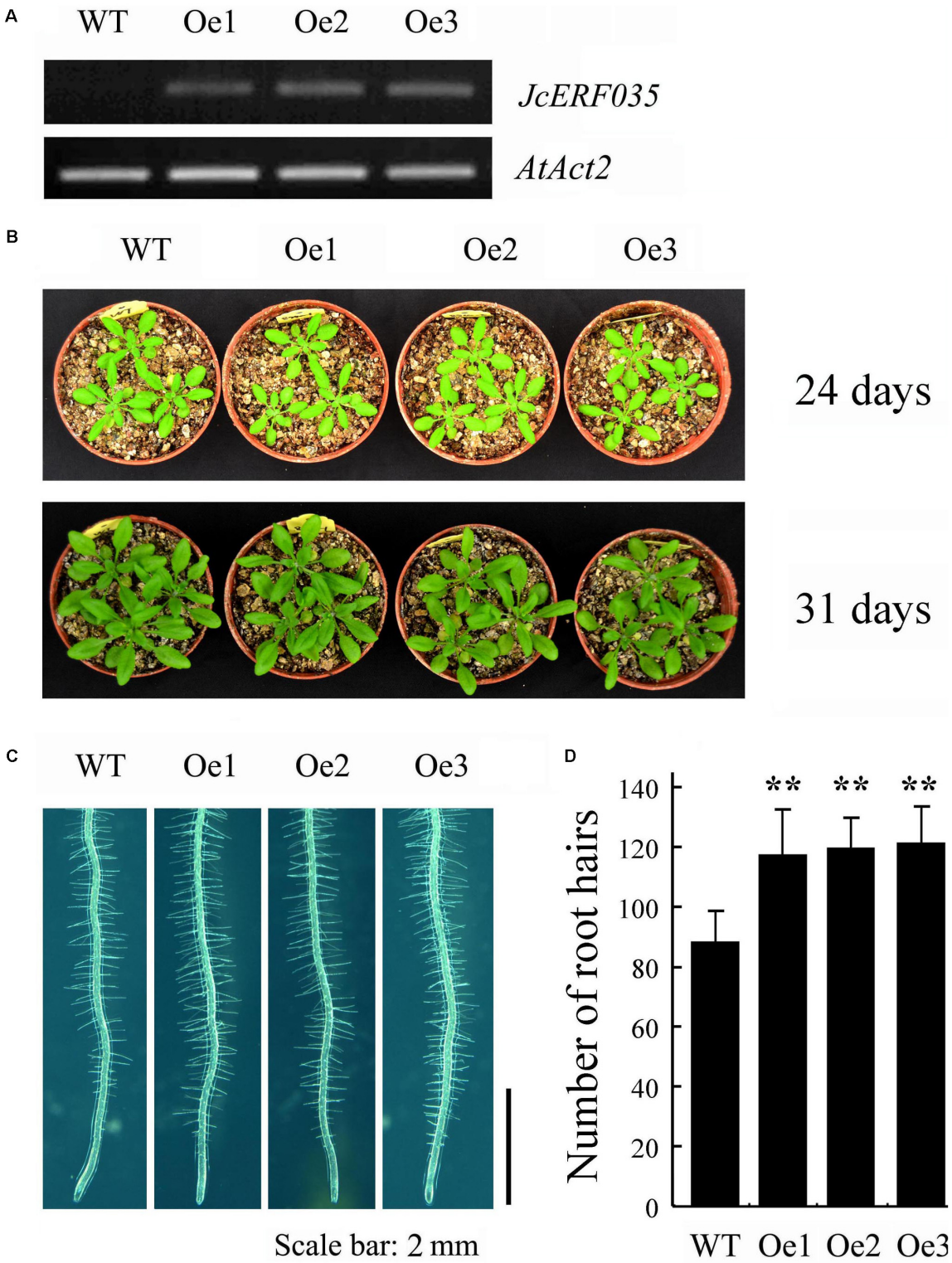

FIGURE 3 | Overexpression of *JcERF035* (*OeJcERF035*) modulates root morphophysiological traits in Arabidopsis under normal conditions. **(A)** Relative expression levels of *JcERF035* transcripts in indicated transgenic lines (Oe1, Oe2, and Oe3) determined by semi-quantitative RT-PCR. **(B)** Plants 24 and 31 days old. **(C)** Phenotypes of root hairs in a 5-mm region of the primary root tip of 4-day-old wild-type and *OeJcERF035* lines grown on 1/2 MS plus 1% sucrose in agar plates. **(D)** Total numbers of root hairs in a 5-mm region of the primary root tip. Values shown are means ± SD from three biological replicates with 30 seedlings in each (Duncan test: $^{**}P < 0.01$).

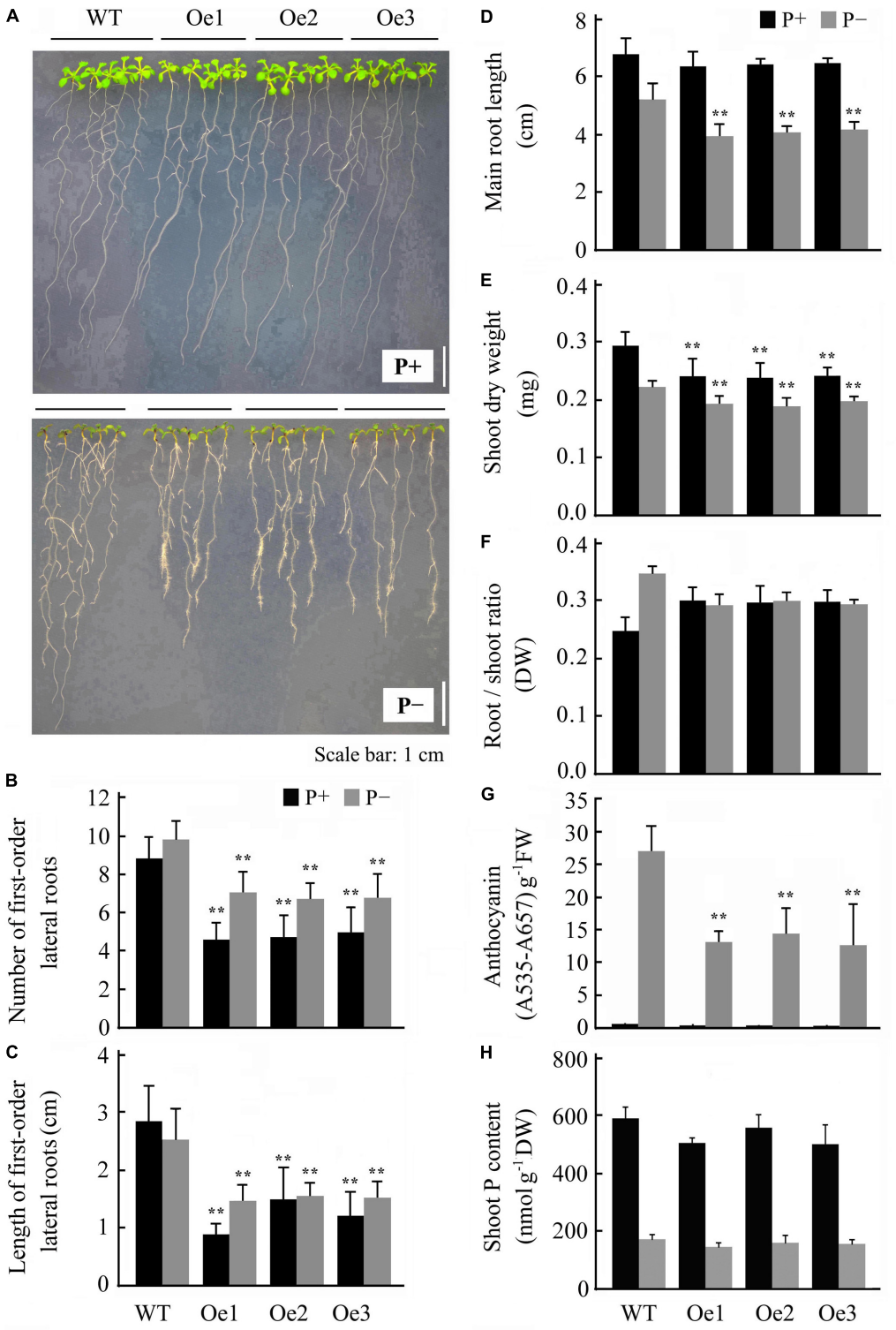

FIGURE 4 | Overexpression of *JcERF035* modulates morphophysiological traits in Arabidopsis under Pi deficiency (P−) conditions at each time. Seedlings were germinated on 1/2 MS plus 1% sucrose medium for 4 days and then transferred to vertically oriented agar plates containing Pi-sufficient (P+) and P− media for 7 days. **(A)** Seedlings grown in P+ and P− agar plates. **(B,C)** Number **(B)** and total length **(C)** of first-order lateral roots. Values are means of $n = 20 \pm$ SD (Duncan test: $^{**}P < 0.01$). **(D)** Primary root length. Values are means of $n = 20 \pm$ SD (Duncan test: $^{**}P < 0.01$). **(E,F)** Dry weights of shoots **(E)** and root–shoot ratios **(F)**. Values are means of $n = 20 \pm$ SD (Duncan test: $^{**}P < 0.01$). **(G,H)** Shoot anthocyanin contents **(G)** and Pi contents **(H)** of seedlings grown on agar plates. Values are means of $n = 3 \pm$ SD (Duncan test: $^{**}P < 0.01$). Asterisks indicate significant differences between transgenic and wild type seedlings under the same growth conditions. DW, dry weight; FW, fresh weight.

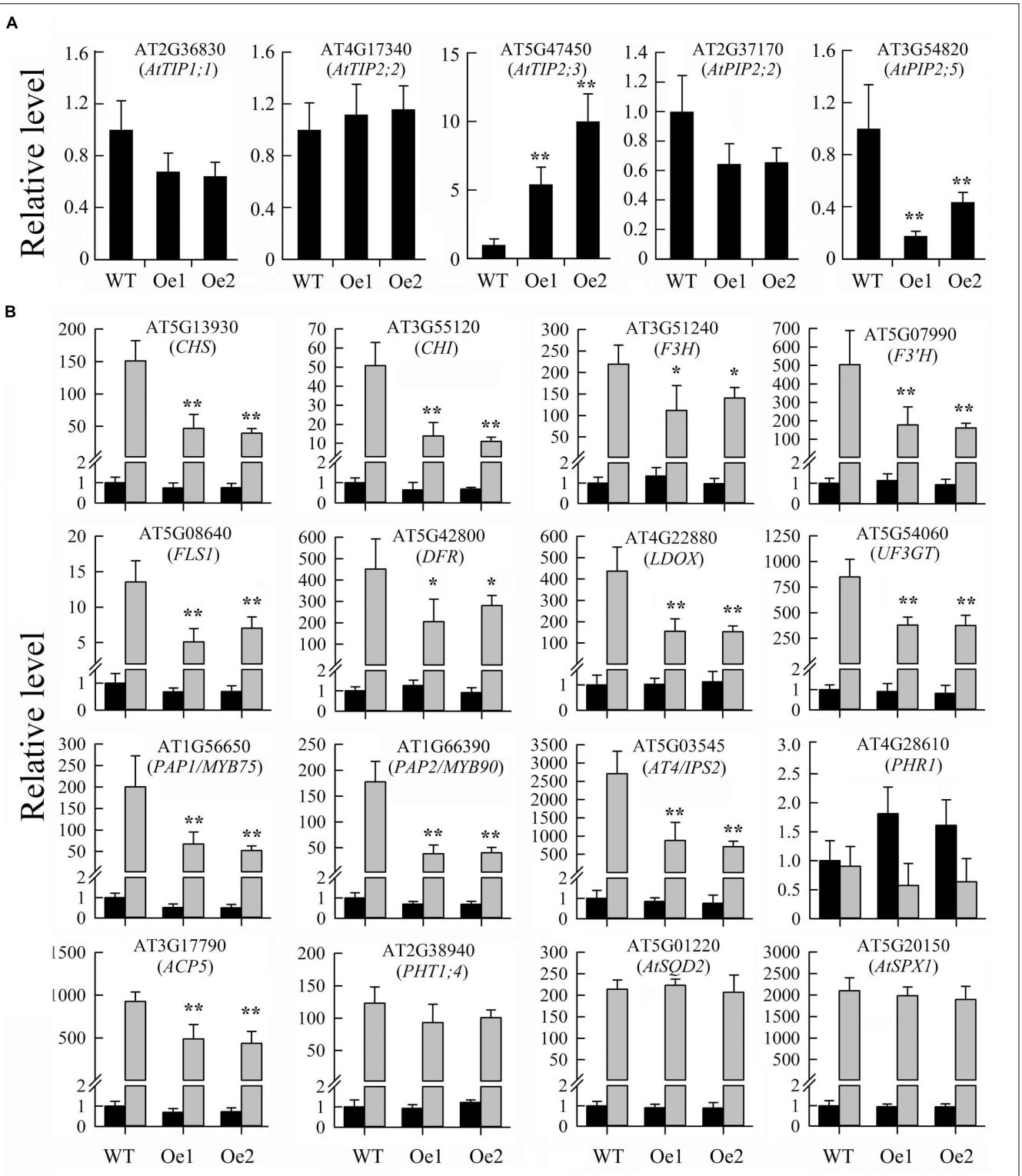

FIGURE 5 | Results of quantitative real-time PCR analysis of gene expression levels in shoots of *OeJcERF035* seedlings: **(A)** Aquaporin genes, and **(B)** anthocyanin biosynthesis-related genes and some PSI genes. Wild-type (WT) and *JcERF035* overexpressing (Oe1 and Oe2) plants were germinated on half-strength MS medium for 5 d, then transferred to vertically oriented agar petri plates containing Pi-sufficient (P+) and Pi-deficient (P–) media for 7 days. Whole shoots were harvested and used for quantitative real-time PCR analysis to determine relative expression levels of genes in the wild type and transgenic lines. The Arabidopsis *AtActin2* (At3g18780) gene was used as a loading control. Expression values for all genes in wild-type plants under P+ conditions were set at 1. Values shown are means ± standard deviations from three biological replicates, each with two technical replicates. Asterisks indicate significant differences between transgenic and wild type seedlings e under the same growth conditions (Duncan test: $*P < 0.05$; $**P < 0.01$). Black columns = P+, gray columns = P–.

expression levels of most genes tested were significantly lower in *OeJcERF035* shoots than in wild-type shoots under Pi starvation conditions (**Figure 5**). These results suggest that the *JcERF035* gene is involved in suppression of Pi starvation-mediated anthocyanin biosynthesis in Arabidopsis.

Next, we analyzed expression levels of several PSI genes. Expression levels of phosphate transporter 1;4 (*PHT1;4*, At2g38940), *PHR1* (At4g28610), sulfoquinovosyldiacylglycerol 2 (*AtSQD2*, At5g01220), and *ATSPX1* (At5g20150) genes were not significantly affected. However, expression levels of *IPS2*/*AT4* (At5g03545) and purple acid phosphatase 17 (*ATPAP17*/*ATACP5*, At3g17790) genes were significantly lower in *OeJcERF035* shoots than in wild-type shoots under Pi starvation conditions (**Figure 5**). These results indicate that the *JcERF035* gene influences the expression of some, but not all, PSI genes in Arabidopsis.

DISCUSSION

Results of this study reveal molecular-level responses of physic nut roots and leaves to Pi deficiency. As reported in rice and Arabidopsis, many of the affected genes play roles in general metabolism. In roots, genes related to Pi release from soil, Pi uptake and transportation, lipid metabolism and the glycolytic bypass were most affected by Pi deficiency. In leaves, genes involved in membrane lipid and fatty acid metabolic pathways and the glycolytic bypass were most affected. In addition, genes involved in Pi transport and phosphatase-encoding genes were affected by Pi deficiency in both roots and leaves. Moreover, many genes involved in cell wall synthesis, cell wall extension and cell expansion were severely down-regulated in physic nut leaves by Pi deficiency. This is consistent with observed reductions in the size of plants' shoots under Pi deficiency. The responses in expression of the *IPS*, miR399, and SPX family genes to Pi deficiency in physic nut were similar to those observed in rice and Arabidopsis (Bari et al., 2006; Secco et al., 2012), suggesting that the miR399/PHO2 inorganic phosphate homeostasis control network is also present in the woody plant physic nut. In Arabidopsis and rice leaves, genes involved in photosynthesis and general carbon metabolism are strongly influenced by Pi deficiency (Wasaki et al., 2006; Müller et al., 2007; Morcuende et al., 2007). We found that few photosynthesis and general carbon metabolism genes were severely influenced by low Pi in physic nut leaves, suggesting that physic nut is less sensitive to Pi starvation than rice and Arabidopsis.

Several differentially regulated genes encoding TFs that may contribute to transcriptional regulation of other genes under low Pi stress have been reported in Arabidopsis, rice, and other plants. In addition, several functionally characterized TFs have shown to be distinguishingly regulated under different Pi concentrations. They were involved in a number of morphological processes responding to Pi availability and in regulating the expression levels of some Pi starvation induced (PSI) genes. In this study, we found that the expression level of *JcERF035* was down-regulated under Pi deficiency (**Figure 2**), indicating that this gene may play a role in Pi nutrition stress responses. Overexpression of *JcERF035* did not seriously inhibit the growth and development of Arabidopsis plants under P+ conditions. Although the *JcERF035*-overexpressing lines displayed some reductions in number and length of lateral roots and shoot biomass (ca. 20%), their primary root lengths, flowering times, and inflorescence lengths were similar to those of wild-type plants. In sharp contrast, in *AtERF070* and *AtMYB62* overexpression lines the primary root length is also reduced and growth is seriously affected according to Devaiah et al. (2009) and Ramaiah et al. (2014).

To decipher the role of *JcERF035* in regulation of Pi starvation responses, three independent *OeJcERF035* Arabidopsis lines were analyzed. Appropriate alterations in root architecture are critical for plant to efficiently absorb and utilize the Pi in soil. The reductions in primary root length, proliferation of both lateral roots and root hairs close to the root apical meristem are typical responses of wild type Arabidopsis plants to Pi starvation (Williamson et al., 2001; Linkohr et al., 2002). The *OeJcERF035* Arabidopsis lines displayed reductions in primary root length, first-order lateral root number and length. Nevertheless, shoots of the *OeJcERF035* lines had similar Pi contents to those of wild-type plants under both P+ and P− conditions, possibly because *OeJcERF035* seedlings had more root hairs than the wild-type seedlings.

Root systems of diverse plant species are more branched and have higher root/shoot ratios under Pi-deficiency than under Pi-sufficiency. These changes in root architecture help to increase root systems' capacities for soil exploration. We found that physic nut plants under P− conditions had 3.78 ± 0.08% lower shoot dry weights than P+ controls, but 9.95 ± 0.21% higher root dry weights. Thus, *JcERF035* may suppress lateral root development, and its down-regulation may promote increases in root system of physic nut plants grown under low Pi conditions, thereby enhancing their soil exploration capacity.

Although the *OeJcERF035* shoots had similar Pi contents to the wild-type shoots, they exhibited less anthocyanin accumulation under P− conditions. Expression levels of genes related to anthocyanin biosynthesis and its regulation, and some PSI genes, were also lower in *OeJcERF035* shoots than in wild-type shoots under P− conditions. These results imply that *JcERF035* might affect these processes independently of Pi content. Pi content-independent anthocyanin accumulation has also been observed in the *bhlh32* mutant of Arabidopsis, which has elevated Pi and anthocyanin contents under Pi-sufficient conditions (Chen et al., 2007). Genes involved in flavonoid and anthocyanin biosynthesis are up-regulated in aerial tissues of P-deficient plants (Hammond et al., 2003; Uhde-Stone et al., 2003; Wu et al., 2003). The accumulation of anthocyanins in the aerial tissues is a characteristic response of P-deficient plants, which is thought to protect nucleic acids from UV damage and chloroplasts from photoinhibitory damage caused by P-limited photosynthesis (Hoch et al., 2001). The down-regulation of the *JcERF035* gene in physic nut leaves might contribute to the biosynthesis and accumulation of flavonoids and anthocyanins in aerial tissues of plants grown under low Pi conditions.

The *JcERF035* gene is a member of subgroup 1b of the ERF family (group A6 of the DREB subfamily) (Tang et al., 2016).

Arabidopsis has eight genes (known as *RAP2.4* genes) assigned to subgroup 1b: ATWIND 1–4, At1g64380, At2g22200, At4g13620, and At4g39780 (Nakano et al., 2006). Products of the *RAP2.4* genes participate in cell dedifferentiation, water balance and oxidative stress responses (Lin R.C. et al., 2008; Iwase et al., 2011; Rae et al., 2011; Zhu et al., 2014; Rudnik et al., 2017). Constitutive overexpression of At1g78080 causes defects in numerous developmental processes regulated by light and ethylene, including root elongation and root hair formation (Lin R.C. et al., 2008). Our previous work revealed that expression of *JcERF035* was down-regulated in physic nut leaves under salinity stress, and its expression in rice reduced expression of GA biosynthesis genes but increased the transgenic seedlings' sensitivity to salt stress (Tang et al., 2017). Similar to the phenotype of overexpressing *JcERF035* rice seedlings, *OeJcERF035* enhanced the sensitivity of transgenic seedlings to the salt stress (**Supplementary Figure S3**). The *OeJcERF035* lines did not show any greater drought tolerance than wild-type controls (data not shown), nor any increase in expression levels of most aquaporin genes. In contrast, overexpression of WIND genes can increase expression levels of most aquaporin genes (Rae et al., 2011; Zhu et al., 2014). These results suggest that the *JcERF035* gene product functions differently from ATWIND in plants. Whether the WIND genes play roles in anthocyanin accumulation in aerial tissues under phosphate starvation conditions in Arabidopsis remains to be studied.

CONCLUSION

The presented study has identified genes with diverse functions that appear to play important roles in adaptations of physic nut to Pi deficiency. The data obtained in this study expand available information on the regulatory and signaling pathways involved in Pi deficiency responses of plants, and should assist elucidation of the molecular basis of adaptation of plants to this stress. The *JcERF035* gene suppresses lateral root formation and phosphate starvation-induced anthocyanin accumulation in leaves. Thus, its down-regulation may promote increases in the root system and anthocyanin accumulation in aerial tissues of physic nut plants under phosphate starvation conditions. Our results indicated that a variety of adaptive changes help plants to cope with Pi deficiency, including induction of genes involved in positive regulatory responses and suppression of genes involved in physiological processes that must be inhibited to avoid Pi depletion.

AUTHOR CONTRIBUTIONS

The research was designed by GW, HJ, YpC, and ML. The experiments were performed by YbC, PW, QZ, and YT, and the data were analyzed by YbC and PW. The manuscript was written by YbC.

FUNDING

This work was supported by funding from the Biological Resources Service Network (Grant No. kfj-brsn-2018-6-008).

SUPPLEMENTARY MATERIAL

The Supplementary Material for this article can be found online at: https://www.frontiersin.org/articles/10.3389/fpls.2018.01186/full#supplementary-material

FIGURE S1 | Sequencing saturation analysis of physic nut roots and leaves under Pi-deficiency (P−) and Pi-sufficient (P+) conditions after treatment for 2 or 16 days.

FIGURE S2 | Results of real-time PCR analysis of changes in expression ratios of the Pi-inducible genes in physic nut leaves and roots after Pi deficiency for 2 and 16 days. The results are based on calculations using two independent loading controls, *JcActin* and H(+)-ATPase, that had steady levels of transcripts in various tissues of physic nut. Since the results of using both loading controls were consistent, results obtained using the *JcActin* gene are presented. Fold changes indicate ratios of expression levels under P− conditions to those recored under P+ conditions at each time point.

FIGURE S3 | *JcERF035* over-expressing plants are more sensitive to salt stress. For salt stress tests, 6-day-old wild-type and transgenic Arabidopsis seedlings were transferred to absorbent cotton infiltrated with Hoagland nutrient solution containing 0 mM (mock), or 150 mM NaCl in glass bottles. Ten days after transfer, the seedlings were photographed **(A)** and the fresh weights of their shoots were measured **(B)**.

TABLE S1 | Primers used in this study.

TABLE S2 | The genes most strongly (≥3-fold) differentially expressed in roots **(A)** and leaves **(B)** under Pi-deficiency 2 and 16 days after the onset of treatment.

TABLE S3 | Expression levels of genes (TPM) involved in Pi homeostasis after 2 and 16 days of the P− and P+ treatments.

REFERENCES

Bari, R., Datt Pant, B., Stitt, M., and Scheible, W. R. (2006). PHO2, microRNA399, and PHR1 define a phosphate-signaling pathway in plants. *Plant Physiol.* 141, 988–999. doi: 10.1104/pp.106.079707

Bates, T. R., and Lynch, J. P. (1996). Stimulation of root hair elongation in *Arabidopsis thaliana* by low phosphorous availability. *Plant Cell Environ.* 19, 529–538. doi: 10.1111/j.1365-3040.1996.tb00386.x

Calderon-Vazquez, C., Ibarra-Laclette, E., Caballero-Perez, J., and Herrera-Estrella, L. (2008). Transcript profiling of *Zea mays* roots reveals gene responses to phosphate deficiency at the plant- and species-specific levels. *J. Exp. Bot.* 59, 2479–2497. doi: 10.1093/jxb/ern115

Chen, Y. F., Li, L. Q., Xu, Q., Kong, Y. H., Wang, H., and Wu, W. H. (2009). The WRKY6 transcription factor modulates PHOSPHATE1 expression in response to low Pi stress in *Arabidopsis*. *Plant Cell* 21, 3554–3566. doi: 10.1105/tpc.108.064980

Chen, Z. H., Nimmo, G. A., Jenkins, G. I., and Nimmo, H. G. (2007). BHLH32 modulates several biochemical and morphological processes that respond to Pi starvation in *Arabidopsis*. *Biochem. J.* 405, 191–198. doi: 10.1042/BJ20070102

Chiou, T. J., and Lin, S. I. (2011). Signaling network in sensing phosphate availability in plants. *Annu. Rev. Plant Biol.* 62, 185–206. doi: 10.1146/annurev-arplant-042110-103849

Clough, S. J., and Bent, A. F. (1998). Floral dip: a simplified method for *Agrobacterium*-mediated transformation of *Arabidopsis*

thaliana. *Plant J.* 16, 735–743. doi: 10.1046/j.1365-313x.1998.00343.x

Dai, X., Wang, Y., Yang, A., and Zhang, W. H. (2012). OsMYB2P-1, an R2R3 MYB transcription factor, is involved in the regulation of phosphate-starvation responses and root architecture in rice. *Plant Physiol.* 159, 169–183. doi: 10.1104/pp.112.194217

Dai, X., Wang, Y., and Zhang, W. H. (2016). OsWRKY74, a WRKY transcription factor, modulates tolerance to phosphate starvation in rice. *J. Exp. Bot.* 67, 947–960. doi: 10.1093/jxb/erv515

Devaiah, B. N., Karthikeyan, A. S., and Raghothama, K. G. (2007a). WRKY75 transcription factor is a modulator of phosphate acquisition and root development in *Arabidopsis*. *Plant Physiol.* 143, 1789–1801. doi: 10.1104/pp.106.093971

Devaiah, B. N., Madhuvanthi, R., Karthikeyan, A. S., and Raghothama, K. G. (2009). Phosphate starvation responses and gibberellic acid biosynthesis are regulated by the MYB62 transcription factor in *Arabidopsis*. *Mol. Plant* 2, 43–58. doi: 10.1093/mp/ssn081

Devaiah, B. N., Nagarajan, V. K., and Raghothama, K. G. (2007b). Phosphate homeostasis and root development in *Arabidopsis* are synchronized by the zinc finger transcription factor ZAT6. *Plant Physiol.* 145, 147–159. doi: 10.1104/pp.107.101691

Dhillon, R. S., Hooda, M. S., Jattan, M., Chawla, V., Bhardwaj, M., and Goyal, S. C. (2009). Development and molecular characterization of interspecific hybrids of *Jatropha curcas* x *J. integerrima*. *Indian J. Biotechnol.* 8, 3 84–390.

Duncan, D. B. (1955). Multiple range and multiple F tests. *Biometrics* 11, 1–42. doi: 10.2307/3001478

Gubitz, G. M., Mittelbach, M., and Trabi, M. (1999). Exploitation of the tropical oil seed plant *Jatropha curcas* L. *Bioresour. Technol.* 67, 73–82. doi: 10.1016/S0960-8524(99)00069-3

Guo, M., Ruan, W., Li, C., Huang, F., Zeng, M., Liu, Y., et al. (2015). Integrative comparison of the role of the PHR1 subfamily in phosphate signaling and homeostasis in rice. *Plant Physiol.* 168, 1762–1776. doi: 10.1104/pp.15.00736

Hammond, J. P., Bennett, M. J., Bowen, H. C., Broadley, M. R., Eastwood, D. C., May, S. T., et al. (2003). Changes in gene expression in Arabidopsis shoots during phosphate starvation and the potential for developing smart plants. *Plant Physiol.* 132, 578–596. doi: 10.1104/pp.103.020941

Hoch, W. A., Zeldin, E. L., and McCown, B. H. (2001). Physiological significance of anthocyanins during autumnal leaf senescence. *Tree Physiol.* 21, 1–8. doi: 10.1093/treephys/21.1.1

Iwase, A., Mitsuda, N., Koyama, T., Hiratsu, K., Kojima, M., Arai, T., et al. (2011). The AP2/ERF transcription factor WIND1 controls cell dedifferentiation in *Arabidopsis*. *Curr. Biol.* 21, 508–514. doi: 10.1016/j.cub.2011.02.020

Lata, C., and Prasad, M. (2011). Role of DREBs in regulation of abiotic stress responses in plants. *J. Exp. Bot.* 62, 4731–4748. doi: 10.1093/jxb/err210

Li, L., Liu, C., and Lian, X. (2010). Gene expression profiles in rice roots under low phosphorus stress. *Plant Mol. Biol.* 72, 423–432. doi: 10.1007/s11103-009-9580-0

Liao, X., Guo, X., Wang, Q., Wang, Y., Zhao, D., Yao, L., et al. (2017). Overexpression of MsDREB6.2 results in cytokinin-deficient developmental phenotypes and enhances drought tolerance in transgenic apple plants. *Plant J.* 89, 510–526. doi: 10.1111/tpj.13401

Lin, R. C., Park, H. J., and Wang, H. Y. (2008). Role of *Arabidopsis* RAP2.4 in regulating light- and ethylene-mediated developmental processes and drought stress tolerance. *Mol. Plant* 1, 42–57. doi: 10.1093/mp/ssm004

Lin, S. I., Chiang, S. F., Lin, W. Y., Chen, J. W., Tseng, C. Y., Wu, P. C., et al. (2008). Regulatory network of microRNA399 and PHO2 by systemic signaling. *Plant Physiol.* 147, 732–746. doi: 10.1104/pp.108.116269

Linkohr, B. I., Williamson, L. C., Fitter, A. H., and Leyser, H. M. (2002). Nitrate and phosphate availability and distribution have different effects on root system architecture of *Arabidopsis*. *Plant J.* 29, 751–760. doi: 10.1046/j.1365-313X.2002.01251.x

Liu, H., Yang, H., Wu, C., Feng, J., Liu, X., Qin, H., et al. (2009). Overexpressing HRS1 confers hypersensitivity to low phosphate-elicited inhibition of primary root growth in *Arabidopsis thaliana*. *J. Integr. Plant Biol.* 51, 382–392. doi: 10.1111/j.1744-7909.2009.00819.x

Liu, X. Q., Liu, C. Y., Guo, Q., Zhang, M., Cao, B. N., Xiang, Z. H., et al. (2015). Mulberry transcription factor MnDREB4A confers tolerance to multiple abiotic stresses in transgenic tobacco. *PLoS One* 10:e0145619. doi: 10.1371/journal.pone.0145619

Marschner, H. (1995). *Mineral Nutrition of Higher Plants*. London: Academic Press.

Misson, J., Raghothama, K. G., Jain, A., Jouhet, J., Block, M. A., Bligny, R., et al. (2005). A genome-wide transcriptional analysis using *Arabidopsis thaliana* Affymetrix gene chips determined plant responses to phosphate deprivation. *Proc. Natl. Acad. Sci. U.S.A.* 102, 11934–11939. doi: 10.1073/pnas.0505266102

Morcuende, R., Bari, R., Gibon, Y., Zheng, W., Pant, B. D., Bläsing, O., et al. (2007). Genome-wide reprogramming of metabolism and regulatory networks of *Arabidopsis* in response to phosphorus. *Plant Cell Environ.* 30, 85–112. doi: 10.1111/j.1365-3040.2006.01608.x

Müller, R., Morant, M., Jarmer, H., Nilsson, L., and Nielsen, T. H. (2007). Genome-wide analysis of the *Arabidopsis* leaf transcriptome reveals interaction of phosphate and sugar metabolism. *Plant Physiol.* 143, 156–171. doi: 10.1104/pp.106.090167

Nagarajan, V. K., Satheesh, V., Poling, M. D., Raghothama, K. G., and Jain, A. (2016). *Arabidopsis* MYB-Related HHO2 exerts a regulatory influence on a subset of root traits and genes governing phosphate homeostasis. *Plant Cell Physiol.* 57, 1142–1152. doi: 10.1093/pcp/pcw063

Nakano, T., Suzuki, K., Fujimura, T., and Shinshi, H. (2006). Genome-wide analysis of the ERF gene family in *Arabidopsis* and rice. *Plant Physiol.* 140, 411–432. doi: 10.1104/pp.105.073783

Parthiban, K. T., Kumar, R. S., Thiyagarajan, P., Subbulakshmi, V., Vennila, S., and Rao, M. G. (2009). Hybrid progenies in Jatropha - a new development. *Curr. Sci. India* 96, 815–823.

Péret, B., Clément, M., Nussaume, L., and Desnos, T. (2011). Root developmental adaptation to phosphate starvation: better safe than sorry. *Trends Plant Sci.* 16, 442–450. doi: 10.1016/j.tplants.2011.05.006

Plaxton, W. C., and Tran, H. T. (2011). Metabolic adaptations of phosphate-starved plants. *Plant Physiol.* 156, 1006–1015. doi: 10.1104/pp.111.175281

Rabino, I., and Mancinelli, A. L. (1986). Light, temperature, and anthocyanin production. *Plant Physiol.* 81, 922–924. doi: 10.1104/pp.81.3.922

Rae, L., Lao, N. T., and Kavanagh, T. A. (2011). Regulation of multiple aquaporin genes in *Arabidopsis* by a pair of recently duplicated DREB transcription factors. *Planta* 234, 429–444. doi: 10.1007/s00425-011-1414-z

Raghothama, K. G. (1999). Phosphate acquisition. *Annu. Rev. Plant Physiol. Plant Mol. Biol.* 50, 665–693. doi: 10.1146/annurev.arplant.50.1.665

Ramaiah, M., Jain, A., and Raghothama, K. G. (2014). Ethylene response factor070 regulates root development and phosphate starvation-mediated responses. *Plant Physiol.* 164, 1484–1498. doi: 10.1104/pp.113.231183

Rehman, S., and Mahmood, T. (2015). Functional role of DREB and ERF transcription factors: regulating stress-responsive network in plants. *Acta Physiol. Plant* 37:178. doi: 10.1007/s11738-015-1929-1

Rubio, V., Linhares, F., Solano, R., Martín, A. C., Iglesias, J., Leyva, A., et al. (2001). A conserved MYB transcription factor involved in phosphate starvation signaling both in vascular plants and in unicellular algae. *Genes Dev.* 15, 2122–2133. doi: 10.1101/gad.204401

Rudnik, R., Bulcha, J. T., Reifschneider, E., Ellersiek, U., and Baier, M. (2017). Specificity versus redundancy in the RAP2.4 transcription factor family of *Arabidopsis thaliana*: transcriptional regulation of genes for chloroplast peroxidases. *BMC Plant Biol.* 17:144. doi: 10.1186/s12870-017-1092-5

Secco, D., Wang, C., Arpat, B. A., Wang, Z., Poirier, Y., Tyerman, S. D., et al. (2012). The emerging importance of the SPX domain-containing proteins in phosphate homeostasis. *New Phytol.* 193, 842–851. doi: 10.1111/j.1469-8137.2011.04002.x

Su, T., Xu, Q., Zhang, F. C., Chen, Y., Li, L. Q., Wu, W. H., et al. (2015). WRKY42 modulates phosphate homeostasis through regulating phosphate translocation and acquisition in *Arabidopsis*. *Plant Physiol.* 167, 1579–1591. doi: 10.1104/pp.114.253799

Tang, Y., Liu, K., Zhang, J., Li, X., Xu, K., Zhang, Y., et al. (2017). JcDREB2, a physic nut AP2/ERF gene, alters plant growth and salinity stress

responses in transgenic rice. *Front. Plant Sci.* 8:306. doi: 10.3389/fpls.2017.00306

Tang, Y., Qin, S., Guo, Y., Chen, Y., Wu, P., Chen, Y., et al. (2016). Genome-wide analysis of the AP2/ERF gene family in physic nut and overexpression of the JcERF011 gene in rice increased its sensitivity to salinity stress. *PLoS One* 11:e0150879. doi: 10.1371/journal.pone.0150879

Thibaud, M. C., Arrighi, J. F., Bayle, V., Chiarenza, S., Creff, A., Bustos, R., et al. (2010). Dissection of local and systemic transcriptional responses to phosphate starvation in *Arabidopsis*. *Plant J.* 64, 775–789. doi: 10.1111/j.1365-313X.2010.04375.x

Uhde-Stone, C., Zinn, K. E., Ramirez-Yáñez, M., Li, A., Vance, C. P., and Allan, D. L. (2003). Nylon filter arrays reveal differential gene expression in proteoid roots of white lupin in response to phosphorus deficiency. *Plant Physiol.* 131, 1064–1079. doi: 10.1104/pp.102.016881

Vance, C. P., Uhde-Stone, C., and Allan, D. L. (2003). Phosphorus acquisition and use: critical adaptations by plants for securing a nonrenewable resource. *New Phytol.* 157, 423–447. doi: 10.1046/j.1469-8137.2003.00695.x

Wang, H., Xu, Q., Kong, Y. H., Chen, Y., Duan, J. Y., Wu, W. H., et al. (2014). *Arabidopsis* WRKY45 transcription factor activates PHOSPHATE TRANSPORTER1;1 expression in response to phosphate starvation. *Plant Physiol.* 164, 2020–2029. doi: 10.1104/pp.113.235077

Wasaki, J., Shinano, T., Onishi, K., Yonetani, R., Yazaki, J., Fujii, F., et al. (2006). Transcriptomic analysis indicates putative metabolic changes caused by manipulation of phosphorus availability in rice leaves. *J. Exp. Bot.* 57, 2049–2059. doi: 10.1093/jxb/erj158

Wasaki, J., Yonetani, R., Kuroda, S., Shinano, T., Yazaki, J., Fujii, F., et al. (2003). Transcriptomic analysis of metabolic changes by phosphorus stress in rice plant roots. *Plant Cell Environ.* 26, 1515–1523. doi: 10.1046/j.1365-3040.2003.01074.x

Williamson, L. C., Ribrioux, S. P., Fitter, A. H., and Leyser, H. M. (2001). Phosphate availability regulates root system architecture in *Arabidopsis*. *Plant Physiol.* 126, 875–882. doi: 10.1104/pp.126.2.875

Wu, P., Ma, L., Hou, X., Wang, M., Wu, Y., Liu, F., et al. (2003). Phosphate starvation triggers distinct alterations of genome expression in Arabidopsis roots and leaves. *Plant Physiol.* 132, 1260–1271. doi: 10.1104/pp.103.021022

Wu, P., Zhou, C., Cheng, S., Wu, Z., Lu, W., Han, J., et al. (2015). Integrated genome sequence and linkage map of physic nut (*Jatropha curcas* L.), a biodiesel plant. *Plant J.* 81, 810–821. doi: 10.1111/tpj.12761

Wu, Z., Xu, X., Xiong, W., Wu, P., Chen, Y., Li, M., et al. (2015). Genome-wide analysis of the NAC gene family in physic nut (*Jatropha curcas* L.). *PLoS One* 10:e0131890. doi: 10.1371/journal.pone.0131890

Wu, Z. Y., Wu, P. Z., Chen, Y. P., Li, M. R., Wu, G. J., and Jiang, H. W. (2015). Genome-wide analysis of the GRAS gene family in physic nut (*Jatropha curcas* L.). *Genet. Mol. Res.* 14, 19211–19224. doi: 10.4238/2015.December.29.31

Xiong, W., Xu, X., Zhang, L., Wu, P., Chen, Y., Li, M., et al. (2013). Genome-wide analysis of the WRKY gene family in physic nut (*Jatropha curcas* L.). *Gene* 524, 124–132. doi: 10.1016/j.gene.2013.04.047

Yang, G., Yu, L., Zhang, K., Zhao, Y., Guo, Y., and Gao, C. (2017). A ThDREB gene from *Tamarix hispida* improved the salt and drought tolerance of transgenic tobacco and *T. hispida*. *Plant Physiol. Biochem.* 113, 187–197. doi: 10.1016/j.plaphy.2017.02.007

Yang, W. T., Baek, D., Yun, D. J., Hwang, W. H., Park, D. S., Nam, M. H., et al. (2014). Overexpression of OsMYB4P, an R2R3-type MYB transcriptional activator, increases phosphate acquisition in rice. *Plant Physiol. Biochem.* 80, 259–267. doi: 10.1016/j.plaphy.2014.02.024

Yi, K., Wu, Z., Zhou, J., Du, L., Guo, L., Wu, Y., et al. (2005). OsPTF1, a novel transcription factor involved in tolerance to phosphate starvation in rice. *Plant Physiol.* 138, 2087–2096. doi: 10.1104/pp.105.063115

Zeng, X. Q., Chow, W. S., Su, L. J., Peng, X. X., and Peng, C. L. (2010). Protective effect of supplemental anthocyanins on *Arabidopsis* leaves under high light. *Physiol. Plant.* 138, 215–225. doi: 10.1111/j.1399-3054.2009.01316.x

Zhang, L., Zhang, C., Wu, P., Chen, Y., Li, M., Jiang, H., et al. (2014). Global analysis of gene expression profiles in physic nut (*Jatropha curcas* L.) seedlings exposed to salt stress. *PLoS One* 9:e97878. doi: 10.1371/journal.pone.0097878

Zhao, Q., Zhang, L., Zhu, S., Zhang, S., Wu, P., Chen, Y., et al. (2012). Effects of several abiotic stresses on photosynthetic rate and other physiological indexes in *Jatropha curcas* L. seedlings. *J. Trop. Subtrop. Bot.* 20, 432–438.

Zhou, C., Chen, Y., Wu, Z., Lu, W., Han, J., Wu, P., et al. (2015). Genome-wide analysis of the MYB gene family in physic nut (*Jatropha curcas* L.). *Gene* 572, 63–71. doi: 10.1016/j.gene.2015.06.072

Zhou, J., Jiao, F., Wu, Z., Li, Y., Wang, X., He, X., et al. (2008). OsPHR2 is involved in phosphate-starvation signaling and excessive phosphate accumulation in shoots of plants. *Plant Physiol.* 146, 1673–1686. doi: 10.1104/pp.107.111443

Zhou, X., Zha, M., Huang, J., Li, L., Imran, M., and Zhang, C. (2017). StMYB44 negatively regulates phosphate transport by suppressing expression of PHOSPHATE1 in potato. *J. Exp. Bot.* 68, 1265–1281. doi: 10.1093/jxb/erx026

Zhu, D., Wu, Z., Cao, G., Li, J., Wei, J., Tsuge, T., et al. (2014). TRANSLUCENT GREEN, an ERF family transcription factor, controls water balance in *Arabidopsis* by activating the expression of aquaporin genes. *Mol. Plant* 7, 601–615. doi: 10.1093/mp/sst152

Conflict of Interest Statement: The authors declare that the research was conducted in the absence of any commercial or financial relationships that could be construed as a potential conflict of interest.

The reviewer LC declared a shared affiliation, though no other collaboration, with several of the authors YbC, QZ, and YT to the handling Editor.

frontiers in Plant Science

ORIGINAL RESEARCH
published: 01 October 2018
doi: 10.3389/fpls.2018.01432

Functional Characterization of Arabidopsis PHL4 in Plant Response to Phosphate Starvation

*Zhen Wang, Zai Zheng, Li Song and Dong Liu**

MOE Key Laboratory of Bioinformatics, Center for Plant Biology, School of Life Sciences, Tsinghua University, Beijing, China

Plants have evolved an array of adaptive responses to cope with phosphate (Pi) starvation. These responses are mainly controlled at the transcriptional level. In Arabidopsis, PHR1, a member of the MYB-CC transcription factor family, is a key component of the central regulatory system controlling plant transcriptional responses to Pi starvation. Its homologs in the MYB-CC family, PHL1 (PHR1-LIKE 1), PHL2, and perhaps also PHL3, act redundantly with PHR1 to regulate plant Pi starvation responses. The functions of PHR1's closest homolog in this family, PHL4, however, have not been characterized due to the lack of its null mutant. In this work, we generated two *phl4* null mutants using the CRISPR/Cas9 technique and investigated the functions of PHL4 in plant responses to Pi starvation. The results indicated that the major developmental, physiological, and molecular responses of the *phl4* mutants to Pi starvation did not significantly differ from those of the wild type. By comparing the phenotypes of the *phr1* single mutant and *phr1phl1* and *phr1phl4* double mutants, we found that PHL4 also acts redundantly with PHR1 to regulate plant Pi responses, but that its effects are weaker than those of PHL1. We also found that the overexpression of *PHL4* suppresses plant development under both Pi-sufficient and -deficient conditions. Taken together, the results indicate that PHL4 has only a minor role in the regulation of plant responses to Pi starvation and is a negative regulator of plant development.

Keywords: PHL4, PHR1, Pi starvation responses, functional redundancy, plant development

OPEN ACCESS

Edited by:
Vagner A. Benedito,
West Virginia University, United States

Reviewed by:
Oswaldo Valdes-Lopez,
Universidad Nacional Autónoma de México, Mexico
Anita Maribel Arenas,
Universidad Austral de Chile, Chile

***Correspondence:**
Dong Liu
liu-d@tsinghua.edu.cn

Specialty section:
This article was submitted to Plant Nutrition, a section of the journal Frontiers in Plant Science

Received: *10 April 2018*
Accepted: *10 September 2018*
Published: *01 October 2018*

Citation:
Wang Z, Zheng Z, Song L and Liu D (2018) Functional Characterization of Arabidopsis PHL4 in Plant Response to Phosphate Starvation. Front. Plant Sci. 9:1432. doi: 10.3389/fpls.2018.01432

INTRODUCTION

Phosphorus (P) is an essential nutrient for all organisms. Phosphate (Pi), the major form of P that plants uptake, however, is quite limiting in soil, often resulting in Pi deficiency in natural ecosystems and agricultural lands (Raghothama, 2000; Nussaume et al., 2011). As sessile organisms, plants have evolved sophisticated strategies to cope with this nutritional stress. When grown under Pi starvation conditions, plants trigger a suite of developmental and metabolic responses in order to sustain their growth and development. Some major adaptive responses include the remodeling of root architecture, i.e., the arrest of primary root growth and the enhanced production of lateral roots and root hairs, the increased activity of high-affinity Pi transporters on the root surface, the induction and secretion of acid phosphatases (APases), and the accumulation of anthocyanins and starches in leaves (Yuan and Liu, 2008; López-Arredondo et al., 2014).

Numerous transcriptomic studies have demonstrated that underlying these developmental and metabolic changes are changes in the levels of a large number of transcripts which include coding genes, microRNAs, and long non-coding RNAs (Hammond et al., 2003; Wu et al., 2003; Misson et al., 2005; Morcuende et al., 2006; Hernández et al., 2007; Müller et al., 2007; Lundmark et al., 2010; O'Rourke et al., 2013; Secco et al., 2013; Yuan et al., 2016). Therefore, a fundamental question about the molecular mechanism that controls plant responses to Pi starvation is "How are the Pi starvation-induced (PSI) transcriptional changes regulated?" Over the last 20 years, this complicated mechanism has been extensively studied (Puga et al., 2017; Wang et al., 2018). In Arabidopsis, Rubio et al. (2001) identified PHR1 (PHOSPHATE STARVATION RESPONSE 1) as the central regulator of plant transcriptional responses to Pi starvation. PHR1 belongs to a MYB-CC protein family that contains 15 members (Bustos et al., 2010) (**Figure 1A**). The proteins in this family share a MYB domain for DNA-binding and a coiled-coil domain that is involved in protein-protein interactions. PHR1 is a transcription factor, and its mRNA and protein levels are not responsive to changes in Pi availability in the environment (Rubio et al., 2001). PHR1 binds to the *cis*-element called P1BS (PHR1-binding sequence) with an imperfect palindromic sequence GNATATNC, which is prevalent in the promoters of many PSI genes. Knockout of *PHR1* greatly reduces the expression of a number of PSI genes and alters several Pi starvation responses. *PHR1* knockout, for example, decreases the cellular Pi content, decreases anthocyanin accumulation in shoots, and reduces the root-to-shoot ratio (Rubio et al., 2001). In contrast, overexpression of *PHR1* increases the expression of PSI genes and consequently increases the cellular Pi content in plants irrespective of Pi regime (Nilsson et al., 2007). The ability of PHR1 to bind to the P1BS element is further regulated by an SPX domain-containing protein, SPX1, which was proposed to be an intracellular Pi sensor through its binding to inositol pyrophosphates instead of Pi (Puga et al., 2014; Wild et al., 2016). PHR1 also has important roles in the interactions between Pi and other essential nutrients, such as sulfate (Rouached et al., 2011), zinc (Khan et al., 2014), and iron (Bournier et al., 2013). Orthologs of PHR1 have been identified in other plant species, including soybean (Xue et al., 2017), oilseed rape (Ren et al., 2012), rice (Zhou et al., 2008; Lv et al., 2014; Wang et al., 2014b; Guo et al., 2015; Ruan et al., 2017), and wheat (Wang et al., 2013), and they function in a similar manner as PHR1 in plant responses to Pi starvation.

In the Arabidopsis MYB-CC family, PHL1 (PHR1-LIKE 1, At5g29000) is closely related to PHR1 (Bustos et al., 2010). Knockout of *PHL1* did not significantly affect plant transcriptional responses to Pi starvation. In the *phr1phl1* double mutant, however, the induction of about 70% of PSI genes at the transcriptomic level was impaired. Also, the Pi starvation-induced phenotypes that were not observed in *phr1* were observed in the *phr1phl1* double mutant. PHL1 can also bind to the P1BS element and form a heterodimer with PHR1 *in vitro*. These results suggested that PHR1 and PHL1 act redundantly and probably cooperatively to regulate plant responses to Pi starvation.

AtPAP10 (ARABIDOPSIS PURPLE ACID PHOSPHATASE 10) is a major Pi starvation-induced secreted APase (Wang et al., 2011, 2014a; Zhang et al., 2014). Both its transcription and protein accumulation are upregulated by Pi starvation. In our search for the transcription factors that regulate *AtPAP10* expression, we identified two proteins that bind to the minimal functional sequence of the *AtPAP10* promoter (Sun et al., 2016). As shown in **Figure 1A**, these two proteins, designated PHL2 (PHR1-LIKE 2, At3g24120) and PHL3 (At4g13640), are also members of the MYB-CC family. They form a separate clade from PHR1 and PHL1 in the phylogenetic tree. Besides sharing a common MYB domain and a coiled-coil domain, PHR1 and PHL1 contain an extra N-terminal region, and PHL2 and PHL3 contain an extra C-terminal region (**Figure 1B**). RNA-seq analysis of Pi deficient-*phl2* indicated that *PHL2* is another key component controlling plant transcriptional response to Pi starvation (Sun et al., 2016). The structural differences among PHR1, PHL1, PHL2, and PHL3 might be responsible for the subtle differences in their functions, in terms of target genes and transcriptional activities.

In the MYB-CC family, the protein encoded by the gene At2g20400, which we named PHL4 (PHR1-LIKE 4) in this study, shares the highest sequence identity with PHR1. The function of PHL4 in regulating plant responses to Pi starvation, however, has not been characterized due to the lack of the *phl4* mutant. In this work, we generated two *phl4* null mutants using the CRISPR/Cas9 technique. We also generated *phr1phl1* and *phr1phl4* double mutants and *PHL4*-overexpressing lines. Our analyses of these lines indicated that PHL4 has only a minor role in regulating plant responses to Pi starvation and is a negative regulator of plant growth and development.

MATERIALS AND METHODS

Plant Materials and Growth Conditions

All Arabidopsis (*Arabidopsis thaliana*) plants used in this study were in the Colombia-0 ecotype background. The T-DNA insertion lines SALK_067629 (*phr1*) and CS832612 (*phl1*) were obtained from the Arabidopsis Biological Resource Center (ABRC). These two mutants have been proved to be null mutants (Nilsson et al., 2007; Bustos et al., 2010). The *phr1phl1* and *phr1phl4* double mutants were generated through genetic crossing. Seeds were surface-sterilized with 20% bleach for 10 min and washed three times with sterilized ultrapure water. The seeds were then sown on agar or agarose plates containing a Pi-sufficient (+Pi) or Pi-deficient (−Pi) medium. The +Pi medium contained half-strength Murashige and Skoog basal salts (Caisson Labs, catalog no. 01170009), half-strength Murashige and Skoog vitamin powder (1000×) (Phyto Technology Laboratories, catalog no. STT0533013A), 1.0% (w/v) sucrose, 0.5% MES, and 1.2% (w/v) agar (Sigma-Aldrich, catalog no. A1296) or 0.8% (w/v) agarose (Gene Company Ltd., catalog no. 111860). In the −Pi medium, half-strength Murashige and Skoog without Pi replaced the Murashige and Skoog basal salts. All experiments used agar-containing media, except for the experiments concerned with

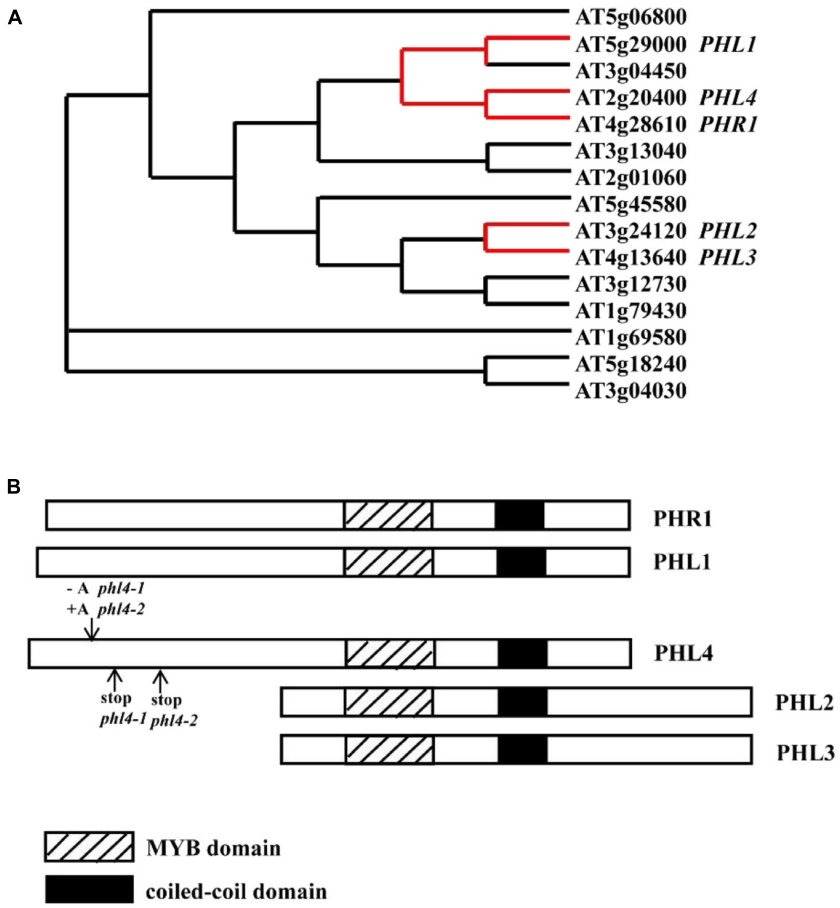

FIGURE 1 | The relative position of PHL4 in the MYB-CC protein family and the mutations in two *phl4* mutant alleles. **(A)** The phylogenetic tree of MYB-CC protein family was generated by an online service[1]. The red lines indicate the positions of *PHR1*, *PHL1*, *PHL2*, *PHL3*, and *PHL4* in the tree. **(B)** Alignment of protein sequences of PHR1, PHL1, PHL2, PHL3, and PHL4. The downward arrow indicated the position where a nucleotide "A" was inserted or deleted due to the gene editing. The upward arrows indicated the positions where the premature stop codon was generated in two mutant alleles. Note that although a similar phylogenetic tree was published by Bustos et al. (2010), we have provided a reconstructed tree to help the reader understand the relationship between PHR1 and PHL1, 2, 3, and 4, and to indicate the positions of the mutation introduced into PHL4 by the CRISPR method.

assessment of root development; in the latter case, agarose-containing media were used to aid in the observation of phenotypes. After seeds were stratified for 2 days at 4°C, the agar plates were placed vertically in a growth room with a photoperiod of 16 h light and 8 h dark at 22 to 24°C. The light intensity was 100 μmol m^{-2} s^{-1}.

Generation of the *phl4* Mutants

Two null mutant alleles of *PHL4* were generated using a CRISPR/Cas9-based genome editing system developed by Yan et al. (2015). The targeting sequence in the *PHL4* gene, which is located in the first exon, was determined using an online service[2]. The synthesized DNA fragment containing the targeting sequence of *PHL4* was cloned to the site between two *Bsa* I restriction enzyme sites in the intermediate vector AtU6-26-sgRNA-SK. The fragment between the *Nhe* I and *Spe* I sites of AtU6-26-sgRNA-SK was then further cloned into the *Spe* I restriction enzyme site in the plant vector pCAMBIA1300-pYAO:Cas9. The resultant construct was transformed into Arabidopsis plants of Columbia-0 background. The primary transformants were selected on kanamycin-containing agar plates and were screened for introduced mutations in *PHL4* by sequencing. The plants with hemizygous mutation in the *PHL4* gene were selfed to produce the homozygous mutants in the next generation. The primers used for construction of gene-editing vectors and verification are listed in **Supplementary Tables 1, 2**.

Histochemical Analysis of GUS Activity

Histochemical analysis of GUS activity was carried out as described by Jefferson et al. (1987). After the reactions were completed, the materials were photographed with a camera attached to a stereomicroscope (Olympus SZ61).

[1] http://www.ebi.ac.uk/Tools/msa/clustalo/

[2] http://www.genome.arizona.edu/crispr/CRISPRsearch.html

Analysis of Root-Associated APase Activity

Histochemical staining of root-associated APase activity was performed as described by Wang et al. (2011). For quantification of root surface-associated APase activity, two roots were excised from two 7-day-old seedlings, and the roots lengths were measured. The excised roots were thoroughly rinsed with distilled water three times, then transferred to a 2.0-mL Eppendorf tube containing 800 mL of reaction buffer (10 mM $MgCl_2$, 50 mM NaAc, 0.1% BCIP, pH 4.9); the tubes with roots were then incubated at 37°C for 1 h before the reaction was terminated by addition of 1 mL of 1M HCl. The samples were centrifuged for 5 min at 10,000 × *g*, and the blue precipitates were re-dissolved in 1M DMSO. Absorbance was measured spectrophotometrically at 635 nm. The root-surface-associated APase activity was expressed as A_{635}/cm root length.

Quantification of Cellular Pi Content and Total P Content

Cellular Pi content and total P content were quantified according to Wang et al. (2011).

Quantification of Anthocyanin Content

Anthocyanins in shoots were extracted with propanol:HCl:H_2O (18:1:81, v/v/v) in the dark at room temperature for 24 h. Absorbance was measured at 530 and 650 nm. Anthocyanin content was expressed as $(A_{530} - A_{650})$/g FW.

Quantitative Real-Time PCR (qPCR) Analyses of PSI Gene Expression

Total RNAs of 8-day-old seedlings were extracted using the Magen HiPure Plant RNA Mini Kit. A 2-μg quantity of the RNAs was reversely transcribed to cDNA using M-MLV reverse transcriptase (Takara). qPCR analyses were carried out using EvaGreen 2 × qPCR MasterMix (ABM) on a Bio-Rad CFX96 real-time PCR detection system. *ACTIN 2* (At3g18780) mRNA was used as an internal control, and the relative expression level of each gene was calculated by the $2^{-\Delta\Delta Ct}$ method (Livak and Schmittgen, 2001). The primers used for qPCR analysis are listed in **Supplementary Table 3**.

Vector Construction and Plant Transformation

For analysis of tissue-specific expression patterns of *PHL4*, a 1,403-bp DNA fragment upstream of the start codon was amplified from genomic DNAs by PCR. During the amplification, the DNA sequences overlapping with the restriction enzyme sites of *Xba* I and *Xma* I of the vector were added to the 5′ and 3′ ends of the PCR products. The amplified fragment was cloned into *Xba* I and *Xma* I sites between the *CaMV 35S* promoter and the GUS reporter gene in the plant transformation vector pBI121 using a one-step isothermal *in vitro* recombination procedure (Gibson et al., 2009). For the overexpression of *PHL4*, a 2,735-bp genomic *PHL4* sequence, including both its 5′ and 3′ untranslated regions (UTRs), was cloned into *Bam*H I and *Sac* I restriction enzyme sites after the *CaMV 35S* promoter in the plant transformation vector pZH01 using the same recombination procedure. For analysis of the subcellular localization of PHL4 protein, a 1,194-bp DNA fragment containing the coding sequence (CDS) of *PHL4* was isolated by PCR from plant cDNAs and was cloned into *Kpn* I and *Pst* I restriction enzyme sites between the *CaMV 35S* promoter and GFP gene in the plant transformation vector pJG053, resulting in the construct of *35S::PHL4-GFP*. To generate the *PHL4::PHL4-GFP* construct, the *35S* promoter on the *35S::PHL4-GFP* vector was replaced by the *PHL4* promoter. All constructs were mobilized into *Agrobacterium tumefaciens* strain GV3101 and transformed into Arabidopsis plants via the flower dip method (Clough and Bent, 1998). The primers used for vector construction are listed in **Supplementary Table 1**.

Luciferase Complementation Imaging (LCI) and Bimolecular Fluorescence Complementation (BiFC) Assays

For LCI assays, the CDSs of *PHL4* and *PHR1* were inserted into the vectors pCAMBIA-nLUC and pCAMBIA-cLUC (Chen et al., 2008), respectively, to generate PHL4-nLUC and cLUC-PHR1 constructs. For BiFC assays, the CDSs of *PHL4* and *PHR1* were individually cloned into the vector nYFP or cYFP (Gibson et al., 2009). The resultant constructs were mobilized into the *A. tumefaciens* strain GV3101 and were used to transform the leaves of *Nicotiana benthamiana*. The LCI and BiFC assays were performed as described by Sun et al. (2016). The primers used for vector construction are listed in **Supplementary Table 4**.

Electrophoretic Mobility-Shift Assay (EMSA)

For EMSA assays, the full-length CDS of *PHL4* was cloned into the *Not* I and *Sal* I sites after the MBP coding sequence in the vector pMAL-c5x. The CDS of the six times-repeated His tag was added to the C-terminus of the PHL4 protein during the PCR amplification of the CDS of *PHL4*. The resultant construct was transformed into *E. coli* strain BL21 (DE3) for protein production. The MBP-PHL4-His recombinant proteins were purified using Ni-NTA agarose beads. The biotin-labeled probes containing twofold P1BS sequence were generated by annealing the biotin-labeled complementary oligonucleotides. The sequences of the oligonucleotides used for generating the probes are listed in **Supplementary Table 5**. With the purified recombinant proteins and biotin-labeled DNA probes, EMSA was performed as described by Sun et al. (2016).

RESULTS

The Expression Patterns of *PHL4*

To investigate the expression patterns of *PHL4*, we fused a 1,403-bp DNA fragment upstream of its start codon to a GUS reporter gene. This DNA fragment included the 5′ UTR, which contains the first intron, and the 966-bp 5′ flanking sequence. The *PHL4::GUS* construct was transformed into wild-type (WT) Arabidopsis plants. The expression patterns of the GUS gene of a

representative line are shown in **Figure 2**. In 8-day-old seedlings, GUS expression was observed in all types of cells of the cotyledon and hypocotyl (**Figure 2A**). GUS expression was detected in the root cap and meristematic zone of both primary and lateral roots but was not detected in the elongation zone of the primary root (**Figures 2B,C**). The GUS gene was strongly expressed in the stele of the maturation zone (**Figure 2D**). In the mature plant, the GUS gene was uniformly expressed in all leaves but was not expressed in the stem (**Figures 2E–G**). In flowers, GUS expression was observed in sepals, filaments, and gynoecia but not in petals or pollen grains (**Figures 2H,I**). In siliques, GUS expression was high at both ends but weak in the middle (**Figure 2J**). Next, we determined whether the expression of *PHL4* was induced by Pi starvation. Both qPCR analysis (**Figure 2K**) and GUS staining assays (**Supplementary Figure 1**) showed that the transcription of *PHL4* was not affected by Pi starvation.

To determine the subcellular localization of the PHL4 protein, we constructed transgenic lines that expressed a PHL4-GFP fusion gene driven by the *35S CaMV* promoter. In the root cells of the transgenic plants, the PHL4-GFP fusion protein was exclusively localized in the nucleus (**Figure 2L**). The localization of PHL4-GFP in the nucleus was confirmed by

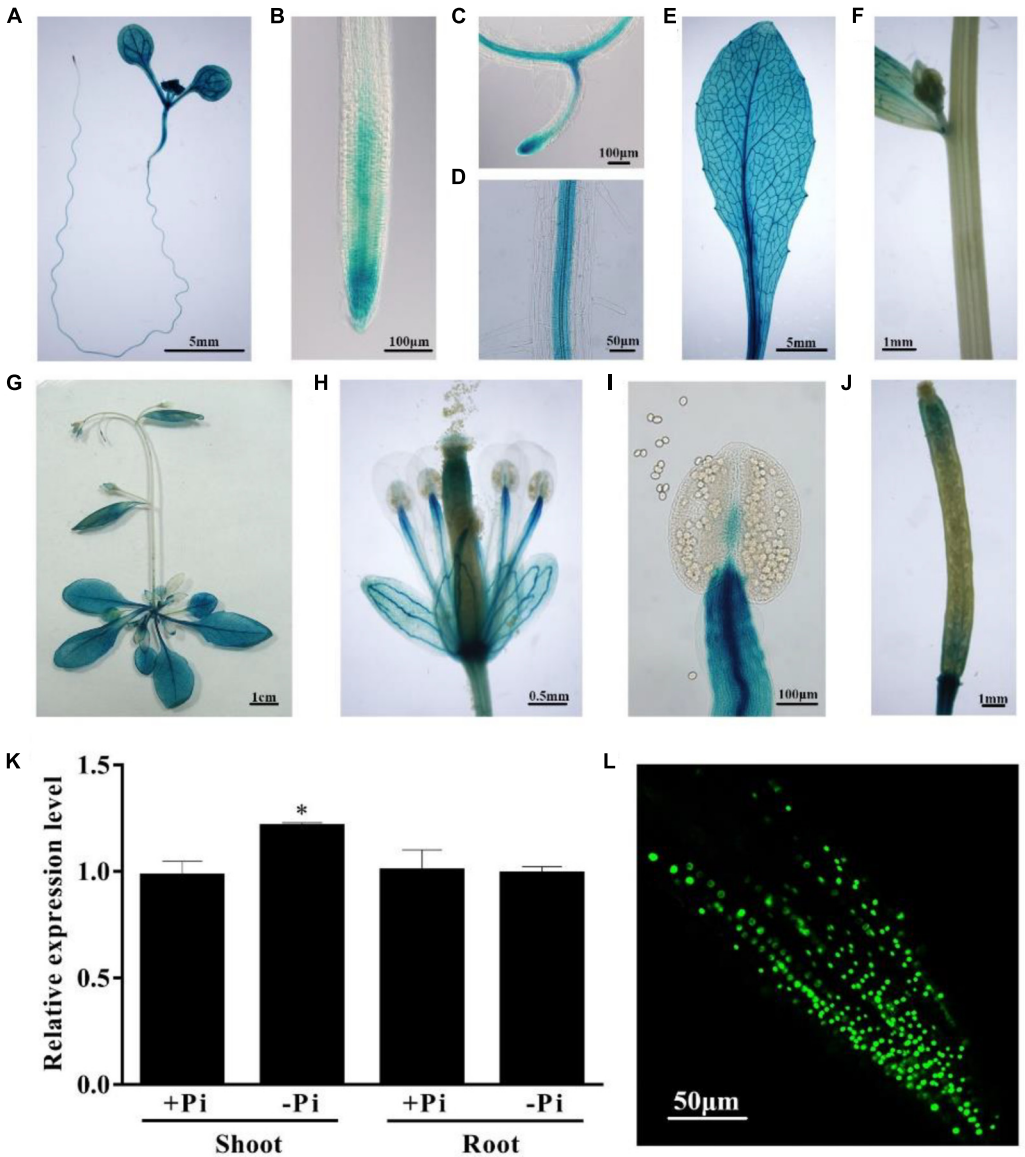

FIGURE 2 | Expression patterns of the *PHL4* gene. **(A–J)** Tissue-specific expression patterns of *PHL4::GUS*. **(A)** An 8-day-old seedling; **(B)** a root tip; **(C)** a newly formed lateral root; **(D)** root mature zone; **(E)** a rosette leaf; **(F)** a stem; **(G)** a 25-day-old mature plant; **(H)** an open flower; **(I)** a stamen; **(J)** a silique. **(K)** Relative expression of the *PHL4* gene in shoots and roots of 8-day-old WT seedlings under +Pi and –Pi conditions as determined by qPCR. Values are the means ± SD of three biological replicates and represent fold changes normalized to transcript levels of the WT on +Pi medium. Means with an asterisk are significantly different from the WT ($P < 0.05$, *t*-test). **(L)** The subcellular localization of the GFP-PHL4 protein in the root tip of a 7-day-old seedling.

transient expression assays in the leaves of *N. benthamiana,* in which the expression of *PHL4-GFP* was driven by either the *35S* promoter or the *PHL4* native promoter (**Supplementary Figure 2A**). Using the *35S::GFP-PHL4* transgenic line, we also found that the subcellular localization and protein abundance of PHL4 were not affected by Pi starvation (**Supplementary Figure 2B**).

Generation of *phl4* Null Mutants

To study the function of *PHL4*, we required *phl4* null mutants for phenotypical characterization. Because the T-DNA knockout mutant of *PHL4* was not available at the Arabidopsis stock centers, we used CRISPR/Cas9 gene editing technique to generate *phl4* mutant alleles. Using this technique, we created four new *PHL4* alleles (*phl4-1* to *phl4-4*, **Supplementary Figure 3**). *phl4-1* had a deletion of one nucleotide 'A' at position 130 after the start codon of the *PHL4* gene, which resulted in a frameshift and generated a premature stop codon at position 169. In *phl4-2*, there was an insertion of one nucleotide 'A' in the same position as in *phl4-1*, which also caused a frameshift and created a premature stop codon at position 258. *phl4-3* had a 24 nucleotides deletion at position 106, which removed eight amino acids, but did not cause a frameshift. *phl4-4* not only had a six nucleotides deletion at position 127, resulting in the loss of two amino acids, but also had a transition of one nucleotide at two positions. The nucleotide transition from G to A at position 115 caused a non-sense mutation and the nucleotide transition from T to C at position 120 caused a conversion from glutamate to lysine. Because the mutations in *phl4-1* and *phl4-2* would cause a truncation of the PHL4 protein, which result in the elimination of both the MYB domain and the coiled-coil domain (**Figure 1B**), therefore, the proteins encoded by *phl4-1* and *phl4-2* would not be functional, even though the levels of *PHL4* mRNA in these two alleles were not significantly altered compared to that of the WT (**Supplementary Figure 4**). As a consequence, *phl4-1* and *phl4-2* were equivalent to null alleles. Therefore, we chose these two alleles for further studies.

Responses of the *phl4* Mutants to Pi Starvation

To determine the roles of *PHL4* in plant responses to Pi starvation, we compared the WT, the *phr1* mutant, and the two *phl4* mutants. The seeds were directly germinated on +Pi and −Pi media. Under Pi sufficiency, the morphologies did not differ among the 10-day-old seedlings (**Figure 3A**). Under Pi deficiency, in contrast, the shoot and root growth of all seedlings were greatly inhibited (**Figure 3A**). The growth inhibition of *phr1*, but not of the two *phl4* mutants, was greater than that of the WT. Enhanced root hair production is a typical response of plants to Pi starvation. The root hair density was similar among the WT, *phr1*, and the two *phl4* mutants; however, *phr1* but not *phl4-1* or *phl4-2* had shorter root hairs than the WT (**Supplementary Figure 5**). No obvious morphological difference was observed among these plants after 5 weeks of growth in soil (**Figure 3C**).

Two additional hallmark responses of plants to Pi starvation are induction and secretion of APases on the root surface and the accumulation of anthocyanins in shoots. We analyzed these two traits for the *phl4* mutants. Root surface-associated APase activity can be detected by histochemical staining using a substrate of APase, BCIP (5-bromo-4-chloro-3-indolyl phosphate). The product of the enzyme reaction forms a blue precipitate. Under Pi deficiency and compared to the WT, secreted APase activity as indicated by BCIP staining was substantially reduced in *phr1* but not in the two *phl4* mutants (**Figure 4A**). This conclusion was further supported by the quantitative analysis of secreted APase activity of these seedlings (**Supplementary Figure 6**). Accumulation of anthocyanins in shoots was also significantly reduced in *phr1* but not in the two *phl4* mutants (**Figure 4B**). Next, we examined the cellular Pi and total P contents in these plants. When the plants were grown on either +Pi or −Pi media, the cellular Pi content of shoots was reduced in *phr1* but not in the two *phl4* mutants relative to the WT (**Figure 4C**). The Pi contents of roots did not significantly differ among the WT, the *phr1* mutant, and the two *phl4* mutants (**Figure 4C**). Although the total P content in shoots was about 15% lower for *phr1* than for the WT under both Pi sufficiency and deficiency (**Figure 4D**), the total P content in roots was lower for *phr1* than for the WT under Pi sufficiency but was higher for *phr1* than for the WT under Pi deficiency (**Figure 4D**). The total P content of roots did not differ between the two *phl4* mutants and the WT under Pi sufficiency or deficiency.

We then analyzed the effect of the *PHL4* mutation on the expression of six PSI marker genes. These PSI genes included a non-coding transcript, *IPS1* (Burleigh and Harrison, 1999); a microRNA, *miR399d* (Fujii et al., 2005); two high-affinity phosphate transporters, *AtPT1* (*Pht1;1*) and *AtPT2* (*Phtl;4*) (Muchhal et al., 1996); a ribonuclease, *RNS1* (Bariola et al., 1994); and an acid phosphatase, *ACP5* (*AtPAP17*) (del Pozo et al., 1999). The induction of these six PSI genes, and especially of *IPS1* and *miRNA399d*, was substantially lower in *phr1* roots than in WT roots (**Figure 5**). In the two *phl4* mutants, however, the induction of expression was unaffected for two of the six genes and was only mildly reduced for four of the six genes.

Taken together, these results indicate that the mutation of the *PHL4* gene had only a minor effect on plant transcriptional responses to Pi starvation. As a consequence, the mutation of the *PHL4* gene did not significantly alter the physiology or development of plants under Pi starvation.

Functional Analysis of the *phr1phl4* Double Mutant

Because the mutation of *PHL4* did not cause obvious phenotypical changes, we wondered whether there was a functional redundancy among the members of the MYB-CC family. To investigate this possibility, we generated a *phr1phl4* double mutant by crossing *phr1* (SALK_067629) with *phl4-2*. The primers used are listed in **Supplementary Table 2**. PHL1 is another close homolog of PHR1 (**Figure 1A**). The mutation of *PHL1* alone does not affect PSI gene expression or cause any other obvious phenotypical changes (Bustos et al., 2010). The combining of the *phr1* and *phl1* mutations, however,

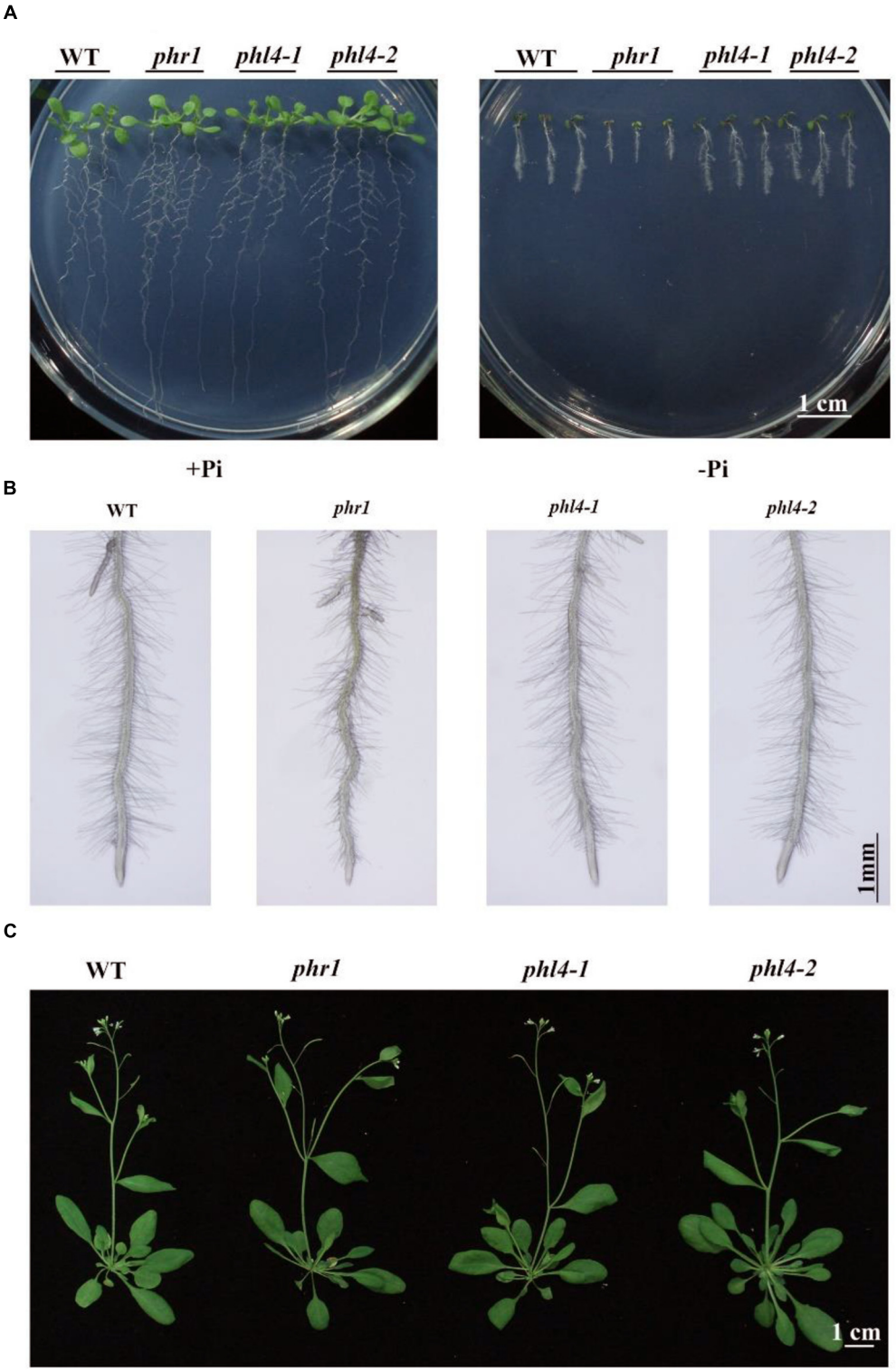

FIGURE 3 | Phenotypic analyses of two *phl4* mutants. **(A)** Morphology of 10-day-old seedlings of the WT, *phr1*, *phl4-1*, and *phl4-2* grown on +Pi and –Pi media. **(B)** Root hairs of 6-day-old seedlings of WT, *phr1*, *phl4-1*, and *phl4-2* grown on –Pi medium. **(C)** Morphology of 5-week-old plants of the WT, *phr1*, *phl4-1*, and *phl4-2* grown in soil.

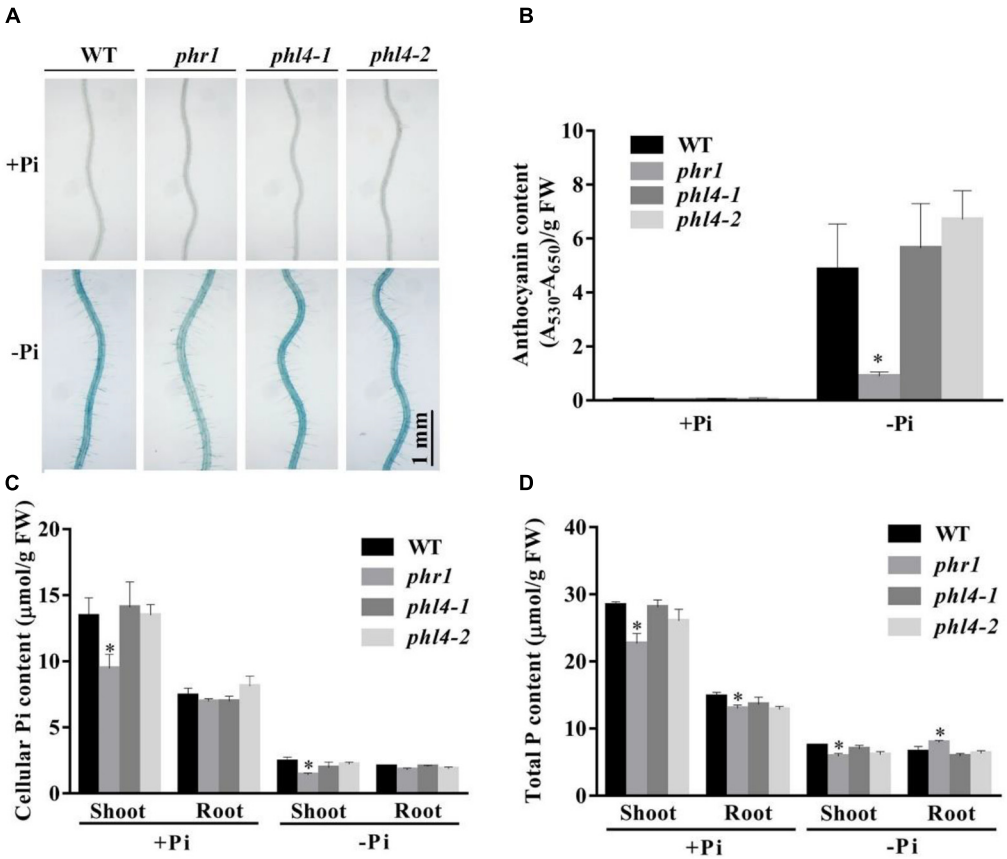

FIGURE 4 | Analyses of root-associated APase activity and contents of anthocyanin, cellular Pi, and total P in the WT, *phr1*, *phl4-1*, and *phl4-2* on +Pi and –Pi media. **(A)** The APase activities revealed by BCIP staining of the root surfaces of 6-day-old seedlings of the WT and various mutants. **(B)** Anthocyanins in the shoots of 12-day-old seedlings of the WT and various mutants. **(C,D)** Cellular Pi and total P contents in the shoots and roots of 12-day-old seedlings of the WT and various mutants. These experiments were repeated three times with similar results. Values represent means ± SD of three replicates. Means with asterisks are significantly different from the WT ($P < 0.05$, *t*-test).

has a synergistic effect on the plant transcriptional responses to Pi deficiency, as well as on other traits, such as root hair development (Bustos et al., 2010). To assess the combined effects of *PHL4* and *PHR1* mutations, we compared the growth phenotypes and plant responses to Pi starvation between *phr1phl1* and *phr1phl4*. When grown on +Pi medium for 10 days, the WT, *phr1*, *phr1phl1*, and *phr1phl4* did not display obvious morphological differences. On −Pi medium, the overall growth was more inhibited for *phr1* than for the WT, and the growth of *phr1phl1* and *phr1phl4* double mutants was more inhibited than that of the *phr1* single mutant. These results indicated a synergistic effect of the double mutation and a similar effect of *PHL1* and *PHL4* mutations on *phr1* (**Figure 6A**). As shown in **Figure 6B**, the WT, *phr1*, and the two double mutants had similar root hair density. Compared to *phr1*, root hair length of *phr1phl1* was further reduced, but such a reduction was not evident for *phr1phl4* (**Figure 6B** and **Supplementary Figure 5**). When grown in soil for 5 weeks, *phr1* and the WT had a similar growth phenotype whereas *phr1phl1* showed a sign of early senescence (**Figure 6C**), which was consistent with that reported by Bustos et al. (2010). The growth phenotype of *phr1phl4* was also similar to that of the WT and *phr1*.

Next, we examined the root-associated APase activity and anthocyanin accumulation in *phr1phl4*. The root-associated APase activity and anthocyanin accumulation in shoots were lower in both *phr1phl1* and *phr1phl4* than in *phr1* but did not significantly differ between *phr1phl1* and *phr1phl4* (**Figures 7A,B**). This conclusion was also supported by the quantitative analyses of the APase activity of these plants (**Supplementary Figure 6**). In terms of cellular Pi and total P contents, the mutation of *PHL1* and *PHL4* had different effects on the *phr1* mutant. Under Pi sufficiency, cellular Pi and total P contents in shoots were lower in *phr1phl1* than in *phr1*; under Pi deficiency, however, cellular Pi and total P contents in shoots were similar in *phr1phl1* and *phr1* (**Figures 7C,D**). In the shoots of *phr1phl4*, however, the levels of cellular Pi and total P were similar to those of *phr1* under both Pi sufficiency and Pi deficiency. In Pi-sufficient roots, levels of cellular Pi and total P in *phr1phl1* and *phr1phl4* were similar to those in *phr1*. In Pi-deficient roots, however, levels of cellular Pi and total P were significantly higher in

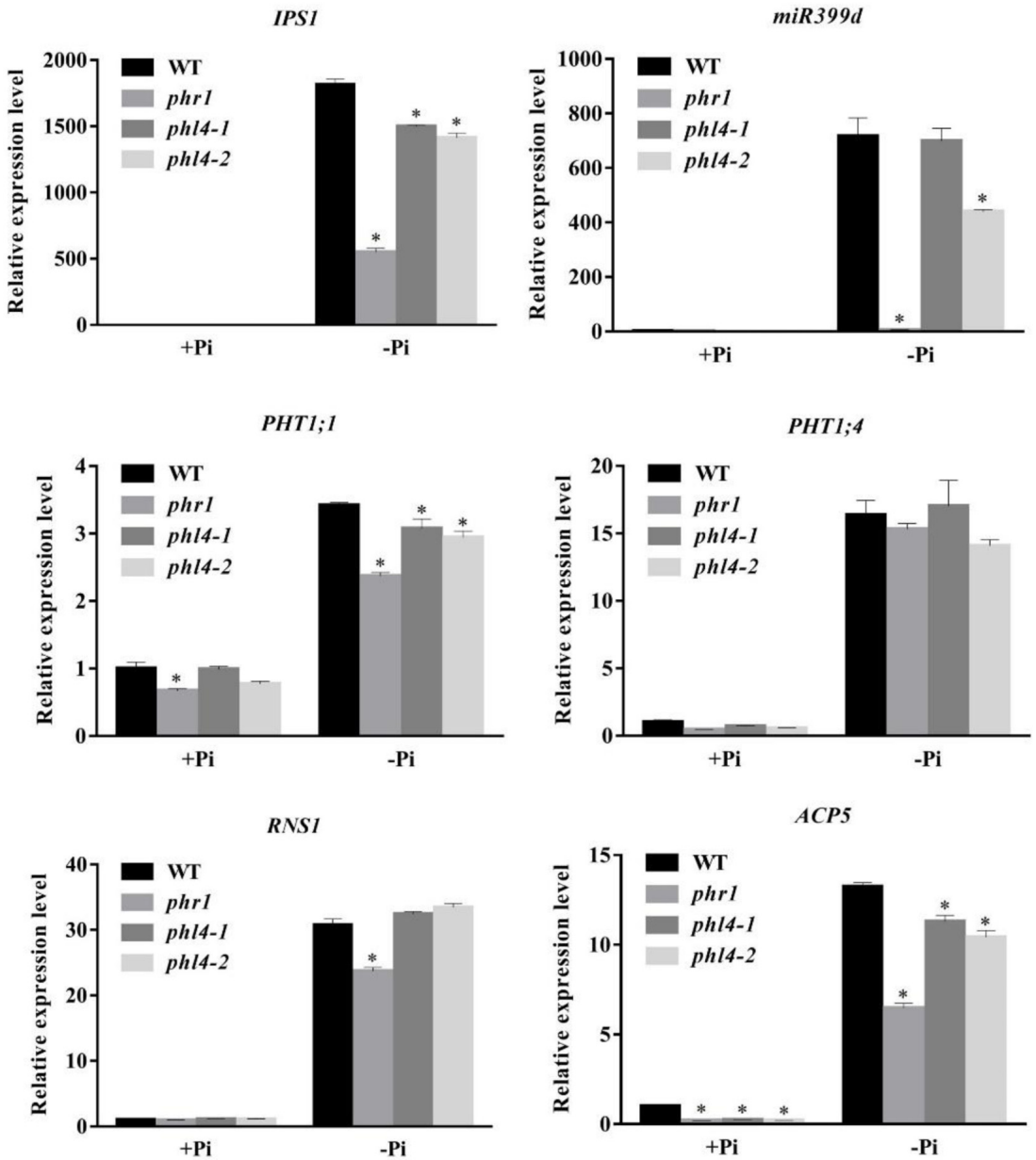

FIGURE 5 | Analyses of PSI gene expression in the WT, *phr1*, *phl4-1*, and *phl4-2*. Roots of 8-day-old seedlings of the WT and other mutants grown on +Pi and –Pi media were used for qPCR analysis. The names of the genes examined are indicated on the top of each panel. Values are the means ± SD of three biological replicates and represent fold changes normalized to transcript levels of the WT on +Pi medium. Means with asterisks are significantly different from the WT ($P < 0.05$, *t*-test).

phr1phl1 than in the WT or *phr1*. Cellular Pi and total P contents did not significantly differ between *phr1phl4* and *phr1*.

We then compared the expression of the six PSI genes in the WT and the three mutants. The induction of all six PSI genes was significantly reduced in *phr1* and was further reduced in *phr1phl1* (**Figure 8**). Although the induction of PSI genes was lower in *phr1phl4* than in *phr1*, the reduction was less in *phr1phl4* than in *phr1phl1*.

These results suggest that, like *PHL1*, *PHL4* acts redundantly with *PHR1* in plant responses to Pi deficiency. The contribution to the response, however, might be less for *PHL4* than for *PHL1*.

Overexpression of *PHL4* Alters Plant Growth and Development

Another way to overcome genetic redundancy in the functional characterization of a given gene is to analyze the phenotypes of its

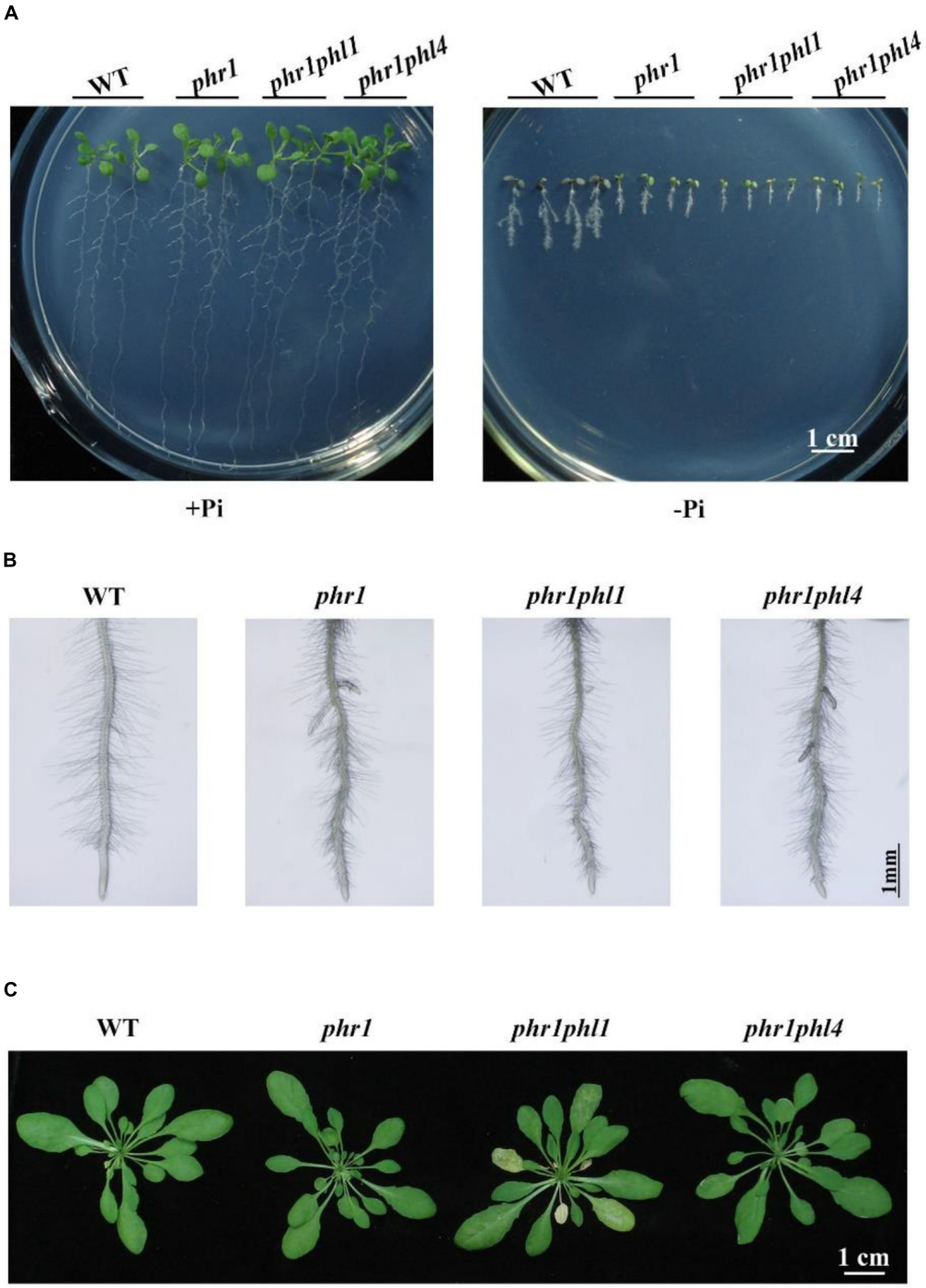

FIGURE 6 | Phenotypic analysis of *phr1phl1* and *phr1phl4* double mutants. **(A)** Morphology of 10-day-old seedlings of the WT, *phr1*, *phr1phl1*, and *phr1phl4* grown on +Pi and –Pi media. **(B)** Root hairs of 6-day-old seedlings of WT, *phr1*, *phr1phl1*, and *phr1phl4* grown on –Pi medium. **(C)** Morphology of 5-week-old plants of the WT, *phr1*, *phr1phl1*, and *phr1phl4* grown in soil. The flower stalks were removed.

overexpressing lines (Weigel et al., 2000). We therefore generated *PHL4*-overexpressing lines (*PHL4 OX*) by transforming *phl4-2* with a genomic sequence of the WT *PHL4* gene driven by a *35S CaMV* promoter. More than 10 independent transgenic lines were generated, and the phenotypes of some representative lines were analyzed. Under both Pi sufficiency and deficiency, *phl4* showed similar growth phenotypes as the WT, while the overall growth of four transgenic lines was greatly impaired (**Figure 9A**). On +Pi medium, the 8-day-old seedlings of these four overexpressing lines had small,

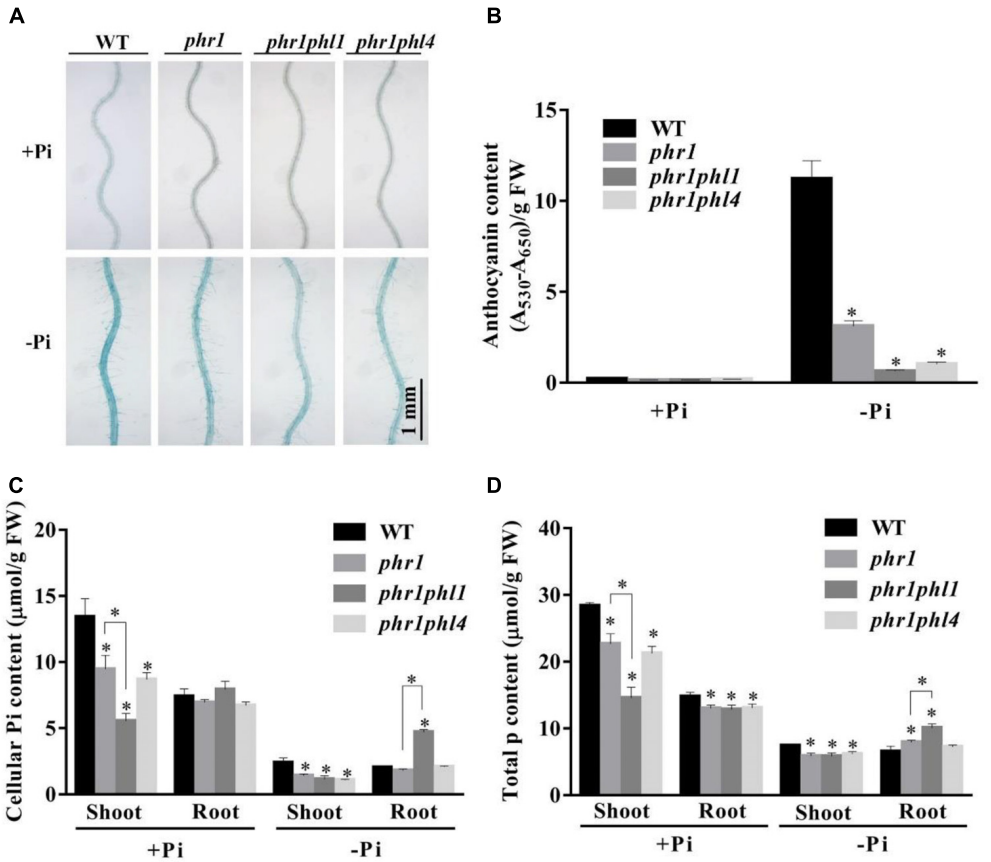

FIGURE 7 | Analyses of root-associated APase activity, anthocyanin, cellular Pi, and total P contents of the WT, *phr1*, *phr1phl1*, and *phr1phl4* on +Pi and –Pi media. **(A)** The APase activities revealed by BCIP staining on the root surfaces of 6-day-old seedlings of the WT and various mutants. **(B)** Anthocyanins in the shoots of 12-day-old seedlings of the WT and various mutants. **(C,D)** Cellular Pi and total P contents in the shoots and roots of 12-day-old seedlings of the WT and various mutants. These experiments were repeated three times with similar results. Values represent means ± SD of three replicates. Means with asterisks are significantly different from the WT ($P < 0.05$, *t*-test). Means with asterisks and thin lines are significant different from each other ($P < 0.05$, *t*-test).

epinastic cotyledons and short primary roots with abnormal gravitropism; on −Pi medium, the *PHL4-OX* seedlings were once again smaller than WT and *phl4* seedlings, but the abnormal gravitropism was no longer evident. Root hair density and root hair length were also significantly lower for these four transgenic lines than for the WT and *phl4* (**Figure 9B** and **Supplementary Figure 5**). When the *PHL4*-overexpressing lines were grown in soil for 5 weeks, they were small with curled and serrated rosette leaves, and had early senescence (**Figures 9C–E**).

In response to Pi starvation, root-associated APase activity was greater in the *PHL4 OX* lines than in the WT or *phl4* as revealed by BCIP staining (**Figure 10A**); however, the quantitative analysis using BCIP as the substrate showed that the total root-associated APase activity per cm root length was similar between the WT and *PHL4 OX* lines (**Supplementary Figure 6**). This was probably due to that the *PHL4 OX* line had less and shorter root hairs and thinner primary root, even though they had stronger BCIP than the WT on their root surface. The anthocyanin contents in shoots were similar in the *PHL4 OX* lines, the WT, and *phl4* (**Figure 10B**). In shoots, the cellular Pi and total P contents were two times greater in two of the overexpressing lines than in the WT or *phl4* grown on either +Pi or −Pi media (**Figures 10C,D**). In roots, the *PHL4 OX* lines also had increased cellular Pi and total P contents, although the increase was less than in the shoots. In response to Pi starvation, the induction of the six typical PSI genes was much higher in the two *PHL4 OX* lines than in the WT or *phl4* (**Figure 11**).

Physical Interaction Between PHL4 and PHR1

Because PHL4 shares the highest sequence homology with PHR1, and because knockout or overexpression of *PHL4* altered the expression of PSI genes, we wondered whether *PHL4* could also bind to the P1BS element in order to regulate gene expression. A MBP (maltose-binding protein)-PHL4-His recombinant protein was produced in *E. coli*, and the fusion protein was purified to homogeneity with an His affinity column. An EMSA demonstrated that PHL4-MBP, but not MBP alone, could form a complex with the biotin-labeled

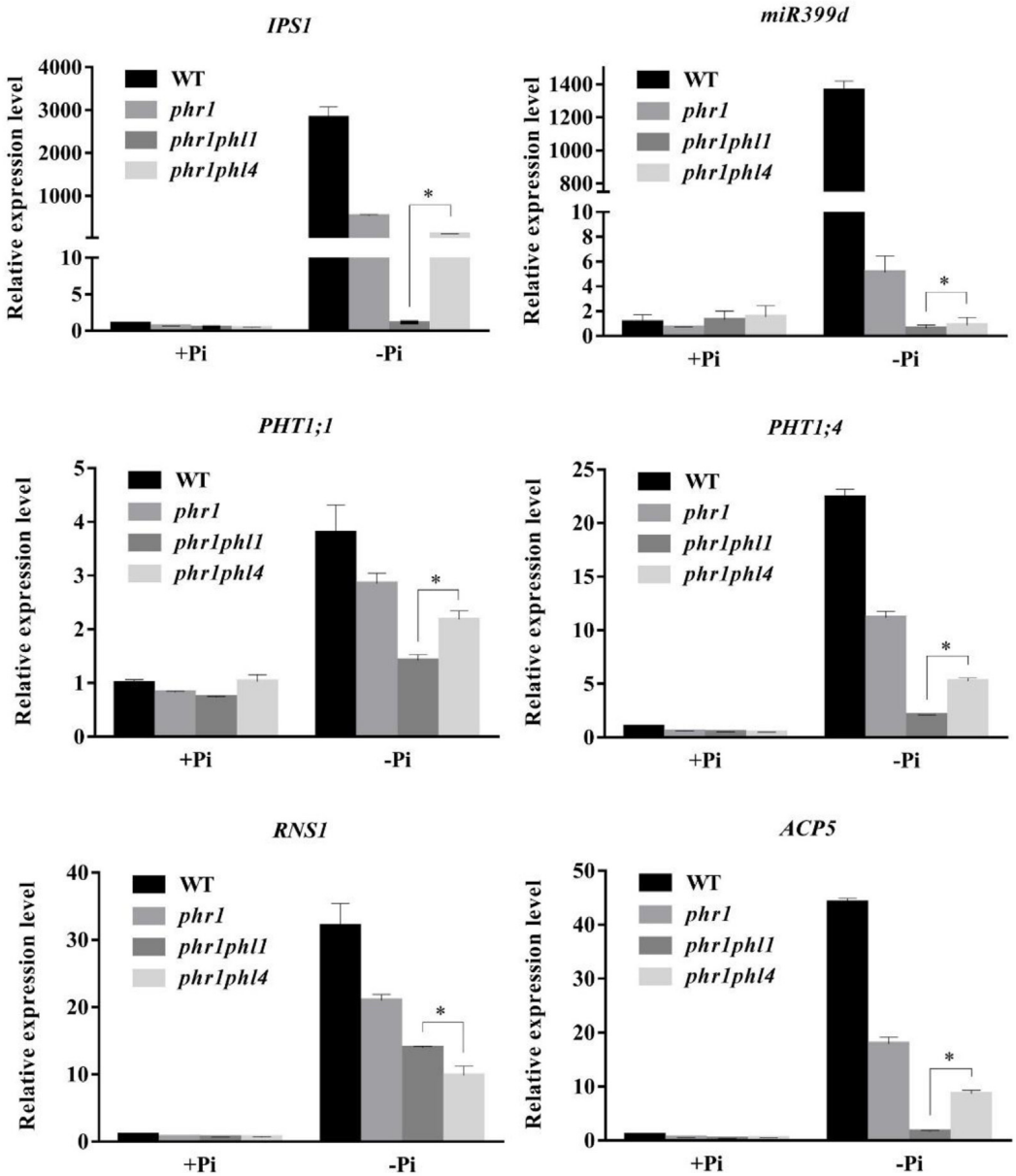

FIGURE 8 | Analysis of PSI gene expression in the WT, *phr1*, *phr1phl1*, and *phr1phl4*. Roots of 8-day-old seedlings of the WT and other mutants grown on +Pi and –Pi media were used for qPCR analysis. The names of the genes examined are indicated on the top of each panel. Values are the means ± SD of three biological replicates and represent fold changes normalized to transcript levels of the WT on +Pi medium. Means with asterisks and thin lines are significantly different from each other ($P < 0.05$, *t*-test).

DNA probe containing the P1BS sequence (**Figure 12A**). An excess of non-labeled DNA probe competed with the labeled DNA for the binding with PHL4-MBP, indicating that such binding was sequence-specific. We next used a luciferase complementary imaging (LCI) assay to determine whether PHL4 can directly interact with PHR1. PHL4 was fused with the N-terminal half of a luciferase (LUC) (PHL4-nLUC), and PHR1 was fused with the C-terminal half of LUC (cLUC-PHR1). These two constructs were co-transformed into the leaves of *N. benthamiana* with proper controls. As positive controls, PHL2 and PHL3 showed a strong interaction (**Figure 12B**), which was previously reported (Sun et al., 2016). In contrast, no reconstituted LUC signals were detected for the pairs of PHL4-nLUC and cLUC or nLUC and cLUC-PHR1. In the leaves in which PHL4-nLUC and cLUC-PHR1 were co-expressed, a moderately strong signal of reconstituted LUC was detected, indicating that PHL4 can interact with PHR1. The interaction between PHL4 and PHR1 was further confirmed by a bimolecular fluorescence complementation (BiFC) assay in the leaves of *N. benthamiana*, and the

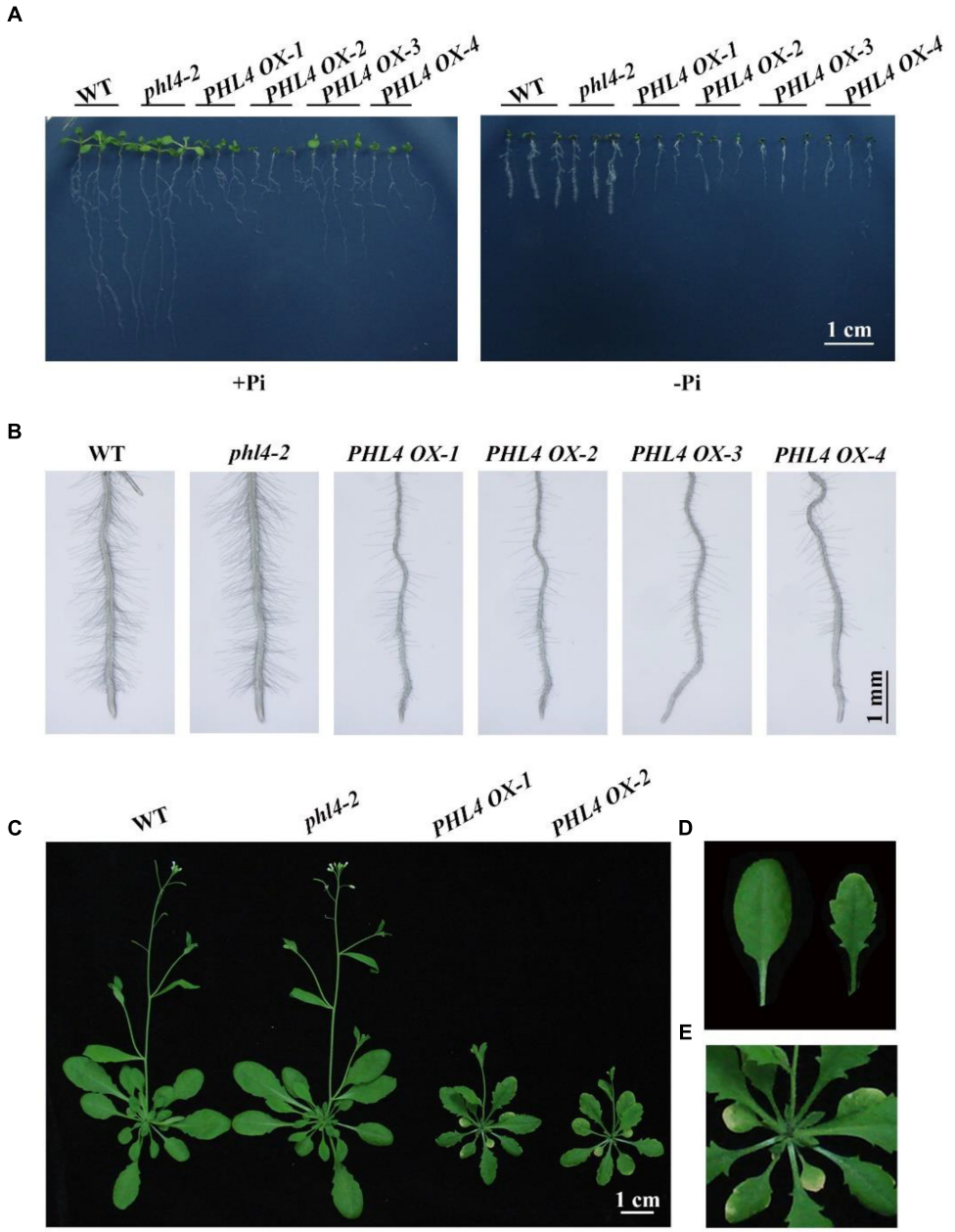

FIGURE 9 | Phenotypic analyses of the *PHL4*-overexpression lines. **(A)** Morphology of 8-day-old seedlings of the WT, *phl4*, and four *PHL4*-overexpression lines grown on +Pi and –Pi media. **(B)** Root hairs of 6-day-old seedlings of the WT, *phl4*, and four *PHL4*-overexpression lines grown on –Pi medium. **(C)** Morphology of 5-week-old seedling of the WT, *phl4*, and two *PHL4*-overexpression lines grown in soil. **(D)** A comparison of the leaf edge of the WT and *PHL4 OX-1*. **(E)** A close view of the rosette of *PHL4 OX-1*.

results showed that the interaction occurred in the nucleus (**Figure 12C**).

DISCUSSION

Plants use many responses to cope with Pi deficiency in the environment. These adaptive responses are controlled by complicated regulatory networks at transcriptional (Bustos et al., 2010), posttranscriptional (Fujii et al., 2005; Bari et al., 2006; Franco-Zorrilla et al., 2007), and posttranslational (Liu et al., 2012; Lin et al., 2013) levels. Among these regulatory processes, a crucial role of transcriptional regulation has been well established by transcriptomic studies (Jain et al., 2012). The functional characterization of the Arabidopsis transcription factor PHR1 and its homologs within the MYB-CC protein family, PHL1 and PHL2, revealed the framework of a central regulatory system controlling plant transcriptional responses to Pi starvation. In

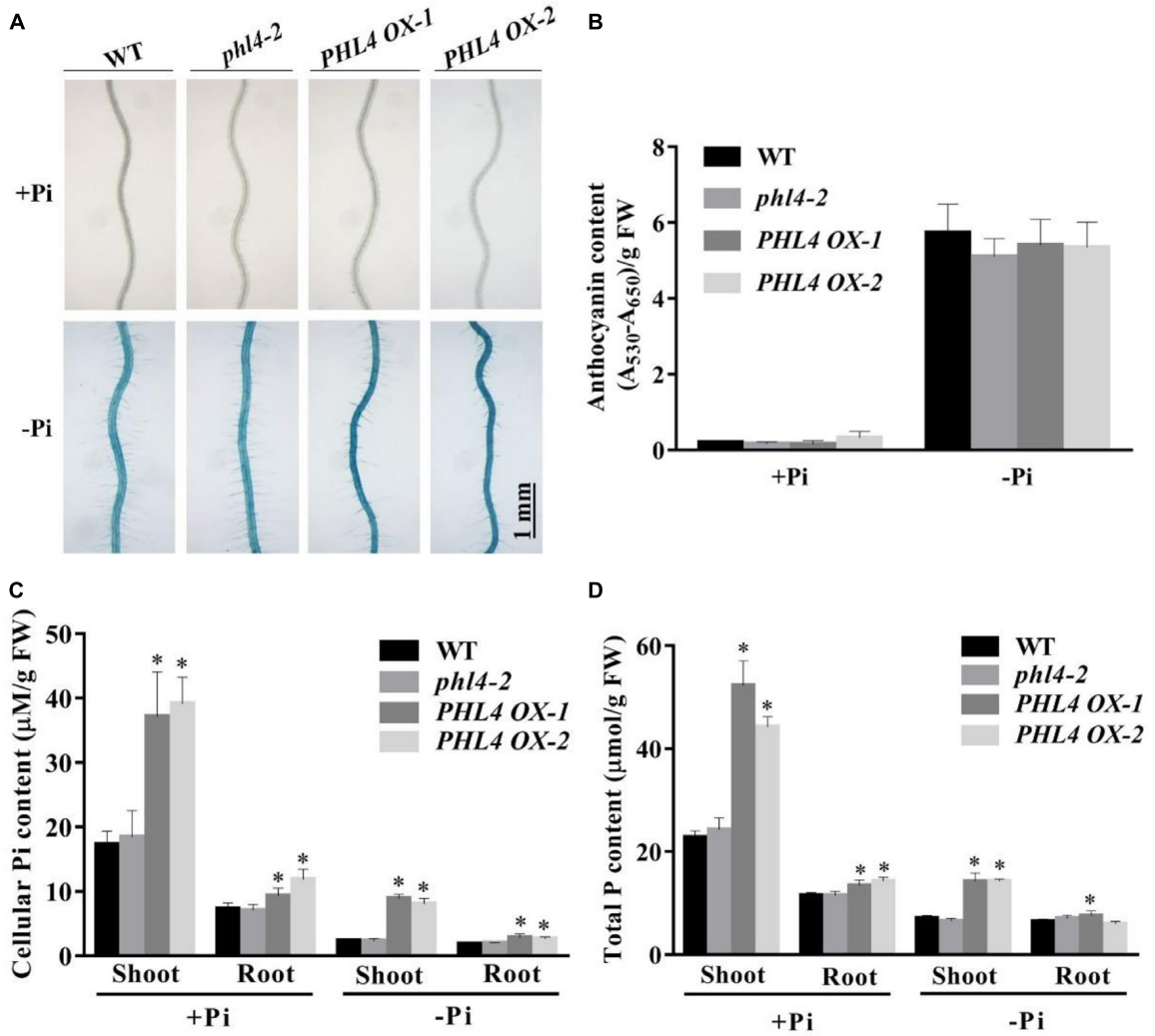

FIGURE 10 | Analyses of root-associated APase activity, anthocyanin, cellular Pi, and total P contents of the two *PHL4*-overexpressing lines (*PHL4 OX-1* and *PHL4 OX-2*) grown on +Pi and –Pi media. **(A)** The APase activities revealed by BCIP staining on the root surfaces of 6-day-old seedlings of the WT, *phl4*, and *PHL4 OX-1* and *-2*. **(B)** Anthocyanins in the shoots of 12-day-old seedlings of the WT, *phl4*, and *PHL4 OX-1* and *-2*. **(C,D)** Cellular Pi and total P contents in the shoots and roots of 12-day-old seedlings of WT, *phl4*, and *PHL4 OX-1* and *-2*. These experiments were repeated three times with similar results. Values represent means ± SD of three replicates. Means with asterisks are significantly different from the WT ($P < 0.05$, *t*-test).

the double knockout mutants *phr1phl1* and *phr1phl2*, however, the expression of PSI genes was not completely abolished (Bustos et al., 2010; Sun et al., 2016), suggesting that other transcription factors in or out of the MYB-CC family also contribute to the regulation of plant transcriptional responses to Pi starvation. In the Arabidopsis MYB-CC protein family, although the PHR1 homologs PHL1, PHL2, and PHL3 have been shown to regulate Pi responses, the functions of the most closely related homolog of PHR1, which we named PHL4 (At2g20400) (**Figure 1A**), had not been previously studied due to the lack of its knockout mutant.

As a first step toward understanding the functions of PHL4 in plant responses to Pi starvation and in plant development, we analyzed the expression patterns of *PHL4* as affected by Pi availability. Our results indicated that PHL4 is localized in the nucleus and that neither its transcription nor its protein abundance is affected by external Pi levels (**Figures 2K,L**). These features are similar to those of PHR1.

To determine the roles of PHL4 in plant responses to Pi starvation, we generated two *phl4* mutant alleles using the CRISPR/Cas9 gene editing technique. The premature stop codons introduced into the *PHL4* gene through gene editing eliminated both the MYB domain and the coiled-coil domain; therefore, the two resultant mutants could be regarded as null alleles (**Figure 1B**). We found that the functional disruption of *PHL4* reduced the expression of only four of the six PSI marker genes examined, and that the reduction was much lower than that observed for the *phr1* mutant (**Figure 5**). Furthermore, although the mutation of *PHL4* somewhat reduced the expression of four PSI marker genes, it did not cause obvious alterations in

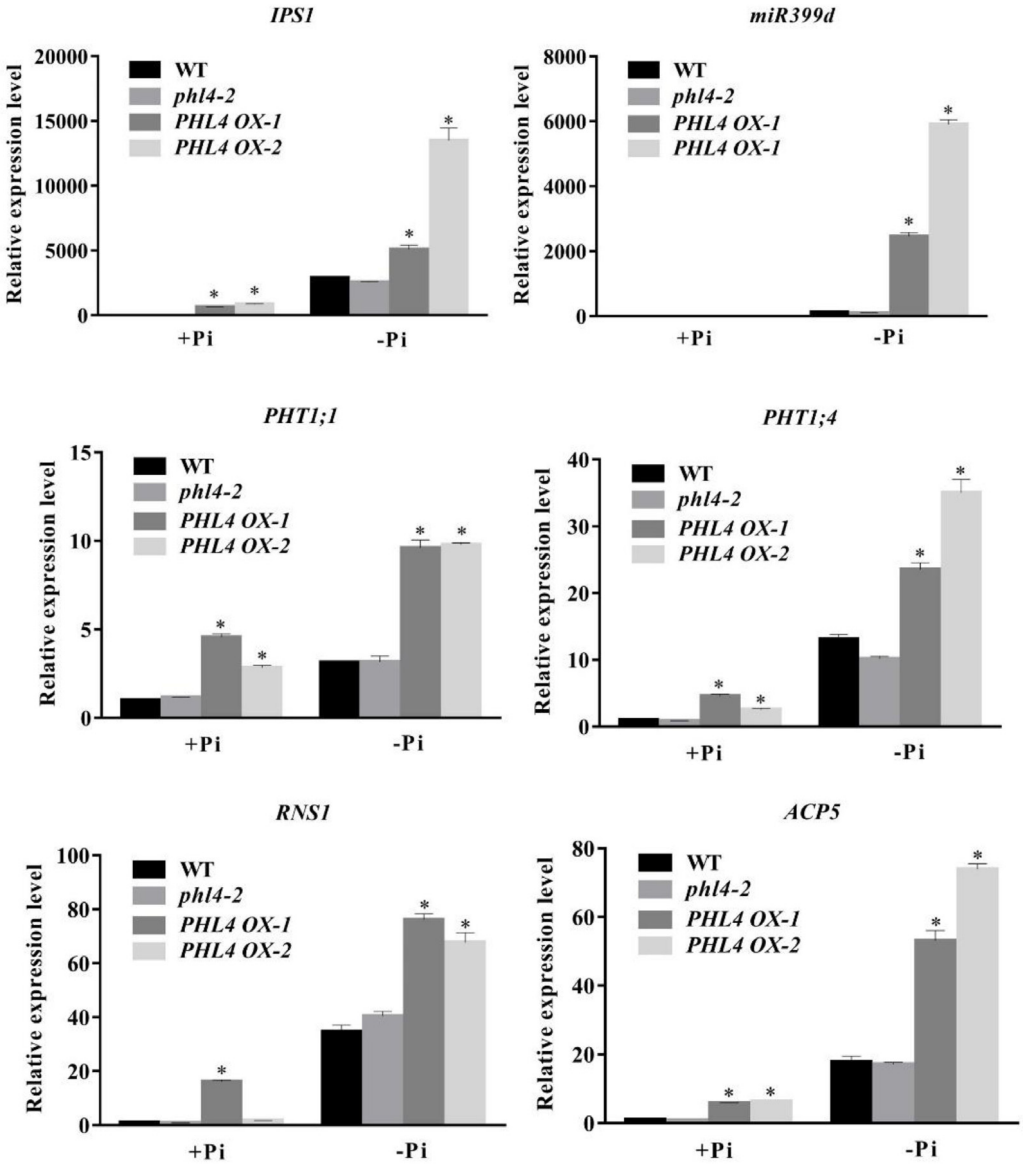

FIGURE 11 | Analyses of PSI gene expression in two *PHL4*-overexpressing lines (*PHL4 OX-1* and *PHL4 OX-2*). Roots of 8-day-old seedlings of the WT, *phl4*, and *PHL4 OX-1* and *-2* grown on +Pi and –Pi media were used for qPCR analysis. The names of the genes examined are indicated on the top of each panel. Values are the means ± SD of three biological replicates and represent fold changes normalized to transcript levels of the WT on +Pi medium. Means with asterisks are significantly different from the WT ($P < 0.05$, *t*-test).

the major hallmark responses to Pi starvation, i.e., mutation of *PHL4* did not affect root architecture (**Figure 3**), root-associated APase activity, the accumulation of anthocyanins in shoots, or the cellular Pi and total P contents in shoot and roots (**Figure 4**). These results suggest that PHL4 has only a minor role in regulating plant responses to Pi starvation.

The mild effect of *PHL4* mutation on plant responses to Pi starvation might be due to the functional redundancy among members of the MYB-CC family. To test this possibility, we generated the *phr1phl4* double mutant and analyzed its phenotypes along with those of the *phr1* single mutant and the *phr1phl1* double mutant. Three different types of effects of *phl1* and *phl4* mutations on *phr1* were observed: First, the *phl1* and *phl4* mutations had similar enhancing effects on certain *phr1* phenotypes. Under Pi deficiency, for example, the growth of *phr1* was more inhibited than that of the WT, and this inhibitory effect was further enhanced and to a similar degree in both *phr1phl1* and *phr1phl4* (**Figure 6A**). Such similar enhancing effects were also observed in *phr1phl1* and *phr1phl4* for the induction of root-associated APase activity (**Figure 7A**) and for the accumulation of anthocyanins in shoots (**Figure 7B**). Second, the enhancing effect was greater for *phl1* than for *phl4* with regard to the expression of six PSI marker genes (**Figure 8**). Third, the *phl1* mutation but not the *phl4* mutation enhanced the following

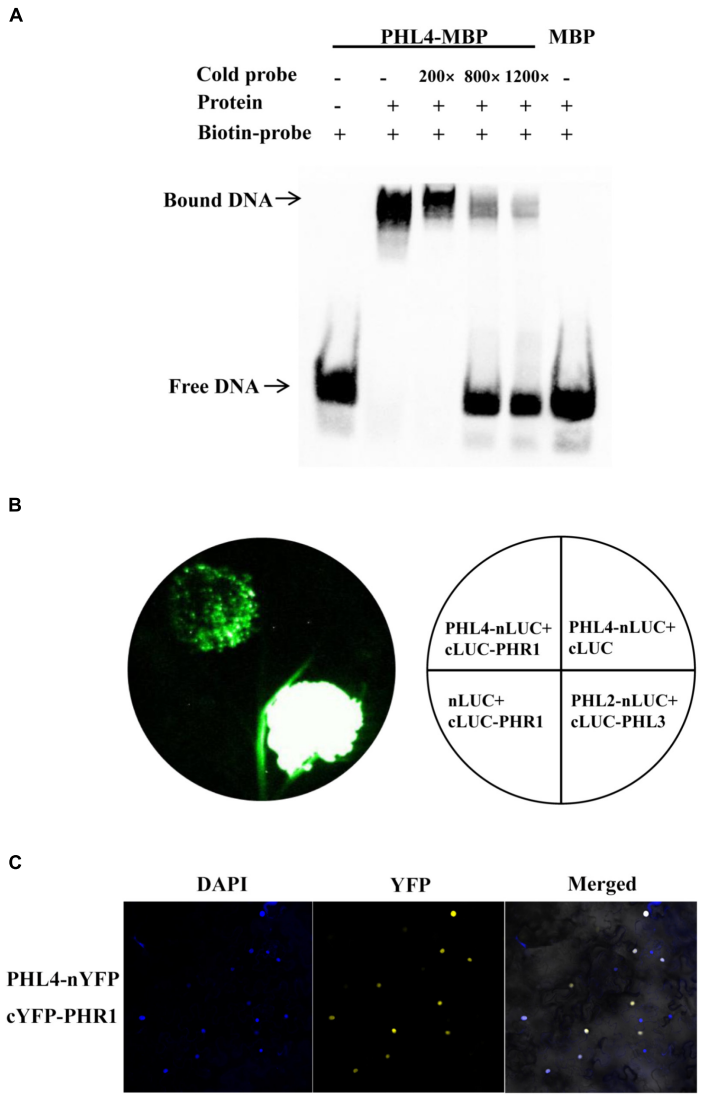

FIGURE 12 | PHL4 binds to the P1BS element and interacts with PHR1. **(A)** EMSA assay showing that PHL4 protein specifically binds to the P1BS element. The experiment was performed using 4 μg of MBP-PHL4 protein and 10 fmol of biotin-labeled DNA probe. The same unlabeled probe was used as the competitor at an excess molar ratio of 200:1, 800:1, and 1200:1 to labeled probe. **(B)** LCI assays for the interaction of PHL4 and PHR1. The constructs PHL4-nLUC and cLUC-PHR1 were co-infiltrated into the leaves of *N. benthamiana*, and LUC signals were recorded 2 d after infiltration. **(C)** BiFC assays for the interaction between PHL4 and PHR1. The constructs PHL4-nYFP and cYFP-PHR1 were co-infiltrated into the leaves of *N. benthamiana*. YFP fluorescence was detected 2 days after infiltration by confocal microscopy. The nuclei were revealed by DAPI staining.

phr1 phenotypes: root hair production by seedlings grown on −Pi medium (**Figure 6B**), early senescence phenotypes of plants grown in soil (**Figure 6C**), and Pi and total P contents in +Pi shoots and −Pi roots (**Figures 7C,D**). Based on these results, we conclude that PHL4 has a smaller role than PHL1 in regulating Pi starvation responses, although PHL4 is more closely related to PHR1 than PHL1.

When analyzing the cellular Pi and total P contents in shoots and roots, we found that the patterns for cellular Pi content were quite similar to those for total P content, indicating that the amount of free Pi in the plant tissues was correlated with the total P content, which includes both free Pi and P incorporated into organophosphates, such as nucleic acids and phospholipids. Rubio et al. (2001) and Bustos et al. (2010) previously noticed that cellular Pi content was decreased in the whole seedlings of *phr1*, and was further decreased in the whole seedlings of the *phr1phl1* double mutant. Nilsson et al. (2007) observed that under Pi deficiency, Pi content but not total P in *phr1* was decreased in shoots and that both Pi and total P contents were increased by about two times in roots, suggesting that PHR1 is involved in Pi translocation from roots to shoots. Under Pi deficiency in our experiments, both Pi and total P contents were decreased in *phr1* shoots, and total P but not cellular Pi was slightly increased in *phr1* roots

(**Figures 7C,D**). This discrepancy between Nilsson et al. (2007) and the current research may be due to the use of hydroponics in their study vs. agar plates in our study. However, we also documented an increase of both Pi and total P contents in the roots of the *phr1phl1* double mutant under Pi deficiency, but not in the roots of *phr1phl4* under Pi deficiency (**Figures 7C,D**). Based on these results, we propose that PHR1 and PHL1 together, but not PHR1 and PHL4 together, function in the regulation of Pi translocation from roots to shoots. PHO1 was previously identified as a key component in regulating Pi translocation from roots to shoots (Poirier et al., 1991). However, whether the over-accumulation of Pi in roots of *phr1phl1* grown under Pi deficiency is linked to PHO1 function requires further investigation.

Another way to overcome genetic redundancy when investigating the functions of a given gene is to study the phenotypes of its overexpressing lines (Weigel et al., 2000). We therefore generated *PHL4 OX* lines using a *35S CaMV* promoter in the *phl4* background. When grown on +Pi medium, the seedlings of four *PHL4 OX* lines had short primary roots that lacked gravitropism and that had small cotyledons with epinasty (**Figure 9A**). On −Pi medium, the *PHL4 OX* seedlings were smaller than the WT, but they regained gravitropism. Under Pi deficiency, root hair development was greatly inhibited in the overexpressing lines (**Figure 9B**). Although *PHL4* is not expressed in root hairs of the WT (**Figure 2D**), *PHL4* might be ectopically overexpressed in trichoblasts of the overexpressing lines, and such ectopic expression may have inhibited root hair initiation and elongation. When grown in soil for 5 weeks, *PHL4 OX* plants were much smaller than WT or *phl4* plants and had yellowish and serrated leaves (**Figure 9C**). The inhibitory effects of *PHL4* overexpression on both shoot and root growth suggest that PHL4 is also a negative regulator of plant growth.

Regarding other plant responses to Pi starvation, the overexpression of *PHL4* enhanced root-associated APase activity (**Figure 10A**), increased tissue Pi and total P contents, especially in shoots (**Figures 10C,D**), and enhanced the expression of all PSI marker genes examined, although the degree of enhancement varied from line to line due to the position effect (**Figure 11**). This enhancement of gene expression caused by the overexpression of *PHL4* is similar to that caused by overexpression of *PHR1* (Nilsson et al., 2007; Sun et al., 2016). However, the enhancement of anthocyanin accumulation in shoots was not observed in the overexpressing lines grown on −Pi medium (**Figure 10B**). When *PHR1* was overexpressed, in contrast, anthocyanin accumulation was enhanced under Pi deficiency. These results suggest that overexpression of *PHL4* affects most but not all plant responses to Pi starvation.

If PHL4 is indeed a transcription factor, it should be able to bind to DNA molecules. PHR1, PHL1, PHL2, and PHL3 were previously demonstrated to bind to the P1BS element (Rubio et al., 2001; Bustos et al., 2010; Sun et al., 2016). Nguyen et al. (2016) studied the regulation of a pollen-specific phospholipase gene, PLA_2-γ. They found that PHL4, which they named γMYB1, and another MYB-CC family member (At3g13040), which they named γMYB2, could bind to the P1BS element on the promoter of the phospholipase gene, PLA2-γ. Our EMSA experiments corroborated that PHL4 can bind to the P1BS element in a sequence-specific manner (**Figure 12A**). Nguyen et al. (2016) also showed that γMYB1 (PHL4) but not γMYB2 has the activity of a transcriptional activator. This is consistent with our finding that the overexpression of *PHL4* enhanced the expression of six PSI genes, all of which carried the P1BS element. PHL1 has been previously shown to form a heterodimer with PHR1 *in vitro* (Bustos et al., 2010). Because PHL4 is most closely related to PHR1, we therefore wondered whether PHL4 could also directly interact with PHR1. Indeed, our LCI and BiFC assays demonstrated that PHL4 could directly interact with PHR1 in the nucleus (**Figures 12B,C**). Because both PHL1 and PHL4 can form a protein complex with PHR1, knockout of either one may be compensated for by the other. This might explain why the *phl1* and *phl4* single mutants did not display an obvious phenotype in plant responses to Pi starvation.

In summary, our analyses of two *phl4* null mutants indicated that PHL4, like PHL1, acts redundantly with PHR1 to regulate plant responses to Pi starvation; however, its role in the PHR1-mediated central regulatory system is only minor. Our comparative study of *phr1phl1* and *phr1phl4* double mutants revealed both overlapping and distinct functions of PHL1 and PHL4 in regulating plant responses to Pi starvation and suggested that the contribution of PHL4 to such regulatory system is less than that of PHL1. Moreover, the phenotypes of *PHL4 OX* lines suggested that PHL4 is a negative regulator of plant growth and development. The next challenge will be to understand how PHL1 and PHL4 differentially act with PHR1 to regulate plant responses to Pi starvation.

AUTHOR CONTRIBUTIONS

ZW, ZZ, and DL conceived and designed the experiments. ZW and LS carried out the experiments. ZW and DL analyzed the data. ZW and DL wrote the manuscript.

FUNDING

This work was supported by funds from National Key R&D Program of China (Grant No. 2016YFD0100700), the National Natural Science Foundation of China (Grant No. 31670256 and 31700217), and the China Postdoctoral Science Foundation (Grant No. 2017M610868).

ACKNOWLEDGMENTS

We thank Dr. Qi Xie of the Institute of Genetics and Developmental Biology, Chinese Academy of Sciences, for kindly providing the CRISPR/Cas9 gene editing constructs.

SUPPLEMENTARY MATERIAL

The Supplementary Material for this article can be found online at: https://www.frontiersin.org/articles/10.3389/fpls.2018.01432/full#supplementary-material

REFERENCES

Bari, R., Datt Pant, B., Stitt, M., and Scheible, W. R. (2006). PHO2, microRNA399, and PHR1 define a phosphate-signaling pathway in plants. *Plant Physiol.* 141, 988–999. doi: 10.1104/pp.106.079707

Bariola, P. A., Howard, C. J., Taylor, C. B., Verburg, M. T., Jaglan, V. D., and Green, P. J. (1994). The *Arabidopsis ribonuclease* gene RNS1 is tightly controlled in response to phosphate limitation. *Plant J.* 6, 673–685. doi: 10.1046/j.1365-313X.1994.6050673.x

Bournier, M., Tissot, N., Mari, S., Boucherez, J., Lacombe, E., Briat, J. F., et al. (2013). Arabidopsis ferritin 1 (AtFer1) gene regulation by the phosphate starvation response 1 (AtPHR1) transcription factor reveals a direct molecular link between iron and phosphate homeostasis. *J. Biol. Chem.* 288, 22670–22680. doi: 10.1074/jbc.M113.482281

Burleigh, S. H., and Harrison, M. J. (1999). The down-regulation of Mt4-Like genes by phosphate fertilization occurs systemically and involves phosphate translocation to the shoots. *Plant Physiol.* 119, 241–248. doi: 10.1104/pp.119.1.241

Bustos, R., Castrillo, G., Linhares, F., Puga, M. I., Rubio, V., Pérez-Pérez, J., et al. (2010). A central regulatory system largely controls transcriptional activation and repression responses to phosphate starvation in Arabidopsis. *PLoS Genet.* 6:e1001102. doi: 10.1371/journal.pgen.1001102

Chen, H., Zou, Y., Shang, Y., Lin, H., Wang, Y., Cai, R., et al. (2008). Firefly luciferase complementation imaging assay for protein-protein interactions in plants. *Plant Physiol.* 146, 368–376. doi: 10.1104/pp.107.111740

Clough, S. J., and Bent, A. F. (1998). Floral dip: a simplified method for agrobacterium-mediated transformation of *Arabidopsis thaliana*. *Plant J.* 16, 735–743. doi: 10.1046/j.1365-313x.1998.00343.x

del Pozo, J. C., Allona, I., Rubio, V., Leyva, A., de la Pena, A., Aragoncillo, C., et al. (1999). A type 5 acid phosphatase gene from Arabidopsis thaliana is induced by phosphate starvation and by some other types of phosphate mobilising/oxidative stress conditions. *Plant J.* 19, 579–589. doi: 10.1046/j.1365-313X.1999.00562.x

Franco-Zorrilla, J. M., Valli, A., Todesco, M., Mateos, I., Puga, M. I., Rubio-Somoza, I., et al. (2007). Target mimicry provides a new mechanism for regulation of microRNA activity. *Nat. Genet.* 39:1033. doi: 10.1038/ng2079

Fujii, H., Chiou, T., Lin, S., Aung, K., and Zhu, J. (2005). A miRNA involved in phosphate-starvation response in Arabidopsis. *Curr. Biol.* 15, 2038–2043. doi: 10.1016/j.cub.2005.10.016

Gibson, D. G., Young, L., Chuang, R., Venter, J. C., Hutchison, C. A. III, and Smith, H. O. (2009). Enzymatic assembly of DNA molecules up to several hundred kilobases. *Nat. Methods* 6, 343–345. doi: 10.1038/nmeth.1318

Guo, M., Ruan, W., Li, C., Huang, F., Zeng, M., Liu, Y., et al. (2015). Integrative comparison of the role of the PHOSPHATE RESPONSE1 subfamily in phosphate signaling and homeostasis in rice. *Plant Physiol.* 168, 1762–1776. doi: 10.1104/pp.15.00736

Hammond, J. P., Bennett, M. J., Bowen, H. C., Broadley, M. R., Eastwood, D. C., May, S. T., et al. (2003). Changes in gene expression in Arabidopsis shoots during phosphate starvation and the potential for developing smart plants. *Plant Physiol.* 132, 578–596. doi: 10.1104/pp.103.020941

Hernández, G., Ramírez, M., Valdés-López, O., Tesfaye, M., Graham, M. A., Czechowski, T., et al. (2007). Phosphorus stress in common bean: root transcript and metabolic responses. *Plant Physiol.* 144, 752–767. doi: 10.1104/pp.107.096958

Jain, A., Nagarajan, V. K., and Raghothama, K. G. (2012). Transcriptional regulation of phosphate acquisition by higher plants. *Cell. Mol. Life Sci.* 69, 3207–3224. doi: 10.1007/s00018-012-1090-6

Jefferson, R. A., Kavanagh, T. A., and Bevan, M. W. (1987). GUS fusions: beta-glucuronidase as a sensitive and versatile gene fusion marker in higher plants. *EMBO J.* 6, 3901–3907. doi: 10.1002/j.1460-2075.1987.tb02730.x

Khan, G. A., Bouraine, S., Wege, S., Li, Y., de Carbonnel, M., Berthomieu, P., et al. (2014). Coordination between zinc and phosphate homeostasis involves the transcription factor PHR1, the phosphate exporter PHO1, and its homologue PHO1;H3 in Arabidopsis. *J. Exp. Bot.* 65, 871–884. doi: 10.1093/jxb/ert444

Lin, W., Huang, T., and Chiou, T. (2013). NITROGEN LIMITATION ADAPTATION, a target of MicroRNA827, mediates degradation of plasma membrane-localized phosphate transporters to maintain phosphate homeostasis in Arabidopsis. *Plant Cell* 25, 4061–4074. doi: 10.1105/tpc.113.116012

Liu, T., Huang, T., Tseng, C., Lai, Y., Lin, S., Lin, W., et al. (2012). PHO2-dependent degradation of PHO1 modulates phosphate homeostasis in Arabidopsis. *Plant Cell* 24, 2168–2183. doi: 10.1105/tpc.112.096636

Livak, K. J., and Schmittgen, T. D. (2001). Analysis of relative gene expression data using real-time quantitative PCR and the $2^{-\Delta\Delta C_T}$ method. *Methods* 25, 402–408. doi: 10.1006/meth.2001.1262

López-Arredondo, D. L., Leyva-González, M. A., González-Morales, S. I., López-Bucio, J., and Herrera-Estrella, L. (2014). phosphate nutrition: improving low-phosphate tolerance in crops. *Annu. Rev. Plant Biol.* 65, 95–123. doi: 10.1146/annurev-arplant-050213-035949

Lundmark, M., Kørner, C. J., and Nielsen, T. H. (2010). Global analysis of microRNA in Arabidopsis in response to phosphate starvation as studied by locked nucleic acid-based microarrays. *Physiol. Plant.* 140, 57–68. doi: 10.1111/j.1399-3054.2010.01384.x

Lv, Q., Zhong, Y., Wang, Y., Wang, Z., Zhang, L., Shi, J., et al. (2014). SPX4 negatively regulates phosphate signaling and homeostasis through its interaction with PHR2 in Rice. *Plant Cell* 26, 1586–1597. doi: 10.1105/tpc.114.123208

Misson, J., Raghothama, K. G., Jain, A., Jouhet, J., Block, M. A., Bligny, R., et al. (2005). A genome-wide transcriptional analysis using *Arabidopsis thaliana* Affymetrix gene chips determined plant responses to phosphate deprivation. *P. Natl. Acad. Sci. U.S.A.* 102, 11934–11939. doi: 10.1073/pnas.0505266102

Morcuende, R., Bari, R., Gibon, Y., Zheng, W., Pant, B. D., Bläsing, O., et al. (2006). Genome-wide reprogramming of metabolism and regulatory networks of Arabidopsis in response to phosphorus. *Plant Cell Environ.* 30, 85–112. doi: 10.1111/j.1365-3040.2006.01608.x

Muchhal, U. S., Pardo, J. M., and Raghothama, K. G. (1996). Phosphate transporters from the higher plant *Arabidopsis thaliana*. *Proc. Natl. Acad. Sci. U.S.A.* 93, 10519–10523. doi: 10.1073/pnas.93.19.10519

Müller, R., Morant, M., Jarmer, H., Nilsson, L., and Nielsen, T. H. (2007). Genome-wide analysis of the Arabidopsis leaf transcriptome reveals interaction of phosphate and sugar metabolism. *Plant Physiol.* 143, 156–171. doi: 10.1104/pp.106.090167

Nguyen, H. T. K., Kim, S. Y., Cho, K., Hong, J. C., Shin, J. S., and Kim, H. J. (2016). A transcription factor γMYB1 binds to the P1BS cis-element and activates PLA2-γ expression with its co-activator γMYB2. *Plant Cell Physiol.* 57, 784–797. doi: 10.1093/pcp/pcw024

Nilsson, L., Müller, R., and Nielsen, T. H. (2007). Increased expression of the MYB-related transcription factor, PHR1, leads to enhanced phosphate uptake in *Arabidopsis thaliana*. *Plant Cell Environ.* 30, 1499–1512. doi: 10.1111/j.1365-3040.2007.01734.x

Nussaume, L., Kanno, S., Javot, H., Marin, E., Pochon, N., Ayadi, A., et al. (2011). Phosphate import in plants: focus on the PHT1 transporters. *Front. Plant Sci.* 2:83. doi: 10.3389/fpls.2011.00083

O'Rourke, J. A., Yang, S. S., Miller, S. S., Bucciarelli, B., Liu, J., Rydeen, A., et al. (2013). An RNA-Seq transcriptome analysis of orthophosphate-deficient white lupin reveals novel insights into phosphorus acclimation in plants. *Plant Physiol.* 161, 705–724. doi: 10.1104/pp.112.209254

Poirier, Y., Thoma, S., Somerville, C., and Schiefelbein, J. (1991). Mutant of Arabidopsis deficient in xylem loading of phosphate. *Plant Physiol.* 97, 1087–1093. doi: 10.1104/pp.97.3.1087

Puga, M. I., Mateos, I., Charukesi, R., Wang, Z., Franco-Zorrilla, J. M., de Lorenzo, L., et al. (2014). SPX1 is a phosphate-dependent inhibitor of PHOSPHATE STARVATION RESPONSE 1 in Arabidopsis. *Proc. Natl. Acad. Sci. U.S.A.* 111, 14947–14952. doi: 10.1073/pnas.1404654111

Puga, M. I., Rojas-Triana, M., de Lorenzo, L., Leyva, A., Rubio, V., and Paz-Ares, J. (2017). Novel signals in the regulation of Pi starvation responses in plants: facts and promises. *Curr. Opin. Plant Biol.* 39, 40–49. doi: 10.1016/j.pbi.2017.05.007

Raghothama, K. G. (2000). Phosphate transport and signaling. *Curr. Opin. Plant Biol.* 3, 182–187. doi: 10.1016/S1369-5266(00)00062-5

Ren, F., Guo, Q., Chang, L., Chen, L., Zhao, C., Zhong, H., et al. (2012). Brassica napus PHR1 gene encoding a MYB-Like protein functions in response to phosphate starvation. *PLoS One* 7:e44005. doi: 10.1371/journal.pone.0044005

Rouached, H., Secco, D., Arpat, B., and Poirier, Y. (2011). The transcription factor PHR1 plays a key role in the regulation of sulfate shoot-to-root flux upon

phosphate starvation in Arabidopsis. *BMC Plant Biol.* 11:19. doi: 10.1186/1471-2229-11-19

Ruan, W., Guo, M., Wu, P., and Yi, K. (2017). Phosphate starvation induced OsPHR4 mediates Pi-signaling and homeostasis in rice. *Plant Mol. Biol.* 93, 327–340. doi: 10.1007/s11103-016-0564-6

Rubio, V., Linhares, F., Solano, R., Martín, A. C., Iglesias, J., Leyva, A., et al. (2001). A conserved MYB transcription factor involved in phosphate starvation signaling both in vascular plants and in unicellular algae. *Genes Dev.* 15, 2122–2133. doi: 10.1101/gad.204401

Secco, D., Jabnoune, M., Walker, H., Shou, H., Wu, P., Poirier, Y., et al. (2013). Spatio-temporal transcript profiling of Rice roots and shoots in response to phosphate starvation and recovery. *Plant Cell* 25, 4285–4304. doi: 10.1105/tpc.113.117325

Sun, L., Song, L., Zhang, Y., Zheng, Z., and Liu, D. (2016). Arabidopsis PHL2 and PHR1 act redundantly as the key components of the central regulatory system controlling transcriptional responses to phosphate starvation. *Plant Physiol.* 170, 499–514. doi: 10.1104/pp.15.01336

Wang, F., Deng, M., Xu, J., Zhu, X., and Mao, C. (2018). Molecular mechanism of phosphate transport and signaling in higher plants. *Semin. Cell Dev. Biol.* 74, 114–122. doi: 10.1016/j.semcdb.2017.06.013

Wang, J., Sun, J., Miao, J., Guo, J., Shi, Z., He, M., et al. (2013). A phosphate starvation response regulator Ta-PHR1 is involved in phosphate signalling and increases grain yield in wheat. *Ann. Bot.* 111, 1139–1153. doi: 10.1093/aob/mct080

Wang, L., Li, Z., Qian, W., Guo, W., Gao, X., Huang, L., et al. (2011). The Arabidopsis purple acid phosphatase AtPAP10 is predominantly associated with the root surface and plays an important role in plant tolerance to phosphate limitation. *Plant Physiol.* 157, 1283–1299. doi: 10.1104/pp.111.183723

Wang, L., Lu, S., Zhang, Y., Li, Z., Du, X., and Liu, D. (2014a). Comparative genetic analysis of Arabidopsis purple acid phosphatases AtPAP10, AtPAP12, and AtPAP26 provides new insights into their roles in plant adaptation to phosphate deprivation. *J. Integr. Plant Biol.* 56, 299–314. doi: 10.1111/jipb.12184

Wang, Z., Ruan, W., Shi, J., Zhang, L., Xiang, D., Yang, C., et al. (2014b). Rice SPX1 and SPX2 inhibit phosphate starvation responses through interacting with PHR2 in a phosphate-dependent manner. *Proc. Natl. Acad. Sci. U.S.A.* 111, 14953–14958. doi: 10.1073/pnas.1404680111

Weigel, D., Ahn, J. H., Blazquez, M. A., Borevitz, J. O., Christensen, S. K., Fankhauser, C., et al. (2000). Activation tagging in Arabidopsis. *Plant Physiol.* 122, 1003–1014. doi: 10.1104/pp.122.4.1003

Wild, R., Gerasimaite, R., Jung, J., Truffault, V., Pavlovic, I., Schmidt, A., et al. (2016). Control of eukaryotic phosphate homeostasis by inositol polyphosphate sensor domains. *Science* 352, 986–990. doi: 10.1126/science.aad9858

Wu, P., Ma, L., Hou, X., Wang, M., Wu, Y., Liu, F., et al. (2003). Phosphate starvation triggers distinct alterations of genome expression in Arabidopsis roots and leaves. *Plant Physiol.* 132, 1260–1271. doi: 10.1104/pp.103.021022

Xue, Y., Xiao, B., Zhu, S., Mo, X., Liang, C., Tian, J., et al. (2017). GmPHR25, a GmPHR member up-regulated by phosphate starvation, controls phosphate homeostasis in soybean. *J. Exp. Bot.* 68, 4951–4967. doi: 10.1093/jxb/erx292

Yan, L., Wei, S., Wu, Y., Hu, R., Li, H., Yang, W., et al. (2015). High-efficiency genome editing in Arabidopsis using YAO promoter-driven CRISPR/Cas9 system. *Mol. Plant* 8, 1820–1823. doi: 10.1016/j.molp.2015.10.004

Yuan, H., and Liu, D. (2008). Signaling components involved in plant responses to phosphate starvation. *J. Integr. Plant Biol.* 50, 849–859. doi: 10.1111/j.1744-7909.2008.00709.x

Yuan, J., Zhang, Y., Dong, J., Sun, Y., Lim, B. L., Liu, D., et al. (2016). Systematic characterization of novel lncRNAs responding to phosphate starvation in *Arabidopsis thaliana*. *BMC Genomics* 17:655. doi: 10.1186/s12864-016-2929-2

Zhang, Y., Wang, X., Lu, S., and Liu, D. (2014). A major root-associated acid phosphatase in Arabidopsis, AtPAP10, is regulated by both local and systemic signals under phosphate starvation. *J. Exp. Bot.* 65, 6577–6588. doi: 10.1093/jxb/eru377

Zhou, J., Jiao, F., Wu, Z., Li, Y., Wang, X., He, X., et al. (2008). OsPHR2 is involved in phosphate-starvation signaling and excessive phosphate accumulation in shoots of plants. *Plant Physiol.* 146, 1673–1686. doi: 10.1104/pp.107.111443

Conflict of Interest Statement: The authors declare that the research was conducted in the absence of any commercial or financial relationships that could be construed as a potential conflict of interest.

frontiers in Plant Science

ORIGINAL RESEARCH
published: 19 November 2018
doi: 10.3389/fpls.2018.01543

Increased Catalase Activity and Maintenance of Photosystem II Distinguishes High-Yield Mutants From Low-Yield Mutants of Rice var. Nagina22 Under Low-Phosphorus Stress

*Yugandhar Poli[1], Veronica Nallamothu[1], Divya Balakrishnan[1], Palakurthi Ramesh[2], Subrahmanyam Desiraju[1], Satendra Kumar Mangrauthia[1], Sitapathi Rao Voleti[1] and Sarla Neelamraju[1]**

[1] ICAR-Indian Institute of Rice Research, Hyderabad, India, [2] Department of Biotechnology, Yogi Vemana University, Kadapa, India

OPEN ACCESS

Edited by:
Alex Joseph Valentine, Stellenbosch University, South Africa

Reviewed by:
Jitender Giri, National Institute of Plant Genome Research (NIPGR), India
Antonio Ferrante, Università degli Studi di Milano, Italy

***Correspondence:**
Sarla Neelamraju
sarla_neelamraju@yahoo.com

Specialty section:
This article was submitted to Plant Nutrition, a section of the journal Frontiers in Plant Science

Received: 12 January 2018
Accepted: 02 October 2018
Published: 19 November 2018

Citation:
Poli Y, Nallamothu V, Balakrishnan D, Ramesh P, Desiraju S, Mangrauthia SK, Voleti SR and Neelamraju S (2018) Increased Catalase Activity and Maintenance of Photosystem II Distinguishes High-Yield Mutants From Low-Yield Mutants of Rice var. Nagina22 Under Low-Phosphorus Stress. Front. Plant Sci. 9:1543. doi: 10.3389/fpls.2018.01543

An upland rice variety, Nagina22 (N22) and its 137 ethyl methanesulfonate (EMS)-induced mutants, along with a sensitive variety, Jaya, was screened both in low phosphorus (P) field (Olsen P 1.8) and in normal field (Olsen P 24) during dry season. Based on the grain yield (YLD) of plants in normal field and plants in low P field, 27 gain of function (high-YLD represented as hy) and 9 loss of function (low-YLD represented as ly) mutants were selected and compared with N22 for physiological and genotyping studies. In low P field, hy mutants showed higher P concentration in roots, leaves, grains, and in the whole plant than in ly mutants at harvest. In low P conditions, F_v/F_m and q_N were 24% higher in hy mutants than in ly mutants. In comparison with ly mutants, the superoxide dismutase (SOD) activity in the roots and leaves of hy mutants in low P fields was 9% and 41% higher at the vegetative stage, respectively, but 51% and 14% lower in the roots and leaves at the reproductive stage, respectively. However, in comparison with ly mutants, the catalase (CAT) activity in the roots and leaves of hy mutants in low P fields was 35% higher at the vegetative stage and 15% and 17% higher at the reproductive stage, respectively. Similarly, hy mutants in low P field showed 20% and 80% higher peroxidase (POD) activity in the roots and leaves at the vegetative stage, respectively, but showed 14% and 16% lower POD activity at the reproductive stage in the roots and leaves, respectively. Marker trait association analysis using 48 simple sequence repeat (SSR) markers and 10 *Pup1* gene markers showed that RM3648 and RM451 in chromosome 4 were significantly associated with grain YLD, tiller number (TN), SOD, and POD activities in both the roots and leaves in low P conditions only. Similarly, RM3334 and RM6300 in chromosome 5 were associated

with CAT activity in leaves in low P conditions. Notably, grain YLD was positively and significantly correlated with CAT activity in the roots and shoots, F_v/F_m and q_N in low P conditions, and the shoots' P concentration and q_N in normal conditions. Furthermore, CAT activity in shoots was positively and significantly correlated with TN in both low P and normal conditions. Thus, chromosomal regions and physiological traits that have a role in imparting tolerance to low P in the field were identified.

Keywords: upland rice variety, EMS-induced mutants, low P condition, antioxidant enzymes, F_v/F_m test

INTRODUCTION

Factors influencing crop growth and productivity, nutrients being the most important, are applied in the form of fertilizers. Among these nutrients, phosphorus (P), secondary to nitrogen (N), plays an essential role in plant growth. Phosphorus fixation is a common problem in the soils of rice fields (Krishnamurthy et al., 2010; Panigrahy et al., 2014; Vandamme et al., 2016; Yugandhar et al., 2018a,b). The applied P is not completely available to plants because of slow diffusion rates and processes such as fixation in alkaline soils with Ca and fixation in acidic soils with Fe and Al. For the farming community, P fertilizers are costly and difficult to access, which cause major concerns for rice cultivation in India and other rice growing countries. Phosphorus fertilizer production is largely dependent on rock phosphate, a nonrenewable resource, and this finite source of P is under the threat of exhaustion.

Low P availability reduces plant height (PH), tiller number (TN), and yield (YLD) attributes such as the number of panicles, grains per panicle, filled grains per panicle, and higher spikelet sterility, thus limiting plant productivity (Veronica et al., 2017). Increase of root acid phosphatase is one of the most common responses to low P conditions, which help plants to hydrolyze organic P into inorganic P and enhance the availability of P to plants (Mehra et al., 2017; Pandey et al., 2017). For this reason, there is a need to develop genotypes that can produce an acceptable grain YLD under low P conditions. In India, the availability of P in most of the cultivated soils is becoming either low or extremely poor (Sanyal et al., 2015), particularly in upland soils.

Phosphate deprivation lowers the leaf photosynthetic oxygen evolution, photosystem II quantum efficiency, and electron transport (Veronica et al., 2017). Reactive oxygen species (ROS) act as signaling molecules under normal physiological conditions and play a vital role in signal transduction. Exposure of plants to low P conditions triggers an increased generation of reactive oxygen intermediates (ROI) or ROS such as O^{2-}, H_2O_2, and OH^- radicals, which are cytotoxic and disrupt the normal metabolism through oxidative damage of lipids, proteins, and nucleic acids, leading to oxidative stress. To manage these ROS outbreaks, plants have evolved intricate antioxidant defense systems, consisting of detoxifying or ROS scavenging enzymatic antioxidants, namely superoxide dismutase (SOD), peroxidase (POD), catalase (CAT), glutathione reductase (GR), and non-enzymatic antioxidants, namely glutathione, ascorbic acid, carotenoids, α-tocopherol, and flavonoids. In rice root tissues, the activities of these three scavenging enzymes (SOD, POD, and CAT) are affected by phosphate deficiency (Juszczuk et al., 2001). Decreased photosynthetic efficiency was reported in low P field conditions, in crops such as rice (Veronica et al., 2017), wheat (Rodríguez et al., 1998), and soybean (Lauer et al., 1989). Veronica et al. (2017) have screened four rice genotypes for antioxidant enzyme activities in 0, 15, 30, 45,and 60 kg/ha of applied P in soil and found that higher CAT activity in the rice cultivar Swarna at the flowering stage led to higher grain YLD in low P conditions. Hussain et al. (2016) reported that P deprivation led to a significant increase in POD and CAT activities in 18-day-old rice hydroponically grown seedlings.

Nagina22, a deep-rooted upland rice variety, tolerant to various biotic and abiotic stresses, was subjected to ethyl methane sulfonate (EMS)-induced mutations. For characterization, 85,000 EMS-induced mutants were generated and maintained under a multi-institutional program (Mithra et al., 2016). Mutants for abiotic stresses such as heat, drought, low-P tolerance, and herbicide resistance were identified (Poli et al., 2013, 2017a,b; Mohapatra et al., 2014; Panigrahy et al., 2014; Lima et al., 2015; Talla et al., 2016; Shoba et al., 2017; Yugandhar et al., 2018a).

In this study, we evaluated different physiological and biochemical traits, including the activity of antioxidant enzymes in the roots and leaves as well as fluorescence parameters in flag leaves. The 27 gain of function (high-YLD represented as hy) and 9 loss of function (low-YLD represented as ly) mutants were compared with N22 and Jaya under normal as well as low P conditions to identify traits that can distinguish hy and ly mutants in low P conditions. In order to establish marker trait associations, mutants were genotyped using simple sequence repeat (SSR) and *Pup1* gene linked markers.

MATERIALS AND METHODS

Field experiments were carried out at ICAR-IIRR (Indian Institute of Rice Research) in 2013. Rice [*Oryza sativa* L. sub group *aus* variety Nagina22 (N22)] and its 137 EMS induced mutants were screened in M4 generation. Of these 137 mutants, 36 mutants were selected based on their grain YLD in low P conditions. Of these 36 mutants, 27 mutants with significantly higher grain YLD than N22 were categorized as hy, and 9 mutants with lower grain YLD or the same YLD as N22 were categorized as ly mutants. These mutants were further characterized for their morpho-agronomical, physiological, and biochemical characteristics.

Plant Material and Screening

Seeds from the 36 mutants selected in M5 generation were sown. After 25 days, each mutant was transferred to both a low P plot and a normal plot. The low P plot at IIRR was maintained without the application of P fertilizers for 35 years (Olsen P 1.8 kg/ha) (Panigrahy et al., 2014). Nitrogen in the form of urea (100 kg/ha), potassium as a muriate of potash (60 kg/ha), and zinc sulfate (12.5 kg/ha) were applied in both plots as basal dose, except N, which was applied in three split doses. Phosphorus as a single super phosphate (60 kg/ha) was applied in the normal plot only. Spacing was maintained at 20 cm between rows and 15 cm between plants. Soil properties of the experimental plots were as described by Panigrahy et al. (2014). The plants were grown to maturity following the normal package of practices (IRRI SES). Nagina22 (wild type) and Jaya (low P sensitive variety) were included as controls. All morphological, physiological, and biochemical observations were made at the time of 50% flowering.

Plant Height (PH)

The PH was measured from the base of the plant to the tip of the main panicle and awns were excluded if present.

Tiller Number (TN)

Tiller number for five plants were recorded on a per plant basis.

Grain Yield (YLD)

Panicles from each treatment were harvested, threshed, cleaned, and sun dried until the moisture content of seeds dropped to 14% and then weighed. Yield was expressed in g/plant.

Chlorophyll a Fluorescence

Chlorophyll a fluorescence parameter, F_v/F_m and electron transport rate (ETR), were recorded in dark adapted leaves in both treatments using a portable PAM-2100 fluorometer (Walz, Effeltrich, Germany).

Phosphorus Concentrations in Roots, Shoots, and Grains

After harvest, the dried roots, shoots, and grains were powdered and digested separately in a mixture of HNO_3, $HClO_4$, and H_2SO_4 (3:1:1) at 350°C for 2 h. After digestion, P concentration was determined using a spectrophotometer by the phosphovanadate method (Hanson, 1950).

Antioxidant Enzymes

Superoxide Dismutase (EC 1.15.1.1), Peroxidase (EC 1.11.1.7), and Catalase (EC 1.11.1.6) Activities

Antioxidant enzymes were estimated at tillering (vegetative stage) and flowering (reproductive stage). Enzyme extracts for SOD, POD, and CAT activities were prepared by freezing the weighed amount (0.1 g) of leaf samples at both the vegetative and flowering stages in liquid nitrogen to prevent proteolytic activity, followed by grinding with 5 ml extraction buffer (0.1 M phosphate buffer, pH 7.5, containing 0.5 mM EDTA). The enzyme extract was centrifuged for 20 min at 15000 g at 4C, and the supernatant was collected and assayed for enzyme activity.

The SOD activity was measured according to the method described by Dhindsa et al. (1981). A volume of 3 ml of SOD reaction mixture consisted of methionine (200 mM), nitro blue tetrazolium chloride (NBT) (2.25 mM), EDTA (3.0 mM), riboflavin (60 μM), sodium carbonate (1.5 M), and phosphate buffer (100 mM, pH 7.8). Tubes were kept under light. The reaction mixture without plant extract and irradiation, served as a blank. The absorbance was recorded at 560 nm. The volume of enzyme extract corresponding to 50% inhibition of the reaction was considered as one enzyme unit. Activity was expressed as units/min/g fresh weight (U/min/g FW). Peroxidase assay was carried out according to the method described by Castillo et al. (1984). A volume of 3 ml of POD assay mixture consisted of 1 ml phosphate buffer (pH 6.1), guaiacol 0.5 ml, H_2O_2 0.5 ml, enzyme 0.1 ml, and water 0.9 ml. An increase in absorbance due to the formation of tetraguaiacol was recorded at 470 nm. The POD activity was measured and expressed as μmol of H_2O_2 reduced per minute per gram FW. The CAT activity was measured according to the method described by Aebi (1984). The CAT assay mixture of 3 ml consisted of 0.05 ml extract, 1.5 ml phosphate buffer (100 mM buffer, pH 7.0), 0.5 ml H_2O_2, and 0.95 ml distilled water. A decrease in the absorbance was recorded at 240 nm. The CAT activity was expressed as μmol of H_2O_2 oxidized per minute per gram FW.

Genotyping

Genomic DNA was extracted from leaves of 36 mutant lines, N22, and Jaya using cetyl trimethyl ammonium bromide extraction buffer. For genotyping, PCR was done with 48 SSR markers (McCouch et al., 2002). The amplified fragments were evaluated as present (1) or absent (0) bands. Single marker analysis was carried out using SMA method in IciMapping v4.1 (www.isbreeding.net) to establish marker trait association.

Statistical Analysis

Two-way analysis of variance (ANOVA) was carried out using Statistix Ver 8.1. The statistical significance of means for all the parameters was determined by the least significant difference (LSD) test. Principal component analysis (PCA) was done to minimize the dimensions of multivariate data into a few principal axes by generating Eigen vectors for each axis and component scores for the traits using PBTools[1] (Version 1.4) and R (R Core Team, 2012).

RESULTS

Screening of Mutants in Normal and Low P Conditions

For further studies, 27 hy and 9 ly mutants were selected based on grain YLD in low P conditions. These mutants were further screened in normal and low P conditions for detailed physiological and biochemical traits. Grain YLD, TN, and PH at maturity, as well as physiological and biochemical traits at both the vegetative and reproductive stages, were recorded.

[1] http://bbi.irri.org/products

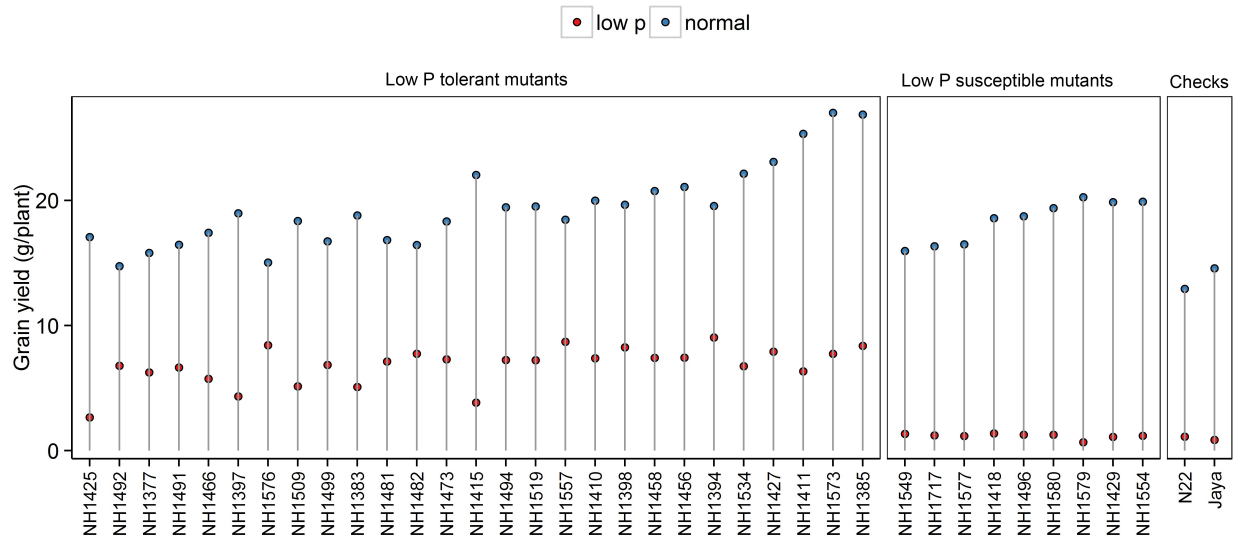

FIGURE 1 | Grain yield (g/plant) in normal and low P conditions in high- and low-yielding mutants.

Grain Yield

Significant reduction in grain YLD was observed in low P conditions compared with normal conditions. In low P conditions, there were significant differences among the mutants and controls. Grain YLD ranged from 3 to 9 g/plant in hy mutants and from 0.66 to 1.37 g/plant in ly mutants. When hy mutants were compared with ly mutants, the ly mutants showed 5.74 times less grain YLD under low P conditions. The YLDs of N22 and Jaya were 1.0 and 0.85 g/plant, respectively (**Figure 1**).

Tiller Number

Tiller numbers were significantly less in low P conditions than in normal conditions. In low P conditions, the differences between hy and ly mutants were significant. In hy mutants, the TN ranged from 8 to 13, and in ly mutants, it ranged from 1 to 4. When hy mutants were compared with ly mutants, the ly mutants showed 73% reduction in TN under low P conditions. The number of tillers per plant in N22 and Jaya were 2 and 1, respectively (**Figure 2**).

Plant Height

Plant height was 30% less in low P conditions when compared with normal conditions. Significant differences were also observed between the hy and ly mutants. PH ranged from 61 cm to 84 cm in hy mutants and from 50 cm to 72 cm in ly mutants. The ly mutants showed a 10% PH reduction under low

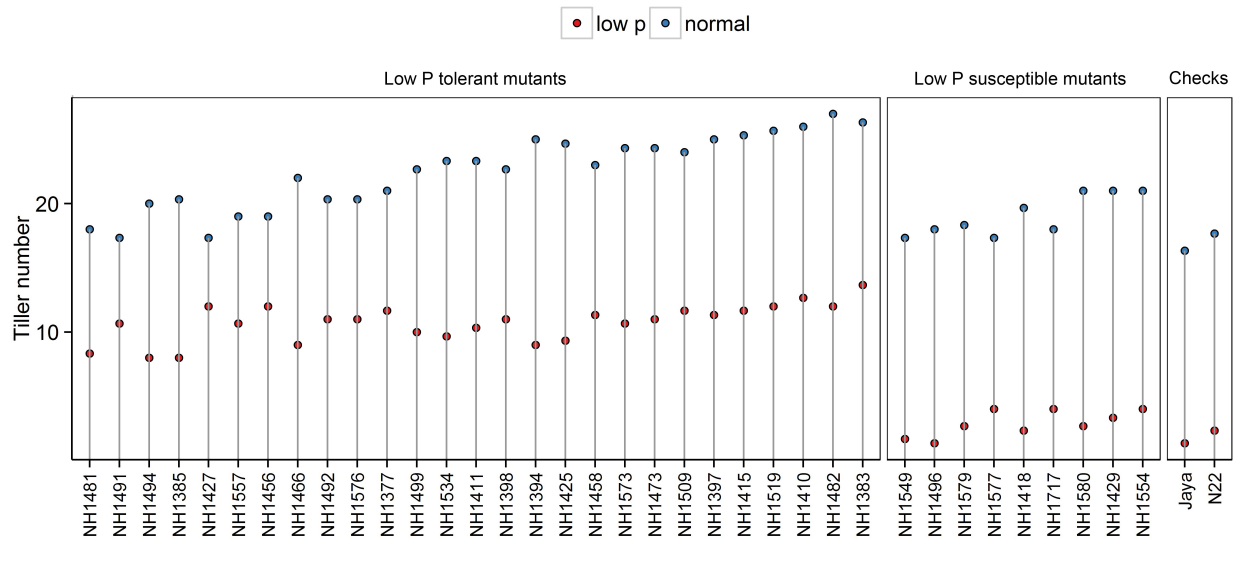

FIGURE 2 | Tiller number in normal and low P conditions in high- and low-yielding mutants.

P conditions when compared with hy mutants. The PH of N22 and Jaya in low P conditions was 71 cm and 53 cm, respectively (**Figure 3**).

Antioxidant Enzyme Activities

The SOD, POD, and CAT (units mg^{-1} protein) activities were measured in the roots and leaves at both the vegetative (tillering stage) and reproductive stages (panicle initiation) in low P and normal conditions (**Supplementary Tables S1**, **S2**). The mean SOD activity in the roots and leaves was threefold more in low P conditions than in normal conditions. At the vegetative stage, differences between mutants were significant. In low P conditions, the average SOD activity in the root and leaves in hy mutants was 9% and 41% higher, respectively, when compared with those in ly mutants (**Figure 4A**).

At the vegetative stage, differences of the POD activity in the roots and leaves were significant between treatments and mutants. In general, the mean POD activity in the roots and leaves was more than four-fold in low P conditions than in normal conditions. The average root POD activity was 6.87 units mg^{-1} protein in hy mutants and 8.29 units mg^{-1} protein in ly mutants. Thus, in low P conditions, the average root POD activity in ly mutants was 20% higher than hy mutants. In low P conditions, the average leaf POD activity was 12.94 units mg^{-1} protein in hy mutants and 6.52 U/min/g FW in ly mutants (**Figure 4C**). Thus, in low P conditions, the average leaf POD activity in hy mutants was 98% higher than in ly mutants. At the vegetative stage, differences of the CAT activity in the roots and leaves were significant between treatments and mutants. The mean CAT activity in the roots and leaves of all 36 mutants was more than three-fold in low P conditions than in normal conditions. In hy mutants, the average CAT activity in the roots and leaves was 22% and 35% more, respectively, than ly mutants in low P conditions (**Figure 4E**).

SOD Activity

The differences of SOD activity were significant between normal and low P conditions, vegetative and reproductive stages, and hy and ly mutants. In comparison with normal conditions, the mean SOD activity in the roots and leavess was threefold more in low P conditions. The mean SOD activity in the roots and leaves was 0.9% and 18% more, respectively, at the reproductive stage in low P conditions when compared with the vegetative stage. The hy mutants exhibited a 51% and 14% decrease of SOD activity in the roots and leaves during the reproductive stage in low P conditions. On the contrary, the SOD activity in the roots and leaves was 15% and 25% more in ly mutants at the reproductive stage. Nagina22 exhibited a 30% and 80% increase of SOD activity in the roots and leaves during the reproductive stage in low P conditions (**Figure 4B**).

POD Activity

Low P conditions triggered significantly more POD activity than normal conditions. The differences of POD activity were significant between the vegetative and reproductive stages and also between hy and ly mutants. In comparison with normal conditions, the mean POD activity in the roots and leaves was ninefold more in low P conditions. The mean POD activity in the roots and leaves was 124% and 185% more at the reproductive stage in low P conditions when compared with the vegetative stage. In low P conditions, the POD activity in the roots and leaves was 14% and 16% higher in ly mutants than in hy mutants. Nagina22 exhibited 115% and 100% more POD activity in the roots and leaves during the reproductive stage in low P conditions (**Figure 4D**).

CAT Activity

The differences of CAT activity were significant between low P and normal conditions, vegetative and reproductive stages, as

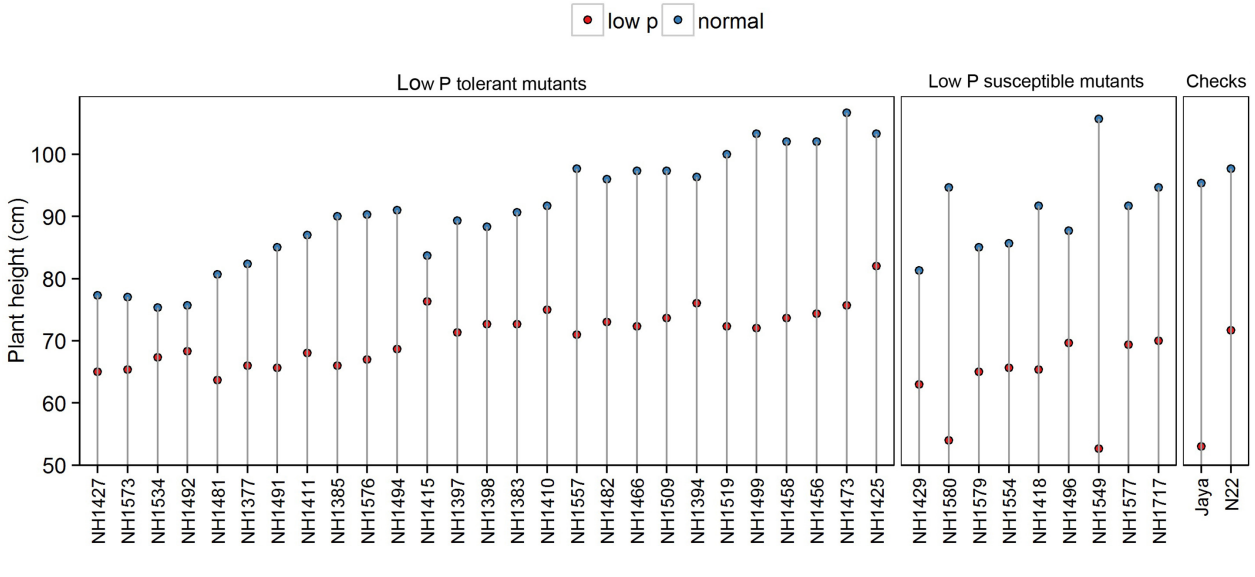

FIGURE 3 | Plant height in normal and low P conditions in high- and low-yielding mutants.

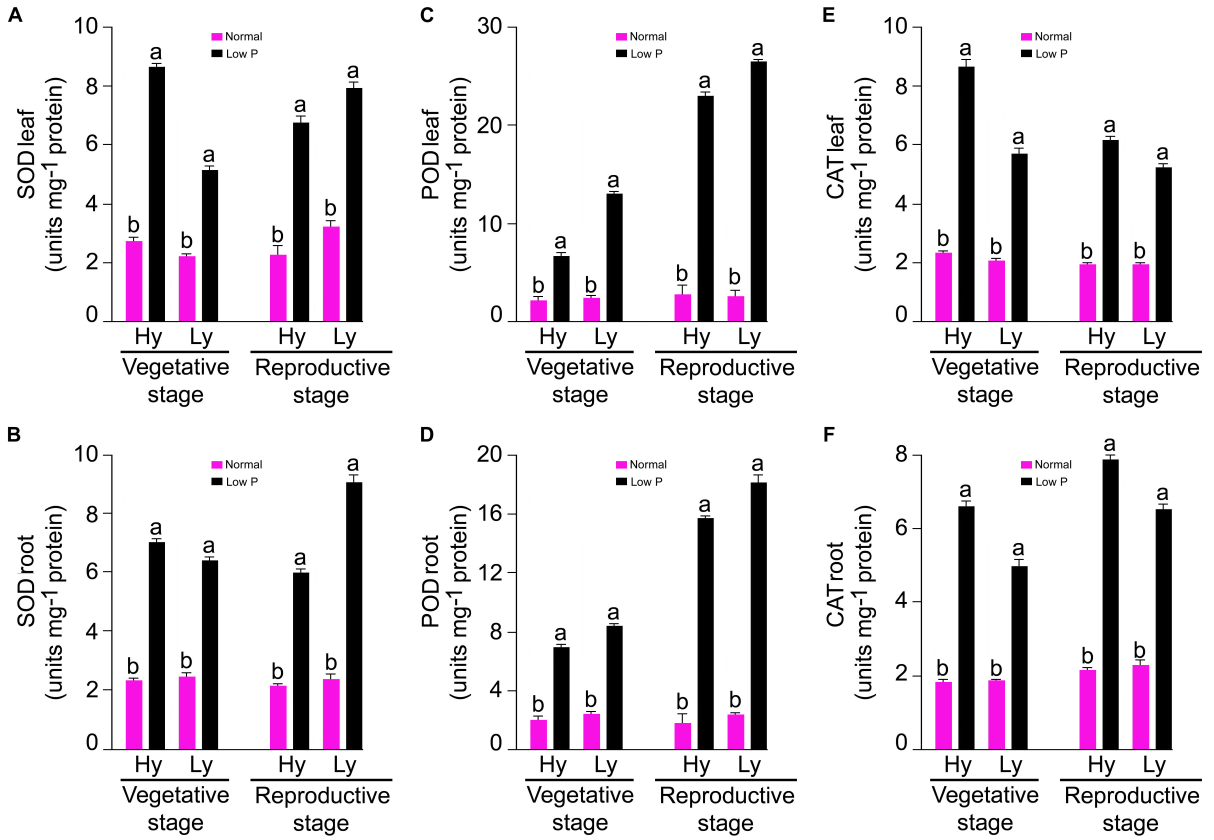

FIGURE 4 | SOD, POD, and CAT activities in leaf **(A,C,E)** and root **(B,D,F)** at vegetative and reproductive stages in high- and low-yielding mutants in normal and low P conditions.

well as between hy and ly mutants. When compared with normal conditions, the mean CAT activity in the roots and leaves was threefold more in low P conditions. The mean CAT activity in the roots and leaves was 22% and 24% more at the reproductive stage in low P conditions than at the vegetative stage. At the reproductive stage, N22 exhibited a 34% and 0.1% increase of CAT activity in the roots and leaves in low P conditions. In comparison with the vegetative stage, CAT activity in ly mutants showed a 15% reduction in roots and a 17% reduction in leaves at the reproductive stage (**Figure 4F**).

Chlorophyll a Fluorescence Parameters

The parameters F_v/F_m and q_N were measured at the reproductive stage only (**Supplementary Table S3**). In comparison with normal conditions, there was a 20% reduction in F_v/F_m and a 15% reduction in q_N in low P conditions. The differences of F_v/F_m and q_N were also significant between hy and ly mutants. In low P conditions, the hy mutants showed 16% higher F_v/F_m and 9% higher q_N when compared with ly mutants (**Figure 5**).

Phosphorous Concentrations in Roots, Leaves, and Grains

The differences in total P concentration in roots, leaves, and grains were significant between low and normal P conditions. Significant differences were also noticed among mutants in low P conditions (**Supplementary Table S4**). The mean root P concentration was significantly higher (63%) in hy mutants when compared with ly mutants. The concentration varied from 0.209 to 2.76 (mg/g DW) in hy mutants and from 0.11 to 0.193 (mg/g DW) in ly mutants. Similarly, in hy mutants, P concentrations were 31% higher in shoots and 39% higher in grains, when compared with those condition in ly mutants in low P conditions. The P concentration range of shoots in hy and ly mutants was 0.309–0.463 (mg/g DW) and 0.213–0.296 (mg/g DW), respectively. Similarly, the P concentration of grains ranged from 1.03 to 1.78 (mg/g DW) in hy mutants and 0.686 to 0.876 (mg/g DW) in ly mutants. Higher P concentration in roots, shoots, and grains eventually led to higher total P concentration in hy mutants. The total P concentration ranged from 1.66 to 4.376 (mg/g DW) in hy mutants and 1.04 to 1.284 (mg/g DW) in ly mutants in low P conditions. Thus, the total P concentration was 43% higher in hy mutants when compared with ly mutants in low P conditions. In N22 and Jaya, the P concentration in roots was 0.23 and 0.17 (mg/g DW), in shoots was 0.34 and 0.26 (mg/g DW), in grains was 0.97 and 0.68 (mg/g DW), and the total P concentration was 1.55 and 1.12 (mg/g DW) respectively, in low P conditions (**Figure 6**).

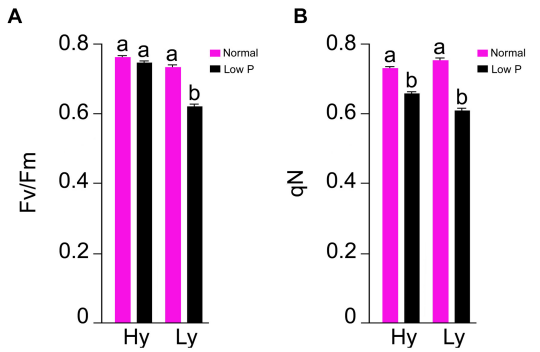

FIGURE 5 | F_v/F_m **(A)** and q_N **(B)** in leaf at reproductive stage in high- and low-yielding mutants in normal and low P conditions.

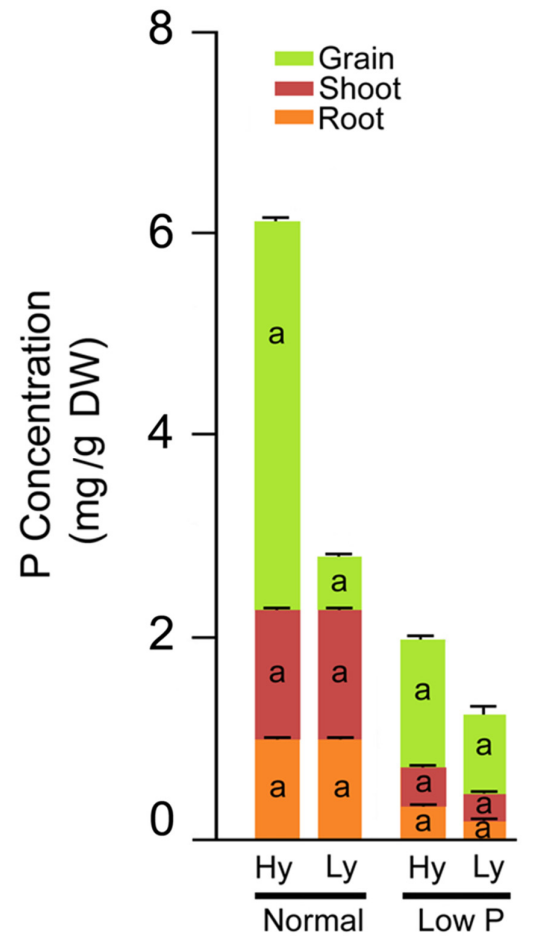

FIGURE 6 | Phosphorus concentration distribution in roots, shoots, and grains in high- and low-yielding mutants in normal and low P conditions.

Correlation Coefficients Among SOD, POD, and CAT Activities

The correlation among traits at the vegetative stage in hy and ly mutants is shown in **Figure 7**. In low P conditions at the vegetative stage, the SOD activity in leaves was positively correlated with the CAT activity in both the roots and shoots. The CAT activity in the roots and leaves was negatively correlated with the POD activity in leaves of hy mutants. On the other hand, in ly mutants, a significant positive correlation was observed between the POD activity and the CAT activity in roots. However, the SOD activity was negatively correlated with the CAT activity in roots. In hy mutants, a significant positive correlation was observed between the CAT activity in the roots and shoots, but a negative correlation was observed between the CAT activity in roots, POD activity in roots, and the SOD activity in leaves at normal conditions. In ly mutants at normal conditions, a positive correlation was observed between the POD activity and the CAT activity in roots, but a highly negative correlation was observed between the CAT activity and the SOD activity in shoots (**Figure 7**). In low P conditions, in hy mutants at the reproductive stage, a positive and significant correlation was found between grain YLD and CAT activity in the roots and shoots, F_v/F_m, and q_N. In normal conditions, grain YLD was positively correlated with concentrations in P shoots and q_N. It is important to note that the CAT activity in shoots was positively and significantly correlated with TN in both low P and normal conditions (**Figure 8**).

Heat Maps and Clustering in Normal and Low P Conditions

Heat maps and clustering of genotypes using different morphological, physiological, and biochemical traits showed a clear grouping of mutants in low P conditions, a specific correlation pattern for all hy mutants, and a reverse pattern for all ly mutants (**Figure 9**). However, in normal conditions, there was no specific pattern of correlation coefficients between hy and ly mutants for any trait (**Figure 10**).

Principal Component Analysis in Normal and Low P Conditions

Principal component analysis was carried out to establish the relationship between various morphological and biochemical traits under low P and normal conditions (**Figure 11**). Among the traits, YLD, PH, and TN were detected as main principal components (PCs) differentiating the mutants into various groups. The TN and PH were positive for PC1 and CAT shoots (CS), CAT roots (CR), and POD in roots (PR) were positive for PC2. The first two PCs showed a cumulative proportion of 93% of the variation, under combined analysis. In low P conditions, the PCA showed that SOD shoots (SS), POD shoots (PS), SOD roots (SR), and PR are the key factors/traits that contribute to low P tolerance and differentiate the mutants as tolerant and sensitive. The cumulative proportion of the first two PCs was 69%. The PS, PR, SS, and SR were captured by PC1 and YLD and TN were captured by PC2. The PCA in normal conditions showed that YLD, TN and SS are the key traits that differentiate the mutants into different groups. The cumulative proportion of the first two PCs was only 40%. YLD, TN, and SS were primarily captured by PC1 and CR and PR were captured by PC2. The PCA also showed a random distribution of genotypes

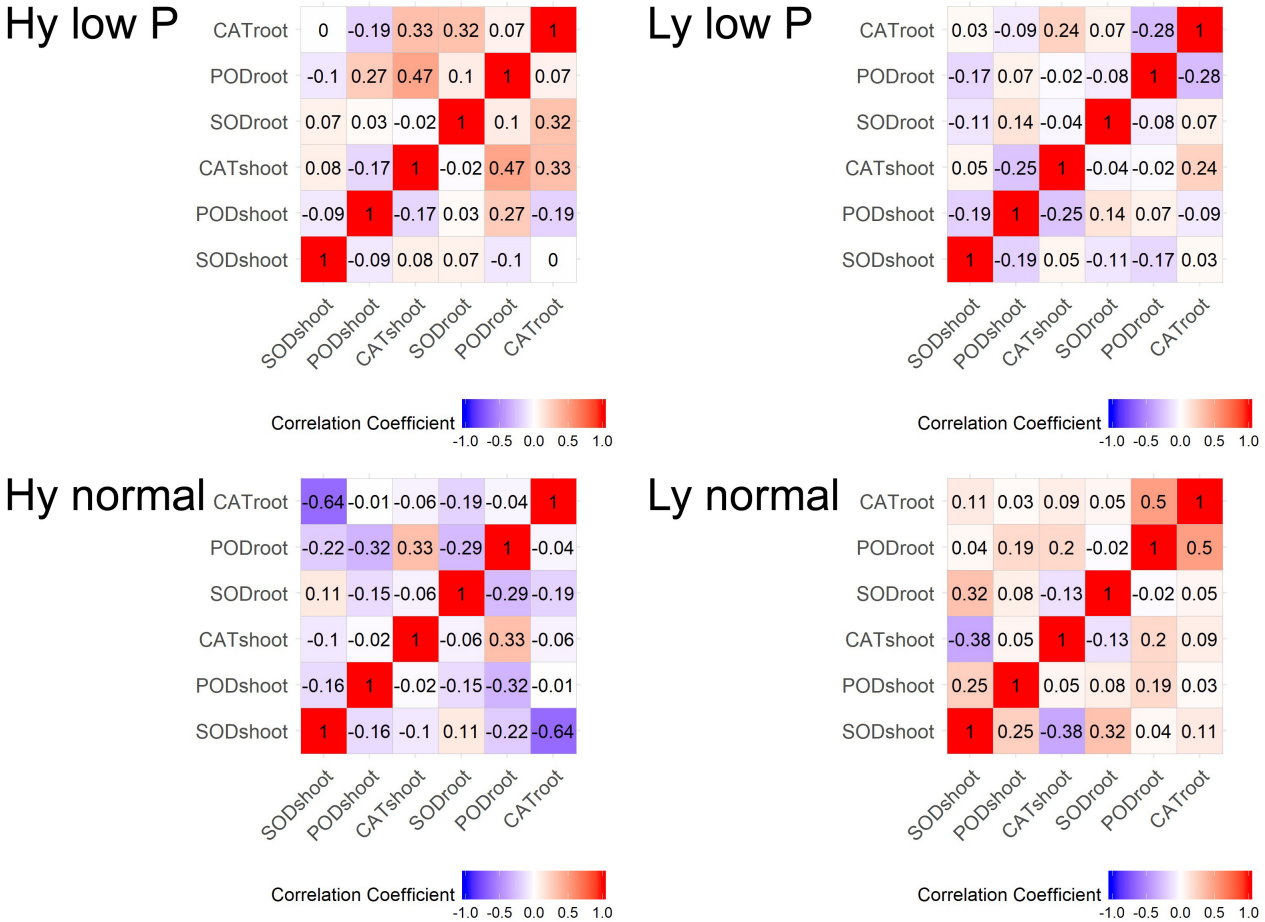

FIGURE 7 | Correlation at vegetative stage in SOD, POD, and CAT activities in high- and low-yielding mutants in normal and low P conditions.

in normal conditions, but clustering was observed in low P conditions. In the combined analysis, mutants grown in low P conditions showed clear groupings, but in normal conditions, mutants showed a random distribution (**Figure 12**).

Marker Trait Associations

Loci RM3648 and RM451 showed significant association with YLD, TN, SOD activity, and POD activity in both the roots and leaves in only low P conditions, whereas loci RM3334 and RM3600 were associated with only CAT activity in leaves in low P conditions.

DISCUSSION

Phosphorus deficiency has become a major challenge because of the declining P resources and the increasing cost of P fertilizers, adding a financial burden on farmers of rice growing countries. Phosphorus, a macronutrient, is required for rice cultivation in large amounts. To tackle the problem of P deficiency, identification and development of rice genotypes that can produce higher YLD even in low P soil is a viable approach.

Field testing and screening of 137 mutants, along with N22, was carried out in low P conditions to identify hy mutants that could perform better than N22. Mutants with heat and low P tolerance were identified in field experiments in previous studies (Poli et al., 2013; Panigrahy et al., 2014). Mutants with higher mean YLD/hill than N22 were categorized as hy mutants and those with lower mean YLD/hill than N22 were categorized as ly mutants in low P conditions. The mutants were selected for further screening based on the YLD/hill in low P conditions, and the other traits such as TN/hill and PH were not considered. It was noted from a previous study that although some mutants had a higher TN, they failed to flower; similarly, mutants that had more PH achieved a poor YLD in low P conditions.

Phenotyping of 36 mutants for PH, TN, and YLD/plant showed that hy mutants are more responsive to P and also showed a significant variation between both conditions. The hy mutants showed a range of variations in their phenotypic expression in low P and normal conditions. Across two test environments, NH1576 (TN) and NH1491 and NH1427 (YLD), the TN (**Figure 2**) and YLD (**Figure 3**) showed a low range of variation, compared with other mutants. These mutants, showing stable YLD performance across different environments, could

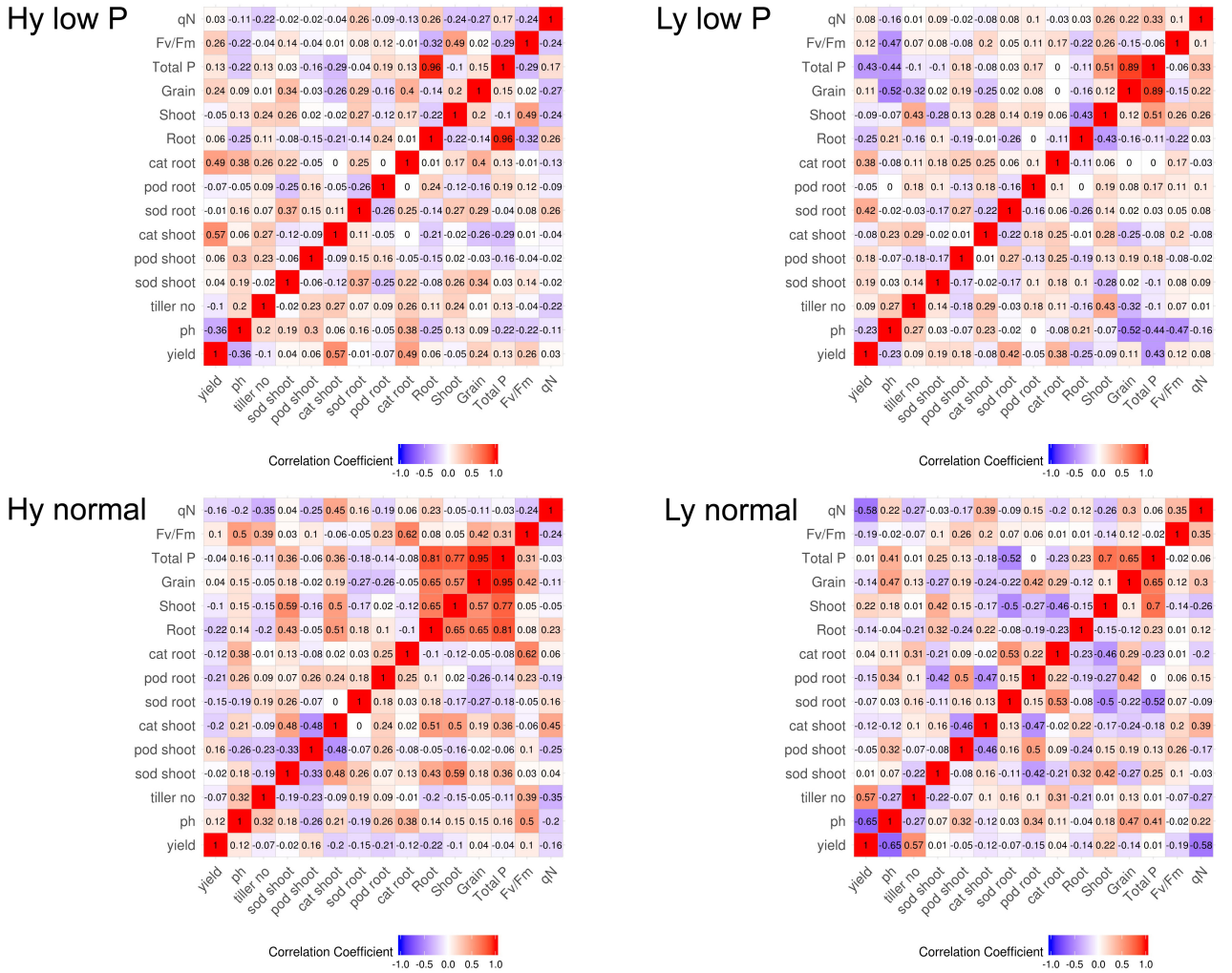

FIGURE 8 | Correlation at reproductive stage in high- and low-yielding mutants in normal and low P conditions.

be tested under multilocation trials to develop low P tolerant varieties.

Low P conditions trigger increased production of ROS in plants. Antioxidant machinery comprising enzymes (SOD, POD, and CAT) and others are produced as defense molecules to neutralize the ROS, whose uncontrolled production could have a devastating impact at the cellular level on the plant. Most studies on the effect of low P conditions on antioxidant systems were carried out in hydroponics (Xu et al., 2007; You et al., 2014), and there are very few reports of the same in soil conditions (Veronica et al., 2017). Therefore, we investigated the impact of low P soil on the antioxidant enzyme activity in the roots and leaves at both vegetative and reproductive stages of selected hy and ly mutants.

Enhanced activities of antioxidant enzymes (SOD, POD, and CAT) act as a coping strategy to scavenge ROS (Munns and Gilliham, 2015). Overexpression of genes involved in ROS detoxification resulted in lower cellular damage and the maintenance of photosynthetic energy capture under saline conditions (Roy et al., 2014). However, it is unknown whether ROS detoxification occurred because of low P stress. In a previous study, 8-day-old seedlings of an indica cultivar Zhenong 966 were subjected to minus (−) P conditions in hydroponics for 16 days. Both SOD and ascorbate peroxidase (APX) in leaves were significantly higher in −P than in plus (+) P. The parameters F_v/F_m and q_N were also reduced significantly in −P (Xu et al., 2007). In another study, Huanghuazhan, an indica cultivar was used to study the effect of −P conditions in hydroponics for 18 days. Antioxidant enzymes, namely SOD, POD, CAT, APX, and GR, were estimated in leaves, and it was concluded that the SOD and CAT activities were significantly higher in −P when compared with +P conditions (Hussain et al., 2016). Our experiment was designed to decipher the activity of antioxidant enzymes in low P field in both the vegetative and reproductive stages as well as in the roots and leaves. Veronica et al. (2017) screened four rice varieties with different P levels in pot experiments up to maturity: Swarna and Akhanphou were tolerant to low

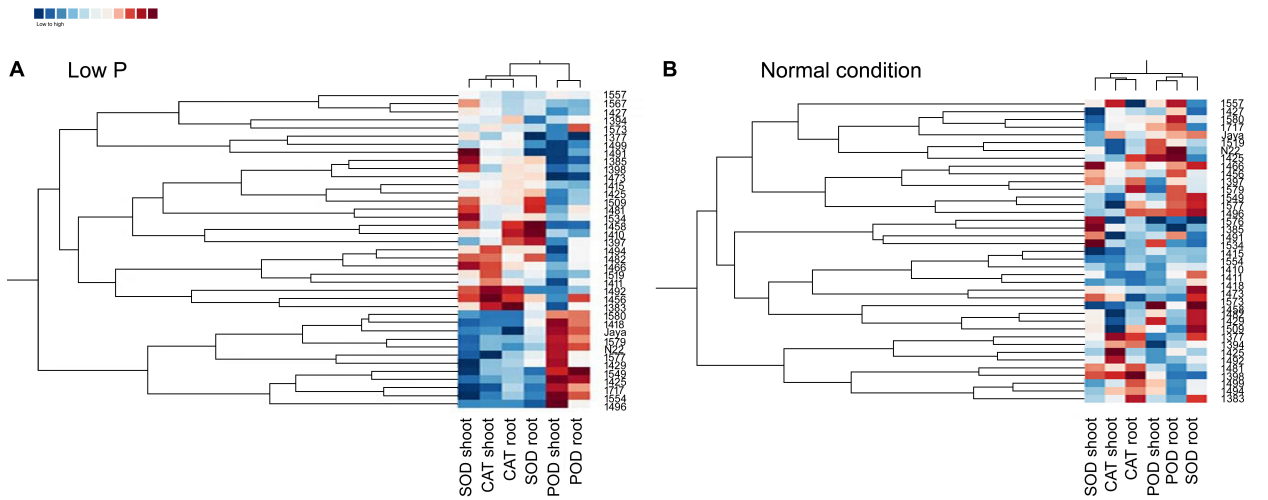

FIGURE 9 | Clustering and correlation at vegetative stage with biochemical assays in selected 36 mutants, N22, and Jaya in normal **(B)** and low P **(A)** conditions.

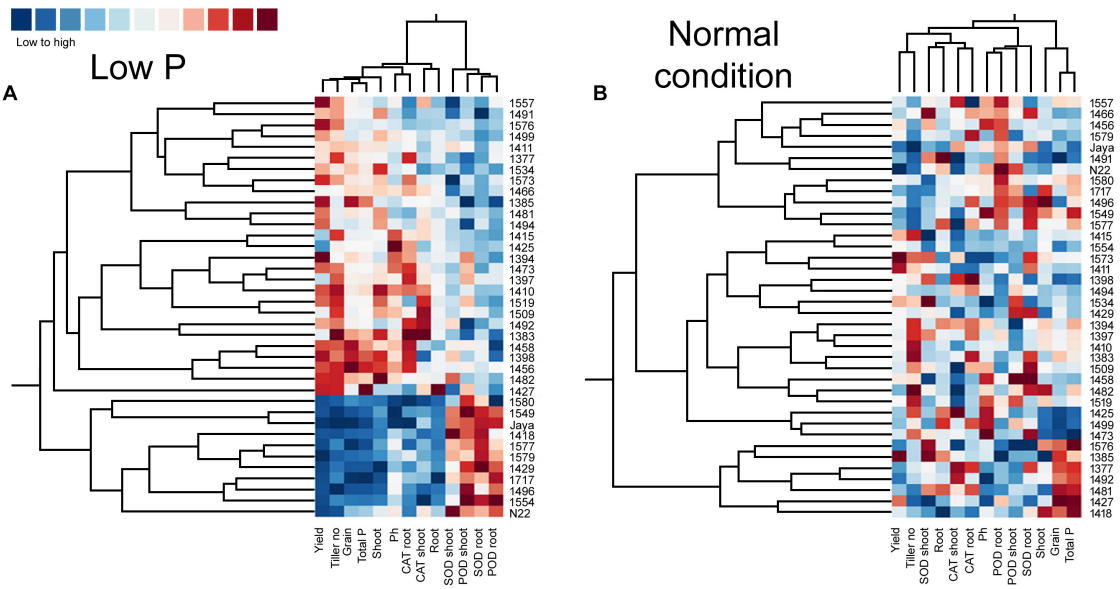

FIGURE 10 | Clustering and correlation at reproductive stage with agronomic traits and biochemical assays in selected 36 mutants, N22, and Jaya in normal **(B)** and low P **(A)** conditions.

P, and MTU1010 and RPBio 226 were sensitive to low P. Antioxidant enzymes were assayed at the reproductive stage with different P levels. The research team concluded that the SOD, POD, and CAT activities were significantly higher in low P conditions for all the genotypes. In tolerant varieties, the higher CAT activity when accompanied with higher F_v/F_m resulted in higher grain YLD in low P conditions. In our experiment, we estimated antioxidant enzymes both at the vegetative and reproductive stages in 27 hy and 9 ly mutants of N22 in low P conditions. Antioxidant enzyme activity and photosynthesis showed association with YLD under low P condition but not in normal condition.

In the vegetative stage, elevated SOD and CAT activities in both the roots and leaves of all hy mutants and higher POD activity in ly mutants were observed in low P conditions. Whereas, at the reproductive stage, hy mutants exhibited lower SOD and POD activities but a higher CAT activity in comparison with ly mutants in both the roots and shoots. These results clearly indicate that hy mutants possessed higher SOD and CAT activities at the early stages and a higher CAT activity at the reproductive stage in both the roots and shoots for scavenging the increased ROS levels in low P conditions.

On the other hand, ly mutants had a higher POD activity but lower SOD and CAT activities and were therefore less efficient in

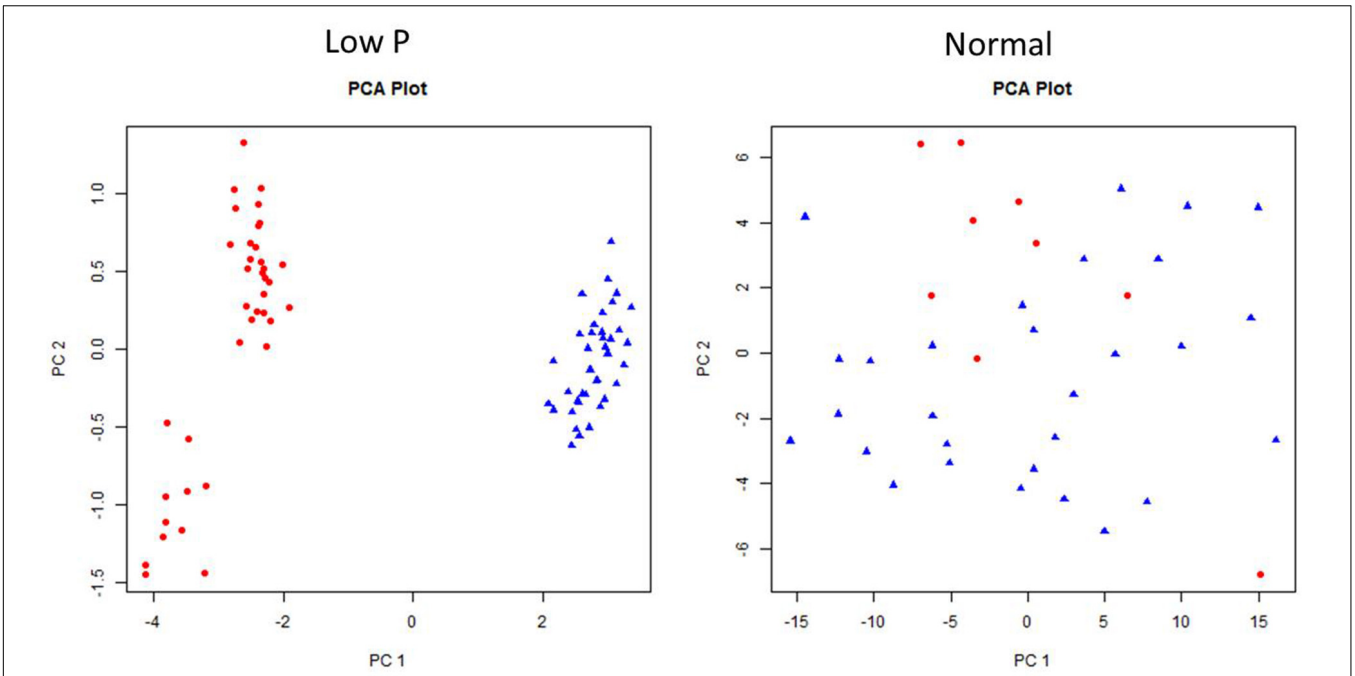

FIGURE 11 | Individual factor map of mutants, N22, and Jaya in low P and normal conditions.

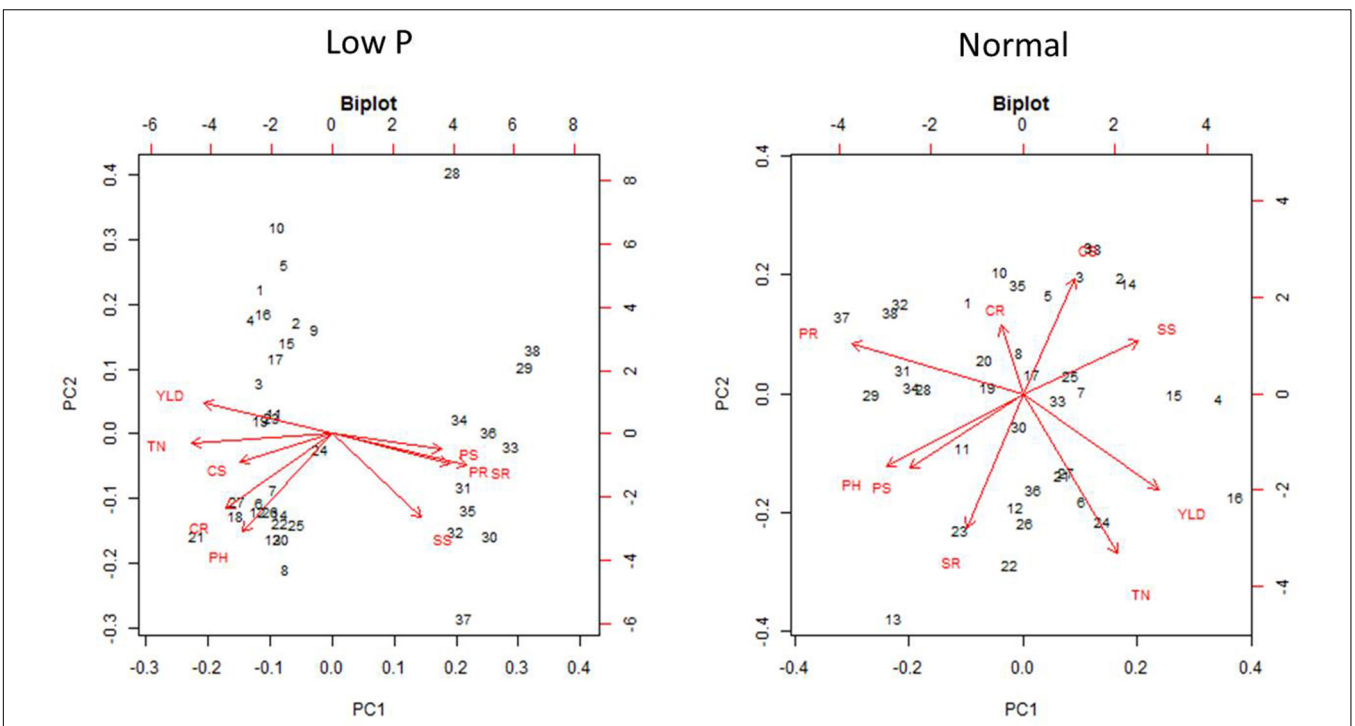

FIGURE 12 | Principal component analysis (PCA) in 36 mutants selected, N22, and Jaya in normal and low P conditions.

scavenging the ROS at the early stages. In ly mutants, a higher POD activity may not be adequate to remove H_2O_2 as rapidly as CAT (Alam and Ghosh, 2018). This is likely to result in the accumulation of H_2O_2 molecules. It was reported that 10 μM of H_2O_2 is sufficient to inhibit 50% of photosynthesis (Kaiser, 1979). Therefore, for the survival of ly mutant plants in low P conditions, a high POD activity alone is insufficient to confer low P tolerance. A higher SOD activity combined with a higher CAT activity at

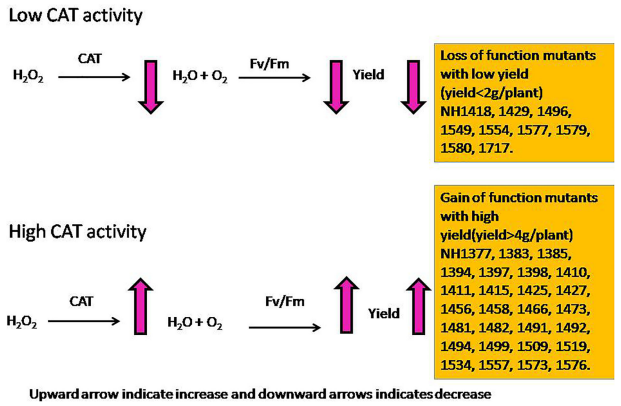

FIGURE 13 | Model diagram of the influence of higher and lower CAT activities on grain yield.

the vegetative stage and a higher CAT activity at the reproductive stage seems to be important for scavenging the increased ROS levels under low P conditions. This may be one of the reasons for better survival and higher YLD of hy mutants under low P conditions.

In the vegetative stage, under low P conditions, in response to the accumulation of ROS, the activity of SOD was increased in both hy and ly mutants that resulted in the accumulation of H_2O_2. The hy mutants showed overall lower antioxidant activity only at the reproductive stage when compared with ly mutants. It is important to note that in low P conditions, the SOD activity was higher in hy mutants than in ly mutants at the vegetative stage, and correspondingly the CAT activity was also higher in hy mutants than in ly mutants at the vegetative stage; so, the ROS were effectively scavenged. However, at the critical reproductive stage, CAT activity in ly mutants could not match with the increased SOD activity. Additionally, CAT activity was increasingly efficient in neutralizing H_2O_2 when compared with POD activity. The POD activity could keep pace with increased SOD in both hy and ly mutants; so, we concluded that the difference is not due to POD but due to CAT at the reproductive stage. In hy mutants under low P conditions, grain YLD was positively and significantly correlated only with CAT in roots and shoots but not with POD and SOD at the reproductive stage. The hy mutants exhibited higher P concentration in roots, shoots, and grains when compared with ly mutants in low P conditions, suggesting that hy mutants had better P uptake and transport mechanisms that helped the mutants to thrive under low P conditions. This may be one of the reasons for the better survival and YLD of hy mutants under low P conditions.

From a physiological point of view, F_v/F_m that represents the PSII photochemistry was reduced under low P conditions, but it was higher in hy mutants than in ly mutants. The hy mutants also had a higher q_N that indicated that excessive excitation energy was lost in the form of heat and minimized the damage caused to photosystem II (Veronica et al., 2017). The hy mutants had higher SOD and CAT activities at the vegetative stage followed by a higher CAT activity at the reproductive stage. Besides, they also had higher F_v/F_m and q_N that indicated that the deleterious effect of low P conditions on PSII mechanism was less in hy mutants. Overall, higher F_v/F_m; qN; and P concentrations in roots, shoots, and grains could probably be the factors promoting hy mutants to cope with the adverse effects of low P conditions. In our study, hy mutants had more CAT activity under low P conditions that resulted in higher F_v/F_m and q_N, which favored these mutants for better survival and seed set. On the other hand, in ly mutants, a higher SOD activity at both the stages enhanced H_2O_2 concentration. However, CAT activity in ly mutants was less at both stages, which resulted in the accumulation of H_2O_2 that inhibited photosynthesis and, thus, reduced grain YLD under low P conditions (**Figure 13**).

Catalase is the most efficient enzyme, which neutralizes H_2O_2 into H_2O and O_2 (Mhamdi et al., 2010; Alam et al., 2014; Veronica et al., 2017), and Kcat of CAT was the highest among all the antioxidant enzymes (Singh et al., 2015). This study indicated that low P stress reduces F_v/F_m in rice, however, mutations in N22 enhanced (in case of hy mutants) or decreased (in case of ly mutants) the activity of CAT, which facilitated the lower reduction of F_v/F_m in hy mutants as compared with ly mutants. This in turn might be an important factor that led to the higher YLD of hy mutants in low P conditions. It would be interesting to further probe into the effects of antioxidants and ROS pathways in low-P tolerance to establish a link between P metabolism and ROS pathways. It can also facilitate developing a ROS based biomarker to identify the genotypes for low-P tolerance in rice. The N22 mutants analyzed in this study are an important genetic resource for carrying out further analyses in this area of research.

Under normal conditions, the first five components accounted for 99.47% of the total variation and morphological traits like PH, YLD, and TN showing high coefficient values in PC1 (79.1%), indicating their major contribution in discriminating accessions, while the remaining variables had weak or no discriminatory power. In contrast, under low P conditions, PCs up to PC5 exhibited 90.17% variation with TN showing the highest coefficient along with SR, YLD, and PR, explaining the variance. TN is used as a surrogate for measuring tolerance to low-P conditions (Wissuwa et al., 1998; Panigrahy et al., 2014; Poli et al., 2017a). These results, therefore, indicate the impact of antioxidant enzymes in differentiating the genotypes under conditions of stress. Even the pooled analysis has shown that POD and SOD activities in roots contributed more toward differentiating genotypes than the morphological traits with high Eigen values for the first PC and indicated the need to identify and improve genotypes with these factors, for better tolerance under conditions of stress. Multivariate analyses conducted from the biochemical and morphological data of recombinant inbred lines (RIL) from contrasting parents, N22 and IR 64, under drought stress also resolved the significant effect of biochemical factors in differentiating tolerant and sensitive lines, and they found that enzyme-morphology correlations were not significant under irrigated control but were significant in conditions of drought. The researchers concluded that GR had a significant and

positive correlation with single plant YLD (SPY) under drought stress but not in normal conditions (Prakash et al., 2016).

Loci RM3648 and RM451 showed significant association with YLD, TN, and SOD and POD activities in both the roots and leaves in low P conditions only. RM3334 and RM3600 were associated with only CAT activity in leaves in low P conditions. The closest genes flanking RM3688 is the oryzain alpha chain precursor (LOC_Os04g55650.1), which is located 5 kb downstream. The gene closest to RM451 is the SNF2 family N-terminal domain containing protein (LOC_Os04g47830.1), which is located 1 kb upstream. RM334 is close to the ankyrin repeat domain-containing protein 28 (LOC_Os05g02130.1), which is located just 124 bp upstream. Close to RM6300 is the mitochondrial import inner membrane translocase subunit Tim17 (LOC_Os05g02060.1), which is located 116 bp downstream. Interestingly, all four genes have a known relationship with antioxidants and are good candidates for establishing a functional link between ROS and low-P tolerance in future studies.

This is the first report to show physiological and biochemical traits together, studying several genotypes (36 mutants + 2 control–N22 and Jaya) in low and normal P conditions, at different growth stages and tissues. Furthermore, the SOD, POD, and CAT activities in the roots and leaves at two stages of crop growth, vegetative and reproductive, as well as the fluorescence parameters, F_v/F_m and q_N, at the reproductive stage were analyzed. Higher SOD and CAT activities at the vegetative stage and a higher CAT activity and F_v/F_m at the reproductive stage are important traits that confer tolerance to low P conditions. This was supported by the high correlation coefficients between SOD and CAT activities at the vegetative stage and CAT activity with grain YLD and F_v/F_m at the reproductive stage, particularly in low P conditions. We have also shown markers associated (RM3648, RM451, RM3334, and RM3600) with antioxidant enzymes, especially in low P conditions. From this study, the useful chlorophyll fluorescence, antioxidant enzymes, and associated markers were identified, which can be useful for the development of low P tolerant genotypes.

AUTHOR CONTRIBUTIONS

SN, SV, SD, SM, and DB designed the research work. YP and VN performed the research. YP, SD, PR, and DB analyzed the data. SN, YP, DB, and SM wrote the manuscript. All authors read and approved the manuscript.

FUNDING

The authors gratefully acknowledge the Department of Biotechnology (DBT), Government of India for their financial support (BT/PR-9264/AGR/02/406(04)/2007 and BT/PR10787/AGIII/103/883/2014) to SN and SM.

ACKNOWLEDGMENTS

We specially thank the network partners, Dr. T. Mohapatra, S. Robin, A. K. Singh, Kuldeep Singh, M. Sheshshayee, and the coordinator, Dr R. P. Sharma. We also thank the Director of ICAR-IIRR for providing institute facilities.

SUPPLEMENTARY MATERIAL

The Supplementary Material for this article can be found online at: https://www.frontiersin.org/articles/10.3389/fpls.2018.01543/full#supplementary-material

REFERENCES

Aebi, H. (1984). Catalase in vitro. *Meth. Enzymol.* 105, 121–126. doi: 10.1016/S0076-6879(84)05016-3

Alam, N. B., and Ghosh, A. (2018). Comprehensive analysis and transcript profiling of *Arabidopsis thaliana* and *Oryza sativa* catalase gene family suggests their specific roles in development and stress responses. *Plant Physiol. Biochem.* 123, 54–64. doi: 10.1016/j.plaphy.2017.11.018

Alam, M. M., Nahar, K., Hasanuzzaman, M., and Fujita, M. (2014). Trehalose-induced drought stress tolerance: a comparative study among different Brassica species. *Plant Omics J.* 7, 271–283. doi: 10.13140/2.1.2883.1366

Castillo, F. I., Penel, I., and Greppin, H. (1984). Peroxidase release induced by ozone in *Sedum album* leaves: involvement of Ca^{2+}. *Plant Physiol.* 74, 846–851. doi10.1104/pp.74.4.846

R Core Team (2012). *R: A Language and Environment for Statistical Computing*. Vienna: R Foundation for Statistical Computing.

Dhindsa, R. A., Plumb, D. P., and Thorpe, T. A. (1981). Leaf senescence: correlated with increased permeability and lipid peroxidation, and decreased levels of superoxide dismutase and catalase. *J. Exp. Bot.* 126, 93–101. doi: 10.1093/jxb/32.1.93

Hanson, W. C. (1950). The photometric determination of phosphorus in fertilizers using the phosphovanado- molybdate complex. *J. Sci. Food Agric.* 1, 172–173. doi: 10.1002/jsfa.2740010604

Hussain, S., Yin, H., Peng, S., Khan, F. A., Khan, F., Sameeullah, M., et al. (2016). Comparative transcriptional profiling of primed and non primed rice seedlings under submergence stress. *Front. Plant Sci.* 7:1125. doi: 10.3389/fpls.2016.01125

Juszczuk, I. M., Wagner, A. M., and Rychter, A. M. (2001). Regulation of alternative oxidase activity during phosphate deficiency in bean roots (*Phaseolus vulgaris*). *Physiol. Plant.* 113, 185–192. doi: 10.1034/j.1399-3054.2001.1130205.x

Kaiser, W. (1979). Carbon metabolism of chloroplasts in the dark. *Planta* 144, 193–200. doi: 10.1007/BF00387270

Krishnamurthy, P., Sreedevi, B., Ram, T., Padmavathi, G., Mahendra, K. R., Raghuveer, R. P., et al. (2010). Evaluation of rice genotypes for phosphorus use efficiency under soil mineral stress conditions. *Oryza* 47, 29–33.

Lauer, M. J., Pallardy, S. G., Belvins, D. G., and Randall, D. D. (1989). Whole leaf carbon exchange characteristics of phosphate deficient soybeans (*Glycine max* L.). *Plant Physiol.* 91, 848–854. doi: 10.1104/pp.91.3.848

Lima, J. M., Nath, M., Dokku, P., Raman, K. V., Kulkarni, K. P., Vishwakarma, C., et al. (2015). Physiological, anatomical and transcriptional alterations in a rice mutant leading to enhanced water stress tolerance. *AoB Plants* 7:plv023. doi: 10.1093/aobpla/plv023

McCouch, S. R., Teytelman, L., Xu, Y., Lobos, K. B., Clare, K., Walton, M., et al. (2002). Development and mapping of 2240 new SSR markers for rice (*Oryza sativa* L.). *DNA Res.* 9, 199–207. doi: 10.1093/dnares/9.6.199

Mehra, P., Pandey, B. K., and Giri, J. (2017). Improvement in phosphate acquisition and utilization by a secretory purple acid phosphatase (OsPAP21b) in rice. *Plant Biotechnol. J.* 15, 1054–1067. doi: 10.1111/pbi.12699

Mhamdi, A., Queval, G., Chaouch, S., Vanderauwera, S., Van Breusegem, F., and Noctor, G. (2010). Catalase function in plants: a focus on *Arabidopsis* mutants as stress-mimic models. *J. Exp. Bot.* 61, 4197–4220. doi: 10.1093/jxb/erq282

Mithra, A. S. V., Kar, M. K., Mohapatra, T., Robin, S., Sarla, N., Seshashayee, M., et al. (2016). DBT propelled national effort in creating mutant resource for functional genomics in rice. *Curr. Sci.* 110, 543–548. doi: 10.18520/cs/v110/i4/543-548

Mohapatra, T., Robin, S., Sarla, N., Sheshashayee, M., Singh, A. K., Singh, K., et al. (2014). EMS induced mutants of upland rice variety nagina22: generation and characterization. *Proc. Indian Natl. Sci. Acad.* 80, 163–172. doi: 10.3389/fpls.2018.01179

Munns, R., and Gilliham, M. (2015). Salinity tolerance of crops-what is the cost? *New Phytol.* 208, 668–673. doi: 10.1111/nph.13519

Pandey, B. K., Mehra, P., Verma, L., Bhadouria, J., and Giri, J. (2017). OsHAD1, a haloacid dehalogenase-like apase, enhances phosphate accumulation. *Plant Physiol.* 174, 2316–2332. doi: 10.1104/pp.17.00571

Panigrahy, M., Rao, D. N., Yugandhar, P., Raju, S. N., Krishnamurthy, P., Voleti, S. R., et al. (2014). Hydroponic experiment for identification of tolerance traits developed by rice Nagina 22 mutants to low-phosphorus in field condition. *Arch. Agron. Soil Sci.* 60, 565–576. doi: 10.1080/03650340.2013.821197

Poli, Y., Basava, R. K., Desiraju, S., Voleti, S. R., Sharma, R. P., and Neelamraju, S. (2017a). Identifying markers associated with yield traits in Nagina22 rice mutants grown in low phosphorus field or in alternate wet/dry conditions. *Aust. J. Crop Sci.* 11, 548–556. doi: 10.1186/1939-8433-6-36

Poli, Y., Basava, R. K., Panigrahy, M., Vinukonda, V. P., Dokula, N. R., Voleti, S. R., et al. (2013). Characterization of a Nagina22 rice mutant for heat tolerance and mapping of yield traits. *Rice* 6:36. doi: 10.1186/1939-8433-6-36

Poli, Y., Veronica, N., Panigrahy, M., Nageswara Rao, D., Subrahmanyam, D., Voleti, S. R., et al. (2017b). Comparing hydroponics, sand, and soil medium to evaluate contrasting rice Nagina 22 mutants for tolerance to phosphorus deficiency. *Crop Sci.* 57, 2089–2097.

Prakash, C., Mithra, S. V. A., Singh, P. K., Mohapatra, T., and Singh, N. K. (2016). Unraveling the molecular basis of oxidative stress management in a drought tolerant rice genotype Nagina 22. *BMC Genomics* 17:774. doi: 10.6084/m9.figshare.c.3624881_d3

Rodríguez, D., Keltjens, W. G., and Goudriaan, J. (1998). Plant leaf area expansion and assimilate production in wheat (*Triticum aestivum* L.) growing under low phosphorus conditions. *Plant Soil* 200, 227–240. doi: 10.1023/A:1004310217694

Roy, S. J., Negrao, S., and Tester, M. (2014). Salt resistant crop plants. *Curr. Opin. Biotechnol.* 26, 115–124. doi: 10.1016/j.copbio.2013.12.004

Sanyal, S. K., Dwivedi, B. S., Singh, V. K., Majumdar, K., Datta, S. C., Pattanayak, S. K., et al. (2015). Phosphorus in relation to dominant cropping sequences in India: chemistry, fertility relations and management options. *Curr. Sci.* 108, 1262–1270

Shoba, D., Raveendran, M., Manonmani, S., Utharasu, S., Dhivyapriya, D., Subhasini, G., et al. (2017). Development and genetic characterization of a novel herbicide (imazethapyr) tolerant mutant in rice (*Oryza sativa* L). *Rice* 10:10. doi: 10.1186/s12284-017-0151-8

Singh, R., Haukka, M., McKenzie, C. J., and Nordlander, E. (2015). High turnover catalase activity of a mixed-valence mn II mn III complex with terminal carboxylate donors. *Eur. J. Inorg. Chem* 2015, 3485–3492. doi: 10.1002/ejic.201500468

Talla, S. K., Panigrahy, M., Kappara, S., Nirosha, P., Neelamraju, S., and Ramanan, R. (2016). Cytokinin delays dark-induced senescence in rice by maintaining the chlorophyll cycle and photosynthetic complexes. *J. Exp. Bot.* 67, 1839–1851. doi: 10.1093/jxb/erv575

Vandamme, E., Wissuwa, M., Rose, T., Dieng, I., Drame, K. N., Fofana, M., et al. (2016). Genotypic variation in grain P loading across diverse rice growing environments and implications for field P balances. *Front. Plant Sci.* 7:1435. doi: 10.3389/fpls.2016.01435

Veronica, N., Subrahmanyam, D., Kiran, T. V., Yugandhar, P., Bhadana, V. P., Padma, V., et al. (2017). Influence of low phosphorus concentration on leaf photosynthetic characteristics and antioxidant response of rice genotypes. *Photosynthetica* 55, 285–293. doi: 10.1007/s11099-016-0640-4

Wissuwa, M., Yano, M., and Ae, N. (1998). Mapping of QTLs for phosphorus-deficiency tolerance in rice (*Oryza sativa* L.). *Theor. Appl. Genet.* 97, 777–783. doi: 10.1007/s001220050955

Xu, X. H., Weng, X. Y., and Yang, Y. (2007). Effect of phosphorus deficiency on the photosynthetic characteristics of rice plants. *Russ. J. Plant Physiol.* 54, 741–748. doi: 10.1134/S1021443707060040

You, L., Wood, S. U., Fritz, S., Guo, Z., See, L., and Koo, J. (2014). *Spatial Production Allocation Model (SPAM) 2005 v2.0*. Available at: http://mapspam.info

Yugandhar, P., Nallamothu, V., Panigrahy, M., Sitaramamma, T., Bhadana, V. P., Voleti, S. R., et al. (2018b). Nagina 22 mutants tolerant or sensitive to low P in field show contrasting response to double P in hydroponics and pots. *Arch. Agron. Soil Sci.* 28:17Z. doi: 10.1080/03650340.2018.1471684

Yugandhar, P., Yafei Sun, Y., Liu, L., Negi, M., Nallamothu, N., Sun, S., et al. (2018a). Characterization of the loss-of-function mutant NH101 for yield under phosphate deficiency from EMS-induced mutants of rice variety Nagina22. *Plant Physiol. Biochem.* 130, 1–13. doi: 10.1016/j.plaphy.2018.06.017

Conflict of Interest Statement: The authors declare that the research was conducted in the absence of any commercial or financial relationships that could be construed as a potential conflict of interest.

frontiers in Plant Science

ORIGINAL RESEARCH
published: 05 February 2019
doi: 10.3389/fpls.2019.00073

Roots and Nodules Response Differently to P Starvation in the Mediterranean-Type Legume *Virgilia divaricata*

Gary G. Stevens[1], María A. Pérez-Fernández[2], Rafael J. L. Morcillo[3], Aleysia Kleinert[1], Paul Hills[4], D. Jacobus Brand[5], Emma T. Steenkamp[6] and Alex J. Valentine[1]**

[1] Department of Botany and Zoology, Stellenbosch University, Matieland, South Africa, [2] Ecology Area, Universidad Pablo de Olavide, Sevilla, Spain, [3] Shanghai Center for Plant Stress Biology, Chinese Academy of Sciences, Shanghai, China, [4] Institute for Plant Biotechnology, Stellenbosch University, Matieland, South Africa, [5] NMR Unit, Central Analytical Facility, Stellenbosch University, Matieland, South Africa, [6] Department of Microbiology and Plant Pathology, Forestry and Agricultural Biotechnology Institute, University of Pretoria, Pretoria, South Africa

OPEN ACCESS

Edited by:
Jose M. Garcia-Mina, University of Navarra, Spain

Reviewed by:
Sylvain Pluchon, Agro Innovation International, Groupe Roullier, France
Andrés Calderín García, Universidade Federal Rural do Rio de Janeiro, Brazil

***Correspondence:**
María A. Pérez-Fernández
maperfer@upo.es
Alex J. Valentine
alexvalentine@mac.com

Specialty section:
This article was submitted to Plant Nutrition, a section of the journal Frontiers in Plant Science

Received: *09 February 2018*
Accepted: *17 January 2019*
Published: *05 February 2019*

Citation:
Stevens GG, Pérez-Fernández MA, Morcillo RJL, Kleinert A, Hills P, Brand DJ, Steenkamp ET and Valentine AJ (2019) Roots and Nodules Response Differently to P Starvation in the Mediterranean-Type Legume Virgilia divaricata. Front. Plant Sci. 10:73. doi: 10.3389/fpls.2019.00073

Virgilia divaricata is a tree legume that grows in the Cape Floristic Region (CFA) in poor nutrient soils. A comparison between high and low phosphate growth conditions between roots and nodules was conducted and evaluated for the plants ability to cope under low phosphate stress conditions in *V. divaricata*. We proved that the plant copes with low phosphate stress through an increased allocation of resources, reliance on BNF and enhanced enzyme activity, especially PEPC. Nodules had a lower percentage decline in P compared to roots to uphold its metabolic functions. These strategies partly explain how *V. divaricata* can sustain growth despite LP conditions. Although the number of nodules declined with LP, their biomass remained unchanged in spite of a plant decline in dry weight. This is achieved via the high efficiency of BNF under P stress. During LP, nodules had a lower % decline at 34% compared to the roots at 88%. We attribute this behavior to P conservation strategies in LP nodules that imply an increase in a metabolic bypass that operates at the PEP branch point in glycolysis. The enhanced activities of nodule PEPC, MDH, and ME, whilst PK declines, suggests that under LP conditions an adenylate bypass was in operation either to synthesize more organic acids or to mediate pyruvate via a non-adenylate requiring metabolic route. Both possibilities represent a P-stress adaptation route and this is the first report of its kind for legume trees that are indigenous to low P, acid soils. Although BNF declined by a small percentage during LP, this P conservation was evident in the unchanged BNF efficiency per weight, and the increase in BNF efficiency per mol of P. It appears that legumes that are indigenous to acid soils, may be able to continue their reliance on BNF via increased allocation to nodules and also due to increase their efficiency for BNF on a P basis, owing to P-saving mechanisms such as the organic acid routes.

Keywords: legumes, nodules, low P, high P allocation of resources, biological nitrogen fixation, conservation strategies, phosphoenolpyruvate carboxylase, phosphate stress

Abbreviations: BNF, biological nitrogen fixation; CFR, Cape Floristic Region; DW, dry weight; FW, fresh weight; HP, high phosphate; LP, low phosphate; MDH, malate dehydrogenase; ME, malic enzyme; NDFA, nitrogen derived from atmosphere; PEP, phosphoenol pyruvate; PEPC, phosphoenolpyruvate carboxylase; P*i*, inorganic phosphate; PK, pyruvate kinase; PP*i*, pyrophosphate; SNAR, specific nitrogen acquisition rate.

INTRODUCTION

The Cape Floristic Region (CFR), found in the south western area of South Africa can be regarded as one of the highest P-impoverished regions of the world and simultaneously a Global Biodiverse Hotspot (Lambers and Shane, 2007). The CFR resembles a typical Mediterranean-type ecosystem usually characterized by sandstone-derived soils (Goldblatt and Manning, 2000), which are acidic, with insufficient nutrients (especially N and P) to sustain normal plant growth (Bordeleau and Prevost, 1994; Von Uexkull and Mutert, 1998; Grigg et al., 2008). In particular, legume species reliant on Biological Nitrogen Fixation (BNF) are highly dependant on P supply, more so than legumes growing on mineral N (Drevon and Hartwig, 1997). For legumes, P not only affects the formation of nodules (Israel, 1993), but limiting P also impacts negatively on the nitrogen fixation process (Schultze et al., 2006; Tsvetkova and Georgiev, 2007). The tree species, *V. divaricata* (Adamson), is a native legume to the CFR and it is distributed over a wide range of P-poor soils from the relatively richer forest margins to poorer Fynbos soils (Coetsee and Wigley, 2013). This implies that the indigenous species may have a range of mechanisms to adapt to variable soil P supply.

These mechanisms, therefore, have evolved adaptations to function optimally under limiting P conditions (Vance et al., 2003). Some strategies are aimed at conserving the use of P, whereas others are directed toward enhanced acquisition and uptake of P (Lajtha and Harrison, 1995; Horst et al., 2001; Vance et al., 2003). Adaptations that conserve the use of P involve a decrease in growth rate, increased growth per unit of P uptake, remobilization of internal P*i*, modification in C-metabolism that bypass P-requiring steps and alternative respiratory pathways (Schachtman et al., 1998; Plaxton and Carswell, 1999; Raghothama, 1999; Uhde-Stone et al., 2003a,b). In legumes, adaptations leading to enhanced P acquisition entail the expression of genes that result in the production of cluster roots. Cluster roots increase the root surface area. This enhances nodule efficiency for P utilization (Le Roux et al., 2008), root exudation of organic acids and acid phosphatase, as well as the induction of numerous transporters (Gilbert et al., 2000; Gilroy and Jones, 2000; Lynch and Brown, 2001; Neumann and Martinoia, 2002; Lamont, 2003; Uhde-Stone et al., 2003a; Vance et al., 2003).

The high sensitivity of legume plants, and indeed the N_2-fixation process to environmental conditions such as acidic soils associated with P deficiency, may result in higher C costs (Mengel, 1994). This concurs with Le Roux et al. (2008), who showed that lupin nodules under P stress acted as stronger C sinks. Nodules are known to have a strong sink capacity for P assimilation during P starvation (Høgh-Jensen et al., 2002). The enhanced nodule cost for P utilization is considered to be an essential coping strategy during P stress (Le Roux et al., 2008). The C sink was found to be more pronounced in plants during symbiosis under low-P conditions (Mortimer et al., 2008). This was shown by a greater growth respiration of low-P plants than high-P plants (Mortimer et al., 2008). The sink effect was also evidenced by the higher photosynthetic rates of host plants (Mortimer et al., 2008). In the case of P stress, the most direct currency is P itself and growth parameters related to P accumulation (Koide and Kabir, 2000).

Physical changes to roots (adjustment of root architecture, root growth, root system composition and mycorrhizal infection) that takes place as a result of P limitations, are complemented by the exudation of a variety of organic compounds (carboxylate anions phenolics, caboxylates, amino acids enzymes, and other proteins), as well as inorganic compounds (protons, phosphate and nutrients) that into the rhizosphere aid the plants in the adaption for a particular nutrient stressed environment (Crowley and Rengel, 1999). The *Fabaceae* family develops cluster roots which are stimulated during phosphate stress. Not only do these species develop cluster roots, but also exude carboxylates which releases P from its bound form, making P more accessible for root uptake (Lambers and Shane, 2007). It was found that during P deficiency, plants exude carboxylates such as citrate, malate, malonate, acetate, fumerate, succinate, lactate, and oxalate in various concentrations (Rengel, 2002). White lupin exudes large amounts of carboxylates in the form of malic- and citric acid to the immediate soil surrounding to release P from its bound form in the soil. These excreted organic acids have the ability to chelate metal cations such as Al^{3++} and Ca^{2+} and immobilize P*i* in the soil, which results in higher P*i* concentrations in the soil up to 1000 fold (Gardner et al., 1983; Dinkelaker et al., 1989; Neumann et al., 2000). The production of these exudates are accomplished by the concerted action of a variety of enzymes, such as the Pyrophosphate (PP*i*), dependent phosphofructokinase (PP*i*-PFK), Phosphoenolpyruvate (PEP) phosphatase and Phosphoenolpyruvate Carboxylase (PEPC). Pyruvate, which is the precursor to many of these substances, can be generated in the cytosol and in the mitochondria. Cytosolic pyruvate is produced from PEP during the glycolytic conversion of ADP to ATP which is catalyzed by pyruvate kinase (PK) (Plaxton, 1996). It is suggested, that when plants experience P stress, that pyruvate synthesis from PEP via PK is restricted (Theodorou and Plaxton, 1993; Plaxton, 1996). However, pyruvate can also be generated from malate when plants make use of a "bypass" route especially during P-limitations. In this "bypass" route, PEP is hydrolyzed to Oxalacetic Acid (OAA) by PEPC and OAA is subsequently converted to malate by Malate Dehidrogenase (MDH). Mitochondrial Malic Enzyme (ME) converts malate into PEP (Plaxton, 1996).

In addition PEPC catalyzes the conversion of phosphoenolpyruvate and bicarbonate to oxaloacetate (OAA) and inorganic phosphate (Chollet et al., 1996). It is believed to play a pivotal role in carbon metabolism in symbiotic nodules of legume roots (Day and Copeland, 1991; Rawsthorne, 2002). The PEPC derived OAA can be converted to malate, via malate dehydrogenase. The generated malate can be fed into the mitochondrial tri-carboxylic acid cycle (TCA) for further metabolism, or metabolized to pyruvate via ME. PEPC plays a crucial role in the assimilation of atmospheric CO_2 during C4 and CAM photosynthesis. PEPC has also been implicated to replenish the citric acid cycle intermediates when carbon skeletons are removed for other metabolic functions like nitrogen assimilation and amino acid biosynthesis when plants

undergo P-stress The induction of PEPC during P-stress also results in elevated levels of organic acids such as malate and citrate in the rhizosphere (O'Leary et al., 2011) and dicarboxylic acids (Streeter, 1991; Tajima et al., 2015). Furthermore, N_2 fixation comes with a high CO_2 loss (Pate et al., 1993), which could account for more than 60% of the carbon allocated to the nodules (Voisin et al., 2007). Plants manage to reincorporate this CO_2 as intermediates to the TCA cycle, and to fuel nodule metabolism, by the combined actions of carbonic anhydrase and PEPC (Vuorinen and Kaiser, 1997; Flemetakis et al., 2003).

Nuclear Magnetic Resonance (NMR) spectroscopy allows for the characterization of the metabolites in plant cells by coupling NMR with ^{13}C stable isotope enrichment, as the ^{12}C isotope is not NMR active. It can be used to determine the metabolite flux in plant cells making it suitable to establish the conditions and compartmentation of these metabolites in plant cells (Chang and Roberts, 1989; Gilbert et al., 2011). Photosynthetic CO_2 fixation discriminates against ^{13}C, therefore mainly the sodium bicarbonate-^{13}C enriched solution supplied as feedstock will be metabolized by the plant. This ^{13}C enrichment allows for the characterization of the resulting metabolic activities in plant cells by NMR. It was shown that this technique could be exploited to determine the metabolite flux in plant cells making it suitable to establish the conditions and compartmentation of these metabolites in plant cells (Chang and Roberts, 1989).

Virgilia is a small tree genus that includes two species *V. divaricata* (Adamson) and *V. oroboides* (P. J. Bergius, T. M. Salter). It is confined to the south-western and southern coastal regions of the CFR (Greinwald et al., 1989). Studies have been conducted on growth and adaptations of legume species native to Mediterranean-type fynbos ecosystems that occur on naturally acidic soils (Muofhe and Dakora, 1999; Spriggs and Dakora, 2008; Power et al., 2010; Kanu and Dakora, 2012). However, information on the physiology of N and P uptake, efficiency and utilization in legume trees in fynbos soils is largely unknown. Although the CFR has a high legume diversity found on the P-poor soils (Goldblatt and Manning, 2000), not much is known about the functional mechanisms which underpin N nutrition within the nodules of these indigenous legumes. The adaptation to P stress may involve a variety of morphological and biochemical mechanisms that are related to enhancing acquisition of soil P, recycling of internal P*i* and conserving available internal P. Recent work from our group has shown that *Virgilia* uses a variety of strategies to adapt to low P conditions. Magadlela et al. (2014) compared two species within the genus *Virgilia*, and demonstrated that *V. divaricata* maintained a high efficiency of BNF, owing to a greater allocation of biomass toward nodules during P deficiency. Vardien et al. (2014) showed that nodules have a high functional plasticity during variable P supply, by recycling organic P via acid phosphatase enzymes and redistributing Fe within the nodule. In the present study we investigated the root system engagement of a non-P requiring metabolic bypass and its implications to nodule efficiency of the indigenous legume *V. divaricata* during variable P supply. We aimed at gathering a better understanding of how nodules manage to sustain their functioning during P-stress. To that end we investigated how PEPC-derived C is metabolized into amino acids and downstream organic acids of P-deficient nodules, using ^{13}C NMR spectroscopy. We hypothesized that plants of *V. divaricata* grown in P-poor soils, have evolved adaptive mechanism which conserve internal P and are designed for maintaining nodule function during P deficiency.

MATERIALS AND METHODS

Plant Growth

Sterile seeds of *V. divaricata* (Silverhill Seeds, Kenilworth, Cape Town, South Africa) were pre-treated with smoke water and water at 50°C for 5 h, to enhance their germination (Soos et al., 2009). Seeds were then allowed to germinate in sterile filter sand in seed-trays placed in a north facing glass house under natural light conditions. Plants were exposed to a photo and thermo period of 10 h sunlight at 25°C and 14 h in darkness at 15°C. Seedlings were transferred to pots with sterile filtered sand after 2 weeks of growth, when the first true leaves had emerged. At this stage, seedlings were harvested and dried and used as the first harvest, from which to calculate growth rates. All plants were inoculated with the nodule forming *Burkholderia phytofirmans*. Inoculation treatments consisted of 500 μl of growth phase broth cultured inoculant at about 1.106 cells ml^{-1}. Plants were divided into two groups, i.e., low (5 μM) –and high (500 μM) phosphate according to the Long Ashton nutrient treatment. Plants received the respective treatments twice per week and were allowed to grow for 8 weeks before harvest. Seedlings were divided into leaves, stems roots and nodules which were, respectively, weighed for their fresh weights. Nodules were kept in Eppendorfs at −80°C until analyzed. The leaves stems and roots were dried in a 50°C until constant weight prior to analysis.

Protein Extraction

Plant material, either roots or nodules, were ground to a fine powder in liquid nitrogen. Proteins from roots and nodules were extracted according to the methods used by Ocaña et al. (1996) and was modified to an extent that 0.5 g of tissue was extracted in 2 ml of extraction buffer consisting of 100 mM Tris–HCl (pH 7.8), 1 mM Ethylenediaminetetraacetic acid (EDTA), 5 mM dithiothreitol (DTT), 20%(v/v)ethylene glycol, plus 2%(m/v) insoluble polyvinylpolypyrrolidone (PVPP) and one Complete Protease Inhibitor Cocktail tablet (Roche Diagnostics, Randburg, South Africa) per 50 ml of buffer. The protein concentration was determined by the NanoDrop Lite Spectrophotometer (Thermo Scientific) where the extraction buffer was used as standard.

Enzyme Assays

All enzyme assays were carried out at 25°C in a multi-well plate reader at a wavelength of 340 nm. All reactions contained 30 μl of the crude extraction mixture in a final volume of 250 μl.

Phosphoenolpyruvate Carboxylase

Phosphoenolpyruvate carboxylase activity was coupled with the NADH-malate dehydrogenase and measuring NADH oxidation at 25°C by monitoring NADH oxidation at 340 nm. The standard assay mixture (pH 8.5) contained 100 mM Tris (pH 8.5), 5 mM

$MgCl_2$, 5 mM $NaHCO_3$, 4 mM PEP, 0.20 mM NADH, and 5 units of MDH (Ocaña et al., 1996). Measurement was carried out against 9 blanks without PEP. Two measurements were taken for each treatment. All reactions were performed in triplicate.

Pyruvate Kinase

Pyruvate kinase was assayed at room temperature (22–24°) by recording at 340 nm the oxidation of NADH. The incubation mixture contained 75 mM Tris–HCl (pH 7.0), 5 mM $MgCl_2$, 20 mM KCl, 1 mM ADP, 3 mM PEP, 0.18 mM NADH and 3 units of lactate dehydrogenase (McCloud et al., 2001), and 2 units of lactate dehydrogenase in a total volume of 1 ml. The blanks consisted of the buffer without ADP.

Malic Enzyme

Malic enzyme activity was assayed by measuring the increase in 340 nm due to the formation of NADH or NADPH. Standard reaction mixture contained 80 mm Tris–HCl (pH 7.5), 2 mm MnCl2, 1 mm malate and 0.4 mm NADP or NAD^+ (Appels and Haaker, 1988).

NADH-Malate Dehydrogenase

The MDH activity was measured in 25 mM KH_2PO_4, 0.2 mM NADH, 0.4 mM oxaloacetate (OAA), pH 7.5 (Appels and Haaker, 1988). 25 mM KH_2PO_4, 0.2 mM NADH, 0.4 mM OAA the rate of disappearance of NADH was monitored at 340 nm before and after addition of oxaloacetate. The former rate served as a measurement of background NADH oxidation which was subtracted from the rate of oxaloacetate-dependent activity. Initial reaction rates have been shown to be proportional to the concentration of enzyme under the conditions used in these experiments. The assay system for measuring the oxidation of malate by NAD^+, catalyzed by malate dehydrogenase, involves the reaction of oxaloacetate with L-glutamate in a subsequent reaction catalyzed by glutamate-oxaloacetate transaminase. The assay system contained 50 mM Tris/HCl, 40 mM L-glutamate, 0.8 mM NAD^+, 4.0 U/ml glutamate oxaloacetate transaminase and 100 mM L-malate, pH 8.0. The reaction rates were measured from the appearance of NADH absorbance at 340 nm. The amount of NADH and oxalacetate formed in the oxidation of malate was stoichiometric 11 with the amount of malate and NAD^+. Initial reaction rates have been shown to be proportional to the concentration of enzyme under the conditions used (Appels and Haaker, 1988).

Citric- and Malic Acid Determination

Citric- and malic acid content for HP and LP nodules and roots were determined using a photometric analyzer (Arena 20XT, Thermo Electron Oy, Finland), which measures the amount of product formed after an enzymatic reaction. The reactions were performed in triplicate. The pH of the samples was adjusted to between 8 and 10 at room temperature. Reactions inside the instrument were performed at 37°C. Citrate and malic acid concentrations were determined by the enzymatic conversion of citrate and malate. In the process, NADH is oxidized which is stoichiometric to the amount of citrate and malate, respectively. NADH is then photometrically determined at 340 nm.

Phosphate Determination

Phosphate analysis was performed on HP and LP samples of roots and nodules For the determination of total P, approximately 0.25 g of the sample material was digested in 7 ml HNO_3 in a Mars CEM microwave digester, then diluted into 50 ml deionized water. P was measured on a Thermo ICAP 6300 ICP-AES after calibration of the instrument with NIST-traceable standards.

Isotope Analysis

Analyses of δ15N were done at the Archeometry Department at the University of Cape Town, where the isotopic ratio of $\delta^{15}N$ was calculated as $\delta = 1000‰$ (Rsample/Rstandard). *R* refers to the molar ratio of the heavier to the lighter isotope of the samples. Standards were similar to those as described by Farquhar et al. (1989). Combustion of the samples were performed in a CHN analyzer (Fisons NA 1500, Series 2, Fisons instruments SpA, Milan, Italy) and the $\delta^{15}N$ values for the nitrogen gas released were determined on a Finnigan Matt 252 mass spectrometer (Finnigan MAT GmbH, Bremen, Germany), which was connected to a CHN analyzer by a Finnigan MAT Conflo control unit. The sample values were corrected by the use of three standards. Two in-house standards (Merck Gel and Nasturtium) were used and the third was the IAEA (International Atomic Energy Agency) standard $(NH_4)_2SO_4$. The percentage of nitrogen derive from atmospheric fixation (%NDFA) was calculated according to Shearer and Kohl (1986), where:

$$\%\text{NDFA} = 100((\delta 15\text{Nreference plant} - \delta 15\textit{Nlegume})/(\delta 15\text{N reference plant} - \text{B}).$$

Wheat (*Triticum aestivum*) was used as reference plant which was grown under the same glasshouse conditions as the legume. The B-value (which was determined as −0.71‰.) refers to the $\delta^{15}N$ natural abundance of the N derived from biological N-fixation of the above-ground tissue of *V. divaricata*, grown in an N-free solution.

^{13}C Enrichment

In order to investigate the metabolism of belowground incorporation and metabolism of ^{13}C labeled bicarbonate in roots and nodules, NMR spectroscopy was used by coupling NMR with ^{13}C stable isotope enrichment at the root-zone level. Plants of *V. divaricata*, were grown in sterile sand culture under two levels of P supply, low (5 μM) P and high (500 μM) P nutrition. At 2 months of age, both the low P and high P plants were supplied with a sodium bicarbonate-^{13}C labeled solution in the pots. The pots were sealed and contained a CO_2 trap, to prevent ^{13}C leakage to the atmosphere. The experimental procedure was as follows. Plants of both treatments were enriched with ^{13}C at the root-zone level, by watering them with a 300 ml solution of sodium bicarbonate-^{13}C labeled (pH 6.8) (Sigma Aldrich Cat # 372382-1G, 99 atom % ^{13}C) (0.215 g/L). A solution of KOH (250 mM) was placed in trays at the bottom of the pots to absorb CO_2 which could escape through soil. Lids, designed with a special opening to cover the sand and below-ground organs, but allow the shoots to be exposed to the atmosphere, were placed on pots immediately after 300 ml of $NaH^{13}CO_3$ solution was fed. These

lids were made completely airtight around the pots. In addition, CO_2 traps were inserted into the lids, to prevent any $NaH^{13}CO_3$ from escaping to the atmosphere. These traps consisted of Soda Lime in 5 ml pipette tips and were inserted in the head space between the lid and soil in pot. The insertion points of traps into the lids were sealed off and made air tight. The run-off volumes of the $NaH_{13}CO_3$ were collected and measured. Pots were then placed on clean trays with fresh KOH. Plants were harvested at 1 h and 2 h intervals after feeding of $NaH^{13}CO_3$. All metabolic processes were stopped by quenching nodulated roots in liquid N_2.

^{13}C NMR

Sample preparation was done as described in Gout et al. (1993). Briefly, 4.5 g of roots and nodules were frozen in liquid N_2 and ground to a powder in 1 ml of 70% (v/v) perchloric acid. The frozen powder was allowed to thaw at −10°C. The thick slurry was the centrifuged at 15000 rpm for 10 min and the supernatant was then neutralized with 2M $KHCO_3$ to pH 5. The supernatant was then centrifuged at 10000 rpm for 10 min to remove $KClO_4$ and then lyophylised and stored in liquid N_2. The lyophilized sample was re-dissolved in 2.5 ml water which contained 10% (v/v) $2H_2O$. The solution was neutralized to pH 7.5, buffered with HEPES and CDTA (50–100 μM) was added to chelate divalent cations. Their respective ^{13}C NMR spectra was recorded at 25°C dissolved in D_2O on a Agilent Inova 600MHz spectrometer utilizing the default pulse sequence parameters in the VnmrJ 4.2 instrument software package.

Calculations

Specific N Absorption Rate

Specific N absorption rate (SNAR) (mg N g^{-1} root DW d^{-1}) is the net N absorption rate per unit root DW as outline in Nielson et al. (2001), and it was calculated as:

$$\mathrm{SNAR} = [(M2 - M1/t2 - t1)] \times [(\log e\, R2 - \log e\, R1)/(R2 - R1)]$$

Where M is the N content per plant, t is the time elapsed between two harvests and R is the root DW.

Belowground Allocation

Belowground allocation refers to the fraction of new biomass partitioned into new roots and nodules over the given growth period. The calculations were done according to

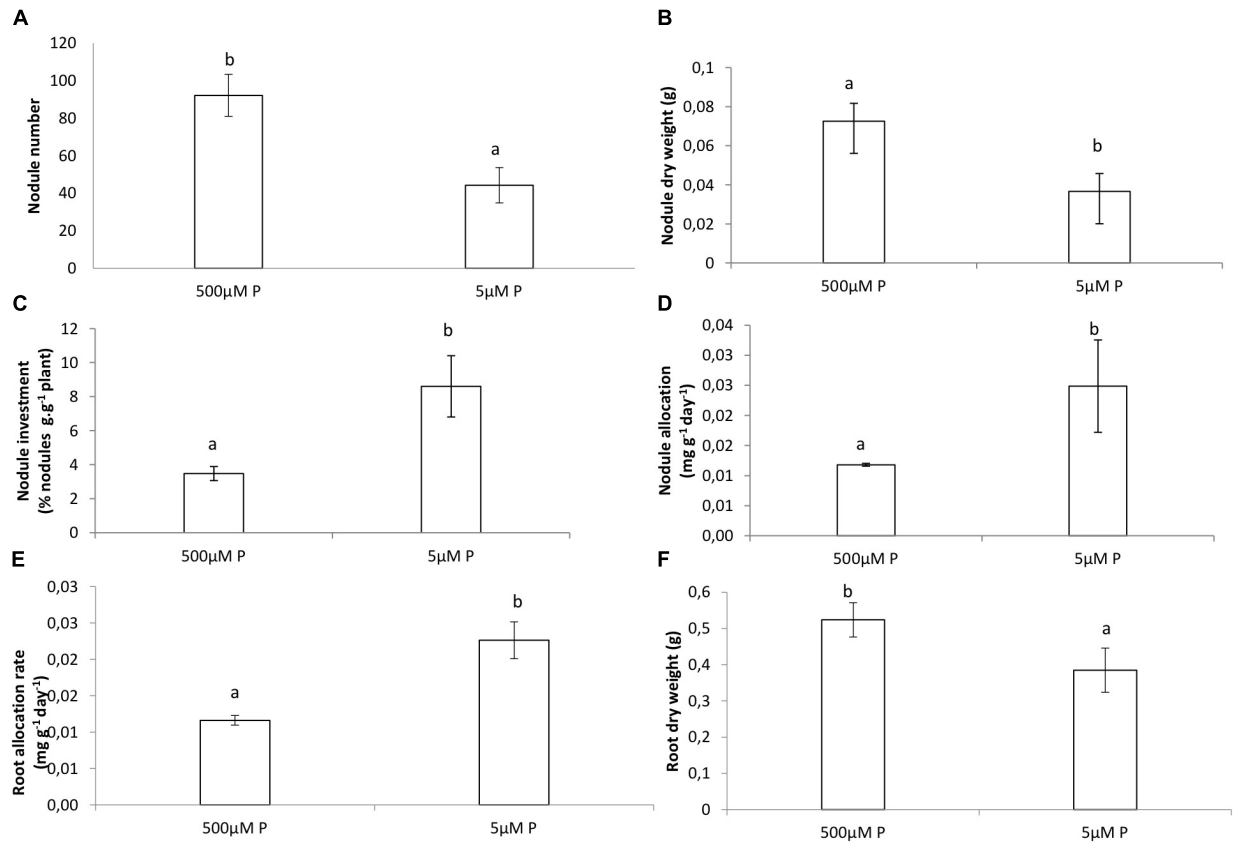

FIGURE 1 | (A) Amount of nodules on roots, **(B)** dry weight of nodules, **(C)** nodule % of plant dry weight, **(D)** nodule allocation rate, **(E)** root allocation rate, **(F)** root dry weight of *Virgilia divaricata* grown under high phosphate (500 μM P) and low phosphate (5 μM P) conditions. Values of four replicates are presented as means ± SE. Different letters indicate significant differences between treatments ($P \leq 0.05$).

Bazzaz and Grace (1997) as follows:

$$df/dt = RGR\ (\partial - Br/Bt)$$

Where RGR is the relative growth rate ($mg.g^{-1}.day^{-1}$) and ∂ is the fraction of new biomass gained during the growth period. Br/Bt is the root weight ratio, based on total plant biomass (Bt) and root biomass (Br).

Statistical Analysis

The effects of the factors and their interactions were tested with an analysis of variance (ANOVA) (KaleidaGraph, Synergy Software, PA, United States). Where the ANOVA revealed significant differences between treatments, the means (6–8) were separated using *post hoc* Tukey's LSD (SuperANOVA for Macintosh, Abacus Concepts, United States) ($P \leq 0.05$).

RESULTS

Biomass

The dry weight (DW) of the roots and nodules was significantly much lower in the LP treatment compared to the HP treatment (**Figures 1A,B,F**). The relative growth rate for roots was much higher for the LP treatment and slightly higher in nodules of the LP treatment compared to the HP treatment (**Figures 1D,E**). However, nodulation in the LP treatment was much lower and more than twice the amount of nodules were formed in the HP treatment (**Figures 1A,B**). The plants allocated more of their resources to nodules and to roots in LP than in HP (**Figures 1C,E**). The allocation of resources for both treatments remained almost similar in the nodules (**Figure 2C**). Internal Pi of roots and nodules was significantly lower in the LP treatments (**Figure 2D**). However, the nodules were more efficient in BNF per dry weight in the LP nodules and there was a decline in %NDFA in the same nodules (**Figures 2A,B**).

Biological Nitrogen Fixation

During low P supply, there was a decline in BNF (%NDFA) compared to the HP supply (**Figure 2A**). However, in spite of the decline in BNF, the efficiency of BNF per unit P was higher in the LP treatment compared to the HP (**Figure 2B**).

Protein and Enzyme Assays

Measurements of PEPC, MDH, and ME in plants grown in LP rended higher values than those obtained in plants grown in HP (**Figures 3A,C,D**). The highest PEPC (**Figure 3A**) activity was

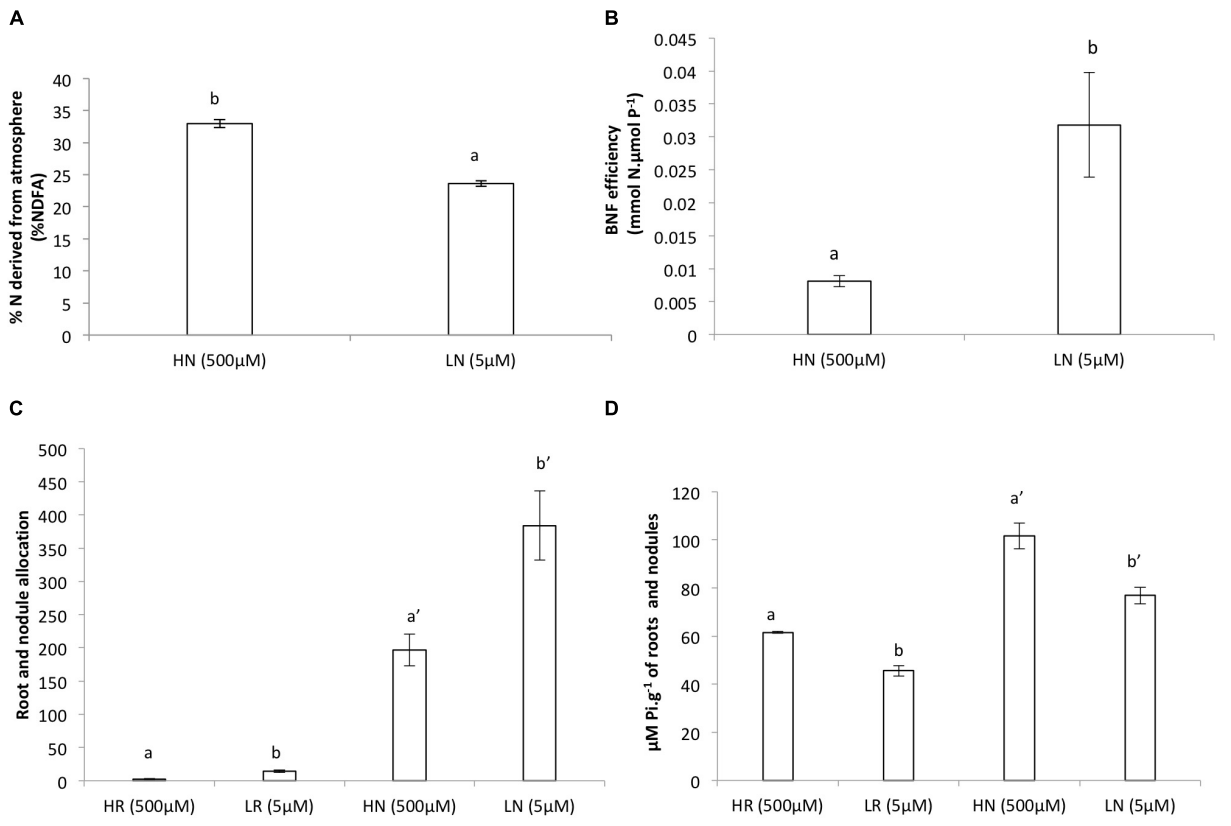

FIGURE 2 | (A) Biological nitrogen fixation (BNF), **(B)** efficiency of biological nitrogen fixation (BNF) per unit of metabolic P in nodules, **(C)** root and nodule allocation, **(D)** internal P*i* of roots and nodules of *V. divaricata*, grown under high phosphate (500 µM P) and low phosphate (5 µM P) conditions. HN (high P nodules), LN (low P nodules, HR (high P roots), and LR (low P roots are compared). Values of four replicates are presented as means ± SE. Different letters indicate significant differences between treatments ($P \leq 0.05$).

in LP roots which was more than four times higher compared to HR roots. PEPC activity in nodules was double compared to HP nodules (**Figure 3A**). PK activity (**Figure 3B**) was higher in the HP conditions compared to the LP conditions. Almost similar PK activity was found for HP in roots and HP in nodules. The PK activity in LP nodules was slightly less than that in HP nodules. PK activity was five times higher in HP roots compared to LP roots (**Figure 3B**). The highest ME activity (**Figure 3C**) was obtained in LP nodules which was double of that in HP nodules. The greatest activity was also found in LP nodules compared to HP nodules (**Figure 3C**). MDH activity per fresh weight was five times higher in LP nodules compared to HP nodules and was more than double in LP roots compared to HP roots (**Figure 3D**).

Organic Acids

Organic acids were higher in roots and nodules receiving the HP treatment (**Figure 4**). The citric acid concentration in HP roots was almost fivefold the amount compared to LP roots (**Figure 4A**). The amount of citric acid found in nodules at HP was double of that in LP (**Figure 4B**). The malic acid concentration in HP roots was one order of magnitude greater than the amount found in LP roots (**Figure 4C**). The amount of malic acid found in nodules at HP was sixfold greater of that in LP (**Figure 4C**).

Inorganic P Data

Higher internal P*i* values were obtained in the HP treatment for both roots and nodules, although we only found significant differences between HP and LP in the concentrations of nodules (**Figures 5A,B**). Phosphate concentration was significantly greater in HP treatments than in LP for both roots and nodules (**Figures 5C,D**).

NMR

An array of ^{13}C NMR spectra was recorded for each individual plant extract. The carbonyl carbon of the different organic acids each appear at a unique chemical shift area, between 175 and 181 ppm, in the respective spectra (**Supplementary Figures S1**−**S4** for partial spectra and **Supplementary Figures S5**, **S6** for full spectra). The unique carbonyl chemical shift of each organic acid were established by running commercial reference solutions of these organic acids (solubilized in D_2O at pH 7.5), under the same conditions as the extract samples. These two signals were consequently assigned to the organic acids malate and citrate, respectively. Much higher (one order of magnitude) relative malate concentrations were found compared to citrate (**Figure 7**). Incorporation of ^{13}C was very noticeable during the first hour with higher relative concentrations and a sharp decline in relative concentration after 2 h of

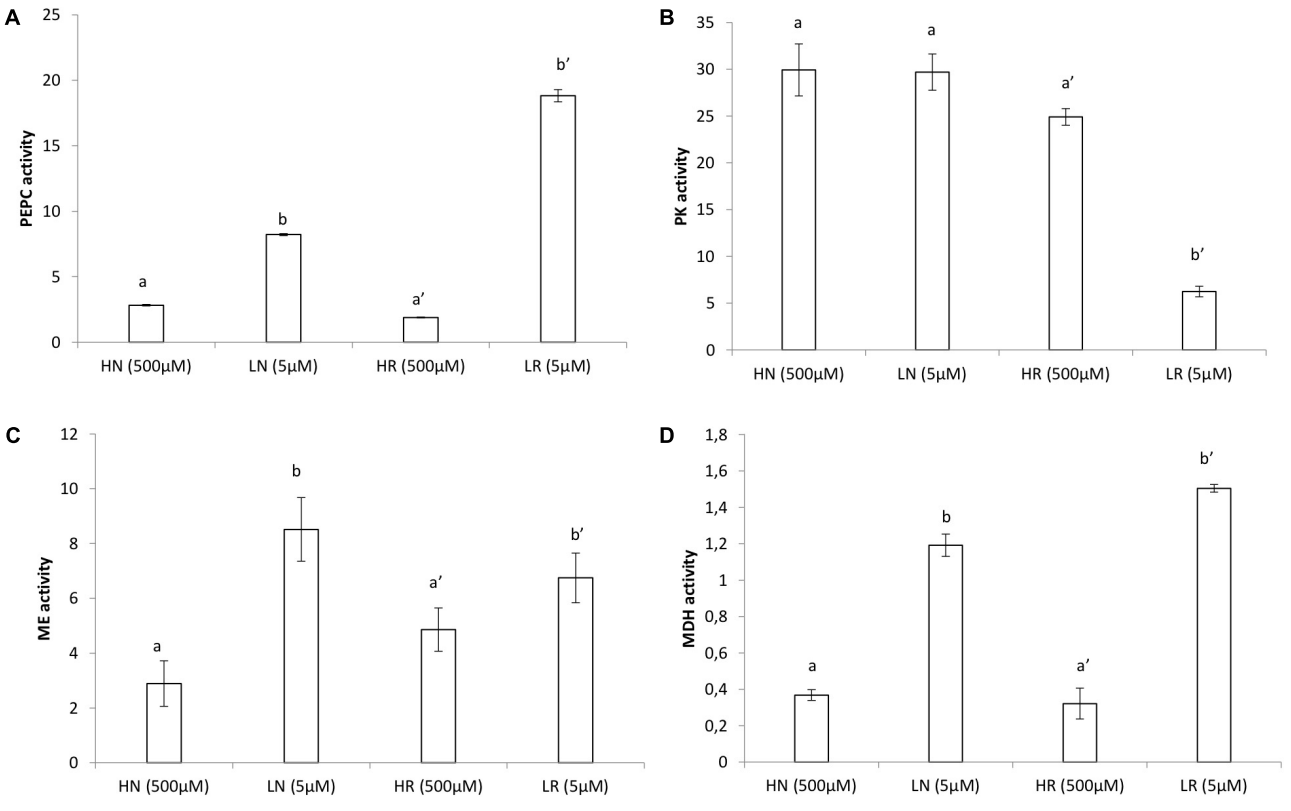

FIGURE 3 | Enzyme activities ($\mu mol.min^{-1}.g^{-1}FW$) in roots and nodules of *V. divaricata* grown under high phosphate (500 µM) and low phosphate (5 µM) conditions **(A)** PEPC, **(B)** PK, **(C)** ME, **(D)** MDH. HN (high P nodules), LN (low P nodules, HR (high P roots), and LR (low P roots are compared). Values of four replicates are presented as means ± SE. Different letters indicate significant differences between treatments ($P \leq 0.05$).

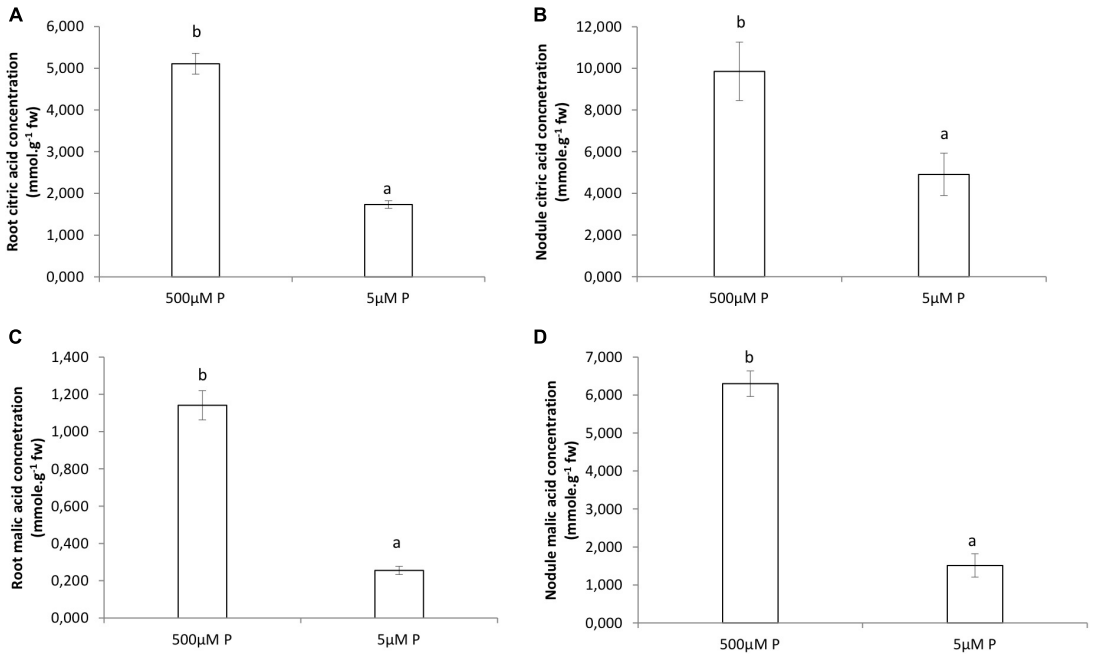

FIGURE 4 | Organic acids concentrations (mg.mol.g^{-1} FW) by GCMS analysis in roots and nodules of *V. divaricata*, grown under high phosphate (500 µM P) and low phosphate (5 µM P) conditions. Citric acid concentration in **(A)** roots, **(B)** nodules. Malic acid concentration in **(C)** roots **(D)**, nodules. Values of four replicates are presented as means ± SE. Different letters indicate significant differences between treatments ($P \leq 0.05$).

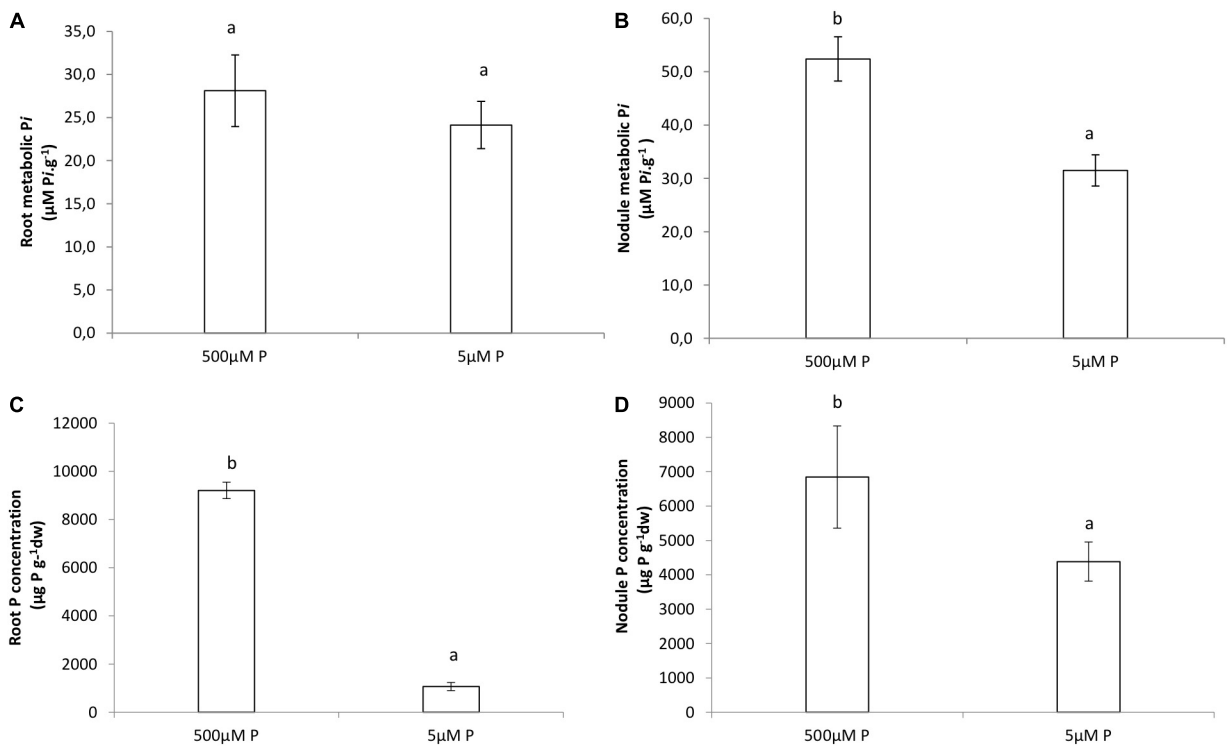

FIGURE 5 | Internal P*i* (µmol P*i*.g^{-1}) of **(A)** roots, **(B)** nodules. Phosphate concentration (mg.kg^{-1}) in **(C)** roots, **(D)** nodules of *V. divaricata* grown under high phosphate (500 µM P) and low phosphate (5 µM P) conditions. Values of four replicates are presented as means ± SE. Different letters indicate significant differences between treatments ($P \leq 0.05$).

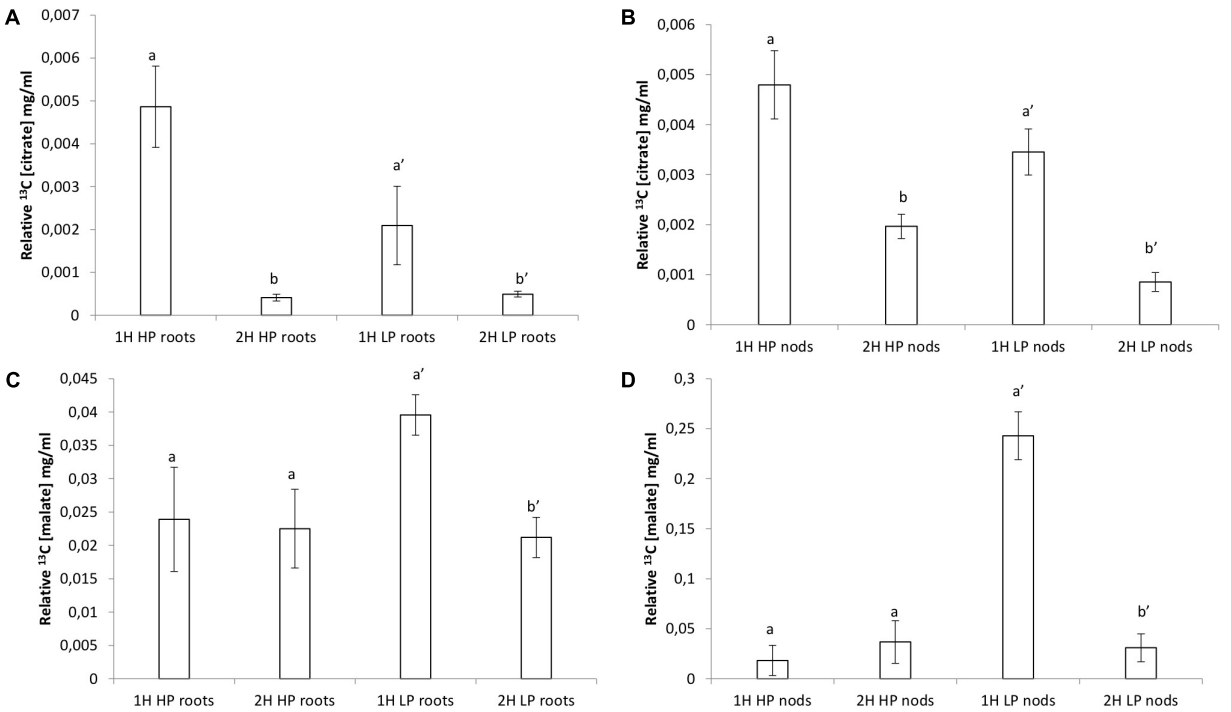

FIGURE 6 | Relative organic acid concentrations (mg.ml^{-1}) found by ^{13}C NMR analysis in roots and nodules of *V. divaricata*, grown under high phosphate (500 μM P) and low phosphate (5 μM P) conditions **(A)** root malate, **(B)** nodule malate, **(C)** root citrate, **(D)** nodules citrate.

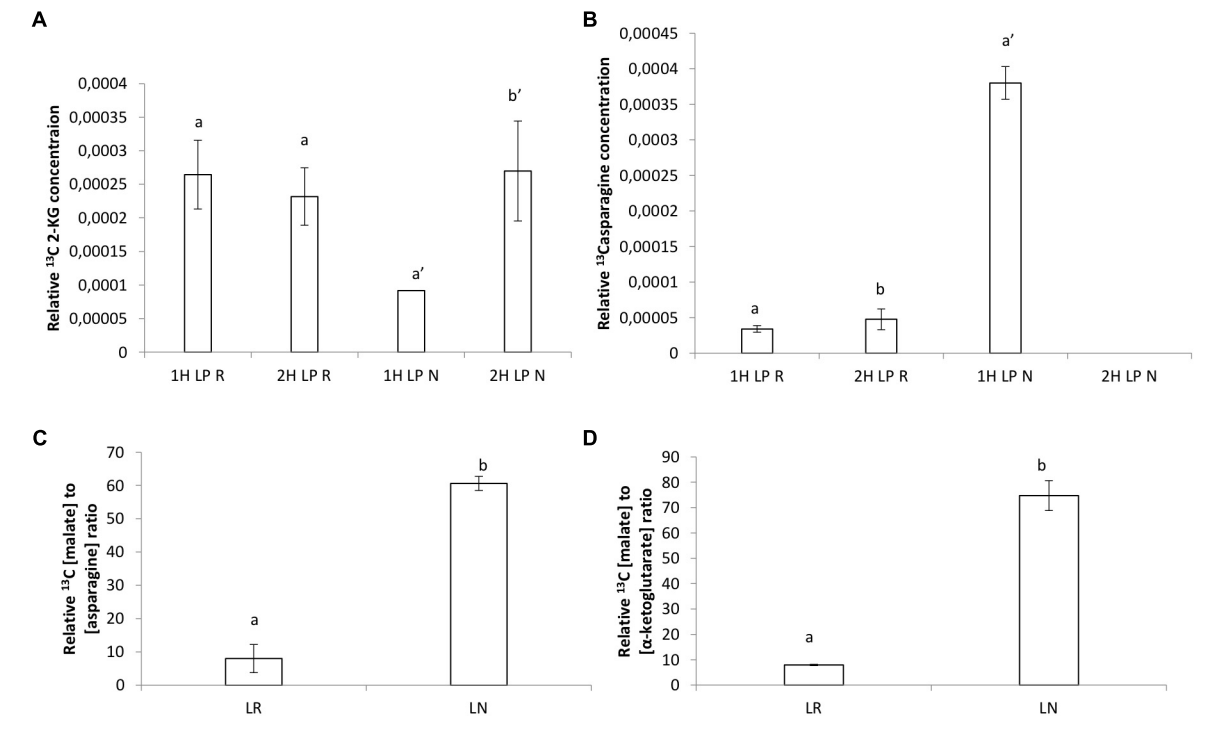

FIGURE 7 | (A) Relative ^{13}C α-ketoglutarate concentration after 1 h, **(B)** relative ^{13}C asparagine concentration after 1 h, **(C)** relative ^{13}C malate converted to asparagine concentration, **(D)** relative ^{13}C malate converted to α-ketoglutarate concentration (mg.ml^{-1})found by ^{13}C NMR analysis in roots and nodules of *V. divaricata*, grown under low phosphate (LP) (5 μM P) conditions.

exposure to ^{13}C, especially citrate (**Supplementary Figures S1**, **S2**).

Citrate levels were significantly higher in HP and LP roots and nodules after 1 h exposure (**Figures 6A,B**). Malate levels remained almost unchanged in HP conditions, however, a significant decline was observed in LP conditions in roots after 2 h of exposure (**Figure 6C**). Malate in nodules remained constant in all treatments without a strong increase after 1 h in LP (**Figure 6D** and **Supplementary Figure S3**). The presence of a keto-group (at 200–220 ppm) could also be observed in a few of the LP root and nodule spectra, which can be assigned to that of 2-ketoglutarate (**Supplementary Figure S4**). The peak at 161 ppm, which was present in all the samples (except in the control sample) can be assigned to ^{13}C bicarbonate which was present in the perfusion medium (Gout et al., 1993). Samples concentrations were corrected by dividing peak areas into the ^{13}C bicarbonate peak area at 161 ppm. Significantly greater concentration of 2-ketoglutarate was recorded in LP nodules after 2 H (**Figure 7A**). Levels of asparagine were very low both in roots and shoots except for the significantly greater concentration measured in LP nodules after 1 h (**Figure 7B**). The relative malate converted to asparagine was significantly greater in the nodules at LP (**Figure 7C**) and the same can be said about the relative malate converted to α-ketoglutarate (**Figure 7D**).

DISCUSSION

During P deficiency, *V. divaricata* nodules experienced less P*i* stress than roots, due to increased metabolic P conservation reactions during organic acid synthesis. Although the BNF declined, the high efficiency of BNF may be underpinned by these altered P conservation pathways and enhanced resource allocation during growth.

In legumes, Biological Nitrogen Fixation (BNF) is highly dependent on phosphate supply, which affects nodule formation (Valentine et al., 2017) as well as the nitrogen fixation process (Schultze et al., 2006; Tsvetkova and Georgiev, 2007). However, certain types of legumes are adapted to fix N_2 efficiently in P-impoverished environment. Particularly, *Virgilia divaricata*, a native legume tree to the Cape Floristic Region of South Africa, with high potential as precursor of Fynbos forests, has evolved to grow under low phosphate stress conditions, through previously unknown mechanisms. Our results indicate that belowground organs, roots and nodules, had a higher resource allocation under LP conditions as a consequence of their potential for greater contribution to mineral nutrition. This concurs with other species during P stress (Almeida et al., 2000) and also with legumes from nutrient poor ecosystems (Magadlela et al., 2014; Vardien et al., 2014), which can be interpreted as a strategy of legumes to adapt to scarce nutrient supply (Araújo et al., 2015).

Although there was a decline in the number of nodules in the LP treatment, the unchanged total nodule mass indicates that plants allocate more resources to existing nodules, thus increasing and maintain their efficiencies during LP conditions. This is supported by the efficiency of nodule functioning (compared to roots), under LP conditions, as reflected in the maintenance or proportionally lower decline of P levels during P stress. This lower decline in P concentration in nodules may also be attributed to the fact that nodules are P scavengers acquiring this nutrient mostly from roots, as reflected in the higher amounts of P and P*i* in nodules compares to roots in the LP-treatment, oriented to maintain their functioning (Jakobsen, 1985; Israel, 1993; Le Roux et al., 2006). Similar findings also indicated that nodule growth and functioning of this species is not limited by P-deficiency in white clover (Almeida et al., 2000) and also concurs with findings for *Medicago truncatula* where the P concentration in nodules seems to be unaffected as most of the P was allocated to the nodules (Sulieman et al., 2010). All these findings support the idea that *V. divaricata* is able to store P in the underground organs as an adaptation to the naturally low P environment where it naturally occurs.

In spite of the decline in BNF, there was an increase in BNF efficiency per mole P. This increase in BNF efficiency during low P supply, suggests that nodules attenuate their BNF capacity, despite low P conditions. It has been suggested that the decrease in nitrogen fixation in P stressed plants, should be viewed in correlation with whole plant growth, while specific nitrogenase activity is still maintained (Schultze, 2003). This idea is supported by various experimental evidences that it is the plant N status which regulates nitrogen fixation rates (Schultze, 2003). In addition, it appears that *V. divaricata* might also be able to shift its acquisition of N from BNF to soil N acquisition. This is reflected in higher mineral N uptake of nodulated roots as evidenced by the increase in specific root system N acquisition rate during P deficiency when BNF declines. This is in contrast to findings by Vardien et al. (2014), where roots showed a decline in mineral N uptake during P deficiency, compared to the current increase of mineral N in the nodulated root system. These differences may reside in the fact that in the current system, both roots and nodules may have contributed to mineral N uptake from soil. It is known that in a nodulated root system, both roots (Magadlela et al., 2014) and nodules can seperately acquire and assimilate mineral/soil N (Becana and Sprent, 1987) within a nodulated root system, which confers additional advantages to the plant growing in extremely poor soils.

Soil derived N is usually taken up in the form of NO_3^- (Lambers and Shane, 2007) and it might be that the roots increase their contribution to acquire N under P limitation. Although root nitrate uptake by roots could be beneficial to plant metabolism, it could also impact negatively on BNF as it might inhibit nitrogenase activity in legume plant nodules. It was shown that nitrate impacts negatively on *Rhizobium*-infection as well as on the ratio of the nodule dry mass to the whole plant mass (Luciński et al., 2002). As BNF is a costly process, it may be more beneficial for legumes from low nutrient ecosystems to take up N via its roots and to reduce energetically costly BNF (Magadlela et al., 2015). Similar trends were also observed in white clover where N concentration was unaffected by P deficiency. It was found in white clover that N_2 fixation increased strongly under P deficiency and that approximately 30% of N was assimilated due to N_2 fixation (Almeida et al., 2000). Similar to the BNF in white clover, we calculated that the nodules in our LP treatment experiment derived approximately 32% of the N from

the atmosphere. The approximate 68% of N might be from soil uptake (whether directly by the nodules or via roots), as the plants were fed with nutrient solution containing NH_4NO_3. In support of the above, we obtained higher specific nitrogen acquisition rate values for naked roots compared to nodulated roots, irrespective the treatment). This could be an indication that the plant would rather utilize soil N instead of utilizing the costly BNF route, which could justify abovementioned findings.

In spite of variable P supply, the unchanged N levels are also reflected in the elevated levels of all major amino acids found in the nodules of the LP treatment compared to the nodules of the HP treatment, and both the treatments for roots. A similar trend was seen in P deficient white clover (Almeida et al., 2000) and *Medicago truncatula* (Sulieman et al., 2010), where elevated levels of all major amino acids were founds, especially asparagine. It appears that aspartate, which serves as a precursor to asparagine, also plays a key role in the maintenance of these processes, as it was the predominant amino acid found in this study (Maxwell et al., 1984; King et al., 1986; Rosendahl et al., 1990). Asparagine, which is usually found in elevated levels during low P conditions, can act as a possible N-feedback regulator to the nodules during P-stress, as it flows from the shoots to the nodules and conveys the message of the shoot nitrogen status to the nodules and modulates their activity according to nutrient status of the plant (Sulieman et al., 2010). In this way the nitrogenase activity can be regulated by asparagine and this trend is also similar in other legumes and non-legumes plants under stress (Steward and Larher, 1980; Lea et al., 2007).

The key to these generated amino acids and other metabolic products during P stress might lie in the operation of the non-adenylated PEPC bypass route. Various studies have implicated this non-adenylated PEPC-bypass route to increase the PEP metabolism during P deficiency (Duff et al., 1989; Theodorou and Plaxton, 1993). Those studies have also found that the PEPC-activity may lead to an increase malate production. Malate could serve as C fuel in bacteroides, which is generated by the combined action of CA, PEPC and MDH (Vance and Heichel, 1991). In addition, malate can be transformed into OAA through MDH and serves as C skeleton to generate Asparagine, which serves as the principle N export compound in temperate legumes (Schultze et al., 2006). The higher accumulation of malate in the nodules compared to the roots (irrespective the treatment), might implicate its role as C fuel for nodules to sustain nodule activity. Similar findings were also observed in white lupin, where higher malate concentrations were also found in nodules compared to roots (Schuller and Werner, 1993). In addition to its role as fuel for nodules, malate as well as citrate can be excreted by roots to chelate metal cations such as Fe^{3+}, Fe^{2+}, Al^{3+}, and Ca^{2+} and in the process it release P from these cations, especially during low P conditions (Neumann and Römheld, 1999). The larger amount of citrate accumulation in roots compared to nodules may be an indication that *V. divaricata* also follows this trend to acquire P.

Although a combined action of all three enzymes (CA, PEPC, and MDH) is needed to generate organic acids for bacterial fuel and for exudation, literature highlights Class1 PEPC as playing a crucial role in the anaplerotic replenishment of tricarboxylic acid cycle intermediates where carbon skeletons are removed for other metabolic functions like nitrogen assimilation and amino acid biosynthesis especially during P-deficiency (Uhde-Stone et al., 2003b; Vance et al., 2003; Shane et al., 2004; O'Leary et al., 2011). When an extremely low level of P in the plant is reached, PEPC (in conjunction with MDH and ME) can theoretically function as a glycolytic enzyme by indirectly bypassing the conventional ADP dependent PK reaction to facilitate continued pyruvate supply to the TCA cycle. In the process, P*i* is also generated and recycled in the P-starved cells (Nagano et al., 1994; Plaxton and Carswell, 1999). *In vitro* root-MDH activity (LP treatment) appears to be the only enzyme to show higher activity over that of nodule-MDH activity. A direct result of this elevated LP root MDH activity might have been the export of malate to nodules which gave rise to the higher malate concentration in nodules, compared to roots). These findings give an indication that P deficiency may impact negatively on the root's metabolic processes resulting in the lower biomass obtained for roots compared to the apparent unaffected nodule metabolism, resulting in an increase in biomass for nodules under P-stress.

CONCLUSION

For legumes such as *V. divaricata* growing in P-poor soils, the continued reliance on BNF is underpinned by several key nodule adaptations. During P deficiency the nodules of *V. divaricata* have an increased allocation of resources and P-conservation mechanisms, which improve the efficiency of nodule BNF. These adaptations form the key to the plant's ability to adapt to poor P environments and thus sustaining its reliance on BNF.

AUTHOR CONTRIBUTIONS

All authors have equally contributed to the manuscript, from its design to finalized the manuscript.

ACKNOWLEDGMENTS

This work is based on the Ph.D. thesis (University of Stellenbosch) of one of the authors, Gary Grant Stevens (GGS). The work first appeared in GGS's thesis and this represents the only medium it has appeared in. This is in line with the university policy (University of Stellenbosch), and the Ph.D. thesis can be accessed online. The authors would like to thank the University of Stellenbosch for the provision of research infrastructure and the DST-NRF Centre of Excellence in Tree Health Biotechnology (CTHB) for funding of this research.

SUPPLEMENTARY MATERIAL

The Supplementary Material for this article can be found online at: https://www.frontiersin.org/articles/10.3389/fpls.2019.00073/full#supplementary-material

FIGURE S1 | A section of the ^{13}C spectra for **(a)** roots after 1 h, **(b)** roots after 2 h grown under high phosphate (500 μM P) conditions of *V. divaricata*.

FIGURE S2 | A section of the ^{13}C spectra of **(a)** roots after 1 h, **(b)** roots after 2 h grown under low phosphate (5 μM P) conditions of *V. divaricata*.

FIGURE S3 | A section of the ^{13}C spectra of **(a)** nodules after 1 h, **(b)** nodules after 2 h grown under high phosphate (500 μM P) conditions of *V. divaricata*.

FIGURE S4 | A section of the ^{13}C spectra of **(a)** nodules after 1 h, **(b)** nodules after 2 h grown under low phosphate (5 μM P) conditions of *V. divaricata*.

FIGURE S5 | A sample of the full ^{13}C spectra of roots after 1 h, from plants grown under high phosphate (500 μM P) conditions of *V. divaricata*.

FIGURE S6 | A sample of the full ^{13}C spectra of nodules after 1 h, from plants grown under high phosphate (500 μM P) conditions of *V. divaricata*.

REFERENCES

Almeida, J. P. F., Hartwig, U. A., Frehner, M., Nösberger, J., and Lüscher, A. (2000). Evidence that P deficiency induces N feedback regulation of symbiotic N2 fixation in white clover (*Trifolium repens*). *J. Exp. Bot.* 51, 1289–1297. doi: 10.1093/jexbot/51.348.1289

Appels, M. A., and Haaker, H. (1988). Identification of cytoplasmic nodules associated forms of malate dehydrogenase involved in the symbiosis between *Rhizobium leguminosarum* and *Pisum sativum*. *Eur. J. Biochem.* 171, 515–522. doi: 10.1111/j.1432-1033.1988.tb13820.x

Araújo, S. S., Beebe, S., Cresp, M., Delbreil, B., González, E. M., Gruber, V., et al. (2015). Abiotic stress response in legumes: strategies used to cope with environmental challenges. *Crit. Rev. Plant Sci.* 34, 237–280. doi: 10.1080/07352689.2014.898450

Bazzaz, F. A., and Grace, J. (1997). *Plant Resource Allocation*. San Diego, CA: Academic Press.

Becana, M., and Sprent, J. I. (1987). Nitrogen fixation and nitrate reduction in the root nodules of legumes. *Physiol. Plant.* 70, 757–765. doi: 10.1111/j.1399-3054.1987.tb04335.x

Bordeleau, L. M., and Prevost, D. (1994). Nodulation and nitrogen fixation in extreme environments. *Plant Soil* 161, 115–125. doi: 10.1007/BF02183092

Chang, K., and Roberts, J. K. M. (1989). Observation of cytoplasmic and vacuolar malate in maize root tips by ’3C-NMR spectroscopy. *Plant Physiol.* 89, 197–203. doi: 10.1104/pp.89.1.197

Chollet, R., Vidal, J., and O’lleary, M. (1996). «Phosphoenolpyruvate carboxylase: a ubiquitous highly regulated enzyme in plants». *Annu. Rev. Plant Physiol. Plant Mol. Biol.* 47, 273–298. doi: 10.1146/annurev.arplant.47.1.273

Coetsee, C., and Wigley, B. J. (2013). *Virgilia divaricata* may facilitate forest expansion in the afrotemperate forests of Southern Cape South Africa. *Koedoe* 55, 1–8. doi: 10.4102/koedoe.v55i1.1128

Crowley, D. E., and Rengel, Z. (1999). “Biology and chemistry of nutrient availability in the rhizosphere,” in *Minera Nutrition of Crops: Fundamental Mechanisms and Implications*, ed. Z. Rengel (New York, NY: Food Products Press), 1–40.

Day, D. A., and Copeland, L. (1991). Carbon metabolism and compartmentation in nitrogen-fixin legume nodules. *Plant Physiol. Biochem.* 29, 185–201.

Dinkelaker, B., Römheld, V., and Marschner, H. (1989). Citric acid excretion and precipitation of calcium citrate in the rhizosphere of white lupin (*Lupinus albus*). *Plant Cell Environ.* 12, 285–292. doi: 10.1111/j.1365-3040.1989.tb01942.x

Drevon, J. J., and Hartwig, U. A. (1997). Phosphorous deficiency increases the Argon-induced decline of nodule nitrogenise activity in soybean and alfalfa. *Planta* 201, 463–469. doi: 10.1007/s004250050090

Duff, S. M. G., Moorhead, G. B., Lefebvre, D. D., and Plaxton, W. C. (1989). Phosphate starvation inducible ‘bypasses’ of adenylate and phosphate dependent glycolytic enzymes in *Brassica nigra* suspension cells. *Plant Physiol.* 90, 1275–1278. doi: 10.1104/pp.90.4.1275

Farquhar, G. D., Ehleringer, J. R., and Hubick, K. T. (1989). Carbon isotope discrimination and photosynthesis. *Annu. Rev. Plant Physiol. Plant Mol. Biol.* 40, 503–537. doi: 10.1146/annurev.pp.40.060189.002443

Flemetakis, E., Dimou, M., Cotzur, D., Aivalakis, G., Efrose, R. C., Kenoutis, C., et al. (2003). A *Lotus japonicus* b-type carbonic anhydrase gene expression pattern suggests distinct physiological roles during nodule development. *Biochim. Biophys. Acta* 1628, 186–194. doi: 10.1016/S0167-4781(03)00142-8

Gardner, W. K., Barber, D. A., and Parbery, D. G. (1983). The acquisition of phosphorus by *Lupinus albus* III. The probable mechanism, by which phosphorus movement in the soil-root interface is enhanced. *Plant Soil* 70, 107–114. doi: 10.1007/BF02374754

Gilbert, A., Silvestre, V., Robin, R. J., Tcherkez, G., and Remaud, G. (2011). A 13C NMR spectrometric method for the determination of intramolecular δ13C values in fructores from plant sucrose samples. *New Phytol.* 191, 579–588. doi: 10.1111/j.1469-8137.2011.03690.x

Gilbert, G. A., Knight, J. D., Vance, C. P., and Allan, D. L. (2000). Proteoid root development of phosphorus deficient lupin is mimicked by auxin and phosphonate. *Ann. Bot.* 85, 921–928. doi: 10.1006/anbo.2000.1133

Gilroy, I., and Jones, D. L. (2000). Through form to function: root hair development and nutrient uptake. *Trends Plant Sci.* 5, 56–60. doi: 10.1016/S1360-1385(99)01551-4

Goldblatt, P., and Manning, J. (2000). *Cape Plants: a Conspectus of the Cape Flora of South Africa. Strelitzia*, Vol. 9. Pretoria: National Botanical Institute.

Gout, E., Bligny, R., Pascal, N., and Douce, R. (1993). 13C nuclear magnetic resonance studies of malate and citrate synthesis and compartmentation in higher plant cells. *J. Biol. Chem.* 268, 3986–3992.

Greinwald, R., Veen, G., Van Wyk, B. E., Witte, L., and Czygan, F. C. (1989). Distribution and taxonomic significance of major alkaloids in the genus *Virgilia*. *Biochem. Syst. Ecol.* 17, 231–238. doi: 10.1016/0305-1978(89)90085-9

Grigg, A. M., Veneklass, E. J., and Lambers, H. (2008). Water relations and mineral nutrition of closely related woody plant species on desert dunes and interdunes. *Aust. J. Bot.* 56, 27–43. doi: 10.1071/BT06205

Høgh-Jensen, H., Schjoerring, J. K., and Soussana, J.-F. (2002). The influence of phosphorus deficiency on growth and nitrogen fixation of white clover plants. *Ann. Bot.* 90, 745–753. doi: 10.1093/aob/mcf260

Horst, W. J., Kamh, M., Jibrin, J. M., and Chude, V. O. (2001). Agronomic measures for increasing P availability to crops. *Plant Soil* 237, 211–223. doi: 10.1023/A:1013353610570

Israel, D. W. (1993). Symbiotic dinitrogen fixation and host-plant growth during development of and recovery from phosphate deficiency. *Plant Physiol.* 88, 294–300. doi: 10.1111/j.1399-3054.1993.tb05502.x

Jakobsen, I. (1985). The role of phosphorus in nitrogen fixation by young pea plants (*Pisum sativum*). *Physiol. Plant.* 64, 190–196. doi: 10.1111/j.1399-3054.1985.tb02334.x

Kanu, S. A., and Dakora, F. D. (2012). Symbiotic nitrogen contribution and biodiversity of root-nodule bacteria nodulating *Psoralea* species in the Cape fynbos. South Africa. *Soil Biol. Biochem.* 54, 68–76. doi: 10.1016/j.soilbio.2012.05.017

King, B. J., Layzell, D. B., and Canvin, D. T. (1986). The role of dark carbon fixation in root nodules of soybean. *Plant Physiol.* 81, 200–205. doi: 10.1104/pp.81.1.200

Koide, R. T., and Kabir, Z. (2000). Extraradical hyphae of the mycorrhizal fungus *Glomus intraradice* can hydrolyse organic phosphate. *New Phytol.* 148, 511–517. doi: 10.1046/j.1469-8137.2000.00776.x

Lajtha, K., and Harrison, A. F. (1995). “Strategies of phosphorus acquisition and conservation by plant species and communities,” in *Phosphorus in the Global Environment: Transfers, Cycles, and Management. SCOPE 54*, ed. H. Tiessen (Chichester: John Wiley and Sons), 139–147.

Lambers, H., and Shane, M. W. (2007). “Role of root clusters in phosphorus acquisition and increasing biological diversity in agriculture,” in *Scale and Complexity in Plant Systems Research: Gene-Plant-Crop Relations*, eds J. H. J. Spiertz, P. C. Struik, and H. H. van Laar (Dordrecht: Springer), 237–250.

Lamont, B. B. (2003). Structure, ecology and physiology of root clusters – a review. *Plant Soil* 248, 1–19. doi: 10.1007/s00442-014-2892-z

Le Roux, M. R., Khan, S., and Valentine, A. J. (2008). Organic acid accumulation may inhibit N2 fixation in phosphorus-stressed lupin nodules. *New Phytol.* 177, 956–964. doi: 10.1111/j.1469-8137.2007.02305.x

Le Roux, M. R., Ward, C. L., Botha, F. C., and Valentine, A. J. (2006). Routes of pyruvate synthesis in phosphorus-deficient lupin roots and nodules. *New Phytol.* 169, 399–408. doi: 10.1111/j.1469-8137.2005.01594.x

Lea, P. J., Sodek, L., Parry, M. A. J., Shewry, P. R., and Halford, N. G. (2007). Asparagine in plants. *Ann. Appl. Biol.* 150, 1–26. doi: 10.1111/j.1744-7348.2006.00104.x

Luciñski, R., Polcyn, W., and Ratajczak, L. (2002). Nitrate reduction and nitrogen fixation in symbiotic association *Rhizobium* — legumes. *Acta Biochim. Pol.* 49, 537–546.

Lynch, J. P., and Brown, K. M. (2001). Topsoil foraging: an architectural adaptation of plants to low phosphorus availability. *Plant Soil* 237, 225–237. doi: 10.1023/A:1013324727040

Magadlela, A., Kleinert, A., Dreyer, L. L., and Valentine, A. J. (2014). Low phosphorus conditions affect the nitrogen nutrition and associated carbon costs of two legume tree species from a Mediterranean-type ecosystem. *Aust. J. Bot.* 62, 1–9. doi: 10.1071/BT13264

Magadlela, A., Steenkamp, E. T., and Valentine, A. J. (2015). Variable P supply affect N metabolism in a legume tree, *Virgilia divaricata*, from nutrient-poor Mediterranean-type ecosystems. *Funct. Plant Biol.* 43, 287–297. doi: 10.1071/FP15262

Maxwell, C. A., Vance, C. P., Heichel, G. H., and Stade, S. (1984). CO2 fixation in alfalfa and birdsfoot trefoil root nodules and partitioning of 14C to the plant. *Crop Sci.* 24, 257–264. doi: 10.2135/cropsci1984.0011183X002400020012x

McCloud, S. A., Smith, R. G., and Schuller, K. A. (2001). Partial purification and characterisation of pyruvate kinase from the plant fraction of soybean root nodules. *Physiol. Plant.* 111, 283–290. doi: 10.1034/j.1399-3054.2001.1110304.x

Mengel, K. (1994). Symbiotic dinitrogen fixation-its dependence on plant nutrition and its ecophysiological impact. *Zeitschrift Pflanzenernährung Bodenkunde* 157, 233–241. doi: 10.1002/jpln.19941570311

Mortimer, P. E., Pérez-Fernández, M. A., and Valentine, A. J. (2008). The role of arbuscular mycorrhizal colonization in the carbon and nutrient economy of the tripartite symbiosis with nodulated *Phaseolus vulgaris*. *Soil Biol. Biochem.* 40, 1019–1027. doi: 10.1016/j.soilbio.2007.11.014

Muofhe, M. L., and Dakora, F. D. (1999). Nitrogen nutrition in nodulated field plants of the shrub tea legume *Aspalathus linearis* assessing using 15N natural abundance. *Plant Soil* 209, 181–186. doi: 10.1023/A:1004514303787

Nagano, M., Hachiya, A., and Ashihara, H. (1994). Phosphate starvation and a glycolytic bypass catalyzed by phosphoenolpyruvate carboxylase in suspension cultured *Catharanthus roseus* cells. *Zeitschrift Naturforschung* 49c, 742–750. doi: 10.1515/znc-1994-11-1208

Neumann, G., and Martinoia, E. (2002). Cluster roots: an underground adaptation for survival in extreme environments. *Trends Plant Sci.* 7, 162–167. doi: 10.1016/S1360-1385(02)02241-0

Neumann, G., Massonneau, A., Langlade, N., Dinkelaker, B., Hengeler, C., Römheld, V., et al. (2000). Physiological aspects of cluster root function and development in phosphorus-deficient white lupin (*Lupinus albus*). *Ann. Bot.* 85, 909–919. doi: 10.1006/anbo.2000.1135

Neumann, G., and Römheld, V. (1999). Root excretion of carboxylic acids and protons in phosphorous deficient plants. *Plant Soil* 211, 121–130. doi: 10.1023/A:1004380832118

Nielson, K. L., Amram, E., and Lynch, J. P. (2001). The effect of phosphorus availability on the carbon economy of contrasting common bean (*Phaseolus vulgaris*) genotypes. *J. Exp. Bot.* 52, 329–339.

Ocaña, A., Cordovilla, M. P., Ligero, F., and Lluch, C. (1996). Phosphoenolpyruvate carboxylase in root nodules of *Vicia faba*: partial purification and properties. *Physiol. Plant.* 97, 724–730. doi: 10.1111/j.1399-3054.1996.tb00537.x

O'Leary, B., Park, J., and Plaxton, W. C. (2011). The remarkable diversity of plant PEPC (phosphoenolpyruvate carboxylase): recent insights into the physiological functions and post-translational controls of non-photosynthetic PEPC's. *Biochem. J.* 436, 15–34. doi: 10.1042/BJ20110078

Pate, J. S., Stewart, G. R., and Unkovich, M. (1993). 15N natural abundance of plant and soil components of a Banksia woodland ecosystem in relation to nitrate utilization, life form, mycorrhizal status and N2-fixing abilities of component species. *Plant Cell Environ.* 16, 365–373. doi: 10.1111/j.1365-3040.1993.tb00882.x

Plaxton, W. C. (1996). The organization and regulation of plant glycolysis. *Annu. Rev. Plant Physiol. Plant Mol. Biol.* 47, 185–214. doi: 10.1146/annurev.arplant.47.1.185

Plaxton, W. C., and Carswell, M. C. (1999). "Metabolic aspects of the phosphate starvation response in plants," in *Plant Responses to Environmental Stresses: From Phytohormones to Genome Reorganization*, ed. H. R. Lerner (New York, NY: Marcel Dekker, Inc), 349–372.

Power, S. C., Cramer, M. D., Verboom, G. A., and Chimphango, S. B. M. (2010). Does phosphate acquisition constraint legume persistence in the fynbos of the cape floristic region? *Plant Soil* 334, 33–46. doi: 10.1007/s11104-010-0311-8

Raghothama, K. G. (1999). Phospahate acquisition. *Annu. Rev. Plant Physiol. Mol. Biol.* 50, 665–693. doi: 10.1146/annurev.arplant.50.1.665

Rawsthorne, S. (2002). Carbon flux and fatty acid synthesis in plants. *Prog. Lipid Res.* 41, 182–196. doi: 10.1016/S0163-7827(01)00023-6

Rengel, Z. (2002). Genetic control of root exudation. *Plant Soil* 245, 59–70. doi: 10.1023/A:1020646011229

Rosendahl, L., Vance, C. P., and Pedersen, W. B. (1990). Products of dark CO2 fixation in pea root nodules support bacteroid metabolism. *Plant Physiol.* 93, 12–19. doi: 10.1104/pp.93.1.12

Schachtman, D. P., Reid, R. J., and Ayling, S. M. (1998). Phosphorus uptake by plants: from soil to cell. *Plant Physiol.* 116, 447–453. doi: 10.1104/pp.116.2.447

Schuller, K. A., and Werner, D. (1993). Phosphorylation of soybean (*Glycine max*) nodule phosphoenolpyruvate carboxylase in vitro decreases sensitivity to inhibition by malate. *Plant Physiol.* 101, 1267–1273. doi: 10.1104/pp.101.4.1267

Schultze, J. (2003). Source-sink manipulations suggests an N-feedback mechanism for the drop in N2 fixation during pod-filling in pea and broad bean. *J. Plant Physiol.* 160, 531–537. doi: 10.1078/0176-1617-00709

Schultze, J., Temple, G., Temple, S., Beschow, H., and Vance, C. P. (2006). White lupin nitrogen fixation under phosphorous deficiency. *Ann. Bot.* 98, 731–740. doi: 10.1093/aob/mcl154

Shane, M. W., Cramer, M. D., Funayama-Noguchi, S., Cawthray, G. R., Millar, A. H., Day, D. A., et al. (2004). Developmental physiology of cluster root carboxylate synthesis and exudation in harsh hakea. Expression of phosphoenolpyruvate carboxylase and the alternative oxidase. *Plant Physiol.* 135, 549–560. doi: 10.1104/pp.103.035659

Shearer, G., and Kohl, D. H. (1986). N2-fixation in field settings: estimations based on natural ∼SN abundance. *Aust. J. Plant Physiol.* 13, 699–756. doi: 10.1071/PP9860699

Soos, V., Juhasz, A., Light, M. E., Van Staden, J., and Balazs, E. (2009). Smoke-water-induced changes of expression pattern in grand rapids lettuce achenes. *Seed Sci. Res.* 19, 37–49. doi: 10.1017/S0960258508187815

Spriggs, A. C., and Dakora, F. D. (2008). Field assessment of symbiotic N2 fixation in wild and cultivated Cyclopia species in the South African fynbos by 15N natural abundance. *Tree Physiol.* 29, 239–247. doi: 10.1093/treephys/tpn021

Steward, G. R., and Larher, F. (1980). "Accumulation of amino acids and related compounds in relation to environmental stress," in *The Biochemistry of Plants*, Vol. 5, ed. B. J. Miflin (London: Academic Press), 609–635.

Streeter, J. G. (1991). Transport and metabolism of carbon and nitrogen in legume nodules. *Adv. Bot. Res.* 18, 129–187. doi: 10.1016/S0065-2296(08)60022-1

Sulieman, S., Fischinger, S. A., Gresshoff, P. M., and Schultze, J. (2010). Asparagine as a major factor in the N-feedback regulation of N2 fixation in *Medicago truncatula*. *Physiol. Plant.* 140, 21–31. doi: 10.1111/j.1399-3054.2010.01380.x

Tajima, Y., Yamamoto, Y., Fukui, K., Nishio, Y., Hashiguchi, K., Usuda, Y., et al. (2015). Effects of eliminating pyruvate node pathways and of coexpression of heterogeneous carboxylation enzymes on succinate production by *Enterobacter aerogenes*. *Appl. Environ. Microbiol.* 81, 929–937. doi: 10.1128/AEM.03213-14

Theodorou, M. E., and Plaxton, W. C. (1993). Metabolic adaptations of plant respiration to nutritional phosphate deprivation. *Plant Physiol.* 101, 339–344. doi: 10.1104/pp.101.2.339

Tsvetkova, G. E., and Georgiev, G. I. (2007). Changes in phosphate fractions extracted from different organs of phosphorous starved nitrogen fixing pea plants. *J. Plant Nutr.* 30, 2129–2140. doi: 10.1080/01904160701700616

Uhde-Stone, C., Gilbert, G., Johnson, J. M. F., Litjens, R., Zinn, K. E., Temple, S. J., et al. (2003a). Acclimation of white lupin to phosphorous deficiency involves enhanced expression of genes related to organic acid metabolism. *Plant Soil* 248, 99–116. doi: 10.1023/A:1022335519879

Uhde-Stone, C., Zinn, K. E., Ramirez-Yáñez, M., Li, A., Vance, C. P., and Allan, D. L. (2003b). Nylon filter arrays reveal differential gene expression in proteoid roots of white lupin in response to phosphorus deficiency. *Plant Physiol.* 131, 1064–1079.

Valentine, A. J., Kleinert, A., and Benedito, V. A. (2017). Adaptive strategies for nitrogen metabolism in phosphate deficient legume nodules. *Plant Sci.* 256, 46–52. doi: 10.1016/j.plantsci.2016.12.010

Vance, C. P., and Heichel, G. H. (1991). Carbon in N2 fixation: limitation or exquisite adaption. *Annu. Rev. Plant Physiol. Mol. Biol.* 42, 373–392. doi: 10.1146/annurev.pp.42.060191.002105

Vance, C. P., Uhde-stone, C., and Allan, D. L. (2003). Phosphorous acquisition and use: critical adaptations by plants for securing a non-renewable resource. *New Phytol.* 157, 423–447. doi: 10.1046/j.1469-8137.2003.00695.x

Vardien, W., Valentine, A. J., Mesjasz-Przybyłowicz, J., Przybyłowicz, W. J., Wang, Y., and Steenkamp, E. T. (2014). Nodules from Fynbos legume *Virgilia divaricata* have high functional plasticity under variable P supply levels. *J. Plant Physiol.* 171, 1732–1739. doi: 10.1016/j.jplph.2014.08.005

Voisin, A.-S., Bourion, V., Duc, G., and Salon, C. (2007). Using an ecophysiological analysis to dissect genetic variability and to propose an ideotype for nitrogen nutrition in pea. *Ann. Bot.* 100, 1525–1536. doi: 10.1093/aob/mcm241

Von Uexkull, H. R., and Mutert, E. (1998). "Global extent, development and economic impact of acid soils," in *Plant-Soil Interaction at Low pH: Principles and Management*, eds R. A. Date, N. J. Grundon, G. E. Payment, and M. E. Probert (Dordrecht: Kluwer Academic Publisher), 5–9.

Vuorinen, A. H., and Kaiser, W. M. (1997). Dark CO_2 carbon dioxide. fixation by roots of willow and barley in media with a high level of inorganic carbon. *J. Plant Physiol.* 151, 405–408. doi: 10.1016/S0176-1617(97)80004-1

Conflict of Interest Statement: The authors declare that the research was conducted in the absence of any commercial or financial relationships that could be construed as a potential conflict of interest.

frontiers in Plant Science

ORIGINAL RESEARCH
published: 19 February 2019
doi: 10.3389/fpls.2019.00183

Interactions Between Light Intensity and Phosphorus Nutrition Affect the P Uptake Capacity of Maize and Soybean Seedling in a Low Light Intensity Area

Tao Zhou[1†], Li Wang[1†], Shuxian Li[1], Yang Gao[1], Yongli Du[1], Li Zhao[2], Weiguo Liu[1] and Wenyu Yang[1,3]**

[1] College of Agronomy, Sichuan Agricultural University, Chengdu, China, [2] Sichuan Coalfield Geological Bureau, Chengdu, China, [3] Key Laboratory of Crop Ecophysiology and Farming System in Southwest, Ministry of Agriculture, Chengdu, China

OPEN ACCESS

Edited by:
Aleysia Kleinert, Stellenbosch University, South Africa

Reviewed by:
Lars Hendrik Wegner, Karlsruhe Institute of Technology (KIT), Germany
Marcellous Le Roux, Stellenbosch University, South Africa

***Correspondence:**
Weiguo Liu
lwgsy@126.com
Wenyu Yang
mssiyangwy@sicau.edu.cn

† These authors have contributed equally to this work

Specialty section:
This article was submitted to Plant Nutrition, a section of the journal Frontiers in Plant Science

Received: *09 May 2018*
Accepted: *05 February 2019*
Published: *19 February 2019*

Citation:
Zhou T, Wang L, Li S, Gao Y, Du Y, Zhao L, Liu W and Yang W (2019) Interactions Between Light Intensity and Phosphorus Nutrition Affect the P Uptake Capacity of Maize and Soybean Seedling in a Low Light Intensity Area. Front. Plant Sci. 10:183. doi: 10.3389/fpls.2019.00183

To capture more nutrients, root systems of maize (*Zea mays* L.) and soybean (*Glycine max* L.) exhibit morphological and physiological plasticity to a localized supply of phosphorus (P). However, the mechanisms of the interaction between light intensity and P affecting root morphological and physiological alterations remain unclear. In the present study, the regulation of P uptake capacity of maize and soybean by light intensity and localized P supply was investigated in a low solar radiation area. The plants were grown under continual and disrupted light conditions with homogeneous and heterogeneous P supply. Light capture of maize and soybean increased under the disrupted light condition. Plant dry weight and P uptake were increased by more light capture, particularly when plants were grown in soil with heterogeneous P supply. Similarly, both localized P supply and disrupted light treatment increased the production of fine roots and specific root length in maize. Both homogeneous P supply and disrupted light treatment increased the malate and citrate exudation in the root of soybean. Across all of the experimental treatments, high root morphological plasticity of maize and root physiological plasticity of soybean were associated with lower P concentrations in leaves and greater sucrose concentrations in roots. It is suggested that the carbon (C), exceeded shoot growth capabilities and was transferred to roots as sucrose, which may serve as both a nutritional signal and a C-substrate for root morphological and physiological changes.

Keywords: photosynthesis, P uptake capacity, root growth, sucrose, maize, soybean, carboxylates

INTRODUCTION

Light intensity plays an important role in determining the performance of individuals in natural communities and the growth and productivity of crops in agroecological systems. In the Sichuan Basin located upstream on the Yangtze River, the range of total solar radiation is 3350–4190 MJ m^{-2} per year and below the annual average of 5900 MJ m^{-2} for China in general. Due to low solar radiation, local crops are sown at low density (maize at 6.0×10^4 plant ha^{-1}, soybean

at 1.2×10^5 plant ha^{-1}, rice at 1.3×10^5 plant ha^{-1}, and wheat at 2.4×10^7 plant ha^{-1}) to circumvent the self-shading within the canopy. Shading is ubiquitous, and all plants are shaded to some degree during their lifetime (Valladares and Niinemets, 2008). Practically, crops capture more light by changing the planting pattern from equal row width distance to narrow-wide row distances rather than decreasing the planting density, as shown in **Supplementary Figure S1** (Liu and Song, 2012). The availability of solar radiation in the narrow row decreases with decreasing row width. However, the light capture of crops in the narrow-wide planting pattern is much higher than that of crops in the equal-width row planting pattern. This might be mostly attributed to the light interception in wide rows (Wang et al., 2017). In addition to the amelioration of light conditions in the wide spacing of the narrow-wide row distance planting pattern, plant phenotypic plasticity may markedly contribute to capture due to minimizing the self-shading effect (Zhu et al., 2015, 2016). Additionally, the leaves of crops maintain a longer green period in the narrow-wide row distance planting pattern than that in the equal-width row distance planting pattern, resulting in leaf area, subsequently, and light capture increased.

It is widely acknowledged that, of the applied fertilizer P each season, crop uptake is only 10–25% (Johnston et al., 2014), as P is strongly bound to soil particles (Hinsinger, 2001; Shen et al., 2011). Roots in soils with low availability and heterogeneous distribution of P show high plasticity to increase the capacity of P acquisition, including root morphological and physiological strategies (Lambers et al., 2006; Shen et al., 2011). For example, cluster-root formation and citrate exudation of *Lupinus albus* were induced by low soil P availability and inhibited by increased P supply (Shen et al., 2003; Li et al., 2008). In many species, including maize and wheat, the heterogeneous distribution of P affects root growth and distribution (Jing et al., 2010; Li L. et al., 2014). The proliferation of roots increases in local nutrient-rich zones because plants stimulate root growth and alter root distribution in response to nutrient-rich zones (Hodge, 2004). However, not all crop species (e.g., Faba bean) show a significant root growth response to localized P supply (Li H.B. et al., 2014; Zhang et al., 2016). Similarly, some species show positive root physiological responses to localized nutrient enrichment (Jackson et al., 1990). Nutrients localized in the soil not only alter root morphology and physiology but also are used as an effective management strategy to determine root distribution in the soil profile. Greater root distribution in wide rows than that in narrow rows in response to localized P supply reduces root competition and increases the acquisition of P from soil (Li Y. et al., 2016; Li H.B. et al., 2016). Hence, the plasticity of root morphology, physiology, and distribution in foraging P is also determined by soil environmental conditions.

Many studies have investigated the contributions of changes in root morphology and physiology for P acquisition in soil environments with low P availability (Rengel and Marschner, 2005; Wang et al., 2009, 2010; Yuan and Chen, 2012; Zhang et al., 2012; Fernandez and Rubio, 2015). Less attention has been paid to understanding how the light aboveground influences root morphology and physiology. Studies indicate that photosynthate is preferentially distributed to shoots during leaf extension to increase the interception of light and decrease the ratios of root to shoot biomass when plants are grown under low light intensity conditions (Gommers et al., 2013; Gundel et al., 2014). Simultaneously, total root length decreased when plants are grown in low light intensities (Samuel and Matthew, 2004; Wissuwa et al., 2005; Sparkes et al., 2008). Light is not only involved in the synthesis and transportation of photosynthate, but also as signal direct regulates root morphology. Such as far-red light detection in the shoot of Arabidopsis regulates lateral root growth through the HY5 transcription factor (Van Gelderen et al., 2018a,b). Root morphology is also altered by shoot P concentration and root sucrose concentration, and the tissue P and sucrose concentration affected by light intensity. High light intensity increases cluster-root formation of white lupine, which is associated with an increase in root sucrose concentration under P-deficient conditions (Cheng et al., 2014). Exogenous supply of sucrose also stimulates the formation of cluster roots, even in P-sufficient conditions (Zhou et al., 2008). High light intensity decreases shoot P concentration, which subsequently increases the total root length, specific root length, and production of fine roots (Cheng et al., 2014; Wen et al., 2017). Root physiology is also affected by light intensity. For example, the expression of the gene *LaPEPC3* (which initiates citrate synthesis) and citrate exudation of white lupine increased with increasing light intensity, independent of the response to changing P supply (Cheng et al., 2014).

In response to low soil P conditions, maize altered root morphology rather than root physiology (Lyu et al., 2016; Wen et al., 2017), whereas soybean positively altered root morphology and root physiology in response to low P soil (Lyu et al., 2016). However, very few studies explore the effect of light intensity aboveground on root morphology and physiology, particularly for maize and soybean, which are widely cultivated crops globally, including in the typically low light intensity areas of southwest China. The primary purpose of this study was to investigate the interactions between heterogeneous shoot light intensity and localized P supply affecting root morphology and physiology associated with an increased ability of maize and soybean P acquisition. Specifically, the hypotheses were that (i), increasing light capture increases photosynthesis and shoot growth rate, which exceeds the P supply ability of roots to leaf, causing growth-induced P starvation in the shoot that produces a systemic signal to induce root proliferation and carboxylate exudation. Furthermore (ii), carbon accumulations in excess of what is required for shoot growth capabilities are transferred to roots as sucrose, which serves as both a nutritional signal and a carbon-substrate for root morphological and physiological changes.

MATERIALS AND METHODS

Experimental Setup

Maize (*Zea mays* L., cv. CD418) and soybean (*Glycine max* L., cv. ND12) were cultivated to investigate their P uptake capacities in response to heterogeneity in light intensity and P in soil. A rhizobox ($24 \times 2 \times 40$ cm, **Figure 1**) experiment with two light condition treatments (continual and disrupted light conditions)

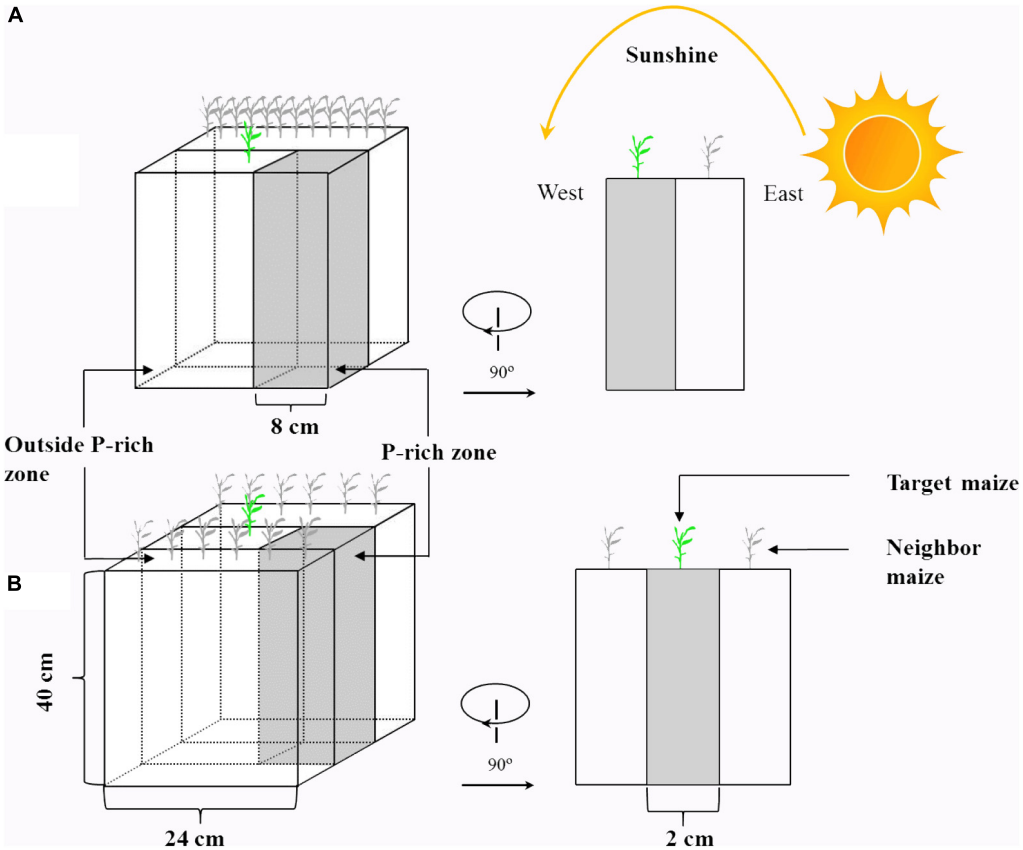

FIGURE 1 | A schematic diagram of the rhizo-box. Shown are: disrupted light condition treatment **(A)** and continual light condition treatment **(B)**. The design of this experiment in maize and soybean was the same, but here only shown for maize to avoid redundancy.

and two P supply treatments was conducted, with three replicates of each treatment. To change the light interception of the experimental plants, two PVC-rhizo-boxes were linked together; the target plants were grown in the one box, and 12 plants of the same species as neighboring for preventing light transmission were grown in the other box. The light interception of the target plants was mostly from the other side with nothing impeding the light (disrupted light condition) (**Figure 1A**). This treatment was designed to simulate plant growth maximally under disrupted light conditions, which simulated conditions as the "narrow-wide row distance planting pattern" in the field (**Supplementary Figure S1**). The continual light treatment was three PVC-rhizo-boxes linked together, with the target plants grown in the middle and the left and right boxes with six plants of the same species, respectively. The target plants intercepted light from the interstices among the neighbor plants (continual light condition) (**Figure 1B**). This treatment was designed to maximally simulate the target plant growth under a continual light condition as the "equal-width row distance planting pattern" in the field. The rhizo-boxes were placed to face to the east and the continual and disrupted light environment in the two treatments were induced by the sun trajectory from east to west (**Figure 1**).

The PVC-rhizo-boxes contained irrigation holes, a viscose fleece for moisture distribution, white plastic foil for a soil covering and a Perspex front lid with screws. All rhizo-boxes were filled with 3 kg of air-dried soil. Phosphorus was supplied as KH_2PO_4 in a homogeneous or heterogeneous pattern. For the heterogeneous P treatment, an 8-cm P-rich layer (1000 g of soil) containing 200 mg of P (200 mg P kg^{-1} soil) was manually mixed and placed at the right of the rhizo-box as the P-rich zone, and the remaining soil without P addition was the background soil (2000 g of soil, outside the P-rich zone) (**Figure 1**). For the homogeneous P treatment, the same total P (200 mg of P) was spread evenly throughout the soil (66 mg P kg^{-1} soil).

The soil was collected from the Renshou experimental station in Sichuan, China, air-dried and passed through a 2-mm sieve. Soil properties were as follow: Olsen-P 3.3 mg kg^{-1}, organic matter 8.7 g kg^{-1}, total N 0.3 g kg^{-1}, available K 85 mg kg^{-1}, available N 7.5 mg kg^{-1} and pH 6.7. To ensure that the nutrient supply was adequate for plant growth, soil was fertilized with basal nutrients at the following rates (mg per box): $Ca(NO_3)_2{\cdot}4H_2O$, 3374; K_2SO_4, 400; $MgSO_4{\cdot}7H_2O$, 130; Fe-EDTA, 17.56; $MnSO_4{\cdot}H_2O$, 20; $ZnSO_4{\cdot}7H_2O$, 30; $CuSO_4{\cdot}5H_2O$, 6; H_3BO_3, 2; and $Na_2MoO_4{\cdot}5H_2O$, 0.5.

Maize and soybean seeds were surface-sterilized in 30% v/v H_2O_2 for 20 min and washed with deionized water before planting. Before planting, all rhizo-boxes were irrigated through the irrigation holes. After 4 days of growth (when the plants

emerged from the soil), the rhizo-boxes were irrigated every day until harvest. The maize and soybean were grown from July 12 to August 20, 2017.

The experiment was conducted in a greenhouse at Sichuan Agricultural University, Chengdu (Latitude: 30°42′ N, Longitude: 103°51′ E). The height of the greenhouse was 6 m, and the top of the greenhouse was covered with thin and transparent plastic to prevent rainfall. Additionally, no plastic was vertically around the greenhouse to maintain the same air temperature inside to outside the greenhouse. The light intensity and air temperature are shown in **Figure 2**.

Plant Harvest and Measurements of Root Morphology

After 40 days of growth, the plants were harvested. Shoots were oven-dried at 105°C for 30 min and at 80°C for 3 days for assays of dry weight and concentrations of P, starch, and sucrose. In the heterogeneous P treatment, roots were separated to the P-rich zone and outside the P-rich zone. In the homogeneous P treatment, the entire root systems were removed from the rhizo-boxes. Roots were washed with deionized water, and then WinRHIZO (WinRHIZO Pro2004, Canada) was used to measure root length and root diameter. Fine roots were defined as roots with a diameter less than 2 mm (Jing et al., 2010). After the determination of root morphology, roots were oven-dried at 105°C for 30 min and at 80°C for 3 days for assays of dry weight and concentrations of P and sucrose.

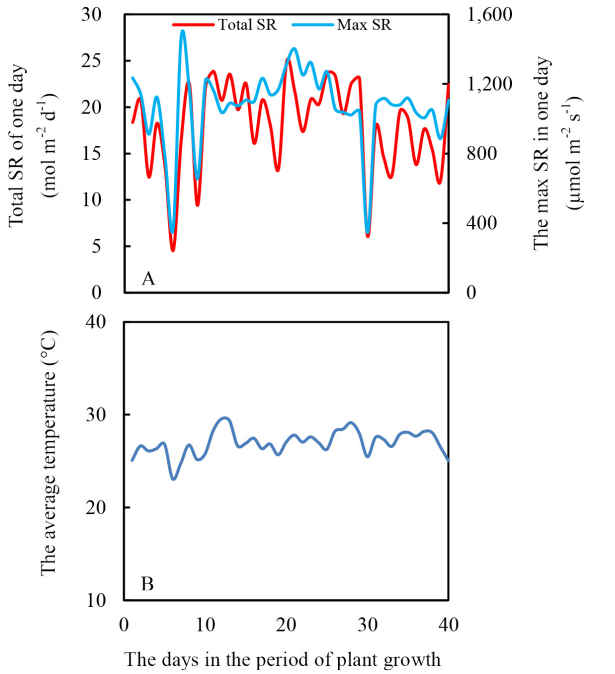

FIGURE 2 | Daily total solar radiation (SR) **(A)** and average air temperature **(B)** during soybean and maize growth period, from July 12th to August 20th in 2017.

Determination of Solar Radiation Interception Rate, Net Photosynthetic Rate, and Concentrations of P, Starch, and Sucrose

Solar radiation interception of plants was measured on all fully expanded leaves using OptoLeaf (Long-term measurement type, Japan) for a week (Kawamura et al., 2005). Net photosynthetic rate (Pn) was measured on the youngest fully expanded leaf using a Li6400 photosynthesis system (Li-COR, Lincoln, NE, United States). Measurements were performed between 10:00 a.m. and 12:00 p.m. on sunny days.

The P concentration in leaf, stem, and root was determined. The material was ground to pass through a 0.149-mm mesh sieve and a 0.3-g sample was wet-digested with concentrated H_2SO_4 and H_2O_2 (30%), and the P was determined by the vanadomolybdate method (Page, 1982).

The extracts of leaves and roots were analyzed after extraction in 80% ethanol (v/v). Sucrose concentration was measured directly in the extract, using resorcinol as the color reagent (Shi et al., 2016). The leaf sample residue after ethanol extraction was washed several times and used for starch analysis following the method of Setter et al. (1994).

Collection and Analysis of Rhizosphere Soil Carboxylates

The soil adhering to the roots was defined as rhizosphere soil. The rhizosphere soil carboxylates were collected following the method of Zhang et al. (2015). Specifically, following removal from the rhizo-boxes, roots were transferred to a tube containing 50 ml of 0.2 μM $CaCl_2$ and were gently shaken to dislodge the rhizosphere soil, followed by shaking for 5–10 s to create homogeneous suspensions. A 10 ml of the suspensions was freeze-dried at −80°C. Then the residue white powder was dissolved with 1 ml of deionized water for carboxylate analysis by high-performance liquid chromatography (HPLC). The HPLC analysis method was according to a previous report (Zhou et al., 2016). The static phase was a 250 × 4.6 mm C18 column (Hypsil, Dalian, China). The mobile phase was 0.5% KH_2PO_4 and 0.5 mM tetrabutylammonium hydrogen sulfate (pH 2.0) with a flow rate of 1 ml min^{-1} at 28°C, and the detection wavelength was 220 nm.

Statistical Analyses

Data from the three replicates were sorted by the Excel (Microsoft) software packages. Analysis of variance (ANOVA) was conducted using the 19.0 statistical software packages (SPSS Institute Inc., United States). Significant differences among means were separated according to LSD at the level of $p \leq 0.05$. Plant growth, Pn, and root length were subjected to one-way ANOVA to assess the effects of light interception and heterogeneous/homogeneous P supply in this study.

RESULTS

Plant Biomass and Root Development

The shoot dry weight of maize significantly increased under disrupted light conditions compared with continual light

conditions irrespective of P supply (**Figure 3A**). Root dry weight density of maize increased when the light intensity changed from continual to disrupted in plant supplied with sufficient P (in the P-rich zone), but was not affected by the light condition when the root was grown with low P supply (outside the P-rich zone) (**Figure 3C**).

The shoot dry weight (**Figure 3B**) and root dry weight density (**Figure 3D**) of soybean generally followed similar tendencies to that of maize in the light and P treatments. However, root dry weight density of soybean was only significantly enhanced under disrupted light in the P-rich zone (**Figure 3D**).

The root length density of maize in the P-rich zone in the heterogeneous treatment was not only higher than the outside the P-rich zone, but also higher than in the homogeneous P treatment (**Figure 4A**). Moreover, this increase was more pronounced under disrupted light condition. The fine roots percentage of maize significantly increased under the disrupted light condition irrespective of P supply, particularly in the P-rich zone (**Figure 4C**). In the P-rich zone, the specific root length of maize significantly enhanced under the disrupted light condition compared to continual light condition (**Figure 4E**).

The root length density (**Figure 4B**) of soybean generally followed similar tendencies to that of maize in the light and P treatments. The fine root percentage and specific root length of soybean significantly increased with exposure to disrupted light conditions as opposed to when light conditions were continual, irrespective of P supply (**Figures 4D,F**). Seemingly, P treatments had no impact on the fine root percentage and specific root length of soybean, with no significant differences noted between the homogeneous P treatment and heterogeneous P treatment (**Figures 4D,F**).

The Carboxylate Concentration in Rhizosphere Soil

The root of maize with adequate P supply exuded more malate and citrate than insufficient P supply (**Figures 5A,C**). Moreover, the malate concentrations, rather than the citrate concentrations, in the rhizosphere soil were elevated substantially under disrupted light condition (**Figures 5A,C**).

On the contrary, the root of soybean with a low P supply exuded more malate and citrate than adequate P supply (**Figures 5B,D**). Furthermore, the trend of rhizosphere soil carboxylates concentrations was reversed in soybean as compared to maize, subjected to the same conditions; i.e., under disrupted light conditions citrate levels increased substantially whereas malate concentrations remained constant (**Figures 5B,D**).

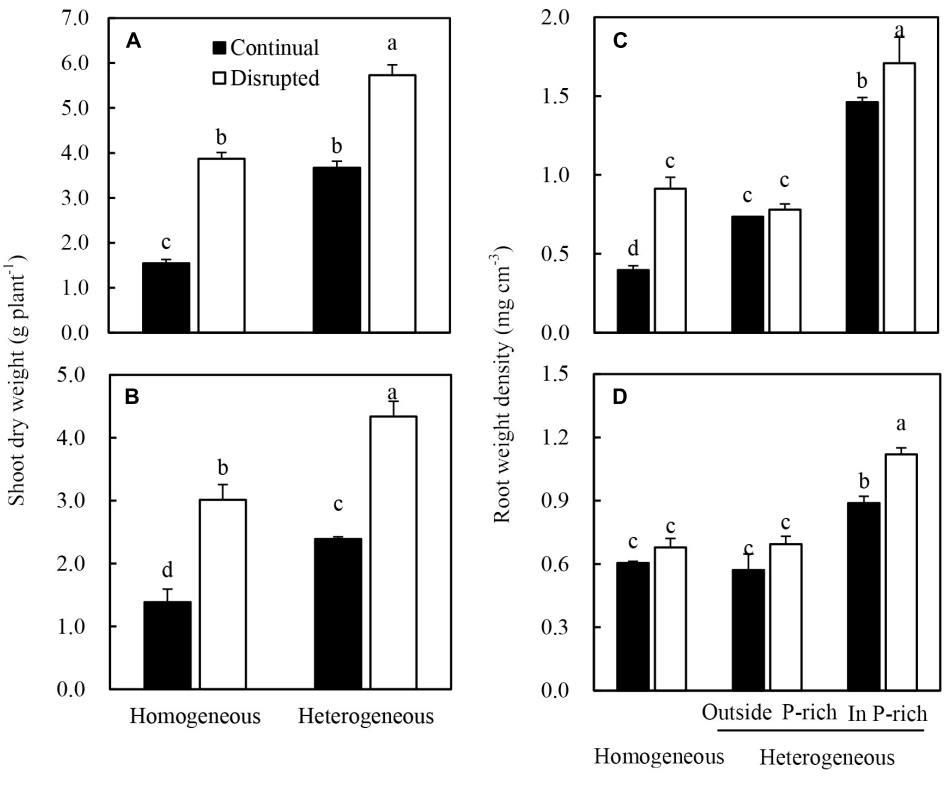

FIGURE 3 | Effect of continual vs. disrupted light condition and homogeneous vs. heterogeneous phosphorus (P) supply on plants shoot dry weight (**A**: maize, **B**: soybean), and on root weight density (**C**: maize, **D**: soybean). Plants were grown in rhizo-box at two P supply treatments (homogeneous = homogeneous P supply, heterogeneous = heterogeneous P supply) and two light conditions (continual = continual light condition, disrupted = disrupted light condition). Data are average of three replicates and bars represent standard errors. Data with different letters are significantly different ($p < 0.05$).

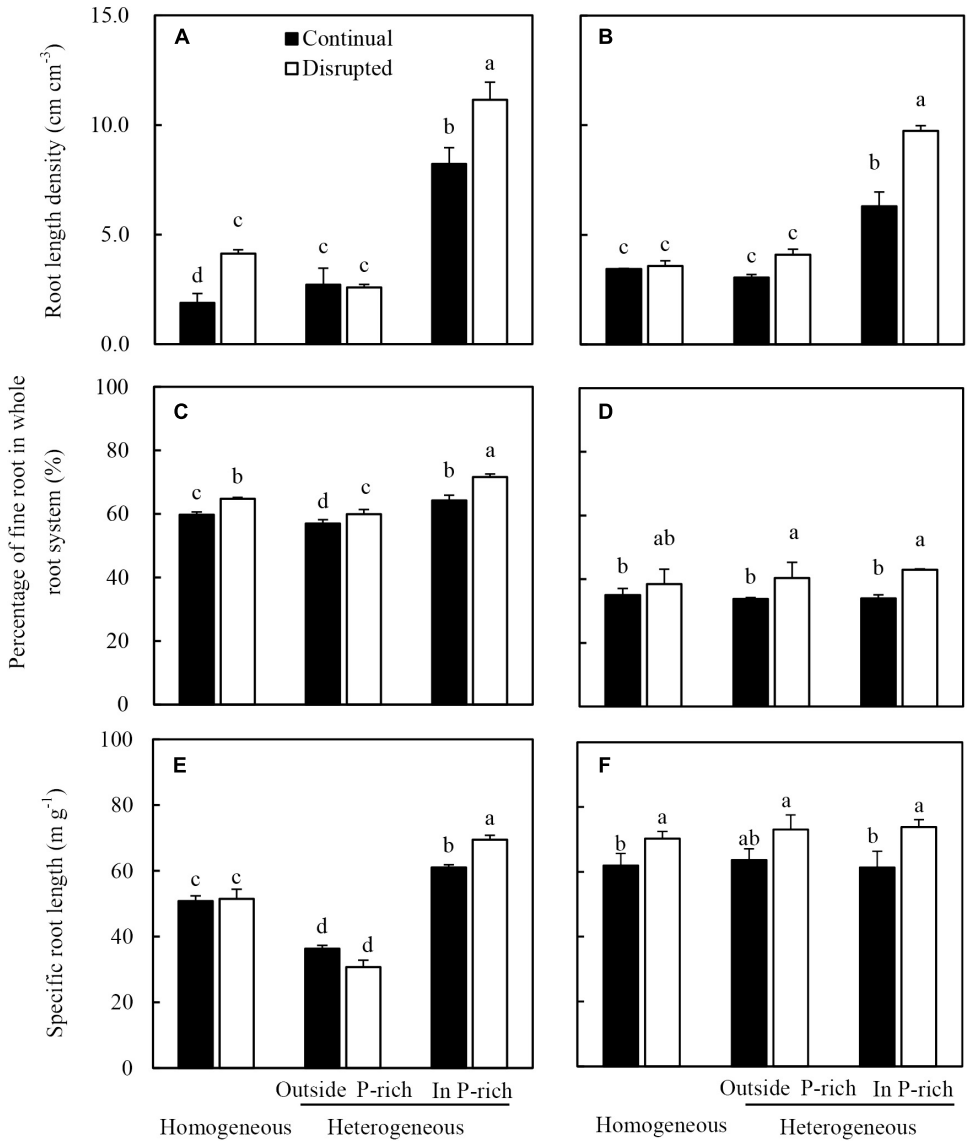

FIGURE 4 | Effect of continual vs disrupted light condition and homogeneous vs. heterogeneous phosphorus (P) supply on root length density (**A**: maize, **B**: soybean), on percentage of fine root in whole root system (**C**: maize, **D**: soybean), and on specific root length (**E**: maize, **F**: soybean). Plants were grown in rhizo-box at two P supply treatments (homogeneous = homogeneous P supply, heterogeneous = heterogeneous P supply) and two light conditions (continual = continual light condition, disrupted = disrupted light condition). Data are average of three replicates and bars represent standard errors. Data with different letters are significantly different ($p < 0.05$). Fine roots were defined as roots with a diameter less than 2 mm.

Additionally, the malate and citrate concentrations in the rhizosphere soil of soybean were 10-fold higher than those of maize, particularly in homogeneous P treatment (**Figures 5A,B**).

Shoot P Status and Root P Uptake Capacity

Maize in the heterogeneous P treatment showed higher leaf P concentration than the homogeneous P treatment (**Figure 6A**). In the heterogeneous P treatment, leaf P concentration of maize decreased under the disrupted light condition compared with the continual light condition. However, leaf P concentrations remained constant in the homogeneous P treatment, irrespective of light conditions (**Figure 6A**). The heterogeneous P treatment and disrupted light condition caused increased shoot P acquisition of maize (**Figure 6C**). The root P concentration of maize in the heterogeneous P treatment, particularly in the P-rich zone was greater than that in the homogeneous P treatment as well as outside the P-rich zone (**Figure 6E**). However, the disrupted light condition, with the exception of the homogeneous P treatment, markedly decreased the root P concentration of maize (**Figure 6E**).

The leaf P concentration (**Figure 6B**), shoot P acquisition (**Figure 6D**) and root P concentration (**Figure 6F**) of soybean

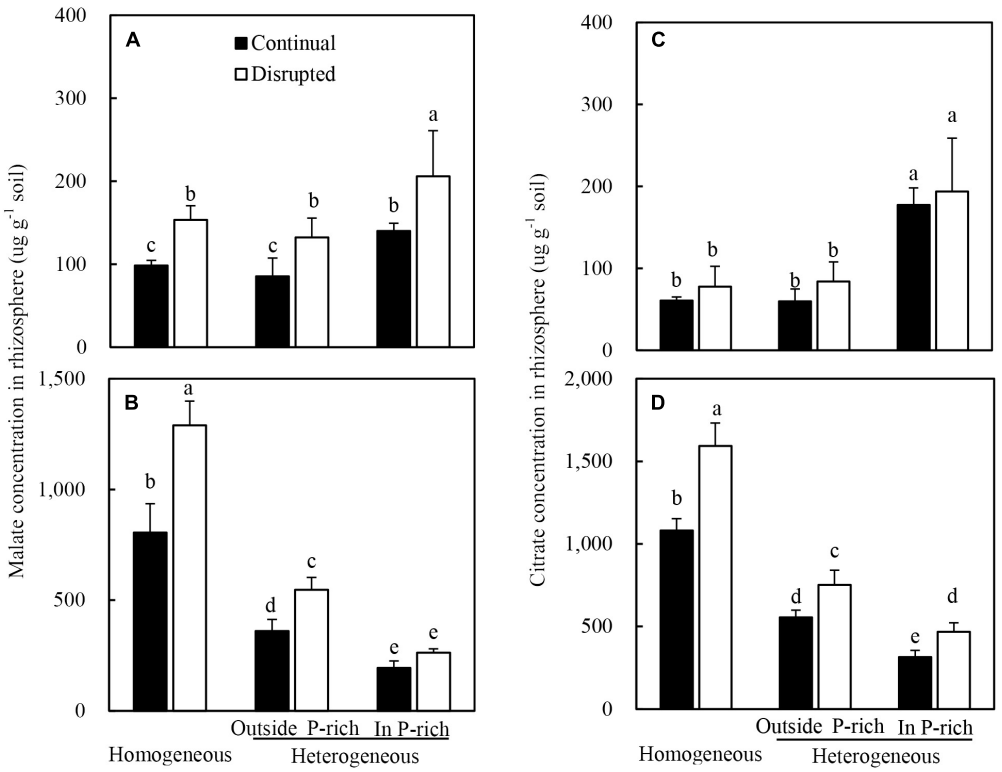

FIGURE 5 | Effect of continual vs disrupted light condition and homogeneous vs. heterogeneous phosphorus (P) supply on rhizosphere soil malate concentration (**A**: maize, **B**: soybean) and on rhizosphere soil citrate concentration (**C**: maize, **D**: soybean). Plants were grown in rhizo-box at two P supply treatments (homogeneous = homogeneous P supply, heterogeneous = heterogeneous P supply) and two light conditions (continual = continual light condition, disrupted = disrupted light condition). Data are average of three replicates and bars represent standard errors. Data with different letters are significantly different ($p < 0.05$).

generally followed similar tendencies as maize under the variable light and P treatments.

Photosynthetic Efficiency and Light Capture of Leaves

Heterogeneous P supply increased the leaf area of maize, consequently, the light interception of plants increased (**Figures 7A,C**). Net photosynthesis (Pn) of maize significantly increased under the disrupted light condition as opposed to continual light condition and also enhanced, particularly under heterogeneous P supply (**Figure 7E**). The increased Pn was correlated with optimized efficiency of light capture, especially under disrupted light conditions (**Figure 7C**).

The leaf area (**Figure 7A**), light interception (**Figure 7D**), and Pn (**Figure 7F**) of soybean generally followed similar tendencies as maize. However, the Pn was not enhanced by heterogeneous P treatment in disrupted light condition.

Carbohydrate Accumulation in Leaves and Roots

Leaf starch concentrations of maize under the continual light condition were higher than those under the disrupted light condition, whilst it decreased in the heterogeneous P treatment compared with homogeneous P treatment (**Figure 8A**). The sucrose concentrations in leaves and roots of maize increased under disrupted light conditions and were also affected by P treatments, with elevated levels under heterogeneous P supply (**Figures 8C,E**). Contrastingly, sucrose concentration in the root of maize in homogeneous P treatment was relatively higher than those of roots either outside or inside the P-rich zone in the heterogeneous P treatment (**Figure 8E**).

Similar trends were found for soybean leaf starch (**Figure 8B**), leaf sucrose (**Figure 8D**) and root sucrose concentration (**Figure 8F**) under the same light and P conditions.

Relationships Between Fine Root Percentage, Rhizosphere Soil Malate Concentration, and Phosphorus Concentration in Leaves, or Sucrose Concentration in Roots

The fine root percentage of maize did not positively correlate to root sucrose concentration (**Figure 9A**) but positively related to the leaf P concentration (**Figure 9C**). The malate concentration in the rhizosphere soil of maize was inversely related to the root sucrose concentration (**Figure 9A**) and positively related to the P concentration in leaf (**Figure 9C**).

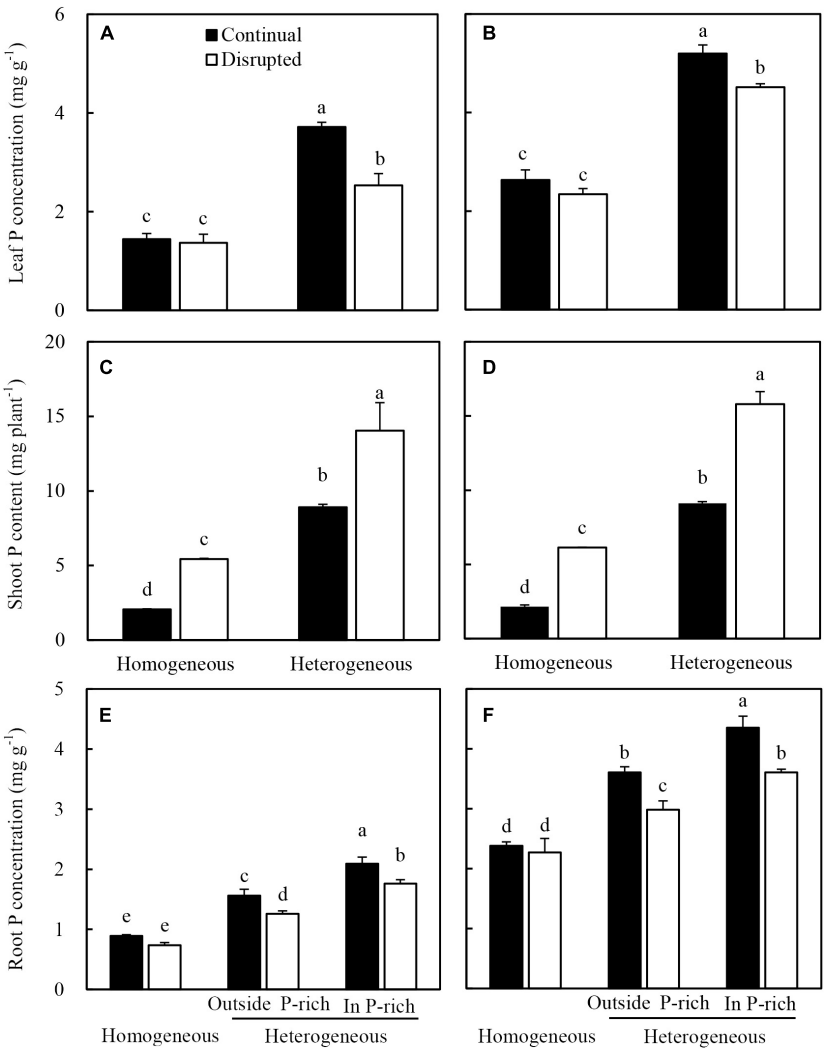

FIGURE 6 | Effect of continual vs. disrupted light condition and homogeneous vs. heterogeneous phosphorus (P) supply on leaf P concentration (**A**: maize, **B**: soybean), on shoot P content (**C**: maize, **D**: soybean), and on root P concentration (**E**: maize, **F**: soybean). Plants were grown in rhizo-box at two P supply treatments (homogeneous = homogeneous P supply, heterogeneous = heterogeneous P supply) and two light conditions (continual = continual light condition, disrupted = disrupted light condition). Data are average of three replicates and bars represent standard errors. Data with different letters are significantly different ($p < 0.05$).

The malate concentration in the rhizosphere soil of soybean was positively related to the root sucrose (**Figure 9B**) and inversely related to the leaf P concentration (**Figure 9D**). In addition, neither root sucrose (**Figure 9B**) nor leaf P concentration (**Figure 9D**) was correlated to the fine root percentage.

DISCUSSION

The Light Capture of Maize and Soybean Increased Under the Disrupted Light Condition

This study was conducted to investigate whether a change in planting pattern in a low light intensity area could increase light capture in leaves, which could possibly augment photosynthesis. In conjunction with how localized P supply could affect the concentration of P and sucrose in plant tissue which increased the P uptake capacity of maize and soybean by regulating root growth.

Wide-narrow row distance planting patterns are widely used by farmers in China. It is a typical system for the region with more than 2.8×10^7 ha of annual crops being intercropped in China (Li et al., 2007). Many studies reported that the increased light capture in border rows resulted in greater yields in strip intercropping than those in mono-cropping (Zhang et al., 2008, 2015; Zhu et al., 2016; Gou et al., 2017; Wang et al., 2017). The light capture of plants in maize/soybean relay strip intercropping was also higher than that of the corresponding mono-crops in southwest China with low solar

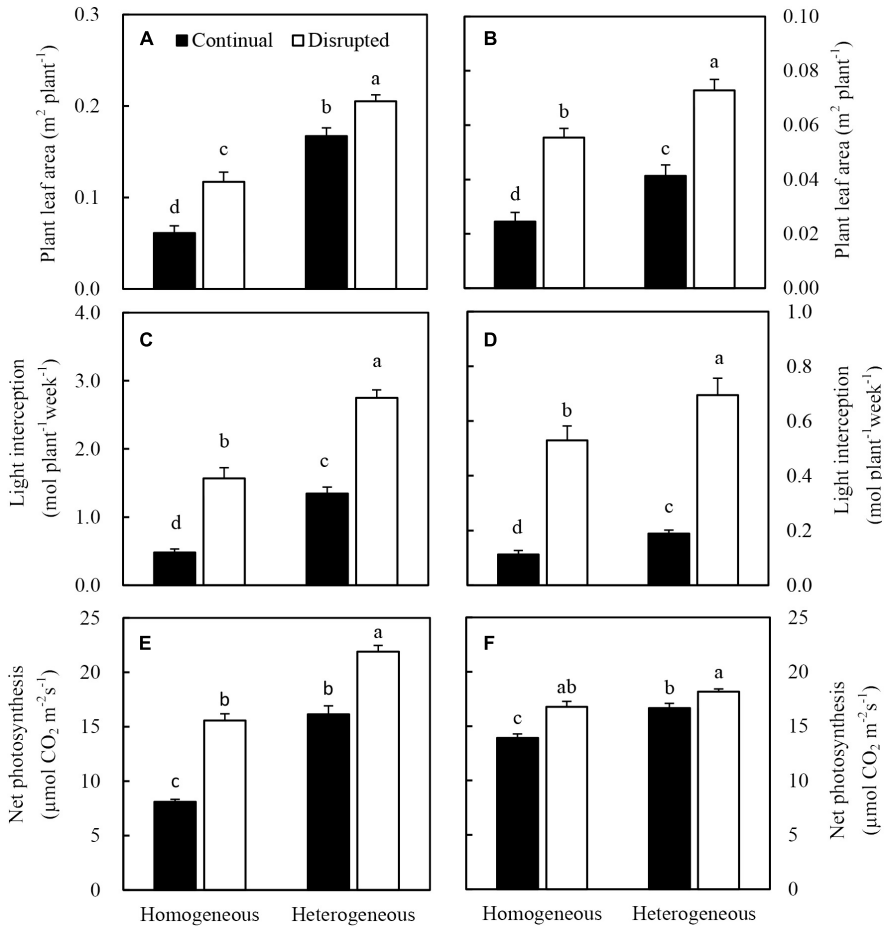

FIGURE 7 | Effect of continual vs disrupted light condition and homogeneous vs. heterogeneous phosphorus (P) supply on plant leaf area (**A**: maize, **B**: soybean), on light interception (**C**: maize, **D**: soybean), and on net photosynthesis rate (**E**: maize, **F**: soybean). Plants were grown in rhizo-box at two P supply treatments (homogeneous = homogeneous P supply, heterogeneous = heterogeneous P supply) and two light conditions (continual = continual light condition, disrupted = disrupted light condition). Data are average of three replicates and bars represent standard errors. Data with different letters are significantly different ($p < 0.05$).

radiation (Gao, 2015; Chen et al., 2016). The observations in this study that the light capture of maize and soybean under the disrupted light condition was higher than those under the continual light condition (**Figures 7C,D**) corroborated results from previous studies. Theoretically, crops in wide-narrow row distance planting patterns obtain a low amount of light capture because half of the leaves on the narrow side are normally shaded by neighboring plants. However, plants showed high phenotypic plasticity to complement light capture in plant mixtures. In a maize/wheat intercropping system, light capture was 23% higher in the maize/wheat system than that of the observed value for monocultures, with 64% of the increase attributable to phenotypic plasticity (Zhu et al., 2015). In the present study, soybean showed high phenotypic plasticity, such as leaves aggregated on one side of non-adjacent plants under the disrupted light condition scenario (**Supplementary Figure S2B**), which might has contributed much to the improved light capture by this crop. Additionally, leaf numbers, single leaf area, and, consequently, total leaf area increased also contributed to the improved light capture under disrupted light condition (**Supplementary Figures S3A–D** and **Figures 7A,B**). Low light and low P aggravated senescence of leaves situated lower down on the main stem, which resulted in a decrease in leaf numbers and area (Lim et al., 2007; Sakuraba et al., 2014) (**Supplementary Figures S1D**, **S2A,C,D**). These results provided evidence in favor of the hypothesis that changes in the planting pattern of maize and soybean from equal-width row distance to narrow-width row distance resulted in improving light capture of crops in low light intensity areas.

Root Morphological Responds to Localized Soil P Supply and Light Condition

To capture more nutrients, root morphological of many species exhibited high plasticity to the localized supply of nutrients (Bilbrough and Caldwell, 1995; Hodge et al., 2000; He et al., 2003; Li H.B. et al., 2014). This also held true for maize in this study,

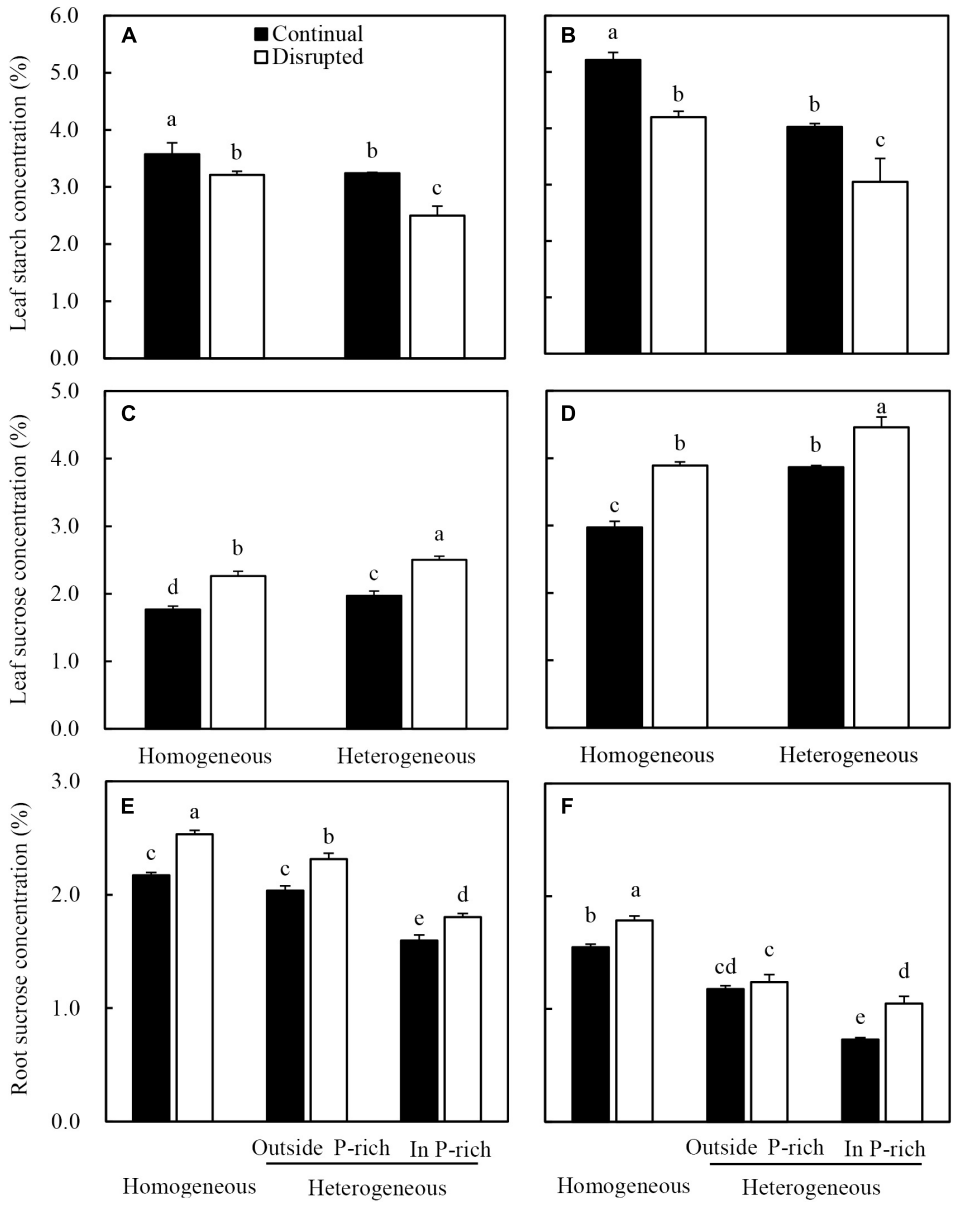

FIGURE 8 | Effect of continual vs. disrupted light condition and homogeneous vs. heterogeneous phosphorus (P) supply on leaf starch concentration (**A**: maize, **B**: soybean), on leaf sucrose concentration (**C**: maize, **D**: soybean), and on root sucrose concentration (**E**: maize, **F**: soybean). Plants were grown in rhizo-box at two P supply treatments (homogeneous = homogeneous P supply, heterogeneous = heterogeneous P supply) and two light conditions (continual = continual light condition, disrupted = disrupted light condition). Data are average of three replicates and bars represent standard errors. Data with different letters are significantly different ($p < 0.05$).

where, heterogeneous supply of P induced root proliferation in the P-rich zone and increased plant P acquisition (Jing et al., 2012; Li et al., 2012; Ma et al., 2013; Zhang et al., 2015). The data reported here were consistent with the observations that P uptake, root length density, and consequently, root dry weight density of maize and soybean increased in the P-rich zone with localized P supply (**Figures 3C,D**, **4A,B**, and **Supplementary Figure S4**). However, the mechanisms of P-dependent changes in root proliferation in response to local P supply were not fully understood (Hodge, 2004; Shen et al., 2011). Generally, root growth was initiated by the signal of low leaf P and high root sucrose concentration (Shane et al., 2003; Hill et al., 2006; Teng et al., 2013). In the present study, the increasing leaf light interception augmented the response of maize and soybean root to the heterogeneous P supply. In heterogeneous P treatment, increased light capture decreased the leaf P concentration of maize and soybean (**Figures 6A,B**), which might be due to increased photosynthesis and shoot growth rate exceeding the P supply ability of roots to leaf, such as high net Pn and sucrose concentration in leaves under disrupted light condition

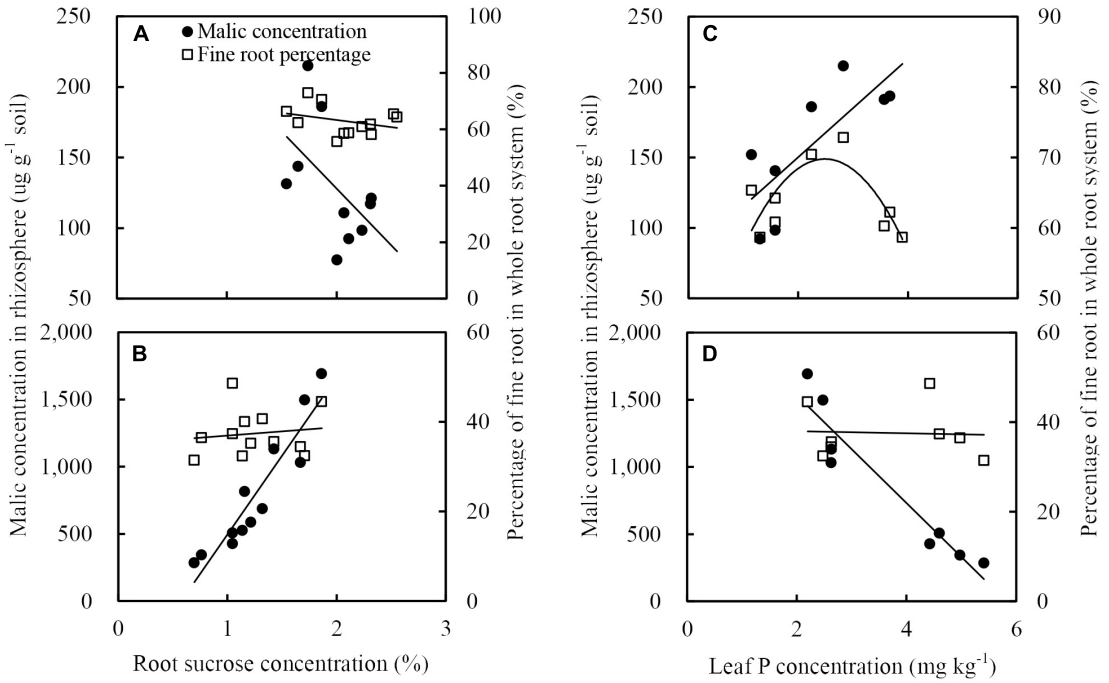

FIGURE 9 | Relationships between soil malate concentration in rhizosphere (black circles) and fine root percentage (open squares), and sucrose concentration in roots (**A**: maize, **B**: soybean), or phosphorus concentration in leaves (**C**: maize, **D**: soybean). There was only showed the relationships between malate concentration in the rhziosphere and sucrose eoncentration in roots, or phosphorus concentration in leaves, because the citrate concentration in rhizosphere soil generally followed similar tendencies to malate.

(**Figures 7A,B**, **8C,D**). Moreover, the root dry weight density and root length density of maize and soybean enhanced under disrupted light condition (**Figures 3C,D**, **4A,B**). Thus, high light may cause growth-induced P starvation in the shoot that produces a systemic signal to induce root growth. These results are consistent with the previous studies on rice and lupine with high light intensity, which induced root growth (Wissuwa et al., 2005; Cheng et al., 2014). In addition, the leaf P concentrations of maize and soybean in homogeneous P treatment were twofold lower than in heterogeneous P treatment (**Figures 6A,B**), but root growth was severely inhibited under homogeneous P supply (**Figures 3C,D**). One possible explanation may be that plant leaf growth under P-deficiency decreased significantly and, subsequently inhibited root growth (Mollier and Pellerin, 1999; Plénet et al., 2000). Therefore, these results provided evidence that favored hypothesis i. In the heterogeneous P treatment, maize and soybean roots presented more sucrose under disrupted light, compared with continual light, resulting relatively great root weight density and root length density (**Figures 3C,D**, **4A,B**). The same results reported previously that the proliferation of roots followed the stimulation of carbohydrate allocation to roots (Watt and Evans, 1999; Hammond and White, 2008; Postma et al., 2014). The sucrose concentrations of maize and soybean roots in the homogeneous P treatment were higher than those in the P-rich zone in heterogeneous P treatment, but the root growth was severely inhibited compared to in the enriched P patch (**Figures 3C,D**, **4A,B**), which might provide evidence to reject hypothesis B. One possible explanation might be that reductions of root growth under P deficiency were not caused by source limitations but were more due to the direct negative effect of low P availability (Wissuwa et al., 2005). The results of root P concentration in the homogeneous and heterogeneous P treatments here were consistent with this view (**Figures 6E,F**).

Furthermore, the localized P supply inducing root proliferation was not only regulated by the signal of leaf P but also root sucrose concentration. Such as in the root-split plants in heterogeneous P treatment, the root growth outside the P-rich zone was lower than the P-rich zone (**Figures 3C,D**, **4A,B**), although the root outside the P-rich zone showed higher sucrose concentration (**Figures 8E,F**). The root proliferation in a nutrient patch depended on the relative concentration of nutrients as it pertains to the rhizosphere vs. bulk soil (Hodge, 2004; Shen et al., 2005; Giehl et al., 2013), and which may also responsive to phytohormone synthesis and transport. For example, ethylene is known to be involved in the regulation of decreasing root gravitropic response under P limitation to increase root proliferation in the P-rich zone (Bonser et al., 1996; Lynch and Brown, 2008). Furthermore, the basipetal flow of auxin was regulated by light intensity which facilitates the root proliferation in P -rich patches (Bhalerao et al., 2002; Costigan et al., 2011).

Localized P supply only increased the fine root percentage and specific root length of maize rather than soybean. Previous studies reported that a localized nutrient (P and nitrogen) supply increased the production of maize fine roots (diameter <0.2 mm) (Jing et al., 2010; Li H.B. et al., 2014; Wen et al., 2017). Root

morphology in response to heterogeneous nutrient supply was influenced by the root diameter. Therefore, fine-rooted species are more responsive to nutrient-rich patches than species with coarse roots (Fitter, 1994; Hodge, 2004). Because plants with fine roots have high specific root length per unit carbon, the metabolic demand per unit of root length in the root system decreased, and therefore, soil P exploration and acquisition increased at a minimal energy cost (Lambers et al., 2006; Zobel et al., 2007; Pang et al., 2009; Lynch, 2015). In this study, most maize roots had a diameter less than 0.2 mm, whereas the root diameter of soybean was more than 0.2 mm, indicating that maize had finer roots than soybean (**Figures 4C,D**). Thus, maize rather than soybean, responded to localized P supply by altering the root architecture for a better interception, as previously reported by Lyu et al. (2016). Similar results also showed that species of Graminaceae (maize and wheat), but not species of Leguminosae (faba bean and chickpea), responded to localized P supply by altering the root architecture for better interception (Li H.B. et al., 2014). A positive relationship was observed between leaf P concentration and fine root percentage of maize, which agreed with the view of the production of fine root in maize affected by leaf P concentration (**Figure 9C**) (Wen et al., 2017). However, the fine root percentage of soybean did not significantly respond to root sucrose (**Figure 9B**) and leaf P concentration (**Figure 9D**), which might be ascribed to soybean response to soil P condition by altering root physiology rather than root morphology (Lyu et al., 2016).

Root Physiological Responds to Light Condition and Localized Soil P Supply

More light capture increased malate and citrate concentration in the rhizosphere of maize and soybean, even under localized P application condition (**Figure 5**). This was consistent with the results obtained in white lupin under high light intensity (Cheng et al., 2014). In this experiment, root sucrose concentration under disrupted light conditions was much higher than continual light conditions, whilst the malate concentration in soybean and maize rhizosphere was positively responded to root sucrose (**Figures 9A,B**). These observations were consistent with the results that root sucrose concentration regulated malate and citrate exudation of maize and soybean, and give credence to findings from a previous study pertaining to citrate exudation of white lupin (Cheng et al., 2014). Other systemic signals could also contribute to the exudation of carboxylates instead of the high light intensity increased carboxylate exudation by translocation of sucrose to roots. This may include low leaf P concentration, which has been found to stimulate root carboxylate exudation (Shen et al., 2005; Li et al., 2008).

However, in this study low leaf P concentration did not stimulate carboxylate exudation in maize root, as reported previously that the increased carboxylate exudation in the rhizosphere of maize was induced by high leaf P concentration (Corrales et al., 2007; Zhang et al., 2015; Liu et al., 2016; Lyu et al., 2016). Localized P supply coincided with increases in the malate and citrate concentrations in the rhizosphere of maize, since external P supply increased the P in leaves (**Figures 5A,C**). This was in agreement with another report on the same species (Wen et al., 2017). Maize showed opposite root carboxylate exudation tendencies to Leguminoseae species regulated by leaf P status (Li H.B. et al., 2014; Lyu et al., 2016). One possible explanation might be that maize responded to P-insufficiency by altering root morphology rather than increasing root exudation, because fibrous roots (e.g., maize) respond to variable P supply through expanding the root surface area to increase the absorption of available P spatially (Lyu et al., 2016; Wen et al., 2017). The carboxylate exudation of maize was markedly lower than that of Leguminoseae species (Pearse et al., 2006, 2007; Rose et al., 2010; Li L. et al., 2014), which provided additional evidence to support that maize responds to P starvation by changing root morphology rather than root physiology.

P deficiency in leaves significantly stimulated the malate and citrate exudation in the rhizosphere of soybean in homogeneous P treatment. In contrast to maize, localized P supply significantly increased the P concentration of leaves and decreased the carboxylate concentration in the rhizosphere of soybean seedlings (**Figure 5B,D**). In addition, a negative relationship was observed between leaf P concentration and malate concentration in the rhizosphere (**Figure 9D**). These results suggested an important influence of localized P supply on soybean root malate and citrate exudation by affecting the leaf P status, which was in agreement with lupin under localized P supply experiment (Shen et al., 2005). It also corresponded well with the observations that leaf P regulated root carboxylate exudation in Leguminoseae species (e.g., faba bean: Li L. et al., 2014, Zhang et al., 2015; white lupine and chickpea: Li L. et al., 2014; Lyu et al., 2016). However, malate and citrate concentration in the outside P-rich zone was higher than in the P-rich zone, which coincided with the observation that the root P outside the enriched P-patch part was lower than in the P-rich zone (**Figure 6F**), indicating a clear effect of the localized P supply on carboxylate exudation.

CONCLUSION

Our results demonstrated that the light capture of maize and soybean under disrupted light conditions were higher than those under continual light conditions in a low solar radiation area. It means that altering planting patterns of crops from equal-width row distance to narrow-width row distance is a useful management strategy to facilitate better light interception, particularly under suboptimal light conditions in low solar radiation areas. The increasing light interception and localized P supply increased maize root proliferation, root morphological plasticity (high fine root percentage, high specific root length) and P uptake capacity. The increased light interception and localized P supply also promoted soybean root growth, but the P supply treatment did not affect the root morphology. However, for soybean, the increased light interception enhanced malate and citrate exudation, which were also induced by concomitant P deficient conditions. The light and P are possibly integrated by maize and soybean through both the P and sucrose concentrations in leaves and roots to determine plant growth.

This study provided new insights into the P uptake capacity of maize and soybean in the "wide-narrow row distance planting pattern," which are important for increasing crop productivity and P fertilizer use efficiency through optimizing planting patterns and soil P supply strategies in low solar radiation areas.

AUTHOR CONTRIBUTIONS

TZ, LW, WL, and WY carried out the design of this research work and writing this manuscript. TZ, LW, and YD carried out the plant cultivation, chemical analysis and statistical analysis of this work. LZ, YG, and SL participated in experiment management.

ACKNOWLEDGMENTS

This work was supported by the National Key Research and Development Program of China (2016YFD0300109-3) and National Natural Science Foundation of China (31771728 and 31671626).

SUPPLEMENTARY MATERIAL

The Supplementary Material for this article can be found online at: https://www.frontiersin.org/articles/10.3389/fpls.2019.00183/full#supplementary-material

FIGURE S1 | The picture showed "wide-narrow row distance planting patterns" of maize **(A)** and soybean **(B)** in the field under low solar radiation area of southwest of China. The picture of **(D)** showed the down leaves of soybean were dropped because of low light interception in continual light condition, but the leaves of soybean keep a longer green period in disrupted light condition **(C)**. The picture of **(E)** showed the soybean was harvested in disrupted light condition (left) and in continual light condition (right).

FIGURE S2 | The picture showed maize **(A)** and soybean **(B)** in continual vs. disrupted light condition and homogeneous vs. heterogeneous phosphorus (P) supply treatment. The soybean showed high phenotypic plasticity **(C,D)**. HomC, homogeneous P supply and continual light condition. HomD, homogeneous P supply and disrupted light condition. HetC, heterogeneous P supply and continual light condition. HetD, heterogeneous P supply and disrupted light condition.

FIGURE S3 | Effect of continual vs. disrupted light condition and homogeneous vs. heterogeneous phosphorus (P) supply on the number of leaves (**A**: maize, **B**: soybean), and on single leaf area (**C**: maize, **D**: soybean). Plants were grown in rhizo-box at two P supply treatments (homogeneous = homogeneous P supply, heterogeneous = heterogeneous P supply) and two light conditions (continual = continual light condition, disrupted = disrupted light condition). Data are average of three replicates and bars represent standard errors. Data with different letters are significantly different ($p < 0.05$).

FIGURE S4 | Effect of continual vs. disrupted light condition and homogeneous vs. heterogeneous phosphorus (P) supply on root P content (**A**: maize, **B**: soybean). Plants were grown in rhizo-box at two P supply treatments (homogeneous = homogeneous P supply, heterogeneous = heterogeneous P supply) and two light conditions (continual = continual light condition, disrupted = disrupted light condition). Data are average of three replicates and bars represent standard errors. Data with different letters are significantly different ($p < 0.05$).

REFERENCES

Bhalerao, R. P., Eklof, J., Ljung, K., Marchant, A., Bennett, M., and Sandberg, G. (2002). Shoot-derived auxin is essential for early lateral root emergence in Arabidopsis seedlings. *Plant J.* 29, 325–332. doi: 10.1046/j.0960-7412.2001.01217.x

Bilbrough, C. J., and Caldwell, M. M. (1995). The effects of shading and N status on root proliferation in nutrient patches by the perennial grass *Agropyron desertorum* in the field. *Oecologia* 103, 10–16. doi: 10.1007/BF00328419

Bonser, A. M., Lynch, J., and Snapp, S. (1996). Effect of phosphorus deficiency on growth angle of basal roots in Phaseolus vulgaris. *New Phytol.* 132, 281–288. doi: 10.1111/j.1469-8137.1996.tb01847.x

Chen, G. P., Wang, X. C., Pu, T., Zeng, H., Chen, C., Peng, W., et al. (2016). Relationship of field microclimate and population yield in maize-soybean relay strip intercropping system. *Acta Agr. Zhejiangensis.* 28, 1812–1821. doi: 10.3969/j.issn.1004-1524.2016.11.02

Cheng, L. Y., Liu, X. Y., Vance, C. P., White, P. J., Zhang, F. S., and Shen, J. B. (2014). Interactions between light intensity and phosphorus nutrition affect the phosphate-mining capacity of white lupin (*Lupinus albus L.*). *J. Exp. Bot.* 65, 2995–3003. doi: 10.1093/jxb/eru135

Corrales, I., Amenos, M., Poschenrieder, C., and Barcelo, J. (2007). Phosphorus efficiency and root exudates in two contrasting tropical maize varieties. *J. Plant Nutr.* 30, 887–900. doi: 10.1080/15226510701375085

Costigan, S. E., Warnasooriya, S. N., Humphries, B. A., and Montgomery, B. L. (2011). Root-localized phytochrome chromophore synthesis is required for photoregulation of root elongation and impacts root sensitivity to jasmonic acid in *Arabidopsis thaliana*. *Plant Physiol.* 157, 1138–1150. doi: 10.1104/pp.111.184689

Fernandez, M. C., and Rubio, G. (2015). Root morphological traits related to phosphorus-uptake efficiency of soybean, sunflower, and maize. *J. Plant Nutr. Soil Sci.* 178, 807–815. doi: 10.1002/jpln.201500155

Fitter, A. H. (1994). "Architecture and biomass allocation as components of the plastic response of root systems to soil heterogeneity," in *Exploitation of Environmental Heterogeneity by Plants*, eds M. J. Hutchings, E. A. John, and A. J. A. Stewart (San Diego, CA: Academic Press), 305–322.

Gao, R. C. (2015). *Study on the Effect of Field Configuration on Light Environment, Light Utilization and Yield in Maize-Soybean Relay Strip Intercropping*. China: Sichuan Agricultural University.

Giehl, R. F. H., Gruber, B. D., and von Wirén, N. (2013). It's time to make changes: modulation of root system architecture by nutrient signals. *J. Exp. Bot.* 65, 769–778. doi: 10.1093/jxb/ert421

Gommers, C. M. M., Visser, E. J. W., St Onge, K. R., Voesenek, L. A. C. J., and Pierik, R. (2013). Shade tolerance: when growing tall is not an option. *Trends Plant Sci.* 18, 65–71. doi: 10.1016/j.tplants.2012.09.008

Gou, F., van Ittersum, M. K., Simon, E., Leffelaar, P. A., van der Putten, P. E. L., Zhang, L., et al. (2017). Intercropping wheat and maize increases total radiation interception and wheat RUE but lowers maize RUE. *Eur. J. Agron.* 84, 125–139. doi: 10.1016/j.eja.2016.10.014

Gundel, P. E., Plerik, R., Mommer, L., and Ballaré, C. L. (2014). Competing neighbors: light perception and root function. *Oecologia* 176, 1–10. doi: 10.2307/24037030

Hammond, J. P., and White, P. J. (2008). Sucrose transport in the phloem: integrating root responses to phosphorus starvation. *J. Exp. Bot.* 59, 93–109. doi: 10.1093/jxb/erm221

He, Y., Liao, H., and Yan, X. L. (2003). Localized supply of phosphorus induces root morphological and architectural changes of rice in split and stratified soil cultures. *Plant Soil* 248, 247–256. doi: 10.1023/A:1022351203545

Hill, J. O., Simpson, R. J., Moore, A. D., and Chapman, D. F. (2006). Morphology and response of roots of pasture species to phosphorus and nitrogen nutrition. *Plant Soil* 286, 1–2. doi: 10.1007/s11104-006-0014-3

Hinsinger, P. (2001). Bioavailability of soil inorganic P in the rhizosphere as affected by root-induced chemical changes: a review. *Plant Soil* 237, 173–195. doi: 10.1023/A:1013351617532

Hodge, A. (2004). The plastic plant: root responses to heterogeneous supplies of nutrients. *New Phytol.* 162, 9–24. doi: 10.1111/j.1469-8137.2004.01015.x

Hodge, A., Stewart, J., Robinson, D., Griffiths, B. S., and Fitter, A. H. (2000). Spatial and physical heterogeneity of N supply from soil does not influence N capture by two grass species. *Funct. Ecol.* 14, 645–653. doi: 10.1046/j.1365-2435.2000.t01-1-00470.x

Jackson, R. B., Manwaring, J. H., and Caldwell, M. M. (1990). Rapid physiological adjustment of roots to localized soil enrichment. *Nature* 344, 58–60. doi: 10.1038/344058a0

Jing, J., Rui, Y., Zhang, F., Rengel, Z., and Shen, J. (2010). Localized application of phosphorus and ammonium improves growth of maize seeding by stimulating root proliferation and rhizosphere acidification. *Field Crop Res.* 119, 355–364. doi: 10.1016/j.fcr.2010.08.005

Jing, J., Zhang, F., Rengel, Z., and Shen, J. (2012). Localized fertilization with P plus N elicits an ammonium-dependent enhancement of maize root growth and nutrient uptake. *Field Crop Res.* 133, 176–185. doi: 10.1016/j.fcr.2012.04.009

Johnston, A. E., Poulton, P. R., Fixen, P. E., and Curtin, D. (2014). Phosphorus: its efficient use in agriculture. *Adv. Agron.* 123, 177–228. doi: 10.1016/B978-0-12-420225-2.00005-4

Kawamura, K., Cho, M., and Takeda, H. (2005). The applicability of a color acetate film for estimating photosynthetic photon flux density in a forest understory. *J. Forest Res.* 10, 247–249. doi: 10.1007/s10310-004-0141-8

Lambers, H., Shane, M. W., Cramer, M. D., Pearse, S. J., and Veneklaas, E. J. (2006). Root structure and functioning for efficient acquisition of phosphorus: matching morphological and physiological traits. *Ann. Bot.* 98, 693–713. doi: 10.1093/aob/mcl114

Li, H. B., Ma, Q. H., Li, H. G., Zhang, F. S., Rengel, Z., and Shen, J. B. (2014). Root morphological responses to localized nutrient supply differ among crop species with contrasting root traits. *Plant Soil* 376, 151–163. doi: 10.1007/s11104-013-1965-9

Li, L., Tilman, D., Lambers, H., and Zhang, F. S. (2014). Plant Diversity and overyielding : insights from belowground facilitation of intercropping in agriculture. *New Phytol.* 203, 63–69. doi: 10.1111/nph.12778

Li, H. B., Zhang, F. S., and Shen, J. B. (2012). Contribution of root proliferation in nutrient-rich soil patch to nutrient uptake and growth of maize. *Pedosphere* 22, 776–784. doi: 10.1016/S1002-0160(12)60063-0

Li, H. G., Shen, J. B., Zhang, F. S., Tang, C. X., and Lambers, H. (2008). Is there a critical level of shoot phosphorus concentration for cluster-root formation in *Lupinus albus*? *Funct. Plant Bio.* 35, 328–336. doi: 10.1071/FP07222

Li, L., Li, S. M., Sun, J. H., Zhou, L. L., Bao, X. G., Zhang, H. G., et al. (2007). Diversity enhances agricultural productivity via rhizosphere phosphorus facilitation on phosphorus-deficient soils. *PNAS* 104, 11192–11196. doi: 10.1073/pnas.0704591104

Li, Y., Niu, S., and Yu, G. (2016). Aggravated phosphorus limitation on biomass production under increasing nitrogen loading: ameta-analysis. *Glob. Chang. Biol.* 22, 934–943. doi: 10.1111/gcb.13125

Li, H. B., Wang, X., Rengel, Z., Ma, Q. H., Zhang, F. S., and Shen, J. B. (2016). Root over-production in heterogeneous nutrient environment has no negative effects on Zea mays shoot growth in the field. *Plant Soil* 409, 405–417. doi: 10.1007/s11104-016-2963-5

Lim, P. O., Kim, H. J., and Gil Nam, H. (2007). Leaf senescence. *Annu. Rev. Plant Biol.* 58, 115–136. doi: 10.1146/annurev.arplant.57.032905.105316

Liu, H., White, P. J., and Li, C. (2016). Biomass partitioning and rhizosphere responses of maize and faba bean to phosphorus deficiency. *Crop Pasture Sci.* 67, 847–856.

Liu, T. D., and Song, F. B. (2012). Maize photosynthesis and microclimate within the canopies at grain-filling stage in response to narrow-wide row planting patterns. *Photosynthetica* 50, 215–222. doi: 10.1007/s11099-012-0011-0

Lynch, J. P. (2015). Root phenes that reduce the metabolic costs of soil exploration: opportunities for 21st century agriculture. *Plant Cell Environ.* 38, 1775–1784. doi: 10.1111/pce.12451

Lynch, J. P., and Brown, K. M. (2008). "Root strategies for phosphorus acquisition," in *The Ecophysiology of Plant-Phosphorus Interactions*, ed. J. P. Hammond (Dordrecht: Springer), 83–116.

Lyu, Y., Tang, H., Li, H., Zhang, F., Rengel, Z., Whalley, W. R., et al. (2016). Major crop species show differential continual between root morphological and physiological responses to variable phosphorus supply. *Front. Plant Sci.* 7:1939.

Ma, Q. H., Zhang, F. S., Rengel, Z., and Shen, J. B. (2013). Localized application of NH4+-N plus P at the seedling and later growth stages enhances nutrient uptake and maize yield by inducing lateral root proliferation. *Plant Soil* 372, 65–80. doi: 10.1007/s11104-013-1735-8

Mollier, A., and Pellerin, S. (1999). Maize root system growth and development as influenced by phosphorus deficiency. *J. Exp. Bot.* 50, 487–497. doi: 10.1093/jxb/50.333.487

Page, A. L. (1982). *Methods of Soil Analysis (Part 2), 2nd Edn*. Madison: American Society of Agronomy.

Pang, J., Ryan, M. H., Tibbett, M., Cawthray, G. R., Siddique, K. H. M., Bolland, M. D. A., et al. (2009). Variation in morphological and physiological parameters in herbaceous perennial legumes in response to phosphorus supply. *Plant Soil* 331, 241–255. doi: 10.1007/s11104-009-0249-x

Pearse, S. J., Veneklaas, E. J., Cawthray, G., Bolland, M. D., and Lambers, H. (2006). Triticum aestivum Shows a greater biomass response to a supply of aluminium phosphate than Lupinus albus, despite releasing fewer carboxylates into the rhizosphere. *New Phytol.* 169, 515–524. doi: 10.1111/j.1469-8137.2005.01614.x

Pearse, S. J., Veneklaas, E. J., Cawthray, G., Bolland, M. D., and Lambers, H. (2007). Carboxylate composition of root exudates does not relate consistently to a crop species' ability to use phosphorus from aluminium, iron or calcium phosphate sources. *New Phytol.* 173, 181–190. doi: 10.1111/j.1469-8137.2006.01897.x

Plénet, D., Etchebest, S., Mollier, A., and Pellerin, S. (2000). Growth analysis of maize field crops under phosphorus deficiency. *Plant Soil* 223, 119–132. doi: 10.1007/s00122-018-3108-4

Postma, J. A., Dathe, A., and Lynch, J. P. (2014). The optimal lateral root branching density for maize depends on nitrogen and phosphorus availability. *Plant Physiol.* 166, 590–602. doi: 10.1104/pp.113.233916

Rengel, Z., and Marschner, P. (2005). Nutrient availability and management in the rhizosphere: exploiting genotypic differences. *New Phytol.* 168, 305–312. doi: 10.1111/j.1469-8137.2005.01558.x

Rose, T. J., Hardiputra, B., and Rengel, Z. (2010). Wheat, canola and grain legume access to soil phosphorus fractions differs in soils with contrasting phosphorus dynamics. *Plant Soil* 326, 159–170. doi: 10.1007/s11104-009-9990-4

Sakuraba, Y., Jeong, J., Kang, M. Y., Kim, J. H., Paek, N. C., and Choi, G. (2014). Phytochrome-interacting transcription factors PIF4 and PIF5 induce leaf senescence in Arabidopsis. *Nat. Commun.* 5:4636. doi: 10.1038/ncomms5636

Samuel, J. W., and Matthew, W. F. (2004). Shade limited root mass and carbohydrate reserves of the federally endangered. *Nat. Plants J.* 5, 27–33. doi: 10.2979/NPJ.2004.5.1.27

Setter, T. L., Ella, E. S., and Valdez, A. P. (1994). Relationship between coleoptile elongation and alcoholic fermentation in rice exposed to anoxia. II. Cultivar differences. *Ann. Bot.* 74, 273–279. doi: 10.1006/anbo.1994.1117

Shane, M. W., De Vos, M., De Roock, S., and Lambers, H. (2003). Shoot P status regulates cluster-root growth and citrate exudation in *Lupinus albus* grown with a divided root system. *Plant Cell Environ.* 26, 265–273. doi: 10.1046/j.1365-3040.2003.00957.x

Shen, J., Li, H., Neumann, G., and Zhang, F. (2005). Nutrient uptake, cluster root formation and exudation of protons and citrate in *Lupinus albus* as affected by localized supply of phosphorus in a split-root system. *Plant Sci.* 168, 837–845. doi: 10.1016/j.plantsci.2004.10.017

Shen, J., Rengel, Z., Tang, C., and Zhang, F. (2003). Role of phosphorus nutrition in development of cluster roots and release of carboxylates in soil-grown *Lupinus albus*. *Plant Soil* 248, 199–206. doi: 10.2307/24129588

Shen, J., Yuan, L., Zhang, J., Li, H., Bai, Z., Chen, X., et al. (2011). Phosphorus dynamics: from soil to plant. *Plant Physiol.* 156, 997–1005. doi: 10.1104/pp.111.175232

Shi, H. R., Wang, B., Yang, P. J., Li, Y. B., and Miao, F. (2016). Differences in sugar accumulation and mobilization between sequential and non-sequential senescence wheat cultivars under natural and drought conditions. *PLoS One* 11:e0166155. doi: 10.1371/journal.pone.0166155

Sparkes, D. L., Berry, P., and King, M. (2008). Effects of shade on root characters associated with lodging in wheat (*Triticum aestivum*). *Ann. Appl. Biol.* 152, 389–395. doi: 10.1111/j.1744-7348.2008.00230.x

Teng, W., Deng, Y., Chen, X., Xu, X., Chen, R., Lv, Y., et al. (2013). Characterization of root response to phosphorus supply from morphology to gene analysis in field-grown wheat. *J. Exp. Bot.* 64, 1403–1411. doi: 10.1093/jxb/ert023

Valladares, F., and Niinemets, Ü (2008). Shade tolerance, a key plant feature of complex nature and consequences. *Annu. Rev. Ecol. Evol. Syst.* 39, 237–257. doi: 10.1146/annurev.ecolsys.39.110707.173506

Van Gelderen, K., Kang, C., Paalman, R. Keuskamp, D., Hayes, S., and Pierik, R. (2018a). Far-red light detection in the shoot regulates lateral root development through the HY5 transcription factor. *Plant Cell* 30, 101–116. doi: 10.1105/tpc.17.00771

Van Gelderen, K., Kang, C., and Pierik, R. (2018b). Light signaling, root development, and plasticity. *Plant Physiol.* 176, 1049–1060. doi: 10.1104/pp.17.01079

Wang, X. R., Shen, J. B., and Liao, H. (2010). Acquisition or utilization, which is more critical for enhancing phosphorus efficiency in modern crop? *Plant Sci.* 179, 302–306. doi: 10.1016/j.plantsci.2010.06.007

Wang, X. R., Wang, Y. X., Tian, J., Lim, B. L., Yan, X. L., and Liao, H. (2009). Overexressing *AtPAP15* enhances phosphorus efficiency in soybean. *Plant Physiol.* 151, 233–240. doi: 10.1104/pp.109.138891

Wang, Z. K., Zhao, X. N., Wu, P. T., Gao, Y., Yang, Q., and Shen, Y. Y. (2017). Border row effects on light interception in wheat/maize strip intercropping systems. *Field Crop Res.* 214, 1–13. doi: 10.1016/j.fcr.2017.08.017

Watt, M., and Evans, J. R. (1999). Linking development and determinacy with organic acid efflux from proteoid roots of white lupin grown with low phosphorus and ambient or elevated atmospheric CO2 concentration. *Plant Physiol.* 120, 705–716. doi: 10.1104/pp.120.3.705

Wen, Z. H., Li, H. G., Shen, J. B., and Rengel, Z. (2017). Maize responds to low shoot P concentration by altering root morphology rather than increasing root exudation. *Plant Soil* 416:37. doi: 10.1007/s11104-017-3214-0

Wissuwa, M., Gamat, G., and Ismail, A. M. (2005). Is root growth under phosphorus deficiency affected by source or sink limitation? *J. Exp. Bot.* 56, 1943–1950. doi: 10.1093/jxb/eri189

Yuan, Z. Y., and Chen, H. Y. H. (2012). A global analysis of fine root production as affected by soil nitrogen and phosphorus. *Proc. R. Soc. B Biol. Sci.* 279, 3796–3802. doi: 10.1098/rspb.2012.0955

Zhang, D. S., Zhang, C. C., Tang, X. Y., Li, H. G., Zhang, F. S., Rengel, Z., et al. (2016). Increased soil phosphorus availability induced by faba bean root exudation stimulates root growth and phosphorus uptake in neighboring maize. *New Phytol.* 209, 823–831. doi: 10.1111/nph.13613

Zhang, L., Van der Werf, W., and Bastiaans, L. (2008). Light interception and utilization in relay intercrops of wheat and cotton. *Field Crop Res.* 107, 29–42. doi: 10.1016/j.fcr.2007.12.014

Zhang, Y., Yu, P., Peng, Y., Li, X., Chen, F., and Li, C. (2012). Fine root patterning and balanced inorganic phosphorus distribution in the soil indicate distinctive adaptation of maize plants to phosphorus deficiency. *Pedosphere* 22, 870–877. doi: 10.1016/S1002-0160(12)60073-3

Zhang, Y. T., Liu, J., Zhang, J. Z., Liu, H. B., Liu, S., Zhai, L. M., et al. (2015). Row ratios of intercropping maize and soybean can affect agronomic efficiency of the system and subsequent wheat. *PLoS One* 10:e0129245. doi: 10.1371/journal.pone.0129245

Zhou, K., Yamagishi, M., Osaki, M., and Masuda, K. (2008). Sugar signaling mediates cluster root formation and phosphorus starvation-induced gene expression in white lupin. *J. Exp. Bot.* 59, 2749–2756. doi: 10.1093/jxb/ern130

Zhou, T., Du, Y. L., Ahmed, S., Liu, T., Ren, M. L., Liu, W. G., et al. (2016). Genotypic differences in phosphorus efficiency and the performance of physiological characteristics in response to low phosphorus stress of soybean in southwest of China. *Front. Plant Sci.* 7:1776. doi: 10.3389/fpls.2016.01776

Zhu, J., Werf, W., van der Vos, J., Anten, N. P. R., Putten, P. E. L., van der, et al. (2016). High productivity of wheat intercropped with maize is associated with plant architectural responses. *Ann. Appl. Biol.* 168, 357–372. doi: 10.1111/aab.12268

Zhu, J. Q., van der Werf, W., Anten, N. P. R., Vos, J., and Evers, J. B. (2015). The contribution of phenotypic plasticity to complementary light capture in plant mixtures. *New Phytol.* 207, 1213–1222. doi: 10.1111/nph.13416

Zobel, R. W., Kinraide, T. B., and Baligar, V. C. (2007). Fine root diameters can change in response to changes in nutrient concentrations. *Plant Soil* 297, 243–254. doi: 10.1007/s11104-007-9341-2

Conflict of Interest Statement: The authors declare that the research was conducted in the absence of any commercial or financial relationships that could be construed as a potential conflict of interest.

Advantages of publishing in Frontiers

OPEN ACCESS
Articles are free to read for greatest visibility and readership

FAST PUBLICATION
Around 90 days from submission to decision

HIGH QUALITY PEER-REVIEW
Rigorous, collaborative, and constructive peer-review

TRANSPARENT PEER-REVIEW
Editors and reviewers acknowledged by name on published articles

Frontiers
Avenue du Tribunal-Fédéral 34
1005 Lausanne | Switzerland

Visit us: www.frontiersin.org
Contact us: frontiersin.org/about/contact

REPRODUCIBILITY OF RESEARCH
Support open data and methods to enhance research reproducibility

DIGITAL PUBLISHING
Articles designed for optimal readership across devices

FOLLOW US
@frontiersin

IMPACT METRICS
Advanced article metrics track visibility across digital media

EXTENSIVE PROMOTION
Marketing and promotion of impactful research

LOOP RESEARCH NETWORK
Our network increases your article's readership